

# Innate immunity and metabolism in the bovine ovarian follicle

Submitted to Swansea University in fulfilment of the requirements for  
the Degree of Doctor of Philosophy

by

Anthony D. Horlock (B. Sc.)



Submitted September 2021

**Swansea University Medical School**  
**Ysgol Feddygaeth Prifysgol Abertawe**



Swansea University  
Prifysgol Abertawe

## Summary


Postpartum uterine disease in dairy cows is associated with reduced fertility. One of the first and most prevalent bacteria associated with uterine disease is *Escherichia coli*. The bacterial endotoxin, lipopolysaccharide (LPS), accumulates in the ovarian follicular fluid of animals with uterine disease. The granulosa cells of the ovarian follicle respond to LPS by secreting pro-inflammatory cytokines, such as interleukin (IL)-1 $\alpha$ , IL-1 $\beta$  and IL-8, and oocyte health is perturbed. Dairy cows also experience metabolic energy stress in the postpartum period, which is associated with an increased risk of developing uterine disease and ovarian dysfunction.

This thesis explored the crosstalk between innate immunity and metabolic energy stress in bovine granulosa cells and cumulus-oocyte complex. Firstly, we found that glycolysis, AMP-activated protein kinase and the mechanistic target of rapamycin, regulate the innate immune responses to LPS in granulosa cells isolated from bovine ovarian follicles. Activation of AMP-activated protein kinase decreased the LPS-induced secretion of IL-1 $\alpha$ , IL-1 $\beta$ , and IL8, and was associated with shortened duration of ERK1/2 and JNK phosphorylation. Next, we found that decreasing the availability of cholesterol or inhibiting cholesterol biosynthesis using short-interfering RNA impaired the LPS-induced secretion of IL-1 $\alpha$  and IL-1 $\beta$  by granulosa cells. Furthermore, metabolic energy stress or inhibiting cholesterol biosynthesis in the bovine cumulus-oocyte complex modulated the innate immune responses to LPS, and perturbed meiotic progression during *in vitro* maturation. Finally, we explored an *in vivo* model of uterine disease in heifers, using RNAseq to investigate alterations to the transcriptome of the reproductive tract. We found that uterine disease altered the transcriptome of the endometrium, oviduct, granulosa cells and oocyte, several months after bacterial infusion; these changes were most evident in the granulosa cells and oocyte of the ovarian follicle.

The findings from this thesis imply that there is crosstalk between innate immunity and metabolism in the bovine ovarian follicle.

**Declaration**

This work has not previously been accepted in substance for any degree and is not being concurrently submitted in candidature for any degree.

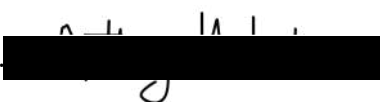
Signed .......... (candidate)

Date .....22.09.2021.....

**Statement 1**

This work is the result of my own investigations, except where otherwise stated. Where correction services have been used, the extent and nature of the correction is clearly marked in a footnote(s).

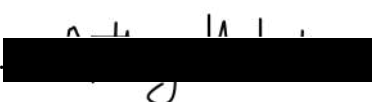
Other sources are acknowledged by footnotes giving explicit references. A bibliography is appended.

Signed .......... (candidate)

Date .....22.09.2021.....

**Statement 2**

I hereby give consent for my thesis, if accepted, to be available for photocopying and for inter-library loan, and for the title and summary to be made available to outside organizations.

Signed .......... (candidate)

Date .....22.09.2021.....

## **Acknowledgements**

The work in this thesis was supported by the Eunice Kennedy Shriver National Institute of Child Health & Human Development of the National Institutes of Health under Award Number R01HD084316, and a Swansea University research studentship. Following disruption to research due to Covid-19, I was supported by the Higher Education Funding Council for Wales (HEFCW) Higher Education and Recovery (HEIR) Fund, and Society for Reproduction and Fertility (SRF) Covid-19 PhD Grant. I am grateful for all the financial support I have received, without which I would not have been able to carry out this research.

I would like to thank my supervisors, Professor Martin Sheldon, Dr Martin Clift, and Dr John Bromfield for their continued support, guidance, and encouragement throughout my PhD. I would also like to thank Nathan Freemantle and Eva Camacho from Kepak for allowing me access to bovine reproductive tracts, and for preparing collections following access restrictions due to Covid-19.

One of the highlights of my PhD was to have the pleasure of visiting the project collaborators at the University of Florida Department of Animal Sciences, where I received training on the isolation, culture, and treatment of bovine cumulus-oocyte complexes. I would also like to thank Dr James Cronin, Dr Sian Owens, and Dr Tom Ormsby for all their advice and technical support over the last 4 years.

Finally, I would like to thank my family for all their support and patience throughout my time in Swansea University.

## List of Figures

Figure 1.1. Structure of the bovine ovary .....	2
Figure 1.2. Components of the bovine ovarian follicle.....	3
Figure 1.3. Synthesis of steroid hormones from cholesterol in the ovarian follicle ....	8
Figure 1.4. Oocyte meiotic progression from interphase to metaphase II .....	10
Figure 1.5. Communication between cumulus granulosa cells and the oocyte .....	12
Figure 1.6. The general structure of lipopolysaccharide in Gram-negative bacteria.	19
Figure 1.7. The TLR4 signalling pathway .....	21
Figure 1.8. Mechanism of inflammasome activation and IL-1 $\beta$ production .....	23
Figure 1.9. Cellular energy homeostasis regulated by AMPK .....	30
Figure 1.10. Mechanisms of AMPK activation in cells.....	31
Figure 1.11. Regulation of mTOR .....	35
Figure 1.12. Sources of cholesterol in cells .....	38
Figure 1.13. The mevalonate pathway of cholesterol biosynthesis .....	39
Figure 2.1. Granulosa cells from dominant follicles have higher expression of <i>LHR</i> than granulosa cells isolated from emerged follicles .....	48
Figure 2.2. Granulosa cells from dominant follicles secrete more oestradiol than granulosa cells isolated from emerged follicles .....	48
Figure 2.3. Cytokine production by granulosa cells increases with cell density .....	49
Figure 2.4. Oocyte meiotic maturation .....	53
Figure 2.5. Representative whole western blot images.....	59
Figure 2.6. Example standard curves for IL-1 $\alpha$ , IL-1 $\beta$ , IL-8, oestradiol, and progesterone ELISAs .....	64
Figure 2.7. The expression of <i>ACTB</i> or <i>RLP19</i> in granulosa cells was not altered by siRNA treatment .....	72
Figure 3.1. Concentrations of glucose in follicular fluid .....	84
Figure 3.2. Glucose availability does not alter the secretion of IL-1 $\alpha$ , IL-1 $\beta$ or IL-8 by granulosa cells.....	86
Figure 3.3. Inhibition of glycolysis with 2-deoxy-D-glucose (2-DG) reduced the secretion of IL-1 $\alpha$ , IL-1 $\beta$ and IL-8 by granulosa cells .....	87
Figure 3.4. Treatment with glucose or 2-DG does not alter cell viability .....	88

Figure 3.5. Manipulation of AMPK and mTOR regulates innate immunity in granulosa cells.....	90
Figure 3.6. Rapamycin and Torin 1 reduce the phosphorylation of p70S6K .....	91
Figure 3.7. Effects of AICAR on phosphorylated AMPK and ACC.....	93
Figure 3.8. Treatment with AICAR increases the abundance of phosphorylated ACC in granulosa cells.....	94
Figure 3.9. Activation of AMPK with AICAR reduced the innate immune response in granulosa cells.....	95
Figure 3.10. Treatment with AICAR does not alter cell viability.....	96
Figure 3.11. AICAR truncates the LPS-stimulated phosphorylation of ERK1/2 and JNK .....	98
Figure 3.12. AICAR truncates the LPS-induced phosphorylation of ERK1/2 and JNK .....	99
Figure 3.13. Inhibition of mTOR with rapamycin did not affect the innate immune response in granulosa cells.....	101
Figure 3.14. Treatment with rapamycin does not alter cell viability .....	102
Figure 3.15. Inhibition of mTOR with Torin 1 reduced the innate immune response in granulosa cells.....	103
Figure 3.16. Torin 1 reduces viability of granulosa cells at higher concentrations .	104
Figure 3.17. Torin 1 did not alter LPS-stimulated phosphorylation of MAPK .....	105
Figure 3.18. Torin 1 did not alter LPS-stimulated phosphorylation of MAPK .....	106
Figure 3.19. Treatment with LPS, AICAR or Torin 1 reduced the secretion of oestradiol and progesterone by granulosa cells from dominant follicles.....	108
Figure 4.1. Ovarian follicles contain mostly HDL cholesterol .....	122
Figure 4.2. Granulosa cells express more SR-BI than LDL receptor .....	123
Figure 4.3. Reducing FBS impairs IL-1 responses in granulosa cells, in response to LPS.....	125
Figure 4.4. Follicular fluid augments the LPS-induced secretion of IL-1 $\alpha$ , IL-1 $\beta$ and IL-8 by granulosa cells.....	126
Figure 4.5. High-density lipoprotein augments the LPS-induced secretion of IL-1 $\alpha$ and IL-1 $\beta$ by granulosa cells.....	128
Figure 4.6. Low-density lipoprotein does not alter the LPS-induced secretion of IL-1 $\alpha$ , IL-1 $\beta$ or IL-8 by granulosa cells.....	129

Figure 4.7. Very low-density lipoprotein does not alter the LPS-induced secretion of IL-1 $\alpha$ , IL-1 $\beta$ or IL-8 by granulosa cells .....	130
Figure 4.8. Methyl- $\beta$ -cyclodextrin treatment reduces the LPS-induced secretion of IL-1 $\alpha$ , IL-1 $\beta$ and IL-8 by granulosa cells .....	132
Figure 4.9. RNA interference in granulosa cells reduces the innate immune response to LPS.....	134
Figure 4.10. RNA interference reduced the gene expression of <i>HMGCR</i> , <i>FDPS</i> or <i>FDFT1</i> .....	135
Figure 4.11. Lovastatin treatment increases the LPS-induced secretion of IL-1 $\alpha$ and IL-1 $\beta$ by granulosa cells .....	137
Figure 4.12. Alendronate treatment increases the LPS-induced secretion of IL-1 $\alpha$ and IL-1 $\beta$ by granulosa cells.....	138
Figure 4.13. Zaragozic acid treatment increases the LPS-induced secretion of IL-1 $\alpha$ and IL-1 $\beta$ by granulosa cells.....	139
Figure 4.14. Treatment of granulosa cells with LPS, lovastatin, alendronate, zaragozic acid or methyl- $\beta$ -cyclodextrin reduce total cellular cholesterol in serum-starved, but not serum containing conditions .....	141
Figure 4.15. Refeeding mevalonate reduced the lovastatin-induced secretion of IL-1 $\alpha$ and IL-1 $\beta$ by granulosa cells .....	143
Figure 4.16. Refeeding FPP reduced the alendronate-induced secretion of IL-1 $\beta$ by granulosa cells.....	144
Figure 4.17. Lovastatin and M $\beta$ CD reduces the LPS-induced abundance of phosphorylated ERK1/2 in granulosa cells from emerged follicles .....	146
Figure 4.18. M $\beta$ CD reduces the LPS-induced abundance of phosphorylated JNK in granulosa cells from dominant follicles .....	147
Figure 4.19. siRNA targeting <i>HMGCR</i> , <i>FDPS</i> or <i>FDFT1</i> reduces the lovastatin augmented LPS response of granulosa cells to LPS .....	149
Figure 4.20. FSH augments inflammatory responses in serum-starved conditions.	152
Figure 4.21. FSH augments inflammatory responses in 2% serum .....	153
Figure 4.22. FSH has limited effects on the innate immune responses to LPS in 10% serum.....	154
Figure 4.23. FSH augments granulosa cell responses to LPS.....	156
Figure 4.24. LH impairs LPS-induced IL-8 secretion by granulosa cells.....	157

Figure 4.25. FSH increases SR-BI in granulosa cells from emerged follicles.....	159
Figure 4.26. FSH increases SR-BI in granulosa cells from dominant follicles .....	160
Figure 4.27. Lovastatin increases in the abundance of SR-BI in granulosa cells ....	161
Figure 4.28. siRNA targeting <i>HMGCR</i> , <i>FDPS</i> or <i>FDFT1</i> does not alter the abundance of SR-BI in granulosa cells .....	162
Figure 5.1. Identification of meiotic status during IVM .....	174
Figure 5.2. LPS induces COC expansion in absence of hormone supplementation	176
Figure 5.3. Glycolysis and AMPK are important for COC expansion .....	177
Figure 5.4. Manipulating energy metabolisms impairs innate immune function of COC's.....	178
Figure 5.5. AICAR impairs meiotic progression in the absence of hormones .....	180
Figure 5.6. 2-DG, AICAR or Torin 1 treatment impairs meiotic progression during IVM.....	181
Figure 5.7. AICAR may induce GVBD failure in bovine oocytes .....	183
Figure 5.8. Cholesterol biosynthesis inhibitors do not alter COC expansion.....	185
Figure 5.9. Inhibiting cholesterol metabolism alters the innate immune function of COC's.....	186
Figure 5.10. Inhibitors of cholesterol biosynthesis impair meiotic progression during IVM.....	187
Figure 6.1. Volcano plots, principal component analysis and heatmap analysis for bacteria-infused and control animals .....	198
Figure 6.2. Volcano plots, principal component analysis and heatmap analysis for bacteria-infused and control animals .....	200
Figure 6.3. Volcano plots, principal component analysis and heatmap analysis for bacteria-infused and control animals .....	202
Figure 6.4. Venn diagram of the common and unique differentially expressed genes 3 months after bacterial infusion.....	204
Figure 6.5. Ingenuity Pathway Analysis of differentially expressed genes.....	205
Figure 6.6. Gene networks of the endometrium affected by bacteria infusion.....	207
Figure 6.7. Gene networks of the oviduct affected by bacteria infusion .....	208
Figure 6.8. Gene networks of the ovarian follicle affected by bacteria infusion....	209
Figure 6.9. Predicted upstream regulators of differentially expressed genes affected by bacteria infusion.....	211
Figure 6.10. Predicted diseases and functions affected by bacteria infusion.....	212



Figure 7.1. Energy stress impairs granulosa cell innate immunity and endocrine function .....	222
Figure 7.2. Alterations to HDL concentrations or cholesterol biosynthesis affect the innate immune responses of granulosa cells to LPS .....	225
Figure 7.3. Proposed effects of energy stress and uterine infection on the ovarian follicle .....	229

### **List of Tables**

Table 2.1. Small molecules used to examine pathways .....	46
Table 2.2. Antibodies used for immunofluorescence .....	52
Table 2.3. Formulation of polyacrylamide gel for SDS-PAGE .....	56
Table 2.4. Formulation of stacking gel for SDS-PAGE .....	56
Table 2.5. Antibodies for western blot .....	57
Table 2.6. Amplex Red working solution .....	66
Table 2.7. siRNA sequence for target gene knockdown .....	68
Table 2.8. Complementary DNA synthesis master mix .....	69
Table 2.9. Components for qPCR .....	70
Table 2.10. qPCR primers used in this thesis .....	71

## List of Abbreviations

- A4 - Androstenedione
- ABCA1 - ATP-binding cassette subfamily A member 1
- ABCG1 - ATP-binding cassette subfamily G member 1
- ACAT - Acetyl-coenzyme A acetyltransferase
- ACC - Acetyl-CoA carboxylase
- ADP - Adenosine diphosphate
- AI - Anaphase I
- AICAR - 5-aminoinidazole-4-carboxamide-riboside-5-phosphate
- AKT - Protein kinase B
- AMPK - Adenosine monophosphate activated protein kinase
- AMP - Adenosine monophosphate
- ANOVA - Analysis of variance
- AP-1 - Activator protein 1
- APS - Ammonium persulfate
- ASC - Apoptosis-associated speck-like protein
- ATP - Adenosine triphosphate
- BCS - Body condition score
- BHB -  $\beta$ -hydroxybutyrate
- BMP15 - Bone morphogenetic protein 15
- BSA - Bovine serum albumin
- CaMKK $\beta$  - Calcium/calmodulin-dependent protein kinase kinase beta
- cAMP - Cyclic adenosine monophosphate
- CD14 - Cluster of differentiation 14
- CEH - Cholesterol ester hydrolase
- CFU - Colony forming units
- CO<sub>2</sub> - Carbon dioxide
- COC - Cumulus-oocyte complex
- Cq - Quantification cycle
- CYP11A1 - Cytochrome P450, family 11, subfamily A, polypeptide 1
- CYP19A1 - Cytochrome P450 Family 19 Subfamily A Member 1 (aromatase)
- D<sub>2</sub>O - Deuterium oxide
- DAMP - Damage-associated molecular pattern

DC (assay) - Detergent compatible (assay)  
DEG - Differentially expressed genes  
Dexamethasone - 1-dehydro-9-fluoro-16-methylhydrocortisone  
dH<sub>2</sub>O - Deionized water  
DMEM - Dulbecco's modified Eagle's medium  
DMSO - Dimethyl sulfoxide  
DNA/cDNA - Deoxyribonucleic acid (complementary DNA)  
DPBS - Dulbecco's phosphate-buffered saline  
*E. coli* - *Escherichia coli*  
E<sub>2</sub> - Oestradiol (1, 3, 5-Estratriene-3, 17β-diol)  
EGF - Epidermal growth factor  
EGTA - Ethylene glycol-bis (β-aminoethyl ether)- N, N, N', N'-tetraacetic acid  
ELISA - Enzyme-linked immunosorbent assay  
ERK1/2 - Extracellular-signal-regulated kinases 1/2  
FBS - Foetal bovine serum  
FDPS - Farnesyl pyrophosphate synthase  
FDFT1 - Farnesyl-diphosphate farnesyltransferase 1  
FGF2 - Basic fibroblast growth factor  
FPP - Farnesyl pyrophosphate  
FSH - Follicle stimulating hormone  
GC - Granulosa cell  
GDF9 - Growth differentiation factor 9  
GnRH - Gonadotropin-releasing hormone  
GV - Germinal vesicle  
GVBD - Germinal vesicle breakdown  
h - Hour  
HDL - High-density lipoprotein  
HEPES - 4-(2-hydroxyethyl)-1-piperazineethanesulfonic acid  
HIF-1α - Hypoxia-inducible factor 1α  
HMG-CoA - 3-hydroxy-3-methylglutaryl-coenzyme A  
HMGCR - 3-hydroxy-3-methylglutaryl-coenzyme A reductase  
HRP - Horseradish peroxidase  
HSDB3 - 3β-Hydroxysteroid dehydrogenase

IFN - Interferon  
IGF-1 - Insulin-like growth factor 1  
IgG - Immunoglobulin G  
IKK - Inhibitor of nuclear factor- $\kappa$ B kinase  
IL-1 $\alpha$  - Interleukin 1 alpha  
IL-1 $\beta$  - Interleukin 1 beta  
IL-8 - Interleukin 8  
INSIG - Insulin-induced gene 1  
IPA - Ingenuity pathway analysis  
IRAK - IL-1 receptor-associated kinase  
IRF3 - Interferon regulatory factor 3  
ITS - Insulin-transferrin selenium  
IVF - *In vitro* fertilisation  
IVM - *In vitro* maturation  
JNK - c-Jun N-terminal kinase  
LDL - Low-density lipoprotein  
LDS - Lipoprotein-deficient serum  
LDLR - Low density lipoprotein receptor  
LH - Luteinising hormone  
LKB1 - Liver kinase B1  
LPS - Lipopolysaccharide  
LXR - Liver X receptor  
LXRE - LXR response elements  
M199 - Medium 199  
MAL - MyD88 adaptor like  
MAPK - Mitogen-activated protein kinase  
MD-2 - Lymphocyte antigen 96 protein  
MI - Metaphase I  
MII - Metaphase II  
Min - minutes  
mRNA - Messenger ribonucleic acid  
mTOR - Mechanistic target of rapamycin  
mTORC1 - Mechanistic target of rapamycin complex 1

mTORC2 - Mechanistic target of rapamycin complex 2  
M $\beta$ CD - Methyl- $\beta$ -cyclodextrin  
MgCl<sub>2</sub> – Magnesium chloride  
MTT - 3-(4,5-dimethylthiazol-2-yl)-2,5-diphenyltetrazolium bromide  
MyD88 - Myeloid differentiation primary response gene 88  
NEB – Negative energy balance  
NEFA - Non-esterified fatty acids  
NF $\kappa$ B - Nuclear factor kappa-light-chain-enhancer of activated B cells  
NLRP3 - NOD-like receptor family, pyrin domain containing 3  
p38 - p38 MAP Kinase  
p70S6K - Ribosomal protein S6 kinase  
P<sub>4</sub> - Progesterone (Pregn-4-ene-3, 20-dione)  
PAMP - Pathogen-associated molecular pattern  
PBS - Phosphate buffered saline  
PCA - Principal component analysis  
PCR - Polymerase chain reaction  
PGE<sub>2</sub> - Prostaglandin E2  
PGF<sub>2 $\alpha$</sub>  - Prostaglandin F2 alpha  
PI3K - Phosphoinositide 3-kinase  
PIPES - piperazine-N, N'-bis (2- ethanesulfonic acid)  
PKA - Protein kinase A  
PKC - Protein kinase C  
PVDF - Polyvinylidene fluoride  
RAPTOR - Regulatory-associated protein of mTOR  
RICTOR - Rapamycin-insensitive companion of mTOR  
RNA - Ribonucleic acid  
RNAseq – RNA sequencing  
RT - Reverse transcriptase  
SCAP – SREBP cleavage-activating protein  
SDS - Sodium dodecyl sulphate  
SDS-PAGE - Sodium dodecyl sulphate polyacrylamide gel electrophoresis  
Sec - Seconds  
SEM - Standard error of the mean

siRNA - Short-interfering RNA  
SGK - Serum/glucocorticoid Regulated Kinase 1  
SR-BI - Scavenger receptor B1  
SREBP - Sterol regulatory element-binding protein  
StAR - Steroidogenic acute regulatory protein  
TAB - Transforming growth factor- $\beta$  activated kinase (TAK) binding protein 1  
TAK - Transforming growth factor- $\beta$  activated kinase  
TANK - TRAF-family-member-associated NF- $\kappa$ B activator  
TBST - Tris-buffered saline Tween-20  
TCA - Tricarboxylic acid cycle  
TEMED - N, N, N', N'-tetramethyl ethylenediamine  
Thr172 - Threonine 172  
TIR domain - Toll/interleukin-1 receptor (TIR) homology domain  
TIRAP - TIR domain-containing adapter protein  
TLR - Toll-like receptor  
TMB - 3,3',5,5'-tetramethylbenzidine  
TNF - Tumour necrosis factor  
TRAF - TNF receptor-associated factor  
TRAM - TRIF-related adaptor molecule  
TRIF - TIR-domain-containing adapter-inducing interferon  
TRIS - Trisaminomethane  
*T. pyogenes* - *Trueperella pyogenes*  
TSC - Tuberous sclerosis complex  
TZP - Transzonal projections  
VEGF - Vascular endothelial growth factor  
VLDL - Very low-density lipoprotein  
ZMP - 5-aminoimidazole-4-carboxamide ribonucleoside monophosphate  
ZP - Zona pellucida  
2-DG - 2-Deoxy-D-glucose  
4EBP1 - Eukaryotic translation initiation factor 4E

## **Publications arising from work presented in the present thesis:**

### **Chapter 3**

**Horlock, A. D., Ormsby, T. J. R., Clift, M. J. D., Santos, J. E. P., Bromfield, J. J., & Sheldon, I. M. (2021).** Manipulating bovine granulosa cell energy metabolism limits inflammation. *Reproduction*. *161*(5), 499-512. <https://doi.org/10.1530/REP-20-0554>

### **Chapter 4**

**Horlock, A. D., Ormsby, T. J. R., Clift, M. J. D., Santos, J. E. P., Bromfield, J. J., & Sheldon, I. M. (2022).** Cholesterol supports granulosa cell inflammatory responses to lipopolysaccharide. *Submitted to Reproduction in January 2022*

### **Chapter 6**

**Horlock, A. D., Piersanti, R. L., Ramirez-Hernandez, R., Yu, F., Ma, Z., Jeong, K. C., Clift, M. J. D., Block, J., Santos, J. E. P., Bromfield, J. J., & Sheldon, I. M. (2020).** Uterine infection alters the transcriptome of the bovine reproductive tract three months later. *Reproduction*, *160*(1), 93-107. <https://doi.org/10.1530/REP-19-0564>

## **Contributions to other publications during thesis:**

**Piersanti, R. L., Horlock, A. D., Block, J., Santos, J. E. P., Sheldon, I. M., & Bromfield, J. J. (2019).** Persistent effects on bovine granulosa cell transcriptome after resolution of uterine disease. *Reproduction*, *158*(1), 35-46. <https://doi.org/10.1530/REP-19-0037>

**Ormsby, T. J. R., Owens, S. E., Horlock, A. D., Davies, D., Griffiths, W. J., Wang, Y., Cronin, J. G., Bromfield, J. J. & Sheldon, I. M. (2021).** Oxysterols protect bovine endometrial cells against pore-forming toxins from pathogenic bacteria. *FASEB*, 2021;00:e21889. <https://doi.org/10.1096/fj.202100036R>

# 1 Introduction

## 1.1 General introduction

Fertility depends on the ovulation of a healthy oocyte, and oocyte health is dependent on the mural granulosa cells that line the ovarian follicle, and the cumulus granulosa cells that surround the oocyte. In the modern dairy cow, the uterus is contaminated with bacteria during the postpartum period, leading to perturbed ovarian function and reduced fertility. During postpartum uterine disease, the bacterial endotoxin lipopolysaccharide (LPS), accumulates in the bovine ovarian follicle. Bovine granulosa cells respond to LPS by secreting cytokines and chemokines, such as interleukin (IL)-1 $\beta$ , IL-6 and IL-8, associated with increased phosphorylation of the mitogen-activated protein kinases (MAPKs), extracellular-signal-regulated kinases 1/2 (ERK1/2) and p38 MAP Kinase (p38) (Bromfield and Sheldon, 2011, Price and Sheldon, 2013, Price et al., 2013).

Metabolic energetic stress, caused by energy demand exceeding supply around the time of parturition and during lactation, impairs immune cell function, perturbs ovarian function, and increases the risk of uterine disease (Beam and Butler, 1997, Hammon et al., 2006, LeBlanc, 2012, Leroy et al., 2008). The bovine ovarian follicle is also exposed to postpartum energy stress, which may impair granulosa cell and oocyte function (Leroy et al., 2004b, Leroy et al., 2004a, Shabankareh et al., 2013, Alves et al., 2014). Cellular energy metabolism is regulated by glycolysis, adenosine monophosphate-activated protein kinase (AMPK) and the mechanistic target of rapamycin (mTOR) (Hardie et al., 2012, Zoncu et al., 2011). Metabolism and immunity are highly integrated, with energetic stress altering immune cell responses to LPS (O'Neill et al., 2016). The link between metabolic energy stress and innate immunity is under-explored in the immune or reproductive systems of cattle at the animal level, and with even less known about the mechanisms at the cellular level. This thesis will focus on the crosstalk between innate immunity and metabolism in the granulosa cells and cumulus-oocyte complex of the bovine ovarian follicle.

The present chapter will discuss the background literature to the thesis. It will start by describing the structure and function of the bovine ovary, before reviewing follicular growth and oocyte maturation. The focus will then shift to the problem of uterine



disease in the dairy cow, and the innate immune responses to LPS. Metabolic energy stress in the modern dairy cow will then be discussed, followed by a description of the regulators of cellular energy metabolism, AMPK and the mTOR. Finally, cellular cholesterol metabolism and the mevalonate pathway of cholesterol biosynthesis will be discussed. The literature review will conclude by setting out the aims and objectives of the thesis.

## **1.2 Ovarian structure and function**

The ovaries are a vital part of the female reproductive system (**Fig. 1.1**). Ovaries have two main functions: to produce fertilizable oocytes with full competence for development, and to secrete the reproductive hormones oestradiol and progesterone, necessary for preparation of the reproductive tract for fertilization and the establishment of pregnancy. The two main types of tissue present in the ovary are the cortex and the medulla. The medulla contains the fibrous tissue, blood vessels and nerves; the cortex surrounds the medulla and contains the ovarian follicles. Within each follicle is an oocyte, surrounded by mural and cumulus granulosa cells, bathed in follicular fluid.

Bovine ovaries develop from gonadal primordia as a thickening of the coelomic epithelium on the ventral-medial surface of the mesonephros at around day 30 of embryo development (Wrobel and Suss, 1998). Gonadal sexual differentiation occurs around day 40 of foetal development in cattle (Erickson, 1966). Primordial germ cells are the undifferentiated gametes that are necessary for the formation of the ovary. Primordial germ cells migrate through the developing hindgut, along the dorsal mesentery to the gonads, rapidly proliferating throughout their migration. Primordial germ cells are mitotically active and represent the pool from which meiotic oocytes develop and differentiate. The germ cells form tight junctions with surface epithelial cells, that go on to become pre-granulosa cells; the germ cells then enter meiosis. The first primordial follicles are formed at day 90 in cows, when the basement membrane forms at the base of the ovigerous cords (Sawyer et al., 2002). Cows have approximately 1 to 3 million oocytes, most of which will undergo atresia during development; there are around 133,000 primordial follicles in each ovary at birth, declining until the cow reaches 15 to 20 years of age (Erickson, 1966).

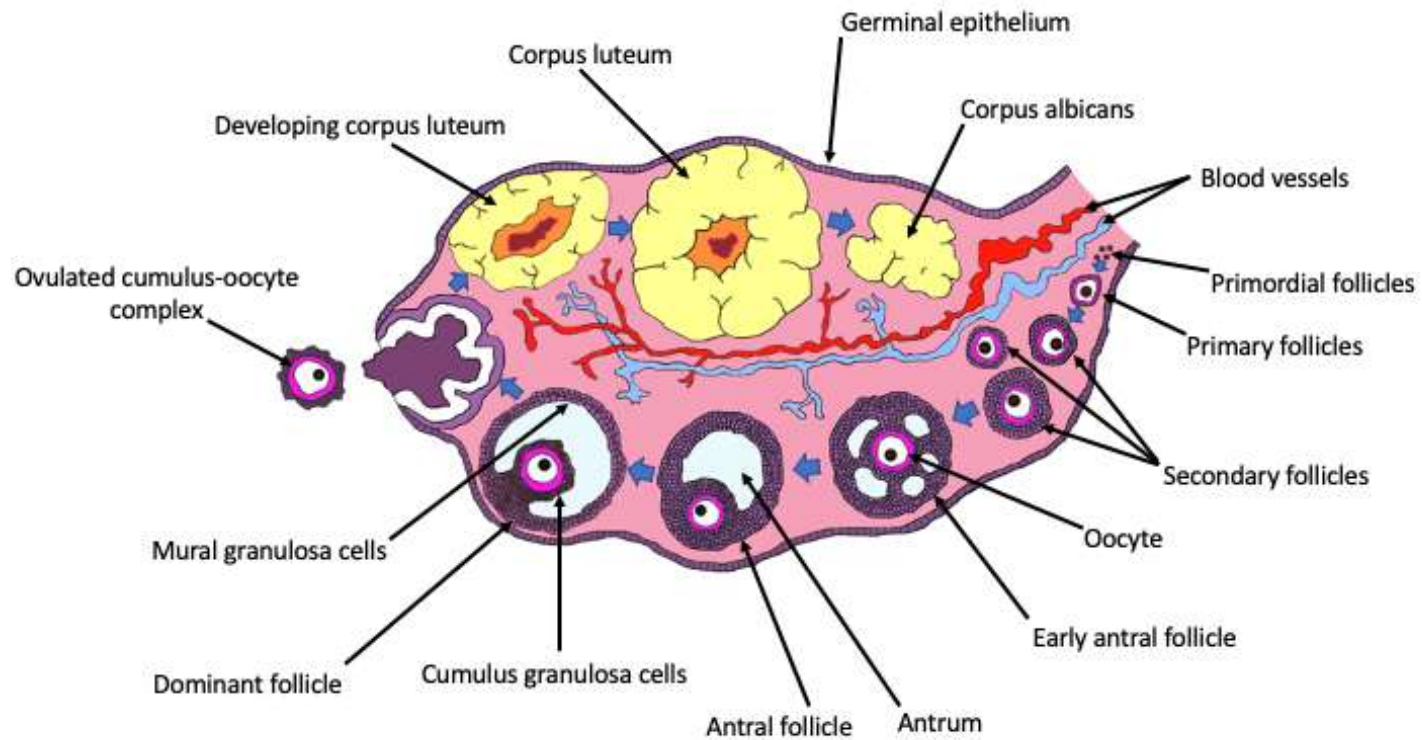


**Figure 1.1. Structure of the bovine ovary**

Structure of the ovary describing the stages of follicular development from primordial follicle to dominant follicle. The dominant follicle ovulates a cumulus-oocyte complex, and the mural granulosa cells luteinize to form the cells of the corpus luteum (Horlock A., 2018).

### 1.3 Follicle structure

Ovarian follicles are the fundamental units of the ovary and are made up of germ cells (oocytes) and somatic cells (granulosa cells and theca cells, along with a basement membrane and follicular fluid (**Fig. 1.2**). Theca cells synthesize androstenedione from cholesterol that is transported across the basement membrane of the ovarian follicle to the mural granulosa cells; androstenedione is then aromatized by mural granulosa cells to produce oestradiol (Ryan et al., 1968, Dorrington et al., 1975, Liu and Hsueh, 1986). Cumulus granulosa cells surround the oocyte, forming the cumulus-oocyte complex, surrounding the oocyte; cumulus cells provide nutrients such as pyruvate and cholesterol to the oocyte (Su et al., 2009). Follicular fluid is a product of blood plasma and secretory products of the granulosa cell and theca cells (Leroy et al., 2004b), and contains metabolites that are essential for oocyte health (Revelli et al., 2009).

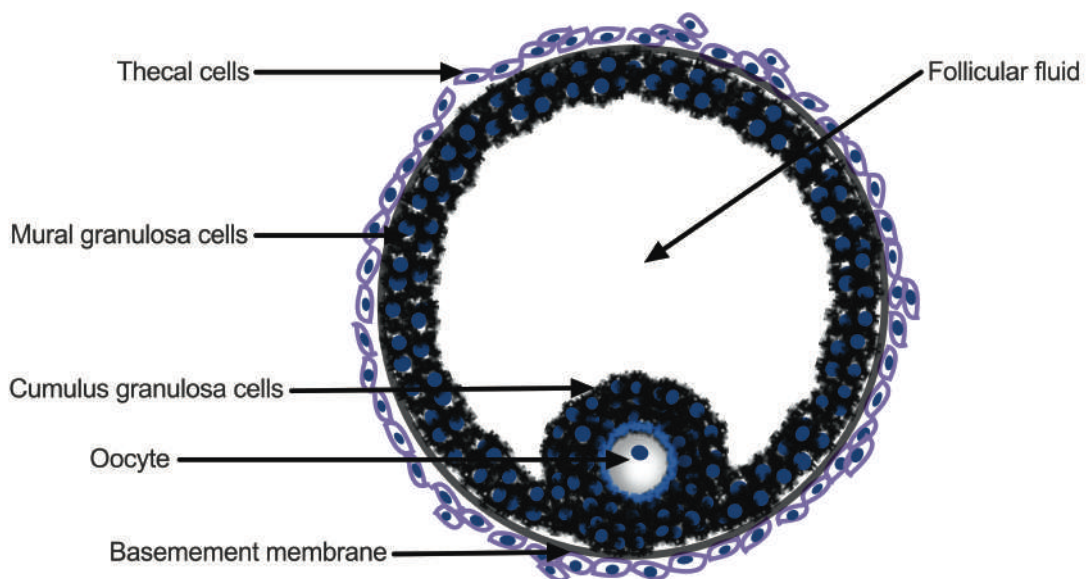


**Figure 1.2. Components of the bovine ovarian follicle**

Structure of the bovine ovarian follicle (Sheldon I M., 2018).

## 1.4 Follicle development

Follicle development from the primordial stage to the ovulation of an antral follicle takes around 150 to 200 days in cattle (Scaramuzzi et al., 2011). Primordial follicles consist of an oocyte, surrounded by a single layer of flattened pre-granulosa cells. The pool of primordial follicles is under inhibitory control by factors, such as anti-Müllerian hormone (Fortune, 2003). Once primordial follicles are released from this inhibitory control, the primordial follicles are activated (Kim, 2012, Wandji et al., 1996). Following activation and release from the primordial pool, granulosa cells increase in numbers and become uniformly cuboidal in shape (Matzuk et al., 2002, Braw-Tal and Yossefi, 1997). There are two to three waves of follicular growth during the bovine oestrous cycle (Fortune, 1994). Each wave consists of the release of a mean of 24 (range, 8 to 41) growing follicles (3 to 4 mm external diameter) from the primordial pool (Ginther et al., 1996), of which three to six follicles grow larger than 5 mm in external diameter (Sirois and Fortune, 1988, Savio et al., 1988),

During the preantral stage, the zona pellucida (ZP), which is absent in primordial follicles, is secreted around the oocyte, as well as increases in the volume of the mitochondria, ribosomes and smooth endoplasmic reticulum (Lundy et al., 1999). There is an increase in the number of granulosa cells, with seven to eight population doublings occurring, and the emergence of the cumulus and mural phenotypes (McNatty et al., 2007). The granulosa cells within the preantral follicle begin to express follicle stimulating hormone (FSH) receptors, although growth at this stage is gonadotrophin independent. The oocyte develops meiotic competence during the preantral to antral transition (Sorensen and Wassarman, 1976). Early antral follicles are most likely to undergo atresia, a selection process regulated by growth factors, cytokines and steroids, resulting in only the most viable oocytes remaining to continue development (Orisaka et al., 2009).

When the follicle has developed two or more layers of granulosa cells, an outer layer of theca cells differentiates, outside of the basement membrane (Young and McNeilly, 2010). At least in mice, the recruitment of theca cells is regulated by the granulosa cells, under the regulation of factors, such as growth differentiation factor 9 (GDF9), secreted by the oocyte (Liu et al., 2015). The theca is divided into two theca layers,

the theca externa, and the theca interna. The theca externa is comprised of fibroblast-like, non-steroidogenic cells that provide structural support to the growing follicle (Magoffin, 2005). The theca interna is highly vascularized and comprised of fibroblasts, endothelial cells, immune cells, and steroidogenic cells, that are the exclusive producer of ovarian androgens (Young and McNeilly, 2010, Hatzirodos et al., 2014a). The steroidogenic cells of the theca interna express luteinizing hormone receptors, and their proliferation, differentiation, and steroidogenesis are mostly under the control of luteinizing hormone (Hatzirodos et al., 2014a). Granulosa cell-derived factors, such as vascular endothelial growth factor (VEGF), basic fibroblast growth factor (FGF2), epidermal growth factor (EGF) and insulin-like growth factor one (IGF-1) are responsible for the establishment and regulation of the theca vascular network (Hatzirodos et al., 2014a). The main functions of the theca layers are to produce androgens for steroidogenesis by granulosa cells, to supply nutrients to the growing follicle via the vascular network, and to provide structural support to the follicle.

Bovine ovarian follicles become gonadotropin-dependent when follicles reach an external diameter of approximately 4 mm, associated with increased expression of FSH receptors (Bao et al., 1997a), and aromatase (cytochrome P450 Family 19 Subfamily A Member 1; CYP19A1) messenger RNA (mRNA) (Xu et al., 1995b). The expression of aromatase mRNA is not detectable in bovine granulosa cells isolated from follicles < 4 mm in external diameter (Xu et al., 1995a). Increased aromatase expression in granulosa cells during the antral stage allows for the synthesis of oestradiol from androstenedione, provided by the theca cells. Without a continuous supply of FSH, bovine ovarian follicles regress and undergo atresia (Gong et al., 1995, Gong et al., 1996). Immunizing cows against gonadotropin-releasing hormone decreases FSH concentrations and prevents the pulsatile secretion of luteinizing hormone (LH), arresting follicular growth at < 4 mm diameter (Crowe et al., 2001).

Antrum formation is associated with the development of fluid-filled cavities between the layers of somatic cells within the follicle (Matzuk et al., 2002). During the time of antrum formation, the granulosa cells differentiate into two populations that are functionally and spatially distinct. The differentiation of granulosa cells is driven by FSH and luteinising hormone, resulting in luteinisation of the mural granulosa cells

that line the walls of the follicle. Oocyte-secreted factors, GDF9 and bone morphogenetic protein 15 (BMP15; formerly known as GDF9 $\beta$ ), actively inhibit the luteinisation of the oocyte's neighbouring granulosa cells, maintaining the cumulus cell phenotype (Eppig et al., 1997, McNatty et al., 2005). Mural granulosa cells express LH receptors, whereas cumulus granulosa cells express very few, if any LH receptors (Amsterdam et al., 1975).

Bovine mural granulosa cells in the future dominant follicle begin to express mRNA for the LH receptor when the follicle reaches an external diameter of approximately 8.5 mm (Xu et al., 1995a, Bao et al., 1997a, Beg et al., 2001). The large amounts of oestradiol, androstenedione and inhibin secreted by the dominant follicle(s), reduces plasma FSH concentrations to below the threshold required to sustain other gonadotrophin-dependent follicles, resulting in atresia of follicles that have not switched over to LH dependence (Scaramuzzi et al., 2011). At the end of a follicle-growth wave, the dominant follicle responds to low progesterone concentrations and the increase in LH pulse frequency, releasing sufficient oestradiol to elicit a surge in LH and FSH which triggers ovulation (Fortune et al., 2001).

### **1.5 Reproductive hormones**

Gonadotrophins and steroid hormones are essential for the development and function of the ovarian follicle. The anterior pituitary gland secretes the gonadotrophins, FSH and LH, in response to gonadotropin-releasing hormone (GnRH). Early in the ovarian cycle, low-frequency GnRH pulses stimulate an increase in FSH concentrations that enhances follicle growth. Follicle-stimulating hormone promotes proliferation and differentiation of the granulosa cells within ovarian follicle to a pre-ovulatory phenotype. High-frequency GnRH pulses at around mid-cycle lead to the "LH surge", triggering ovulation and formation of the corpus luteum (Richards and Pangas, 2010). The "LH surge" is triggered by oestradiol, produced by the mural granulosa cells of the developing follicle; oestradiol both inhibits GnRH production and causes the high-frequency GnRH pulses.

Steroid hormones are synthesized from cholesterol (**Fig. 1.3**), which is imported into theca cells in the form of high-density lipoproteins (HDL) and low-density

lipoproteins (LDL), through binding scavenger receptor B1 (SR-BI) and LDL receptors on the theca cell membrane. Intracellular cholesterol can also be synthesized *de novo* via the mevalonate pathway (Bloch, 1965). Cholesterol metabolism will be discussed in more detail in *Section 1.14*.

Free cellular cholesterol is transported across the mitochondrial membrane by the steroidogenic acute regulatory protein (StAR), the rate-limiting step in steroidogenesis, and is activated, inhibited and regulated by trophic hormones (e.g. LH), transcription factors, and growth factors (e.g., insulin-like growth factor I (IGF-I)) (Walsh et al., 2012b). Cholesterol is converted into pregnenolone by cytochrome P450 Family 11 Subfamily A Member 1 (CYP11A1), which then diffuses out of the mitochondria. Pregnenolone is then converted into progesterone and androstenedione by enzymes in the cytoplasm. Granulosa cells do not synthesise oestradiol from cholesterol, instead they rely on the theca cells to provide androstenedione that is converted into oestradiol by the aromatase enzyme (Eppig, 1991, Richards, 1994). The LH surge triggers the transformation of granulosa and theca cells into luteal cells (luteinization) and thus a switch from oestradiol synthesis to progesterone synthesis (Drummond, 2006). Progesterone is mostly synthesized by the corpus luteum following the rupture of the dominant follicle at ovulation.

Oestradiol and progesterone are the hormones that are most associated with ovarian function. However, many other hormones and growth factors are essential for normal follicle development and ovulation. Some examples include granulosa cell-derived factors, such as VEGF, FGF2, EGF and IGF-1, which are essential for the establishment and regulation of the theca vascular network. Oocyte-derived factors, such as GDF9 and BMP15, are implicated in many functions, such as actively maintaining the cumulus cell phenotype, regulating theca cell differentiation, promoting the proliferation of granulosa cells, and expansion of the cumulus-oocyte complex (Sanfins et al., 2018). Prostaglandins, secreted by the uterus influence the function of the corpus luteum, with prostaglandin E2 (PGE<sub>2</sub>) preventing and prostaglandin F2 alpha (PGF<sub>2α</sub>) promoting luteolysis, respectively.

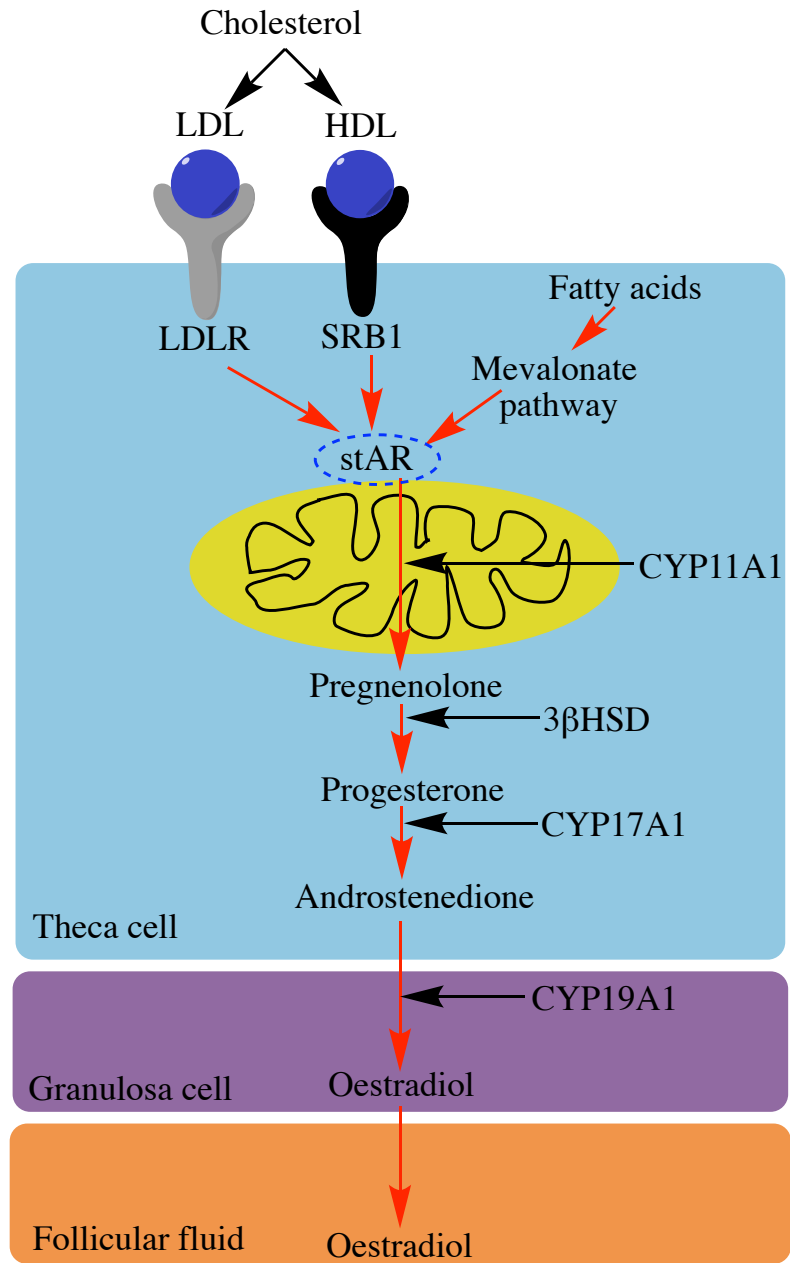


**Figure 1.3. Synthesis of steroid hormones from cholesterol in the ovarian follicle**

LDL: low-density lipoprotein; HDL: high-density lipoprotein; LDLR: low density lipoprotein receptor; SRB1: scavenger receptor B1; StAR: steroidogenic acute regulatory protein (adapted from (Walsh et al., 2012b)).



## 1.6 Oocyte maturation

Oocyte maturation is the process by which oocytes acquire the ability to support the subsequent stages of development, and can be divided into two main processes, nuclear and cytoplasmic maturation (Ferreira et al., 2009). The process of nuclear maturation in the oocyte begins during foetal development and is not completed until fertilization. Oocytes enter the meiotic cell cycle during foetal life and arrest at prophase I in primordial follicles until they develop through to the antral stage of growth. The preovulatory surge of LH initiates the resumption of meiotic maturation in the fully grown oocyte (**Fig. 1.4**). The preovulatory LH surge triggers an increase in maturation promoting factor, releasing the oocyte from meiotic arrest, resulting in both nuclear and cytoplasmic maturation. In addition to resumption of meiotic maturation, the LH surge is also associated with the formation of a hyaluronan-rich matrix, leading to cumulus expansion (Chen et al., 1990, Fulop et al., 2003). At ovulation, the oocyte completes the first meiotic division and proceeds to the second meiotic division, where meiosis is arrested at metaphase II until fertilisation.

During *in vitro* maturation (IVM), germinal vesicle breakdown (GVBD) takes around 6 to 8 h in cows (Conti and Franciosi, 2018) and is characterised by folding and fragmentation of the nuclear membrane, and disappearance of the nuclear pores. Following GVBD, the chromosomes align along the first metaphasic plate and the microtubules assemble into a spindle to reach metaphase I (MI) at around 10 to 15 h of IVM (Conti and Franciosi, 2018). The bivalent homologous chromosomes then migrate to the opposite poles of the spindle during anaphase I (AI) at around 16 to 17 h of IVM (Koyama et al., 2014), and become surrounded by a nuclear membrane during telophase I. Finally, the first polar body forms and is extruded from the oocyte, and the reassembling of the meiotic spindle along the equatorial plane occurs during metaphase II (MII), at around 22 to 24 h of IVM. The oocyte arrests at MII until fertilisation. Concomitant with nuclear maturation, oocytes also undergo cytoplasmic maturation. During cytoplasmic maturation, oocytes undergo extensive remodelling and redistribution of organelles, such as the cytoskeleton, mitochondria, the Golgi complex and cortical granules (Ferreira et al., 2009).

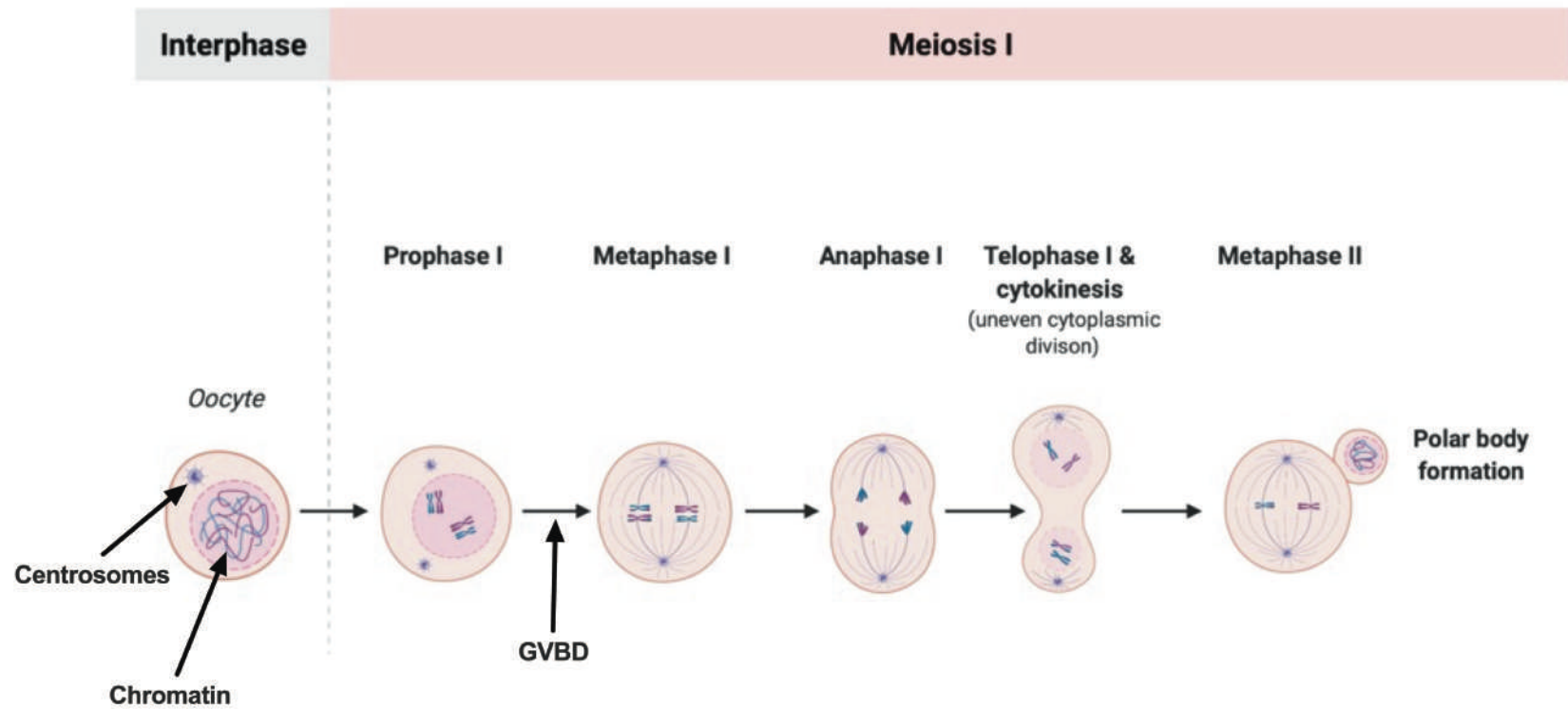


**Figure 1.4. Oocyte meiotic progression from interphase to metaphase II**

During foetal development, oocytes progress from interphase I to prophase I, where they arrest until the antral stage of follicle development. Following the preovulatory LH surge, oocytes progress from prophase I to metaphase II, where they are arrested until fertilization. GVBD, germinal vesicle breakdown (Horlock A., 2020; Created with BioRender.com).

## 1.7 Bi-directional communication

The zona pellucida (ZP) is composed of glycoproteins and forms an extracellular matrix that surrounds the oocyte (Rankin et al., 2001). The ZP glycoproteins, ZP1, ZP2 and ZP3, combine to form a layer around the oocyte which is up to 15  $\mu\text{m}$  thick (Cohen et al., 1992). There is bi-directional communication between the oocyte and the surrounding granulosa and cumulus cells via transzonal projections (TZPs; **Fig 1.5**), which are essential for the coordinated development of the oocyte and somatic cells within the follicle (Matzuk et al., 2002). The TZPs extend from the cumulus granulosa cells, traverse the ZP and terminate on the oocyte cell surface, allowing for the delivery of small molecules ( $< 1$  kDa) and paracrine factors (e.g. leptin) from granulosa cells to the oocyte and from the oocyte to granulosa cells (e.g. GDF9 and BMP15) (Hussein et al., 2006, Albertini et al., 2001). The delivery of these factors is thought to be modulated by FSH through the remodelling of the microtubule cytoskeleton (Albertini et al., 2001).

Gap junction channels between oocytes and cumulus granulosa cells consist of the connexin 37 protein; mural-mural and mural-cumulus cell gap junctions are also formed by the connexin 43 protein (Su et al., 2009). Gap junctions allow for the transport of ions (e.g. calcium), metabolites (e.g. pyruvate), amino acids and signalling molecules (e.g. cyclic adenosine monophosphate (cAMP)) between the cells of the follicle (Su et al., 2009). In ZP2-null mice, only a thin ZP is synthesized and cannot be sustained in pre-ovulatory follicles; ZP1-null mice have reduced fecundity, and ZP3-null mice are sterile (Rankin et al., 2001).

Oocytes are deficient in their ability to take up glucose (Purcell et al., 2012), carry out glycolysis (Su et al., 2009, Biggers et al., 1967, Sugiura et al., 2007) or cholesterol biosynthesis (Su et al., 2008), therefore they outsource this function to the surrounding cumulus granulosa cells. Oocytes regulate glycolysis and cholesterol biosynthesis in cumulus cells by releasing paracrine factors, such as GDF9, BMP15 or fibroblast growth factor to promote the expression of genes encoding glycolytic and cholesterol biosynthesis enzymes (Sugiura et al., 2005, Sugiura et al., 2007, Su et al., 2008).

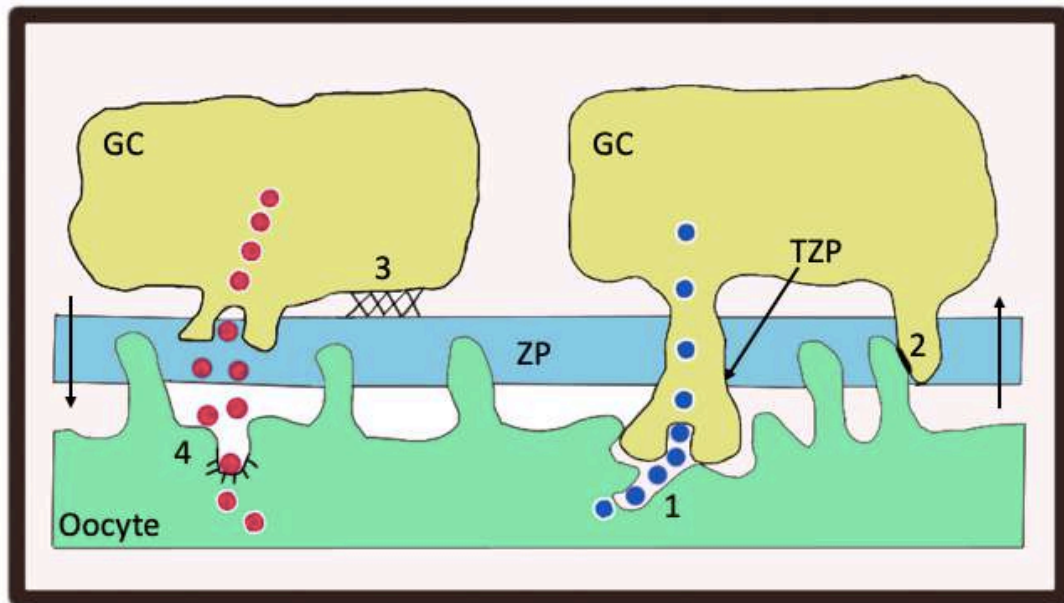


**Figure 1.5. Communication between cumulus granulosa cells and the oocyte**

(1) Endocytosis of oocyte-derived factors, such as GDF9 at attached sites of TZPs to the oolemma. (2) Gap junctions allowing for the direct communication between granulosa cells and the oocyte. (3) Correct orientation of TZPs is achieved by granulosa-zona pellucida anchoring. (4) Receptor-mediated endocytosis of granulosa cell-derived factors by the oocyte. GC: Granulosa cell; ZP: Zona pellucida; TZP: Transzonal projection; Granulosa cell factors (red circles); Oocyte-secreted factors (blue circles). Adapted from (Albertini et al., 2001).

## 1.8 Uterine Disease and infertility

Approximately 40% of dairy cattle suffer bacterial uterine infections following parturition (Sheldon et al., 2009), and disrupted ovarian function and infertility is observed in cows suffering these infections (Sheldon et al., 2002). The estimated cost of uterine infection to the dairy industry, in term of lost milk production, delayed conception and treatment costs is €1.4 billion/year and \$650 million/year to the European Union and United States, respectively (Sheldon et al., 2009).

Contamination of the uterus with bacteria is ubiquitous following parturition, with approximately 40% developing metritis, 30% developing subclinical endometritis and approximately 15% of dairy cattle developing clinical endometritis (Sheldon et al., 2009, LeBlanc et al., 2002). Metritis typically occurs within 21 days of parturition and is characterized by a purulent uterine discharge, often accompanied by a fetid odour (Sheldon et al., 2009). There are three grades of metritis: (i) grade one metritis where animals have an enlarged uterus and a purulent uterine discharge, (ii) grade two metritis where animals experience additional symptoms, such as decreased milk yield and a fever  $> 39.5^{\circ}\text{C}$ , and (iii) grade three metritis where animals display additional signs, such as decreased appetite (Sheldon et al., 2009). Subclinical endometritis is characterized by uterine samples containing neutrophils between 5.5% and 10% of the total cells (Kasimanickam et al., 2004, Santos et al., 2009). Clinical endometritis is characterized by the presence of a pus within the uterus and a purulent discharge, which is often detectable in the vagina 21 days or more postpartum (Sheldon, 2020, Sheldon et al., 2019a). Clinical endometritis is graded on a three-point scale: (i) grade 0, clear or translucent mucus, (ii) grade 1, mucus containing flecks of pus, (iii) grade 2, mucus containing  $\leq 50\%$  pus, and (iv) grade 3, mucus containing  $> 50\%$  pus (Sheldon et al., 2009).

Clinical disease usually resolves following treatment, or spontaneously resolves after one to two months. However, the importance of endometritis is that even after resolution of the disease, animals remain less fertile than unaffected animals. Compared with unaffected animals, a history of endometritis increases the interval to first insemination by approximately 11 days, delays conception by 32 days, and nearly doubles involuntary culling (Borsberry and Dobson, 1989, LeBlanc et al., 2002).

The most prevalent bacteria isolated from the uteri of postpartum dairy cows with uterine disease are *Escherichia coli* and *Trueperella pyogenes* (Sheldon et al., 2002, Williams et al., 2007). The strains of *E. coli* that cause uterine disease in cattle are genetically different to strains that are found in the gastrointestinal tract, more invasive for endometrial stromal cells, and twice as adherent as *E. coli* isolated from clinically unaffected animals (Sheldon et al., 2010).

Cows with uterine disease have compromised fertility, often displaying irregular ovarian cycles, a prolonged postpartum luteal phase and delayed onset of ovarian cyclicity (Ribeiro et al., 2013, Opsomer et al., 1998). Holstein heifers that received an infusion of LPS into the uterus had suppressed LH surge and did not ovulate (Peter et al., 1989). In a study of 70 postpartum dairy cows, the diameter of the first dominant follicle was smaller, dominant follicle growth was slower, and plasma oestradiol concentrations were lower in animals with a higher bacterial score, compared with animals with standard bacterial scores (Sheldon et al., 2002). Furthermore, following ovulation of the dominant follicle, the first postpartum corpus luteum was slightly smaller and peripheral plasma progesterone concentrations were much lower in cows with a higher uterine pathogen growth density at day 7 postpartum, compared with cows that had a lower uterine pathogen growth density (Williams et al., 2007).

Postpartum uterine infection is associated with inflammation of the endometrium with infiltration of neutrophils and macrophages. *In vivo*, the expression of pro-inflammatory cytokines in the endometrium, such as *IL1A*, *IL1B*, *IL6* and *IL8* are higher in cows with uterine disease (Herath et al., 2009, Chapwanya et al., 2012). *Ex vivo* cultures of bovine endometrium secrete IL-1 $\beta$ , IL-6 and IL-8 in response to challenge with *E. coli* (Borges et al., 2012). Additionally, *in vitro* cultures of bovine endometrial and stromal cells increase the expression of pro-inflammatory cytokines in response to LPS via Toll-like receptor 4 (Cronin et al., 2012).

The mechanisms linking postpartum uterine infections and persistent infertility in cattle are not known. However, potential mechanisms include disruption to the endocrine system, perturbed endometrial environment to be able to support implantation and embryo development, and perturbed ovarian function and reduced oocyte quality (Bromfield et al., 2015).

## 1.9 Lipopolysaccharide in the ovarian follicle

Animals with uterine disease have LPS in their follicular fluid (Cheong et al., 2017, Herath et al., 2007, Piersanti et al., 2019a). The concentrations of LPS found in the follicular fluid of healthy postpartum cows ranged from 0 to 0.8 ng/mL, whereas the concentrations of LPS found in the follicular fluid of cows diagnosed with subclinical endometritis ranged from 4.3 to 875.2 ng/mL (Herath et al., 2007). *In vivo*, intrafollicular injections with 1 µg/ml LPS reduced follicle growth rate and delayed ovulation (Gindri et al., 2019).

It has been reported that pre-ovulatory bovine follicles do not contain professional immune cells (Spanel-Borowski et al., 1997). However, a recent study detected the presence of multiple professional immune cells, such as lymphocytes, eosinophils, mast cells, neutrophils, monocytes, macrophages and dendritic cells in pre-ovulatory follicles (24 h before ovulation) (Abdulrahman Alrabiah et al., 2021). Cultured bovine granulosa cells isolated from emerged or dominant follicles are generally free from immune cell contamination, evidenced by the lack of expression of the major histocompatibility complex class II when analysed by flow cytometry (Price and Sheldon, 2013, Price et al., 2013, Bromfield and Sheldon, 2011). However, granulosa cells isolated from emerged or dominant follicles express mRNA encoding Toll-like receptor 4 (TLR4) and the accessory molecules myeloid differentiation factor-2 (MD-2) and cluster of differentiation-14 (CD14), suggesting that granulosa cells may have immune capabilities (Herath et al., 2007). Furthermore, treatment of granulosa cells isolated from emerged or dominant follicles with LPS is associated with increased expression of TLR4, MD-2 and CD14 mRNA (Shimizu et al., 2012b). Granulosa cells from emerged or dominant follicles express the mRNA for all ten TLRs and respond to LPS by secreting the cytokines IL-1 $\beta$  and IL-6, and the chemokine IL-8 (Price et al., 2013, Price and Sheldon, 2013). Treatment of granulosa cells from emerged or dominant with LPS is also associated with activation of MAPKs, with increased abundance of phosphorylated ERK1/2 and p38 in cell lysates (Price and Sheldon, 2013, Price et al., 2013, Bromfield and Sheldon, 2011).

In addition to stimulation of innate immunity, treatment of granulosa cells isolated from dominant follicles with LPS reduces the secretion of oestradiol and progesterone,

associated with decreased abundance of aromatase or LH receptor mRNA and protein, compared with control (Price et al., 2013, Herath et al., 2007); this suggests crosstalk between innate immunity and endocrine function in bovine granulosa cells.

Accumulation of LPS in follicular fluid may directly affect the cumulus granulosa cells and oocyte of the cumulus-oocyte complex (COC). For example, IVM of bovine oocytes in the follicular fluid of cows diagnosed with subclinical endometritis had fewer oocytes that reached the cleaved or blastocyst stage of development, compared with IVM in the follicular fluid of cows without subclinical endometritis (Heidari et al., 2019). Similarly, when bovine oocytes are matured in the follicular fluid or plasma from cows with LPS-induced mastitis, fewer oocytes developed to the blastocyst stage, compared with oocytes matured in the plasma or follicular fluid from cows that had been saline treated (Roth et al., 2020). Recently, using an *in vivo* model of clinical endometritis in Holstein heifers, oocytes were collected from emerged follicles and underwent *in vitro* fertilization and embryo culture; fewer oocytes developed to morulae stage from bacteria-infused animals, compared with vehicle-infused animals (Dickson et al., 2020).

Temporal regulation of COC expansion is essential for ovulation and fertilization (Russell and Robker, 2007). Treatment with LPS during IVM induces COC expansion in the absence of gonadotrophin stimulation (Bromfield and Sheldon, 2011). Like mural granulosa cells, mouse COCs express the molecular machinery (*Tlr4*, *Myd88*, *Cd14*, *Ly96* (MD-2)), necessary to detect and respond to LPS (Liu et al., 2008, Shimada et al., 2006). Treatment with LPS is associated with increased expression of *TLR4* mRNA and protein in bovine COCs, and secretion of IL-1 $\beta$ , TNF $\alpha$ , and IL-6 (Zhao et al., 2019, Bromfield and Sheldon, 2011). Treatment with LPS also induces meiotic failure in bovine oocytes, defined as oocytes that do not reach the M-phase of meiosis II or display perturbed meiotic structures such as aberrant spindles, chromosomal ejection, parthenogenic activation or germinal vesicle breakdown failure (Bromfield and Sheldon, 2011, Zhao et al., 2017b, Magata and Shimizu, 2017). Additionally, LPS treatment of bovine oocytes induces oxidative stress, apoptosis, and decreases parthenogenic development (Zhao et al., 2019, Sheldon et al., 2019b).



## 1.10 Innate immunity

The innate immune system is an organism's non-specific defence against infection that can be activated rapidly, within hours of detection of a pathogen. The components of the innate immune system include external physical barriers, humoral innate immunity and cell-mediated innate immunity, which are conserved amongst jawed vertebrates (Riera Romo et al., 2016). Physical barriers include skin or external mucous secretions; humoral innate immunity includes the production of cytokines, acute phase proteins or antimicrobial peptides; cell-mediated immunity includes phagocytic or cytotoxic cells (Riera Romo et al., 2016). Correct functioning of the innate immune system depends on the ability to differentiate between self and non-self, by recognizing pathogen-associated molecular patterns (PAMPS) (Medzhitov and Janeway, 2002).

Pathogen-associated molecular patterns allow the host to detect an infection and initiate the immune response to kill and clear the pathogen. Activation of Toll-like receptors by PAMPs triggers an intracellular signalling cascade, leading to the production of immune mediators, including pro-inflammatory cytokines and chemokines (Akira and Hemmi, 2003). One of the most studied PAMPs, LPS, is part of the outer membrane of Gram-negative bacteria, such as *E. coli*, that binds to Toll-like receptor 4 (TLR4) (Mazgaeen and Gurung, 2020).

Innate immunity also has a role in the resolution of tissue damage. The female reproductive tract needs to sense danger because there is significant disruption to tissue homeostasis caused by infection, damage, and insemination. The immune system detects damaged or stressed cells through the detection of damage-associated molecular patterns (DAMPs), such as IL-1 $\alpha$ . Under normal physiological conditions, DAMPs are normally sequestered intracellularly and therefore are hidden from recognition by the immune system; DAMPs can also be components of the extracellular matrix, such as hyaluronan. When cells become damaged, through stress or injury, these DAMPs are released into the extracellular environment where they are detected by the immune system which then mounts an inflammatory response.

### 1.10.1 Toll-like receptors

Toll-like receptors, discovered in the 1990's, are membrane-bound proteins involved in the recognition of pathogens and damage molecules (Poltorak et al., 1998, Hoshino et al., 1999). Toll was first discovered in *Drosophila* and are evolutionarily conserved between insects and humans (Akira et al., 2001). Toll-like receptors act as pattern-recognition receptors and are involved in the recognition of PAMPS from bacteria, viruses and fungi, and DAMPs, from cell damage. Stimulation of TLRs are necessary for the activation of the innate immune response to infection and required for adaptive immunity (Moresco et al., 2011). Ten TLRs have been identified in humans and cows (Davies et al., 2008, Herath et al., 2009), and 12 identified in mice (Kawai and Akira, 2010). Each TLR binds to a different bacterial PAMP and are located on either the cell surface or intracellularly. Cell-surface located TLRs are TLR1, TLR2, TLR4, TLR5, TLR6 and TLR10, whereas TLR3, TLR7, TLR8 and TLR9 are located intracellularly (Moresco et al., 2011).

### 1.10.2 Lipopolysaccharide

Gram-negative bacteria are characterized by their cell wall structure (**Fig. 1.6**). The membrane of Gram-negative bacteria is composed of three main layers: the outer membrane, peptidoglycan layer and an inner membrane (Glauert and Thornley, 1969). Gram-positive bacteria do not possess the outer membrane, but instead have a thick layer of peptidoglycan. The structure of the membrane is what distinguished Gram-negative bacteria from Gram-positive bacteria. The outer membrane of Gram-negative bacteria is a lipid bilayer, with phospholipids confined to the inner leaflet of the membrane and the outer membrane composed of glycolipids, principally lipopolysaccharide (Silhavy et al., 2010). Lipopolysaccharide is the major outer surface membrane component present in almost all Gram-negative bacteria and consists of three principal domains: a hydrophobic lipid A moiety, a core of oligosaccharides and a distal region of polysaccharide, known as the O antigen (Zhang et al., 2013). The lipid A moiety of LPS has been shown to be immunostimulatory.

## Gram negative bacteria cell wall structure

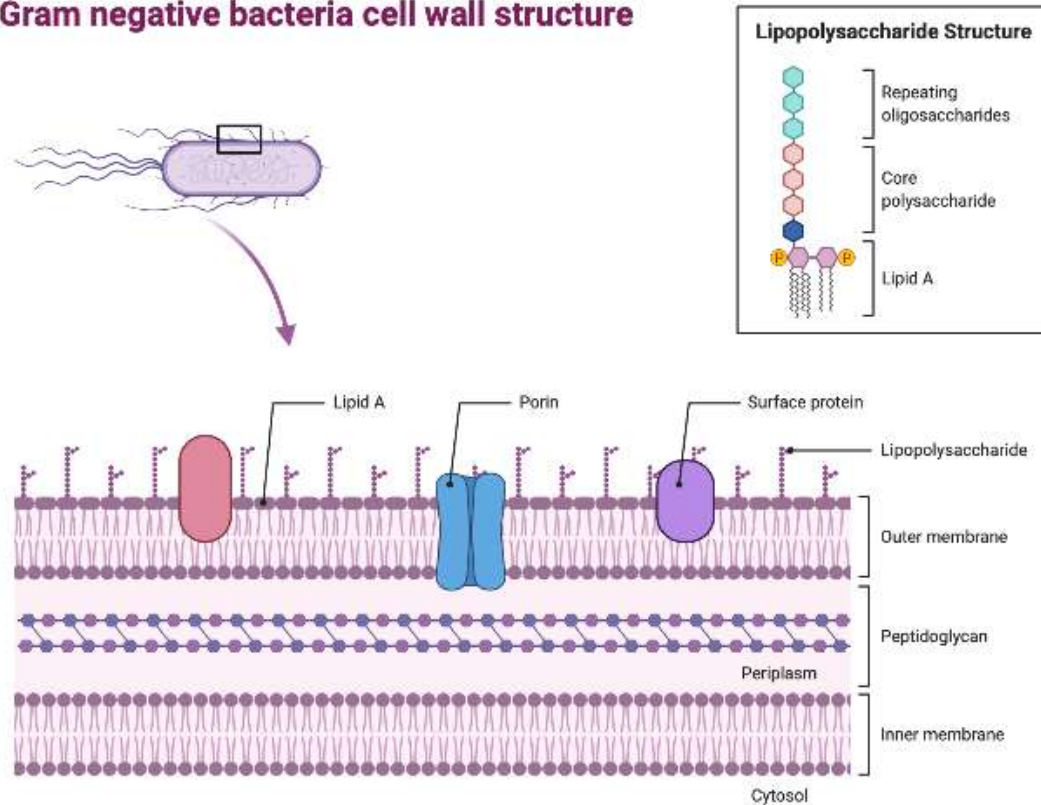


**Figure 1.6. The general structure of lipopolysaccharide in Gram-negative bacteria**

The structure of lipopolysaccharide and its location in the cell wall of Gram-negative bacteria (Horlock A., 2020; Adapted from template in BioRender.com).

### 1.10.3 Toll-like receptor 4 signalling

The LPS released from Gram-negative bacterial associates with LPS-binding protein, an acute phase molecule (Tobias et al., 1986). Lipopolysaccharide then binds to CD14, which interacts with the MD-2-TLR4 complex to initiate cellular responses (**Fig. 1.7**) (Triantafilou et al., 2002, da Silva Correia et al., 2001). Myeloid differentiation factor-2 is necessary for TLR4 to bind to LPS, and CD14 allows for the differentiation between smooth (long O-polysaccharide chains) and rough (lacking O-polysaccharide chains) LPS chemotypes (Moresco et al., 2011).

Specific biological responses are triggered by individual TLRs. The differences in TLR responses are explained by the presence of TIR (Toll/interleukin-1 receptor) domain-containing adaptor molecules, such as Myeloid differentiation primary response gene 88 (MyD88), MAL (MyD88 adaptor like), TRIF (TIR domain-containing adaptor protein inducing IFN- $\beta$ ) and TRAM (TRIF-related adaptor molecule) (O'Neill and Bowie, 2007, Kawai and Akira, 2010). There are two main pathways that are activated by TLR signalling, the myeloid differentiation primary response gene 88 (MyD88)-dependent pathway and the MyD88-independent pathway (TRIF-dependent pathway). All TLRs use the MyD88-dependent pathway, except TLR3 that uses the MyD88-independent pathway (Yamamoto et al., 2003). Activation of the MyD88 pathway leads to the production of pro-inflammatory cytokines, whereas the MyD88-independent (TRIF-dependent) pathway leads to the induction of type I interferons, as well as pro-inflammatory cytokines (Akira et al., 2006).

Toll-like receptor 4 is the only TLR that uses both the MyD88-dependent and MyD88-independent pathways (**Fig. 1.7**). The MyD88-dependent pathway starts with the binding of LPS to TLR4 resulting in the recruitment of MAL and MyD88 to the plasma membrane, and the recruitment of the IL-1 receptor associated kinases (IRAK), IRAK4, IRAK1 and IRAK2 (Kawagoe et al., 2008). The IRAK proteins then interact with the tumour necrosis factor receptor-associated factor 6 (TRAF6), which recruits transforming growth factor- $\beta$  activated kinase (TAK) binding protein 1 (TAB1) and TAB2, leading to the activation of TAK1 by phosphorylation. Activation of TAK1 leads to phosphorylation of the inhibitor of nuclear factor- $\kappa$ B kinase (IKK) or the

mitogen-activated protein kinases, ERK1/2, p38 and c-Jun N-terminal kinase (JNK), leading to activation of nuclear factor  $\kappa$ B (NF- $\kappa$ B) or activator protein 1 (AP-1), respectively. Activation of NF- $\kappa$ B or AP-1 leads to increased expression of genes encoding pro-inflammatory cytokines, such as IL-1 $\beta$ , IL-6 and TNF $\alpha$  (Kawai and Akira, 2007, Liu et al., 2017). The MyD88-independent (TRIF-dependent) pathway starts with association of TRIF with TLR4 and TRAM, leading to activation of TRAF-family-member-associated NF- $\kappa$ B activator (TANK) binding kinase 1 (TBK1), via TNF receptor-associated factor 3 (TRAF3) (Akira et al., 2006). Activation of TBK1 leads to the phosphorylation of interferon regulatory factor 3 (IRF3), resulting in the induction of type 1 interferon genes.

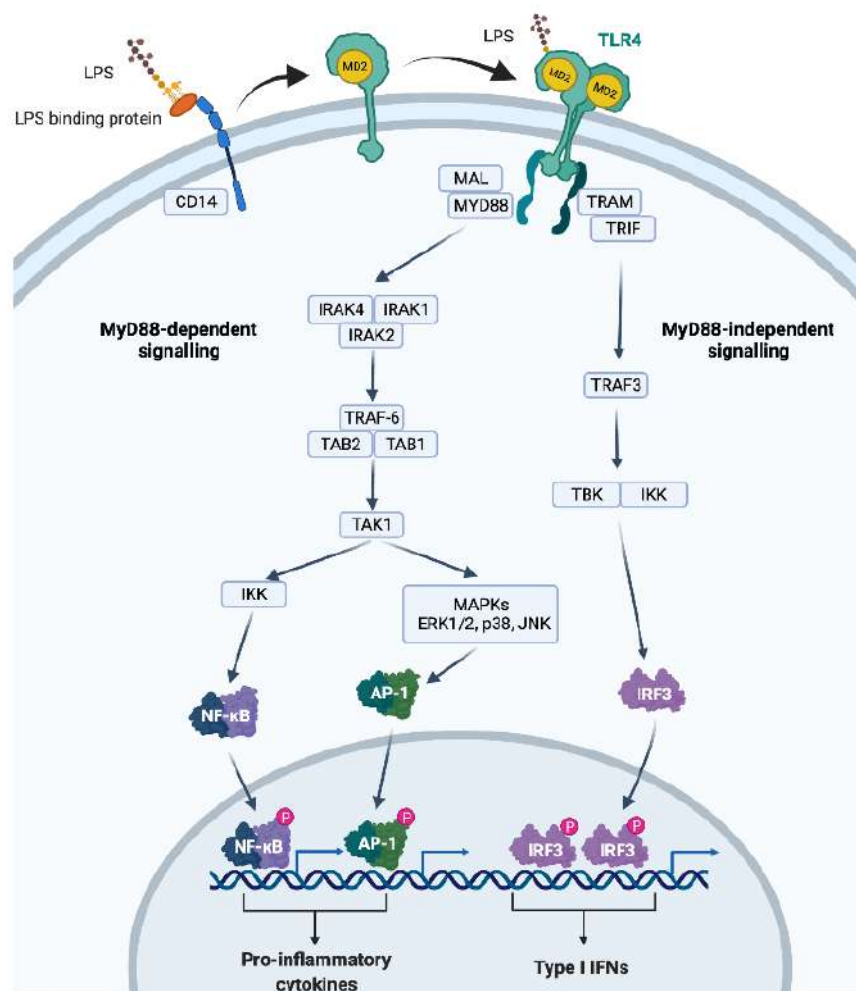


**Figure 1.7. The TLR4 signalling pathway**

Lipopolysaccharide activates TLR4 via the MyD88-dependent and MyD88-independent pathways, leading to the induction of pro-inflammatory cytokines or type I interferons (IFNs). Horlock A., 2021; Created with BioRender.com.

#### 1.10.4 Cytokines and Chemokines

Cytokines evolved as intracellular messengers in invertebrates before the appearance of receptors and signalling cascades, where they are involved in host defence and repair (Dinarello, 2007). Cytokines are defined as small, soluble signalling proteins or glycoproteins (< 30 kDa) that have specific effects on interactions and communication between cells. There are several families of cytokines including the interleukins, chemokines, interferons, tumour necrosis factors (TNFs) and growth factors. The important role of cytokines in ovarian physiology are becoming increasingly apparent.

Binding of LPS to TLR4 activates signalling pathways, leading to the transcription of genes encoding pro-inflammatory cytokines (e.g., *IL1A*, *IL1B*, *IL6* and *TNFA*), chemokines (e.g., *IL8* and *CXCL1*) or prostaglandin E<sub>2</sub> (*PTGS2*) (Liu et al., 2017, Takeuchi and Akira, 2010, Uematsu et al., 2002). The cytokine IL-6 is a 21 to 28 kDa protein which is critical for the maturation of B-cells into antibody-producing cells, the activation of T cells and the secretion of acute phase proteins by the liver (Turner et al., 2014a). The chemokine IL-8 is a 6 to 8 kDa protein responsible for the chemotactic migration of immune cells to the site of inflammation (Turner et al., 2014a).

Interleukin-1 $\alpha$  and IL-1 $\beta$  play an essential role in inflammation and the immune response, stimulating activation and proliferation of B and T lymphocytes, synthesis of acute phase proteins in the liver, and prostaglandins (Gerard et al., 2004). Interleukin-1 alpha and IL-1 $\beta$  are translated as 31 kDa precursor proteins, that are then cleaved to 17 kDa proteins and bind to the IL-1 receptor, triggering similar biological responses. However, where only the cleaved form of IL-1 $\beta$  is biologically active and can bind to the IL-1 receptor, both forms of the IL-1 $\alpha$  protein are biologically active (Kim et al., 2013, Di Paolo and Shayakhmetov, 2016). Interleukin-1 $\alpha$  is normally considered to be an intracellular cytokine, that is released upon cell damage (Kim et al., 2013). For example, bovine endometrial or stromal cells treated with 0.1  $\mu$ g/ml LPS accumulate IL-1 $\alpha$  intracellularly, but do not secrete it into culture supernatants (Healy et al., 2014). However, IL-1 $\alpha$  can function as a membrane-bound cytokine, an intracellular cytokine, or be secreted out of the cell (Malik and Kanneganti, 2018).

### 1.10.5 Inflammasome activation

The pro-inflammatory cytokine IL-1 $\beta$  is mainly produced by activated macrophages and monocytes in response to TLR activation. Excessive concentrations of IL-1 $\beta$  are associated with septic shock and autoimmune disorders (Mariathasan et al., 2004). Canonical inflammasomes are composed of an inflammasome sensor protein, apoptosis-associated speck-like protein containing a caspase activation and recruitment domain (ASC), and pro-caspase-1 (Mariathasan et al., 2004). The mechanism for the induction of IL-1 $\beta$  secretion can be divided into two steps, the induction of pro-IL-1 $\beta$  and caspase-1 activation (Franchi et al., 2009). Caspase-1 is the IL-1 $\beta$  converting enzyme responsible for the cleavage of the inactive pro-IL-1 $\beta$  into active IL-1 $\beta$ . One of the most characterized inflammasome complexes is the Nod-like receptor pyrin domain containing 3 (NLRP3) inflammasome (**Fig. 1.8**). The NLRP3 inflammasome is tightly regulated and cannot be induced by a single microbial ligand, therefore, robust activation of caspase-1 requires an additional activation signal, such as extracellular adenosine triphosphate (ATP) (Franchi et al., 2009). Activation of TLR4 by LPS induces the expression of NLRP3, pro-IL-1 $\beta$  and pro-caspase 1; the second activation signal by PAMPs, DAMPs, or ATP triggers formation of the NLRP3 inflammasome (Zheng et al., 2020).

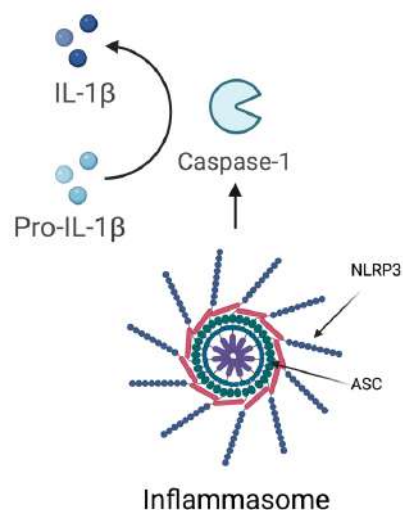


**Figure 1.8. Mechanism of inflammasome activation and IL-1 $\beta$  production**

IL-1 $\beta$ , interleukin 1 beta; NLRP3, Nod-like receptor pyrin domain containing 3; ASC, apoptosis-associated speck-like protein containing a caspase activation and recruitment domain (Horlock A., 2021; Created with BioRender.com).

### 1.10.6 Ovulation as an inflammatory reaction

During ovulation, follicles become hyperaemic (highly vascularized), produce large amounts of prostaglandins and a hyaluronan-rich matrix, in a similar manner to that generated during inflammation and wound repair (Richards et al., 2008). Physiological events within the ovary, including ovulation and formation and regression of the corpus luteum, are inflammatory-like processes (Espey, 1980). Ovulation is associated with the release of cytokines such as IL-1, IL-6 and IL-8, and damage of the hyaluronan extracellular matrix (Richards et al., 2008, Espey, 1980).

Interleukin-1 is involved in ovulation processes and oocyte maturation and may be involved in protease synthesis, prostaglandin, and nitric oxide production, as well as regulation of ovarian steroidogenesis (Gerard et al., 2004, Terranova and Rice, 1997). In the bovine ovarian follicle, growth from preantral to small antral follicles is associated with increased expression of *IL1A* and *IL1B*, whilst growth from small antral to large antral follicles is associated with increased *IL1B*, but reduced *IL1A* expression (Passos et al., 2016). The cytokine IL-1 $\beta$  promotes the development of primordial follicles and contributes to the maintenance of early follicle survival, potentially through the phosphatidylinositol 3-kinase (PI3K) pathway and initiation of NF- $\kappa$ B (Passos et al., 2016).

Treatment of bovine granulosa cells isolated from 1 to 5 mm diameter follicles with IL-1 $\beta$  decreased the FSH-induced secretion of oestradiol; however, the FSH-induced secretion of oestradiol was not affected in granulosa cells isolated from > 8 mm follicles, following IL-1 $\beta$  treatment (Spicer and Alpizar, 1994). However, another study found that treatment with IL-1 $\beta$  reduced the FSH-induced secretion of oestradiol and progesterone was decreased in granulosa cells isolated from > 8 mm, but not < 5 mm follicles (Baratta et al., 1996). Treatment of rat granulosa cells with IL-1 $\beta$  decreased the FSH-induced secretion of estrogen and progesterone (Donesky et al., 1998).

Synthesis of hyaluronan and cumulus expansion are induced by IL-1 $\beta$  (Kokia et al., 1993), and IL-1 antagonism blocks cumulus expansion and ovulation in rats (Simón



et al., 1994). Mouse cumulus cells utilize endogenous ligands of TLR4, such as hyaluronan during the final stages of oocyte maturation and expansion of the cumulus-oocyte complex (Shimada et al., 2008). Activation of TLR4 by hyaluronic acid induces the expression of *Il6* mRNA, an autocrine regulator of mouse cumulus cell function (Liu et al., 2009). In the rabbit ovary, IL-1 $\beta$  treatment is associated with induction of ovulation and oocyte meiotic maturation, but reduced fertilization and embryonic development, in the absence of gonadotrophin stimulation (Takehara et al., 1994). Similarly, treatment of rat ovaries with IL-1 $\beta$  increased the LH-induced ovulation rate (Brännström et al., 1993). In contrast, treatment with IL-1 receptor agonist suppresses ovulation in the rat (Simón et al., 1994) and mare (Martoriati et al., 2003).

Interleukin-1 $\alpha$  may be involved in repair of the ovarian surface because IL-1 $\alpha$  stimulates the expression of *IL6* and *IL8* on the ovarian surface, associated with increased cellular proliferation (Rae et al., 2004, Jabbour et al., 2009). Interleukin-1 $\alpha$  may also be involved in the regulation of ovulation because treatment of bovine granulosa cells with recombinant IL-1 $\alpha$  increased IL-6 secretion, associated with increased phosphorylation of ERK and p38 (Yang et al., 2017). Supporting this, IL-1 $\alpha$  knockout mice have lower expression of genes encoding IL-1 $\beta$ , IL-6 and TNF $\alpha$  in the ovaries, compared with wild-type control mice (Uri-Belapolsky et al., 2014).

The chemokine IL-8 is involved in the recruitment of leukocytes, aiding in the formation of the bovine corpus luteum following ovulation (Jientaweeboon et al., 2011). Interleukin-8 may also have a role in vascularization of the rat follicle because injection of IL-8 is associated with increased follicular growth and capillary density (Goto et al., 2002). Treatment of bovine granulosa cells isolated from large follicles (> 8.5 mm external diameter) with recombinant IL-8 decreased the FSH-induced secretion of oestradiol, associated with decreased abundance of aromatase; however, treatment with IL-8 increased the LH-induced secretion of progesterone, associated with increased abundance of StAR (Shimizu et al., 2012a).

### 1.11 Energy stress in the dairy cow

Dairy cows are also under significant metabolic energy stress during the postpartum period because they cannot consume enough food to meet the energetic demands of lactation. The metabolic energy demand of lactation is three times the resting metabolic rate (Butler and Smith, 1989). The maintenance requirements of a typical dairy cow is ~ 65 MJ/d, whereas the energy requirement for milk production is ~ 5MJ/L milk (Sheldon et al., 2018). As a result of negative energy balance (NEB), body fat and muscle are catabolised to meet the energy requirements (Bauman and Currie, 1980, Coffey et al., 2004). This period of NEB may last up to 20 weeks in cattle during the postpartum period (Beever et al., 2001).

Negative energy balance in dairy cows result in the increased mobilization of body fat, decreased plasma glucose concentrations, and reduced hormone concentrations. A comparison in the metabolites and hormone plasma concentrations between dairy cows under mild negative energy balance and severe negative energy balance revealed lower glucose (4.1 vs. 2.7 mmol/L), oestradiol (2.2 vs. 1.6 pg/ml) and IGF-1 (51.4 vs. 10.6 ng/ml) concentrations (Wathes et al., 2009, Fenwick et al., 2008a). Additionally, cows under severe NEB experienced increased plasma  $\beta$ -hydroxybutyrate (BHB; 0.5 vs. 3.7 mM) and non-esterified fatty acid concentrations (NEFA; 0.3 vs. 1.4 mM), compared with cows under mild negative energy balance (Wathes et al., 2009, Fenwick et al., 2008a). A recent study analysed blood samples from 69,161 cows across 1748 UK farms for the markers of NEB: serum BHB, NEFA and glucose concentrations; 52% of UK dairy cows experience NEB during late pregnancy and 75.2% experienced NEB in the first 20 days after calving (Macrae et al., 2019). Additionally, NEB is associated with increased insulin resistance in cattle (Oikawa and Oetzel, 2006, Bell and Bauman, 1997).

Negative energy balance and the concurrent metabolic changes contribute to the impaired reproductive performance observed in dairy cows (Canfield and Butler, 1990, Butler, 2000). The interactions between NEB and the hypothalamus-pituitary axis have been well documented. One of the major effects of NEB is reduced LH pulse frequency and amplitude, leading to impaired steroidogenesis and anovulation (Butler, 2003, Butler, 2000, Butler et al., 1981, Jorritsma et al., 2005). Additionally, NEB

reduces the ovarian responsiveness to LH stimulation (Butler, 2001). A study of 334 high yielding dairy cows found that 49% experienced ovarian dysfunction, and the two most frequent dysfunctions were delayed cyclicity and a prolonged luteal phase (Opsomer et al., 1998, Opsomer et al., 2000). Early resumption of ovarian cyclicity postpartum has been associated with improved reproductive performance. A recent study of 52 pregnant Holstein dairy cows, found that there was greater negative energy balance, greater insulin resistance, fewer LH pulses, and reduced follicular fluid androstenedione and oestradiol concentrations in cows that did not ovulate in the first postpartum follicular wave, compared to cows that ovulated (Cheong et al., 2016).

Cows with NEB can be monitored using body condition scores (BCS) following parturition, an indirect measure of NEB commonly used in dairy herds (Wildman et al., 1982). The BCS of cows is a good measure of subcutaneous fat which is an important fuel for energy production in postpartum cows (Ayres et al., 2009). Cows with a lower BCS score during early lactation are at a greater risk for low fertility (Pryce et al., 2001). Poor BCS decreases the likelihood that the developing follicle will reach pre-ovulatory size or ovulate (Beam and Butler, 1999). Cows that lose body weight in the first 3 weeks of lactation display lower numbers of viable and transferable good quality embryos after a superovulation treatment at 100 days postpartum (Carvalho et al., 2014). Higher losses of BCS in the postpartum period are associated with increased incidence of postpartum problems, such as metritis (Wang et al., 2019) or endometritis (Roche et al., 2013, Dubuc et al., 2010, Carneiro et al., 2014) in dairy cows.

Negative energy balance perturbs ovarian follicle growth and function and increases the risk of uterine disease (Beam and Butler, 1997, Hammon et al., 2006, LeBlanc, 2012, Leroy et al., 2008). Decreases in serum glucose concentrations are reflected in the follicular fluid, suggesting that negative energy balance may affect the availability of glucose within the ovarian follicle (Leroy et al., 2004a, Leroy et al., 2004b). Postpartum NEB may have long term effects on fertility by negatively affecting the developing follicle or oocyte (Britt, 1992). Many of the altered blood metabolites that are associated with NEB, such as glucose, BHB, NEFA, cholesterol and IGF-1, are reflected in the follicular fluid from the dominant follicles of postpartum dairy cows (Leroy et al., 2004a, Leroy et al., 2004b, Echtenkamp et al., 1990).

The plasma concentrations of total cholesterol (Quiroz-Rocha et al., 2009, Esposito et al., 2014, Cavestany et al., 2005), high-density (HDL), low-density (LDL) and very-low density (VLDL) lipoproteins (Kessler et al., 2014) also decrease around parturition in dairy cows. Unfortunately, decreases in plasma total cholesterol concentrations are further exacerbated by negative energy balance in the postpartum period (Kim and Suh, 2003, Ruegg et al., 1992, Esposito et al., 2014). Decreased serum cholesterol concentrations are associated with increased incidence of uterine diseases, such as metritis or endometritis in the postpartum period (Bogado Pascottini and LeBlanc, 2020, Paiano et al., 2019). Changes to serum total cholesterol or HDL concentrations are reflected in the follicular fluid concentrations of total cholesterol (Leroy et al., 2004b, Leroy et al., 2004a, Shabankareh et al., 2013, Alves et al., 2014) or HDL cholesterol (Gautier et al., 2010).

Negative energy balance may prevent cows from mounting effective immune responses to bacterial infection in the postpartum period (Wathes et al., 2009, McCarthy et al., 2010, Morris et al., 2009, Ingvarsten and Moyes, 2013). Postpartum Holstein-Friesian dairy cows under severe NEB had lower numbers of white blood cells and lymphocytes, compared with cows under mild NEB (Wathes et al., 2009). Negative energy balance because of lactation is a factor in the immunosuppression of cows in the postpartum period (Goff, 2006). Lactating postpartum dairy cows had fewer lymphocytes around calving, and impaired lymphocyte function, compared with postpartum mastectomized cows (Kimura et al., 2002). In another study, the mammary tissue of lactating dairy cows was inoculated with *Streptococcus uberis* to induce mastitis, under either NEB or positive energy balance; transcriptome analysis revealed that the most affected canonical pathways associated with energy status were related to immune function, such as IL-8 signalling and glucocorticoid signalling pathways (Moyes et al., 2010).

Whilst there is evidence of the associations between NEB and immunity in cows, the link between metabolic energy stress and innate immunity is under-explored in the immune or reproductive systems of cattle, and even less is known about the mechanisms at the cellular level.

## 1.12 AMP-activated protein kinase (AMPK)

Adenosine triphosphate is the main source of energy for most cellular processes. The first enzyme in glycolysis, hexokinase, controls the rate of conversion of glucose to pyruvate, to supply the tricarboxylic acid (TCA) cycle and generate ATP. In nutrient-replete conditions (**Fig. 1.9A**), sufficient energy is available to drive anabolic processes, such as cholesterol synthesis and lipid synthesis.

AMP-activated protein kinase is the principal sensor of cellular energy and is present in essentially all eukaryotic cells (Hardie et al., 2012, Garcia and Shaw, 2017). The role of AMPK in cells is to restore energy homeostasis in response to energetic stress (Hardie et al., 2012). Energy stress causes an increase in the ratio of adenosine diphosphate to ATP, which is always accompanied by an increase in the ratio of AMP:ATP (Gowans et al., 2013). During nutrient-deprived conditions (**Fig. 1.9B**), increased ratios of AMP:ATP results in phosphorylation of AMPK at Threonine 172 (Thr172), which stimulates catabolic pathways such as glycolysis, and inhibits anabolic pathways that consume ATP, such as protein synthesis, fatty acid synthesis and cholesterol biosynthesis (Hardie et al., 2012). Phosphorylated AMPK inhibits mTOR, which further limits anabolic pathways (Hardie et al., 2012, Zoncu et al., 2011), and 3-hydroxy-3-methylglutaryl-coenzyme A reductase (HMGCR), the rate limiting enzyme in cholesterol biosynthesis (Clarke and Hardie, 1990).

AMP-activated protein kinase is a serine/threonine heterotrimeric kinase, composed of three subunits, the catalytic  $\alpha$  subunit and the  $\beta$  and  $\gamma$  regulatory subunits (**Fig. 1.10**), and the genes of these subunits are highly conserved across eukaryotic species (Hardie et al., 2003). Binding of AMP to the  $\gamma$ -subunit of AMPK causes a conformational change in the  $\alpha$ -subunit, allowing for phosphorylation of the  $\alpha$ -subunit at Thr172, resulting in the activation of AMPK. Phosphorylation at Thr172 results in > 100-fold increase in the activity of AMPK in cell-free assays (Hawley et al., 1996). Upstream regulators of AMPK include liver kinase B1 (LKB1) and calmodulin-dependent protein kinase kinase- $\beta$  (CaMKK $\beta$ ) (Hawley et al., 2003, Hawley et al., 2005). Pharmaceutical compounds, such as 5-aminoimidazole-4-carboxamide-riboside-5-phosphate (AICAR) also activate AMPK (Corton et al., 1995).

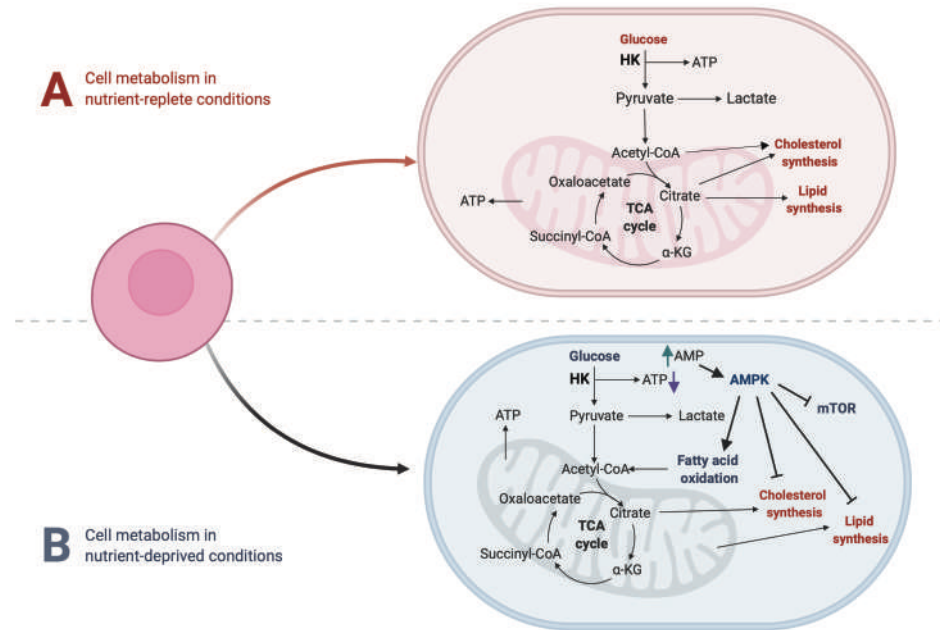


**Figure 1.9. Cellular energy homeostasis regulated by AMPK**

(A) In nutrient-replete conditions, cellular energy is produced via ATP production driven by glycolysis and the TCA cycle. (B) In nutrient-deprived conditions, less ATP can be produced via glycolysis and the TCA cycle, leading to an increased AMP:ATP ratio and activation of AMPK. Activation of AMPK inhibits anabolic pathways that consume ATP, such as mTOR, cholesterol synthesis and lipid synthesis. Activation of AMPK also stimulates catabolic pathways that produce ATP, such as fatty acid oxidation. AMP, adenosine monophosphate; ATP, adenosine triphosphate; HK, hexokinase; AMPK, adenosine monophosphate activated protein kinase; mTOR, mechanistic target of rapamycin (Horlock A., 2021; Adapted from template in BioRender.com).

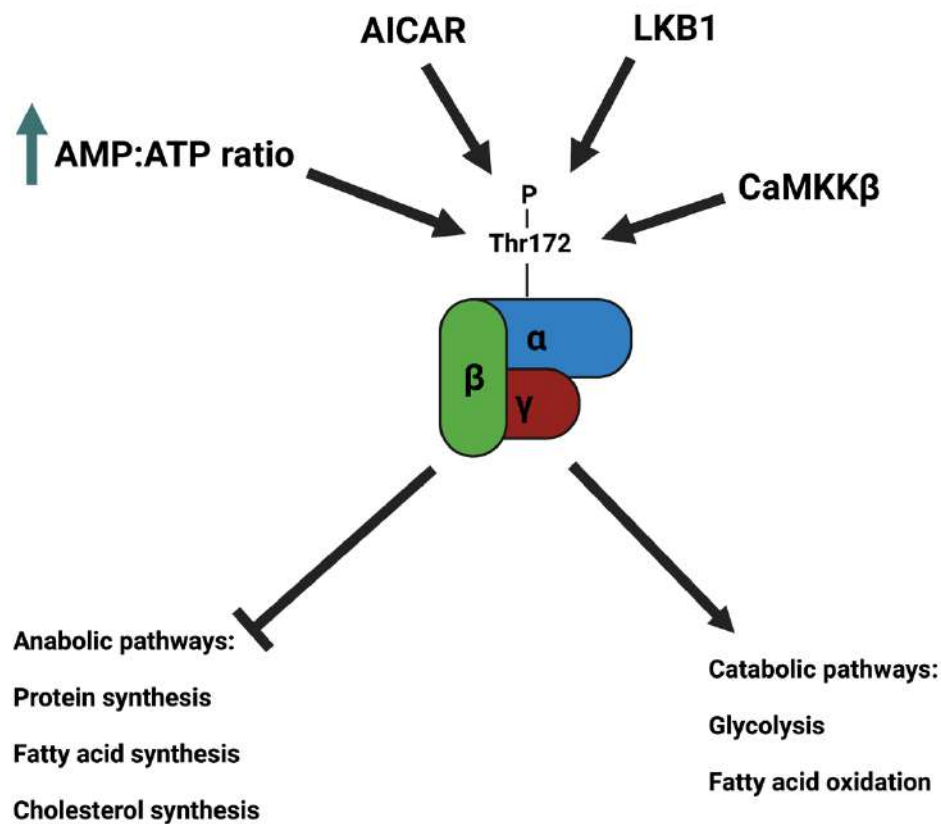


**Figure 1.10. Mechanisms of AMPK activation in cells**

AMP-activated protein kinase is a serine/threonine heterotrimeric kinase, composed of three subunits, the catalytic  $\alpha$  subunit and the  $\beta$  and  $\gamma$  regulatory subunits. Upstream regulators of AMPK by phosphorylation of the  $\alpha$ -subunit at Thr172. Activation of AMPK inhibits anabolic pathways that consume ATP, such as protein synthesis, fatty acid synthesis and cholesterol synthesis; activation of AMPK also promotes catabolic pathways that generate ATP, such as glycolysis and fatty acid oxidation. AMPK, AMP-activated protein kinase; AICAR, aminoimidazole-4-carboxamide-riboside-5-phosphate; LKB1, liver kinase B1; CaMKK $\beta$ , calmodulin-dependent protein kinase kinase- $\beta$ . (Adapted from (Garcia and Shaw, 2017))

### 1.12.1 AMPK in granulosa cells

The role of AMPK in female reproduction is becoming increasingly apparent, providing a link between metabolism and fertility (Nguyen, 2019, Bertoldo et al., 2015, Yang et al., 2020). Bovine granulosa cells, theca cells and oocytes express both isoforms of the AMPK  $\alpha$ -subunit ( $\alpha_1$  and  $\alpha_2$ ) and the AMPK  $\beta$ -subunit ( $\beta_1$  and  $\beta_2$ ) (Tosca et al., 2007a). Therefore, there may be an important role for AMPK in reproductive function, linking energy balance with the gonadal axis (Bertoldo et al., 2015).

Studies using bovine granulosa cells suggest that AMPK may regulate steroidogenesis. Bovine granulosa cells treated with the AMPK activators metformin or AICAR have increased phosphorylation of AMPK (Thr172) and its downstream target, acetyl-CoA carboxylase (ACC), and is associated with reduced secretion of oestradiol and progesterone (Tosca et al., 2007a). Similar results have been observed in rat granulosa cells, where treatment with AICAR is associated with reduced progesterone secretion (Tosca et al., 2005). Treatment of bovine granulosa cells with metformin is associated with a decrease in the abundance of  $3\beta$ -hydroxysteroid dehydrogenase (HSD3B), CYP11A1, and stAR (Tosca et al., 2007a). Additionally, metformin treatment is associated with decreased abundance of phosphorylated ERK1/2 and p38 proteins (Tosca et al., 2007a), suggesting a possible link between immunity and metabolic energy stress in granulosa cells.

There may also be a role for AMPK in the regulation of granulosa cell proliferation. Treatment of bovine granulosa cells with metformin is associated with reduced IGF-1 induced proliferation and protein synthesis, and decreased phosphorylation of the downstream target of the mechanistic target of rapamycin Complex 1 (mTORC1), ribosomal protein S6 kinase (p70S6K), but not the mechanistic target of rapamycin Complex 2 (mTORC2) downstream target, protein kinase B (Akt) (Tosca et al., 2010). Utilizing an adenoviral vector, to overexpress dominant-negative AMPK $\alpha_1$  in granulosa cells, the authors were able abolish the effects of metformin on the IGF-1 induced reductions in cell proliferation and phosphorylation of p70S6K (Tosca et al., 2010).



### 1.12.2 AMPK in the oocyte

The role of AMPK in the maturation of oocytes appears to be species-specific (Bertoldo et al., 2015). Activation of AMPK blocks nuclear maturation in bovine (Bilodeau-Goeseels et al., 2007, Tosca et al., 2007b) and porcine (Mayes et al., 2007) oocytes. However, activation of AMPK in mouse oocytes stimulates the resumption of meiosis (Chen et al., 2006, Downs et al., 2002, Downs and Chen, 2006).

Treatment of porcine COCs or oocytes with AICAR arrested ~ 90% of oocytes at the germinal vesicle (GV) stage of meiosis, and treatment with AICAR, 5-aminoimidazole-4-carboxamide ribonucleoside monophosphate (ZMP) or metformin reduced COC expansion (Santiquet et al., 2014). Similarly, treatment of porcine oocytes with AICAR, ZMP or metformin also arrested the majority of oocytes at the GV stage of meiosis (Mayes et al., 2007). Treatment of bovine COCs with metformin arrested ~ 80% at the GV stage of meiosis and reduced COC expansion, compared with control COCs (Tosca et al., 2007b). Similarly, treatment of bovine COCs or denuded oocytes with AICAR or metformin arrested most oocytes at the GV stage of meiosis (Bilodeau-Goeseels et al., 2007).

Conversely, in mice, treatment of COCs or denuded oocytes with AICAR stimulates meiotic maturation (Downs et al., 2002). Treatment of mouse oocytes with AICAR stimulated the resumption of meiosis, and inhibition of AMPK with compound C inhibited the resumption of meiosis (Chen et al., 2006, Downs and Chen, 2006). The effects of AMPK activation are different in rats, where treatment with AICAR only marginally stimulated the resumption of meiosis in COCs and had no effect in denuded oocytes (Downs, 2011).

The effects of AMPK activation in human oocytes are not known. However, the similarities between humans and cows in regard to folliculogenesis, characteristics of the dominant follicle, the response to ovarian stimulation, IVM and similarities in embryo development make the cow a good animal model to study human oocyte competence (Sirard, 2017).

### 1.13 Mechanistic Target of Rapamycin (mTOR)

Mechanistic Target of Rapamycin is a 289 kDa protein belonging to the phosphoinositide 3-kinase (PI3K) family and is at the interface between growth and starvation, allowing organisms to sense energy and nutrient abundance and to control growth and homeostasis (Zoncu et al., 2011, Yang et al., 2014). There are two mTOR complexes, mTOR Complex 1 (mTORC1) and mTOR Complex 2 (mTORC2). The assembly of mTORC1 is dependent on the presence of regulatory protein associated with mTOR (Raptor) (Kim et al., 2002), whereas mTORC2 is dependent on the presence of rapamycin insensitive companion of mTOR (Rictor) (Sarbasov et al., 2004).

The four regulatory inputs: nutrients, growth factors, energy and stress are integrated by mTORC1 (**Fig. 1.11**). The role of mTORC1 is to promote translation and protein synthesis, mainly through its substrates ribosomal protein S6 kinase (p70S6K) and the eukaryotic translation initiation factor 4E-binding protein 1 (4EBP1). The anabolic processes of protein, nucleotide lipid synthesis and the anabolic support pathways (Warburg effect) are promoted by mTORC1, while the catabolic processes of autophagy, lysosomal degradation, fatty acid oxidation are inhibited by mTORC1 (Ben-Sahra and Manning, 2017). These processes would still occur in the absence of mTORC1; however, its activation provides the link between growth signals and elevated biosynthetic processes. When nutrients are abundant, mTOR signals the cell to enhance protein synthesis, activating protein kinase pathways which regulate cells survival, anabolism, and cell cycle progression. In a nutrient deficit, mTOR senses lower amino acids, and is inhibited via AMPK, and these processes are inhibited, and autophagy recycles intracellular organelles to provide an alternative source of amino acids and substrates for energy production (Zoncu et al., 2011, Nicklin et al., 2009).

The role of mTORC2 (**Fig. 1.11**) is less understood than mTORC1, although it is known to have important roles as a mediator of cytoskeletal organization and polarization, as well as the regulation of cell survival, cell cycle progression and anabolism through the activation of its main targets, protein kinase B (AKT), serum and glucocorticoid-induced protein kinase (SGK) and protein kinase C (PKC) (Jacinto et al., 2004).

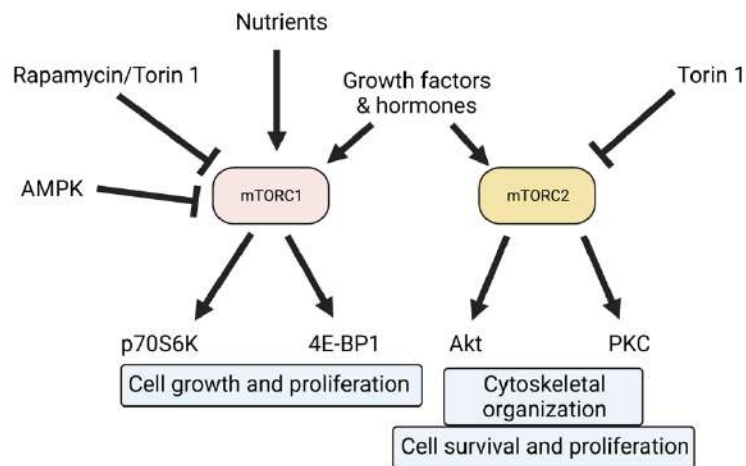


**Figure 1.11. Regulation of mTOR**

mTORC1, mechanistic target of rapamycin complex 1; mTORC2, mechanistic target of rapamycin complex 2; p70S6K, ribosomal protein S6 kinase; 4E-BP1, eukaryotic translation initiation factor 4E-binding protein 1; Akt, protein kinase B; PKC, protein kinase C. (Adapted from (Mao and Zhang, 2018))

### 1.13.1 mTOR in granulosa cells

There is growing interest in the role of mTOR in female reproduction and this has been the subject of recent reviews (Guo and Yu, 2019, Correia et al., 2020). Ovulation depends on the proliferation and growth of granulosa cells, and disruption of this process leads to anovulation (Kayampilly and Menon, 2007). Studies suggest that mTOR is a positive regulator of granulosa cell proliferation. In rat granulosa cells, FSH increased the phosphorylation of p70S6K through an ERK1/2-dependent pathway (Kayampilly and Menon, 2007). In mice, inhibition of mTOR with rapamycin led to reduced granulosa cell proliferation and reduced follicle growth *in vitro* (Yaba et al., 2008). Treatment of spontaneously immortalized rat granulosa cells with rapamycin resulted in a concentration-dependent slowing of granulosa cell proliferation, without induction of cell death (Yu et al., 2011). Experiments with primary rat granulosa cells found that mTOR is activated by FSH, via the PI3-kinase/AKT signalling pathway, resulting in an increase in the transcription of genes that control cellular growth, proliferation and glucose metabolism; the results of this study indicate that FSH-stimulated mTOR activation results in the induction of the

lutinizing hormone receptor and other proteins essential for differentiation of granulosa cells into the pre-ovulatory phenotype (Alam et al., 2004).

In bovine luteal cells, activation of the LH receptor results in the phosphorylation of the mTOR substrates ribosomal protein S6 kinase (S6K1) and eukaryotic translation initiation factor 4E binding protein 1 (4EBP1), suggesting that LH-stimulated mTOR activation may contribute to the differentiation of granulosa cells into luteal cells (Hou et al., 2010).

### **1.13.2 mTOR in the oocyte**

In granulosa cells, growth signals, such as oocyte-derived growth factors (GDF9 and BMP15) and endocrine factors (FSH, LH, oestradiol) are integrated by mTOR to execute follicular growth (Yu et al., 2012). The GDF9 and GDF9-BMP15 heterodimers have been shown to promote the survival and development of COCs in mice by enabling the oocyte-dependant activation of mTOR signalling in cumulus cells; cumulus cell survival and oocyte developmental competence are compromised when mTOR in COCs was inhibited with Torin 1 (Guo et al., 2016). *In vivo*, treatment of mice with rapamycin is associated with reduced numbers of ovulated oocytes (Yu et al., 2011). Oocyte-specific conditional knockout of mTOR compromised oocyte meiosis and developmental competence, *in vivo* (Guo et al., 2018b). Additionally, knockout of mTOR in primordial mouse oocytes causes a shift in granulosa cell morphology to a Sertoli cell-like phenotype (Guo et al., 2018b). The tumour suppressor tuberous sclerosis complexes, Tsc1 and Tsc2, are negative regulators of mTORC1. Mutant mice lacking the *Tsc1* or *Tsc2* gene in oocytes experience elevated mTORC1 activity and overactivation of the entire pool of primordial follicles, potentially leading to infertility (Adhikari et al., 2010, Adhikari et al., 2009).

There may be a role for mTORC2 in folliculogenesis because oocyte-specific deletion of *Rictor* in mice is associated with increased follicle atresia, along with a decrease in the follicular pool and decreased serum oestradiol concentrations (Chen et al., 2015). Inhibition of mTOR in mouse oocytes with the dual mTORC1/mTORC2 inhibitor Torin 1 compromised developmental competence, with a reduction in the rate of fertilization and blastocyst development (Guo et al., 2016).

## 1.14 Cholesterol metabolism

Cholesterol is an essential component of many cellular processes such as in the production of steroids, vitamin D, bile acids and lipoproteins, and therefore, the synthesis, uptake and efflux of cholesterol are tightly regulated in cells (Goldstein and Brown, 1990). Cholesterol constitutes about 30 to 40 mol% of the plasma membrane of cells and is important for membrane organization and function (Ikonen, 2008, van Meer et al., 2008, Semrau et al., 2009, Levental and Veatch, 2016).

Cholesterol can be derived from several sources (**Fig. 1.12**): (1) via the uptake of cholesterol from LDL or HDL by the low-density lipoprotein receptor (LDLR) or scavenger receptor class B member I (SR-BI), respectively; (2) via *de novo* cholesterol biosynthesis; (3) from cholesterol esters stored in lipid droplets via cholesterol ester hydrolase (Brown and Goldstein, 1976, Goldstein and Brown, 1990, Connelly and Williams, 2003, Acton et al., 1996, Hu et al., 2010a, Shen et al., 2014).

Cellular cholesterol homeostasis is regulated by the sterol regulatory element-binding proteins (SREBPs) (Brown and Goldstein, 1997). There are three isoforms of SREBPs, SREBP-1a, SREBP1c, and SREBP-2, with the latter involved in regulation of cholesterol and lipid synthesis. In the endoplasmic reticulum, SREBP-2 is bound to the SREBP cleavage-activating protein (SCAP). When intracellular cholesterol concentrations are depleted, SCAP escorts SREBP-2 to the Golgi apparatus, where it undergoes proteolytic cleavage at site-1 and site-2 protease to generate the nuclear forms that activate genes for cholesterol biosynthesis and uptake (Goldstein et al., 2006). When intracellular cholesterol concentrations increase, cholesterol binds to SCAP, triggering the binding of SCAP to the insulin-induced gene 1 (INSIG), preventing transport of SCAP to the Golgi, thus preventing the activation of genes involved in cholesterol biosynthesis and uptake (Goldstein et al., 2006).

Excess intracellular cholesterol is either converted into cholesterol esters by acyl-coenzyme A: cholesterol acyltransferase (ACAT) and stored as lipid droplets, or removed from the cell by the ATP-binding cassette transporter A1 (ABCA1) or the ATP-binding cassette transporter G1 (ABCG1) (Luo et al., 2020). Oxysterols, such as 25-hydroxycholesterol and 27-hydroxycholesterol, are cholesterol derivatives that

regulate cholesterol homeostasis (Schroepfer, 2000, Luo et al., 2020). Oxysterols act via the Liver X receptors (LXRs), LXR $\alpha$  and LXR $\beta$  (Janowski et al., 1996, Lehmann et al., 1997) to promote cholesterol efflux by upregulating ABCA1 and ABCG1, and suppress *de novo* cholesterol synthesis, via inhibition of HMG-CoA reductase (HMGCR) (Hu et al., 2010b).

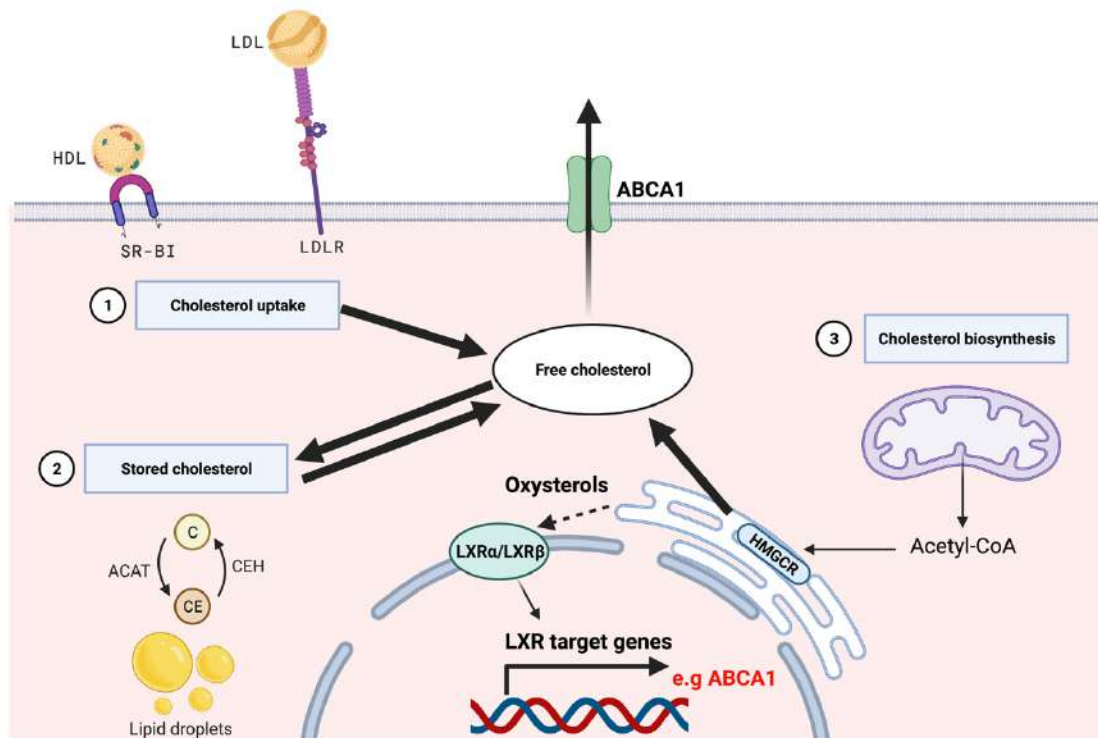


**Figure 1.12. Sources of cholesterol in cells**

Cells can obtain cholesterol from three main sources: (1) the uptake of extracellular cholesterol from HDL or LDL via SR-BI or LDLR, respectively (2) from cholesterol stored in lipid droplets or (3) cholesterol biosynthesis via the mevalonate pathway. Increased intracellular cholesterol in the cell leads to increased concentrations of oxysterols, activating LXRs and the activation of target genes, such as the cholesterol efflux transporter, ABCA1. ACAT, acyl-coenzyme A: cholesterol acyltransferase; CEH, cholesterol ester hydrolase; HMGCR, HMG-CoA reductase; LXR, liver X receptor; C, cholesterol; CE, cholesterol ester; HDL, high-density lipoprotein; LDL, low-density lipoprotein; SR-BI, scavenger receptor class B type I; LDLR, low-density lipoprotein receptor; ABCA1, ATP-binding cassette transporter A1. (Adapted from (Luo et al., 2020)).

### 1.14.1 The mevalonate pathway

In eukaryotes, cholesterol is synthesized from isoprenoids which are produced via the mevalonate pathway (**Fig. 1.13**) (Goldstein and Brown, 1990, Lombard and Moreira, 2011). All steroidogenic cells are capable of carrying out *de novo* cholesterol synthesis (Hu et al., 2010a). The mevalonate pathway of cholesterol biosynthesis starts by the condensing of two molecules of acetyl-CoA to acetoacetyl-CoA, which is then converted to 3-hydroxy-3-methyl-glutaryl-CoA (HMG-CoA) by HMG-CoA synthase, and then converted into mevalonate by the by rate limiting enzyme in the mevalonate pathway, HMGCR (**Fig. 1.13**); farnesyl pyrophosphate synthase (FDPS) converts mevalonate to geranyl phosphate and then farnesyl pyrophosphate (FPP), which is then converted to squalene by farnesyl diphosphate farnesyltransferase 1 (FDFT1) followed by another series of enzyme reactions to yield cholesterol (Bloch, 1965, Sharpe and Brown, 2013).

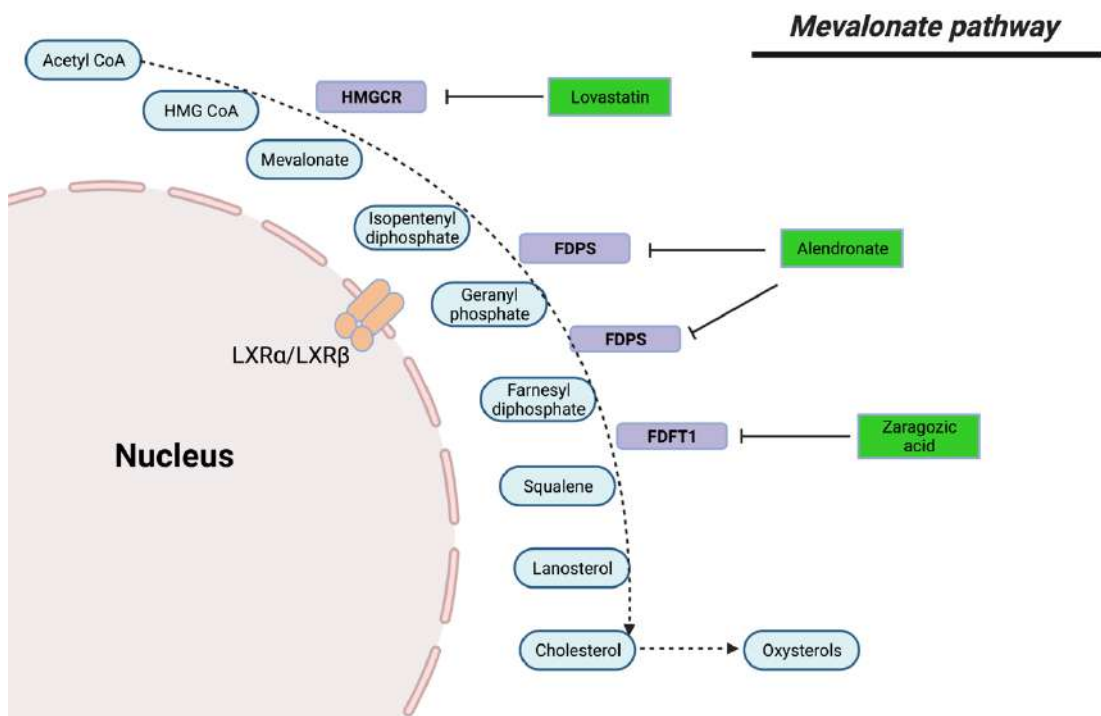


**Figure 1.13. The mevalonate pathway of cholesterol biosynthesis**

Diagram of the mevalonate pathway showing the key enzymes leading to the synthesis of cholesterol (adapted from (Healey et al., 2016).

### 1.14.2 Cholesterol metabolism in granulosa cells

The current understanding of cholesterol metabolism in granulosa cells mostly comes from studies investigating luteinized granulosa cells and steroidogenesis. However, little is known about cholesterol metabolism in bovine granulosa cells because prior to luteinization, granulosa cells aromatize androstenedione provided by the theca cells that surround the follicle to synthesize oestradiol (Ryan et al., 1968, Dorrington et al., 1975, Liu and Hsueh, 1986).

The ovarian basement membrane is permeable to proteins up to 300 kDa and is thought to exclude LDL (~3500 kDa) and VLDL (6000 to 27000 kDa) until vascularization, at around the time of ovulation (Jaspard et al., 1996, Le Goff, 1994, Shalgi et al., 1973). Therefore, HDL (175 to 500 kDa) is the only class of lipoprotein that has been detected in follicular fluid in bovine (Savion et al., 1982, Brantmeier et al., 1987), porcine (Chang et al., 1976), and human (Simpson et al., 1980, Jaspard et al., 1996) follicles.

Bovine granulosa cells express lower abundance of mRNA encoding SR-BI, compared with luteinized bovine granulosa cells, with a 5-fold increase in expression over 5 days of culture, *in vitro* (Rajapaksha et al., 1997). Additionally, treatment of un-luteinized bovine granulosa cells with HDL has no significant effect on progesterone secretion, suggesting that granulosa cells cannot utilize HDL for steroidogenesis prior to luteinization (O'Shaughnessy et al., 1990). Following luteinization, treatment of bovine luteal cells with HDL or LDL is associated with increased progesterone secretion (Bao et al., 1997b, Bao et al., 1995) and proliferation (Bao et al., 1995). Similarly, in porcine granulosa cells, there is low expression of SR-BI at the mRNA and protein level, which increases following luteinization (Miranda-Jimenez and Murphy, 2007). Non-luteinized rat granulosa cells may not have the capability to utilize cholesterol from HDL because they do not take up radiolabelled HDL or fluorescent cholesterol esters, and do not appear to express SR-BI (Azhar et al., 1998a). However, luteinized rat granulosa cells take up radiolabelled HDL or fluorescent cholesterol esters, express higher abundance of SR-BI and secrete more progesterone in response to treatment with HDL (Azhar et al., 1998a). Knockdown of *SRBI* in a human granulosa cell line (HGL5) was associated with lower progesterone



secretion and lower expression of genes encoding StAR and HSD3B1 (Kolmakova et al., 2010).

Intracellular lipid droplets may be a source of cholesterol for progesterone synthesis in bovine luteal cells. In response to LH stimulation, bovine luteal cells secrete progesterone, associated with increased hydrolysis of cholesterol esters within lipid droplets by hormone sensitive lipase (Plewes et al., 2020).

### **1.15 Aims and hypotheses**

Concurrent metabolic energy stress and uterine bacterial infections are associated with impaired ovarian function in postpartum dairy cows (Leroy et al., 2008, Sheldon et al., 2019a, Sheldon et al., 2002). Multiple Gram-negative bacteria infect the postpartum uterus, and lipopolysaccharide has been shown to accumulate in the dominant follicle of animals with uterine disease (Herath et al., 2007). Granulosa cells from emerged or dominant follicles secrete IL-1 $\beta$ , IL-6 and IL-8 in response to LPS (Price et al., 2013, Price and Sheldon, 2013, Bromfield and Sheldon, 2011). The aim of the present thesis was to explore whether there is evidence for crosstalk between innate immunity and metabolic energy stress in the granulosa cells and cumulus-oocyte complex of the bovine ovarian follicle. In this thesis, we used ultrapure lipopolysaccharide from *E. coli* 0111: B4 as a model toxin because it is free from contaminating lipoproteins, therefore only activates TLR4 (Hirschfeld et al., 2000).

In *Chapter 3*, we start by investigating the crosstalk between innate immunity and metabolism in bovine granulosa cells. Our hypothesis was that manipulating glycolysis, AMPK, or mTOR to mimic energy stress, would impair the innate immune responses of granulosa to LPS. To test this hypothesis, we altered the availability of glucose or used small molecule inhibitors to inhibit glycolysis, activate AMPK or inhibit mTOR, and measured the LPS-induced secretion of IL-1 $\alpha$ , IL-1 $\beta$  and IL-8. We also investigated the effects of activating AMPK or inhibiting mTOR on the LPS-induced activation of MAPKs.

In *Chapter 4*, we investigated the effects of limiting cholesterol metabolism on the granulosa cell innate immune responses to LPS. The first hypothesis of this chapter

was that decreasing the availability of cholesterol would impair the innate immune responses to LPS in granulosa cells. To test this hypothesis, we reduced the availability of exogenous cholesterol or depleted cholesterol with methyl- $\beta$ -cyclodextrin. We then treated granulosa cells with HDL, LDL or VLDL cholesterol. The second hypothesis of this chapter was that inhibiting the cholesterol biosynthesis pathway in granulosa cells would impair the innate immune responses of granulosa cells to LPS. To test this hypothesis, we inhibited the cholesterol biosynthesis pathway using short-interfering RNA or small molecule inhibitors. Following this, we measured the LPS-induced secretion of IL-1 $\alpha$ , IL-1 $\beta$  and IL-8. We also investigated the effects of some of the treatments on the abundance of SR-BI or HMGCR, or on the LPS-induced activation of MAPKs.

In *Chapter 5*, we explored the effects of energy stress or limiting cholesterol metabolism on the innate immune response of the bovine cumulus-oocyte complex (COC) to LPS. The hypothesis of this chapter was that energy stress or decreasing the availability of cholesterol would alter the innate immune responses of COCs to LPS. To explore the crosstalk between innate immune function and energy stress in the COC, we used small molecule inhibitors to inhibit glycolysis, activate AMPK or inhibit mTOR. To explore the crosstalk between innate immune function and cholesterol metabolism in the COC, we used small molecule inhibitors of the cholesterol biosynthesis pathway. Following IVM, we measured the LPS-induced secretion of IL-1 $\alpha$ , IL-1 $\beta$  and IL-8. In addition to measuring the accumulation of pro-inflammatory cytokines, we also assessed COC expansion and meiotic progression following treatments as markers of oocyte health.

Finally, in *Chapter 6*, we exploited an *in vivo* model of endometritis in cattle to investigate the potential long-term effects of uterine disease on transcriptome of the ovary. For comparison, we also explored the changes in the transcriptome across the bovine reproductive tract. The hypothesis of this chapter was that intrauterine infusion of pathogenic bacteria, *in vivo*, would lead to changes in the transcriptome of the reproductive tract in dairy cattle several months later. To test this hypothesis, Holstein heifers received intrauterine infusion of pathogenic bacteria that induced clinical endometritis, and the tissues of the endometrium, oviduct, granulosa cells and oocytes were collected several months later and subject to RNA-sequencing.

## 2 General Materials and Methods

The experiments presented in this thesis used primary granulosa cells isolated from emerged (4 to 8 mm in diameter) or dominant (> 8.5 mm in diameter) bovine ovarian follicles, or cumulus-oocyte complexes isolated from emerged follicles. Cells were challenged with ultrapure LPS from *E. coli* 0111: B4 (#tlrl-3pelps; Invivogen, Toulouse, France), which is associated with bacterial infection. The secretion of pro-inflammatory cytokines or hormones were measured in cell-free supernatants, and protein or RNA was extracted from cells to measure the activation of immune pathways, or the expression of genes associated with immunity or physiology. For granulosa cells and COCs, the crosstalk between energy or cholesterol metabolism and innate immunity was explored. For cumulus-oocyte complexes, the effects of the treatments on oocyte health were also explored by assessing cumulus expansion and meiotic status, following *in vitro* maturation (IVM).

### 2.1 Granulosa cell isolation

Ovaries were collected from cattle after slaughter and processing, during the normal work of a commercial slaughterhouse, with approval from the United Kingdom Department for Environment, Food and Rural Affairs under the Animal By-products Registration (EC) No. 1069/2009 (registration number U1268379/ABP/OTHER).

Ovaries were collected from post pubertal, non-pregnant, healthy mixed breed beef cattle within 15 min of slaughter at a local slaughterhouse and transported directly to the laboratory. The ovaries were transported to the laboratory in Medium 199 (M199; Thermo Fisher Scientific, Paisley, UK), containing 1% Antibiotic, Antimycotic Solution (Merck, Gillingham, UK) and 0.1% bovine serum albumin (BSA; Merck), heated to 38.5°C and stored in a thermos flask. For transport medium, powdered M199 (Thermo Fisher Scientific) was reconstituted with 500 ml ultrapure water, and pH adjusted to 7.1 to 7.4. Ovaries from between 10 to 20 animals were pooled for each experiment. Ovaries were processed for collection of mural granulosa cells within 90 min of excision. Only healthy follicles, with clear follicular fluid and no evidence of haemorrhage were used.

## 2.2 Isolation of bovine granulosa cells

On returning to the laboratory, the ovaries were rinsed in 70% ethanol, followed by a brief rinse in sterile phosphate-buffered saline (PBS; Thermo Fisher Scientific, Loughborough, UK), before aspiration of the mural granulosa cells from follicles. Granulosa cells were isolated, as described previously, with minor modifications (Bromfield and Sheldon, 2011, Price et al., 2013, Price and Sheldon, 2013). Emerged (4 to 8 mm diameter) or dominant (> 8.5 mm diameter) follicles were aspirated using a sterile 20-gauge needle and 2 ml or 5 ml endotoxin-free syringe, respectively (BD Medical, Oxford, UK), into 30 ml collection medium (0.5% w/v BSA, 25 mM HEPES (4-[2-hydroxyethyl] piperazine-1-ethanesulfonic acid), containing 1% Antibiotic, Antimycotic Solution, 0.005% w/v heparin (all Merck) in Medium 199), in 90 mm petri dishes (Fisher), warmed to 37.5°C on a slide warmer. The granulosa cell suspensions were then collected into sterile 50 ml centrifuge tubes (Greiner Bio-One, Gloucester, UK) and centrifuged for 10 min at  $700 \times g$  (Eppendorf 5810R, Cambridge, UK) to produce a cell pellet. Following this, any red blood cells were lysed with the addition of 1 ml of sterile-filtered water (Merck) for 1 min, following which, 29 ml of M199 culture medium containing 10% heat-inactivated fetal bovine serum (FBS; Biosera, Ringmer, UK), 1% Antibiotic, Antimycotic Solution (Merck), 1% insulin-transferrin-selenium (ITS) (Corning, Palo Alto, CA), 1% GlutaMAX (Thermo Fisher Scientific) was added and centrifuged again at  $700 \times g$  for 10 min (Eppendorf 5810R). The cells were resuspended in 10 ml of culture medium and counted using a Coulter-counter (Beckman Coulter, Indianapolis, U.S.), at the 8 to 17  $\mu\text{m}$  size range. A density of 750,000 cells per well were seeded into 24-well plates (TPP) in 0.5 ml per well of granulosa cell culture medium.

All cells were cultured at 38.5°C, in a humidified atmosphere of air containing 5% CO<sub>2</sub> in an incubator only used for primary cells. The same batch of FBS was used throughout the thesis and had previously been batch tested to ensure minimal stimulation of pro-inflammatory cytokines and chemokines. Collection media was filtered through a 0.2  $\mu\text{m}$  filter and stored in the base of the 250 ml filter unit (TPP).

### 2.3 Granulosa cell culture and treatments

Following an initial 18 h culture period to allow the granulosa cells to adhere to the wells of the plates, the medium was aspirated, and the cells were cultured with vehicle or treatments in 0.5 ml of granulosa cell culture medium. The rationale was to use small molecules to manipulate glycolysis, AMPK, mTOR or cholesterol metabolism, and then challenge the cells with LPS to evaluate inflammation (**Table 2.1**). Treatments were diluted to the required concentration in warm culture medium and vortexed immediately before use. Cell treatments were added at double concentration in 0.5 ml/well for the indicated time, before the addition of 0.5 ml/well of control medium or medium containing LPS at a final concentration of 1 µg/ml LPS for a further 24 h. After 24 h LPS challenge, supernatants were stored at -20°C in micro-centrifuge tubes (Alpha Labs, Hampshire, UK) for cytokine analysis by ELISA.

We used ultrapure LPS because it is free from contaminating lipoproteins, therefore only activates TLR4 (Hirschfeld et al., 2000). The LPS was reconstituted in endotoxin-free water (provided with the LPS) to a concentration of 5 mg/ml, and vortexed for 10 min. The LPS was then further diluted in endotoxin-free water to a final concentration of 1 mg/ml and stored at -20°C, in salinized vials (Merck). The concentration and duration of LPS challenge was based on previous experiments using a range of concentrations of 1 ng/ml to 10 µg/ml LPS, and on IL-1β, IL-6 and IL-8 responses to 1 µg/ml LPS in bovine granulosa cells isolated from emerged or dominant follicles (Bromfield and Sheldon, 2011, Price et al., 2013, Price and Sheldon, 2013). Throughout this thesis, we used a relatively high concentration of 1 µg/ml LPS to stimulate robust inflammatory responses. Prior to use, the LPS was defrosted at room temperature, sonicated for 3 min and vortexed for 1 min prior to dilution to the required concentration in warm culture medium. The LPS solution was then vortexed for 1 min before cell challenge.

Granulosa cells have limited responses to PAMPs when cultured in the absence of serum (Bromfield and Sheldon, 2011). Unfortunately, serum diminishes FSH responsiveness and oestradiol producing capability, and results in granulosa cell luteinisation. Most of the experiments in this thesis were carried out in the presence of serum over 48 h, to detect the responses to LPS whilst minimizing luteinisation.

**Table 2.1. Small molecules used to examine pathways**

Name	Target	Manufacturer	Code	Treatment period before challenge	Solvent	Working concentration
2-DG	Hexokinase II	Merck	D3179	2 h	H <sub>2</sub> O	0.05 to 1 mM
AICAR	AMPK	Merck	A9978	2 h	H <sub>2</sub> O	0.01 to 1 mM
Rapamycin	mTOR	Bio-Techne	1292/1	2 h	DMSO	5 to 500 nM
Torin 1	mTOR	Bio-Techne	4247/10	2 h	DMSO	10 to 150 nM
Dexamethasone	Glucocorticoid receptor	Merck	D4902	2 h	DMSO	1 µM
Lovastatin	HMGCR	Merck	PHR1285	24 h	DMSO	0.01 to 10 µM
Alendronate	FDPS	Merck	126855	24 h	DMSO	0.5 to 20 µM
Zaragozic acid	FDFT1	Merck	Z2626	24 h	DMSO	0.5 to 20 µM
Methyl-β-cyclodextrin	Cholesterol	Merck	C4555	24 h	H <sub>2</sub> O	0.1 to 1 mM
Mevalonate	HMGCR	Merck	90469	24 h	DMSO	0 to 100 µM
Farnesol pyrophosphate	FDPS	Merck	F6892	24 h	Methanol: ammonia solution	0 to 50 µM
Human HDL	SR-BI	Merck	437641	24 h	N/A	0 to 100 µg/ml
Human LDL	LDLR	Invitrogen	L3486	24 h	N/A	0 to 50 µg/ml
Human VLDL	VLDLR	Merck	437647	24 h	N/A	0 to 10 µg/ml

## 2.4 Validation of granulosa cell phenotypes

Granulosa cells from 4 to 8 mm diameter follicles are representative of the homogenous pool of follicles containing granulosa cells that are FSH-responsive and LH-unresponsive, and only granulosa cells from follicles over 8.5 mm (external diameter) express the luteinizing hormone receptor (Xu et al., 1995a). To confirm that granulosa cells from 4 to 8 mm diameter follicles represent emerged follicles and > 8.5 mm diameter follicles represent dominant follicles, the expression of *FHSR* and *LHR* were analysed by quantitative polymerase chain reaction (qPCR) (**Fig. 2.1**). Granulosa cells were treated for 48 h in 0.5 ml of granulosa cell culture medium, washed with 200  $\mu$ l ice cold PBS, lysed using 350  $\mu$ l RLT buffer and stored at  $-80^{\circ}\text{C}$ , prior to analysis by qPCR (protocol described in *Section 2.21*). We selected a 48 h treatment period to match and exceed the treatment period we used in major experiments throughout this thesis. Granulosa cells from both 4 to 8 mm and > 8.5 mm diameter follicles expressed *FHSR* (**Fig. 2.1**). Granulosa cells from >8.5 mm diameter follicles expressed more *LHR* ( $P < 0.01$ ), compared with granulosa cells from emerged follicles.

Additionally, we also cultured granulosa cells for 48 h in 1 ml of granulosa cell culture medium, containing 1 ng/ml highly purified FSH (A. F. Parlow, National Hormone and Peptide program, Torrance, California) and  $10^{-7}$  M androstenedione (Merck), to stimulate the production of oestradiol and progesterone by granulosa cells, as previously described (Gutierrez et al., 1997). The concentrations of oestradiol and progesterone were measured by ELISA (protocol described in *Section 2.16*). We found that granulosa cells from > 8.5 mm diameter follicles secreted more oestradiol into the medium than granulosa cells from 4 to 8 mm diameter follicles ( $P < 0.001$ ; **Fig. 2.2A**), confirming previous studies (Spicer et al., 2002, Gutierrez et al., 1997, Roberts and Echterkamp, 1994). We did not detect any difference in the secretion of progesterone into the medium between granulosa cells from 4 to 8 mm and > 8.5 mm diameter follicles ( $P = 0.14$ ; **Fig. 2.2B**). Luteinization of granulosa cells is a concern when culturing in the presence of serum (10% FBS). Luteinized bovine granulosa cells secrete more progesterone, and less oestradiol than un-differentiated granulosa cells (Henderson and Moon, 1979). Therefore, it can be inferred that in this culture model, the granulosa cells have not yet differentiated into luteal cells.

Together, these data suggests that the follicle diameters selected for this thesis are representative of granulosa cells from emerged or dominant follicles. From this point in the thesis, granulosa cells will be referred to as isolated from either emerged or dominant follicles.

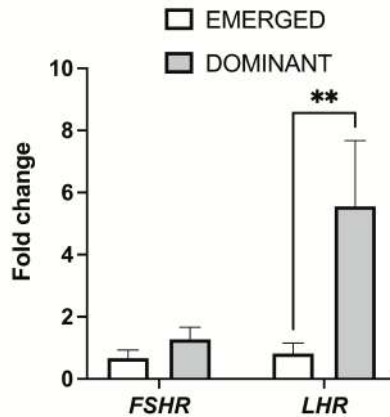


**Figure 2.1. Granulosa cells from dominant follicles have higher expression of *LHR* than granulosa cells isolated from emerged follicles**

Granulosa cells were cultured for 48 h in granulosa cell culture medium. The expression of *FSHR* and *LHR* mRNA was measured by qPCR and expressed as fold change, relative to *ACTB*. Data are presented as mean (SEM) and represent 3 independent experiments. The relative expression of *FSHR* or *LHR* were compared using t test; \*\* P < 0.01.

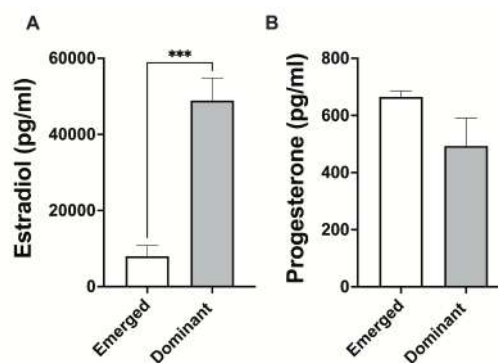


**Figure 2.2. Granulosa cells from dominant follicles secrete more oestradiol than granulosa cells isolated from emerged follicles**

Granulosa cells were cultured for 48 h in granulosa cell culture medium, containing 1 ng/ml highly purified FSH and  $10^{-7}$  M androstenedione, and the accumulation of oestradiol (A) or progesterone (B) were measured in supernatants. Data are presented as mean (SEM) and represent 4 independent experiments. Data was compared using t test, \*\*\* P < 0.001.



## 2.5 Optimal granulosa cell culture conditions for inflammatory responses

To determine the optimal culture conditions for examining inflammatory protein responses, granulosa cells were isolated from emerged or dominant follicles and plated at three different seeding densities: 375,000, 750,000 and 1,500,000 cells/well of a 24-well plate and established for 18 h before challenge for 24 h with 1  $\mu$ g/well LPS (Fig. 2.3). The secretion of IL-1 $\alpha$ , IL-1 $\beta$  or IL-8 was measured by ELISA (protocol described in Section 2.13 to Section 2.15). Granulosa cells from emerged or dominant follicles, plated at a density of 1,500,000 cells/well accumulated more IL-1 $\alpha$  ( $P < 0.05$ ), compared with granulosa cells plated at 375,000 cells/well. From dominant follicles, there was more accumulation of IL-1 $\beta$  ( $P < 0.05$ ) by granulosa cells plated at 1,500,000 cells/well, compared with granulosa cells plated at 375,000 cells/well. Therefore, we concluded that a seeding density of 750,000 cells/well was sufficient to stimulate robust innate immune responses to LPS, as previously described (Bromfield and Sheldon, 2011, Price and Sheldon, 2013, Price et al., 2013, Herath et al., 2007).

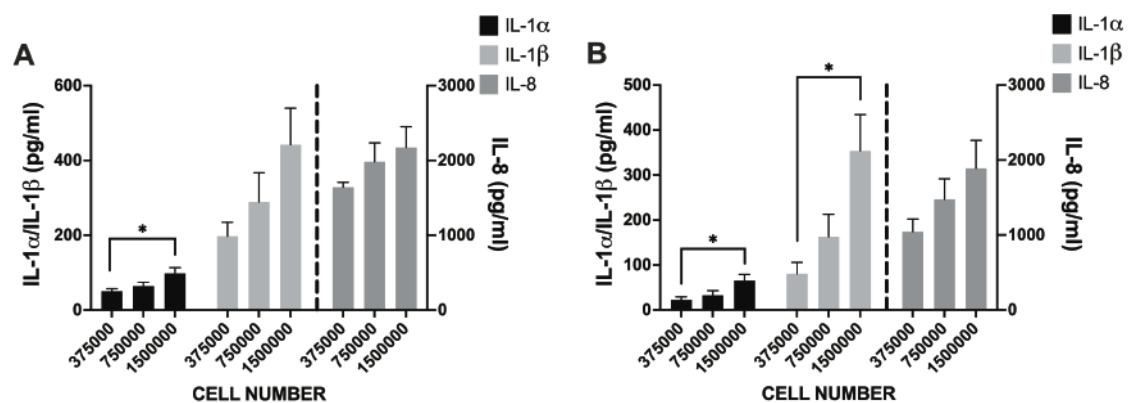


**Figure 2.3. Cytokine production by granulosa cells increases with cell density**

Granulosa cells were isolated from emerged (A) or dominant follicles (B), and seeded at 375,000, 750,000 or 1,500,000 cells/well, before 24 h challenge with 1  $\mu$ g/ml LPS. After 24 h the supernatants were collected and the accumulation of IL-1 $\alpha$ , IL-1 $\beta$  and IL-8 were measured by ELISA. Data are presented as mean (SEM) and represent at least 4 independent experiments. Data were analysed by one-way ANOVA using Dunnett's post hoc test. \*,  $P < 0.05$ .

## **2.6 Cumulus-oocyte complex treatment and in vitro maturation**

Following aspiration of emerged follicles, cumulus-oocyte complexes (COCs) were immediately collected from the petri dish using a Wiretrol pipette (Drummond Scientific Company, Broomall, PA), under a dissecting microscope. An average of 200 COCs from 20 to 40 ovaries were pooled into collection medium without heparin. The COCs were washed twice in collection medium without heparin and groups of 10 to 50 COCs were matured in organ culture dishes (Corning Falcon) for 22 h in 0.5 ml of oocyte maturation medium (0.25 mM pyruvate (Merck), 0.4 mM glutamine (Merck), 1% ITS, 1% Antibiotic, Antimycotic Solution, 10% FBS, all in M199), containing 2 µg/ml oestradiol (Merck) and 20 µg/ml highly purified bovine FSH, as previously described (Bromfield and Sheldon, 2011, Piersanti et al., 2019b). Cumulus-oocyte complexes were matured in a humidified incubator of air at 38.5°C under 5% CO<sub>2</sub> in control oocyte maturation medium or medium containing the treatments described in *Chapter 5*.

## **2.7 Assessment of COC expansion**

Following 22 h IVM, COCs were examined for cumulus expansion, from Grade 0 to Grade 4, using previously reported criteria (Vanderhyden et al., 1990, Funsho Fagbohun and Downs, 1990, Downs, 1989, Whitty et al., 2021): Grade 0 COCs have no response, with cumulus cells adhered to the IVM dish; Grade 1 COCs are unexpanded in a spherical shape; Grade 2, only the outermost layer of cumulus cells are expanded; Grade 3 COCs were mostly expanded; Grade 4 COCs were fully expanded and spongy in appearance.

## **2.8 Cumulus-oocyte complex fixation**

Cumulus-oocyte complexes were fixed in 4% paraformaldehyde for 10 min at 37.5°C, prior to transfer into microtubule stabilising buffer (deionized water (dH<sub>2</sub>O) containing 100 mM piperazine-N, N'-bis (2- ethanesulfonic acid) (PIPES), 5 mM magnesium chloride (MgCl<sub>2</sub>), 2.5 mM ethylene glycol-bis (β-aminoethyl ether)- N, N, N', N'-tetraacetic acid (EGTA), 2% formaldehyde, 0.1% Triton-X-100, 1 mM Taxol, 10 U/ml aprotinin and 50% deuterium oxide (D<sub>2</sub>O); all Merck) for 45 min at 37.5°C, and stored

in wash/block solution (PBS containing 0.2% sodium azide, 0.2% powdered milk, 2% normal goat serum, 1% BSA, 0.1M glycine, 0.1% Triton-X-100) at 4°C for up to 2 weeks.

## **2.9 Immunofluorescence and confocal microscopy**

Cumulus-oocyte complexes were washed once in wash/block solution and up to 10 COCs/well were transferred into each well of a 96-well round-bottom microplate (Thermo Fisher Scientific) into 50 µl/well wash/block solution containing mouse anti- $\alpha$ -tubulin and mouse anti- $\beta$ -tubulin (**Table 2.2**) and incubated overnight at 4°C with gentle agitation. Samples were then washed twice in wash solution and detection was performed using goat anti-mouse-Alexa-488 secondary (**Table 2.2**), in combination with Phalloidin-Alexa-555 (1:100; #A34055; Invitrogen) and 1 µg/ml Hoechst 33342 (#H1399; Invitrogen), for the detection of F-actin and nucleic acids, respectively. Samples were incubated for 1 h at room temperature with gentle agitation.

To mount the COCs ready for imaging, samples were washed twice in wash solution and transferred onto frosted polysine microscope slides (VWR). A small amount of wax was placed onto the corners of a 24 x 50 mm borosilicate coverglass to prevent compression of samples. Mounting media (50% PBS, 50% glycerol containing 1 µg/ml Hoechst 33342) was added under the coverslip via capillary action.

**Table 2.2. Antibodies used for immunofluorescence**

Target peptide/protein	MW (kDa)	Manufacturer and code	RRID	Dilution	Species raised in and clonality
$\alpha$ -tubulin	50	Bio-technie NB100-690	AB_521686	1:100	Mouse monoclonal
$\beta$ -tubulin	50	Invitrogen 32-2600	AB_2533072	1:100	Mouse monoclonal
IgG Highly Cross-Absorbed Secondary Antibody, Alexa-488	N/A	Invitrogen A32723	AB_2633275	1:400	Goat anti-mouse polyclonal

### 2.9.1 Assessment of meiotic status

Cumulus-oocyte complexes were analysed on a Zeiss LSM 710 confocal microscope using a 40x Plan-Apochromat objective ( $n_a = 1.3$ ), KrArg (405,488 nm) and HeNe (543 nm) lasers to collect three channel z-stacks through the oocyte. Oocytes were analysed using Zen software (Zeiss, Jena, Germany). Oocyte meiotic status was assessed according to the criteria described in *Chapter 1*. Oocytes with evidence of a polar body and a bipolar spindle with condensed chromatids were evaluated as MII oocytes (Combelles et al., 2002, Bromfield and Sheldon, 2011). Germinal vesicle breakdown (GVBD) is characterised by folding and fragmentation of the nuclear membrane, and disappearance of the nuclear pores (**Fig. 2.4**). Following GVBD, the chromosomes align along the first metaphasic plate and the microtubules assemble into a spindle to reach metaphase I (MI). The bivalent homologue chromosomes then migrate to the opposite poles of the spindle during anaphase I (AI) and becomes surrounded by a nuclear membrane during telophase I. Finally, the first polar body forms and is extruded from the oocyte and the reassembling of the meiotic spindle along the equatorial plane occurs during metaphase II (MII).

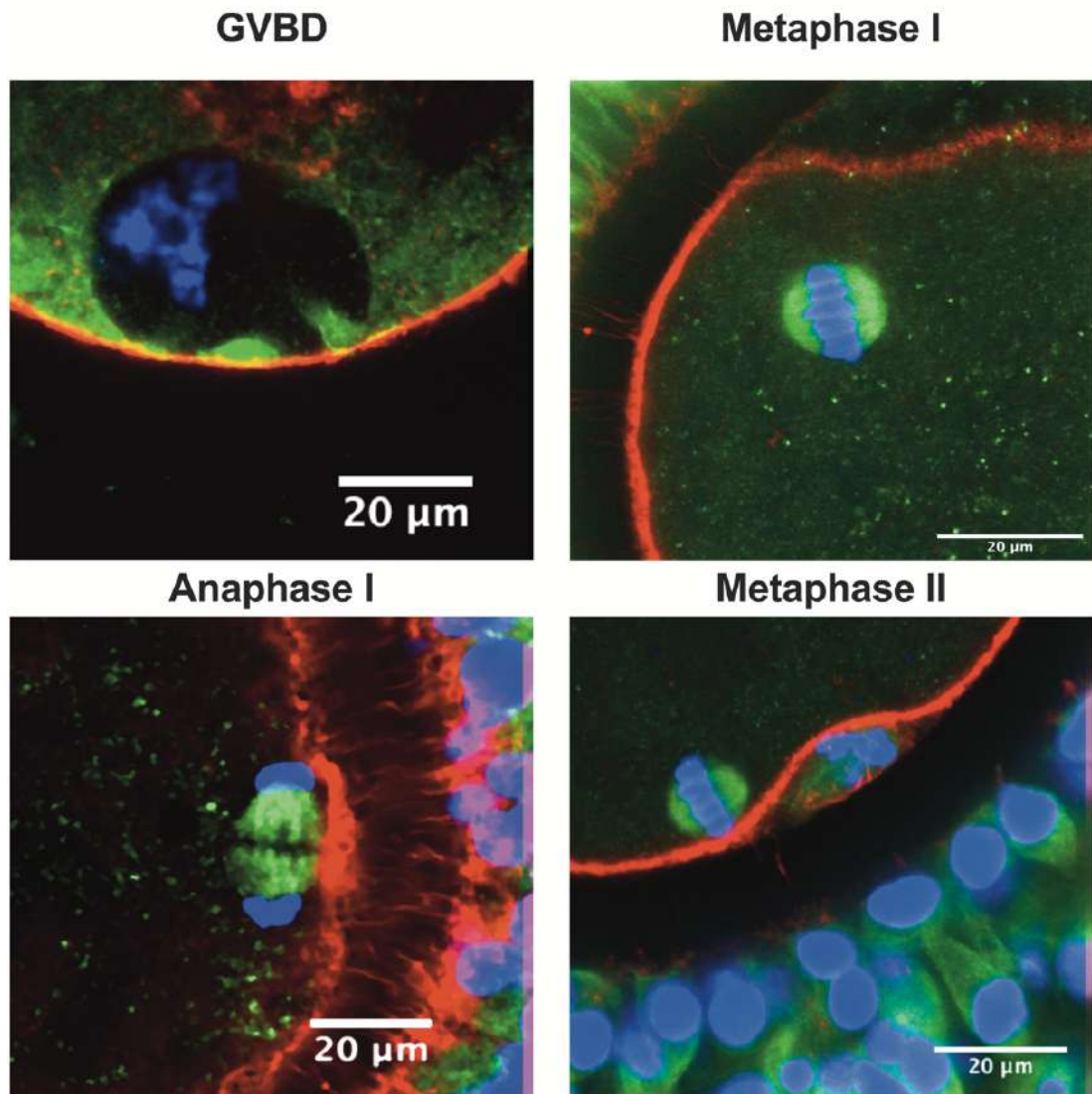


**Figure 2.4. Oocyte meiotic maturation**

Germinal vesicle breakdown (GVBD) is characterised by condensed chromatin surrounded by a ring around the nucleolus. During metaphase I (MI), the chromosomes align along the first metaphase plate and the microtubules assemble into a spindle. At anaphase I (AI), the chromosomes are segregated to opposite poles of the bipolar spindle. Finally, at metaphase II (MII), the oocyte extrudes the polar body and the MII spindle reassembles with the chromosomes aligned along the equatorial plane.

## 2.10 Protein extraction and quantification

Granulosa cells were washed with 350  $\mu$ l of ice-cold PBS before being lysed with 100  $\mu$ l Phosphosafe Extraction Reagent (Novagen, Madison, US) per well of a 24-well plate (TPP). Adherent cells were scraped from each well using the base of a sterile pipette tip (Starlab, Milton Keynes, UK) and lysates transferred to 1.5 ml tubes (Eppendorf, Stevenage, UK). The tubes were centrifuged at  $13,000 \times g$  at  $4^{\circ}\text{C}$  for 10 min and the lysate transferred to fresh iced tubes, without disturbing the pellet. The lysate was then quantified for protein abundance and stored at  $-20^{\circ}\text{C}$ .

The detergent compatible (DC) assay (Bio-Rad, Hercules, CA, USA) was used to quantify the concentration of protein in each sample, as per manufacturer's instructions. Briefly, standards of bovine serum albumin (Merck) were diluted from 0.5 to 2.5 mg/ml. A volume of 5  $\mu$ l of either samples or standards were added in duplicate to the wells of a 96-well Nunclon plate (TPP). The alkaline copper tartrate solution (Reagent A; Bio-Rad) was made up of 20  $\mu$ l of Reagent S (Bio-Rad) for every 1 ml of Reagent A, and vortexed to mix. A volume of 25  $\mu$ l of Reagent A was added to each well containing samples or standard, followed by the addition of 200  $\mu$ l of Reagent B, a dilute Folin reagent (Bio-Rad). The plate was incubated for 15 min in the dark and the absorbance measured at 750 nm on a microplate reader (POLARstar Omega, BMG Labtech, Offenburg, Germany). The inter- and intra-assay coefficients of variation for the DC Assay were  $< 2\%$  and  $< 3\%$ , respectively.

## 2.11 SDS-PAGE

Samples were mixed in a 1:5 ratio with Laemmli sample buffer, vortexed and heated for 10 min at  $95^{\circ}\text{C}$ . A 12% polyacrylamide gel (made in-house) was constructed (**Table 2.3**) in a gel mould and left to polymerize for 30 min, following which a stacking gel (**Table 2.4**) was constructed and placed in a mini trans-blot PROTEAN electrophoresis cell (Bio-Rad). The tank was filled with running buffer (25 mM Tris (Melford), 192 mM glycine (Merck), 0.1% w/v SDS (VWR), in deionized water), and 10  $\mu$ l of Precision Plus All Blue Protein standard (Bio-Rad) was added to the first lane,

and a total of 10 µg/lane of sample protein added to the remaining wells. Electrophoresis was carried out at 180 V for 40 min (PowerPac basic, Bio-Rad).

## 2.12 Western Blot

Polyvinylidene difluoride (PVDF) membrane (GE Healthcare, Chalfont, St Giles, UK) was immersed in 100% methanol (Thermo Fisher Scientific) for 30 s until translucent, followed by dH<sub>2</sub>O for 2 min. Filter paper (Bio-Rad) was equilibrated in transfer buffer (25 mM Tris (Melford Labs, Ipswich, UK), 192 mM glycine (Merck), 20% w/v methanol (Thermo Fisher Scientific) in deionized water). The transfer cassette (Bio-Rad) was then assembled, and protein was transferred at 25 V for 30 min. The PVDF membrane was then removed from the cassette and blocked in 5% BSA in TBST (Merck; 20 mM Tris (Melford Labs), 125 mM NaCl (Thermo Fisher Scientific), 0.1% w/v Tween-20 (Merck) in deionized water) for 1 h at room temperature. The membrane was then washed for 5 sec in TBST, before being incubated with primary antibody (**Table 2.5**) overnight at 4°C. The membrane was washed 3 x 5 min with TBST, incubated with secondary antibody for 1 h at room temperature and then washed again 3 x 5 min with TBST and placed into the ChemiDoc XRS system (Bio-Rad). Clarity Western ECL substrate (Bio-Rad) was dispensed onto the membrane and the image was captured using Quantity One software (Bio-Rad) up until the point of saturation. Following imaging, the membrane was stripped with Restore Western Blot Stripping Buffer (Thermo Fisher Scientific) for 7 min at room temperature, re-blocked and re-stained with the appropriate primary or secondary antibodies.

### 2.12.1 Western Blot Quantification

Images were captured using a ChemiDoc XRS System (Bio-Rad). Representative whole blot images are presented in **Figure 2.5**. The background-normalised peak band density was measured in the images for each protein using Fiji (Schindelin et al., 2012); target protein bands were normalised to β-actin or α-tubulin; when antibodies were available, phosphorylated proteins were normalised to their cognate total protein.

**Table 2.3. Formulation of polyacrylamide gel for SDS-PAGE**

Reagent	7.5%	10%	12%	15%	Storage
Water	5 ml	4.2 ml	3.5 ml	2.5 ml	N/A
4 x Tris and SDS (Separating buffer)	2.5 ml	2.5 ml	2.5 ml	2.5 ml	RT
30% Acrylamide	2.5 ml	3.3 ml	4 ml	5 ml	4°C
APS (10% solution)	100 µl	100 µl	100 µl	100 µl	4°C
Temed	10 µl	10 µl	10 µl	10 µl	RT

**Table 2.4. Formulation of stacking gel for SDS-PAGE**

Water	1.75 ml
4 x Tris and SDS	0.75 ml
30% Acrylamide	0.5 ml
APS (10% solution)	50 µl
Temed	3 µl



**Table 2.5. Antibodies for western blot**

Target peptide/protein	Band size (kDa)	Manufacturer and code	RRID	Dilution	Species raised in and clonality	Species reactivity
Diphosphorylated ERK1/2	42/44	Merck M8159	AB_477425	1:1000	Mouse monoclonal	Mouse, <i>Xenopus</i> , <i>Drosophila</i> , <i>Caenorhabditis elegans</i> , Rat, Yeast, Hamster, Bovine, Human
ERK1/2	42/44	Abcam 17942	AB_2297336	1:1000	Rabbit polyclonal	Mouse, Rat, Human
Phospho p38 (pThr180/pTyr182)	39	Acris AP05898PU-N	AB_1620514	1:1000	Rabbit polyclonal	Bovine, Canine, Chicken, Human, Monkey, Mouse, Rat, Zebrafish
P38	40	Cell Signaling 8690	AB_10999090	1:1000	Rabbit monoclonal	Human, Mouse, Rat, Hamster, Monkey, Bovine, Pig
Phospho JNK	46/54	Cell Signaling 9251	AB_331659	1:1000	Rabbit polyclonal	Human, Mouse, Rat, Hamster, Monkey, <i>Drosophila</i> , Bovine, Yeast
JNK	46/54	Cell Signaling 9152	AB_2250373	1:1000	Rabbit polyclonal	Human, Mouse, Rat, Monkey
Phospho-AMPK $\alpha$ (Thr172)	62	Cell Signaling 2535	AB_10622186	1:1000	Rabbit monoclonal	Human, Mouse, Rat, Hamster, Monkey, <i>Drosophila</i> , Yeast
AMPK $\alpha$	62	Cell Signaling 5831	AB_331250	1:1000	Rabbit monoclonal	Human, Mouse, Rat, Monkey, Bovine
Phospho-ACC1 (Ser79)	265	Cell Signaling 3661	AB_330337	1:1000	Rabbit polyclonal	Human, Mouse, Rat, Monkey
ACC1	265	Cell Signaling 3662	AB_2219400	1:1000	Rabbit polyclonal	Human, Mouse, Rat, Monkey, Bovine
Phospho-p70S6K (Thr421/Ser424)	70/85	Cell Signaling 9234	AB_2269803	1:1000	Rabbit polyclonal	Human, Mouse, Rat, Monkey

p70S6K	70/85	Cell Signaling 9202	AB_331676	1:1000	Rabbit polyclonal	Human, Mouse, Rat, Monkey
LDLR	120/160	Bio-techn NBP1-78159	AB_11016939	1:500	Mouse monoclonal	Human, Rat, Pig, Bovine
SR-BI	82	Bio-techn NB400-101	AB_10107658	1:1000	Rabbit polyclonal	Human, Mouse, Rat, Bovine, Hamster, Monkey
HMGCR	97	Abcam ab174830	AB_2749818	1:1000	Rabbit monoclonal	Mouse, Rat, Human
Beta-actin	42	Abcam ab8226	AB_306371	1:1000	Mouse monoclonal	Mouse, Rat, Human
Alpha tubulin	52	Cell Signaling 2125	AB_2619646	1:1000	Rabbit monoclonal	Human, Mouse, Rat, Monkey, <i>Drosophila</i> , Zebrafish, Bovine, Pig
Mouse IgG-HRP linked	N/A	Cell Signaling 7076	AB_330924	1:2500	Horse polyclonal	N/A
Rabbit IgG-HRP linked	N/A	Cell Signaling 7074	AB_2099233	1:2500	Goat polyclonal	N/A

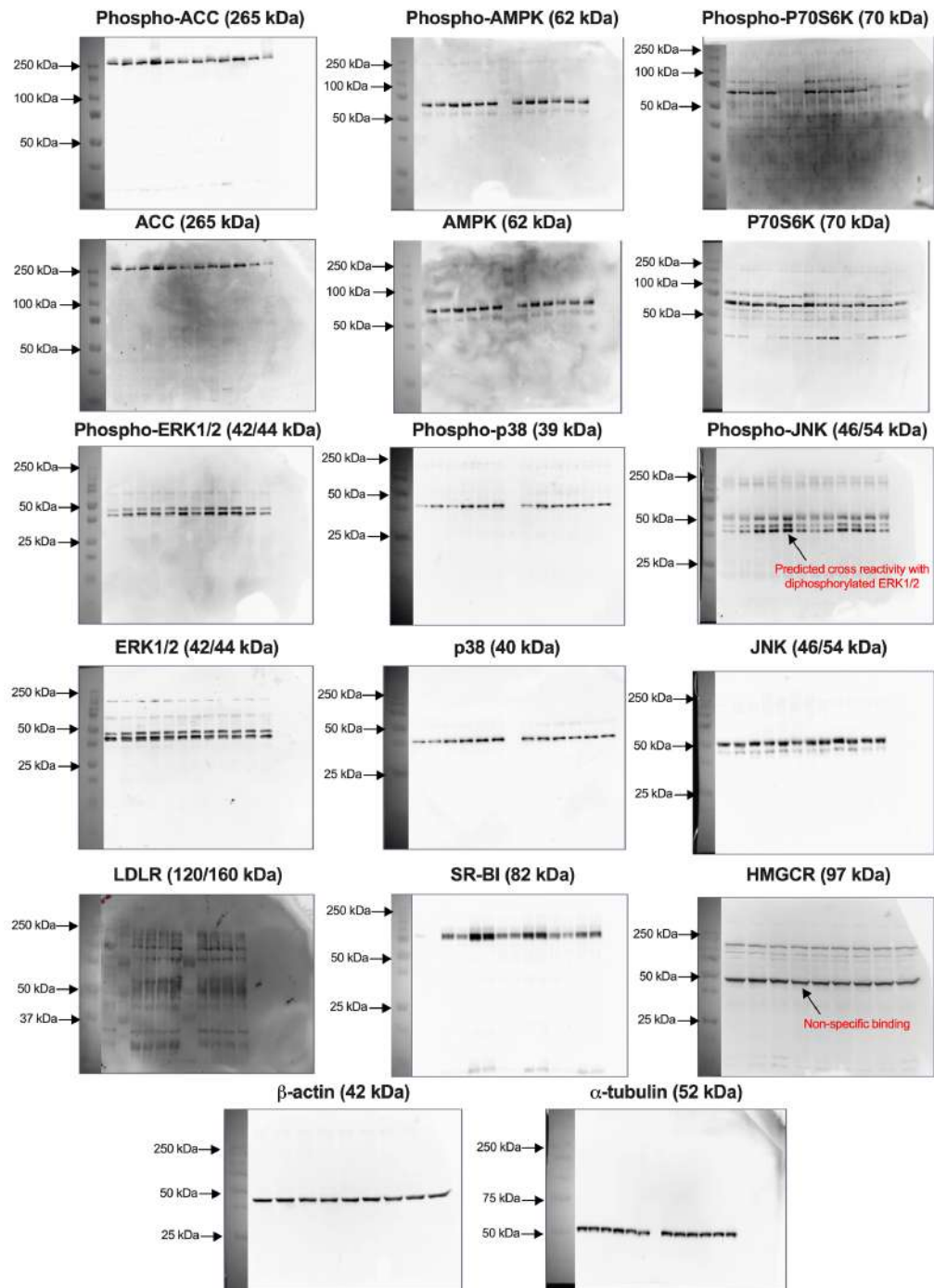


**Figure 2.5. Representative whole western blot images**

Western blot images were captured using the ChemiDoc XRS system for each of the antibodies used in this thesis. Images are representative of western blots carried out on protein isolated from emerged or dominant follicles. Prior to imaging, an epi-white image of the blot was captured, so that the protein size ladder could be cropped alongside the U.V image; the membrane was not moved between the epi-white and U.V. light imaging steps, so that the size markers could be matched to the size of the detected protein.

### **2.13 Bovine IL-1 $\beta$ ELISA**

The accumulation of IL-1 $\beta$  in culture supernatants was measured using a bovine-specific ELISA (Thermo Fisher Scientific; RRID: AB\_283324). The bovine IL-1 $\beta$  ELISA does not cross-react with recombinant bovine IL-2, IL-4, IL-6, IL-8, IFN $\gamma$ , or TNF $\alpha$  (< 0.5%). Coating antibody was diluted 1:100 in carbonate-bicarbonate buffer (0.2M made using carbonate-bicarbonate capsules (Merck), in deionized water) and 50  $\mu$ l added to each well of a half-area 96-well microplate (Greiner Bio-One). The plate was sealed and incubated at room temperature overnight on a shaker, after which, each well was aspirated and 150  $\mu$ l of blocking buffer (4% BSA (Merck), 5% sucrose (Merck) in PBS (Gibco)) added to each well and incubated for 1 h at room temperature on a shaker. Reconstituted protein standard was diluted 1:2 in reagent diluent (4% BSA in PBS; 0.2  $\mu$ M filtered) and a further six 1:2 dilutions in reagent diluent made (the concentration of the highest standard of IL-1 $\beta$  was 2000 pg/ml). Supernatants were defrosted overnight at 4°C. The blocking buffer was aspirated, and 50  $\mu$ l of either standard or sample was added to each well in duplicate, the plate sealed and incubated for 1 h at room temperature on a shaker. Each well was aspirated and washed three times with wash buffer (0.05% Tween20 (Merck) in PBS) and dried thoroughly by blotting onto paper towels. Detection antibody was diluted 1:100 in reagent diluent and 50  $\mu$ l added to each well. The plate was sealed and incubated on a plate shaker for 1 h at room temperature. After a further three washes, streptavidin-horseradish peroxidase (HRP) was diluted 1:400 in reagent diluent, 50  $\mu$ l added to each well and the plate sealed and incubated for 30 min in the dark on a shaker at room temperature. After a final wash, 50  $\mu$ l of substrate solution was added to each well, the plate sealed and incubated for 20 min in the dark on a shaker at room temperature. The reaction was stopped through the addition of 50  $\mu$ l stop solution to each well.

### **2.14 Bovine IL-8 ELISA**

An ultrasensitive bovine IL-8 ELISA was developed in-house (Cronin et al., 2015). The IL-8 ELISA has no reported cross-reactivity with biologically meaningful concentrations of bovine IL-1 $\beta$ , IL-10, TNF $\alpha$ , IFN $\gamma$ , or CCL2 (Cronin et al., 2015). Mouse anti-sheep IL-8 capture antibody (#MCA1660; Bio-Rad; RRID: AB\_322152) was dissolved 1:400 to a concentration of 2.5  $\mu$ g/ml in carbonate-bicarbonate buffer

and 50 µl/well added to a half-area 96-well plate (Greiner Bio-One), sealed, and incubated on a shaker overnight at room temperature. Each well was aspirated, washed three times with wash buffer using a plate washer (LT-3500; Labtech). The plate was blocked with 150 µl/well of reagent diluent (4% fish-skin gelatin (Merck) in D-PBS; 0.2 µM filtered) and incubated on a shaker for 1 h at room temperature. Recombinant bovine IL-8 protein standards (4000 to 62.5 pg/ml; RP0023B; Kingfisher Biotech, Saint Paul, USA) were prepared from a 50 µg/ml stock solution by diluting 1:250 in reagent diluent, followed by a further 1:50 dilution in reagent diluent to make up the top standard of 4000 pg/ml. This was followed by further 1:2 serial dilutions in reagent diluent. Supernatants were defrosted overnight at 4°C and vortexed before use. The plate was washed three times, and 50 µl/well of either standard or sample was added in duplicate and incubated for 1.5 h on a shaker at room temperature. Rabbit anti-sheep IL-8 detection antibody (#AHP425; Bio-Rad; RRID: AB\_322153), containing 10% mouse serum (Merck) was diluted 1:700 in reagent diluent to a final concentration of 0.145 µg/ml. The plate was washed three times, and 50 µl/well of detection antibody was added and incubated on a shaker for 2 h at room temperature. A further three washes were performed, goat anti-rabbit immunoglobulins/HRP antibody (#P0448; Dako, Glostrup, Denmark; RRID: AB\_2617138) was diluted 1:6000 to a concentration of 0.042 µg/ml in reagent diluent, and 50 µl/well added and the plate incubated on a shaker in the dark for 1 h at room temperature. After a final wash step, 50 µl/well of substrate solution (1:1 mix of H<sub>2</sub>O<sub>2</sub> and tetramethylbenzidine; BD Biosciences) was added and incubated for 10 min in the dark. The reaction was stopped by adding 50 µl/well of stop solution (0.5 M sulphuric acid).

### **2.15 Bovine IL-1α ELISA**

An ultrasensitive bovine IL-1α ELISA was developed in-house (Healy et al., 2014). Cross-reactivity was <1% for recombinant bovine IL-10, CCL2, IL-6, IL-1β, IFN-γ and TNFα (Healy et al., 2014). Polyclonal rabbit anti-bovine IL-1α capture antibody (#PB0331B; Kingfisher Biotech; RRID: AB\_2833237) was dissolved in carbonate-bicarbonate buffer to a concentration of 2 µg/ml and 50 µl/well added to a half-area 96-well plate (Greiner Bio-One), sealed, and incubated on a shaker overnight at room temperature. Each well was aspirated and washed three times with wash buffer (0.05% Tween20 (Merck) in PBS) and dried thoroughly by blotting onto paper towels. The

plate was blocked with 150  $\mu$ l/well of reagent diluent (4% fish-skin gelatine (Merck) in PBS; 0.2  $\mu$ M filtered) and incubated on a shaker for 1 h at room temperature. Recombinant bovine IL-1 $\alpha$  protein standards (800 to 12.5 pg/ml; RP0097B; Kingfisher Biotech) were prepared from a 10  $\mu$ g/ml stock solution by diluting 1:250 in reagent diluent, followed by a further 1:50 dilution in reagent diluent to make up the top standard of 800 pg/ml. This was followed by further 1:2 serial dilutions in reagent diluent. Supernatants were defrosted overnight at 4°C and vortexed before use. The plate was washed three times, 50  $\mu$ l/well of either standard or sample was added in duplicate and incubated for 1.5 h on a shaker at room temperature. Biotinylated polyclonal anti-bovine IL-1 $\alpha$  detection antibody (#PBB0332B; Kingfisher Biotech; RRID: AB\_2833238) was diluted in reagent diluent to a concentration of 0.2  $\mu$ g/ml. The plate was washed three times, and 50  $\mu$ l/well of detection antibody was added and incubated on a shaker for 2 h at room temperature. After a further three washes, Avidin-HRP (#18410051; Fisher Scientific) was diluted 1:500 in reagent diluent, 50  $\mu$ l added to each well and incubated for 30 min in the dark on a shaker at room temperature. After a final wash step, 50  $\mu$ l/well of substrate solution (1:1 mix of H<sub>2</sub>O<sub>2</sub> and tetramethylbenzidine; BD Biosciences) was added and incubated for 15 min in the dark. The reaction was stopped by adding 50  $\mu$ l/well of stop solution.

The concentrations of the cytokines were determined using a spectrophotometer (POLARstar Omega) measuring absorbance at 450 nm and 550 nm and analysed using the associated software (MARS data analysis v3.2 R3, Omega). The software determined the concentrations by plotting the optical density against the concentrations of the standards (pg/ml). A seven-point standard curve was created using a 4-parameter fit model of the blank-corrected raw data. The software then uses this to calculate the unknown concentrations of cytokines from this standard curve. Example standard curves for IL-1 $\alpha$ , IL-1 $\beta$  and IL-8 are provided in **Figure 2.6**.

The limits of detection for IL-1 $\alpha$ , IL-1 $\beta$ , and IL-8 were 12.5, 31.3, 62.5 pg/ml, respectively. The inter- and intra-assay coefficients of variation for IL-1 $\alpha$ , IL-1 $\beta$  and IL-8 were all < 7% and < 9%, respectively.

## 2.16 Oestradiol and Progesterone ELISA (DRG Diagnostics)

The accumulation of oestradiol and progesterone were measured in cell culture supernatants using commercial kits (DRG Diagnostics, Marburg, Germany); these are competitive ELISAs, and the intensity of colour developed is inversely proportional to the concentration of oestradiol or progesterone in the sample. All reagents were allowed to equilibrate to room temperature and were used according to manufacturer's instructions. All samples were diluted 1:20 in sterile PBS and vortexed prior to analysis.

To measure the accumulation of oestradiol (#EIA-2693; RRID: AB\_2889185), 25 µl of oestradiol standard (0, 25, 100, 250, 500, 1000 and 2000 pg/ml) or sample was added in duplicate to the wells of the Microtiter plate (pre-coated with an anti-rabbit polyclonal antibody for oestradiol) provided with the kit. Following this, 100 µl of enzyme conjugate (oestradiol conjugated to horseradish peroxidase) was added to each well and mixed thoroughly. The plate was then incubated for 90 min at room temperature. The contents of the wells were then washed three times with 200 µl of wash solution, with residual liquid being expelled through striking the plate on absorbent paper. Then, 50 µl of substrate solution (tetramethylbenzidine) was added to each well and the plate incubated for 30 min at room temperature. The enzymatic reaction was stopped by the addition of 50 µl stop solution (0.5 M sulphuric acid).

To measure the accumulation of progesterone (#EIA-1561; RRIB: AB\_2833253), 25 µl of progesterone standard (0, 0.3, 1.25, 2.5, 5.0, 15 and 40 ng/ml) or sample was added in duplicate to the wells of the Microtiter plate (pre-coated with an anti-rabbit polyclonal antibody for progesterone) provided with the kit and incubated for 5 min at room temperature. Then, 200 µl of enzyme conjugate (progesterone conjugated to horseradish peroxidase) was added to the wells and mixed thoroughly. The plate was then incubated for 1 h at room temperature. The contents of the wells were then washed three times with 200 µl wash buffer, with residual liquid expelled through striking the plate on absorbent paper. Then, 200 µl/well of substrate solution (tetramethylbenzidine) was added to each well and incubated for 15 min at room temperature. The reaction was stopped by the addition of 100 µl stop solution (0.5 M sulphuric acid).

Absorbance was measured using a spectrophotometer at 450 nm and 620 nm, within 10 min of stopping the reaction. Example standard curves are provided in **Figure 2.6**. The inter- and intra-assay coefficients of variation for oestradiol and progesterone were < 3% and < 6 %, respectively.

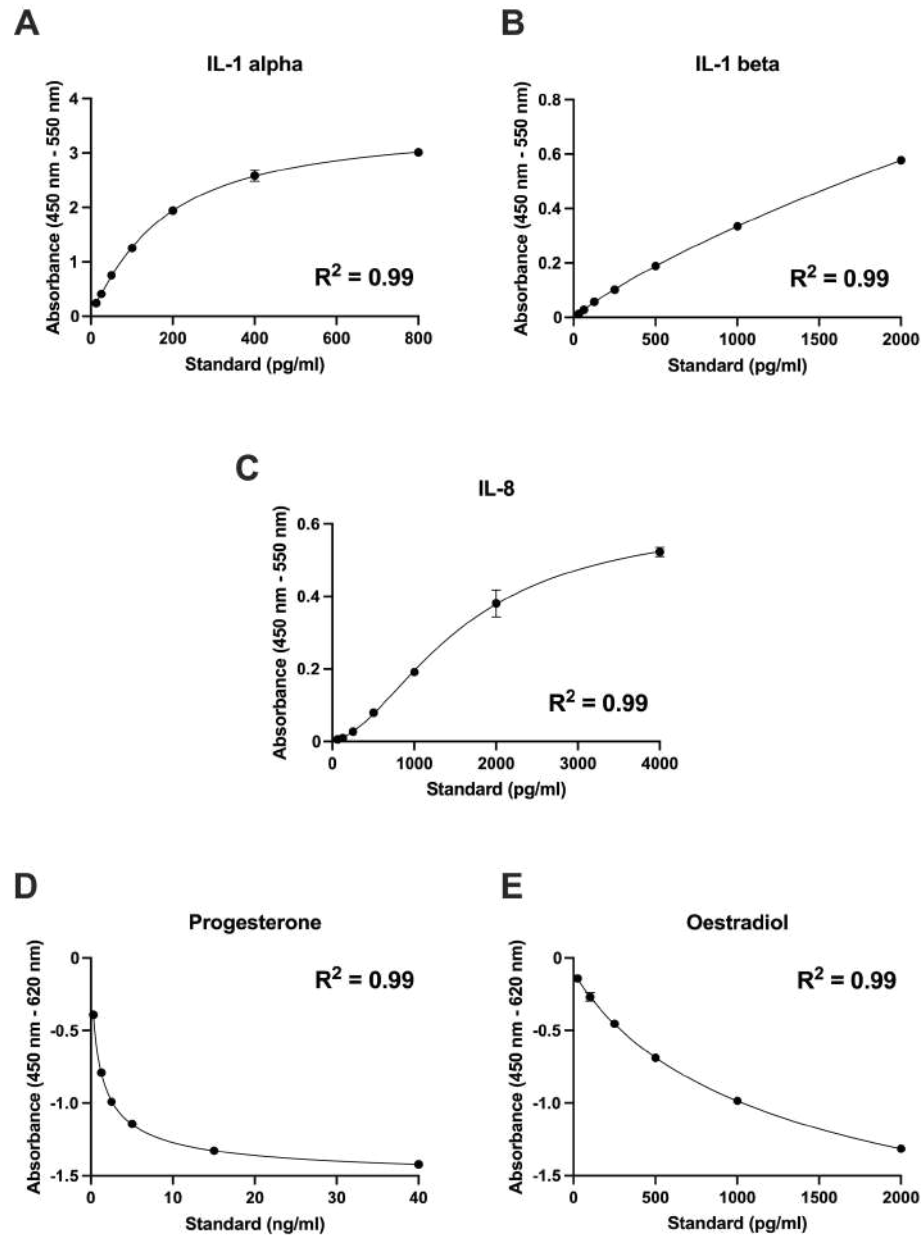


**Figure 2.6. Example standard curves for IL-1 $\alpha$ , IL-1 $\beta$ , IL-8, oestradiol, and progesterone ELISAs**

Standard curves were generated using the 4-parameter fit function of the spectrophotometer software (MARS data analysis). Example standard curves are presented for each ELISA, and  $R^2$  values are presented on each graph.



## **2.17 Quantification of glucose and cholesterol concentrations**

Follicular fluid glucose was analysed using a colorimetric method (Randox Daytona Plus, Randox Laboratories Ltd., Crumlin, UK). Glucose concentrations were determined after enzymatic oxidation in the presence of glucose oxidase; the intensity of the final colour is directly proportional to the glucose concentration, measured at OD<sub>505</sub>. The reportable range for glucose on the RX Daytona Plus is 0.2 to 46.5 mM/L. The reported inter- and intra-assay coefficients of variation for glucose quantification were 1.98% and 2.08%, respectively.

Follicular fluid total cholesterol concentrations were analysed with the cholesterol oxidase-enzymatic endpoint method (Randox Daytona Plus). The concentration of cholesterol is determined after enzymatic hydrolysis and oxidation. The reportable range for cholesterol on the RX Daytona Plus is 0.65 to 16 mM/L.

## **2.18 Extraction of HDL and LDL cholesterol**

High-density lipoprotein and low-density lipoproteins were extracted from the follicular fluid, FBS or lipoprotein-deficient serum using 2X LDL/VLDL Precipitation Buffer (Abcam, Cambridge, UK). Briefly, 100 µl of sample was mixed with 100 µl of 2X Precipitation Buffer in 1.5 ml Eppendorf tubes and incubated for 10 min at room temperature. The HDL fraction was isolated by centrifuging the samples for 10 min at  $2,000 \times g$  and transferred into fresh Eppendorfs. The precipitate was centrifuged once more for 10 min at  $2000 \times g$  to remove any HDL fraction left in the sample. The LDL/VLDL fraction was isolated by resuspending the precipitate in 200 µl PBS and vortexing thoroughly. Samples were diluted 1:100 in 1X cholesterol assay buffer and quantified using the Amplex Red Cholesterol Assay Kit (Invitrogen), described below. The recovery of HDL or LDL was  $> 78\%$  and  $> 92\%$ , respectively.

## 2.19 Amplex Red cholesterol assay

Total cellular cholesterol concentrations were quantified using the Amplex Red Cholesterol Assay Kit (Thermo Fisher Scientific), according to manufacturer's instructions. Following the treatment period, granulosa cells were washed with 250  $\mu$ l/well of ice-cold PBS and collected in 300  $\mu$ l/well of 1X cholesterol assay buffer into 1.5 ml Eppendorf tubes and kept on ice. The samples were homogenised by passing 10 times through a 19-gauge needle and 2 ml syringe, before sonicating for 10 min in a sonicating water bath.

A cholesterol standard curve was generated by diluting 5.17 mM cholesterol reference standard in 1X Reaction Buffer to produce cholesterol concentrations from 0 to 20  $\mu$ M. Briefly, 25  $\mu$ l of standards or samples were added in duplicate to the wells of a black 96-well half-area plate (VWR), followed by the addition of 25  $\mu$ l/well of Amplex Red working solution. The components of the Amplex Red working solution are listed in **Table 2.6**. The plate was incubated at 38.5°C for 30 min in the dark and fluorescence was measured on a microplate reader using an excitation of 530 nm and emission of 590 nm. Cholesterol concentrations were analysed using the Omega software, using a 4-parameter fit based on the standard curve. The inter- and intra-assay coefficients of variation for the Amplex Red Cholesterol Assay were both < 6%. Cellular cholesterol concentrations were normalized to cellular total protein concentrations, as previously described (Nicholson and Ferreira, 2009).

**Table 2.6. Amplex Red working solution**

Component	Volume for 100 assays ( $\mu$ l)
Amplex Red reagent	37.5
Horseradish peroxidase	25
Cholesterol oxidase from <i>Streptomyces</i>	25
Cholesterol esterase from <i>Pseudomonas</i>	2.5
1X Reaction buffer	2410

## 2.20 MTT assay

Granulosa cell viability was estimated using an MTT (3-(4-(4,5-Dimethylthiazol-2-yl)-2,5-diphenyltetrazolium bromide) assay, as previously described (Mosmann, 1983). A working concentration of 0.5 mg/ml MTT in M199 medium was made from a stock solution of 5 mg/ml MTT (Merck) in D-PBS. Following the treatment period, supernatants were removed from the 24-well plate, and 250 µl of the MTT solution was added to each well and incubated for 1 h at 37.5°C, under 5% CO<sub>2</sub>. Following incubation, the MTT medium was discarded, and 300 µl of dimethyl sulphoxide (DMSO; Merck) was added to each well to lyse the cells. The plate was placed on a rocker for 5 min, following which 50 µl of lysed cell suspension was added in duplicate to a 96-well plate (TPP). The absorbance was measured at 570 nm using a spectrophotometer (POLARstar Omega) and associated software (MARS data analysis v3.2 R3, Omega).

## 2.21 Short interfering RNA (siRNA)

Short interfering RNA (siRNA) was designed for bovine genes *HMGCR*, *FDPS*, or *FDFT1* using the SiDESIGN Center package (Thermo Fisher Scientific; **Table 2.7**), as described and previously validated (Griffin et al., 2017, Healey et al., 2016). Knockdown of target genes was carried out by transfection, using Lipofectamine RNA-iMax (Invitrogen). Target siRNA or ON-TARGETplus Non-targeting Control Pool scramble siRNA (Horizon Discovery, Cambridge, UK) was dissolved in siRNA buffer (Horizon Discovery) to a final concentration of 20 µM. All siRNA knockdowns were carried out under a Class II hood using a CoolRack to keep reagents cool. Briefly, 2 µl of 20 µM scramble or target siRNA and 4.5 µl Lipofectamine was added to 300 µl OptiMEM reduced serum media (Thermo Fisher Scientific) and mixed by briefly vortexing. The siRNA was then incubated for 15 min to allow for the formation of lipid droplets and complex formation of the siRNA into micelles. A total of 900 µl of antibiotic-free granulosa cell culture medium was added to each well of the 24-well plate, before the addition of 100 µl vehicle (OptiMEM), scramble siRNA, or respective siRNA treatment. Cells were then incubated at 38.5°C for 24 h prior to LPS challenge, or 48 h prior to collection of RNA for validation by qPCR, as previously described (Healey et al., 2016).

**Table 2.7. siRNA sequence for target gene knockdown**

<b>Gene</b>	<b>Sense</b>	<b>Anti-Sense</b>
<i>HMGCR</i>	CAGCAUGGAUUAUUGAACAAUU	UUGUUCAAUAUCCAUGCUG
<i>FDPS</i>	GCACAGACAUCCAGGACAAUU	UUGUCCUGGAUGUCUGUGCUU
<i>FDFT1</i>	GCGAGAAGGGAGAGAGUUUUU	AAACUCUCUCCCUUCUCGC

### 2.21.1 RNA extraction

Granulosa cell RNA was extracted using the RNeasy Mini Kit (Qiagen, GmbH), according to manufacturer's instructions. Briefly, cells were washed with 200  $\mu$ l ice cold PBS and lysed using 350  $\mu$ l RLT buffer. Cells were scraped using the base of a 200  $\mu$ l pipette tip and collected into a 2 ml DNase/RNase-free syringe by passing the lysate 10 times through a 19-gauge needle. The cell lysate was transferred to a 1.5 ml Eppendorf tube and 350  $\mu$ l of 70% molecular grade ethanol (Merck) was added to the lysate and mixed with repeat pipetting. A total of 700  $\mu$ l of lysate was added to a RNeasy mini spin column in a 2 ml collection tube, centrifuged at  $8,000 \times g$  for 15 s and the flow through discarded. Then, 700  $\mu$ l of Buffer RW1 was added to the spin column and centrifuged again at  $8,000 \times g$  for 15 s, and the flow through discarded. Following this, 500  $\mu$ l Buffer RPE was added to the spin column and centrifuged at  $8,000 \times g$  for 15 s and the flow through discarded. Another 500  $\mu$ l Buffer RPE was added to the spin column and centrifuged at  $8,000 \times g$  for 2 min and the flow through discarded. The spin column was then placed into a fresh collection tube and centrifuged at full speed ( $16,000 \times g$ ) for 1 min. The spin column was then placed into a 1.5 ml collection tube and 30  $\mu$ l of RNase-free water was added directly to the membrane of the column and centrifuged at  $8,000 \times g$  for 1 min. To maximise the RNA concentration, the 30  $\mu$ l of water from the previous step was added to the membrane of the column again and centrifuged at  $8,000 \times g$  for 1 min. The tubes containing RNA were placed immediately on ice and quantified on a NanoDrop spectrophotometer (ND-100 Spectrometer, Labtech International, Uckfield, UK), before storage at  $-80^{\circ}\text{C}$ . Samples were assumed to be free from contamination because the ratios obtained at 260/280 nm and 260/230 nm were between 1.8 and 2.2.

### 2.21.2 cDNA synthesis and elimination of genomic DNA

Handling of RNA and DNA was carried out in a dedicated laminar flow hood, using sterile filter pipette tips (Starlab), 200  $\mu$ l microfuge tubes, 0.5 ml, and 2 ml Eppendorf tubes, all of which were certified to be RNase, DNase, DNA, and pyrogen free. The hood and all items, including pipettes were wiped with RNaseZap (Thermo Fisher Scientific) prior to use. Complimentary DNA (cDNA) was synthesized using the QuantiTect Reverse Transcription kit (Qiagen). Briefly, the RNA stock was diluted in RNase-free water in a 200  $\mu$ l microfuge tube to provide up to 1  $\mu$ g of RNA in 12  $\mu$ l final volume. Then, 2  $\mu$ l of gDNA wipeout buffer was added to the tube, mixed and briefly microcentrifuged and incubated for 2 min at 42°C using a thermal cycler (T100 Thermal Cycler, Bio-Rad). A reverse-transcription master mix was made up containing 1  $\mu$ l Quantiscript Reverse Transcriptase, 4  $\mu$ l Quantiscript RT Buffer (5 x) and 1  $\mu$ l RT Primer Mix per reaction (**Table 2.8**). A total of 6  $\mu$ l of the reverse-transcription master mix was added to the 14  $\mu$ l of RNA template, briefly microcentrifuged and incubated in a thermal cycler for 15 min at 42°C, followed by 3 min at 95°C to inactivate the Quantiscript Reverse Transcriptase. The cDNA was then placed immediately on ice until further use.

**Table 2.8. Complementary DNA synthesis master mix**

Reagent	Volume ( $\mu$ l)
Quantiscript® Reverse Transcriptase	1
5 x Quantiscript RT	4
RT Primer Mix	1

### 2.21.3 Quantitative PCR

The QuantiFast SYBR Green PCR kit (Qiagen) was used to carry out quantitative PCR (qPCR), allowing the use of primers with different melting points. A total reaction volume of 25  $\mu$ l/well was prepared for qPCR, with 1.5  $\mu$ l of RNase-free water used as a no template control (**Table 2.9**). A master mix was prepared for each gene target by adding 450  $\mu$ l SYBR Green master mix, 378  $\mu$ l RNase-free water, 9  $\mu$ l of forward

primer (10  $\mu$ M) and 9  $\mu$ l of reverse primer (10  $\mu$ M) to a 2 ml Eppendorf tube and vortexed thoroughly. Three master mixes (each containing a pair of primers) are enough for one 96-well PCR plate (Bio-Rad). The primers used in this thesis have been validated and published previously (**Table 2.10**). A total of 75  $\mu$ l of each master mix was added to one 0.5 ml Eppendorf tube for each sample, in addition to 5  $\mu$ l of cDNA. Each sample was vortexed thoroughly before 25  $\mu$ l was added each well of a PCR plate in triplicate. In addition to the samples, the cDNA from control granulosa cells (from emerged or dominant follicles) was used to generate a 10-fold serial dilution to create a standard curve. Negative controls, containing the master mix with water instead of sample were used to verify that the primers were specific and check whether dimers were being formed. The plate was sealed and centrifuged at  $2,000 \times g$  for 1 min, before being placed in a PCR machine (CFX Connect Real-Time PCR Detection System, Bio-Rad) using the following program: initial denaturation of 95°C for 5 min, followed by 40 cycles of 2-step cycling: 10 s denaturation at 95°C and 30 s annealing at 60°C. Data were analysed using CFX Manager Software (Bio-Rad). The software was used to calculate the expression of the target gene relative to the reference RNA, and normalized to the two housekeeping genes, *ACTB* and *RLP19*. To confirm that the expression of *ACTB* or *RLP19* was not altered following siRNA treatment, the raw quantification cycle (Cq) values were analysed following qPCR (**Fig. 2.7**).

**Table 2.9. Components for qPCR**

<b>Component</b>	<b>Volume (<math>\mu</math>l)</b>
2 x QuantiFast SYBR Green PCR Master Mix	12.5
Forward Primer	0.25
Reverse Primer	0.25
RNase-free water	10.5
cDNA	1.5
<b>Total volume</b>	<b>25</b>

**Table 2.10. qPCR primers used in this thesis**

<b>Gene</b>	<b>Sense</b>	<b>Anti-Sense</b>	<b>Accession</b>	<b>Reference</b>
<i>ACTB</i>	CAGAAGGACTCGTACGTGGG	TTGGCCTTAGGGTTCAGGG	NM_173979.3	(Griffin et al., 2017, Coussens and Nobis, 2002, Bromfield and Sheldon, 2011)
<i>RPL19</i>	TGTTTTTCCGGCATCGAGCCCG	ATGCCAACTCCCGCCAGCAGAT	NM_001040516.2	(Griffin et al., 2017, Griffin et al., 2018, Dickson et al., 2020)
<i>FSHR</i>	AATCTACCTGCTGCTCATAGCCTC	TTTGCCAGTCGATGGCATAG	NM_174061.1	(Price and Sheldon, 2013, Hosoe et al., 2011)
<i>LHCGR</i>	AGAGTGAAGTGAAGTGGCTGG	CAACACGGCAATGAGAGTAG	NM_174381.1	(Price and Sheldon, 2013, Calder et al., 2003)
<i>HMGCR</i>	TGAGATCCGGAGGATCCGAG	CAGATGGTCAGCGTCACTGT	NM_001105613.1	(Griffin et al., 2017)
<i>FDPS</i>	ATGACGGGTAAGATCGGCAC	TTCTGCCCATAGTTCTCCTGC	NM_177497.2	(Griffin et al., 2017, Griffin et al., 2018)
<i>FDFT1</i>	GGCACCTGAGGAGTTCTAC	GCATACTGCATGGCGCATTT	NM_001013004.1	(Griffin et al., 2017, Griffin et al., 2018)

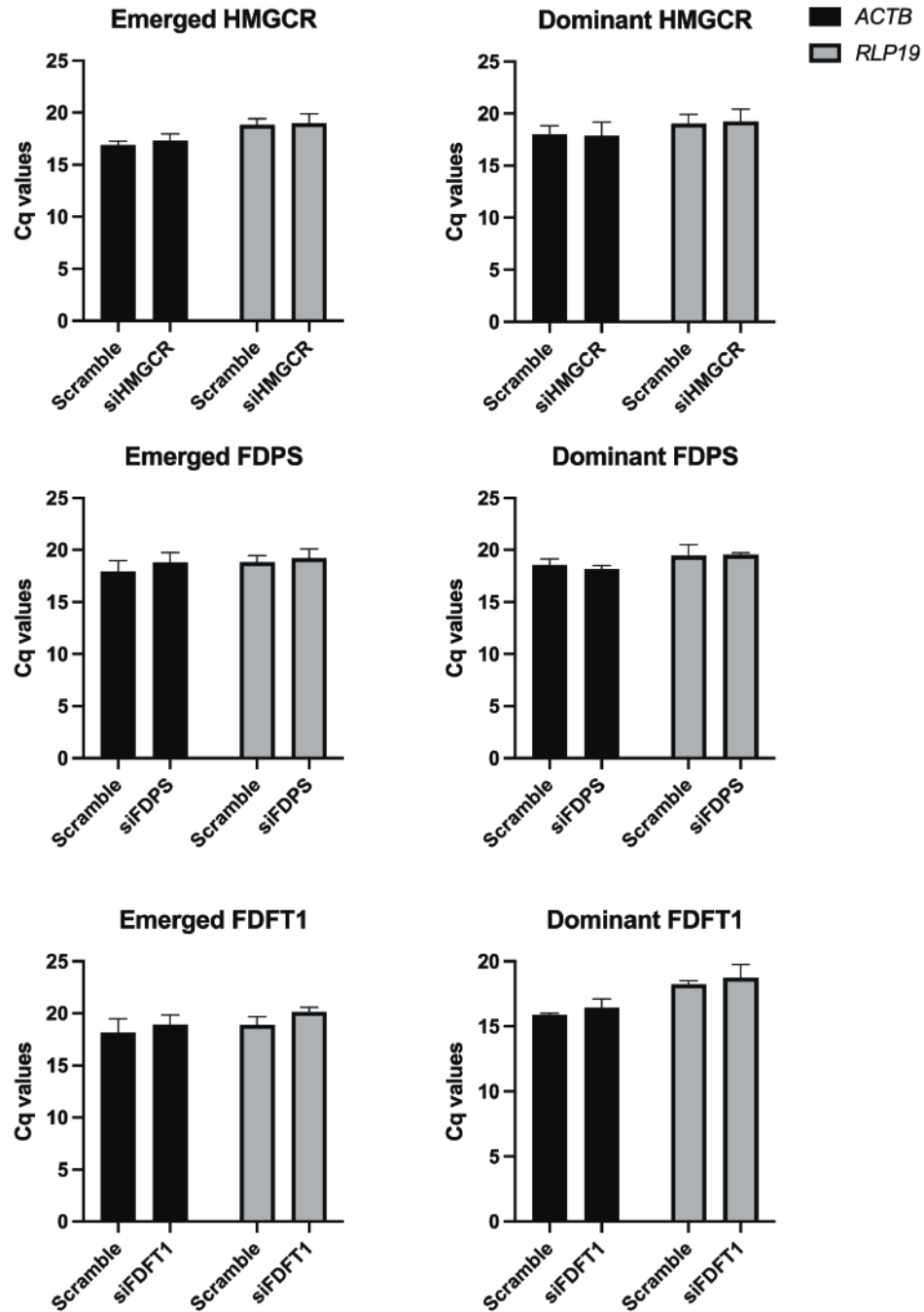


**Figure 2.7. The expression of *ACTB* or *RLP19* in granulosa cells was not altered by siRNA treatment**

Granulosa cells were transfected for 48 h with scramble or siRNA targeting *HMGCR*, *FDPS*, or *FDFT1*. The genes *ACTB* and *RLP19* were used as housekeeping genes to normalize the qPCR data. To confirm that the siRNA treatments did not alter the expression of the housekeeping genes, the raw Cq values were inspected. Data are presented as mean (SEM) and represents 3 independent experiments. Mean values were compared using two-way ANOVA.



## **2.22 Model of clinical endometritis in Holstein heifers**

In this thesis (*Chapter 6*), we exploited the data generated following RNA sequencing (RNAseq) of the tissues of the bovine female reproductive tract collected several months after the intrauterine infusion of control intrauterine infusion or intrauterine pathogenic bacteria that induced clinical endometritis. The model of endometritis described below was developed and carried out by the project collaborators at the University of Florida Dairy Research Unit (Gainesville, FL, USA), and subsequently published (Piersanti et al., 2019c). No *in vivo* work, or sample processing was carried out by me in the production of *Chapter 6*; RNAseq data was kindly provided by Dr John Bromfield (University of Florida) for analysis. A summary of the *in vivo* model of endometritis, sample collection and RNA sequencing are provided in *Sections 2.22.1 to 2.22.5*.

### **2.22.1 Ethical statement**

The University of Florida Institutional Animal Care and Use Committee approved all animal procedures (protocol number 201508884), which were conducted from June to October 2017 at the University of Florida Dairy Research Unit (Gainesville, FL, USA).

### **2.22.2 Animal model of endometritis**

Virgin Holstein heifers, 11 to 13 months old received a control intrauterine infusion (n = 6) or intrauterine pathogenic bacteria that induced clinical endometritis (n = 4). Animals were clinically healthy prior to the experiment. Estrous cycles were synchronized, and animals were blocked by age and weight, and randomly assigned to intrauterine infusion of control sterile medium (n = 6), or bacteria (n = 4), using *E. coli* MS499 (Goldstone et al., 2014b) and *T. pyogenes* MS249 (Goldstone et al., 2014a).. Clinical endometritis was induced 4 to 6 days after uterine infusion in the bacterial-infusion animals but not in controls as evidenced by pus detectable in the vagina (median endometritis grade 3 vs.  $\leq 1$ ). The presence of clinical endometritis was confirmed by visualising pus in the uterine lumen of bacteria-infused animals using transrectal ultrasonography, whereas control animals had no evidence of fluid or echogenic material in the uterus. Infection was also verified by increased abundance

of bacterial total 16S RNA in the vaginal mucus of bacteria-infused animals compared with control animals.

### **2.22.3 Collection of reproductive tract tissues**

Reproductive tracts were collected 94 days after bacterial infusion, as previously described (Horlock et al., 2020). Starting 80 days after infusion, the oestrous cycles of all animals were synchronized, with the second GnRH administered 6 days before sample collection, to induce ovulation. Briefly, endometrium as either caruncular tissue or intercaruncular tissue was dissected away from underlying myometrium, and oviduct samples were collected by extrusion of either the ampulla or isthmus into a collection vessel. Granulosa cells were isolated from dominant follicles > 8 mm diameter by aspiration, and follicle aspirates were centrifuged at  $500 \times g$  to isolate the granulosa cells. Samples of caruncular and intercaruncular endometrium, oviduct isthmus and ampulla, and granulosa cells were snap frozen in liquid nitrogen and stored at  $-80^{\circ}\text{C}$ . Technical problems prevented collection of the oviduct from one bacteria-infused animal and the intercaruncular endometrium from a separate bacteria-infused animal.

### **2.22.4 Ovum pickup**

Ovum pick-up was performed on day 60 relative to treatment. Briefly, ovum pick-up was performed using transvaginal ultrasound guided follicle aspiration. A 20 G aspiration needle attached to a vacuum pump was introduced into the oocyte pick-up handle and using ultrasound guidance all follicles with exception of the dominant follicle, were aspirated. Cumulus cells were stripped from the oocytes by manually pipetting, and the zona pellucida of denuded oocytes were subsequently removed using 0.1% protease from *Streptococcus griseus* (Sigma-Aldrich). Zona-free oocytes were snap frozen and stored at  $-80^{\circ}\text{C}$  until further processing.

### **2.22.5 RNA sequencing**

Isolation of RNA was carried out at the University of Florida Dairy Research Unit. Briefly, endometrial (caruncular and intercaruncular tissue), oviduct (isthmus and

ampulla) and granulosa cell sample RNA was extracted using the RNeasy Mini kit (Qiagen), and oocyte RNA was extracted using the RNeasy Micro kit (Qiagen), according to the manufacturer's instructions. Total RNA with a 28S:18S ratio  $> 1$  and RNA integrity number  $\geq 7$  were used for RNAseq library construction.

The RNA library construction and sequencing were performed at the Interdisciplinary Centre for Biotechnology Research, University of Florida. The transcripts of *Bos taurus* (76,341 sequences) retrieved from the NCBI genome database (GCF\_002263795.1) were used as reference sequences for RNAseq analysis. The RNAseq data was deposited in NCBI's Gene Expression Omnibus database and is accessible through GEO Series accession number GSE140469 <https://www.ncbi.nlm.nih.gov/geo/query/acc.cgi?acc=GSE140469>. Gene expression was compared between the bacteria-infused and control animals by counting the number of mapped reads for each transcript (Yao and Yu, 2011).

## **2.23 RNA sequencing (RNAseq) analysis**

### **2.23.1 Volcano plots**

Volcano plots were generated in GraphPad Prism version 8.4.1 (GraphPad Software). A volcano plot is a type of scatterplot that can allow for the quick visualization of genes with large fold changes, that are also statistically significant. Volcano plots display statistical significance (P-value) versus the magnitude of change (fold-change) on the y and x axes, respectively.

### **2.23.2 Principal component analysis**

Principal component analysis (PCA) was performed using the online tool, Clustvis (<https://biit.cs.ut.ee/clustvis/>) (Metsalu and Vilo, 2015). The PCA reduces the dimensionality of high dimension data to single principal components that still contain most of the information in the dataset. The PCA plot is a 2-dimensional scatterplot of the correlations (or not) between DEGs between samples. Principal components represent directions of the data that explain the most variance, allowing for the differences between the observations to be more visible. The first principal component

(PC1) accounts for the largest possible variance in the data. The second principal component (PC2) accounts for the second largest variance in the data, with the condition that it is uncorrelated with the first principal component.

### **2.23.3 Heatmaps**

Heatmaps were generated for the DEGs of individual animals with Heatmapper (<http://www.heatmapper.ca>) (Babicki et al., 2016), using Euclidean distance and average linkage, which are commonly used for displaying gene expression data (Quackenbush, 2001). A Heatmap is a data matrix that can visualise commonly regulated DEGs between samples using a colour gradient, with each row representing a gene and each column representing a sample. The colour and intensity of the boxes represent changes of gene expression, with red representing increased gene expression and green representing decreased gene expression.

### **2.23.4 Venn diagrams**

Venn diagrams were generated using jvenn to compare the DEGs amongst tissues (<http://jvenn.toulouse.inra.fr/app/index.html>) (Bardou et al., 2014). The list of DEGs for each sample is presented as a transparent shape, and the overlap between the shapes indicates the DEGs that are shared between the samples. Within individual shapes, the count of DEGs that are unique to the sample are displayed, and where the shapes intersect, the count of DEGs that are common between samples are displayed.

### **2.23.5 Ingenuity Pathway Analysis (IPA)**

Ingenuity Pathway Analysis (IPA version 10, Qiagen, Hilden, Germany) was used to interpret data from RNAseq (Kramer et al., 2014). A core analysis was performed to identify signalling and metabolic canonical pathways, upstream regulators, networks and diseases and functions associated with the differentially expressed genes (DEGs) present in the dataset. The reference set of genes for the core analysis were taken from the Ingenuity Knowledge base, derived from scientific literature, experimental datasets, and public databases. All node types and data sources were included, all direct and indirect interactions were considered, all species were considered,

experimentally observed predictions were included, and all mutations were considered. The cut-offs for the analysis were set at  $-\log P > 1.3$  and  $\log_2$  fold change (FC) of  $\leq -2$  or  $\geq 2$ , and corresponding z-scores were calculated to predict activation status. The IPA software calculated a “P-value of overlap” using a Right-Tailed Fisher’s Exact Test that predicts whether molecules in the dataset overlap with a particular disease, function, network, or pathway. However, this P-value cannot determine the directional of the changes of the molecules. IPA also calculates a “z-score” that predicts the activation or inhibition of canonical pathways, upstream regulators and diseases and functions in the treatment group, compared with the control group. Canonical pathways, upstream regulators of DEGs, and predicted diseases and functions were identified by z-scores  $\geq 2$  or  $\leq -2$  and were considered significant predictors of activation or inhibition of DEGs, respectively (Hatzirodos et al., 2014b, Piersanti et al., 2019a). Gene networks were identified by assessing the number of DEGs in each network, and gene network scores were calculated by the software (a network score of  $\geq 2$  gives 99% confidence the network was not identified by chance).

## 2.24 Statistical analysis

Graphs were created using GraphPad Prism version 9.21 (GraphPad Software, San Diego, California). The statistical unit was each independent culture of granulosa cells or cumulus-oocyte complexes, collected on separate days and pooled from the ovaries of 10 to 20 animals. Statistical analysis was performed using GraphPad Prism, with significance attributed when  $P < 0.05$ . Data were presented as the mean and standard error of the mean (SEM). Normality was assessed using the Shapiro-Wilks test, with data assumed to be normally distributed when  $P > 0.05$ . Comparison between treatments were compared using one-way or two-way analysis of variance (ANOVA), followed by Dunnett’s or Bonferroni post hoc test, or t test, as reported in *Results* and figure legends. In experiments using a range of treatment concentrations, P-values are reported; where different treatments are compared, significant differences are presented as: \*  $P < 0.05$ , \*\*  $P < 0.01$ , \*\*\*  $P < 0.001$ . Pearson correlation was used to evaluate the correlation between follicle size and follicular fluid glucose concentrations. Cumulus-oocyte complex expansion was analysed using chi-squared test in SPSS Version 26 (SPSS Inc, Chicago, USA).

### 3 AMPK and mTOR regulate the innate immune response of granulosa cells

#### 3.1 Introduction

Ovarian follicle function is often perturbed by energy stress and bacterial infections in postpartum dairy cows (Leroy et al., 2008, Sheldon et al., 2019a, Sheldon et al., 2002). Granulosa cells in ovarian follicles are exposed to energy stress when cows are unable to consume enough food to meet their energetic demands around the time of parturition and during lactation. These granulosa cells are then exposed to LPS if Gram-negative bacteria proliferate in the uterus, mammary gland, or rumen during the postpartum period (Bromfield et al., 2015, Piersanti et al., 2019a). Within ovarian follicles, the granulosa cells mount innate immune responses to LPS (Bromfield and Sheldon, 2011, Herath et al., 2007). However, whether energy stress alters granulosa cell inflammatory responses to LPS is unclear.

Granulosa cells are central to the emergence and development of 4 to 8 mm diameter ovarian follicles, selection, and growth of dominant follicles > 8.5 mm in diameter, and ovulation of competent oocytes (Fortune, 1994, Ginther et al., 1996). However, postpartum uterine disease reduces follicle growth rate and oestradiol secretion, inhibits ovulation, and reduces conception rates (LeBlanc et al., 2002, Sheldon et al., 2019a, Sheldon et al., 2002). Animals with uterine disease have LPS in their follicular fluid, and intrafollicular injections with LPS reduces follicle growth rate and delays ovulation (Cheong et al., 2017, Gindri et al., 2019, Herath et al., 2007, Piersanti et al., 2019a). Other potential sources of follicular fluid LPS include mastitis, ruminal acidosis, and intestinal barrier dysfunction (Bidne et al., 2018, Dosogne et al., 2002, Khafipour et al., 2009). When LPS binds to TLR4, immune cells release inflammatory cytokines, such as interleukins IL-1 and IL-6, and the chemokine IL-8 (Moresco et al., 2011). Bovine granulosa cells express *TLR4*, and LPS activates MAPK signalling and stimulates the production of IL-1 $\beta$ , IL-6 and IL-8 (Bromfield and Sheldon, 2011, Herath et al., 2007, Price and Sheldon, 2013, Price et al., 2013). As well as being pro-inflammatory mediators, IL-1 $\alpha$ , IL-1 $\beta$  and IL-8 affect ovarian follicle growth and function (Gerard et al., 2004, Spicer and Alpizar, 1994, Uri-Belapolsky et al., 2014).

Energetic stress, caused by energy demand exceeding supply around the time of parturition and during lactation, impairs immune cell function, perturbs ovarian follicle growth and function, and increases the risk of uterine disease (Beam and Butler, 1997, Hammon et al., 2006, LeBlanc, 2012, Leroy et al., 2008). Inflammatory responses to LPS are also energetically demanding. An extra 2.1 Kg/d glucose is required to respond to LPS infusion, which is comparable with 2.7 Kg/d glucose to produce 40 litres of milk (Habel and Sundrum, 2020, Kvidera et al., 2017). Cellular energy metabolism is regulated by glycolysis, AMPK and mTOR (Hardie et al., 2012, Murray et al., 2015, O'Neill et al., 2016, Zoncu et al., 2011). The first enzyme in glycolysis, hexokinase, controls the rate of conversion of glucose to pyruvate, to supply the Krebs cycle and generate ATP. During energy stress, increased ratios of AMP:ATP results in phosphorylation of AMPK, which stimulates catabolic pathways such as glycolysis, and inhibits anabolic pathways that consume ATP, such as protein synthesis (Hardie et al., 2012). Phosphorylated AMPK also inhibits mTOR, which further limits anabolic pathways (Hardie et al., 2012, Zoncu et al., 2011). Metabolism and immunity are highly integrated, with energetic stress altering immune cell responses to LPS (Dror et al., 2017, Lachmandas et al., 2016, Murray et al., 2015, O'Neill et al., 2016). An example of immunometabolism is that inhibiting glycolysis with 2-deoxy-D-glucose suppresses LPS-stimulated IL-1 $\beta$  in murine macrophages (Tannahill et al., 2013). However, the role of immunometabolism in the ovary is unclear.

This chapter explored whether energy stress alters inflammatory responses to LPS in granulosa cells. The hypothesis was that manipulating glycolysis, AMPK or mTOR to mimic energy stress in bovine granulosa cells limits the inflammatory responses to LPS. To test this hypothesis, granulosa cells were isolated from emerged and dominant ovarian follicles. Granulosa cells were treated with small molecules to inhibit glycolysis, activate AMPK, or inhibit mTOR, and then challenged the cells with LPS to measure inflammatory responses via the accumulation of IL-1 $\alpha$ , IL-1 $\beta$  and IL-8.

## 3.2 Methods

### 3.2.1 Granulosa cell culture and treatment

Granulosa cells were isolated from emerged (4 to 8 mm diameter) or dominant (> 8.5 mm diameter) follicles as described in *Chapter 2*. Briefly, granulosa cells were plated in 24-well plates at a density of 750,000 cells in 0.5 ml of culture media and incubated for 18 h at 38.5°C, in a humidified atmosphere of air containing 5% CO<sub>2</sub>, to allow the cells to adhere. The medium was then aspirated, and the cells were cultured with vehicle or treatments in 0.5 ml of granulosa cell culture medium. The first enzyme in the glycolysis pathway, hexokinase, was inhibited by treating cells for 2 h with 50 to 1000 µM 2-deoxy-D-glucose (2-DG) to model energy stress, as previously described (Tannahill et al., 2013, Zhao et al., 2017c).

Energy stress activates AMPK, so AMPK was activated by treating cells for 2 h with 0.01 to 1 mM 5-amino-4-imidazolecarboxamide ribonucleoside (AICAR), as described previously (Corton et al., 1995); and validated previously by showing that AICAR stimulated phosphorylation of AMPK in bovine granulosa cells (Tosca et al., 2007a). Subsequent experiments used 1 mM AICAR, based on the preceding experiment, and the use of 1 mM AICAR to activate AMPK in granulosa cells from rats, chickens and cattle (Tosca et al., 2007a, Tosca et al., 2005, Tosca et al., 2006), and bovine endometrial cells (Turner et al., 2016).

As AMPK inhibits mTOR, the role of mTOR was explored by treating cells for 2 h with the mTOR Complex 1 (mTORC1) inhibitor rapamycin (5 to 500 nM) and the mTORC1/2 inhibitor 1-[4-[4-(1-Oxopropyl)-1-piperazinyl]-3-(trifluoromethyl)phenyl]-9 (3-quinolinyl)-benzo[h]-1,6-naphthyridin-2(1H)-one (Torin 1; 10 to 150 nM), as described previously (Oshiro et al., 2004, Thoreen et al., 2009). Subsequent experiments used 500 nM rapamycin and 50 nM Torin 1, based on the preceding experiment, and the use of similar concentrations to investigate responses to LPS in human leukocytes (Zhang et al., 2019), and the use of 100 nM Torin 1 in mouse granulosa cells (Shen et al., 2017). A glucocorticoid, 1 µM dexamethasone, was used as a reference anti-inflammatory agent (Bhattacharyya et al., 2007).



To explore the requirements for glucose, granulosa cells were treated for 24 h with a range of concentrations of glucose (0 to 5 mM) added to glucose-free DMEM (Thermo Fisher Scientific; glucose-free M199 was not available), supplemented with 10% FBS (supplying 0.79 mM glucose at final concentration), 1% Antibiotic Antimycotic Solution, 1% ITS and 2 mM glutamine (Gibco).

Following each treatment period, the cells were challenged for 24 h by adding either 0.5 ml of either granulosa cell culture medium (control) or medium providing a final concentration of 1 µg/ml ultrapure LPS. As the hypothesis was that treatments might reduce inflammation, a relatively high concentration of 1 µg/ml LPS was used to stimulate robust inflammatory responses, as previously described (Bromfield and Sheldon, 2011, Price and Sheldon, 2013, Price et al., 2013).

To explore the crosstalk between energy stress, innate immunity and endocrine function, granulosa cells were treated with 2-DG (1 mM), AICAR (1 mM), rapamycin (500 nM), Torin 1 (50 nM) or dexamethasone (1 µM), in the presence of  $10^{-7}$  M androstenedione (Merck) and 1 ng/ml of highly purified bovine FSH (A. F. Parlow, National Hormone and Peptide program, Torrance, California), to stimulate the production of oestradiol and progesterone by granulosa cells, as previously described (Gutierrez et al., 1997).

At the end of each experiment, granulosa cell supernatants were collected for the measurement of IL-1 $\alpha$ , IL-1 $\beta$  and IL-8 by ELISA, and cell viability was estimated using the MTT assay or cell lysates were collected for western blotting. Each experiment was performed on at least 3 independent occasions, with each replicate using the granulosa cells pooled from the ovaries of 10 to 20 animals.

### **3.2.2 Measurement of cytokines and hormones**

The accumulation of IL-1 $\alpha$ , IL-1 $\beta$  and IL-8 was measured in supernatants, as described in *Chapter 2*. The concentrations of oestradiol and progesterone were measured in supernatants using a commercial assay, according to manufacturer's instructions (DRG International), as described in *Chapter 2*.

### 3.2.3 MTT assay

The MTT assay for cell viability as described in *Chapter 2*. Briefly, cells were incubated with fresh media containing 0.5 mg/ml MTT (Merck) for 1 h at 37.5°C, in a humidified atmosphere of air containing 5% CO<sub>2</sub>. The medium was then aspirated, washed with D-PBS before cell lysis with dimethyl sulfoxide (DMSO). The absorbance was measured at 570 nm using a microplate reader (POLARstar Omega; BMG).

### 3.2.4 Western blotting

Granulosa cells from emerged or dominant ovarian follicles were treated for 24 h in granulosa cell culture medium with vehicle, 1 mM 2-deoxy-D-glucose, 1 mM AICAR, 500 nM rapamycin or 50 nM Torin 1m with the effect of 1 µg/ml LPS also examined. In addition to the 24 h treatments, granulosa cells were also treated with 1 mM AICAR for 0, 10, 20, 30, 60 or 120 min to examine the activation of AMPK and acetyl-CoA-carboxylase (ACC). Secondly, the effects of AICAR or Torin 1 treatment followed by LPS challenge on MAPK signalling was examined, because LPS induces MAPK signalling in granulosa cells (Bromfield and Sheldon, 2011, Price et al., 2013, Price and Sheldon, 2013). Granulosa cells from emerged or dominant follicles were treated for 2 h with 1 mM AICAR or 50 nM Torin 1, and then challenged for 0, 10, 20, 30, 60 or 120 min with medium containing a final concentration of 1 µg/ml LPS.

At the end of all experiments, granulosa cells were washed with 300 µl of ice-cold phosphate buffered saline (PBS) and lysed with 100 µl of PhosphoSafe Extraction Reagent (Novagen), followed by protein extraction and quantification using the DC Assay, followed by western blot, as described in *Chapter 2*. Briefly 10 µg/lane of protein was probed overnight to quantify the abundance of phospho-P70S6 kinase, P70S6 kinase, phospho-ACC, ACC, phospho-AMPK, AMPK, diphosphorylated ERK1/2, ERK1/2, phospho-p38, phospho-JNK and JNK (**Table 2.5**). Protein reactivity was assessed by enhanced chemiluminescence (Clarity Western ECL substrate; Bio-Rad). After imaging, membranes were stripped for 7 min with Restore Western Blot Stripping Buffer (Fisher Scientific) and re-probed with another primary antibody, or with 1:1000 dilution β-actin or α-tubulin to normalise protein loading.

Images were captured using a ChemiDoc XRS System (Bio-Rad). The background-normalised peak band density was measured in the images for each protein using Fiji (Schindelin et al., 2012); target protein bands were normalised to  $\beta$ -actin or  $\alpha$ -tubulin; when antibodies were available, phosphorylated proteins were normalised to their cognate total protein.

### **3.2.5 Glucose quantification**

Follicular fluid was aspirated from a total of 48 emerged or dominant follicles, from at least fifteen animals, and the concentration of glucose was determined using a colorimetric method (Randox Daytona Plus, Randox Laboratories Ltd.), as described in *Chapter 2*.

### **3.2.6 Statistics**

The statistical unit was each independent culture of granulosa cells, collected on separate days and pooled from the ovaries of 10 to 20 animals. Statistical analysis was performed using GraphPad Prism version 9.21 (GraphPad Software). Data were analysed using one-way or two-way ANOVA, using Dunnett's post hoc test, or Pearson's correlation, as reported in *Results*. Data are presented as mean (SEM) from at least three independent experiments, and  $P < 0.05$  was considered significant.

### 3.3 Results

#### 3.3.1 Follicular fluid glucose concentrations

The physiological concentrations of glucose in the bovine follicular fluid isolated from dominant follicles ranged from 0.73 to 5.7 mM ( $n = 48$ ; mean =  $3.06 \pm 0.18$  mM; **Fig. 3.1**; top panel), which is similar to the previously reported ranges of 1.4 to 5 mM (Leroy et al., 2004a, Orsi et al., 2005, Nishimoto et al., 2009, Sutton-McDowall et al., 2010, Sutton-McDowall et al., 2005). The concentrations of glucose in follicular fluid are also similar to the  $\sim 4$  mM found in peripheral plasma of cows (Wathes et al., 2009).

Follicular fluid was aspirated and pooled from follicles of varying sizes (2 to 20 mm diameter) and the concentrations of glucose were quantified (**Fig 3.1**; bottom panel). It was necessary to pool the follicular fluid from the smaller follicles of the same sizes, because the Randox Clinical Analyser required 100  $\mu$ l volume. The concentrations of glucose measured were correlated with follicle size ( $R^2 = 0.70$ ;  $P < 0.001$ ). These findings are similar to what have been reported previously (Leroy et al., 2004a).

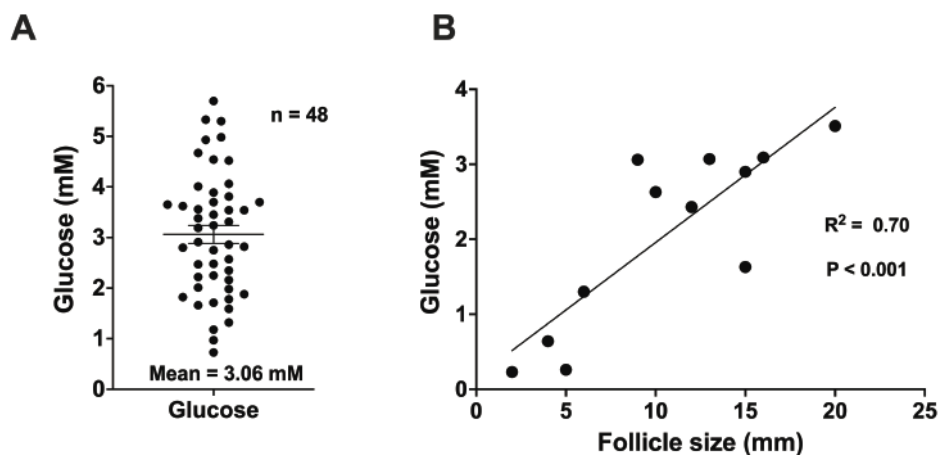


**Figure 3.1. Concentrations of glucose in follicular fluid**

(A) Follicular fluid was aspirated from 48 follicles from the ovaries of 15 animals and the concentration of glucose was measured using the Randox Daytona plus clinical analyser. (B) Follicular fluid was aspirated from follicles of different sizes and the concentrations of glucose were quantified using the Randox Daytona plus clinical analyser. Individual points are one sample measurement; mean (SEM) is indicated on the graph.

### 3.3.2 Glucose availability does not alter the innate immune response

Granulosa cells from emerged (**Fig. 3.2A, C, E**) or dominant follicles (**Fig. 3.2B, D, F**) were cultured for 24 h in medium (glucose and glutamine-free DMEM; Gibco), containing a range of concentrations of glucose (0 to 5 mM), with glutamine (2.5 mM) and 10% FBS (supplying 0.79 mM glucose). Granulosa cells were then challenged for 24 h with control medium or medium containing 1  $\mu\text{g/ml}$  LPS. Glucose availability did not alter the LPS-induced secretion of IL-1 $\alpha$ , IL-1 $\beta$  or IL-8. Additionally, cell viability was not altered by glucose concentration (**Fig. 3.4A-B**). This data implies that glucose availability does not regulate the innate immune function of granulosa cells.

### 3.3.3 Treatment with 2-DG impairs the innate immune response

Granulosa cell defences are important if ovarian follicles are exposed to LPS during the postpartum period, and yet there is often concurrent energy stress (Beam and Butler, 1997, Cheong et al., 2017, Leroy et al., 2004b, Piersanti et al., 2019a). The glycolysis inhibitor 2-DG was used to model of energy stress, as described previously (Lee et al., 2020, Tannahill et al., 2013, Zhao et al., 2017c). Granulosa cells isolated from emerged or dominant follicles were treated with vehicle or 2-DG prior to, and then during a 24 h challenge with control medium or medium containing 1  $\mu\text{g/ml}$  LPS. Treatment with 2-DG reduced the LPS-induced secretion of IL-1 $\alpha$ , IL-1 $\beta$  and IL-8 by granulosa cells from both emerged ( $P < 0.01$ ; **Fig. 3.3A, C, E**) and dominant ( $P < 0.05$ ; **Fig. 3.3B, D, F**) follicles. Additionally, cell viability was not altered by 2-DG concentration (**Fig. 3.5C-D**). Specifically, compared with vehicle, treatment with 500  $\mu\text{M}$  2-DG reduced the LPS-induced secretion of IL-1 $\alpha$  by  $> 80\%$ , IL-1 $\beta$  by  $> 90\%$  and IL-8 by  $> 65\%$  for granulosa cells from emerged and dominant follicles.

These data provide evidence that inhibiting glycolysis to mimic energy stress limited LPS-induced inflammation in granulosa cells from both emerged and dominant follicles.

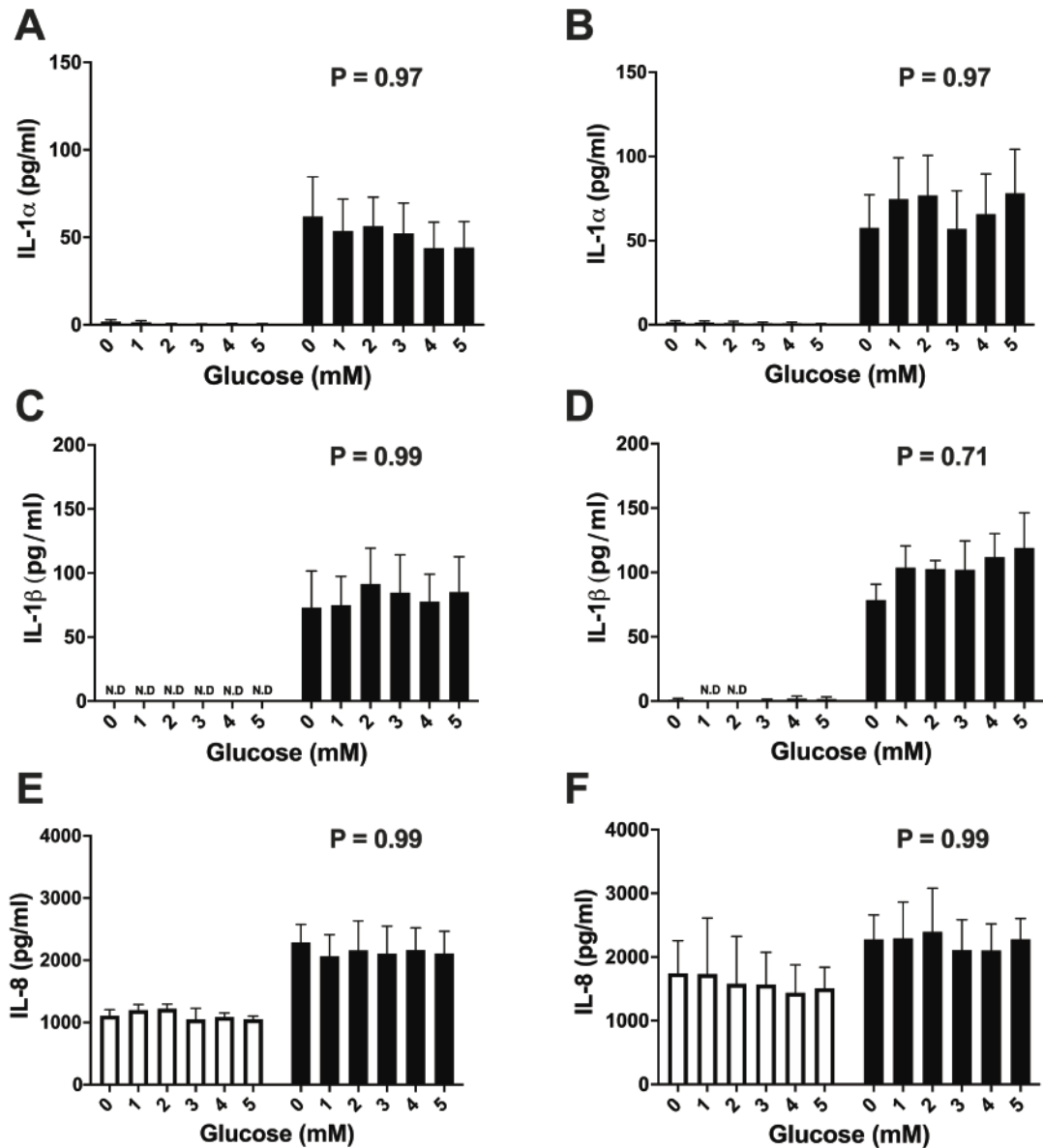


**Figure 3.2. Glucose availability does not alter the secretion of IL-1 $\alpha$ , IL-1 $\beta$  or IL-8 by granulosa cells**

Granulosa cells from emerged (A, C E) or dominant (B, D, F) follicles were treated with the indicated concentration of glucose for 24 h. Granulosa cells were then challenged for 24 h with control medium (white bars) or medium containing 1  $\mu$ g/ml LPS (black bars), in the presence of the treatments. Supernatants were collected and the accumulation of IL-1 $\alpha$  (A-B), IL-1 $\beta$  (C-D) and IL-8 (E-F) measured by ELISA. Data are presented as mean (SEM) and represents 4 independent experiments. Mean values were compared using two-way ANOVA, and P values reported for the effect of treatment on responses to LPS. N.D = below limits of detection.

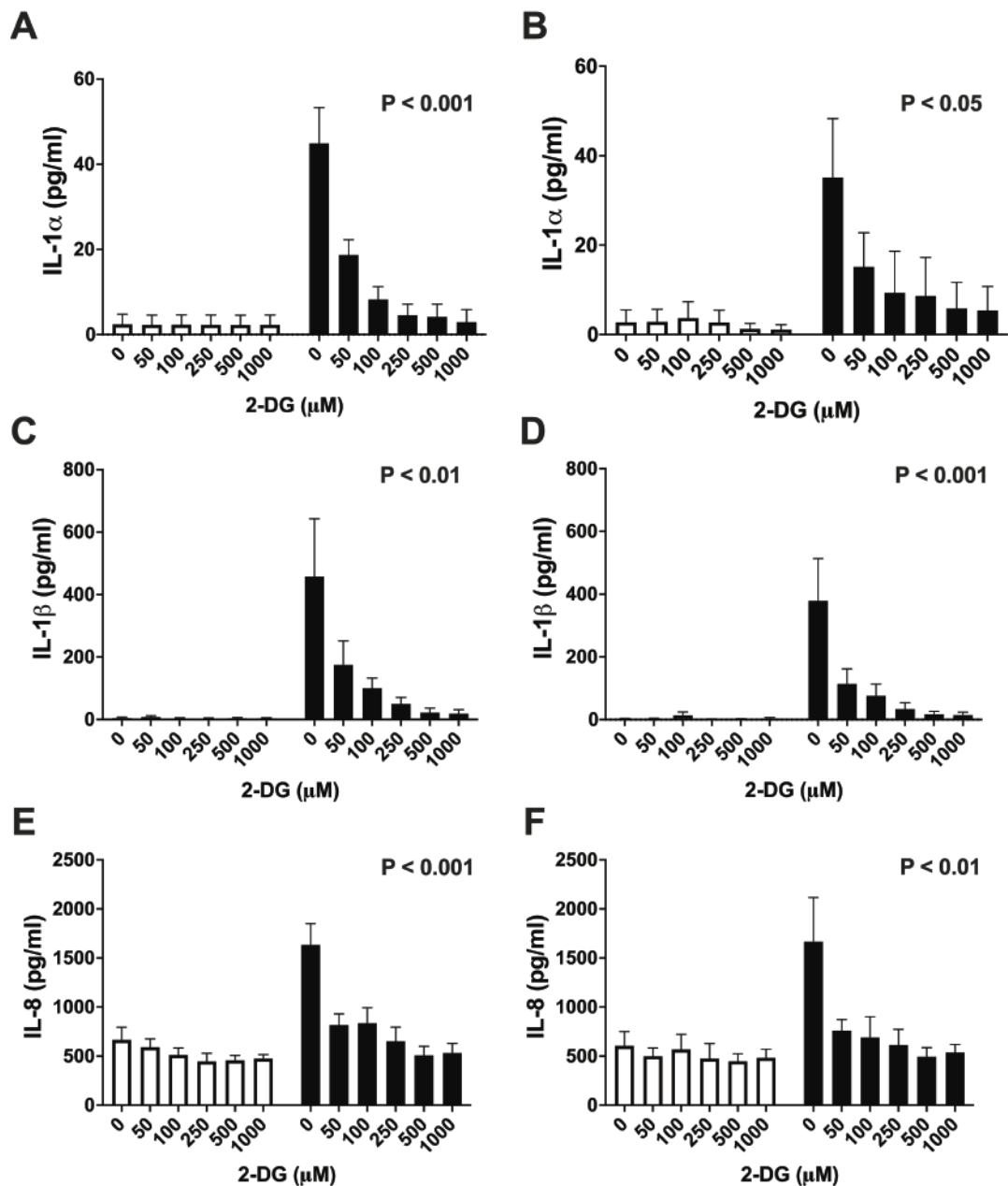


**Figure 3.3. Inhibition of glycolysis with 2-deoxy-D-glucose (2-DG) reduced the secretion of IL-1 $\alpha$ , IL-1 $\beta$  and IL-8 by granulosa cells**

Granulosa cells from emerged (A, C, E) or dominant (B, D, F) follicles were treated for 2 h with the indicated final concentration of 2-DG. Granulosa cells were then challenged for 24 h with control medium (white bars) or medium containing 1  $\mu$ g/ml LPS (black bars), in the presence of the treatments. Supernatants were collected and the accumulation of IL-1 $\alpha$  (A-B), IL-1 $\beta$  (C-D) and IL-8 (E-F) measured by ELISA. Data are presented as mean (SEM) and represents 4 independent experiments. Mean values were compared using two-way ANOVA, and P values reported for the effect of treatment on responses to LPS.

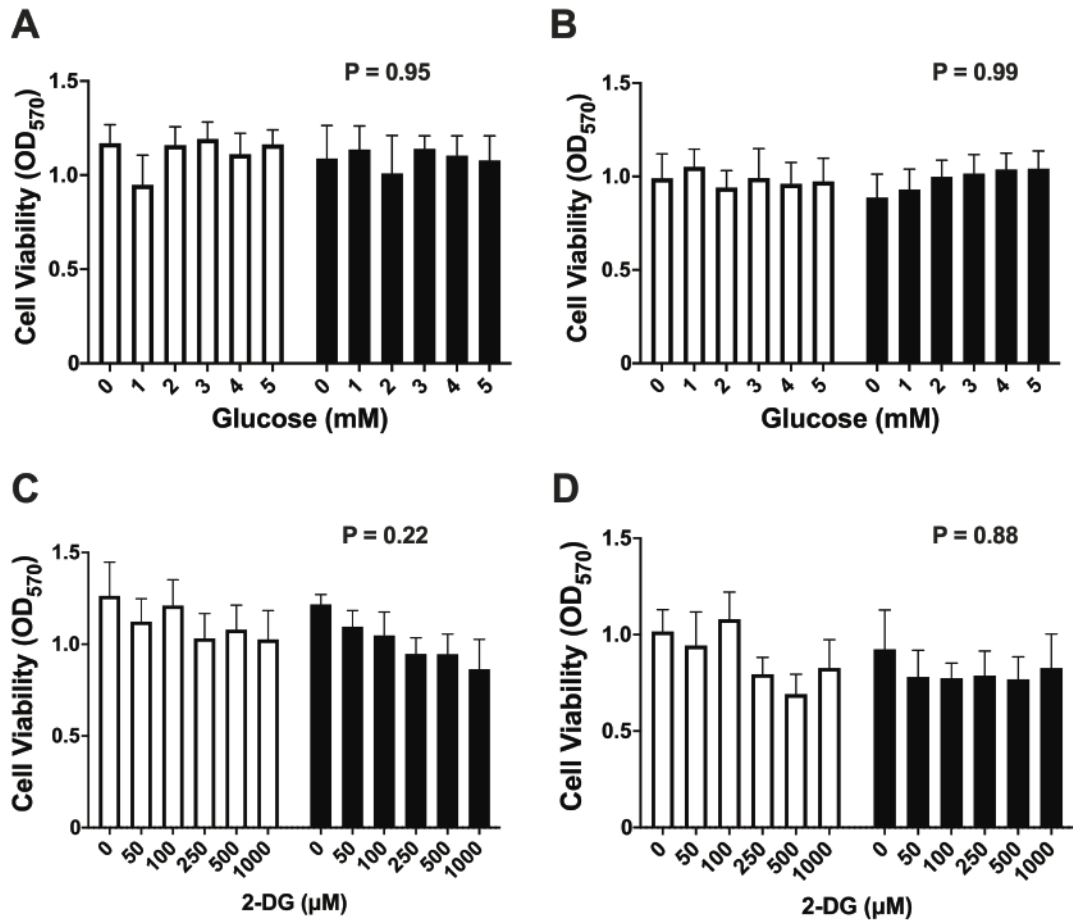


**Figure 3.4. Treatment with glucose or 2-DG does not alter cell viability**

Granulosa cells from emerged (A, C) or dominant (B, D) follicles were treated for 24 h with vehicle or the indicated percentages of glucose (A, B) or 2-DG (C, D). Granulosa cells were then challenged for 24 h with control medium (white bars) or medium containing 1 μg/ml LPS (black bars) in the continued presence of the treatments. Cell viability was estimated by MTT assay. Data are presented as mean (SEM) from 4 independent experiments. Data were analysed by two-way ANOVA, and P values reported for the effect of treatment on responses to LPS.



### 3.3.4 AMPK and mTOR reduced granulosa cell inflammatory responses to LPS

Cellular energy metabolism is regulated by AMPK and mTOR with energy stress activating AMPK and inhibiting mTOR in cells (Hardie et al., 2012, Zoncu et al., 2011). To screen for effects of AMPK and mTOR, granulosa cells were treated for 2 h prior to and during a 24 h LPS challenge, with 1 mM AICAR to activate AMPK, 500 nM rapamycin to inhibit mTORC1 or 50 nM Torin 1 to inhibit mTORC1 and mTORC2; 1  $\mu$ M dexamethasone was used as a reference anti-inflammatory agent (Bhattacharyya et al., 2007). Treatment with AICAR reduced the LPS-induced secretion of IL-1 $\alpha$ , IL-1 $\beta$  and IL-8, by granulosa cells from emerged ( $P < 0.05$ ) **Fig. 3.5A, C, E** and dominant ( $P < 0.001$ ; **Fig. 3.5B, D, F**) follicles, compared with control. Rapamycin did not reduce LPS-induced inflammation, but Torin 1 reduced IL-1 $\alpha$  and IL-1 $\beta$  in granulosa cells from emerged ( $P < 0.05$ ; **Fig. 3.5A, C**) and dominant ( $P < 0.5$ ; **Fig. 3.5B, D**) follicles. The reference anti-inflammatory agent, dexamethasone, was at least as effective as AICAR or Torin 1 in reducing the LPS-induced secretion of IL-1 $\alpha$  and IL-1 $\beta$  by granulosa cells from emerged ( $P < 0.01$ ; **Fig. 3.5A, C**) and dominant ( $P < 0.05$ ; **Fig. 3.5B, D**) follicles. However, like Torin 1, dexamethasone did not reduce the LPS-induced secretion of IL-8 by granulosa cells from either follicle size (**Fig. 3.5E, F**).

It was next considered whether reducing inflammation by inhibiting glycolysis, activating AMPK, or inhibiting mTOR simply reflected reduced protein synthesis because these can reduce phosphorylation of p70S6K, which induces protein synthesis (Kimura et al., 2003). In granulosa cells from emerged (**Fig. 3.6A, C**) and dominant (**Fig. 3.6B, D**) follicles, rapamycin and Torin 1 alone reduced the abundance of phosphorylated p70S6K ( $P < 0.05$ ), however treatment with LPS, 2-DG or AICAR did not alter the phosphorylation of p70S6K. Furthermore, the findings were further supported by experiments where Torin 1, but not AICAR reduced the amount of protein per culture well in granulosa cells from emerged (Torin 1,  $1.49 \pm 0.04$  mg protein vs. AICAR,  $2.03 \pm 0.06$  mg or control,  $2.19 \pm 0.12$  mg;  $P < 0.05$ , ANOVA,  $n = 4$ ) and dominant (Torin 1,  $1.32 \pm 0.12$  mg protein vs. AICAR,  $1.52 \pm 0.05$  or control,  $1.51 \pm 0.09$  mg;  $P < 0.05$ , ANOVA,  $n = 4$ ) follicles.

Together, these observations suggest that activating AMPK may limit granulosa cells inflammatory responses to LPS independently of protein synthesis and inhibiting mTOR may limit inflammatory responses by reducing protein synthesis.

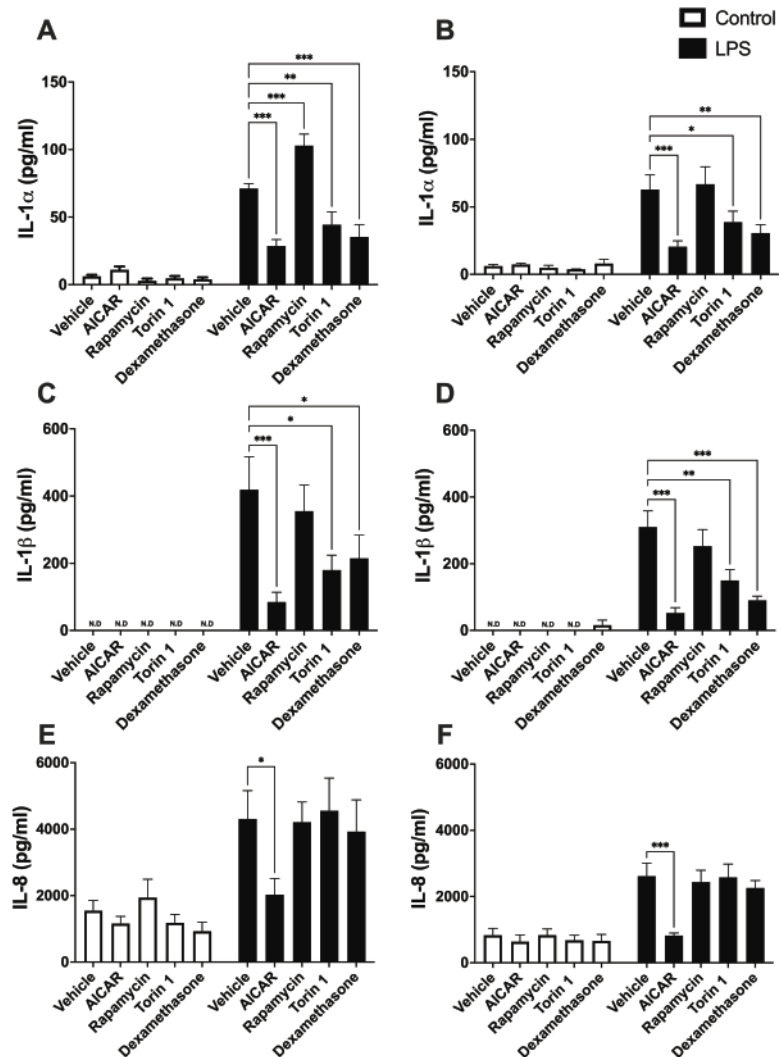


**Figure 3.5. Manipulation of AMPK and mTOR regulates innate immunity in granulosa cells**

Granulosa cells from emerged (A, C, E) or dominant (B, D, F) follicles treated for 2 h with vehicle, AICAR (1 mM), rapamycin (500 nM), Torin 1 (50 nM) or dexamethasone (1 μM). Granulosa cells were then challenged for 24 h with control medium (white bars) or medium containing 1 μg/ml LPS (black bars), in the presence of the treatments. Supernatants were collected and the accumulation of IL-1α (A-B), IL-1β (C-D) and IL-8 (E-F) measured by ELISA. Data are presented as mean (SEM) and represents 4 independent experiments. Mean values were compared using two-way ANOVA, using Dunnett's post hoc test. Values differ from vehicle, \*\*\* P < 0.001, \*\* P < 0.01, \* P < 0.05. N.D = below limits of detection.

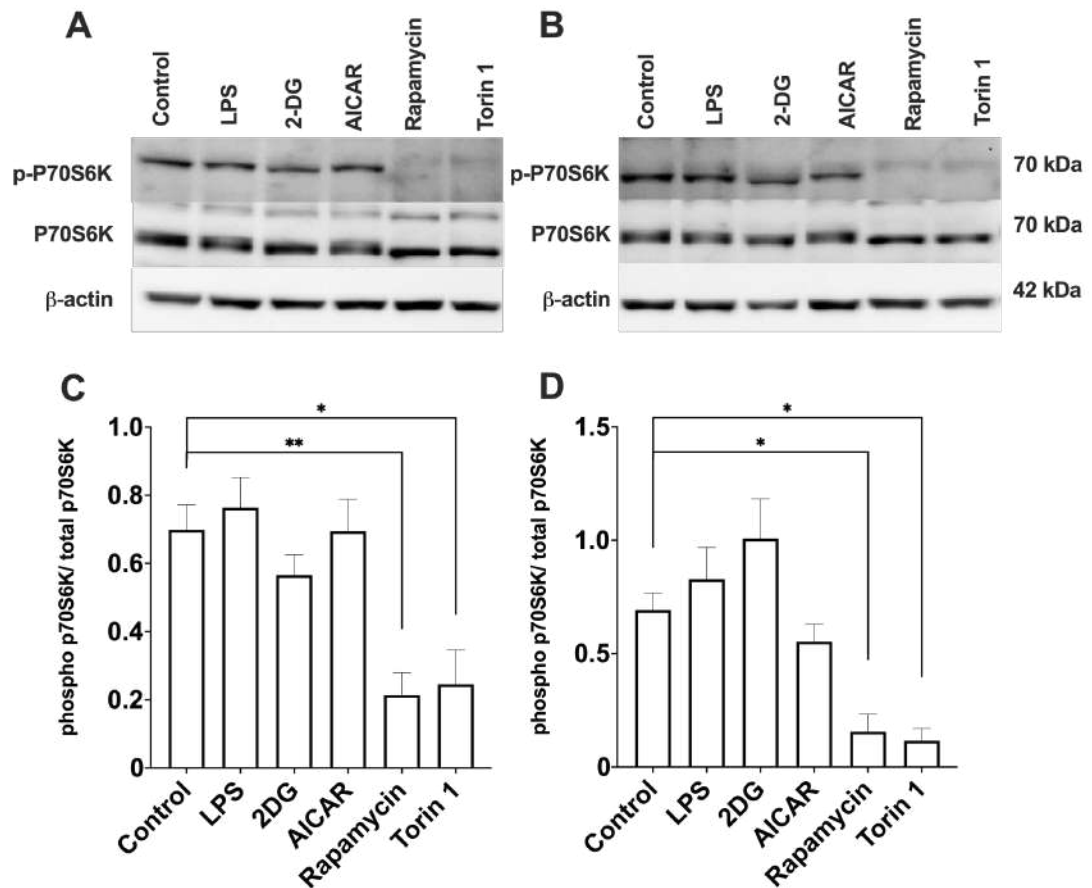


**Figure 3.6. Rapamycin and Torin 1 reduce the phosphorylation of p70S6K**

Granulosa cells from emerged (A, C) or dominant (B, D) follicles were treated for 24 h with control, 1 $\mu$ g/ml LPS, 1 mM 2-DG, 1 mM AICAR, 500 nM rapamycin or 50 nM Torin 1, and the phosphorylation p70S6 Kinase (p70S6K) analysed by western blot. A representative blot showing treatments with bands corresponding to phosphorylated p70S6 kinase (Thr421/Ser424), total p70S6 Kinase and  $\beta$ -actin (A). The band densities for p-p70S6K and p70S6K were first quantified relative to  $\beta$ -actin, and then p70S6K was quantified relative to total p70S6K (C-D). Data are presented as mean (SEM) of 3 independent experiments. Values differ from control by one-way ANOVA, using Dunnett's post hoc test. Values differ from control, \*\*  $P < 0.01$ , \*  $P < 0.05$ .

### 3.3.5 Treatment with AICAR impairs granulosa cell responses to LPS.

To further investigate the effect of manipulating cellular energy metabolism, AICAR was used to activate AMPK (Corton et al., 1995), as validated previously in bovine granulosa cells by phosphorylation of AMPK (Tosca et al., 2007a). The activity of AICAR was confirmed for granulosa cells by evaluating the phosphorylation of acetyl-CoA carboxylase (ACC), which is a biomarker for activation of AMPK (Gonzalez et al., 2020, Hardie et al., 2012). Treating granulosa cells with AICAR induced the phosphorylation of ACC within 2 h in granulosa cells from both emerged ( $P < 0.01$ ; **Fig. 3.7A**) and dominant ( $P < 0.05$ ; **Fig. 3.7B**) follicles. Surprisingly, AMPK phosphorylation was not altered over the 2 h period (**Fig. 3.7C-D**). The phosphorylation of ACC was still evident after 24 h of AICAR treatment ( $P < 0.05$ ; **Fig. 3.8**); although LPS, 2-DG, rapamycin or Torin 1 did not alter ACC phosphorylation.

Granulosa cells were treated with a range of concentrations of AICAR for 2 h prior to and during a 24 h LPS challenge. Treatment with AICAR reduced the LPS-induced secretion of IL-1 $\alpha$ , IL-1 $\beta$  and IL-8 in granulosa cells from emerged ( $P < 0.01$ ; **Fig. 3.9A, C, E**) and dominant ( $P < 0.05$ ; **Fig. 3.9B, D, F**) follicles. Specifically, treatment with 0.5 mM AICAR reduced the LPS-induced secretion of IL-1 $\alpha$  by  $> 60\%$ , IL-1 $\beta$  by 75% and IL-8 by  $> 20\%$  by granulosa cells from both emerged and dominant follicles. Cell viability was not altered by AICAR treatment (**Fig. 3.10A-B**).

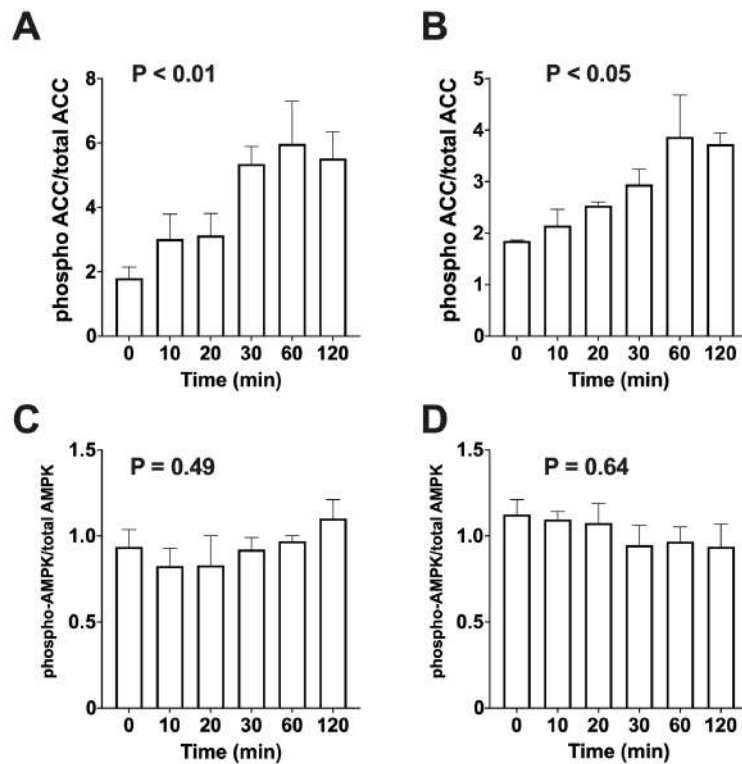
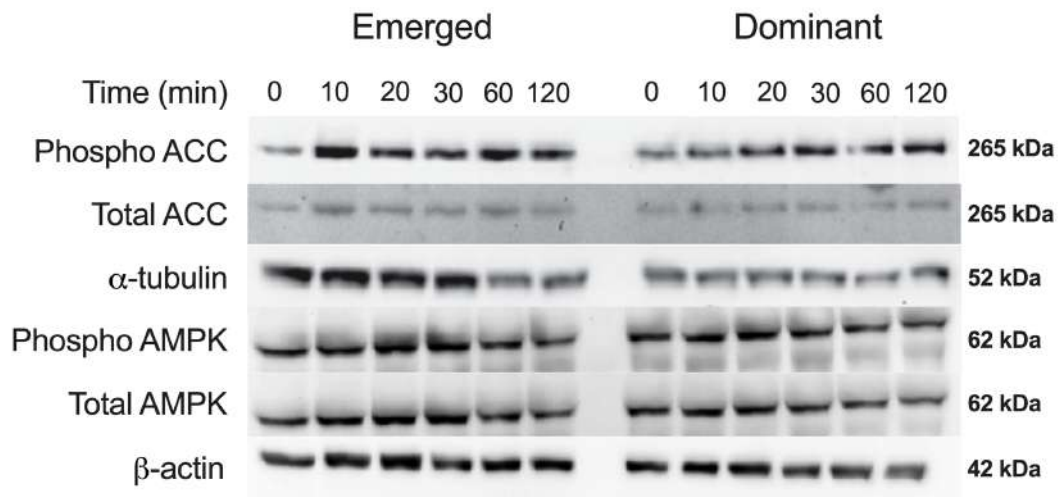


**Figure 3.7. Effects of AICAR on phosphorylated AMPK and ACC**

Granulosa cells from emerged (A, C) or dominant (B, D) follicles were treated in culture medium with vehicle, or for the indicated times with 1 mM AICAR and the phosphorylation of acetyl-CoA carboxylase (ACC) and AMP-activated protein kinase (AMPK) analysed by western blot. Representative western blots of phosphorylated ACC, total ACC, phosphorylated AMPK, total AMPK,  $\alpha$ -tubulin, and  $\beta$ -actin are shown. Data are presented as mean (SEM) of 3 independent experiments. Mean values were compared using one-way ANOVA. P values reported for the effect of treatment compared with time 0.

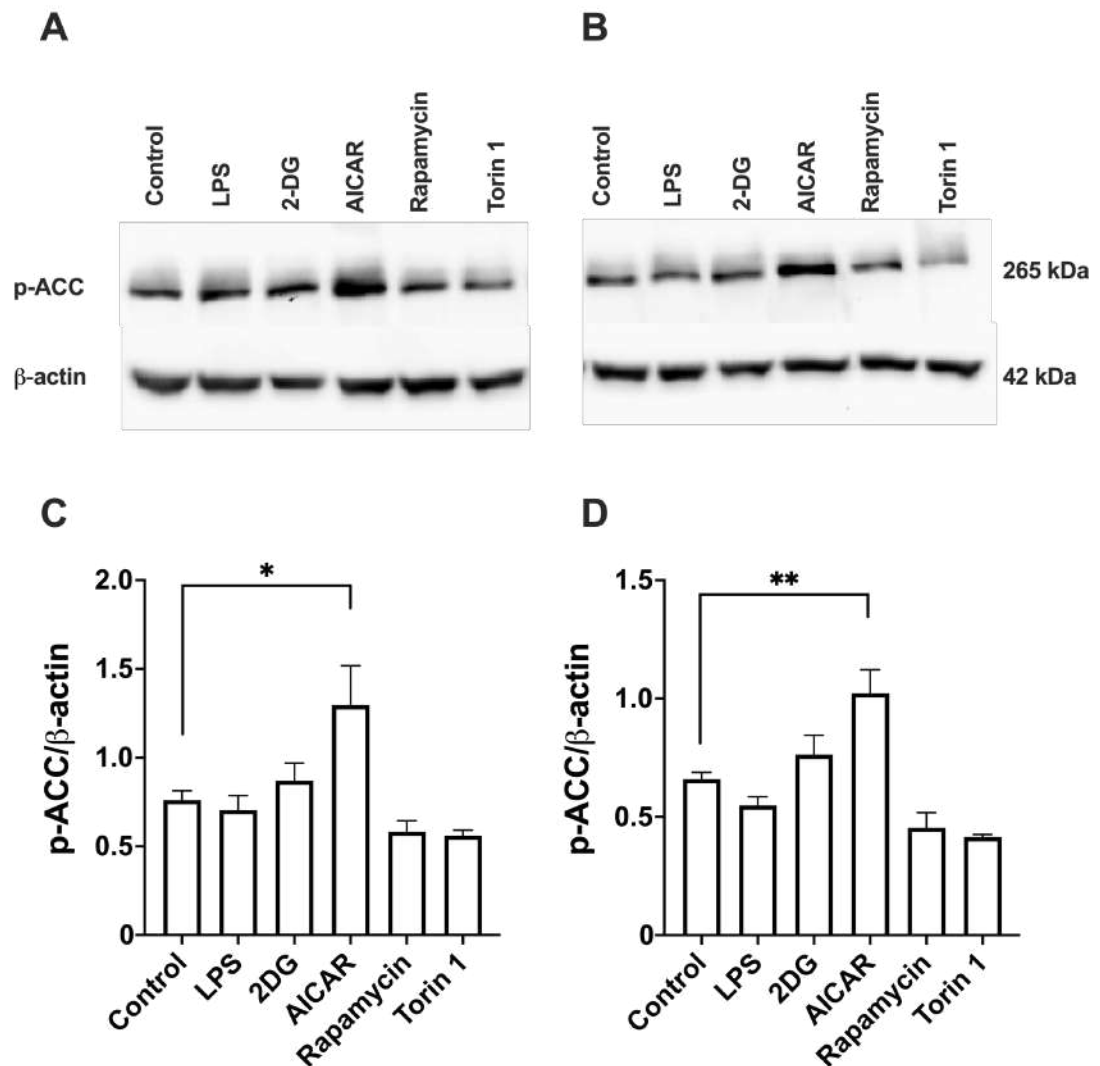


**Figure 3.8. Treatment with AICAR increases the abundance of phosphorylated ACC in granulosa cells**

Granulosa cells from emerged (A, C) or dominant (B, D) follicles were treated for 24 h with control, 1 µg/ml LPS, 1 mM 2-DG, 1 mM AICAR, 500 nM rapamycin or 50 nM Torin 1, and the phosphorylation ACC analysed by western blot. Representative blots showing treatments with bands corresponding to phosphorylated ACC and β-actin (A-B). The band densities for p-ACC were quantified relative to β-actin, (C-D). Data are presented as mean (SEM) from 3 independent experiments. Data were analysed using one-way ANOVA, using Dunnett's post hoc test. Values differ from control; \*\* P < 0.01, \* P < 0.05.

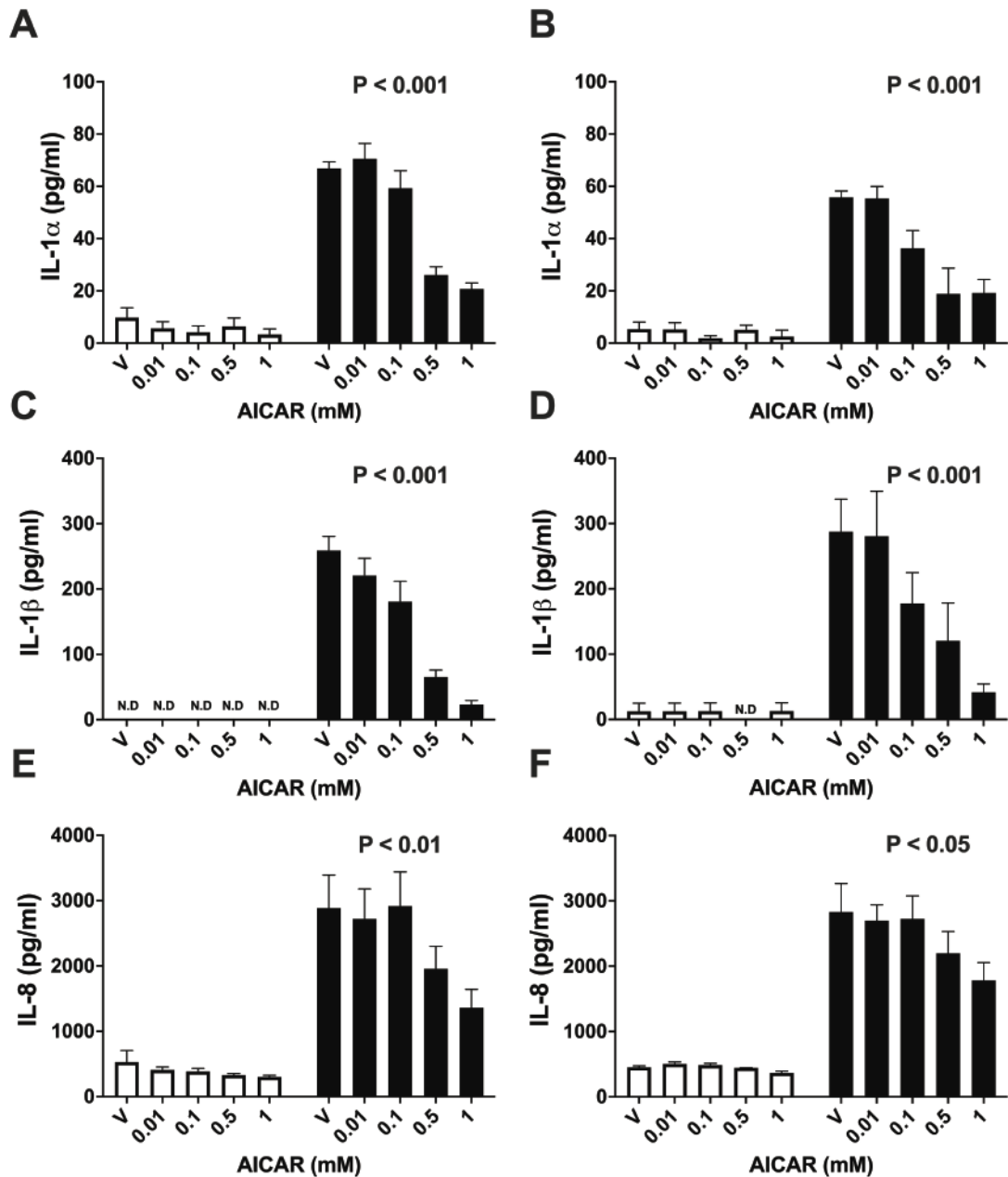


**Figure 3.9. Activation of AMPK with AICAR reduced the innate immune response in granulosa cells**

Granulosa cells from emerged (A, C, E) or dominant (B, D, F) follicles were treated for 2 h with vehicle or the indicated final concentrations of AICAR. Granulosa cells were then challenged for 24 h with control medium (white bars) or medium containing 1  $\mu$ g/ml LPS (black bars). Supernatants were collected and the accumulation of IL-1 $\alpha$  (A–B), IL-1 $\beta$  (C–D) and IL-8 (E–F) measured by ELISA. Data are presented as mean (SEM) and represents 4 independent experiments. Mean values were compared using two-way ANOVA, and P values reported for the effect of treatment on responses to LPS.

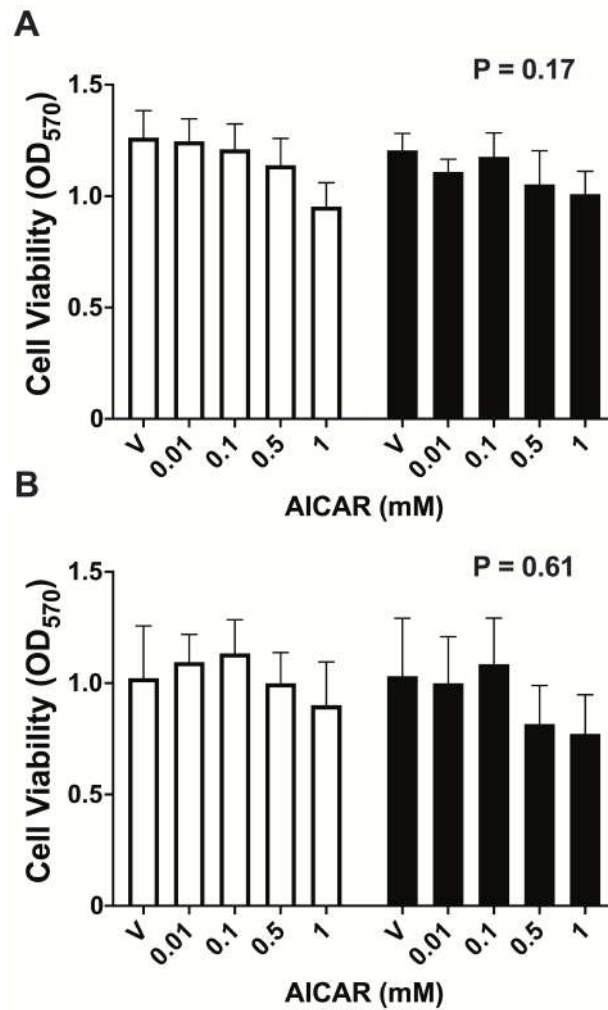


**Figure 3.10. Treatment with AICAR does not alter cell viability**

Granulosa cells from emerged (A) or dominant (B) follicles were treated for 2 h with vehicle or the indicated concentrations of AICAR. Granulosa cells were then challenged for 24 h with control medium (white bars) or medium containing 1  $\mu\text{g/ml}$  LPS (black bars) in the continued presence of the treatments. Cell viability was estimated by MTT assay. Data are presented as mean (SEM) from 4 independent experiments. Data were analysed by one-way ANOVA, and P values reported for the effect of treatment on responses to LPS.



### **3.3.6 AICAR truncates the LPS-induced phosphorylation of ERK1/2 and JNK.**

Lipopolysaccharide stimulates the phosphorylation of ERK1/2 and p38 in granulosa cells within 30 min (Bromfield and Sheldon, 2011, Price and Sheldon, 2013, Price et al., 2013). In the present study, granulosa cells were treated for 2 h with vehicle or 1 mM AICAR, and then challenged for up to 120 min with LPS. There was LPS-induced phosphorylation of ERK1/2 in granulosa cells from emerged (**Fig. 3.11**) and dominant (**Fig. 3.12**) follicles. Although there was no significant effect of treatment with AICAR, there was a shorter duration of ERK1/2 phosphorylation in cells treated with AICAR than vehicle for cells from emerged (time x treatment,  $P < 0.001$ ) and dominant (time x treatment,  $P < 0.05$ ) follicles. Treatment with AICAR stimulated p38 phosphorylation in granulosa cells from emerged and dominant follicles, but there was no significant effect of time or time x treatment (**Fig. 3.11**; **Fig. 3.12**).

The phosphorylation of JNK in response to LPS was also examined. There was LPS-induced phosphorylation of JNK in granulosa cells from emerged (**Fig. 3.11**) and dominant (**Fig. 3.12**) follicles. Treatment with AICAR stimulated JNK phosphorylation in granulosa cells from both follicles. Furthermore, there was a shorter duration of JNK phosphorylation in cells treated with AICAR than vehicle for granulosa cells from emerged (time x treatment,  $P < 0.05$ ) and dominant (time x treatment,  $P < 0.01$ ) follicles. These experiments provide evidence that AICAR reduced inflammatory responses to LPS and truncated the LPS-induced phosphorylation of ERK1/2 and JNK.

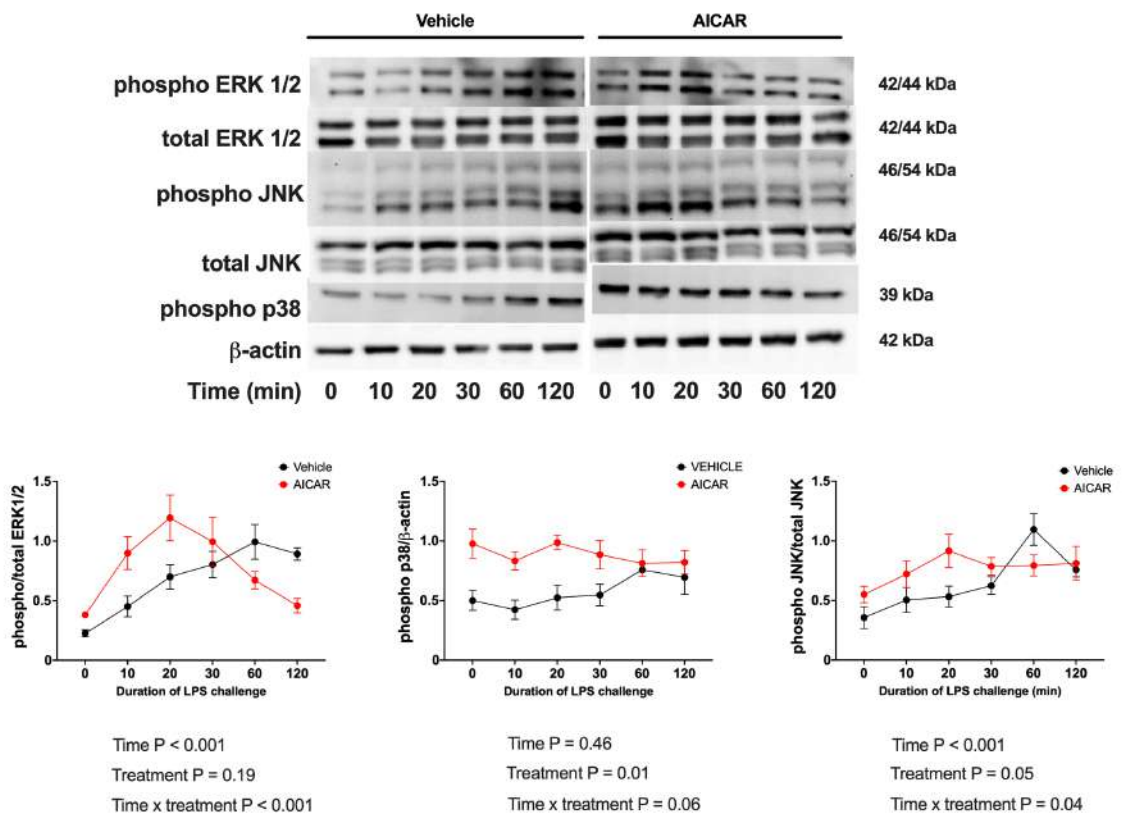


**Figure 3.11. AICAR truncates the LPS-stimulated phosphorylation of ERK1/2 and JNK**

Granulosa cells from emerged follicles were treated for 2 h with granulosa cell culture medium containing vehicle or medium containing AICAR (1 mM), before challenge with LPS for 0, 10, 20, 30, 60 or 120 min, and the phosphorylation of ERK1/2, p38 and JNK analysed by western blot. Representative blots showing vehicle and AICAR, with bands corresponding to diphosphorylated ERK1/2, ERK1/2, phosphorylated p38 (Thr180/Tyr182), phosphorylated JNK, JNK or  $\beta$ -actin. Band intensities for phosphorylated ERK1/2 were quantified relative to ERK1/2; phosphorylated p38 was quantified relative to  $\beta$ -actin. Phosphorylated JNK were quantified relative to JNK. Data are presented as mean (SEM) of 4 independent experiments. Mean values were compared using two-way ANOVA and P values are reported.

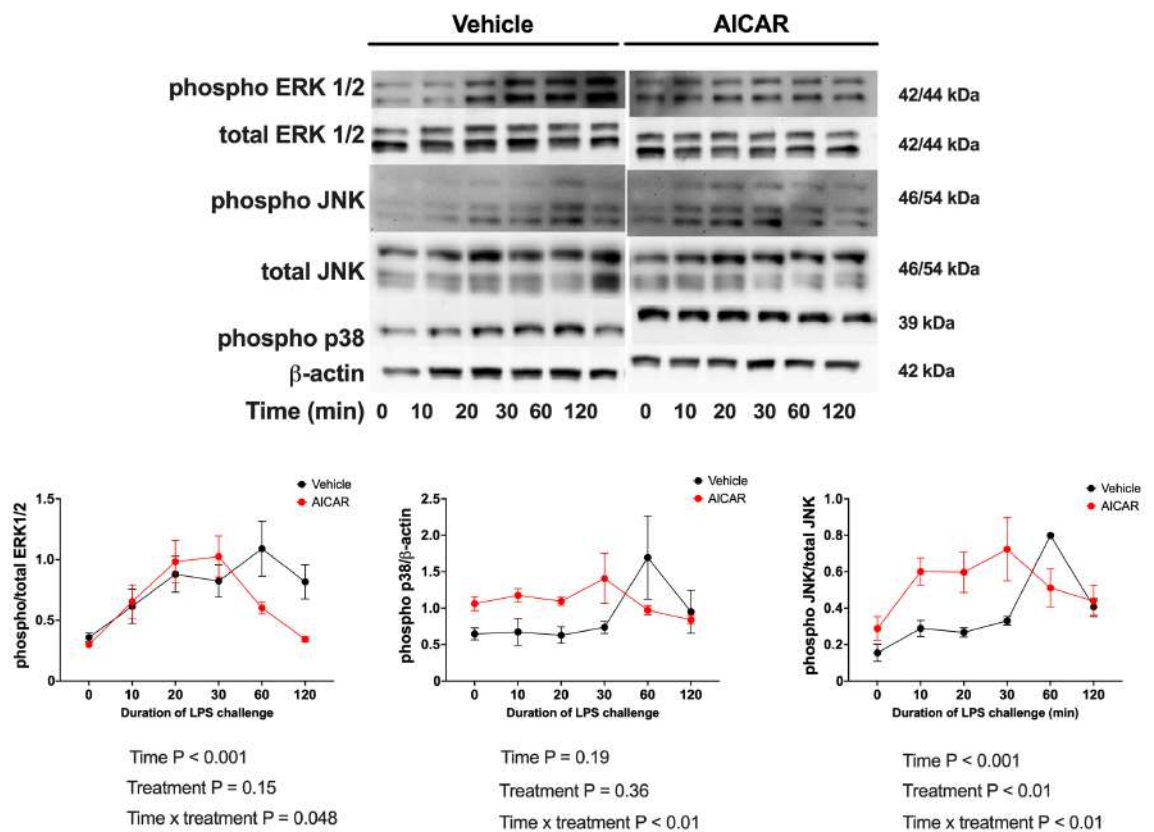


**Figure 3.12. AICAR truncates the LPS-induced phosphorylation of ERK1/2 and JNK**

Granulosa cells from dominant follicles were treated for 2 h with granulosa cell culture medium containing vehicle or medium containing AICAR (1 mM), before challenge with LPS for 0, 10, 20, 30, 60 or 120 min, and the phosphorylation of ERK1/2, p38 and JNK analysed by western blot. Representative blots showing vehicle and AICAR, with bands corresponding to diphosphorylated ERK1/2, ERK1/2, phosphorylated p38 (Thr180/Tyr182), phosphorylated JNK, JNK or β-actin. Band intensities for phosphorylated ERK1/2 were quantified relative to ERK1/2; phosphorylated p38 was quantified relative to β-actin. Phosphorylated JNK were quantified relative to JNK. Data are presented as mean (SEM) of 4 independent experiments. Mean values were compared using two-way ANOVA and P values are reported.

### 3.3.7 Torin 1 limited granulosa cell IL-1 responses to LPS.

The role of mTOR in granulosa cell responses was then explored because activation of AMPK in turn inhibits mTOR (Hardie et al., 2012, Zoncu et al., 2011). Granulosa cells were treated for 2 h with vehicle, or a range of concentrations of the mTORC1 inhibitor rapamycin (Oshiro et al., 2004), or the dual mTORC1 and mTORC2 inhibitor Torin 1 (Thoreen et al., 2009), followed by a 24 h LPS challenge, in the presence of the treatments. Rapamycin did not alter the inflammatory responses to LPS in granulosa cells from emerged (Fig. 3.13A, C, E) or dominant (Fig. 3.13B, D, F) follicles, and did not affect cell viability (Fig. 3.14A-B). Treatment with Torin 1 reduced the LPS-induced secretion of IL-1 $\alpha$  and IL-1 $\beta$ , but not IL-8, by granulosa cells from emerged ( $P < 0.01$ ; Fig. 3.15A, C, E) and dominant ( $P < 0.05$ ; Fig. 3.15B, D, F) follicles. Specifically, compared with vehicle, treatment with 50 nM Torin 1 reduced the LPS-induced secretion of IL-1 $\alpha$  by  $> 65\%$  and IL-1 $\beta$  by  $> 50\%$  in granulosa cells. Although the highest concentrations of Torin 1 reduced cell viability by up to 10%, treatment with 50 nM Torin 1 did not alter the cell viability of granulosa cells (Fig. 3.16).

### 3.3.8 Torin 1 did not alter LPS-induced phosphorylation of MAPKs

To explore whether Torin 1 altered the LPS-induced phosphorylation of MAPKs. Granulosa cells were treated for 2 h with vehicle or 50 nM Torin 1, and then challenged for up to 120 min with LPS. There was LPS-induced phosphorylation of ERK1/2 and JNK in granulosa cells from emerged follicles (Fig. 3.17), and phosphorylation of ERK1/2, p38 and JNK in granulosa cells from dominant follicles (Fig. 3.18). However, unlike AMPK, Torin 1 did not alter the duration of ERK1/2, p38 or JNK phosphorylation.

Together, the data in *Section 3.38* and *Section 3.39* suggest that whilst Torin 1 reduced the IL-1 responses to LPS, Torin 1 did not alter duration of LPS-induced phosphorylation of MAPKs.

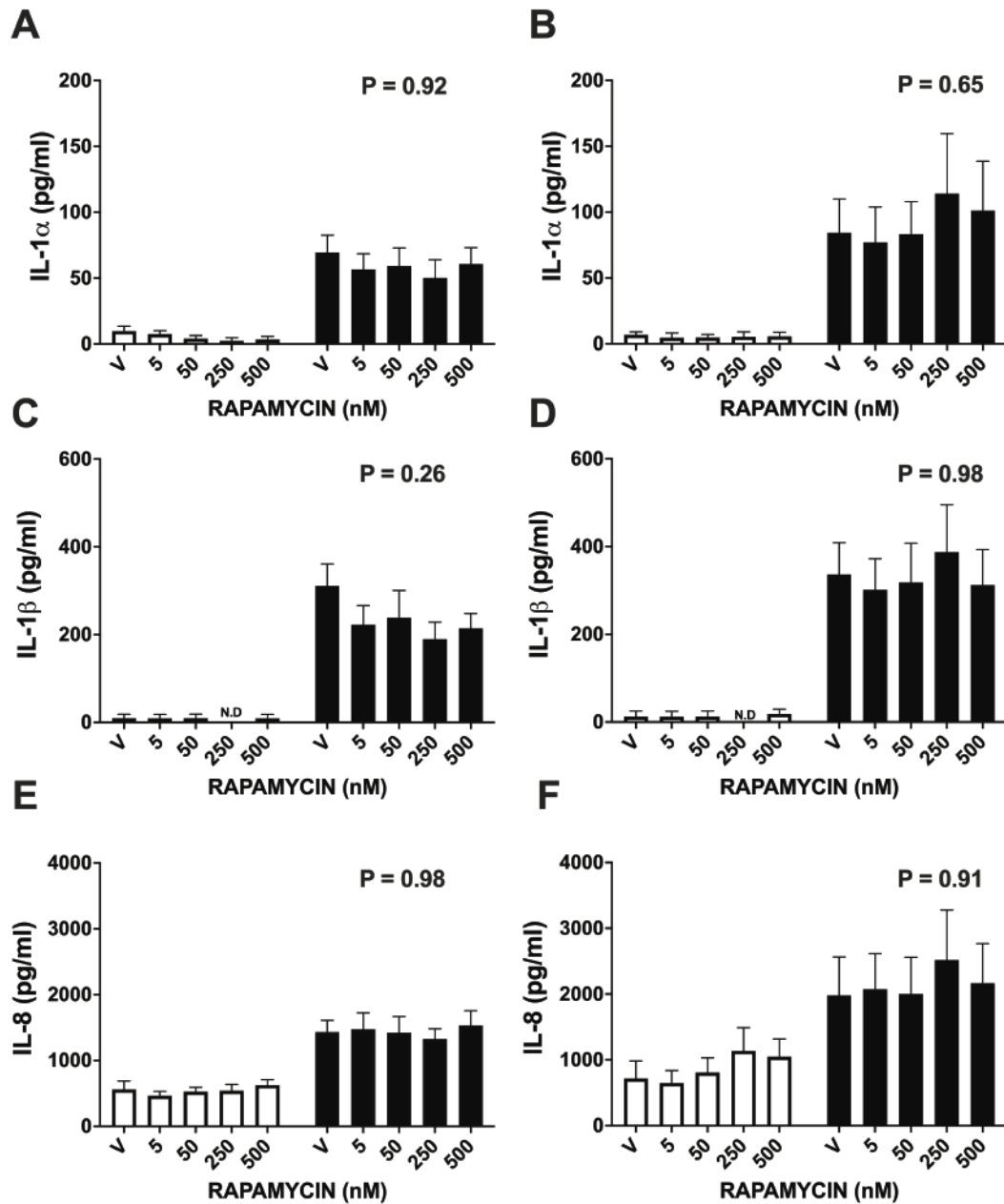


**Figure 3.13. Inhibition of mTOR with rapamycin did not affect the innate immune response in granulosa cells**

Granulosa cells from emerged (A, C, E) or dominant (B, D, F) follicles were treated for 2 h with vehicle or the indicated final concentration of rapamycin. Granulosa cells were then challenged for 24 h with control medium (white bars) or medium containing 1  $\mu$ g/ml LPS (black bars). Supernatants were collected and the accumulation of IL-1 $\alpha$ , IL-1 $\beta$  and IL-8 measured by ELISA. Data are presented as mean (SEM) and represents 4 independent experiments. Mean values were compared using two-way ANOVA, and P values reported for the effect of treatment on responses to LPS. N.D = below limit of detection.

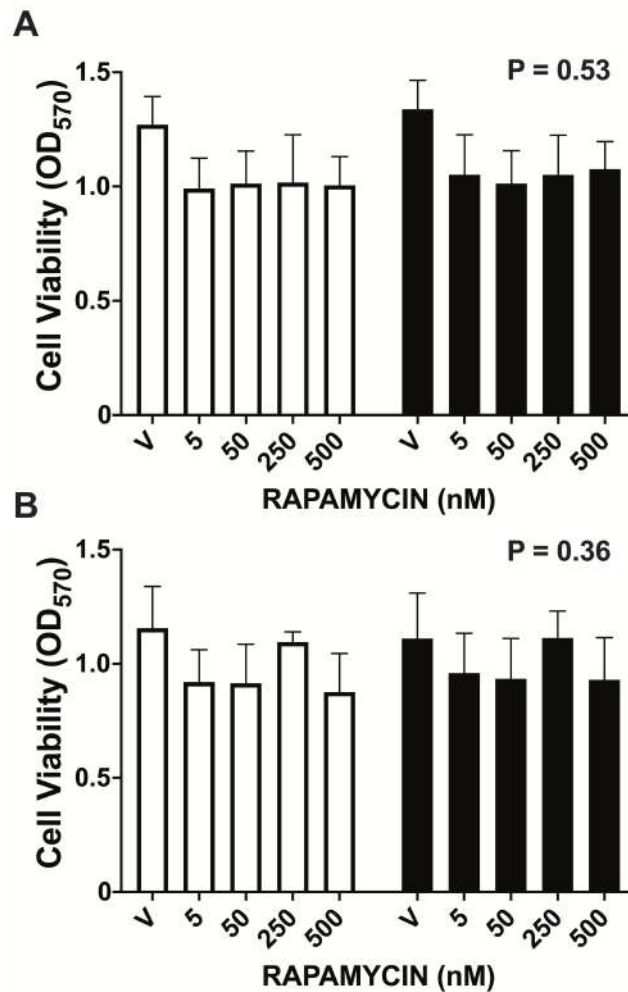


**Figure 3.14. Treatment with rapamycin does not alter cell viability**

Granulosa cells from emerged (A) or dominant (B) follicles were treated for 2 h with vehicle or the indicated concentrations of rapamycin. Granulosa cells were then challenged for 24 h with control medium (white bars) or medium containing 1  $\mu\text{g/ml}$  LPS (black bars) in the continued presence of the treatments. Cell viability was estimated by MTT assay. Data are presented as mean (SEM) from 4 independent experiments. Data were analysed by one-way ANOVA, and P values reported for the effect of treatment on responses to LPS.

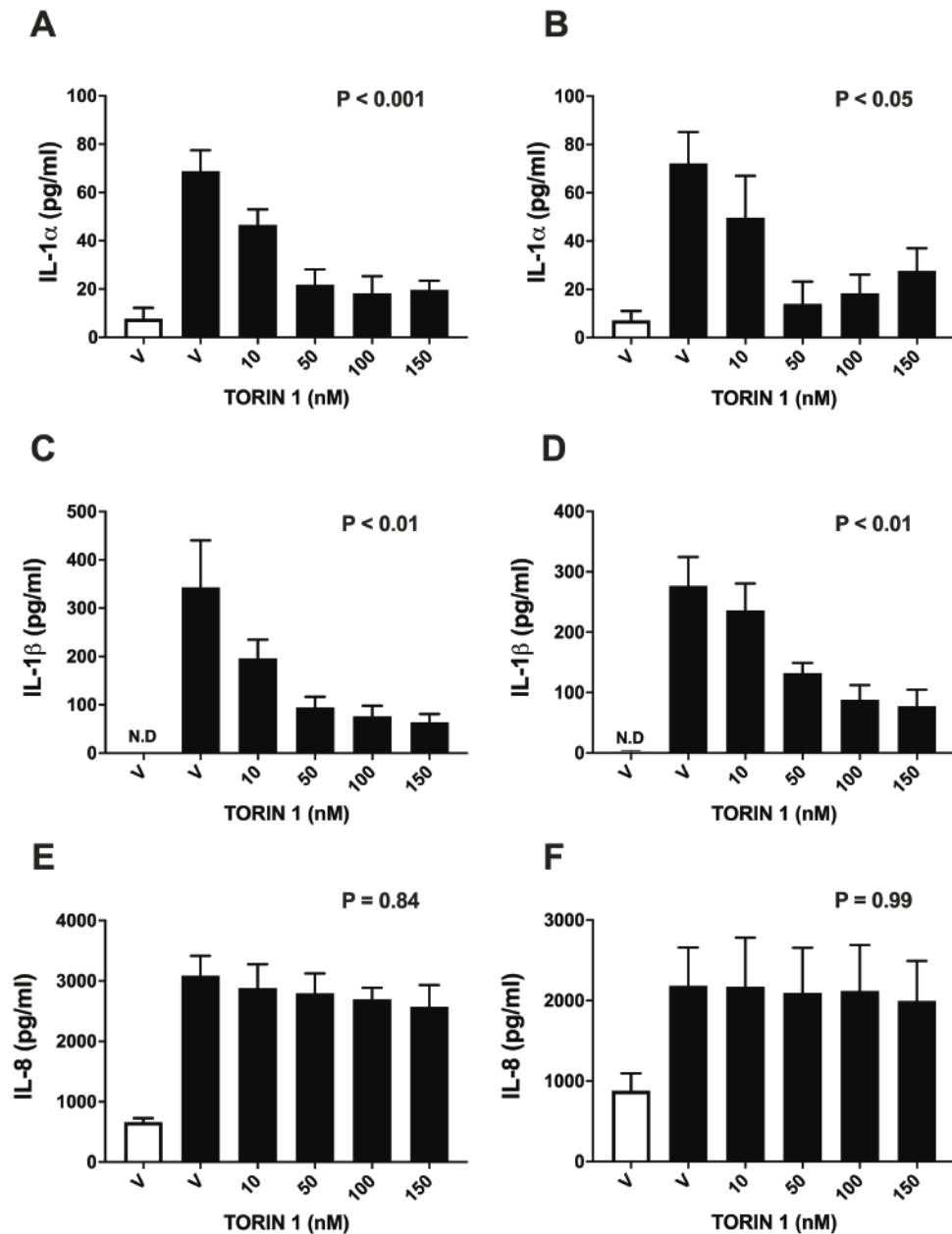


**Figure 3.15. Inhibition of mTOR with Torin 1 reduced the innate immune response in granulosa cells**

Granulosa cells from emerged (A, C, E) or dominant (B, D, F) follicles were treated for 2 h with vehicle or culture media containing the indicated final concentrations of Torin 1. Granulosa cells were then challenged for 24 h with control medium (white bars) or media containing 1  $\mu$ g/ml LPS (black bars). Supernatants were collected and the accumulation of IL-1 $\alpha$ , IL-1 $\beta$  and IL-8 measured by ELISA. Data are presented as mean (SEM) and represents 4 independent experiments. Mean values were compared using one-way ANOVA, and P values reported for the effect of treatment on responses to LPS. N.D = below limit of detection.

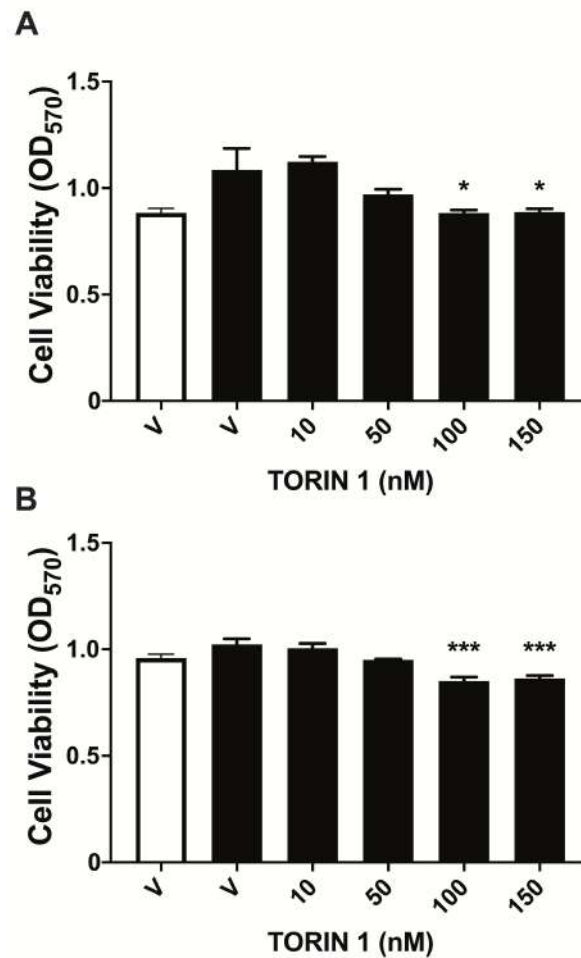


**Figure 3.16. Torin 1 reduces viability of granulosa cells at higher concentrations**

Granulosa cells from emerged (A) or dominant (B) follicles were treated for 24 h with vehicle or culture media containing the indicated final concentrations of Torin 1. Granulosa cells were then challenged for 24 h with control medium (white bars) or media containing 1 µg/ml LPS (black bars). Cell viability was estimated by MTT assay. Data are presented as mean (SEM) from 4 independent experiments. Data were analysed by one-way ANOVA using Dunnett's post hoc test. \*\*\* P < 0.001, \* P < 0.05



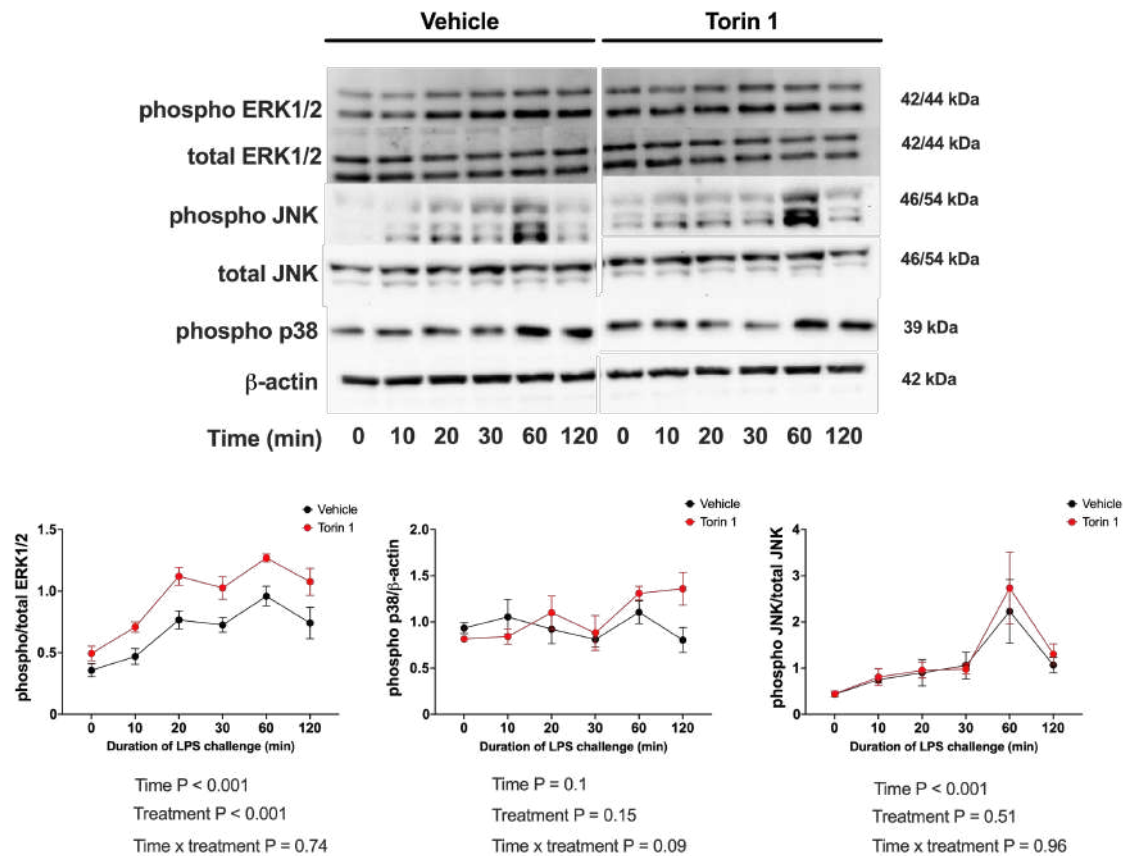


**Figure 3.17. Torin 1 did not alter LPS-stimulated phosphorylation of MAPK**

Granulosa cells from emerged follicles were treated for 2 h with granulosa cell culture medium containing vehicle or medium containing Torin 1 (50 nM), before challenge with LPS for 0, 10, 20, 30, 60 or 120 min, and the phosphorylation of ERK1/2, p38 and JNK analysed by western blot. Representative blots showing vehicle and Torin 1, with bands corresponding to diphosphorylated ERK1/2, ERK1/2, phosphorylated p38 (Thr180/Tyr182), phosphorylated JNK, JNK or  $\beta$ -actin. Band intensities for phosphorylated ERK1/2 were quantified relative to ERK1/2; phosphorylated p38 was quantified relative to  $\beta$ -actin. Phosphorylated JNK were quantified relative to JNK. Data are presented as mean (SEM) of 4 independent experiments. Mean values were compared using two-way ANOVA and P values are reported.

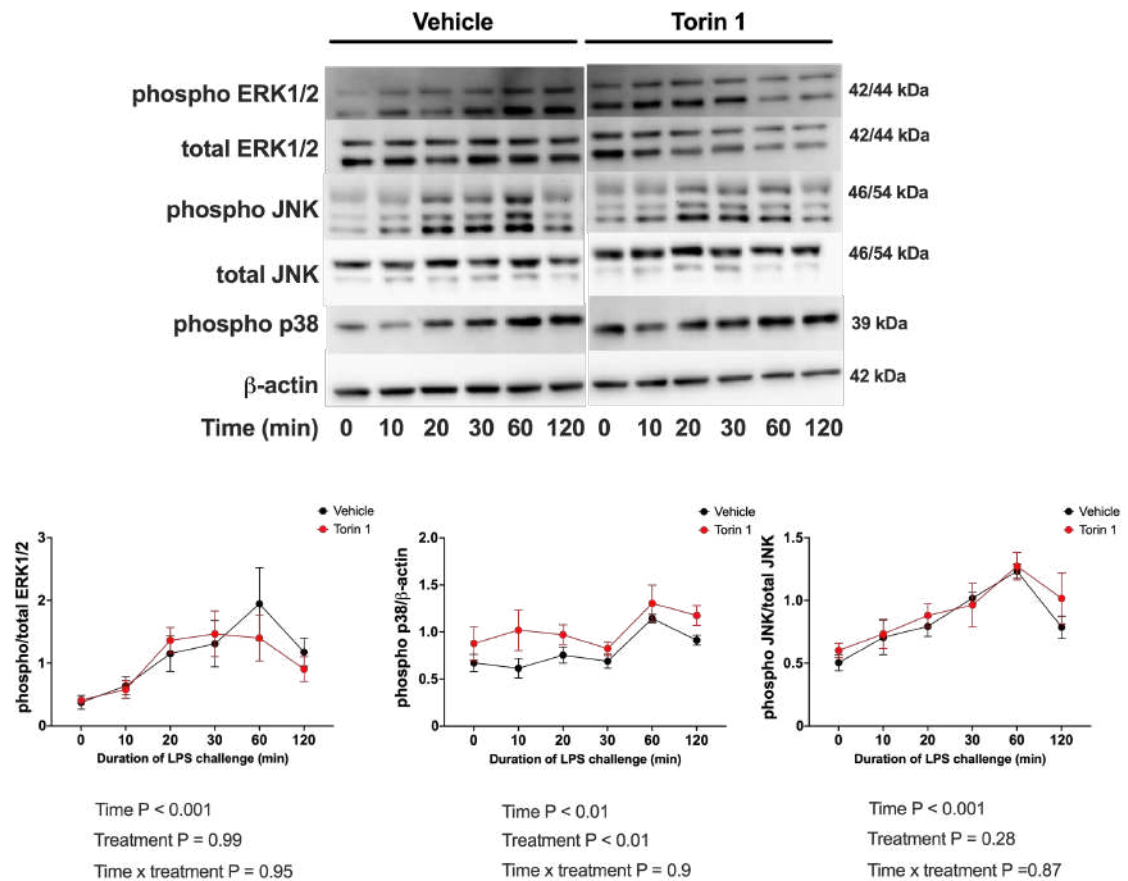


**Figure 3.18. Torin 1 did not alter LPS-stimulated phosphorylation of MAPK**

Granulosa cells from dominant follicles were treated for 2 h with granulosa cell culture medium containing vehicle or medium containing Torin 1 (50 nM), before challenge with LPS for 0, 10, 20, 30, 60 or 120 min, and the phosphorylation of ERK1/2, p38 and JNK analysed by western blot. Representative blots showing vehicle and Torin 1, with bands corresponding to diphosphorylated ERK1/2, ERK1/2, phosphorylated p38 (Thr180/Tyr182), phosphorylated JNK, JNK or  $\beta$ -actin. Band intensities for phosphorylated ERK1/2 were quantified relative to ERK1/2; phosphorylated p38 was quantified relative to  $\beta$ -actin. Phosphorylated JNK were quantified relative to JNK. Data are presented as mean (SEM) of 4 independent experiments. Mean values were compared using two-way ANOVA and P values are reported.

### 3.3.9 Energy stress impairs the endocrine function of granulosa cells

Finally, the interactions between energy stress and endocrine function were investigated because as steroidogenic cells, granulosa cells carry out an essential role in ovarian function. To measure the accumulation of oestradiol and progesterone, cells were cultured in granulosa cell culture medium with the addition of  $10^{-7}$  M androstenedione (Merck) and 1 ng/ml of highly purified bovine FSH. To screen for the effects of AMPK and mTOR on endocrine function, granulosa cells were treated with vehicle, 1  $\mu$ g/ml LPS, 1 mM 2-DG, 1 mM AICAR, 500 nM rapamycin, or 50 nM Torin 1 (**Fig. 3.19**)

Challenge with LPS reduced the secretion of oestradiol by granulosa cells from emerged follicles by 50% ( $P < 0.001$ ), but not granulosa cells from dominant follicles ( $P = 0.50$ ). Lipopolysaccharide also reduced the secretion of progesterone by granulosa cells from emerged ( $P < 0.001$ ) and dominant ( $P < 0.05$ ) follicles by >26%.

Treatment with 2-DG reduced the secretion of oestradiol by granulosa cells from emerged follicles ( $P < 0.01$ ) but not granulosa cells from dominant follicles, or the secretion of progesterone by granulosa cells from either follicle size. Treatment with AICAR reduced the secretion of oestradiol and progesterone by granulosa cells from both emerged ( $P < 0.001$ ) and dominant ( $P < 0.05$ ) follicles. Rapamycin treatment decreased the secretion of oestradiol by granulosa cells from emerged follicles ( $P < 0.001$ ), but not dominant follicles, and decreased the secretion of progesterone by granulosa cells from both follicle sizes ( $P < 0.001$ ). Torin 1 treatment decreased the secretion of oestradiol ( $P < 0.05$ ) and progesterone ( $P < 0.001$ ) by granulosa cells from both emerged and dominant follicles.

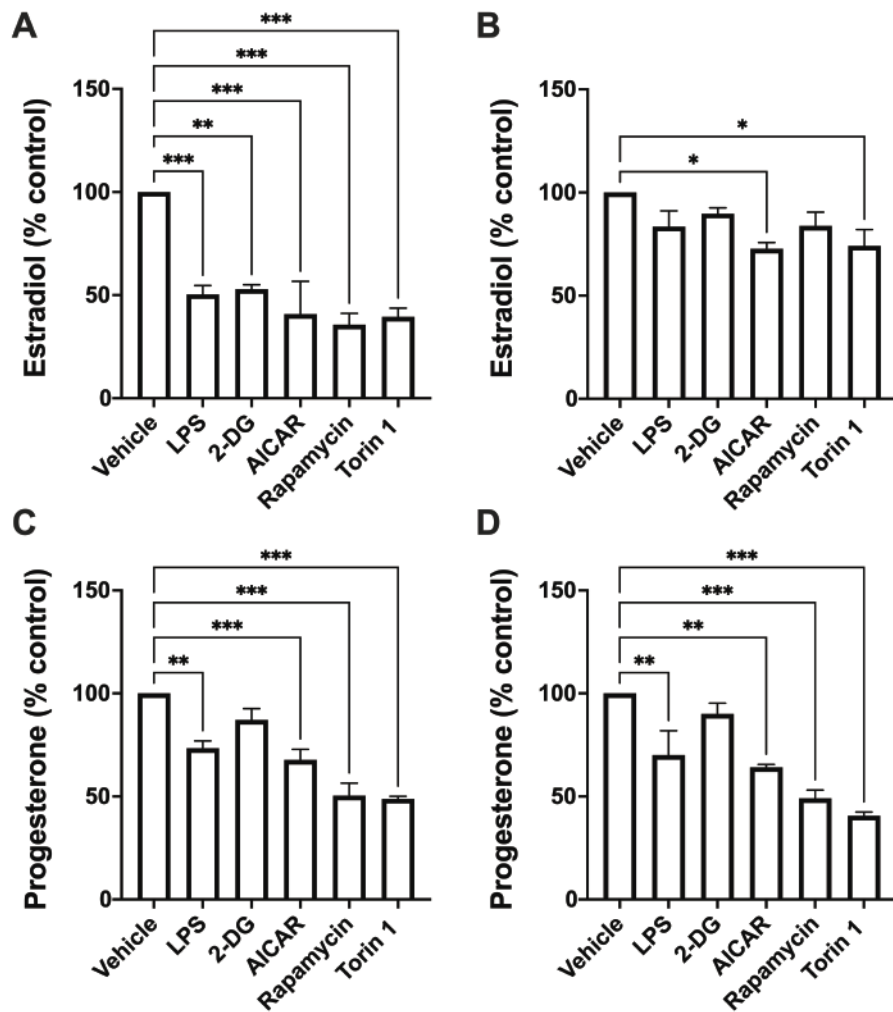


**Figure 3.19. Treatment with LPS, AICAR or Torin 1 reduced the secretion of oestradiol and progesterone by granulosa cells from dominant follicles**

Granulosa cells from emerged (A, D) or dominant (B, D) follicles were treated for 24 h with granulosa cells culture medium containing vehicle, LPS (1  $\mu\text{g/ml}$ ), AICAR (1 mM) or Torin 1 (50 nM) and the accumulation of oestradiol or progesterone was measured by ELISA. Data are presented as mean (SEM) from 3 independent experiments. Data were analysed using one-way ANOVA, using Dunnett's post hoc test. Values differ from control; \*\*\*  $P < 0.001$ , \*\*  $P < 0.01$ , \*  $P < 0.05$ . N.D = below limit of detection.

### 3.4 Discussion

Innate immunity and energy stress are both important in granulosa cells because ovarian follicles are often exposed to LPS after parturition, which is when cows are unable to consume enough food to meet their energy requirements (Beam and Butler, 1997, Leroy et al., 2004b, Cheong et al., 2017, Piersanti et al., 2019c). In the present chapter, we found that LPS stimulated the secretion of IL-1 $\alpha$ , IL-1 $\beta$  and IL-8, which was associated with phosphorylation of ERK1/2 and JNK. The main finding of this chapter was that energy stress limited the innate immune responses of bovine granulosa cells. Inflammatory responses to LPS were limited by the glycolysis inhibitor 2-deoxy-D-glucose, the AMPK activator AICAR, or the mTOR inhibitor Torin 1. Furthermore, AICAR truncated LPS-induced phosphorylation of ERK1/2 and JNK. The effects of manipulating energy metabolism were similar for granulosa cells isolated from emerged or dominant follicles. Collectively, these data provide evidence for an immunometabolism crosstalk in granulosa cells and implies that energy stress limits ovarian follicle defences.

We first mimicked energy stress by inhibiting hexokinase with 2-deoxy-D-glucose to prevent glycolysis (Tannahill et al., 2013, Zhao et al., 2017a, Lee et al., 2020). Inhibiting glycolysis reduced LPS-induced secretion of IL-1 $\alpha$ , IL-1 $\beta$  and IL-8 by granulosa cells from emerged or dominant follicles. This reduced inflammation is similar to findings with murine macrophages, where inhibiting hexokinase reduced the LPS-induced secretion of IL-1 $\beta$  (Tannahill et al., 2013). Inhibiting hexokinase or depleting glucose and glutamine, also limit LPS-induced IL-1 $\beta$ , IL-6 and IL-8 secretion in bovine endometrial tissue (Turner et al., 2016, Noleto et al., 2017). When follicular fluid was collected from cows 63 days postpartum, intrafollicular IL-8 and LPS concentrations were correlated as might be expected, but more interestingly intrafollicular IL-8 and glucose concentrations were also correlated ( $r^2 = 0.77$ ) (Piersanti et al., 2019a). Transcriptomic analysis has also suggested that energy stress also impairs inflammatory responses to LPS in postpartum cows (Girard et al., 2015).

Cellular energy metabolism is regulated by AMPK and MTOR in most eukaryotic cells (Zoncu et al., 2011, Hardie et al., 2012, Murray et al., 2015, O'Neill et al., 2016). The energy sensor AMPK is activated by energy stress or by small molecules such as

AICAR (Tosca et al., 2007a, Tosca et al., 2010, Hardie et al., 2012). Activating AMPK regulates energy metabolism by stimulating glucose uptake, glycolysis, and the Krebs cycle to produce ATP (Hardie et al., 2012). Activating AMPK also inhibits mTOR and pathways that consume ATP, including inhibition of lipid metabolism via phosphorylation of acetyl-CoA carboxylase. In the present chapter, AICAR increased phosphorylation of acetyl-CoA carboxylase, confirming previous observations that AICAR activates AMPK in bovine granulosa cells. More importantly, treatment with AICAR reduced LPS-induced secretion of IL-1 $\alpha$ , IL-1 $\beta$  and IL-8 in granulosa cell, with 0.5 mM AICAR reducing LPS-stimulated secretion of IL-1 $\alpha$  by > 60%, IL-1 $\beta$  by > 75% and IL-8 by > 20%. Our finding agrees with previous observations that AICAR reduces LPS-induced secretion of TNF- $\alpha$  and IL-6 in murine neutrophils, and IL-1 $\beta$ , IL-6 and IL-8 in bovine endometrial tissue (Zhao et al., 2008, Turner et al., 2016). Surprisingly, the responses to LPS and the effects of energy stress in the present chapter were similar for granulosa cells from both emerged and dominant follicles, despite developmental differences between these follicle sizes (Fortune, 1994, Ginther et al., 1996). This consistent immunometabolism effect may reflect the evolutionary importance of integrating defence with metabolism.

One concern was that the reductions in inflammation were simply caused by reduced protein synthesis. However, AICAR did not inhibit phosphorylation of p70S6K or reduce total cellular protein. Instead, AICAR reduced duration of LPS-induced phosphorylation of ERK1/2 and JNK. This observation is similar to a reduction in FSH-induced phosphorylation of ERK1/2 when granulosa cells were treated with metformin, which also activates AMPK (Tosca et al., 2007a, Tosca et al., 2010). Activating AMPK can in turn regulate energy metabolism by inhibiting mTOR (Zoncu et al., 2011, Hardie et al., 2012). We found that granulosa cell IL-1 $\alpha$  and IL-1 $\beta$  responses to LPS were reduced by Torin 1, but not rapamycin, and MAPK phosphorylation was unaffected. The different IL-1 responses between Torin 1 and rapamycin may be because Torin 1 inhibits both mTORC1 and mTORC2 (Oshiro et al., 2004, Thoreen et al., 2009). Another possibility is that Torin 1 reduced the phosphorylation of p70S6K and the amount of total cellular protein.

The observation that depleting glucose did not limit inflammatory responses to LPS was unexpected because the responses to LPS are energetically expensive (Kvidera et al., 2017). Bovine granulosa cells have the capability to take up glucose because they express the mRNA for the glucose transporters, GLUT1 and GLUT3, at comparable levels to organs such as the brain or heart; mRNA for GLUT4 is also present, but at much lower levels (Nishimoto et al., 2006). Negative energy balance in cattle is associated with increased insulin resistance, the impaired tissue sensitivity and responsiveness to insulin (Oikawa and Oetzel, 2006, Bell and Bauman, 1997). In the present thesis, we cultured granulosa cells in the presence of insulin, therefore, the lack of effect of glucose depletion on granulosa cell inflammation might be due to differential effects of 2-DG or limiting the availability of glucose on GLUT expression or cellular metabolism.

It has also been reported that directly inhibiting glycolysis with 2-deoxy-D-glucose has widespread impacts on cell metabolism (Tannahill et al., 2013, O'Neill et al., 2016). Future studies could investigate whether components of the glycolysis pathway or Krebs cycle impinge directly on granulosa cell inflammatory responses because acetyl-CoA, succinate and fumarate all regulate inflammation in immune cells (Ryan et al., 2019). Another intriguing observation worthy of further investigation is that whilst AICAR, Torin 1 and dexamethasone reduced LPS-induced IL-1 secretion, only AICAR reduced IL-8, which may reflect the differences in the regulation of IL-1 and IL-8 production or secretion (Hoffmann et al., 2002).

We also provide evidence that energy stress may impair endocrine function because oestradiol and progesterone secretion by granulosa cells was impaired by treatment with AICAR, confirming previous observations that found that AICAR treatment reduced the secretion of oestradiol and progesterone by bovine granulosa cells (Tosca et al., 2007a), and progesterone secretion by rat granulosa cells (Tosca et al., 2005). There may be a role for mTOR in endocrine function of granulosa cells because we found that treatment with Torin 1 also decreased the secretion of oestradiol and progesterone by granulosa cells from both emerged and dominant follicles.

In conclusion, granulosa cell inflammatory responses to LPS were limited by manipulating cellular energy metabolism using a glycolysis inhibitor, an AMPK activator, or an mTOR inhibitor. Specifically, in cells isolated from emerged and dominant follicles, 2-DG and AICAR limited LPS-induced IL-1 $\alpha$ , IL-1 $\beta$  and IL-8 secretion, and Torin 1 limited IL-1 $\alpha$  and IL-1 $\beta$ . These observations are an example of immunometabolism, linking cellular energy metabolism with innate immunity in granulosa cells. Our findings also imply that energy stress compromises ovarian follicle immune defences and endocrine function, which may reduce the capability of cows to cope with effect of infections on fertility. The findings of *Chapter 3* are summarized in **Figure 7.1**.



## 4 Manipulating cholesterol homeostasis alters innate immune responses in granulosa cells

### 4.1 Introduction

In postpartum cattle there is an increased metabolic demand for lactation, and the plasma concentrations of total cholesterol (Quiroz-Rocha et al., 2009, Esposito et al., 2014, Cavestany et al., 2005), HDL, LDL and VLDL (Kessler et al., 2014) decrease around parturition. Unfortunately, decreases in plasma total cholesterol concentrations are further exacerbated by negative energy balance in the postpartum period (Kim and Suh, 2003, Ruegg et al., 1992, Esposito et al., 2014). There is also an association between decreased serum cholesterol concentrations and increased incidence of uterine diseases, such as metritis or endometritis in the postpartum period (Bogado Pascottini and LeBlanc, 2020, Paiano et al., 2019). Interestingly, changes to serum total cholesterol or HDL concentrations are reflected in the follicular fluid concentrations of total cholesterol (Leroy et al., 2004b, Leroy et al., 2004a, Shabankareh et al., 2013, Alves et al., 2014) or HDL cholesterol (Gautier et al., 2010), respectively.

The permeability of the follicle membrane to proteins up to 300 kDa is thought to exclude LDL (~3500 kDa) and VLDL (6000 to 27000 kDa) until vascularization, at around the time of ovulation (Jaspard et al., 1996, Le Goff, 1994, Shalgi et al., 1973). Therefore, HDL (175 to 500 kDa) is the only class of lipoprotein that has been detected in follicular fluid in bovine (Savion et al., 1982, Brantmeier et al., 1987), porcine (Chang et al., 1976), and human (Simpson et al., 1980, Jaspard et al., 1996) follicles. Follicular fluid concentrations of HDL increase with follicle size and concentrations range between 30 and 45% of plasma concentrations, depending on follicle size (Brantmeier et al., 1987).

Cellular proliferation is associated with increased cholesterol synthesis for new membrane synthesis (Batetta and Sanna, 2006, Chen, 1984). Granulosa cells proliferate rapidly during follicle growth, with multiple layers of granulosa cells lining the inside of the growing follicle (Scaramuzzi et al., 2011). Granulosa cells also proliferate rapidly *in vitro*; therefore, they may have a high demand for cholesterol for

membrane biogenesis. Depletion of mevalonate by inhibiting HMGCR is associated with decreased cellular growth and proliferation, as well as DNA replication (Siperstein, 1984, Sinensky and Logel, 1985). Blocking cholesterol biosynthesis reduces proliferation and is associated with cell cycle arrest in human leukaemia lymphocyte (HL-60) cells (Fernandez et al., 2005).

Bovine granulosa cells express mRNA encoding LDL receptors (LDLR) and Scavenger receptor B1 (SR-BI) (Argov et al., 2005), and the expression of SR-BI mRNA increases at around 72 h of culture (Yamashita et al., 2011). However, previous studies have suggested that bovine granulosa cells display little or no endocrine response to HDL prior to luteinization (O'Shaughnessy et al., 1990, Bao et al., 1995), perhaps because they have lower expression of SR-BI mRNA compared with luteal cells (Rajapaksha et al., 1997). Additionally, bovine granulosa cells express the metabolic machinery necessary to synthesize cholesterol *de novo* (Bertevello et al., 2018). However, little is known about the contribution of *de novo* cholesterol biosynthesis to granulosa cell function prior to luteinization.

Cholesterol constitutes about 30% of the plasma membrane in cells (Das et al., 2014), and is essential for TLR4 signalling (Triantafilou et al., 2002). Following LPS stimulation, TLR4, MyD88 and JNK are recruited into the lipid rafts where they interact with the LPS-CD14 complex, leading the activation of the TLR4 signalling pathway (Triantafilou et al., 2002). Disruption of lipid rafts, using the cholesterol depleting agent, methyl- $\beta$ -cyclodextrin (M $\beta$ CD), inhibits LPS-induced TNF $\alpha$  production in human monocytes (Triantafilou et al., 2002). Knockout bone-marrow derived macrophages for the cholesterol efflux proteins ABCA1 or ABCG1 have increased total cellular cholesterol, and increased cholesterol-rich microdomains in the plasma membrane, associated with increased TLR4 expression and inflammatory responses to LPS (Yvan-Charvet et al., 2008, Zhu et al., 2008, Koseki et al., 2007).

The mevalonate pathway of cholesterol biosynthesis has become the target of therapy to reduce cholesterol synthesis and treat hypercholesterolemia (Goldstein and Brown, 1990). Statins are generally considered to be anti-inflammatory in humans (Jain and Ridker, 2005, Weitz-Schmidt, 2002). However, at the cellular level, it has been reported that statins can augment pro-inflammatory responses in macrophages

(Matsumoto et al., 2004), bone-marrow derived macrophages (Sun and Fernandes, 2003), peripheral blood mononuclear cells (Montero et al., 2000, Coward et al., 2006), and THP-1 cells (Massonnet et al., 2009, Kuijk et al., 2008, Liao et al., 2013).

Granulosa cells are exposed to the bacterial endotoxin, LPS, that accumulates in the follicular fluid of cows with postpartum uterine infections (Herath et al., 2007). Bovine granulosa cells mount innate immune responses to LPS via TLR4 and secrete IL-1 $\alpha$ , IL-1 $\beta$  and IL-8, associated with increased phosphorylation of the MAPKs, ERK1/2, p38 and JNK (Bromfield and Sheldon, 2011, Price and Sheldon, 2013, Price et al., 2013, Horlock et al., 2021). Innate immunity and metabolism are intricately linked (O'Neill et al., 2016). In *Chapter 3*, we found that energy stress compromised the inflammatory response to LPS in bovine granulosa cells. However, it is unclear whether changes in granulosa cell cholesterol affects the inflammatory response to LPS.

Here, we explored whether altering the availability of cholesterol or inhibiting cholesterol biosynthesis in bovine granulosa cells altered the innate immune responses to LPS. Our first hypothesis was that decreasing the availability of cholesterol would impair the innate immune responses to LPS in granulosa cells. To test this hypothesis, we measured the concentration of cholesterol, HDL and LDL/VLDL in fetal bovine serum (FBS) or follicular fluid (FF) and altered their availability prior to LPS challenge and the measurement of IL-1 $\alpha$ , IL-1 $\beta$  and IL-8. We also treated granulosa cells with the cholesterol lowering agent, methyl- $\beta$ -cyclodextrin, prior to LPS challenge and measurement of IL-1 $\alpha$ , IL-1 $\beta$  and IL-8.

Our second hypothesis was that inhibiting the cholesterol biosynthesis pathway in granulosa cells would impair the innate immune responses of granulosa cells to LPS. To test this hypothesis, we used short-interfering RNA (siRNA) targeting the mevalonate pathway enzymes HMGCR, FDPS or FDFT1, prior to LPS challenge. We also used the small molecule inhibitors, lovastatin, alendronate or zaragozic acid to inhibit cholesterol biosynthesis in granulosa cells, prior to LPS challenge and measurement of IL-1 $\alpha$ , IL-1 $\beta$  and IL-8.

## **4.2 Methods**

### **4.2.1 Granulosa cell culture.**

Granulosa cells were isolated from emerged and dominant follicles, as described in *Chapter 2*. Granulosa cells were plated in 24-well plates at a density of 750,000 cells in 0.5 ml of culture media and cultured for 18 h at 38.5°C, in a humidified atmosphere of air containing 5% CO<sub>2</sub>. The medium was then aspirated, and the cells were cultured with vehicle or treatments in 0.5 ml of granulosa cell culture medium. For some experiments, granulosa cells were treated in serum-free medium, or medium containing 2% or 10% FBS, as indicated in figure legends.

### **4.2.2 Measurement of HDL and LDL cholesterol in FBS and follicular fluid**

Follicular fluid was aspirated from a total of 47 emerged or dominant follicles, from at least 15 animals, and the concentration of cholesterol was determined using the cholesterol oxidase-endpoint method (Randox Daytona Plus), as previously described (Piersanti et al., 2019a). The reportable range for cholesterol on the RX Daytona Plus is 0.65 to 16 mM/L.

High- and low-density lipoproteins were separated from samples using LDL/VLDL precipitation buffer (Abcam), and the concentrations of total cholesterol, HDL and LDL/VLDL were quantified for follicular fluid, FBS or lipoprotein-deficient serum (LDS; Merck), using the Amplex Red Cholesterol Assay (Life Technologies), as described in *Chapter 2*. Total cellular cholesterol concentrations were normalized to cellular total protein concentrations, as previously described (Nicholson and Ferreira, 2009, Pospiech et al., 2021). Measurements were normalized to percentage of control before analysis.

### **4.2.3 Treatment of granulosa cells with FBS or follicular fluid**

Granulosa cells were treated for 24 h with vehicle or a range of percentages of heat-inactivated FBS (Biosera; 0, 1%, 2%, 5%, 8% or 10%), or follicular fluid (0, 1%, 2%, 3%, 4% or 5%) aspirated and pooled from five dominant follicles, in serum-free

granulosa cell culture medium. Granulosa cells were then challenged with serum-free control medium or serum-free medium containing 1 µg/ml LPS, in the continued presence of FBS or follicular fluid, respectively.

#### **4.2.4 Treatment of granulosa cells with HDL, LDL and VLDL cholesterol**

Granulosa cells were treated for 24 h with vehicle or a range of concentrations of human HDL (0, 5, 10, 25, 50 or 100 µg/ml; Merck), LDL from human plasma (0, 5, 10, 25 or 50 µg/ml; Invitrogen) or human VLDL (0, 1, 2, 5 or 10 µg/ml; Merck) for 24 h in serum-free granulosa cell culture medium. Granulosa cells were then challenged for 24 h with serum-free control medium or serum-free medium containing 1 µg/ml LPS, in the continued presence of the treatments. Human HDL and LDL have previously been used to investigate steroidogenesis in human (Azhar et al., 1998b), bovine (Savion et al., 1981) and rat granulosa cells (Reaven et al., 1995). Serum-free conditions were used to avoid the confounding factors of free cholesterol, HDL, LDL or VLDL that are present in FBS.

#### **4.2.5 Inhibition of cholesterol biosynthesis**

In this study, HMGCR, FDPS or FDFT1 were inhibited using lovastatin, alendronate or zaragozic acid, respectively (Wasko et al., 2011, Mok and Lee, 2020). Granulosa cells were treated for 24 h in granulosa cell culture medium (containing 10% FBS) with vehicle or a range of concentrations of lovastatin (0, 0.01, 0.1, 1 or 10 µM), alendronate (0, 0.5, 5, 10 or 20 µM) or zaragozic acid (0, 0.5, 5, 10, or 20 µM). Granulosa cells were then challenged with control medium or medium containing 1 µg/ml LPS, in the continued presence of the inhibitors.

Cholesterol inhibitor experiments were carried out in the presence of 10% FBS to maintain robust granulosa cell inflammatory responses (Bromfield and Sheldon, 2011). The maximal concentration of lovastatin selected were informed by concentrations used in human and rat granulosa cells (Rung et al., 2005). The concentrations of alendronate and zaragozic acid selected were similar to those previously used with bovine endometrial stromal cells (Griffin et al., 2017). A 24 h treatment period for the inhibitors was chosen based on previous studies using statins,

bisphosphonates or zaragozic acid (Healey et al., 2016, Kuijk et al., 2008, Pospiech et al., 2021). To explore the effects of re-feeding mevalonic acid or farnesyl pyrophosphate (FPP) on the granulosa cell responses to LPS, cells were treated in granulosa cell culture medium (containing 10% FBS) with vehicle or lovastatin (10  $\mu$ M) or alendronate (10  $\mu$ M) for 24 h, in combination with a range of concentrations of mevalonic acid (20, 50 or 100  $\mu$ M) or farnesyl diphosphate (1, 10 or 50  $\mu$ M), respectively. Granulosa cells were then challenged with control medium or medium containing 1  $\mu$ g/ml LPS, in the continued presence of the treatments. The concentrations of mevalonic acid or FPP were selected based on previous studies (Healey et al., 2016, Monick et al., 2003).

#### **4.2.6 Cholesterol sequestration with methyl- $\beta$ -cyclodextrin**

To deplete the total cellular cholesterol concentrations in culture media, granulosa cells were treated for 24 h in granulosa cell culture media (containing 10% FBS) with vehicle or a range of concentrations of M $\beta$ CD (0, 0.1, 0.2, 0.5 or 1 mM) for 24 h, prior to 24 h challenge with control medium or medium containing 1  $\mu$ g/ml LPS, in the continued presence of M $\beta$ CD. The maximal concentration of M $\beta$ CD selected was previously used with bovine endometrial stromal cells (Healey et al., 2016).

#### **4.2.7 Treatment of granulosa cells with FSH or LH**

To investigate the crosstalk between innate immunity and endocrine function, granulosa cells were treated for 24 h in serum-free medium containing a range of concentrations of highly purified follicle-stimulating hormone (FSH; 0, 1, 5, 10, 100, or 1000 ng/ml) or luteinizing hormone (LH; 0, 2, 4, 6, 8, or 10 ng/ml). For some experiments, the effect of FSH (2.5  $\mu$ g/ml), alone or in combination with androstenedione (A4;  $10^{-7}$  M) on the innate immune responses to LPS was explored. The concentrations of FSH were selected based on physiological concentrations, and previous studies using bovine granulosa cells (Price and Sheldon, 2013, Price et al., 2013, Bromfield and Sheldon, 2011, Gong et al., 1993). The concentrations of LH selected were based on the physiological concentrations found in bovine follicular fluid (Fortune and Hansel, 1985, Henderson et al., 1982). The concentration of

androstenedione ( $10^{-7}$  M) was selected, as previously described (Gutierrez et al., 1997).

#### 4.2.8 Western blotting

Firstly, granulosa cells from emerged or dominant follicles cultured for 48 h in granulosa cell culture medium containing 10% FBS and examined for the presence of SR-BI or LDLR. Secondly, the effects of lovastatin or M $\beta$ CD treatment followed by LPS challenge on MAPK signalling was examined, because LPS induces MAPK signalling in granulosa cells (Bromfield and Sheldon, 2011, Price et al., 2013, Price and Sheldon, 2013). Based on the results in *Chapter 3*, a 60 min duration of LPS challenge was selected where the LPS-induced phosphorylation of ERK1/2, p38 and JNK were at their maximum. Granulosa cells from emerged or dominant follicles were treated for 24 h with 10  $\mu$ M lovastatin or 1 mM M $\beta$ CD, and then challenged for 60 min with medium containing a final concentration of 1  $\mu$ g/ml LPS. Thirdly, to explore the effects of FSH or serum on the abundance of SR-BI and HMGCR, granulosa cells were treated for 48 h with control, androstenedione (A4;  $10^{-7}$  M), FSH (2.5  $\mu$ g/ml) or FSH + androstenedione (2.5  $\mu$ g/ml and  $10^{-7}$  M, respectively) in medium containing 0%, 2% or 10% FBS. Then, to examine the effects of lovastatin treatment on SR-BI expression, granulosa cells were treated for 48 h with control or 10  $\mu$ M lovastatin and proteins collected for analysis by western blot. Finally, to explore the effects of siRNA on the abundance of SR-BI, granulosa cells were treated 48 h with scramble or siRNA targeting *HMGCR*, *FDPS* or *FDFT1*.

At the end of all experiments, granulosa cells were washed with 300  $\mu$ l of ice-cold phosphate buffered saline (PBS) and lysed with 100  $\mu$ l of PhosphoSafe Extraction Reagent (Novagen), followed by protein quantification (DC Assay; Bio-Rad) and western blot, as described in *Chapter 2*. Briefly, 10  $\mu$ g/lane of protein was probed overnight to quantify the abundance of SR-BI, LDLR, HMGCR, diphosphorylated ERK1/2, ERK1/2, phospho-p38, p38, phospho-JNK and JNK (**Table 2.5**). Protein reactivity was assessed by enhanced chemiluminescence (Clarity Western ECL substrate; Bio-Rad). After imaging, membranes were stripped for 7 min with Restore western Blot Stripping Buffer (Fisher Scientific) and re-probed with another primary

antibody, or with 1:1000 dilution  $\beta$ -actin (Abcam) or  $\alpha$ -tubulin (Cell Signaling) to normalise protein loading. Images were captured using a ChemiDoc XRS System (Bio-Rad). The background-normalised peak band density was measured in the images for each protein using Fiji (Schindelin et al., 2012); target protein bands were normalised to  $\beta$ -actin or  $\alpha$ -tubulin; when antibodies were available, phosphorylated proteins were normalised to their cognate total protein.

#### **4.2.9 ELISA**

The accumulation of IL-1 $\alpha$ , IL-1 $\beta$  and IL-8 was measured in supernatants, as described in *Chapter 2*. The limits of detection for IL-1 $\alpha$ , IL-1 $\beta$ , and IL-8 were 12.5, 31.3, 62.5 pg/ml, respectively. The inter- and intra-assay coefficients of variation for IL-1 $\alpha$ , IL-1 $\beta$  and IL-8 were all < 7% and < 9%, respectively.

#### **4.2.10 MTT Assay**

The MTT assay for cell viability was carried out as described in *Chapter 2*. Briefly, cells were incubated in M199 media containing 0.5 mg/ml MTT (Merck) for 1 h at 37.5°C, in a humidified atmosphere of air containing 5% CO<sub>2</sub>. The medium was then aspirated, washed with D-PBS before cell lysis with dimethyl sulfoxide (DMSO). The absorbance was measured at 570 nm using a microplate reader (POLARstar Omega; BMG).

#### **4.2.11 Short interfering RNA**

Granulosa cells were transfected with Lipofectamine RNA-iMax (Invitrogen) and small interfering RNA (siRNA), as described in *Chapter 2*. The siRNA targeting *HMGCR*, *FDPS* or *FDFT1* were designed using Dharmacon SiDESIGN Center (Thermo Scientific) and published previously (Healey et al., 2016, Griffin et al., 2017). Cells were transfected using scramble siRNA (Horizon Discovery) or siRNA targeting *HMGCR*, *FDPS* or *FDFT1* (*Chapter 2*; **Table 2.7**). Briefly, 750,000 cells/well in 24-well culture plates were cultured for 30 min in 900  $\mu$ l of antibiotic-free granulosa cell culture medium (containing 10% FBS), prior to the addition 100  $\mu$ l OptiMEM



(Thermo Fisher Scientific), containing 2 µl of 20 µM scramble or target siRNA and 1.5 µl Lipofectamine RNA-iMax for 24 h. Following transfection, granulosa cells were challenged for 24 h in granulosa cell culture medium (containing 10% FBS) with vehicle or 1 µg/ml LPS and supernatants collected for measurement of IL-1 $\alpha$ , IL-1 $\beta$  and IL-8. To validate the efficiency of siRNA, granulosa cells were transfected for 48 h prior to the collection of RNA for analysis by qPCR.

At the end of each experiment, granulosa cell supernatants were collected for the measurement of IL-1 $\alpha$ , IL-1 $\beta$  and IL-8 by ELISA, and cell viability was estimated using the MTT assay or RNA was collected for qPCR. Each experiment was performed on at least 3 independent occasions, with each replicate using the granulosa cells pooled from the ovaries of 10 to 20 animals.

#### **4.2.12 Quantitative PCR (qPCR)**

Granulosa cells were washed in 200 µl of ice-cold PBS and lysed using 350 µl of buffer RLT and scraped using the base of a sterile 200 µl tip. Total RNA was extracted using the RNeasy Mini kit (Qiagen), as described in *Chapter 2*. Total RNA was quantified using a NanoDrop spectrophotometer. Complementary DNA (cDNA) was synthesised from 1 µg RNA using the QuantiTect Reverse Transcription kit (Qiagen), as described in *Chapter 2*. The mRNA encoding the genes *HMGCR*, *FDPS* and *FDFT1* were measured by qPCR and expression was normalised to the reference genes *ACTB* and *RLP19*. Sequences for the primers have been published previously and are detailed in **Table 2.10** (*Chapter 2*).

#### **4.2.13 Statistics**

The statistical unit was each independent culture of granulosa cells, collected on separate days and pooled from the ovaries of 10 to 20 animals. Statistical analysis was performed using GraphPad Prism version 9.21 (GraphPad Software). Data were analysed using t test or one-way or two-way ANOVA, using Dunnett's post hoc test, as reported in *Results*. Data are presented as mean (SEM) from at least three independent experiments, and  $P < 0.05$  was considered significant.

### 4.3 Results

#### 4.3.1 Follicular fluid contains mostly HDL cholesterol

The concentration of total cholesterol in bovine follicular fluid was  $1.5 \pm 0.05$  mM (Fig. 4.1A). In the present study, the predominant lipoprotein measured in the follicular fluid of animals was HDL with higher concentrations present in emerged ( $323 \pm 30$   $\mu\text{g/ml}$ ) than dominant ( $307 \pm 31$   $\mu\text{g/ml}$ ) follicles; small concentrations of LDL/VLDL were also measured in emerged ( $42 \pm 13$   $\mu\text{g/ml}$ ) and dominant ( $29 \pm 9$   $\mu\text{g/ml}$ ) follicles (Fig. 4.1B). In FBS, the concentrations of total cholesterol, HDL and LDL/VLDL were  $818 \pm 108$   $\mu\text{g/ml}$ ,  $151 \pm 6$   $\mu\text{g/ml}$ , and  $110 \pm 6$   $\mu\text{g/ml}$ , respectively. As a negative control, in lipoprotein-deficient serum (LDS), the concentrations of total cholesterol, HDL and LDL/VLDL were  $49 \pm 2$   $\mu\text{g/ml}$ ,  $20 \pm 5$   $\mu\text{g/ml}$  and  $3 \pm 2$   $\mu\text{g/ml}$ , respectively.

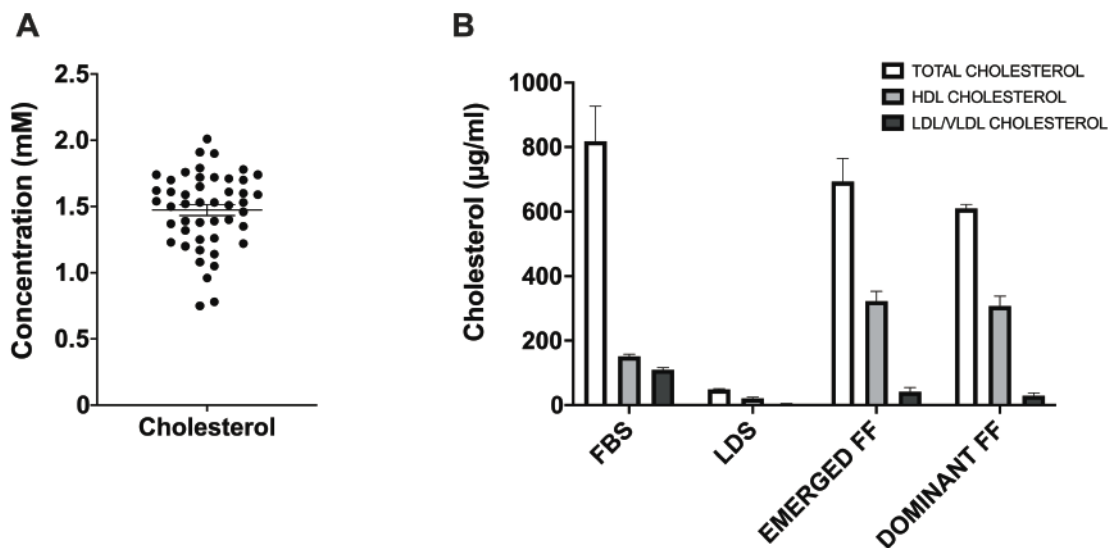


**Figure 4.1. Ovarian follicles contain mostly HDL cholesterol**

Follicular fluid was aspirated from the follicles of beef heifers, and the concentration of total cholesterol quantified using the Randox Daytona Plus Clinical Analyser (A). Total cellular cholesterol, HDL and LDL/VLDL cholesterol was isolated from fetal bovine serum (FBS), lipoprotein-deficient serum (LDS), emerged follicular or dominant follicular fluid and quantified using the Amplex Red cholesterol Assay (B). Data are presented as mean (SEM) from (A) 47 follicles or (B) 3 independent experiments.

### 4.3.2 Granulosa cells express receptors for HDL and LDL uptake

Previously, mRNA for the genes encoding LDLR and SR-BI have been detected in granulosa cells from small (4 to 5 mm diameter) follicles, however, the expression of SR-BI begins to increase around 72 h of culture (Yamashita et al., 2011). The presence of LDLR or SR-BI at the protein level, has not been identified in bovine granulosa cells. To determine whether granulosa cells express scavenger receptor BI (SR-BI) or LDL receptor (LDLR), granulosa cells were cultured for 24 h in granulosa cell culture media (containing 10% FBS), lysed and proteins extracted for analysis by western blot. Granulosa cells from both emerged and dominant follicles express SR-BI and LDLR (Fig. 4.2). Interestingly, granulosa cells from both emerged and dominant follicles expressed more SR-BI protein than LDLR protein (Fig. 4.2;  $P < 0.001$ ). These data suggests that HDL is the predominant lipoprotein present in the follicular fluid of emerged and dominant follicles, and that granulosa cells possess the SR-BI receptors necessary for HDL uptake.

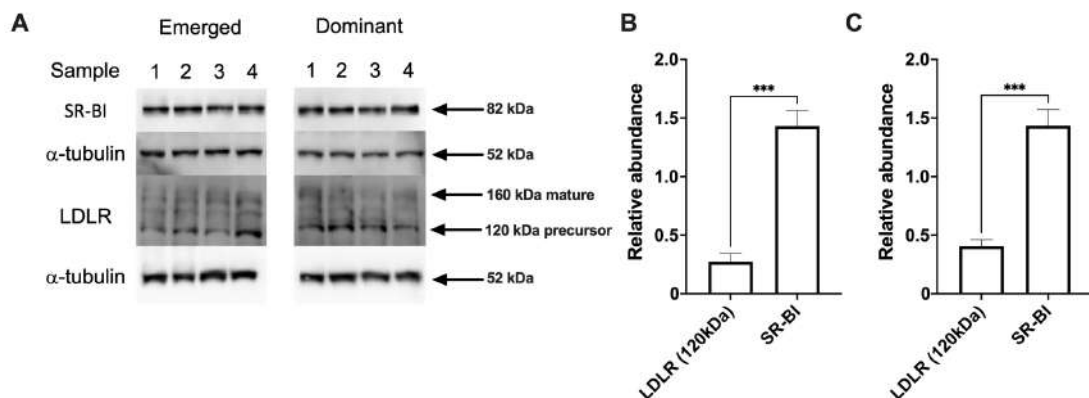


**Figure 4.2. Granulosa cells express more SR-BI than LDL receptor**

The abundance of SR-BI and LDLR in granulosa cells from emerged or dominant follicles was quantified by western blot (A). Granulosa cells were established for 18 h, and then cultured for 48 h in granulosa cell culture medium (containing 10% FBS). The relative abundance of SR-BI and the precursor form of LDLR was quantified (B). Data are presented as mean (SEM) from 4 independent experiments. Data were analysed using t test; \*\*\*  $P < 0.001$ .

### 4.3.3 Factors present in fetal bovine serum or follicular fluid regulate granulosa cell responses to LPS

Granulosa cells cultured in serum-free conditions have previously been shown to have limited responses to LPS (Bromfield and Sheldon, 2011). We treated granulosa cells with the indicated concentrations of FBS (10% providing ~217  $\mu$ M cholesterol) or follicular fluid (5% providing ~75  $\mu$ M cholesterol).

Treatment with less FBS decreased the LPS-induced secretion of IL-1 $\alpha$  and IL-1 $\beta$ , but not IL-8 by granulosa cells from both emerged (**Fig. 4.3A, C**) and dominant (**Fig. 4.3B, D**) follicles. Treatment with more follicular fluid increased the LPS-induced secretion of IL-1 $\alpha$  and IL-8 by granulosa cells from both emerged (**Fig. 4.4A, E**) and dominant (**Fig. 4.4B, F**) follicles. There was a trend for an increase in the LPS-induced secretion of IL-1 $\beta$  following treatment with 4% follicular fluid by granulosa cells from emerged follicles ( $P = 0.06$ ; **Fig. 4.4C**) and following treatment with 5% follicular fluid in granulosa cells from dominant follicles ( $P = 0.12$ ; **Fig. 4.4D**).

Treatment with FBS did not alter the cell viability of granulosa cells from emerged (0% FBS,  $0.91 \pm 0.06$  OD<sub>570</sub> vs. 10% FBS,  $0.83 \pm 0.03$  OD<sub>570</sub>;  $P = 0.08$ , ANOVA,  $n = 3$ ) or dominant (0% FBS,  $0.79 \pm 0.11$  OD<sub>570</sub> vs. 10% FBS,  $0.86 \pm 0.07$  OD<sub>570</sub>;  $P = 0.96$ , ANOVA,  $n = 3$ ) follicles. Additionally, treatment with follicular fluid did not alter cell the cell viability of granulosa cells from emerged (0% FF,  $0.91 \pm 0.06$  OD<sub>570</sub> vs. 5% FF,  $0.83 \pm 0.04$  OD<sub>570</sub>;  $P = 0.2$ , ANOVA,  $n = 3$ ) or dominant (0% FF,  $0.79 \pm 0.11$  OD<sub>570</sub> vs. 5% FF,  $0.65 \pm 0.08$  OD<sub>570</sub>;  $P = 0.78$ , ANOVA,  $n = 3$ ) follicles.

These data suggests that there are factors present in FBS and follicular fluid that may regulate the innate immune responses of granulosa cells to LPS.

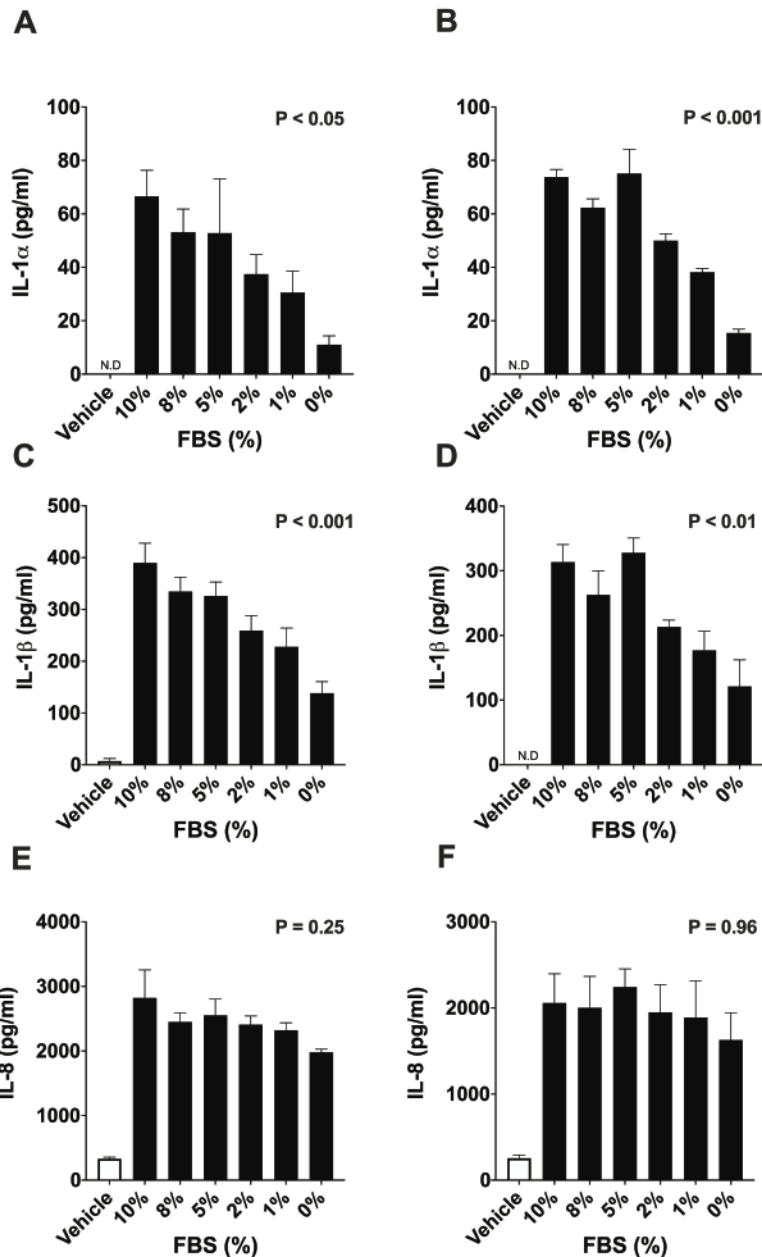


**Figure 4.3. Reducing FBS impairs IL-1 responses in granulosa cells, in response to LPS**

Granulosa cells from emerged (A, C, E) or dominant (B, D, F) follicles were treated for 24 h with vehicle or the indicated final percentage of FBS in serum-free media. Granulosa cells were then challenged for 24 h with control medium (white bars) or medium containing 1  $\mu$ g/ml LPS (black bars), in the continued presence of the treatments. Supernatant IL-1 $\alpha$  (A, B), IL-1 $\beta$  (C, D) or IL-8 (E, F) were measured by ELISA. Data are presented as mean (SEM) from 3 independent experiments. Mean values were compared using one-way ANOVA, and P values reported for the effect of treatment on responses to LPS. N.D = below limit of detection.

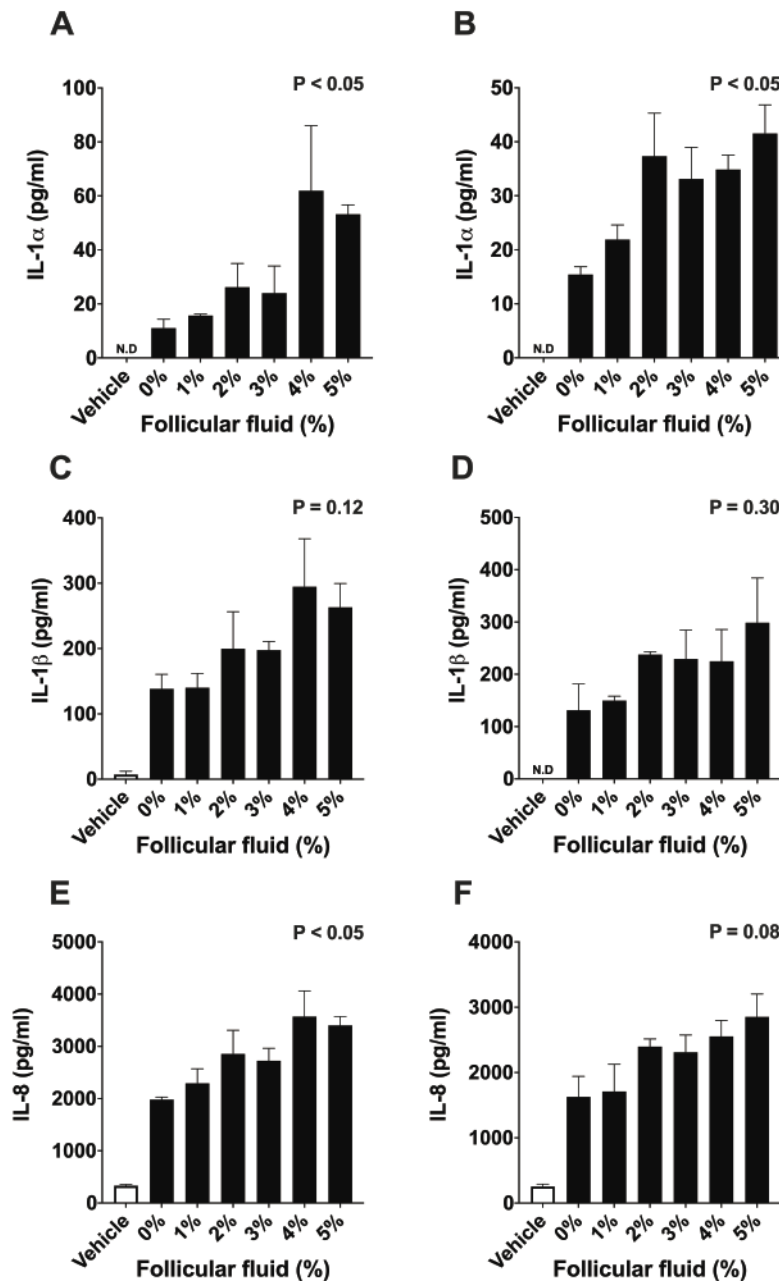


**Figure 4.4. Follicular fluid augments the LPS-induced secretion of IL-1 $\alpha$ , IL-1 $\beta$  and IL-8 by granulosa cells**

Granulosa cells from emerged (A, C, E) or dominant (B, D, F) follicles were treated for 24 h with vehicle or the indicated final percentage of follicular fluid in serum-free media. Granulosa cells were then challenged for 24 h with control medium (white bars) or medium containing 1  $\mu$ g/ml LPS (black bars), in the continued presence of the treatments. Supernatant IL-1 $\alpha$  (A, B), IL-1 $\beta$  (C, D) or IL-8 (E, F) were measured by ELISA. Data are presented as mean (SEM) from 3 independent experiments. Mean values were compared using one-way ANOVA, and P values reported for the effect of treatment on responses to LPS. N.D = below limit of detection.

#### 4.3.4 High density lipoprotein augments granulosa cell IL-1 responses to LPS

Granulosa cells were treated for 24 h with a range of concentrations of HDL cholesterol (0, 5, 10, 20, 50 or 100  $\mu\text{g/ml}$ ) in serum-free culture media, followed by 24 h challenge with control media or 1  $\mu\text{g/ml}$  LPS. The concentrations of HDL used are like those used previously in bovine luteal cells (Carroll et al., 1992, Bao et al., 1997b). Treatment with HDL augmented the LPS-induced secretion of IL-1 $\alpha$  and IL-1 $\beta$  by granulosa cells from emerged (**Fig. 4.5A, C**) and dominant (**Fig. 4.5B, D**) follicles. The secretion of IL-8 was not altered by HDL treatment (**Fig. 4.5E-F**). Specifically, treatment with 100  $\mu\text{g/ml}$  of HDL increased the secretion of IL-1 $\alpha$  by > 300% and IL-1 $\beta$  by 160% by granulosa cells.

Granulosa cells were treated for 24 h with a range of concentrations of LDL (0, 5, 10, 25 or 50  $\mu\text{g/ml}$ ) or VLDL (0, 1, 2, 5 or 10  $\mu\text{g/ml}$ ) cholesterol in serum-free culture media, followed by 24 h challenge with control media or 1  $\mu\text{g/ml}$  LPS. The concentrations of LDL are similar to those used previously in bovine luteal (Bao et al., 1997b), granulosa cells (Zhang et al., 2015), and similar to what we measure to be present in follicular fluid (50  $\mu\text{g/ml}$  = 126  $\mu\text{M}$ ). Additionally, in bovine luteal cells, saturation of the LDL receptors is observed at a concentration of 100  $\mu\text{g/ml}$  (Savion et al., 1981). Treatment with LDL or VLDL did not alter the LPS-induced secretion of IL-1 $\alpha$  (**Fig. 4.6A-B; Fig. 4.7A-B**), IL-1 $\beta$  (**Fig. 4.6C-D; Fig. 4.7C-D**) or IL-8 (**Fig. 4.6E-F; Fig. 4.7E-F**) by granulosa cells. Treatment with HDL did not alter the cell viability of granulosa cells from emerged (0  $\mu\text{g/ml}$  HDL,  $0.91 \pm 0.04$  OD<sub>570</sub> vs. 100  $\mu\text{g/ml}$  HDL,  $0.75 \pm 0.04$  OD<sub>570</sub>;  $P = 0.3$ , ANOVA,  $n = 5$ ) or dominant (0  $\mu\text{g/ml}$  HDL,  $0.82 \pm 0.06$  OD<sub>570</sub> vs. 100  $\mu\text{g/ml}$  HDL,  $0.74 \pm 0.03$  OD<sub>570</sub>;  $P = 0.6$ , ANOVA,  $n = 5$ ) follicles. Treatment with LDL did not alter the cell viability of granulosa cells from emerged (0  $\mu\text{g/ml}$  LDL,  $0.93 \pm 0.23$  OD<sub>570</sub> vs. 50  $\mu\text{g/ml}$  LDL,  $0.82 \pm 0.02$  OD<sub>570</sub>;  $P = 0.97$ , ANOVA,  $n = 3$ ) or dominant (0  $\mu\text{g/ml}$  LDL,  $0.68 \pm 0.09$  OD<sub>570</sub> vs. 50  $\mu\text{g/ml}$  LDL,  $0.69 \pm 0.01$  OD<sub>570</sub>;  $P = 0.86$ , ANOVA,  $n = 3$ ) follicles. Treatment with VLDL did not alter the cell viability of granulosa cells from emerged (0  $\mu\text{g/ml}$  VLDL,  $0.93 \pm 0.23$  OD<sub>570</sub> vs. 10  $\mu\text{g/ml}$  VLDL,  $0.74 \pm 0.1$  OD<sub>570</sub>;  $P = 0.93$ , ANOVA,  $n = 3$ ) or dominant (0  $\mu\text{g/ml}$  VLDL,  $0.68 \pm 0.09$  OD<sub>570</sub> vs. 10  $\mu\text{g/ml}$  VLDL,  $0.72 \pm 0.15$  OD<sub>570</sub>;  $P = 0.97$ , ANOVA,  $n = 3$ ) follicles.

These data suggest that there may be a role for HDL, but not LDL or VLDL in the innate immune responses of granulosa cells to LPS.

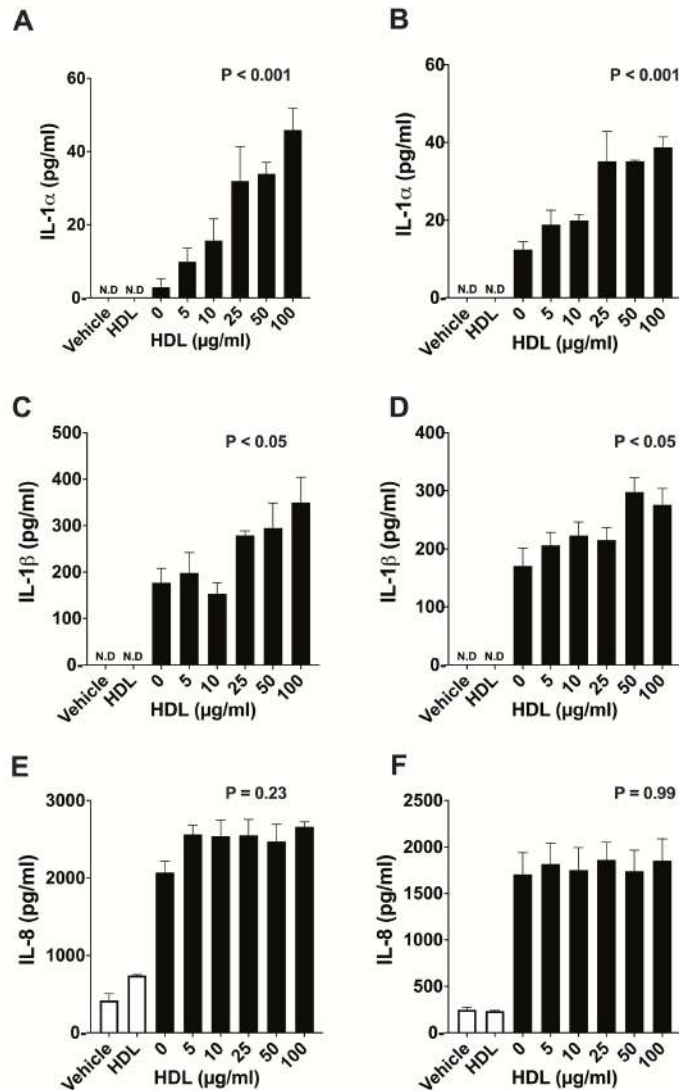


**Figure 4.5. High-density lipoprotein augments the LPS-induced secretion of IL-1 $\alpha$  and IL-1 $\beta$  by granulosa cells**

Granulosa cells from emerged (A, C, E) or dominant (B, D, F) follicles were treated for 24 h with vehicle, HDL (100  $\mu\text{g/ml}$ ) or the indicated final concentrations of HDL in serum-free media. Granulosa cells were then challenged for 24 h with control medium (white bars) or medium containing 1  $\mu\text{g/ml}$  LPS (black bars), in the continued presence of the treatments. Supernatant IL-1 $\alpha$  (A, B), IL-1 $\beta$  (C, D) or IL-8 (E, F) were measured by ELISA. Mean values were compared using one-way ANOVA, and P values reported for the effect of treatment on responses to LPS. N.D = below limit of detection.



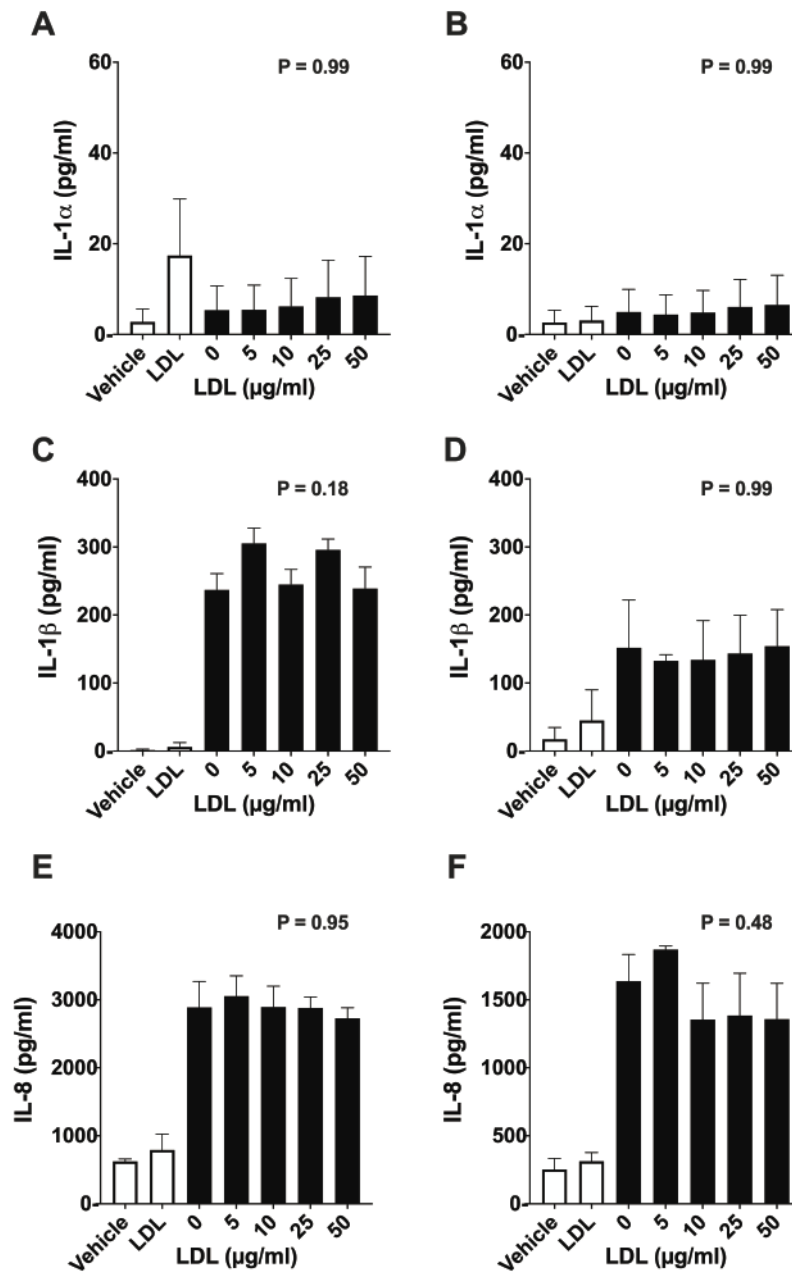


**Figure 4.6. Low-density lipoprotein does not alter the LPS-induced secretion of IL-1 $\alpha$ , IL-1 $\beta$  or IL-8 by granulosa cells**

Granulosa cells from emerged (A, C, E) or dominant (B, D, F) follicles were treated for 24 h with vehicle, LDL (50  $\mu$ g/ml) or the indicated concentrations of LDL in serum-free media. Granulosa cells were then challenged for 24 h with control medium (white bars) or medium containing 1  $\mu$ g/ml LPS (black bars) in the continued presence of the treatments. The accumulation of supernatant IL-1 $\alpha$  (A, B), IL-1 $\beta$  (C, D) and IL-8 (E, F) were measured by ELISA. Data are presented as mean (SEM) from 3 independent experiment. Data were analysed by one-way ANOVA, and P values reported for the effect of treatment on responses to LPS.

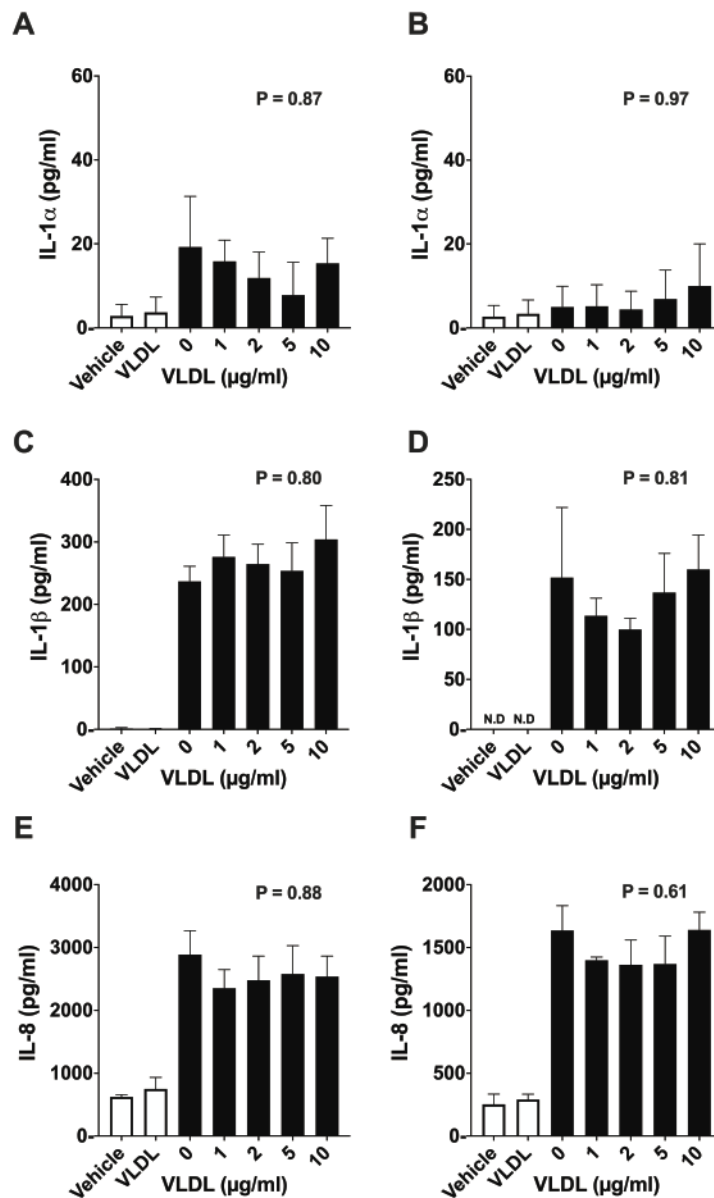


**Figure 4.7. Very low-density lipoprotein does not alter the LPS-induced secretion of IL-1 $\alpha$ , IL-1 $\beta$  or IL-8 by granulosa cells**

Granulosa cells from emerged (A, C, E) or dominant (B, D, F) follicles were treated for 24 h with vehicle, VLDL (10  $\mu$ g/ml) or the indicated concentrations of VLDL in serum-free media. Granulosa cells were then challenged for 24 h with control medium (white bars) or medium containing 1  $\mu$ g/ml LPS (black bars) in the continued presence the treatments. The accumulation of supernatant IL-1 $\alpha$  (A, B), IL-1 $\beta$  (C, D) and IL-8 (E, F) were measured by ELISA. Data are presented as mean (SEM) from 3 independent experiment. Data were analysed by one-way ANOVA, and P values reported for the effect of treatment on responses to LPS. N.D = below limit of detection.

#### 4.3.5 Depletion of available cholesterol impairs granulosa cell responses to LPS.

There are three pools of cholesterol in the plasma membrane of cells: the essential pool, a sphingomyelin sequestered pool, and a labile pool (Das et al., 2014). *In vitro*, the labile cholesterol pool can be depleted using M $\beta$ CD, a cyclic oligosaccharide that binds cholesterol (Kilsdonk et al., 1995, Christian et al., 1997). Methyl- $\beta$ -cyclodextrin was mixed to the indicated concentrations in granulosa cell culture medium, containing 10% FBS, 5 min prior to cell treatments. Granulosa cells were treated for 24 h with a range of concentrations of M $\beta$ CD (0, 0.1, 0.2, 0.5, 1 mM). Granulosa cells were then challenged for 24 h with control media or media containing 1  $\mu$ g/ml LPS, in the continued presence of the treatments. A glucocorticoid, 1  $\mu$ M dexamethasone, was used as a reference anti-inflammatory agent (Bhattacharyya et al., 2007).

Treatment with M $\beta$ CD reduced the LPS-induced secretion of IL-1 $\alpha$  (**Fig. 4.8A-B**) and IL-1 $\beta$  (**Fig. 4.8C-D**) by granulosa cells from both emerged and dominant follicles. However, treatment with M $\beta$ CD reduced the LPS-induced secretion of IL-8 in emerged (**Fig. 4.8E**), but not dominant (**Fig. 4.8F**) follicles. Specifically, treatment with 1 mM M $\beta$ CD reduced the LPS-induced secretion of IL-1 $\alpha$  by 82%, IL-1 $\beta$  by > 52% and IL-8 by 20%.

Treatment with M $\beta$ CD did not alter the amount of protein per culture well in granulosa cells from emerged (control,  $2.1 \pm 0.36$  mg protein vs. M $\beta$ CD,  $1.9 \pm 0.33$  mg;  $P = 0.72$ , ANOVA,  $n = 4$ ) and dominant (control,  $1.5 \pm 0.2$  mg protein vs. M $\beta$ CD,  $1.2 \pm 0.29$ ;  $P = 0.50$ , ANOVA,  $n = 4$ ). Additionally, treatment with M $\beta$ CD did not alter cell viability of granulosa cells from emerged (control,  $0.9 \pm 0.02$  OD<sub>570</sub> vs. M $\beta$ CD,  $1.0 \pm 0.06$  OD<sub>570</sub>;  $P = 0.07$ , ANOVA,  $n = 4$ ) or dominant (control,  $0.64 \pm 0.1$  OD<sub>570</sub> vs. M $\beta$ CD,  $0.94 \pm 0.09$  OD<sub>570</sub>;  $P = 0.09$ , ANOVA,  $n = 4$ ) follicles.

These data suggest that the availability of cholesterol may be important in the innate immune function of granulosa cells.

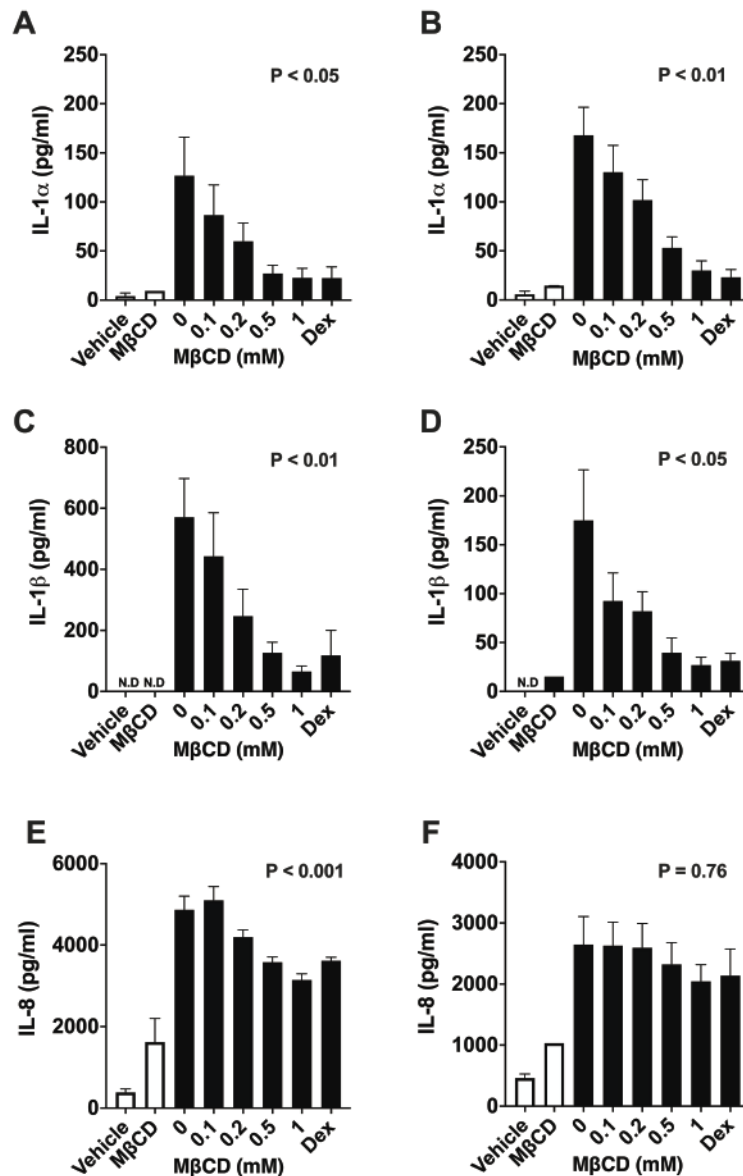


**Figure 4.8. Methyl- $\beta$ -cyclodextrin treatment reduces the LPS-induced secretion of IL-1 $\alpha$ , IL-1 $\beta$  and IL-8 by granulosa cells**

Granulosa cells from emerged (A, C, E) or dominant (B, D, F) follicles were treated for 24 h with vehicle, methyl- $\beta$ -cyclodextrin (M $\beta$ CD; 1 mM), dexamethasone (Dex; 1  $\mu$ M) or the indicated concentrations of M $\beta$ CD. Granulosa cells were then challenged for 24 h with control medium (white bars) or medium containing 1  $\mu$ g/ml LPS in the continued presence of the treatments. The accumulation of supernatant IL-1 $\alpha$  (A, B), IL-1 $\beta$  (C, D) and IL-8 (E, F) were measured by ELISA. Data are presented as mean (SEM) from 4 independent experiments. Mean values were compared using one-way ANOVA, and P values reported for the effect of treatment on responses to LPS. N.D = below limit of detection.

#### 4.3.6 RNA interference of mevalonate pathway enzymes impairs granulosa cell responses to LPS

Short interfering RNA (siRNA) has previously been used in bovine stromal and epithelial cells to reduce the expression of *HMGCR*, *FDPS* or *FDFTI* (Healey et al., 2016, Griffin et al., 2017, Griffin et al., 2018).

Granulosa cells were transfected with scramble siRNA or siRNA targeting *HMGCR*, *FDPS* or *FDFTI* for 24 h in antibiotic-free granulosa cell culture medium (containing 10% FBS), prior to 24 h challenge control medium (containing 10% FBS) or medium containing 1 µg/ml LPS (containing 10% FBS). Surprisingly, compared to scramble, siRNA knockdown of any one of the RNA encoding mevalonate pathway enzymes reduced the secretion of IL-1 $\alpha$ , IL-1 $\beta$  and IL-8 by granulosa cells from emerged (**Fig. 4.9A, C, E**) and dominant (**Fig. 4.9B, D, F**) follicles. Specifically, knockdown of *HMGCR* reduced the LPS-induced secretion of IL-1 $\alpha$  by > 69%, IL-1 $\beta$  by > 35% and IL-8 by > 62%; knockdown of *FDPS* reduced the LPS-induced secretion of IL-1 $\alpha$  by > 35%, IL-1 $\beta$  by 57% and IL-8 by > 36%; knockdown of *FDFTI* reduced the LPS-induced secretion of IL-1 $\alpha$  by > 40%, IL-1 $\beta$  by > 46% and IL-8 by > 55% (**Fig. 4.9**).

Quantitative PCR was used to validate the efficiency of siRNA knockdowns of the RNA targets (**Fig. 4.10**). Unfortunately, only knockdowns of *HMGCR* (**Fig. 4.10B**) and *FDPS* (**Fig. 4.10D**) in granulosa cells from dominant follicles showed a statistically significant reduction in expression. There was a trend for decrease in the expression of *HMGCR*, *FDPS* and *FDFTI* following knockdown in granulosa cells from emerged follicles (**Fig. 4.10A, C, E**), as well as for *FDFTI* in granulosa cells from dominant follicles (**Fig. 4.10F**). When converted to percentage of scramble control, reductions could be observed in the expression of *HMGCR* (emerged, 26% reduction; dominant, 33% reduction), *FDPS* (emerged, 45% reduction; dominant, 71% reduction) and *FDFTI* (emerged, 30% reduction; dominant, 40% reduction). Treatment with siRNA did not reduce the cell viability of granulosa cells from either follicle size (emerged, ANOVA P = 0.84, n = 5; dominant, ANOVA P = 0.26, n = 3).

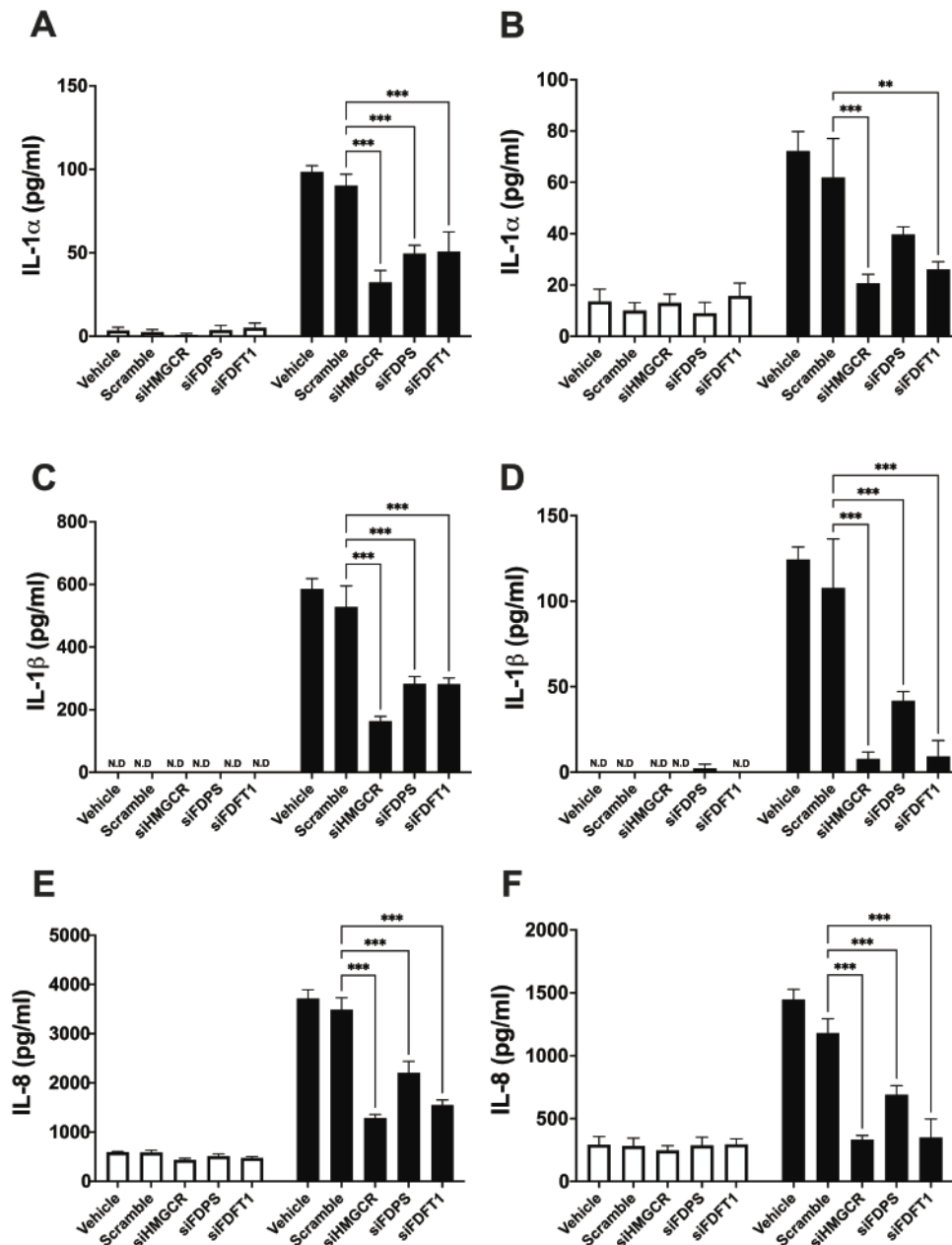


**Figure 4.9. RNA interference in granulosa cells reduces the innate immune response to LPS**

Granulosa cells from emerged (A, C, E) or dominant (C, D, F) follicles were transfected with scramble siRNA or siRNA targeting *HMGCR*, *FDPS* or *FDFT1* for 24 h. Granulosa cells were then challenged for 24 h with control medium or medium containing 1  $\mu\text{g/ml}$  LPS. The accumulation of IL-1 $\alpha$  (A-B), IL-1 $\beta$  (C-D) or IL-8 (E-F) was measured by ELISA. Data are presented as mean (SEM) from at least 4 independent experiments. Data were analysed by two-way ANOVA using Dunnett's post hoc test; values differ from scramble, \*\*\*  $P < 0.001$ , \*\*  $P < 0.01$ , \*  $P < 0.05$ . N.D = below limit of detection.

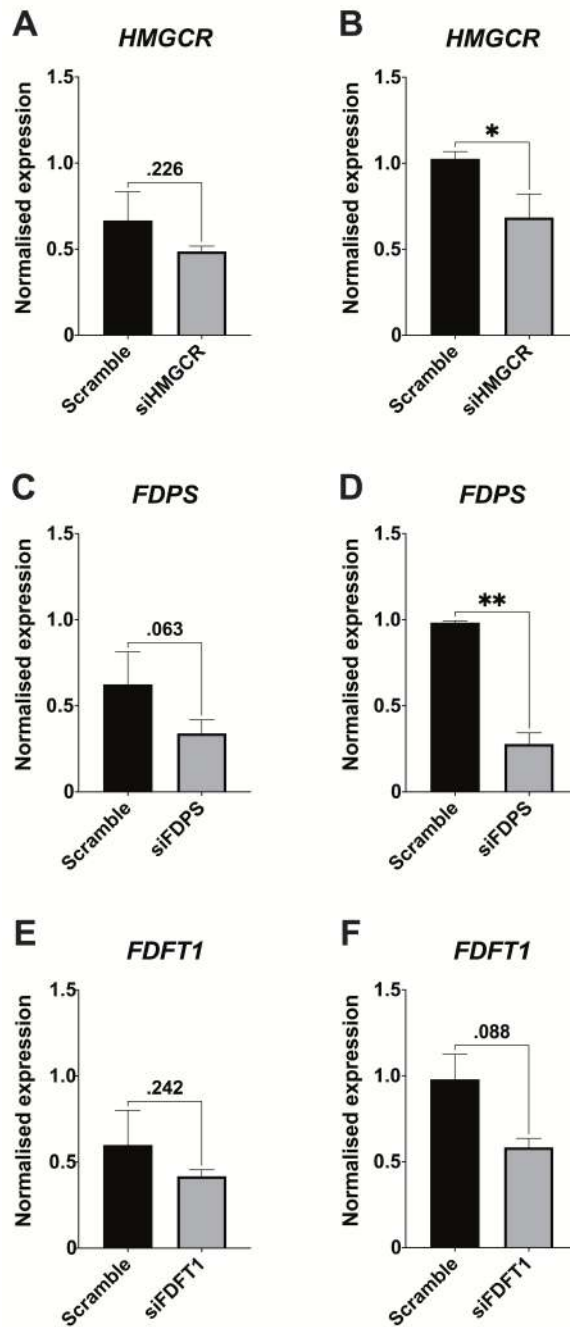


**Figure 4.10. RNA interference reduced the gene expression of *HMGCR*, *FDPS* or *FDFT1***

Granulosa cells from emerged (A, C, E) or dominant (B, D, F) follicles were transfected with scramble siRNA or siRNA targeting *HMGCR* (A, B), *FDPS* (C, D) or *FDFT1* (E, F) for 48 h and gene expression measured by qPCR. Data are presented as mean (SEM) from three independent experiments. Gene expression was normalised against *ACTB* and *RLP19*. Data were analysed by t test from 3 independent experiments; values differ from scramble, \*\* P < 0.01; \*P < 0.05. Where differences are not significant, P values are displayed.

#### **4.3.7 Inhibitors of the mevalonate pathway augment granulosa cell responses to LPS.**

We used inhibitors lovastatin, alendronate or zaragozic acid to inhibit HMGCR, FDPS or FDFT1, respectively. Treatments were carried out in medium containing 10% FBS. Dexamethasone, (1  $\mu$ M), was used as a reference anti-inflammatory agent (Bhattacharyya et al., 2007, Horlock et al., 2021).

Treatment with lovastatin, alendronate or zaragozic acid increased the LPS-induced secretion of IL-1 $\alpha$  and IL-1 $\beta$  by granulosa cells from emerged (**Fig. 4.11A, C; Fig. 4.12A, C; Fig. 4.13A, C**) and dominant (**Fig. 4.11B, D; Fig. 4.12B, D; Fig. 4.13B, D**) follicles. Specifically, treatment with 10  $\mu$ M lovastatin increased the LPS-induced secretion of IL-1 $\alpha$  by > 292% and IL-1 $\beta$  by 212%; treatment with 10  $\mu$ M alendronate increased the LPS-induced secretion of IL-1 $\alpha$  by > 145% and IL-1 $\beta$  by 121%; treatment with 10  $\mu$ M zaragozic acid increased the LPS-induced secretion of IL-1 $\alpha$  by > 19% and IL-1 $\beta$  by 8%.

Treatment with lovastatin, alendronate or zaragozic acid did not alter the LPS-induced secretion of IL-8 by granulosa cells from either follicle size (**Fig. 4.11E, F; Fig. 4.12E, F; Fig. 4.13E, F**). Treatment with 10  $\mu$ M lovastatin, 10  $\mu$ M alendronate, or 10  $\mu$ M zaragozic acid did not alter cell viability (emerged, ANOVA P = 0.1, n = 5; dominant, ANOVA P = 0.76, n = 3) or protein abundance (emerged, ANOVA P = 0.92, n = 5; dominant, ANOVA P = 0.95, n = 5).

These data suggest that small molecule inhibitors of cholesterol biosynthesis increase the IL-1 responses to LPS in granulosa cells.



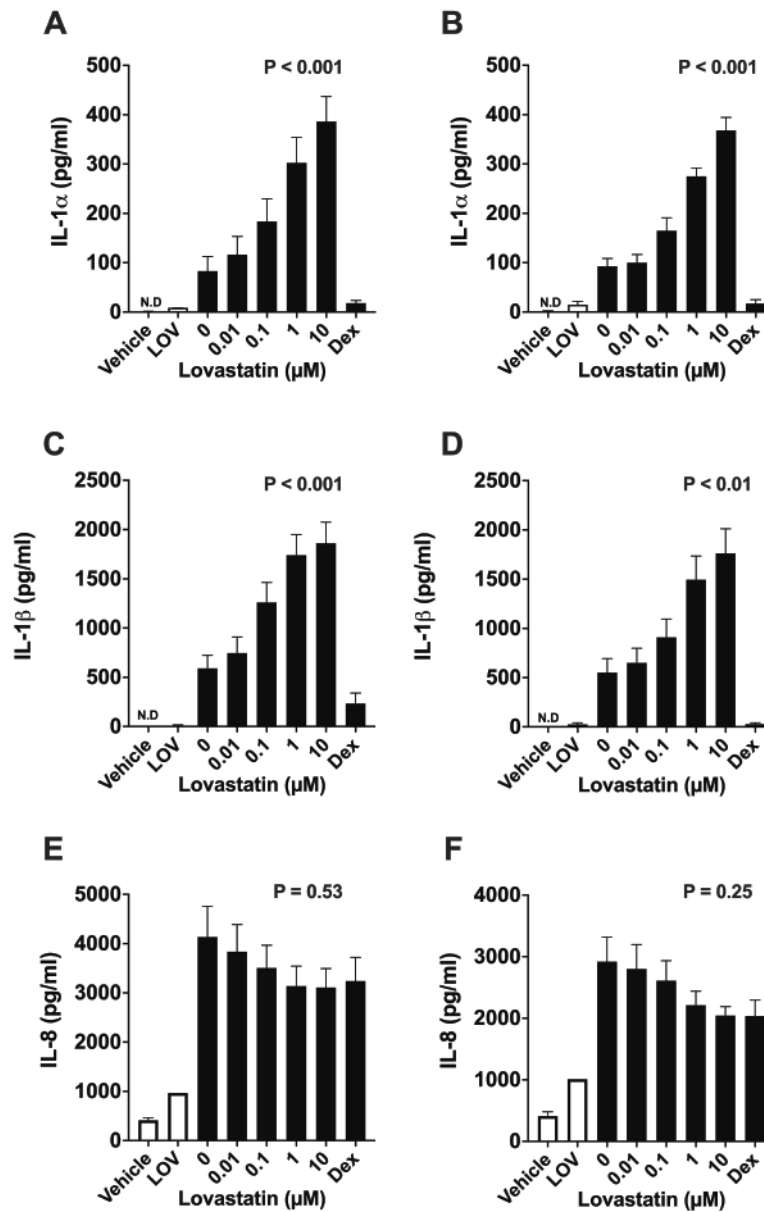


**Figure 4.11. Lovastatin treatment increases the LPS-induced secretion of IL-1 $\alpha$  and IL-1 $\beta$  by granulosa cells**

Granulosa cells from emerged (A, C, E) or dominant (B, D, F) follicles were treated for 24 h with vehicle, lovastatin (LOV; 10  $\mu$ M), dexamethasone (Dex; 1  $\mu$ M) or the indicated concentrations of lovastatin. Granulosa cells were then challenged for 24 h with control medium (white bars) or medium containing 1  $\mu$ g/ml LPS (black bars), in the continued presence of the treatments. Supernatant IL-1 $\alpha$  (A, B), IL-1 $\beta$  (C, D) or IL-8 (E, F) were measured by ELISA. Data are presented as mean (SEM) from at least 3 independent experiments. Mean values were compared using one-way ANOVA, and P values reported for the effect of treatment on responses to LPS. N.D = below limit of detection.

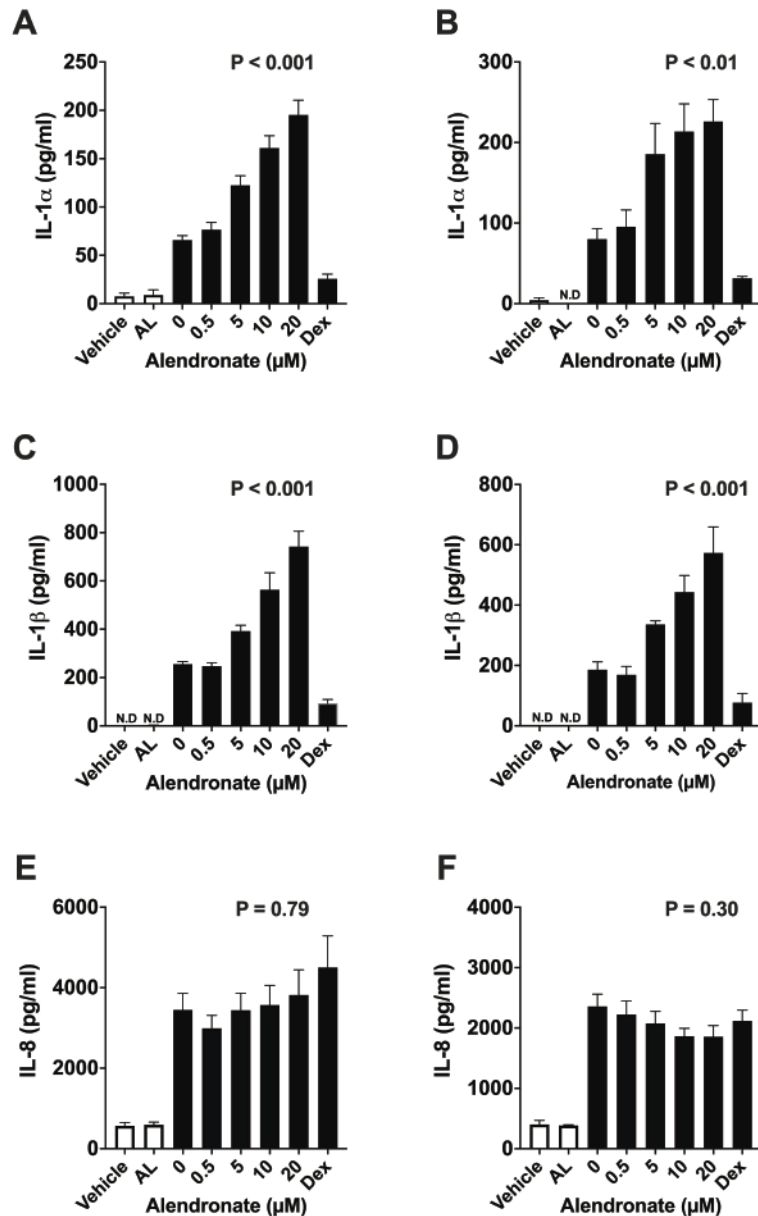


**Figure 4.12. Alendronate treatment increases the LPS-induced secretion of IL-1 $\alpha$  and IL-1 $\beta$  by granulosa cells**

Granulosa cells from emerged (A, C, E) or dominant (B, D, F) follicles were treated for 24 h with vehicle, alendronate (AL; 10  $\mu$ M), dexamethasone (Dex; 1  $\mu$ M) or the indicated concentrations of alendronate. Granulosa cells were then challenged for 24 h with control medium (white bars) or medium containing 1  $\mu$ g/ml LPS (black bars), in the continued presence of the treatments. Supernatant IL-1 $\alpha$  (A, B), IL-1 $\beta$  (C, D) or IL-8 (E, F) were measured by ELISA. Data are presented as mean (SEM) from at least 3 independent experiments. Mean values were compared using one-way ANOVA, and P values reported for the effect of treatment on responses to LPS. N.D. = below limit of detection.

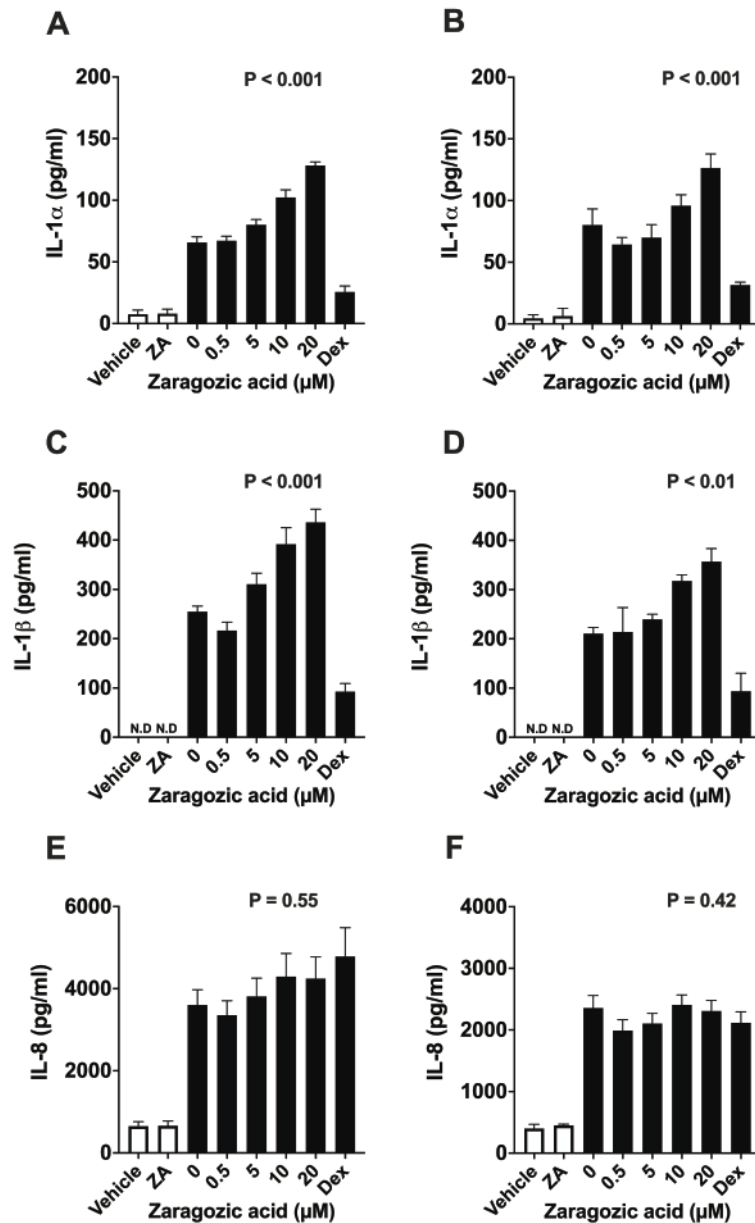


**Figure 4.13. Zaragozic acid treatment increases the LPS-induced secretion of IL-1 $\alpha$  and IL-1 $\beta$  by granulosa cells**

Granulosa cells from emerged (A, C, E) or dominant (B, D, F) follicles were treated for 24 h with vehicle, zaragozic acid (ZA; 10  $\mu$ M), dexamethasone (Dex; 1  $\mu$ M) or the indicated concentrations of zaragozic acid. Granulosa cells were then challenged for 24 h with control medium (white bars) or medium containing 1  $\mu$ g/ml LPS (black bars), in the continued presence of the treatments. Supernatant IL-1 $\alpha$  (A, B), IL-1 $\beta$  (C, D) or IL-8 (E, F) were measured by ELISA. Data are presented as mean (SEM) from at least 3 independent experiments. Mean values were compared using one-way ANOVA, and P values reported for the effect of treatment on responses to LPS. N.D. = below limit of detection.

#### **4.3.8 Inhibitors of the mevalonate pathway reduce cellular cholesterol in serum-free conditions.**

To investigate whether treatment with lovastatin, alendronate or zaragozic acid decrease total cellular cholesterol concentrations, granulosa cells were treated for 48 h with 1 µg/ml LPS, 10 µM lovastatin, 10 µM alendronate, 10 µM zaragozic acid or 1 mM methyl-β-cyclodextrin in either serum-free culture medium or culture medium containing 10% FBS.

In serum-free conditions, treatment with lovastatin decreased the cholesterol concentrations by ~ 25%, alendronate by ~ 20%, zaragozic acid by ~ 17% and methyl-β-cyclodextrin by ~ 37% in granulosa cells from emerged and dominant follicles (**Fig. 4.14A**). Interestingly, treatment with 1 µg/ml LPS decreased cellular cholesterol concentrations by ~ 15%.

When granulosa cells were treated with the compounds in serum-containing conditions (10% FBS), the reductions in total cellular cholesterol concentrations were reversed. There were no significant changes to cellular cholesterol concentrations by any of the treatments in granulosa cells from dominant follicles (**Fig. 4.14B**). Surprisingly, treatment of granulosa cells from emerged follicles with alendronate increased cholesterol concentrations by ~ 39% ( $P < 0.05$ ). There was also a trend for an increase in cellular cholesterol concentrations following treatment with zaragozic acid ~ 34% ( $P = 0.09$ ).

These data indicate that inhibitors of the cholesterol biosynthesis pathway or methyl-β-cyclodextrin decrease total cellular cholesterol concentrations in serum-free, but not serum-containing conditions., possibly due to the presence of cholesterol in FBS (providing ~217 µM cholesterol at final concentration).

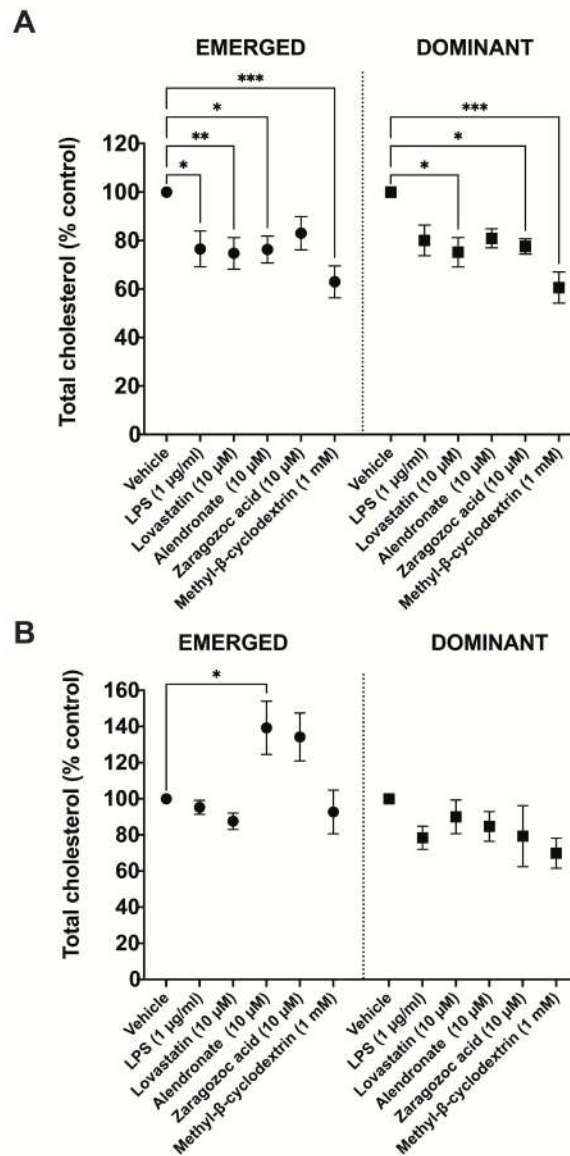


**Figure 4.14. Treatment of granulosa cells with LPS, lovastatin, alendronate, zaragozic acid or methyl-β-cyclodextrin reduce total cellular cholesterol in serum-starved, but not serum containing conditions**

Granulosa cells from emerged (left panel) or dominant (right panel) follicles were treated for 24 h with vehicle, lovastatin (10 µM), alendronate (10 µM), zaragozic acid (10 µM) or methyl-β-cyclodextrin (1 mM) in serum-free medium (A) or medium containing 10% FBS (B). Granulosa cells were then challenged with serum-free control medium (A) or control medium containing 10% FBS (B). The concentrations of total cellular cholesterol were measured by Amplex Red Cholesterol Assay. Data are presented as percentage of control (SEM) from at least 4 independent experiments. Data were analysed by two-way ANOVA using Dunnett's post hoc test. Values differ from vehicle, \*\*\*  $P < 0.001$ , \*\*  $P < 0.01$ , \*  $P < 0.05$ .

### 4.3.9 Re-feeding mevalonic acid or FPP partially reverse mevalonate inhibitor effects on IL-1

HMG-CoA reductase (HMGCR) converts HMG-CoA into mevalonate, which is followed by a series of enzymatic steps, converting mevalonate into isoprenoids, and isoprenoids into FPP by farnesyl diphosphate synthase (FDPS). Statins, such as lovastatin inhibit HMGCR and deplete mevalonate, whereas bisphosphonates such as alendronate deplete FPP.

Lovastatin treatment increased the LPS-induced secretion of IL-1 $\alpha$  ( $P < 0.05$ ) and IL-1 $\beta$  ( $P < 0.01$ ) by granulosa cells from emerged and dominant follicles (**Fig. 4.15**). Treatment with mevalonic acid reduced the lovastatin-induced secretion of IL-1 $\alpha$  ( $P < 0.001$ ) and IL-1 $\beta$  ( $P < 0.05$ ) by granulosa cells from emerged follicles (**Fig. 4.15A, C**), but not dominant follicles (**Fig. 4.15B, D**).

Alendronate treatment increased the LPS-induced secretion of IL-1 $\alpha$  ( $P < 0.001$ ) and IL-1 $\beta$  ( $P < 0.001$ ) by granulosa cells from emerged follicles (**Fig. 4.16A, C**), and increased the LPS-induced secretion of IL-1 $\beta$  ( $P < 0.05$ ) by granulosa cells from dominant follicles (**Fig. 4.16B, D**). Treatment with FPP decreased the alendronate-induced secretion of IL-1 $\beta$  by granulosa cells from emerged ( $P < 0.05$ ) and there was a trend for a decreased in IL-1 $\beta$  secretion by granulosa cells from dominant follicles ( $P = 0.12$ ) (**Fig. 4.16**).

Together, these data provide evidence that the augmentation of the IL-1 response to LPS in granulosa cells was due to the inhibition of HMGCR or FDPS by lovastatin or alendronate, respectively.

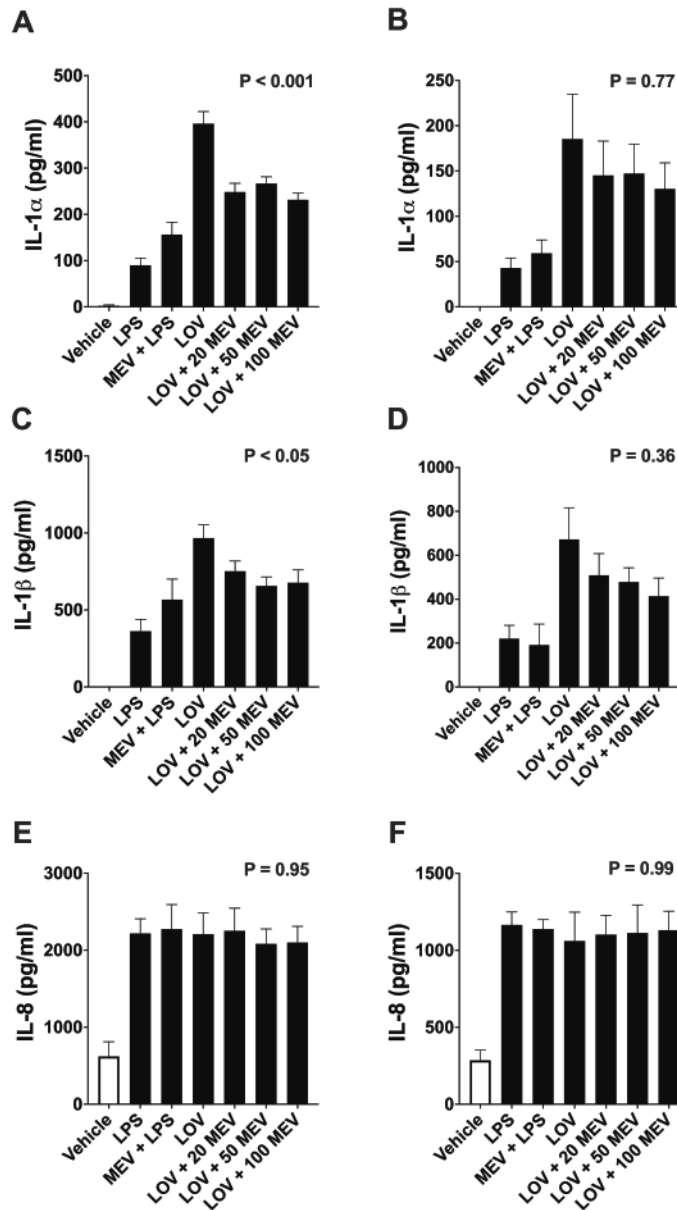


**Figure 4.15. Refeeding mevalonate reduced the lovastatin-induced secretion of IL-1 $\alpha$  and IL-1 $\beta$  by granulosa cells**

Granulosa cells from emerged (A, C, E) or dominant (B, D, F) follicles were treated for 24 h with vehicle or lovastatin (LOV) in combination with the indicated concentrations of mevalonic acid (MEV). Granulosa cells were then challenged with control medium (white bars) or medium containing 1  $\mu$ g/ml LPS (black bars), in the continued presence of the treatments. Supernatant IL-1 $\alpha$  (A, B), IL-1 $\beta$  (C, D) or IL-8 (E, F) were measured by ELISA. Data are presented as mean (SEM) from at least 3 independent experiments. Data were analysed using one-way ANOVA, and P values reported for the effect of treatment on responses to LOV. N.D = below limit of detection.

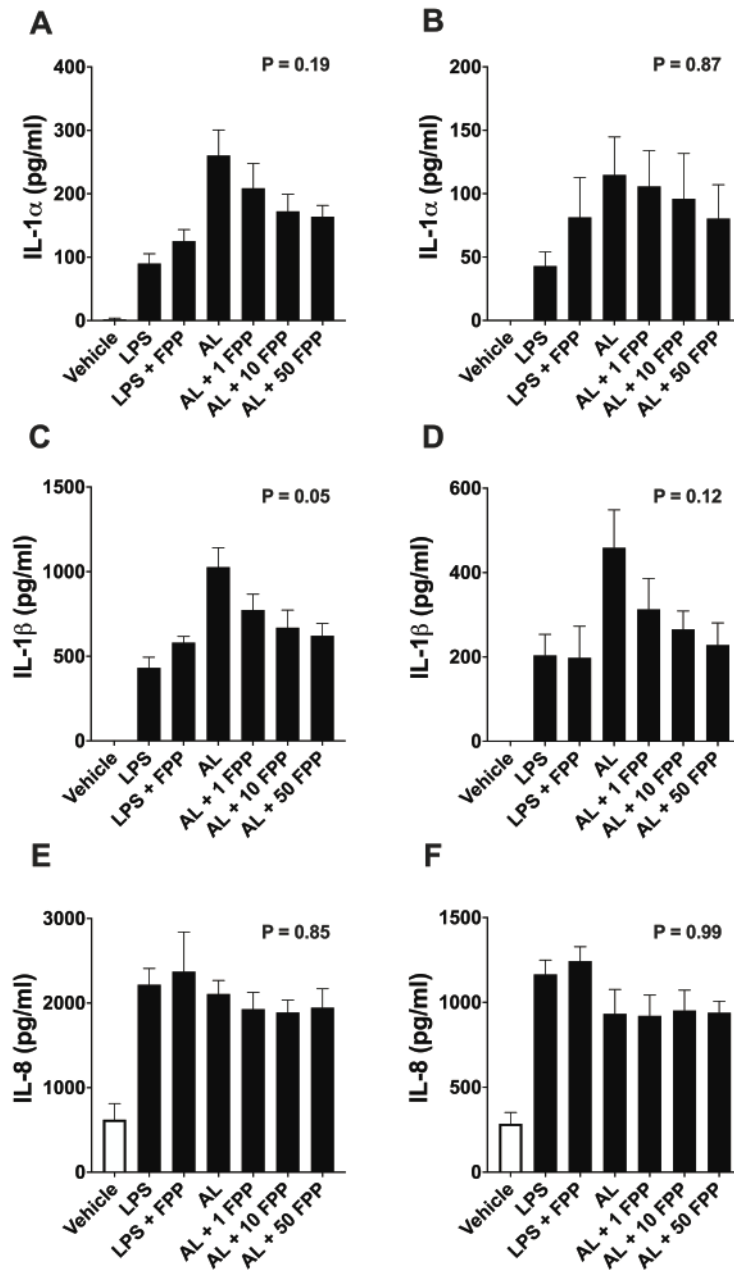


**Figure 4.16. Refeeding FPP reduced the alendronate-induced secretion of IL-1 $\beta$  by granulosa cells**

Granulosa cells from emerged (A, C, E) or dominant (B, D, F) follicles were treated for 24 h with vehicle or alendronate (AL) in combination with the indicated concentrations of farnesyl pyrophosphate (FPP). Granulosa cells were then challenged with control medium (white bars) or medium containing 1  $\mu$ g/ml LPS (black bars), in the continued presence of the treatments. Supernatant IL-1 $\alpha$  (A, B), IL-1 $\beta$  (C, D) or IL-8 (E, F) were measured by ELISA. Data are presented as mean (SEM) from at least 3 independent experiments. Data were analysed using one-way ANOVA, and P values reported for the effect of treatment on responses to AL. N.D = below limit of detection.



#### **4.3.10 Lovastatin or methyl- $\beta$ -cyclodextrin do not alter LPS-induced MAPK activation.**

Granulosa cell responses to LPS are associated with an increase in the phosphorylation of MAPKs, such as ERK1/2 and p38 (Price and Sheldon, 2013, Price et al., 2013, Bromfield and Sheldon, 2011). In the previous chapter, the phosphorylation of ERK1/2, p38 and JNK was increased within 2 h of LPS challenge; specifically, maximal phosphorylation of MAPKs was observed at 60 min following challenge with LPS. Treatment with AICAR shortened the duration of LPS-induced ERK1/2 and JNK phosphorylation. Therefore, the effects of lovastatin or M $\beta$ CD treatment on the LPS-induced phosphorylation of ERK1/2, p38 and JNK was investigated.

Granulosa cells were treated for 24 h with vehicle, lovastatin (10  $\mu$ M) or M $\beta$ CD (1 mM) and challenged for 60 min with 1  $\mu$ g/ml LPS. Compared with vehicle, LPS increased the phosphorylation of ERK1/2 (emerged,  $P < 0.001$ ; dominant,  $P < 0.05$ ), p38 (emerged,  $P < 0.001$ ; dominant,  $P < 0.01$ ) and JNK (emerged,  $P < 0.01$ ; dominant,  $P < 0.05$ ) in granulosa cells from emerged (**Fig. 4.17**) and dominant (**Fig. 4.18**) follicles.

Surprisingly, treatment with lovastatin or methyl- $\beta$ -cyclodextrin reduced the LPS-induced phosphorylation of ERK1/2 in granulosa cells from emerged follicles but did not alter the phosphorylation of p38 or JNK (**Fig. 4.17**). There were no differences in MAPK phosphorylation with lovastatin treatment in granulosa cells from dominant follicles, however methyl- $\beta$ -cyclodextrin decreased the LPS-induced phosphorylation of JNK (**Fig. 4.18**).

These data suggest that the altered IL-1 responses to LPS seen with lovastatin or methyl- $\beta$ -cyclodextrin treatment may not be mediated via altered MAPK phosphorylation.

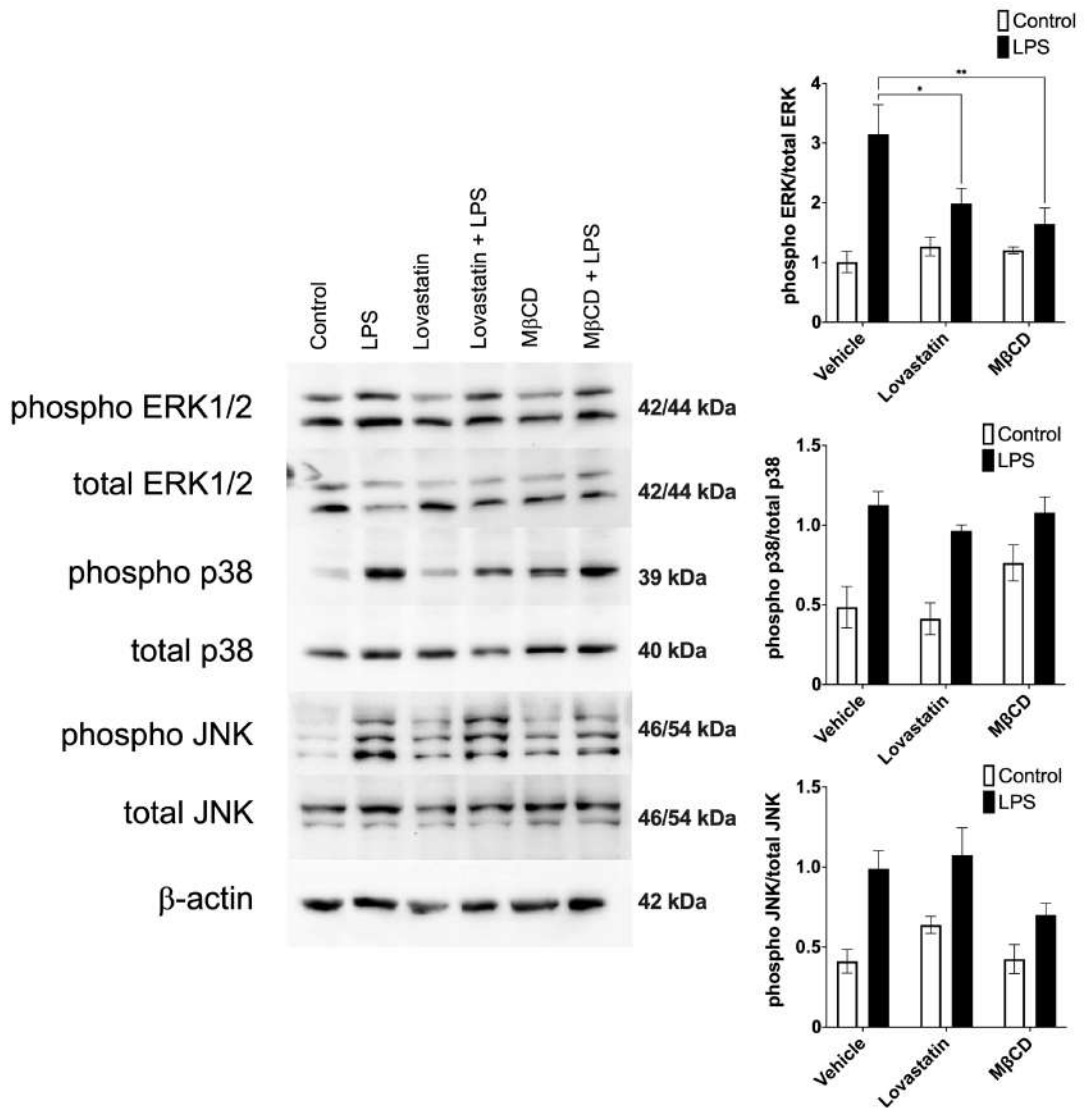


**Figure 4.17. Lovastatin and MβCD reduces the LPS-induced abundance of phosphorylated ERK1/2 in granulosa cells from emerged follicles**

Granulosa cells from emerged follicles were treated for 48 h with granulosa cell culture medium containing vehicle, lovastatin (10 μM) or MβCD (1 mM) prior to challenge for 60 min with either control medium or medium containing 1 μg/ml LPS and the abundance of phosphorylated ERK1/2, p38 or JNK analysed by western blot. Representative western blots of phospho ERK1/2, ERK1/2, phospho p38, p38, phospho JNK, JNK and β-actin are shown on the left. Quantification of band densities normalised to the total protein are presented on the right. Data are presented as mean (SEM) from 3 independent experiments. Data were analysed by two-way ANOVA using Dunnett's post hoc test. Values differ from control, \*\* P < 0.01, \* P < 0.05.

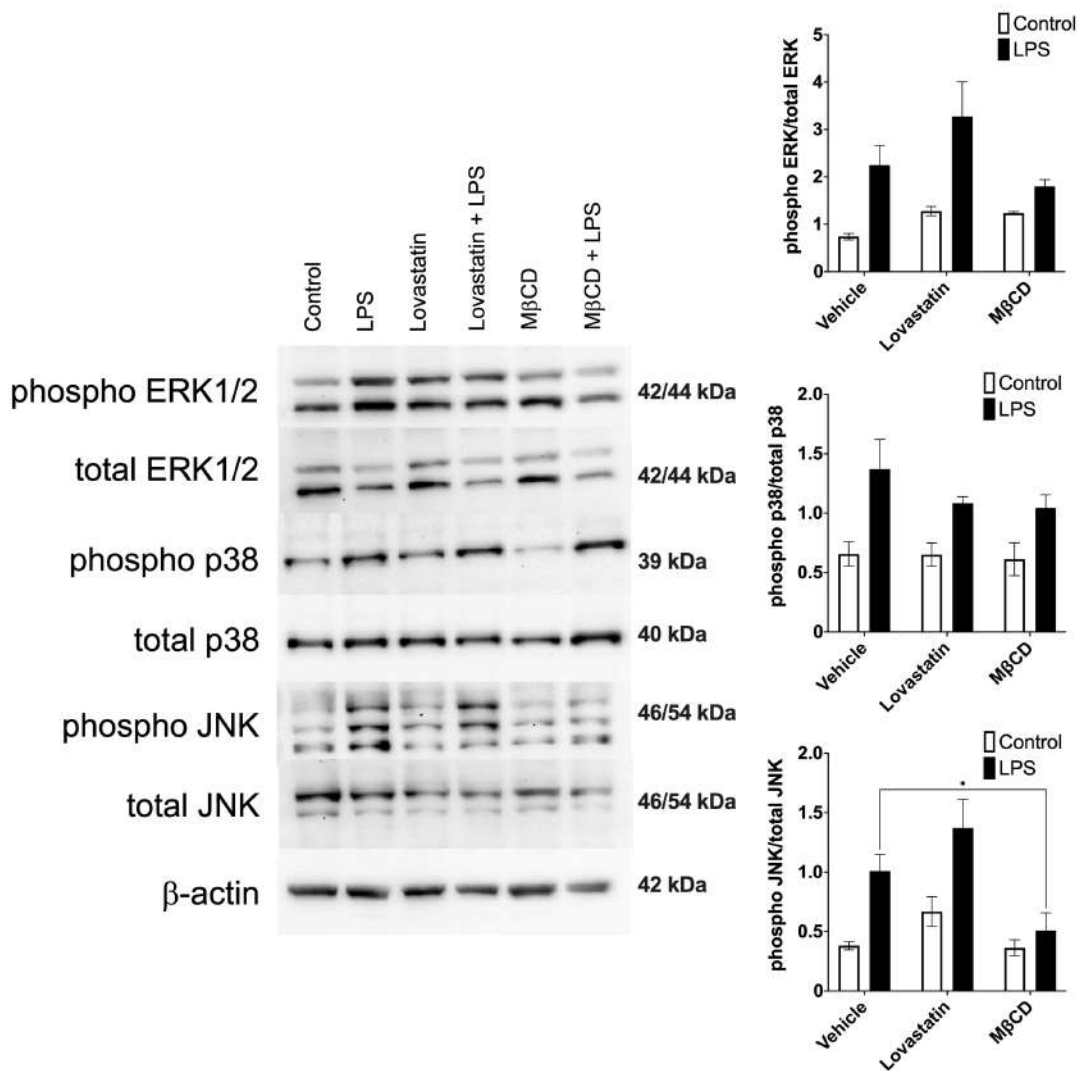


**Figure 4.18. M $\beta$ CD reduces the LPS-induced abundance of phosphorylated JNK in granulosa cells from dominant follicles**

Granulosa cells from dominant follicles were treated for 48 h with granulosa cell culture medium containing vehicle, lovastatin (10  $\mu$ M) or M $\beta$ CD (1 mM) prior to challenge for 60 min with either control medium or medium containing 1  $\mu$ g/ml LPS and the abundance of phosphorylated ERK1/2, p38 or JNK analysed by western blot. Representative western blots of phospho ERK1/2, ERK1/2, phospho p38, p38, phospho JNK, JNK and  $\beta$ -actin are shown on the left. Quantification of band densities normalised to the total protein are presented on the right. Data are presented as mean (SEM) from 3 independent experiments. Data were analysed by two-way ANOVA using Dunnett's post hoc test. Values differ from control, \*  $P < 0.05$ .

#### **4.3.11 RNA interference reduces the lovastatin augmented LPS responses in granulosa cells**

In an attempt to resolve the conflicting granulosa cell responses to pharmaceutical inhibitors of cholesterol biosynthesis and siRNA targeting *HMGCR*, *FDPS* or *FDFT1*, we combined the treatments. Following 24 h siRNA interference, we treated granulosa cells with control, LPS, or LPS in combination with lovastatin.

Similar to the results reported in *Section 4.3.6*, siRNA targeting *HMGCR*, *FDPS* or *FDFT1* reduced the LPS-induced secretion of IL-1 $\alpha$ , IL-1 $\beta$  and IL-8 by granulosa cells from emerged and dominant follicles (**Fig. 4.19**). Additionally, similar to the results reported in *Section 4.3.7*, lovastatin treatment increased the LPS-induced secretion of IL-1 $\alpha$  ( $P < 0.05$ ; **Fig. 4.19A-B**) and IL-1 $\beta$  ( $P < 0.05$ ; **Fig. 4.19C-D**), in vehicle or scramble treated granulosa cells, from both emerged and dominant follicles.

However, treatment with lovastatin did not overcome the effects of siRNA treatment targeting *HMGCR*, *FDPS* or *FDFT1* on the LPS-induced secretion of IL-1 $\alpha$ , IL-1 $\beta$  and IL-8 by granulosa cells from either follicle size. Although the effects of siRNA or lovastatin treatment produce seemingly opposing effects on the innate immune function of granulosa cells, their effects on inflammation may still be mediated via alteration in the function of the mevalonate pathway enzymes *HMGCR*, *FDPS* or *FDFT1*, rather than entirely off target-effects of the statin inhibitor on IL-1 responses.

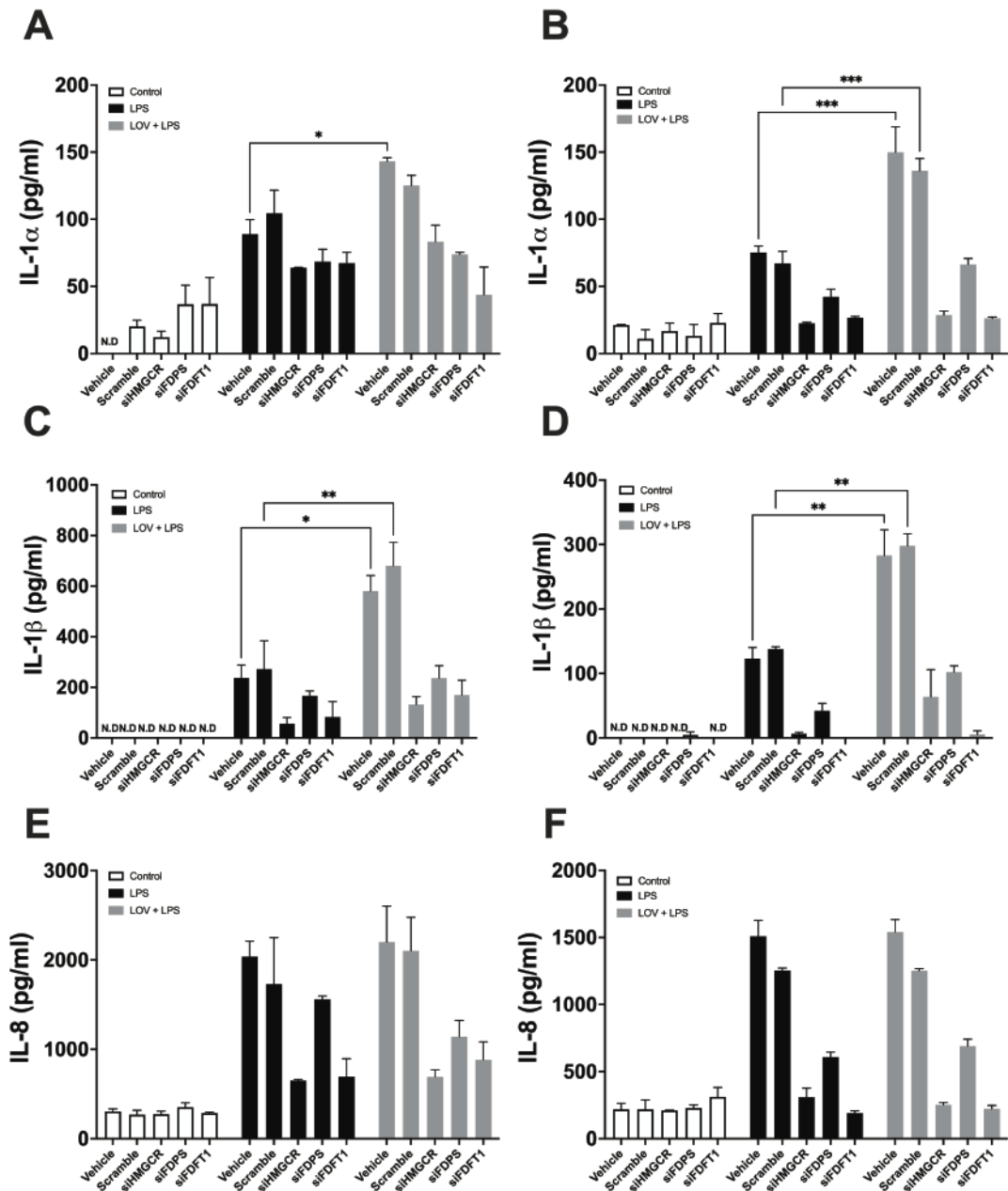


**Figure 4.19. siRNA targeting *HMGCR*, *FDPS* or *FDFT1* reduces the lovastatin augmented LPS response of granulosa cells to LPS**

Granulosa cells from emerged (A, C, E) or dominant (C, D, F) follicles were transfected with scramble siRNA or siRNA targeting *HMGCR*, *FDPS* or *FDFT1* for 24 h. Granulosa cells were then challenged for 24 h with control medium (white bars), medium containing 1  $\mu\text{g/ml}$  LPS (black bars) or medium containing 10  $\mu\text{M}$  lovastatin combined with 1  $\mu\text{g/ml}$  LPS (grey bars). The accumulation of IL-1 $\alpha$  (A-B), IL-1 $\beta$  (C-D) or IL-8 (E-F) was measured by ELISA. Data are presented as mean (SEM) from 2 independent experiments. Data were analysed by two-way ANOVA using Dunnett's post hoc test. Values differ from scramble, \*\*\*  $P < 0.001$ , \*\*  $P < 0.01$ , \*  $P < 0.05$ .

#### 4.3.13 FSH augments the innate immune responses of granulosa cells to LPS

Previously, treatment with 2.5 µg/ml FSH increased the LPS-induced secretion of IL-6 and IL-8 by bovine granulosa cells isolated from emerged follicles (Bromfield and Sheldon, 2011), suggesting a link between innate immunity and endocrine function. Additionally, treatment with FSH was associated with increased intracellular total cholesterol concentrations and increased abundance of HMGCR in bovine granulosa cells from small antral follicles (3 to 5 mm external diameter) (Reverchon et al., 2014), suggesting that FSH may increase cholesterol biosynthesis in cells. Therefore, to further explore the crosstalk between FSH and innate immunity, granulosa cells were treated for 24 h with control, androstenedione (A4;  $10^{-7}$  M), FSH (2.5 µg/ml) or A4 and FSH combined ( $10^{-7}$  M and 2.5 µg/ml, respectively), followed by 24 h challenge with vehicle or 1 µg/ml LPS. The treatments were carried out in serum-free medium (**Fig. 4.20**), medium containing 2% FBS (**Fig. 4.21**) or medium containing 10% FBS (**Fig. 4.22**).

In serum-starved conditions, treatment with FSH, or FSH in combination with A4, increased the LPS-induced secretion of IL-1 $\alpha$  ( $P < 0.05$ ; **Fig. 4.20A-B**) and IL-1 $\beta$  ( $P < 0.01$ ; **Fig. 4.20C-D**) by granulosa cells from both emerged and dominant follicles. Treatment with FSH increased the LPS-induced secretion of IL-8 by granulosa cells from emerged ( $P < 0.001$ ; **Fig. 4.20E**), but not dominant (**Fig. 4.20F**) follicles. However, treatment with FSH in combination with A4, increased the LPS-induced secretion of IL-8 by granulosa cells from dominant follicles ( $P < 0.05$ ; **Fig. 4.20F**).

In medium containing 2% FBS, treatment with FSH, or FSH in combination with A4, increased the LPS-induced secretion of IL-1 $\alpha$  ( $P < 0.001$ ; **Fig. 4.21B**) and IL-1 $\beta$  ( $P < 0.01$ ; **Fig. 4.21D**) by granulosa cells from dominant follicles. Treatment with FSH in combination with A4, increased the LPS-induced secretion of IL-1 $\alpha$  by granulosa cells from emerged follicles ( $P < 0.05$ ; **Fig. 4.21A**). The LPS-induced secretion of IL-1 $\beta$  by granulosa cells from emerged follicles (**Fig. 4.21C**), or the LPS-induced secretion of IL-8 from either follicle size (**Fig. 4.21E-F**), was not altered following treatment with FSH, or FSH in combination with A4.

In medium containing 10% FBS, treatment FSH in combination with A4, decreased the LPS-induced secretion of IL-1 $\beta$  from dominant follicles ( $P < 0.05$ ; **Fig. 4.22B**), and there was a trend for a decrease in the secretion of IL-1 $\beta$  by granulosa cells from emerged follicles (**Fig. 4.22C**;  $P = 0.054$ ). Similarly, there was a trend for a decrease in the LPS-induced secretion of IL-1 $\alpha$  by granulosa cells from emerged (**Fig. 4.22A**;  $P = 0.06$ ) and dominant (**Fig. 4.22B**;  $P = 0.1$ ) follicles, following treatment with FSH in combination with A4. The LPS-induced secretion of IL-8 (**Fig. 4.22E-F**) was not altered following treatment with FSH, or FSH in combination with A4.

These data suggest that FSH augments the innate immune responses to LPS in granulosa cells in serum-free conditions. However, the presence of serum diminishes the effect of FSH on granulosa cell innate immune responses, suggesting potential inhibitory effects by serum factors.

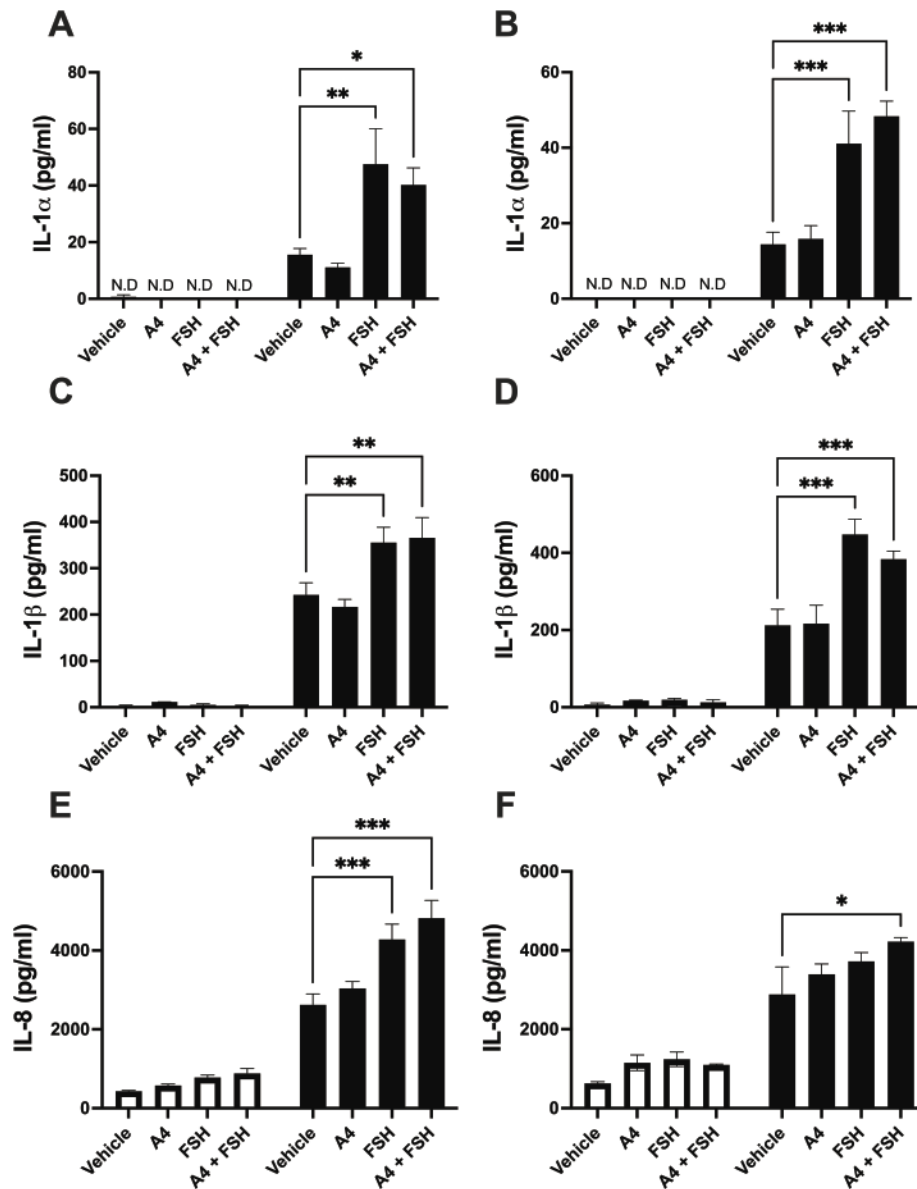


**Figure 4.20. FSH augments inflammatory responses in serum-starved conditions**

Granulosa cells from emerged (A, C, E) or dominant (B, D, F) follicles were treated for 24 h with granulosa cell culture medium containing vehicle, androstenedione (A4;  $10^{-7}$  M), FSH (2.5  $\mu\text{g/ml}$ ) or FSH + androstenedione (2.5  $\mu\text{g/ml}$  +  $10^{-7}$  M) in serum-free medium. Granulosa cells were then challenged for 24 h with serum-free control medium (white bars) or serum-free medium containing 1  $\mu\text{g/ml}$  LPS in the continued presence of the treatments. The accumulation of supernatant IL-1 $\alpha$  (A, B), IL-1 $\beta$  (C, D) and IL-8 (E, F) were measured by ELISA. Data are presented as mean (SEM) from 4 independent experiments. Data were analysed by two-way ANOVA using Dunnett's post hoc test. Values differ from LPS control; \*\*\*  $P < 0.001$ , \*\*  $P < 0.01$ , \*  $P < 0.05$ . N.D = below limit of detection.



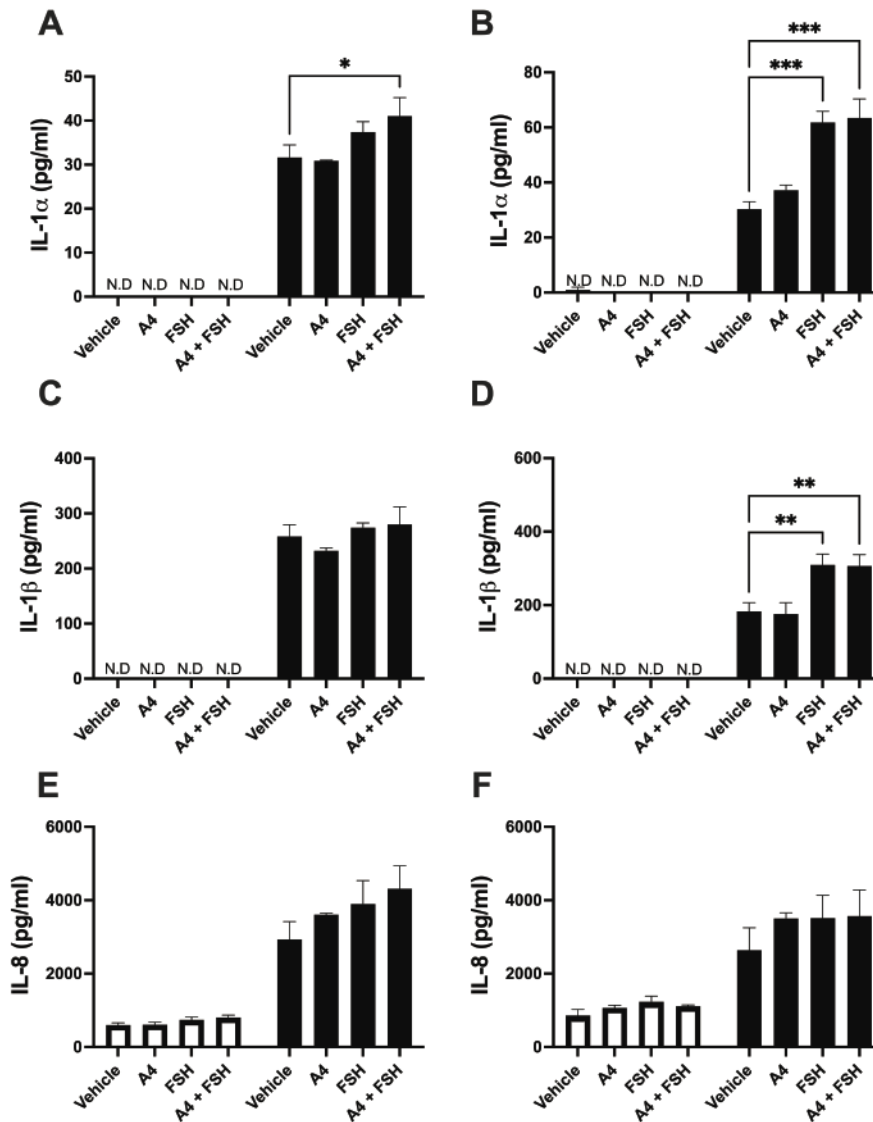


**Figure 4.21. FSH augments inflammatory responses in 2% serum**

Granulosa cells from emerged (A, C, E) or dominant (B, D, F) follicles were treated for 24 h with granulosa cell culture medium containing vehicle, androstenedione (A4;  $10^{-7}$  M), FSH (2.5  $\mu\text{g/ml}$ ) or FSH + androstenedione (2.5  $\mu\text{g/ml}$  +  $10^{-7}$  M) in medium containing 2% FBS. Granulosa cells were then challenged for 24 h with control medium (containing 2% FBS; white bars) or medium containing 1  $\mu\text{g/ml}$  LPS (containing 2% FBS; black bars) in the continued presence of the treatments. The accumulation of supernatant IL-1 $\alpha$  (A, B), IL-1 $\beta$  (C, D) and IL-8 (E, F) were measured by ELISA. Data are presented as mean (SEM) from 4 independent experiments. Data were analysed by two-way ANOVA using Dunnett's post hoc test. Values differ from LPS control; \*\*\*  $P < 0.001$ , \*\*  $P < 0.01$ , \*  $P < 0.05$ . N.D = below limit of detection.

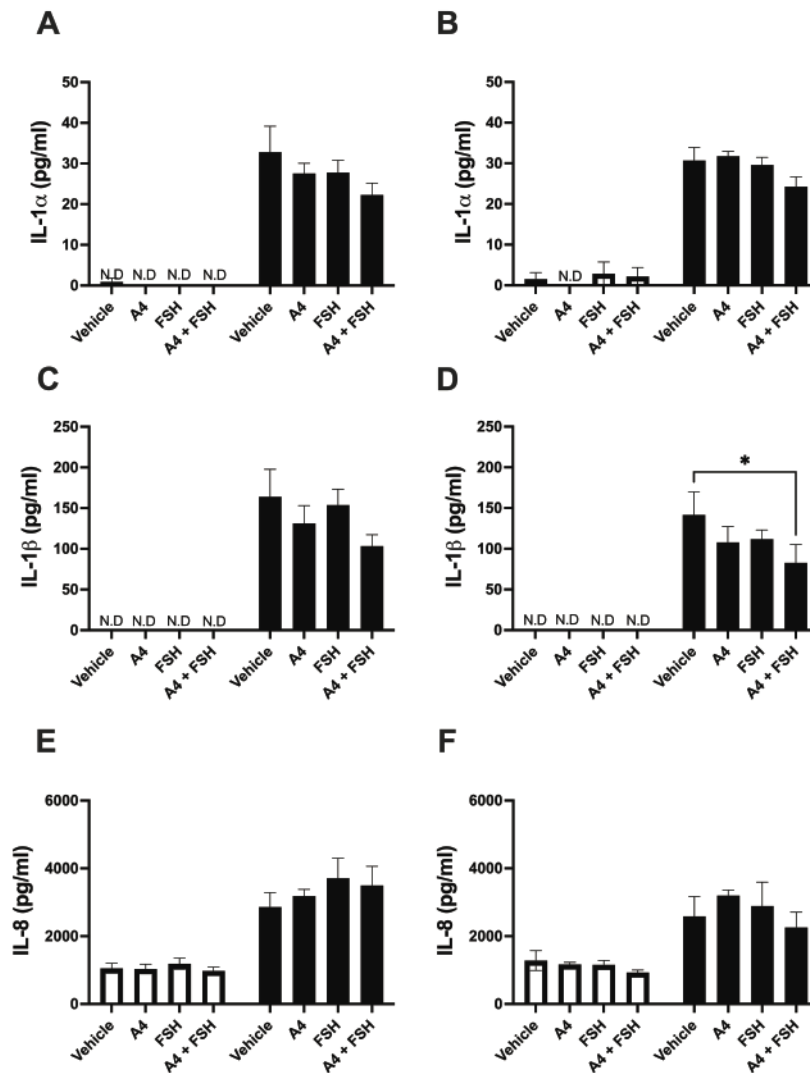


**Figure 4.22. FSH has limited effects on the innate immune responses to LPS in 10% serum**

Granulosa cells from emerged (A, C, E) or dominant (B, D, F) follicles were treated for 24 h with granulosa cell culture medium containing vehicle, androstenedione (A4;  $10^{-7}$  M), FSH (2.5  $\mu\text{g/ml}$ ) or FSH + androstenedione (2.5  $\mu\text{g/ml}$  +  $10^{-7}$  M) in medium containing 10% FBS. Granulosa cells were then challenged for 24 h with control medium (containing 10% FBS; white bars) or medium containing 1  $\mu\text{g/ml}$  LPS (containing 10% FBS; black bars) in the continued presence of the treatments. The accumulation of supernatant IL-1 $\alpha$  (A, B), IL-1 $\beta$  (C, D) and IL-8 (E, F) were measured by ELISA. Data are presented as mean (SEM) from 3 independent experiments. Data were analysed by two-way ANOVA using Dunnett's post hoc test. Values differ from LPS control; \*\*\*  $P < 0.001$ , \*\*  $P < 0.01$ , \*  $P < 0.05$ . N.D = below limit of detection.

#### 4.3.14 FSH, but not LH augments granulosa cell responses to LPS

The effects of FSH on the innate immune responses of granulosa cells were most apparent when granulosa cells were treated in serum-starved conditions (**Fig. 4.20**). Therefore, to further explore the crosstalk between gonadotrophins and innate immunity in granulosa cells, we treated granulosa cells from emerged or dominant follicles with increasing concentrations of FSH (**Fig. 4.23**) or LH (**Fig. 4.24**) in serum-starved conditions.

In granulosa cells from emerged follicles, treatment with increasing concentrations of FSH increased the LPS-induced secretion of IL-1 $\beta$  and IL-8 ( $P < 0.001$ ; **Fig. 4.23B, D**). Specifically, treatment with 100 ng/ml FSH increased the LPS-induced secretion of IL-1 $\beta$  and IL-8 by 33% and 39%, respectively. Unfortunately, the secretion of IL-1 $\alpha$  was below the limit of detection of the assay. In granulosa cells from dominant follicles, treatment with increasing concentrations of FSH increased the LPS-induced secretion of IL-1 $\alpha$ , IL-1 $\beta$  and IL-8 ( $P < 0.001$ ; **Fig. 4.23A, C, E**). Specifically, treatment with 100 ng/ml FSH increased the LPS-induced secretion of IL-1 $\alpha$ , IL-1 $\beta$  and IL-8 by 65%, 57% and 30%, respectively.

In granulosa cells from emerged follicles, treatment with increasing concentrations of LH reduced the LPS-induced secretion of IL-8 ( $P < 0.001$ ; **Fig. 4.24D**). Specifically, treatment with 8 ng/ml LH reduced the LPS-induced secretion of IL-8 by 33%. The LPS-induced secretion of IL-1 $\beta$  was not altered following treatment with LH in granulosa cells from emerged follicles (**Fig. 4.24B**). Unfortunately, the secretion of IL-1 $\alpha$  was below the limit of detection of the assay. In granulosa cells from dominant follicles, treatment with increasing concentrations of LH altered the LPS-induced secretion of IL-8 ( $P < 0.05$ ; **Fig. 4.24E**). Specifically, treatment with 2 ng/ml LH reduced the LPS-induced secretion of IL-8 by 34%. The LPS-induced secretion of IL-1 $\alpha$  or IL-1 $\beta$  was not altered following treatment with LH in granulosa cells from dominant follicles (**Fig. 4.24A, C**).

These data suggest that FSH may regulate the innate immune responses to LPS in granulosa cells. However, regulation of the innate immune responses to LPS by LH are less clear.

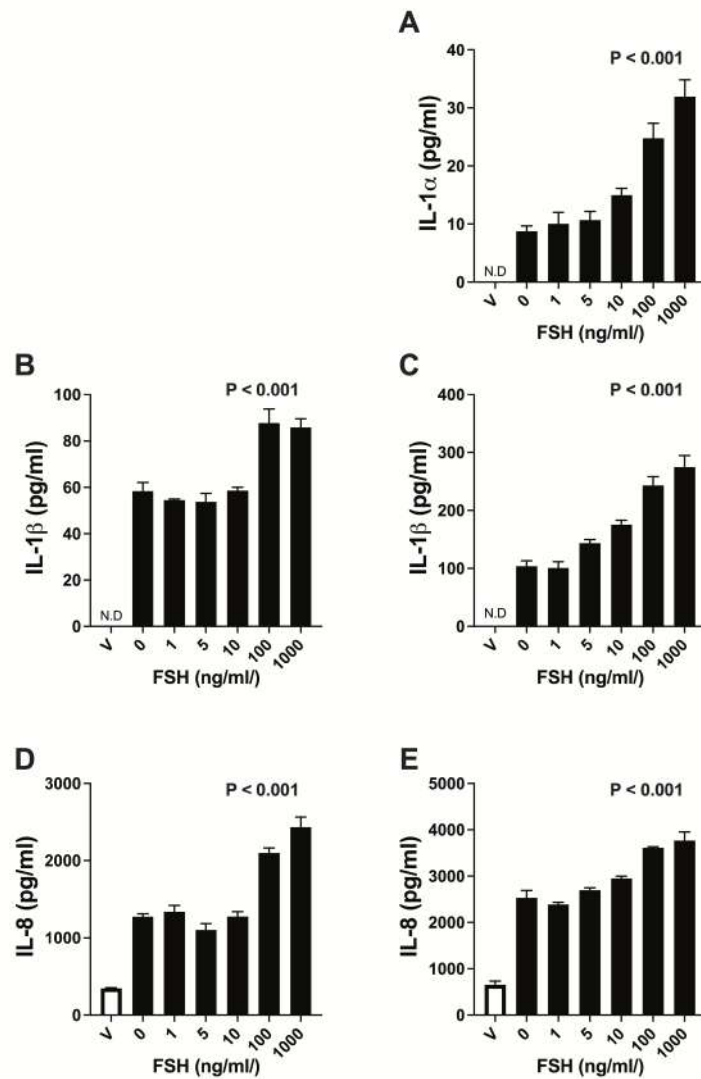


**Figure 4.23. FSH augments granulosa cell responses to LPS**

Granulosa cells from emerged (B, D) or dominant (A, C, E) follicles were treated for 24 h with vehicle, or the indicated concentrations of FSH in serum-free medium. Granulosa cells were then challenged for 24 h with serum-free control medium (white bars) or serum-free medium containing 1  $\mu$ g/ml LPS (black bars) in the continued presence of the treatments. The accumulation of supernatant IL-1 $\alpha$  (A, B), IL-1 $\beta$  (C, D) and IL-8 (E, F) were measured by ELISA. Data are presented as mean (SEM) from 3 independent experiments. Mean values were compared using one-way ANOVA, and P values reported for the effect of treatment on responses to LPS. N.D = below limit of detection.

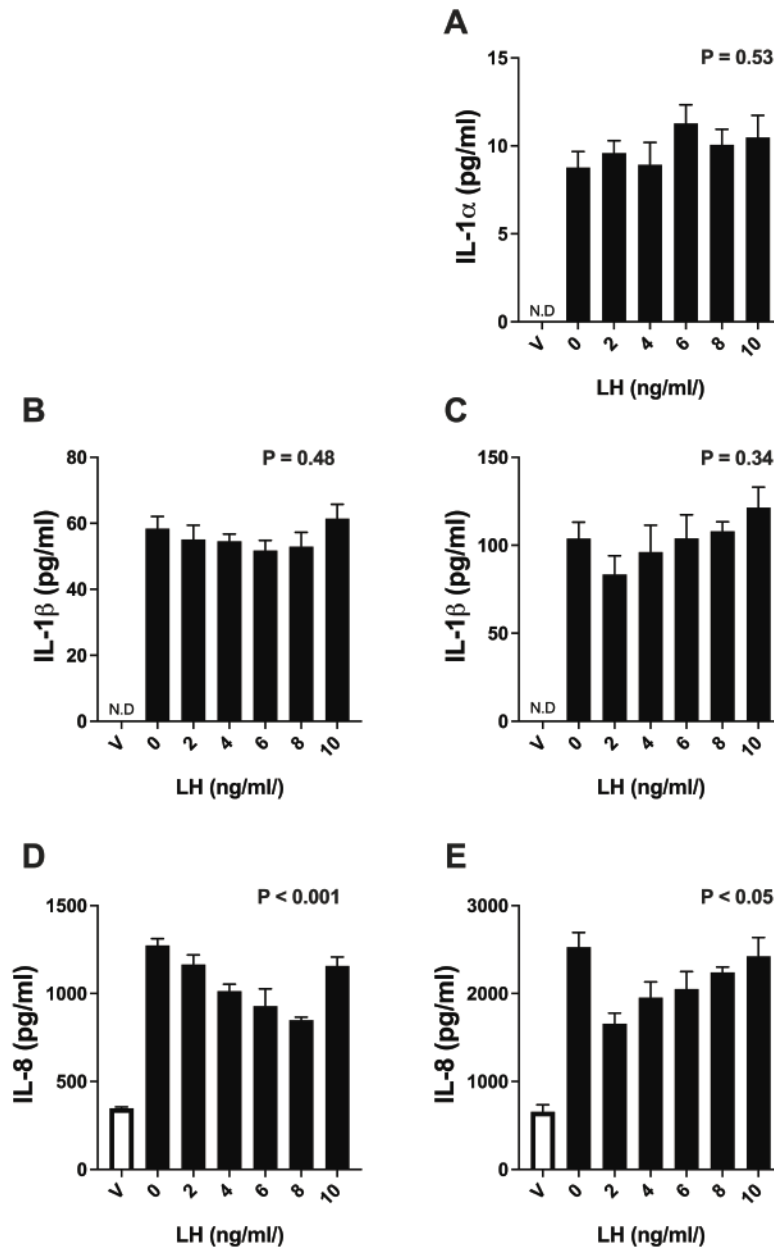


**Figure 4.24. LH impairs LPS-induced IL-8 secretion by granulosa cells**

Granulosa cells from emerged (B, D) or dominant (A, C, E) follicles were treated for 24 h with vehicle, or the indicated concentrations of LH in serum-free medium. Granulosa cells were then challenged for 24 h with serum-free control medium (white bars) or serum-free medium containing 1  $\mu$ g/ml LPS (black bars) in the continued presence of the treatments. The accumulation of supernatant IL-1 $\alpha$  (A, B), IL-1 $\beta$  (C, D) and IL-8 (E, F) were measured by ELISA. Data are presented as mean (SEM) from 3 independent experiments. Mean values were compared using one-way ANOVA, and P values reported for the effect of treatment on responses to LPS. N.D = below limit of detection.

#### 4.3.15 FSH increases the abundance of SR-BI and HMGCR in granulosa cells

Granulosa cells from emerged (**Fig. 4.25**) or dominant (**Fig. 4.26**) follicles were treated for 48 h with control, androstenedione (A4;  $10^{-7}$  M), FSH (2.5  $\mu$ g/ml) or A4 and FSH combined ( $10^{-7}$  M and 2.5  $\mu$ g/ml, respectively), in serum-free medium, medium containing 2% FBS or medium containing 10% FBS, and the abundance of SR-BI or HMGCR was quantified by western blot.

Treatment of granulosa cells from emerged follicles with FSH or FSH and androstenedione, in serum-free medium or medium containing 2% FBS, increased the abundance of SR-BI ( $P < 0.05$ ). However, there was no significant effect of FSH on the abundance of SR-BI in medium containing 10% FBS. Treatment with FSH in combination with A4, increased the abundance of HMGCR in serum-free medium ( $P < 0.05$ ). However, the abundance of HMGCR was not altered by treatment with FSH in medium containing 2% or 10% FBS. Treatment with androstenedione did not alter the abundance of SR-BI or HMGCR in granulosa cells under any of the treatment conditions (0, 2 or 10% FBS).

Treatment of granulosa cells from dominant follicles with FSH, or FSH and androstenedione, in medium containing 0 or 2% FBS, increased the abundance of SR-BI ( $P < 0.001$ ). Additionally, treatment with FSH, in combination with androstenedione increased the abundance of SR-BI in medium containing 10% FBS ( $P < 0.05$ ). None of the treatment conditions alter the abundance of HMGCR in granulosa cells from dominant follicles. Treatment with androstenedione did not alter the abundance of SR-BI or HMGCR in granulosa cells under any of the treatment conditions (0, 2 or 10% FBS).

These data suggest that FSH may increase the abundance of SR-BI in granulosa cells, perhaps to take up additional cholesterol from HDL for steroidogenesis.

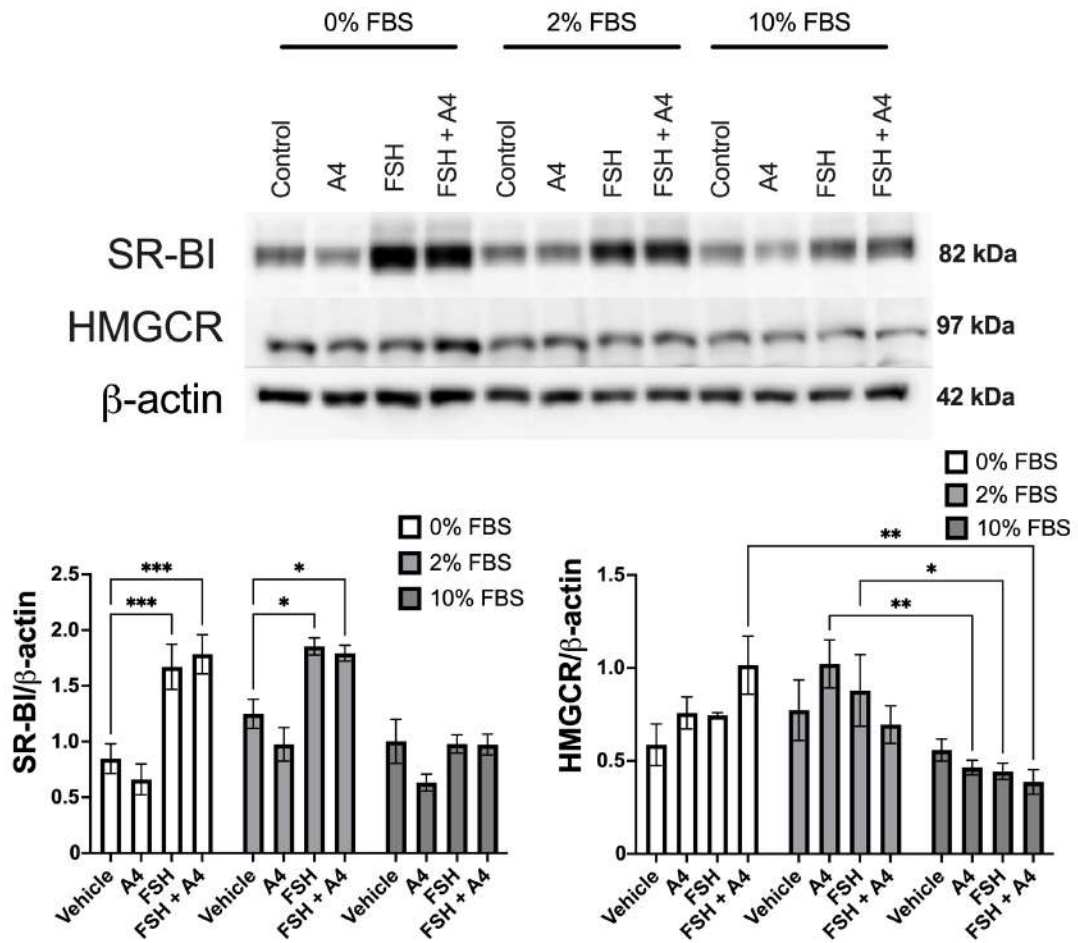


**Figure 4.25. FSH increases SR-BI in granulosa cells from emerged follicles**

Granulosa cells from emerged follicles were treated 48 h with granulosa cell culture medium containing vehicle, androstenedione (A4;  $10^{-7}$  M), FSH ( $2.5 \mu\text{g/ml}$ ) or FSH + androstenedione ( $2.5 \mu\text{g/ml} + 10^{-7}$  M) in medium containing 0%, 2% or 10% FBS. Following treatment, the abundance of SR-BI and HMGCR were quantified by western blot. Data are presented as mean (SEM) from 3 independent experiment. Data were analysed by two-way ANOVA using Dunnett's post hoc test. Values differ from control; \*\*\*  $P < 0.001$ , \*\*  $P < 0.01$ , \*  $P < 0.05$ .

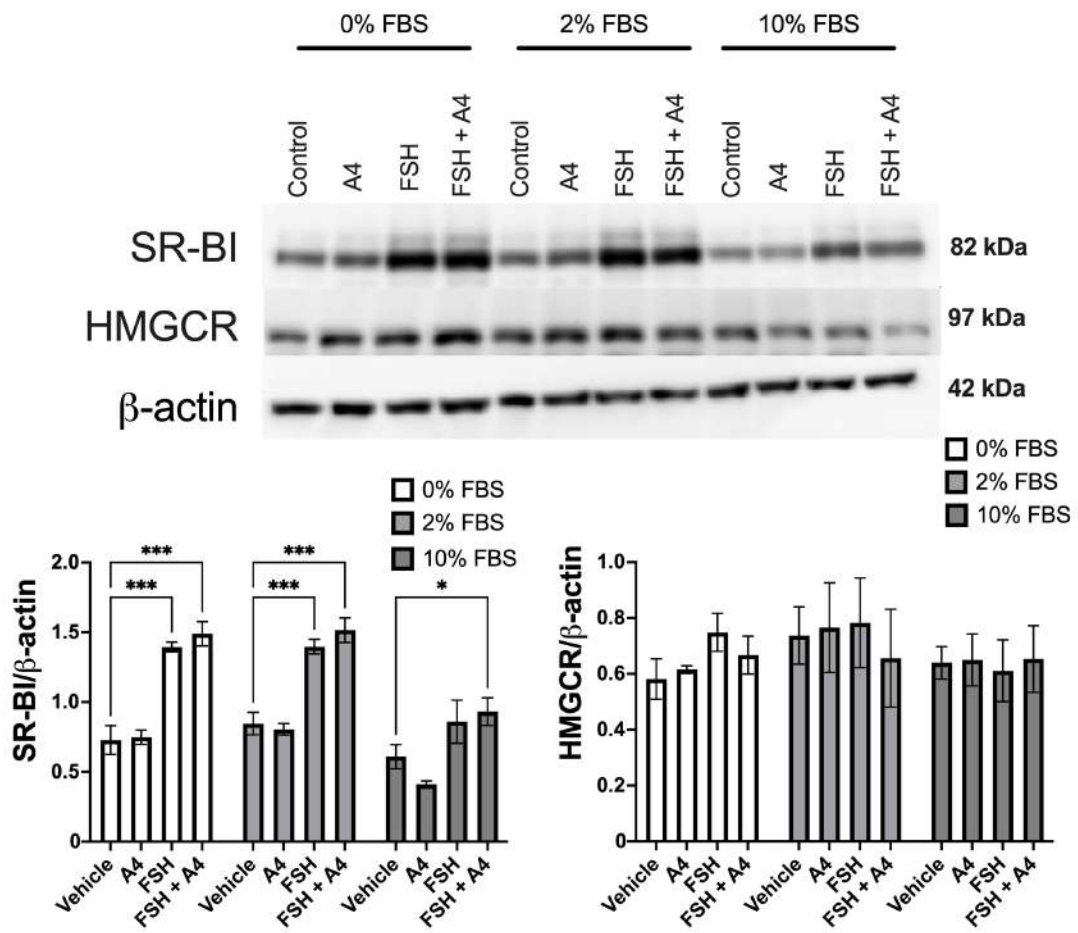


**Figure 4.26. FSH increases SR-BI in granulosa cells from dominant follicles**

Granulosa cells from dominant follicles were treated 48 h with granulosa cell culture medium containing vehicle, androstenedione (A4;  $10^{-7}$  M), FSH (2.5  $\mu$ g/ml) or FSH + androstenedione (2.5  $\mu$ g/ml +  $10^{-7}$  M) in medium containing 0%, 2% or 10% FBS. Following treatment, the abundance of SR-BI and HMGCR were quantified by western blot. Data are presented as mean (SEM) from 3 independent experiment. Data were analysed by two-way ANOVA using Dunnett's post hoc test. Values differ from control; \*\*\*  $P < 0.001$ , \*  $P < 0.05$ .



#### 4.3.16 Lovastatin increases HDL receptor expression in granulosa cells

All cells must maintain a homeostatic balance in cholesterol concentrations so that there is sufficient cholesterol for essential cell processes, whilst avoiding an excess of cholesterol that can be toxic to the cell (Luo et al., 2020). We wanted to explore whether statins that inhibit HMGCR might upregulate the uptake of lipoproteins to compensate for the reduction in *de novo* synthesis. To test this, granulosa cells were treated for 24 h with either granulosa cell culture media or 10  $\mu$ M lovastatin, and the abundance of SR-BI protein was quantified by western blot (Fig. 4.27). Granulosa cells treated with lovastatin had increased abundance of SR-BI protein, compared with control cells ( $P < 0.05$ ). These data suggest that treatment with lovastatin upregulated SR-BI in granulosa cells, potentially increasing the uptake of cholesterol esters from HDL into the cells.

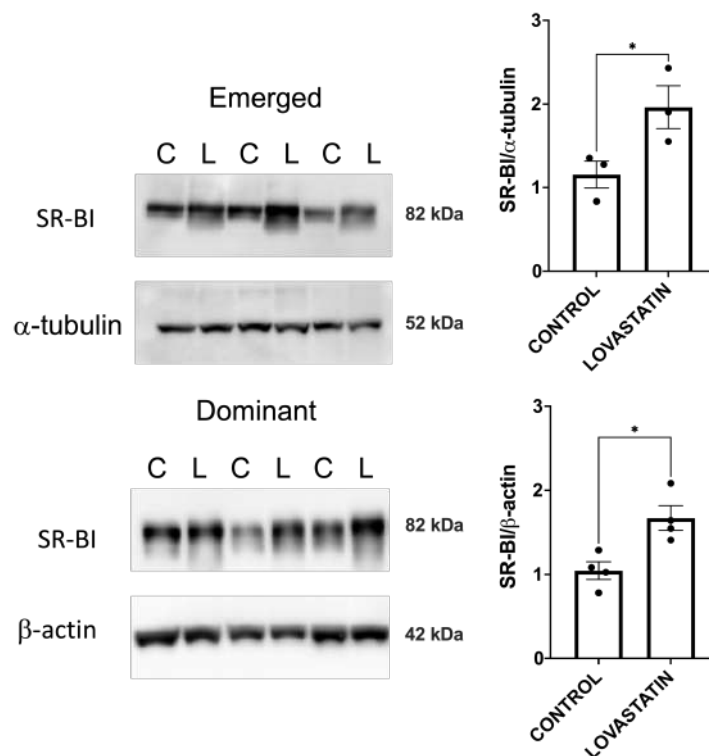


**Figure 4.27. Lovastatin increases in the abundance of SR-BI in granulosa cells**

Granulosa cells from emerged (top) or dominant (bottom) follicles were treated for 48 h with granulosa cells culture medium containing control or lovastatin (10  $\mu$ M), and the abundance of SR-BI quantified by western blot (left panels). Data are presented as mean (SEM) from 3 independent experiments (right panels). Data were analysed by t test. Values differ from control \*  $P < 0.05$ .

#### 4.3.17 siRNA interference of mevalonate pathway enzymes does not alter SR-BI abundance

We then wanted to determine whether the effects of lovastatin on the abundance of SR-BI would be mirrored when granulosa cells were treated with siRNA targeting *HMGCR*, *FDPS* or *FDFT1*. Granulosa cells from emerged (Fig. 4.28A) or dominant follicles (Fig. 4.28B) were treated 48 h with scramble or siRNA targeting *HMGCR*, *FDPS* or *FDFT1* and the abundance of SR-BI was quantified by western blot. We found that none of the siRNA treatments altered the abundance of SR-BI.

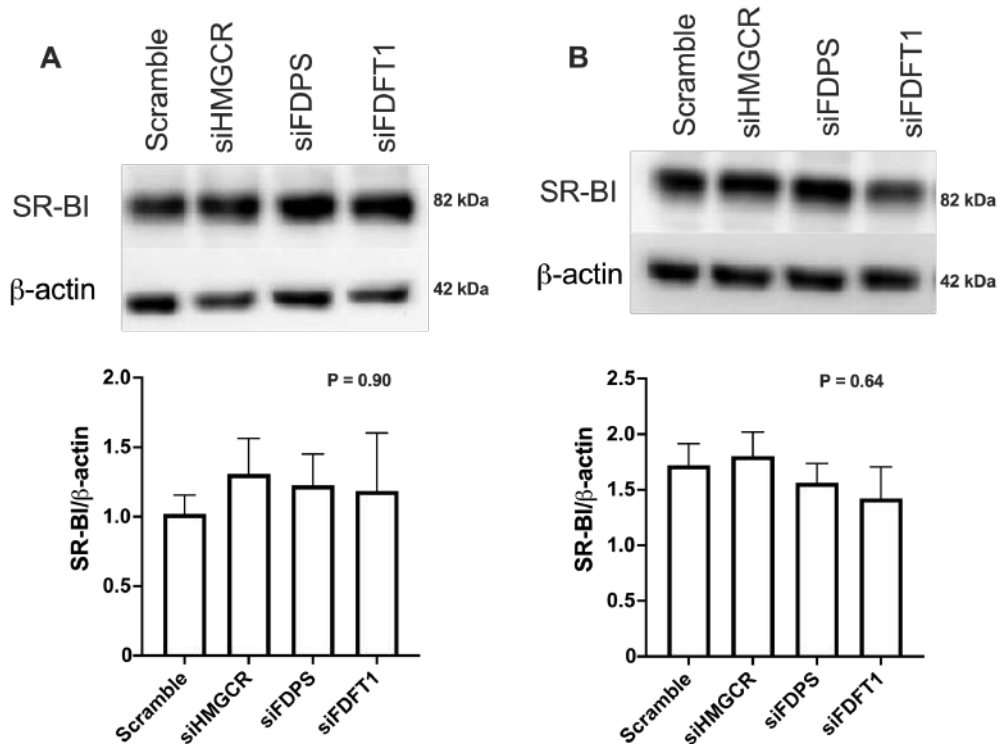


**Figure 4.28. siRNA targeting *HMGCR*, *FDPS* or *FDFT1* does not alter the abundance of SR-BI in granulosa cells**

Granulosa cells from emerged (A) or dominant (B) follicles were treated 48 h with granulosa cell culture medium containing scramble or siRNA targeting *HMGCR*, *FDPS* or *FDFT1*, and the abundance of SR-BI was quantified by western blot. Data are presented as mean (SEM) from 3 independent experiment. Data were analysed using one-way ANOVA, and P values reported for the effect of treatment compared with scramble.

#### 4.4 Discussion

In the present chapter, we found that limiting the availability of cholesterol impaired the innate immune response to LPS in granulosa cells from both emerged and dominant follicles. Initially, we found that reducing the availability of cholesterol by reducing the FBS content of the culture medium or altering cholesterol abundance by supplementing serum-free medium with follicular fluid, impaired the innate immune responses of granulosa cells to LPS. We then found that increasing the availability of HDL, but not LDL or VLDL, augmented the LPS-induced secretion of IL-1 $\alpha$  and IL-1 $\beta$  by granulosa cells. Additionally, depleting cholesterol using methyl- $\beta$ -cyclodextrin also impaired the innate immune responses to LPS in granulosa cells. Next, we found that limiting cholesterol biosynthesis by using siRNA to reduce the expression of *HMGCR*, *FDPS* or *FDFT1* impaired the LPS-induced secretion of IL-1 $\alpha$ , IL-1 $\beta$  and IL-8 by granulosa cells. Surprisingly, small molecule inhibitors of cholesterol biosynthesis increased the LPS-induced secretion of IL-1 $\alpha$  and IL-1 $\beta$  by granulosa cells. We then found that FSH, but not LH, augmented the LPS-induced secretion of IL-1 $\alpha$ , IL-1 $\beta$  and IL-8 in granulosa cells, however, these effects appeared to be diminished by the presence of serum. Finally, we implicated the HDL receptor, SR-BI, as a regulator of innate immunity in granulosa cells because lovastatin and FSH, but not siRNA interference, increased the abundance of SR-BI protein.

Follicular fluid concentrations of cholesterol were like those previously measured in the follicular fluid of Holstein Friesian dairy cows (Leroy et al., 2004a, Piersanti et al., 2019a, Walsh et al., 2012b). It has been previously reported that HDL is the only class of lipoprotein found in the follicular fluid of bovine follicles (Brantmeier et al., 1987). We found that the follicular fluid concentrations of HDL were similar to a recent study that aspirated follicular fluid from the largest follicle, *in vivo* (de Campos et al., 2017). Surprisingly, we also detected LDL/VLDL in follicular fluid. However, HDL was the most predominant lipoprotein present in the follicular fluid of both emerged and dominant follicles. The presence of LDL/VLDL in follicular fluid is surprising however, LDL and VLDL cholesterol have been detected previously in follicular fluid of cows (Argov et al., 2004) and women (Von Wald et al., 2010). It has been suggested that granulosa cells could be the source of LDL or VLDL in follicular fluid (Gautier

et al., 2010, Dunning et al., 2014), however this was not the focus of the present chapter.

Granulosa cells may have the capability to take up cholesterol from both HDL and LDL because they express the LDLR and SR-BI receptors. Not surprisingly, we found that the abundance of SR-BI was higher than the abundance of LDLR in granulosa cells. Treatment of granulosa cells with HDL increased the LPS-induced secretion of IL-1 $\alpha$  and IL-1 $\beta$  in granulosa cells. Conditions in humans, such as hypercholesterolaemia and atherosclerosis are associated with cholesterol accumulation in plasma and an increased inflammatory environment (Tall and Yvan-Charvet, 2015). High density lipoproteins are usually considered to be anti-inflammatory, and associated with cholesterol efflux out of the cell (Tall and Yvan-Charvet, 2015). However, granulosa cells are steroidogenic cells, relying on the supply of cholesterol from HDL to fuel steroidogenesis following luteinization (O'Shaughnessy et al., 1990, Bao et al., 1997b, Bao et al., 1995). Additionally, treatment with HDL has been shown to increase the secretion of TNF $\alpha$  by THP-1 cells (Thompson and Kitchens, 2006), and in human and murine macrophages (van der Vorst et al., 2017, Fu et al., 2019). In agreement with the relatively low abundance of LDLR in granulosa cells, we did not find any significant changes in the granulosa cell responses to LPS following treatment with LDL or VLDL. Therefore, we suggest that there may be an important role for HDL in the innate immune function of granulosa cells.

Interestingly, we found that FSH increased the innate immune responses to LPS in serum-free conditions. However, increasing the amount of FBS in the culture medium appeared to diminish the effects of FSH on the granulosa cell innate immune responses to LPS. These findings are similar to what has been observed in cultured rat granulosa cells where treatment with FSH increased the expression of functional LH receptors, which was completely abolished by the presence of serum (rat, horse, porcine, human or calf serum) (Erickson et al., 1983). Additionally, treatment of rat granulosa cells with FSH in serum-free medium resulted in 25-fold more progesterone and estrogen per cell, compared with granulosa cells cultured in medium containing 5% serum (Orly et al., 1980). The authors of these two studies suggest that either the presence of metabolic hormones in serum may be preventing the actions of FSH, or FSH-induced

steroidogenesis may be negatively regulated by growth-related processes (Erickson et al., 1983, Orly et al., 1980).

Little is known about *de novo* synthesis of cholesterol in bovine granulosa cells because prior to luteinization, granulosa cells aromatize androstenedione provided by the theca cells that surround the follicle (Ryan et al., 1968, Dorrington et al., 1975, Liu and Hsueh, 1986). In humans, mevalonate kinase deficiency is a disorder characterised by disruption of the mevalonate pathway, accumulation of mevalonic acid and chronic inflammation (Pontillo et al., 2010, Favier and Schulert, 2016, Akula et al., 2016). We found that siRNA targeting *HMGCR*, *FDPS* or *FDFT1* impaired the innate immune responses to LPS in granulosa cells. Previously, siRNA targeting *FDFT1* in bovine endometrial stromal cells reduced the LPS-induced secretion of IL-6 and IL-8, however siRNA targeting *HMGCR* increased the LPS-induced secretion of IL-6 and IL-8 (Healey et al., 2016). In this study, the efficiency of the knockdowns was lower than previously reported in bovine endometrial stromal cells, using these siRNA constructs (Griffin et al., 2017). The lower knockdown efficiency in the present study may reflect the steroidogenic nature of granulosa cells. Despite the low efficiencies of the mRNA knockdowns, the effects on the innate immune response of granulosa cell to LPS were striking.

Surprisingly, we found that using pharmaceutical inhibitors of cholesterol biosynthesis had the opposite effect to siRNA, increasing the LPS-induced secretion of IL-1 $\alpha$  and IL-1 $\beta$  in granulosa cells. Additionally, refeeding granulosa cells with either mevalonic acid or FPP following treatment with lovastatin or alendronate, respectively, partially reversed the effects of the inhibitor on the LPS-induced IL-1 secretion. A recent study in human peripheral blood mononuclear cells found that treatment with simvastatin increased the LPS-induced secretion of IL-1 $\beta$ , and increased the mRNA expression of *IL1A* and *IL1B*, associated with decreased protein geranylation (Akula et al., 2016). Similarly, in THP-1 cells (Liao et al., 2013, Kuijk et al., 2008) and human peripheral blood mononuclear cells (Massonnet et al., 2009, Frenkel et al., 2002, Mandey et al., 2006, Montero et al., 2000), statin treatment increased IL-1 responses to PAMPs, and re-feeding with mevalonic acid or geranylgeranyl pyrophosphate abolished the effects.

Granulosa cell inflammatory responses are associated with increased phosphorylation of ERK1/2, p38 and JNK within 2 h of LPS challenge (Price and Sheldon, 2013, Price et al., 2013, Bromfield and Sheldon, 2011, Horlock et al., 2021). Therefore, we wondered whether the increases in the LPS-induced secretion of IL-1 following lovastatin treatment, or the depletion of cellular cholesterol by methyl- $\beta$ -cyclodextrin was due to modulation of MAPK activity. Although there was some modulation of LPS-induced ERK phosphorylation following lovastatin or methyl- $\beta$ -cyclodextrin treatment in granulosa cells from emerged follicles and modulation of LPS-induced JNK phosphorylation in granulosa cells from dominant follicles, it is unlikely that this could explain the changes in IL-1 that these treatments are associated with. One possibility is that lovastatin is activating the inflammasome, that is directly involved in IL-1 $\beta$  secretion and indirectly involved in IL-1 $\alpha$  secretion (Fettelschoss et al., 2011, Yazdi and Drexler, 2013, Groß et al., 2012).

Next, we explored whether the increased LPS-induced IL-1 secretion following treatment with HDL or inhibitors of cholesterol biosynthesis might be linked. Interestingly, we found that treatment of granulosa cells with lovastatin was associated with an increase in the expression of SR-BI. Similarly, treatment of murine macrophages with pitavastatin increased the expression of SR-BI and HDL binding (Han et al., 2004), and treatment of human umbilical vein epithelial cells with simvastatin also increased SR-BI expression (Kimura et al., 2008). We suggest that in response to the inhibition of cholesterol biosynthesis, granulosa cells may increase their expression of SR-BI to take up additional cholesterol from HDL to maintain cholesterol homeostasis. The finding that treatment with inhibitors of cholesterol biosynthesis did not reduce cellular total cholesterol concentrations in media containing 10% FBS supports this. The uptake of cholesterol esters from HDL has been positively linked to the expression of SR-BI protein in rat granulosa cells (Azhar et al., 1998a). We infer that the inhibition of HMGCR with lovastatin may activate homeostatic mechanism that increases the expression of SR-BI and cholesterol ester uptake via HDL, which may activate the inflammasome leading to increased IL-1 secretion; to test this hypothesis, future studies might also test the effects of lovastatin on the innate immune responses of granulosa cells in serum-free medium.

The contradictory results between the inhibitors of the cholesterol biosynthesis enzymes, and siRNA knockdown of the mRNA encoding the genes of the enzymes is interesting. Treatment of human breast cancer cells (MCF-7 and T47D cells) with statins has been shown to increase the abundance of HMGCR protein, an effect that can be reversed by siRNA targeting *HMGCR* (Gobel et al., 2019). Induction of HMGCR protein and mRNA by statins has also been observed in mouse liver cells and Chinese hamster ovary cells (CHO7 cells) (Jiang et al., 2018). It is possible that the contradictory results we observed may be due to an upregulation of the enzymes in a compensatory manner against the inhibitors. Off-target effects of the inhibitors have also been reported (Huang et al., 2019), and are another possible explanation for the LPS-induced increased IL-1 secretion in this study. However, we found that siRNA treatment, prior to lovastatin treatment, reversed the statin-augmented secretion of IL-1, in response to LPS. This suggests that the statin effects may not be entirely due to off-target effects. Further studies are needed to elucidate the mechanism by which cholesterol biosynthesis inhibitors increase IL-1 responses to LPS in granulosa cells.

Interestingly, in addition to increased innate immune responses to LPS, we found that treatment with either FSH or lovastatin was associated with increased abundance of SR-BI in granulosa cells. Previously, treatment with FSH increased the abundance of SR-BI in rat granulosa cells (Lai et al., 2013); treatment with simvastatin increased the abundance of SR-BI in human umbilical vein endothelial cells. However, the effects of FSH on the immune response were more apparent in conditions without exogenous HDL supplied by FBS. Therefore, the increased innate immune responses to LPS may not be solely due to increased cholesterol uptake via HDL but may reflect crosstalk between innate immunity and SR-BI. Increased abundance of SR-BI is usually associated with anti-inflammatory responses (Vasquez et al., 2017). Mice that are deficient in hepatic SR-BI have increased serum LPS concentrations compared with control mice, suggesting that hepatic SR-BI may have a role in the clearance of LPS during sepsis (Guo et al., 2014). Additionally, LPS-clearance through SR-BI has been proposed in studies using mouse hepatocytes (Cai et al., 2008), and HeLa cells (Vishnyakova et al., 2003). Macrophages deficient in SR-BI secrete more pro-inflammatory cytokines in response to LPS, associated with increased MAPK signalling (Cai et al., 2012).

However, in support of our findings, SR-BI has been associated with pro-inflammatory responses. Scavenger receptors can act as co-receptors, presenting ligands to Toll-like receptors (Vasquez et al., 2017). Lipopolysaccharide may be a ligand for SR-BI (Shen et al., 2018, Morin et al., 2015). For example, lipopolysaccharide binds to CLA-1, a human SR-BI analogue, and is internalized independently, or in association with HDL (Vishnyakova et al., 2003). Overexpression of CLA-1 in HeLa cells is associated with increased LPS uptake and an increase in the LPS-induced secretion of IL-8 (Baranova et al., 2012). Transgenic mice, overexpressing SR-BI demonstrated 2 to 3-fold higher concentrations of LPS-induced serum cytokine concentrations, such as IL-6, compared with wild-type controls (Baranova et al., 2016). Additionally, blocking SR-BI with synthetic amphipathic helical peptides impairs the LPS-induced secretion of IL-6 and IL-8 by THP-1 cells (Bocharov et al., 2004).

There is emerging evidence of the crosstalk between innate immunity and reverse cholesterol transport (Azzam and Fessler, 2012). In non-steroidogenic cells, SR-BI is usually involved in reverse cholesterol transport, removing excess cholesterol from cells (Trigatti et al., 1999). Lipopolysaccharide treatment of human macrophages impairs reverse cholesterol transport, reducing cholesterol efflux from the cells (McGillicuddy et al., 2009). However, granulosa cells are steroidogenic cells, and SR-BI delivers cholesterol to cells for storage or the synthesis of steroid hormones (Gwynne and Strauss, 1982, Azhar et al., 1998a). Internalization of LPS via SR-BI and presentation to the inflammasome is one potential mechanism by which FSH or small molecule inhibitors of cholesterol biosynthesis might increase the IL-1 responses observed. Future experiments might explore the role of SR-BI in the innate immune responses of granulosa cells following treatment with statins or FSH by designing siRNA targeting bovine *SCARB1*.

In conclusion, we provide evidence that reduced cholesterol availability to granulosa cells in the postpartum period or impaired cholesterol biosynthesis during energy stress may impair the defences of the ovarian follicle to infections. The findings of *Chapter 3* are summarized in **Figure 7.2**.



## **5 Manipulating energy metabolism or the mevalonate pathway alters cumulus-oocyte complex responses to LPS and impairs oocyte health**

### **5.1 Introduction**

Ovarian follicle function is often perturbed by bacterial infections in postpartum dairy cows (Sheldon et al., 2019a, Sheldon et al., 2002). The bacterial endotoxin, LPS, accumulates in the follicular fluid of animals with uterine disease (Herath et al., 2007, Piersanti et al., 2019a). Like mural granulosa cells, bovine cumulus granulosa cells of the COC express *TLR4* and respond to LPS by secreting cytokines, such as IL-1 $\beta$ , IL-6 and TNF $\alpha$  (Bromfield and Sheldon, 2011, Zhao et al., 2019). Lipopolysaccharide treatment is also associated with a reduction of the bovine primordial ovarian follicle pool (Bromfield and Sheldon, 2013). Additionally, treatment with LPS is associated with impaired meiotic progression of bovine oocytes to the MII stage, *in vitro* (Magata and Shimizu, 2017, Zhao et al., 2017b, Bromfield and Sheldon, 2011).

The Britt hypothesis suggests that energy stress during follicle growth might reduce oocyte competence in dairy cows (Britt, 1992). The oocyte must regulate its microenvironment to ensure it is provided with the nutrition and hormones that it requires for development (Eppig et al., 1997). The oocyte does this through the maintenance of its cumulus cell population (Sutton et al., 2003, Sugiura et al., 2005). Bovine oocytes are deficient in their ability to take up glucose (Sutton-McDowall et al., 2010). As COCs mature, their requirements for glucose increase, with mature bovine COCs requiring twice as much glucose, oxygen, and pyruvate as immature oocytes (Sutton et al., 2003). Glucose is important during IVM and can have profound effects on the developmental capacity of the bovine oocyte (Sutton-McDowall et al., 2004). Similarly, mouse oocytes are deficient in their ability to take up glucose (Purcell et al., 2012), or carry out glycolysis (Su et al., 2009, Biggers et al., 1967, Sugiura et al., 2007), therefore they outsource this function to the surrounding cumulus granulosa cells. Mouse oocytes regulate glycolysis in cumulus cells by releasing paracrine factors to promote the expression of genes encoding glycolytic enzymes (Sugiura et al., 2005, Sugiura et al., 2007). The effects of glucose restriction can be mimicked using the glycolysis inhibitor, 2-deoxy-D-glucose. For example, treatment of mouse

COCs with 2-DG mimicked the effects of glucose restriction, impairing COC expansion and meiotic resumption (Han et al., 2012).

Energy stress is sensed at the cellular level by AMPK, signalling the cell to reduce anabolic, ATP consuming pathways (Hardie et al., 2012). Studies have shown that AMPK mRNA and protein is present in bovine cumulus granulosa cells and oocytes (Tosca et al., 2007b, Bilodeau-Goeseels et al., 2007). The activation of AMPK in bovine (Tosca et al., 2007b, Bilodeau-Goeseels et al., 2007) and porcine (Mayes et al., 2007) oocytes block nuclear maturation. For example, treatment of bovine COCs with the AMPK activator metformin is associated with decreased cumulus cell expansion and arrested 80% of oocytes at the germinal vesicle stage of meiosis (Tosca et al., 2007b). Additionally, treatment of bovine COCs or denuded oocytes with the AMPK activators, AICAR or metformin, arrests oocytes at the GV stage of meiosis (Bilodeau-Goeseels et al., 2007).

Phosphorylated AMPK also inhibits mTOR, which further limits anabolic pathways (Hardie et al., 2012, Zoncu et al., 2011). There is emerging evidence of the role of mTOR in female reproduction (Correia et al., 2020, Guo and Yu, 2019). Treatment of mice with the mTOR inhibitor rapamycin is associated with fewer ovulated oocytes (Yu et al., 2011). Additionally, oocyte-specific conditional knockout of mTOR has been shown to compromise oocyte meiosis and developmental competence in mice (Guo et al., 2018b). Mutant mice lacking the genes that encode *Tsc1* or *Tsc2*, that negatively regulate mTOR activity, experience elevated mTORC1 activity and overactivation of the entire pool of primordial follicles, potentially leading to infertility (Adhikari et al., 2010, Adhikari et al., 2009). Inhibition of mTOR in mouse oocytes with the dual mTORC1/mTORC2 inhibitor Torin 1 compromises oocyte developmental competence, with a reduction in the rate of fertilization and blastocyst development (Guo et al., 2016).

Phosphorylated AMPK also inhibits 3-hydroxy-3-methyl-glutaryl-CoA reductase (HMGCR), the rate limiting enzyme in cholesterol biosynthesis (Clarke and Hardie, 1990). HMG-CoA reductase catalyses the conversion of HMG-CoA into mevalonate. A series of enzymes, including farnesyl pyrophosphate synthase (FDPS) converts mevalonate to farnesyl pyrophosphate (FPP), which is then converted to squalene by

farnesyl diphosphate farnesyltransferase 1 (FDFT1), followed by another series of enzyme reactions to yield cholesterol (Bloch, 1965, Sharpe and Brown, 2013). Mouse oocytes are deficient in their ability to carry out cholesterol biosynthesis, therefore the cumulus cells must provide cholesterol (Su et al., 2008). Cellular cholesterol may be obtained via HDL or LDL mediated uptake, or via *de novo* cholesterol biosynthesis (Brown and Goldstein, 1976, Goldstein and Brown, 1990, Connelly and Williams, 2003, Acton et al., 1996). The supply of cholesterol to the oocyte might be important because depleting cellular cholesterol with methyl- $\beta$ -cyclodextrin prevents mouse embryonic development *in vitro* (Comiskey and Warner, 2007). Interestingly, female mice lacking the HDL receptor, SR-BI are infertile, accumulate excess cholesterol *in vivo*, and oocytes spontaneously resume meiosis, escaping MII arrest (Yesilaltay et al., 2014). Similarly, mouse oocytes that are treated with cholesterol-loaded methyl- $\beta$ -cyclodextrin to increase cholesterol concentrations activate prematurely and escape MII arrest, *in vitro* (Yesilaltay et al., 2014).

In *Chapter 3*, we demonstrated that energy stress impairs the innate immune responses to LPS by bovine granulosa cells isolated from emerged or dominant follicles. Then, in *Chapter 4*, we demonstrated that deficits in cholesterol, or disruption to cholesterol biosynthesis impairs the innate immune responses to LPS by bovine granulosa cells isolated from emerged and dominant follicles. Therefore, we wanted to explore how disruption to energy or cholesterol metabolism might affect the COC and oocyte. The hypothesis of this chapter is that energy stress or decreasing the availability of cholesterol would alter the innate immune response of the COC to LPS. To test this hypothesis, we manipulated energy metabolism using 2-DG, AICAR or Torin 1 to inhibit glycolysis, activate AMPK, or inhibit mTOR, respectively. We also inhibited cholesterol biosynthesis using lovastatin, alendronate or zaragozic acid, to inhibit HMGCR, FDPS or FDFT1, respectively. We then measured the LPS-induced secretion of IL-1 $\alpha$ , IL-1 $\beta$  and IL-8. Cumulus oocyte expansion is essential for ovulation and is indicative of oocyte quality (Larsen et al., 1996, Sutton-McDowall et al., 2004, Ozturk, 2020), and the ability of an oocyte to resume meiosis and reach metaphase II is a key indicator of oocyte competence (Sirard et al., 2006). Therefore, in addition to assessing secretion of pro-inflammatory cytokines by COCs, we assessed the effects of the treatments on COC expansion and meiotic progression.

## 5.2 Methods

### 5.2.1 Cumulus oocyte culture and treatment

Cumulus-oocyte complexes (COCs) were pooled from 20 to 40 ovaries and subject to IVM, as described in *Chapter 2*. Up to 50 COCs were immediately transferred into 500  $\mu$ l IVM medium in 1 ml organ culture dishes (Corning Falcon) containing control, 1 mM 2-DG, 1 mM AICAR or 50 nM Torin 1, 10  $\mu$ M lovastatin, 10  $\mu$ M alendronate or 10  $\mu$ M zaragozic acid, in the presence or absence of 1  $\mu$ g/ml LPS. *In vitro* maturation (IVM) was then carried out for 22 h, as previously described (Bahrami et al., 2019, Koyama et al., 2014, Sirard et al., 1989, Zhao et al., 2019). Some experiments were performed in the absence of hormone supplementation (2  $\mu$ g/ml oestradiol and 20  $\mu$ g/ml FSH), as previously described (Bromfield and Sheldon, 2011). IVM was carried out in a humidified incubator at 38.5°C, under 5% CO<sub>2</sub>. Following IVM, supernatants were collected and stored at -20°C for subsequent analysis by ELISA; cumulus expansion was assessed, as described in *Chapter 2*; COCs were fixed and stored at 4°C for up to 2 weeks, prior to assessment of meiotic status.

### 5.2.2 ELISA

The accumulation of IL-1 $\alpha$ , IL-1 $\beta$  and IL-8 was measured in supernatants, as described in *Chapter 2*. The limits of detection for IL-1 $\alpha$ , IL-1 $\beta$ , and IL-8 were 12.5, 31.3, 62.5 pg/ml, respectively. The inter- and intra-assay coefficients of variation for IL-1 $\alpha$ , IL-1 $\beta$  and IL-8 were all < 7% and < 9%, respectively.

### 5.2.3 COC fixation

Cumulus-oocyte complexes were fixed in 4% paraformaldehyde for 10 min at 37°C, prior to transfer into microtubule stabilising buffer (dH<sub>2</sub>O containing 100 mM PIPES, 5 mM MgCl<sub>2</sub>, 2.5 mM EGTA, 2% formaldehyde, 0.1% Triton-X-100, 1 mM Taxol, 10 U/ml aprotinin and 50% D<sub>2</sub>O; Merck) for 45 min at 37°C, and stored in wash/block solution (PBS containing 0.2% sodium azide, 0.2% powdered milk, 2% normal goat serum, 1% BSA, 0.1M glycine, 0.1% Triton-X-100) at 4°C for up to 2 weeks.

#### 5.2.4 COC fixation and assessment of meiotic status

Cumulus-oocyte complexes were fixed in 4% paraformaldehyde and probed overnight at 4°C with mouse anti- $\alpha$ -tubulin (1:100; Bio-technie) and mouse anti- $\beta$ -tubulin (1:100; Invitrogen), as described in *Chapter 2*. Samples were then probed with anti-mouse-Alexa-488 secondary (1:400; Molecular Probes), in combination with Phalloidin-Alexa-555 (1:100; Molecular Probes) and 1  $\mu$ g/ml Hoechst 33342 (Molecular Probes), for the detection of F-actin and nucleic acids, respectively. Samples were then washed and mounted onto polysine microscope slides (VWR) in mounting media (50% PBS, 50% glycerol containing 1  $\mu$ g/ml Hoechst 33342).

Cumulus-oocyte complexes were analysed on a Zeiss LSM 710 confocal microscope using a 40x Plan-Apochromat objective (na=1.3), KrArg (405,488 nm) and HeNe (543 nm) lasers to collect three channel z-stacks through the oocyte. Oocytes were analysed using Zen software (Zeiss, Jena, Germany). Oocyte meiotic status was assessed according to the criteria described in **Figure 5.1**. Oocytes with evidence of a polar body and a bipolar spindle with condensed chromatids were evaluated as MII oocytes (Combelles et al., 2002, Bromfield and Sheldon, 2011).

#### 5.2.5 Statistics

A total of 615 COCs were used across all experiments. Data are presented as arithmetic means and SEM. Statistical analysis was performed using GraphPad Prism version 9.21 (GraphPad Software) or SPSS (SPSS Inc, Chicago, USA). Expansion of COCs was analysed using Chi-squared analysis. The rate of meiotic failure was analysed with one-way ANOVA, using Dunnett's post hoc test. To compare inflammatory responses, data were analysed by one-way ANOVA with Dunnett's post hoc test to compare treatments with control.  $P < 0.05$  was considered significant.

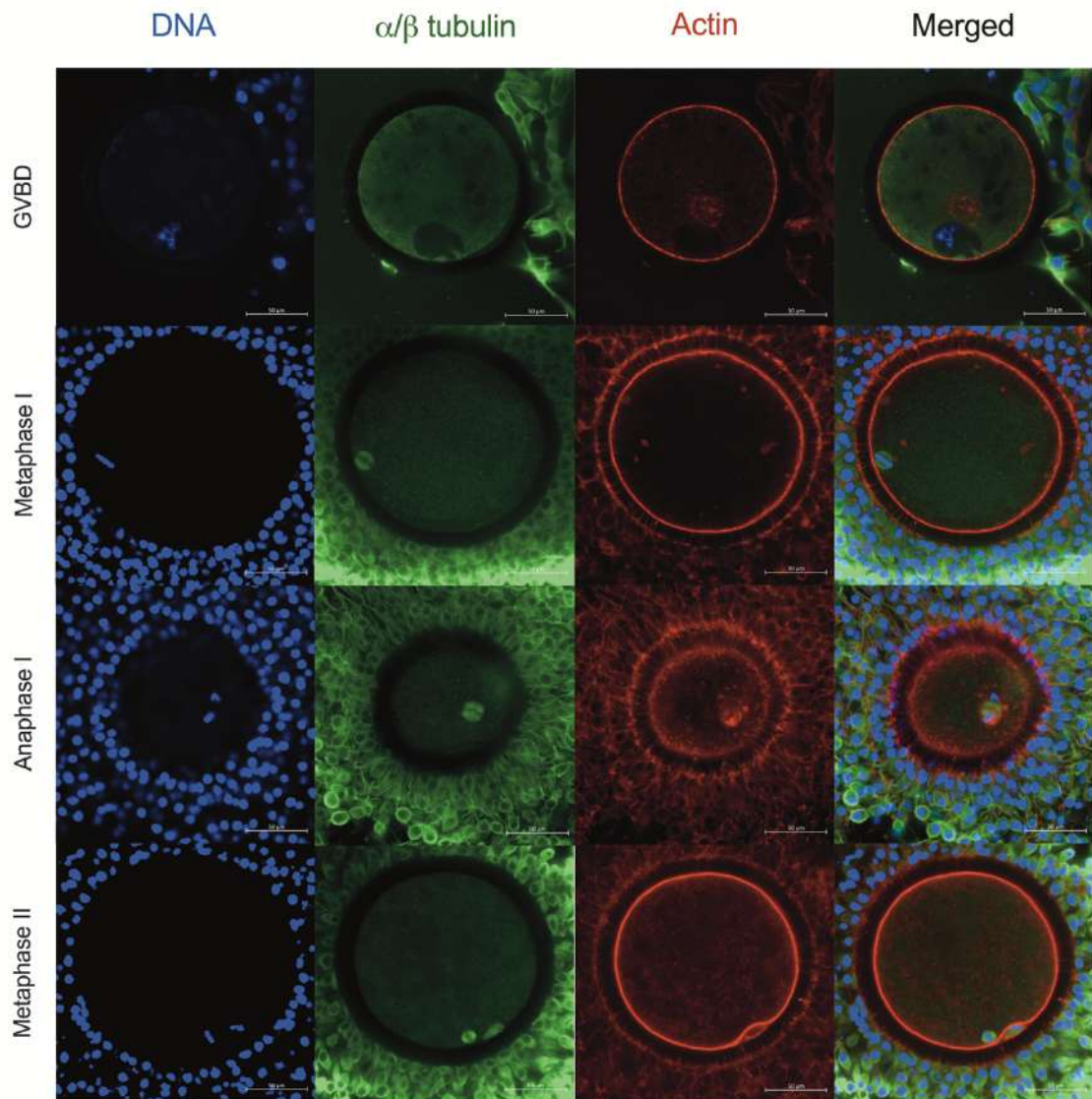


**Figure 5.1. Identification of meiotic status during IVM**

Bovine oocytes underwent IVM for 22 h, prior to fixation in 4% paraformaldehyde and antibody staining for  $\alpha$ -tubulin and  $\beta$ -tubulin (green), phalloidin for actin (red), and Hoechst 33342 for nucleic acid detection (blue); a merged image is also displayed. During IVM, there are 4 main stages of meiotic progression: germinal vesicle breakdown (GVBD; top row), metaphase I (MI; second row), anaphase I (AI; third row) and metaphase II (MII; bottom row). Scale bare represents 50  $\mu$ m.

## 5.3 Results

### 5.3.1 Effects of energy stress or LPS on COC expansion

Following 22 h IVM, COCs that were treated with Control, 2-DG, AICAR or Torin 1 (without hormone supplementation), in the presence or absence of LPS, were imaged (**Fig 5.2A**), and the expansion assessed from Grade 0 to Grade 4 (**Fig. 5.2B**). Chi-squared analysis revealed that there was a significant effect of treatment on COC expansion ( $\chi^2$  (df = 6, n = 160) = 18.66,  $P < 0.01$ ). Specifically, there were more COCs at Grade 0 at the end of IVM following treatment with 2-DG, compared with control. Additionally, there was a significant effect of LPS ( $\chi^2$  (df = 4, n = 80) = 50.53,  $P < 0.001$ ), with more COCs progressing to Grade 3 or 4, compared with vehicle.

Cumulus-oocyte complexes that were treated with Control, 2-DG, AICAR or Torin 1 (with hormone supplementation), in the presence or absence of LPS, were imaged (**Fig. 5.3A**), and expansion assessed (**Fig. 5.3B**). Chi-squared analysis revealed that there was a significant effect of treatment on COC expansion ( $\chi^2$  (df = 12, n = 160) = 162.94,  $P < 0.001$ ). Treatment with 2-DG or AICAR impaired COC expansion, with fewer COCs reaching Grade 3 or Grade 4, compared with control. There was no significant effect of LPS alone on COC expansion, however, there was a significant effect of LPS on AICAR treated COCs ( $\chi^2$  (df = 1, n = 80) = 3.91,  $P < 0.05$ ), with more COCs assessed as Grade 1, compared with AICAR treatment alone.

These results confirm that LPS stimulates COC expansion in the absence of hormone supplementation, as previously reported (Bromfield and Sheldon, 2011). When IVM was carried out in the presence of hormone stimulation, treatment with 2-DG or AICAR impaired COC expansion.

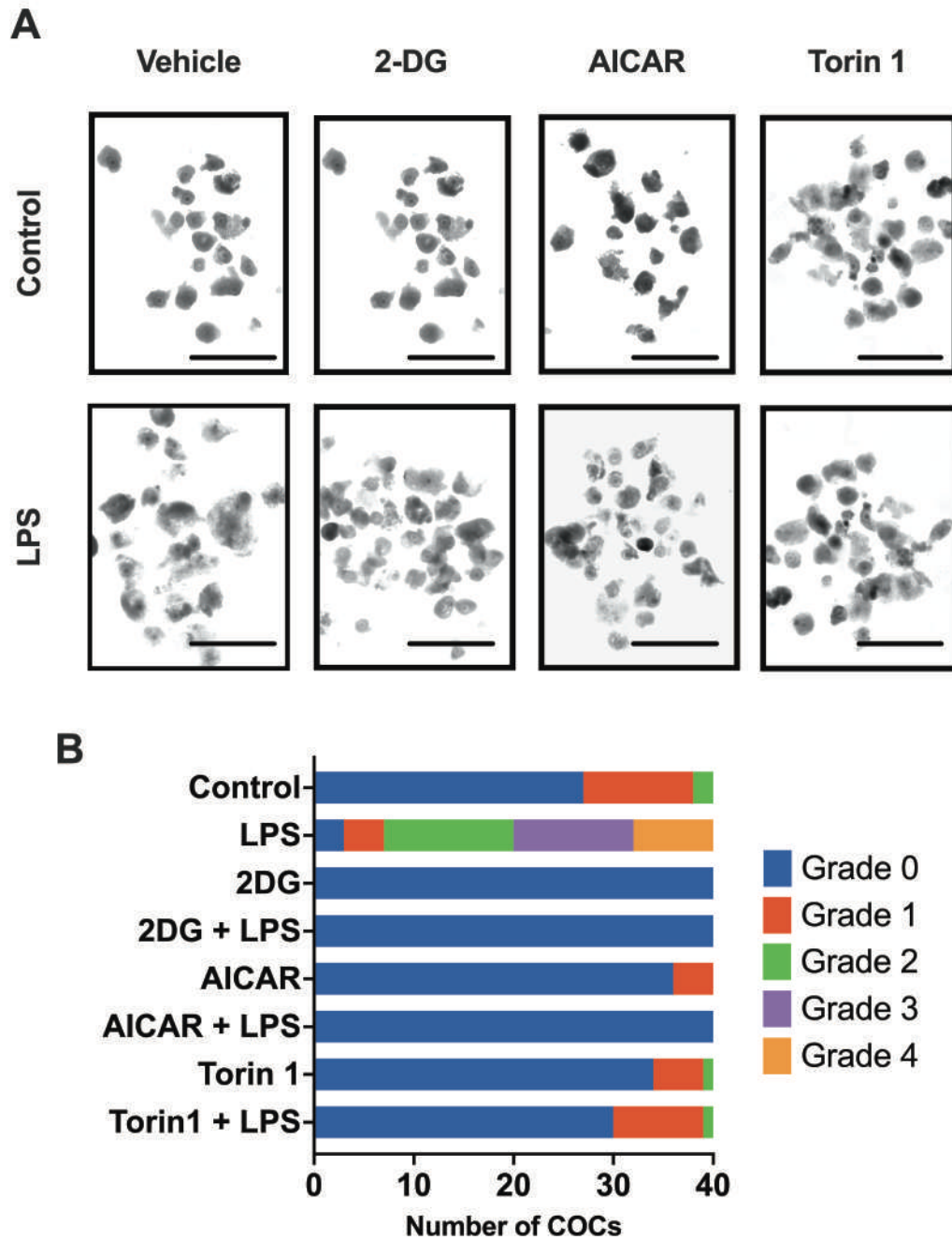


**Figure 5.2. LPS induces COC expansion in absence of hormone supplementation**

Cumulus-oocyte complexes were treated in IVM medium containing control, 1 mM 2-DG, 1 mM AICAR or 50 nM, and challenged with vehicle or 1  $\mu$ g/ml LPS for 22 h. Following IVM, expansion was assessed (A). Forty COCs were assessed per treatment, with a total of 320 COCs assessed over 4 independent occasions. Data are presented as a spine plot, with the number of COCs in each Grade displayed: Grade 0 (blue), Grade 1 (red), Grade 2 (green), Grade 3 (purple) or Grade 4 (orange) (B). Scale bar represents 1 mm.



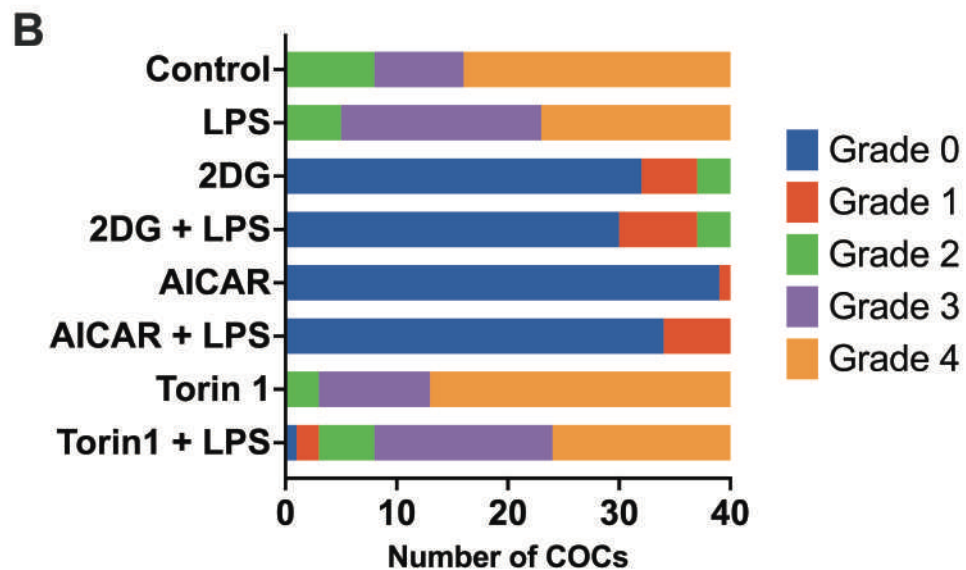
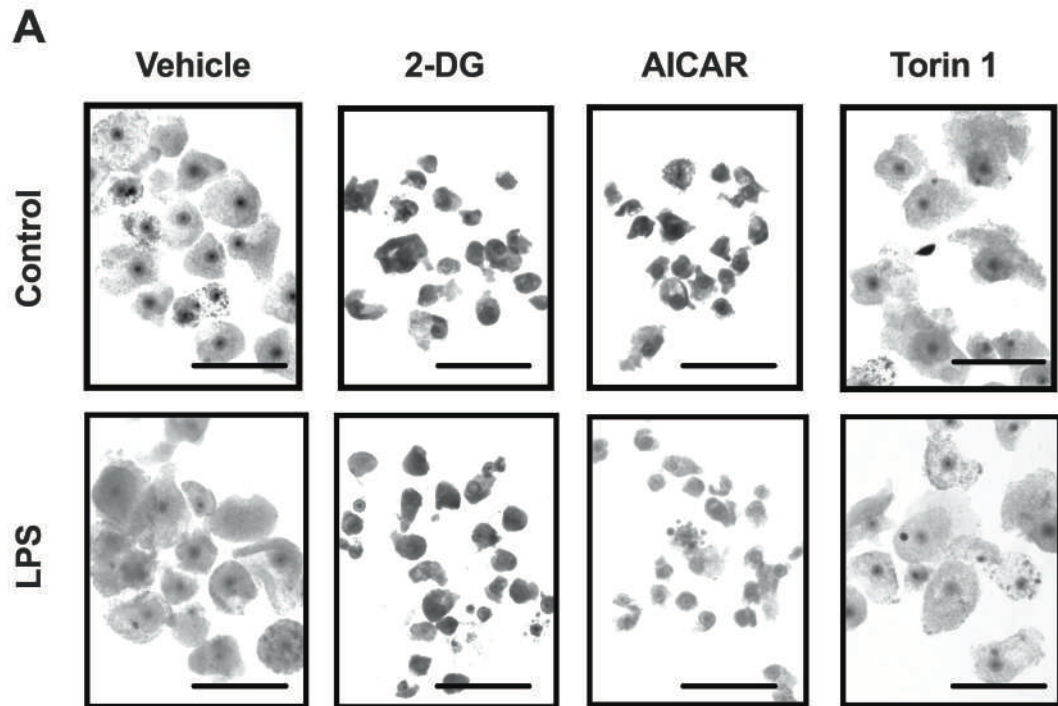


**Figure 5.3. Glycolysis and AMPK are important for COC expansion**

Cumulus-oocyte complexes were treated in IVM medium (supplemented with 20  $\mu\text{g/ml}$  FSH and 2  $\mu\text{g/ml}$  oestradiol) containing control, 1 mM 2-DG, 1 mM AICAR or 50 nM, and challenged with vehicle or 1  $\mu\text{g/ml}$  LPS for 22 h. Following IVM, expansion was assessed (A). Forty COCs were assessed per treatment, with a total of 320 COCs assessed over 4 independent occasions. Data are presented as a spine plot, with the number of COCs in each Grade displayed: Grade 0 (blue), Grade 1 (red), Grade 2 (green), Grade 3 (purple) or Grade 4 (orange) (B). Scale bar represents 1 mm.

### 5.3.2 Manipulating glycolysis, AMPK or mTOR impairs the immune response of COCs to LPS.

Groups of 50 COCs (with hormone supplementation) were treated for 22 h with control, 1 mM 2-DG, 1 mM AICAR or 50 nM Torin 1, in the presence or absence of 1 µg/ml LPS (Fig. 5.4). Bovine COCs secreted IL-1β and IL-8 in response to LPS ( $P < 0.001$ ), but not IL-1α ( $P = 0.96$ ). Treatment with 2-DG, AICAR or Torin 1 reduced the LPS-induced secretion of IL-1β and IL-8 in COCs ( $P < 0.05$ ). Specifically, 2-DG reduced the secretion of IL-1β to levels that were not detectable and reduced the secretion of IL-8 by 28%. Treatment with AICAR also reduced the secretion of IL-1β to levels that were not detectable and reduced the secretion of IL-8 by 28%. Treatment with Torin 1 reduced the LPS-induced secretion of IL-1β by 91% and the LPS-induced secretion of IL-8 by 16%.

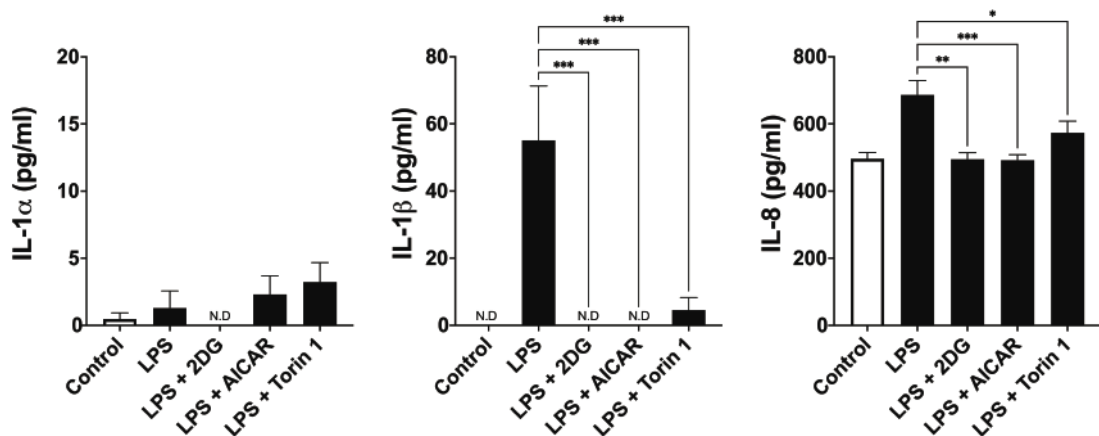


**Figure 5.4. Manipulating energy metabolisms impairs innate immune function of COC's**

Groups of 50 COCs were treated with IVM medium (supplemented with 20 µg/ml FSH and 2 µg/ml oestradiol) containing control, 1 mM 2-DG, 1 mM AICAR or 50 nM Torin 1, in combination with vehicle or 1 µg/ml LPS for 22 h. The accumulation of IL-1α, IL-1β or IL-8 was then assessed by ELISA. Data are presented as mean (SEM) and represent 5 independent experiments. Mean values were compared using one-way ANOVA, using Dunnett's post hoc test. Values differ from LPS, \*\*\*  $P < 0.001$ , \*\*  $P < 0.01$ , \*  $P < 0.05$ .

### 5.3.3 Manipulating glycolysis, AMPK or mTOR impairs the meiotic competence of bovine oocytes

Cumulus-oocyte complexes were treated for 22 h with vehicle, 1 µg/ml LPS, 1 mM 2-DG, 1 mM AICAR or 50 nM Torin 1. Treatments were carried out using either IVM medium without hormone supplementation (**Fig. 5.5**), or IVM media supplemented with hormone supplementation (20 µg/ml FSH and 2 µg/ml oestradiol: **Fig. 5.6**). Following IVM, oocytes were subjected to confocal microscopy to determine meiotic status. In total, 312 oocytes were assessed across 10 different treatment groups.

In the absence of hormonal stimulation, 52% of vehicle oocytes were deemed to have failed meiosis (**Fig. 5.5**). With the limited number of oocytes assessed, we used one-way ANOVA to compare the effects of the treatments on the rate of meiotic failure. There were no significant differences between the meiotic status of oocytes treated with LPS, 2-DG, or Torin 1, compared with vehicle (**Fig. 5.5A**). However, treatment with AICAR, increased the rate of meiotic failure to 96% ( $P < 0.05$ ; **Fig. 5.5A**). On inspection of the meiotic stages (**Fig. 5.5B**), it was observed that treatment with AICAR arrested 96% of oocytes at the GVBD stage (vehicle, 52% vs. AICAR, 96%).

In the presence of hormonal stimulation, 20% of vehicle oocytes were deemed to have failed meiosis (**Fig. 5.6**). With the limited number of oocytes assessed, we used one-way ANOVA to compare the effects of the treatments on the rate of meiotic failure. There was no significant effect of LPS on the rate of meiotic failure, but the rate of meiotic failure did increase to 40%. However, treatment with 2-DG, AICAR or Torin 1 increased the rate of meiotic failure, to 70%, 97% and 73%, respectively ( $P < 0.001$ ; **Fig. 5.6A**). On inspection of the meiotic stages (**Fig. 5.6B**), 2-DG arrested most oocytes at the GVBD (vehicle, 3% vs. 2-DG, 27%) and MI stage of meiosis (vehicle, 8% vs. 2-DG, 33%). AICAR treatment arrested most oocytes at the GVBD stage of meiosis (vehicle, 3% vs. AICAR, 90%). Torin 1 treatment arrested most oocytes at the AI stage of meiosis (vehicle, 8% vs. Torin 1, 41%).

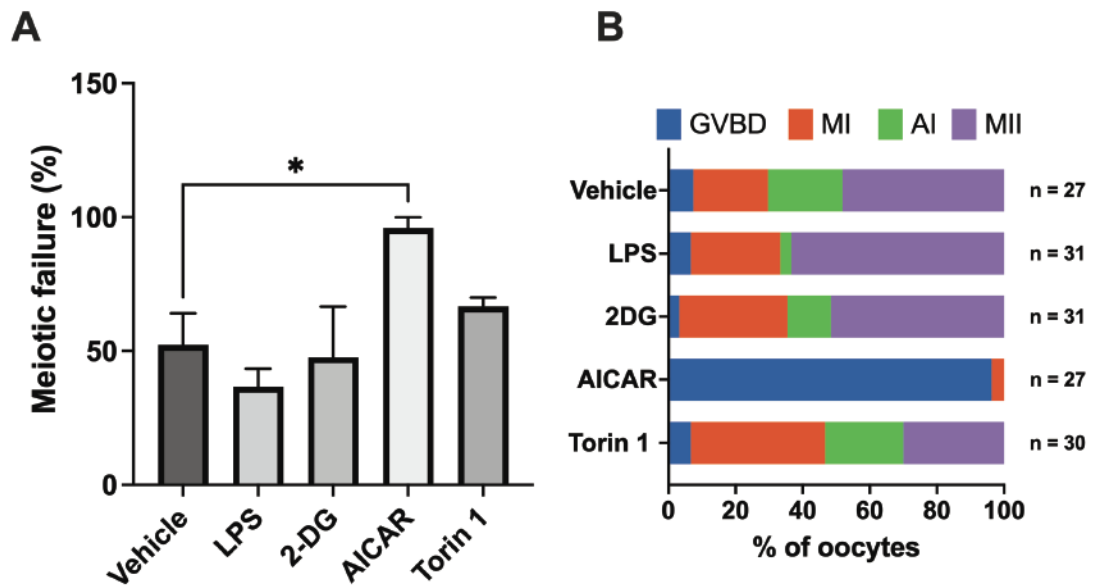


**Figure 5.5. AICAR impairs meiotic progression in the absence of hormones**

Cumulus oocyte complexes were treated in IVM medium without hormone supplementation with vehicle, 1  $\mu\text{g/ml}$  LPS, 1 mM 2-DG, 1 mM AICAR or 50 nM Torin 1 for 22 h. Oocytes that did not progress to the MII phase of meiosis were deemed to have failed meiosis (A). Oocytes were assessed for meiotic progression using confocal microscopy, according to four main criteria: germinal vesicle breakdown (GVBD), metaphase I (MI), anaphase I (AI) or metaphase II (MII) (B). Data are presented as mean (SEM) from at least four independent experiments. Mean values were compared using one-way ANOVA, using Dunnett's post hoc test. Values differ from treatment, \*  $P < 0.05$ .

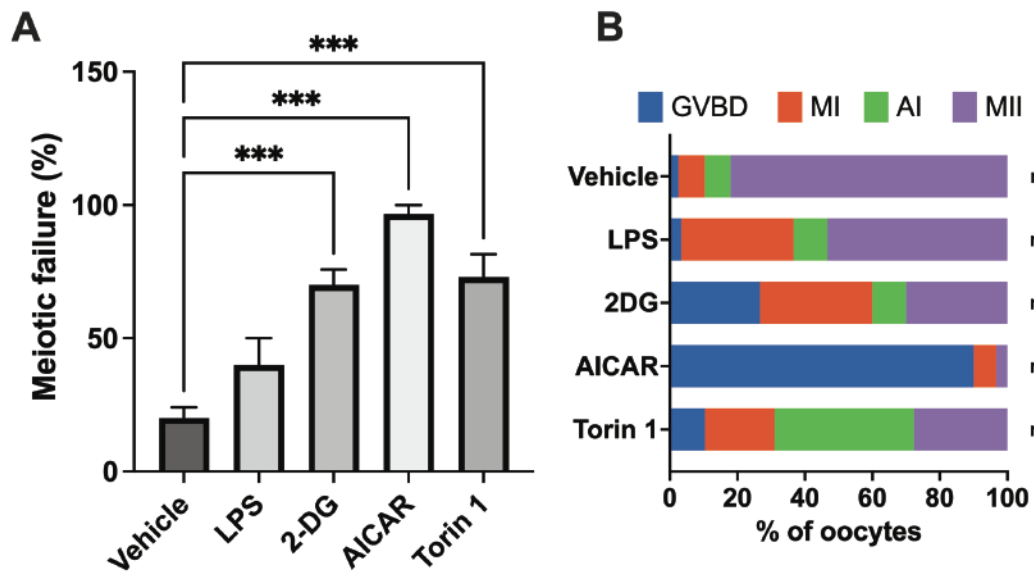


**Figure 5.6. 2-DG, AICAR or Torin 1 treatment impairs meiotic progression during IVM**

Cumulus oocyte complexes were treated in IVM medium (supplemented with 20  $\mu\text{g/ml}$  FSH and 2  $\mu\text{g/ml}$  oestradiol) with vehicle, 1  $\mu\text{g/ml}$  LPS, 1 mM 2-DG, 1 mM AICAR or 50 nM Torin 1 for 22 h. Oocytes that did not progress to the MII phase of meiosis were deemed to have failed meiosis (A). Oocytes were assessed for meiotic progression using confocal microscopy, according to four main criteria: germinal vesicle breakdown (GVBD), metaphase I (MI), anaphase I (AI) or metaphase II (MII) (B). Data are presented as mean (SEM) from at least four independent experiments. Mean values were compared using one-way ANOVA, using Dunnett's post hoc test. Values differ from treatment, \*\*\*  $P < 0.001$ .

#### **5.3.4 AICAR treatment causes abnormal nuclear actin in bovine oocytes**

Interestingly, following treatment with AICAR, we noticed the presence of actin filaments around the chromatin that did not appear to be organized (**Fig. 5.7**). In the absence of hormonal supplementation, following AICAR treatment or AICAR treatment in combination with LPS, 19% (5/27) and 25% (4/16) of the oocytes displayed an abnormal nuclear actin, respectively. In the presence of hormonal supplementation, following AICAR treatment or AICAR treatment in combination with LPS, 7% (2/30) and 3% (1/30) of the oocytes displayed an abnormal nuclear actin, respectively. The control treatment groups appeared normal, and there were no instances of abnormal nuclear actin observed in oocytes cultured with (0/49) or without hormonal supplementation (0/27). Unfortunately, due to the low number of oocytes assessed, the GVBD failure observed in this study was not statistically significant. These data suggest that AICAR treatment may be associated with an increase in the occurrence of disorganized actin filaments in the oocyte.

It is widely accepted that during mammalian oocyte development, there are dynamic changes in the actin cytoskeleton. In addition to the formation of the actin cap, cytoplasmic actin density and the thickness of cortical actin increase during oocyte maturation (Namgoong and Kim, 2016). These data imply that AMPK may be involved in actin re-organization and cytoskeletal dynamics in bovine oocytes during maturation, which warrants further study.

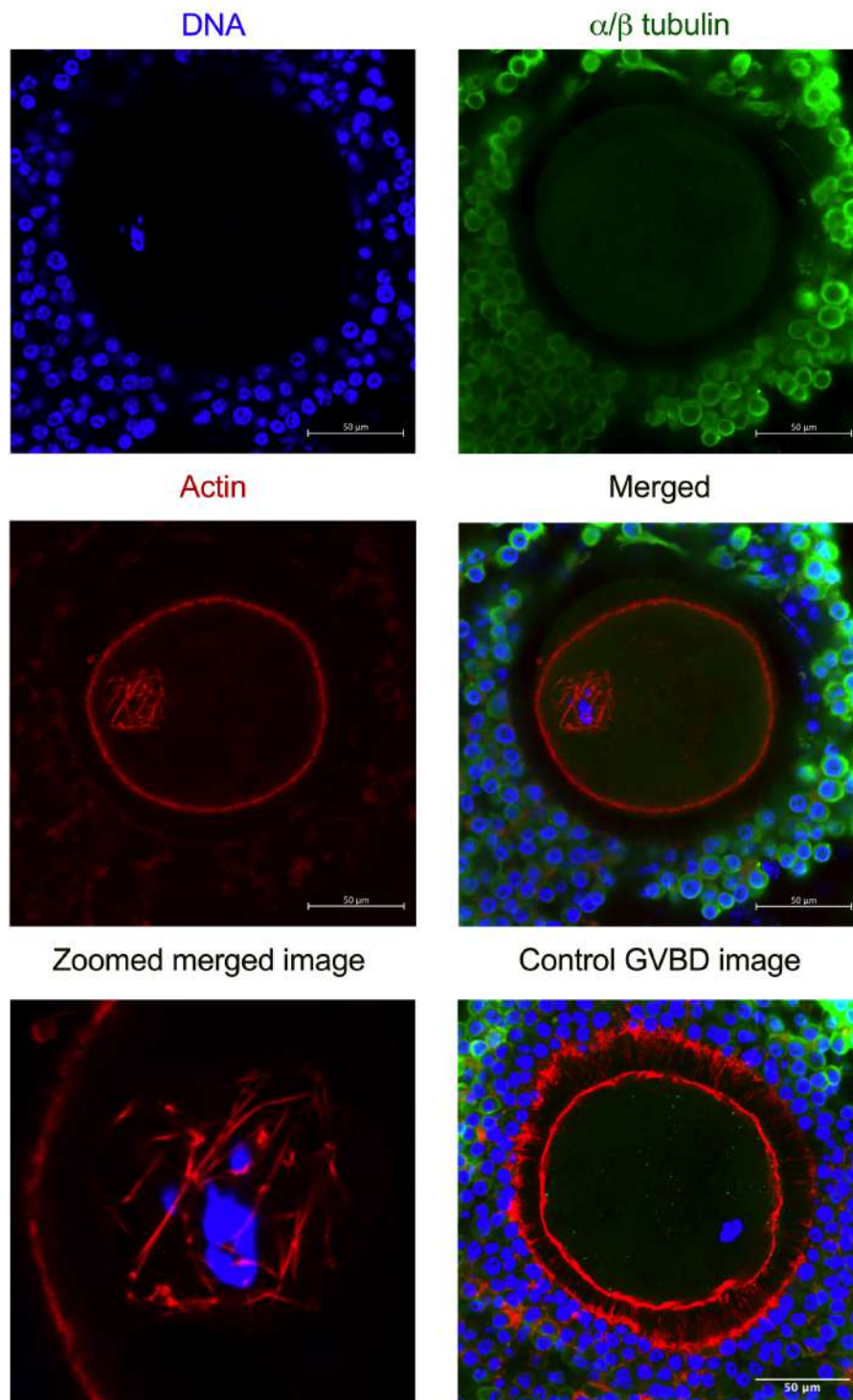


**Figure 5.7. AICAR may induce GVBD failure in bovine oocytes**

Cumulus-oocyte complexes were treated with AICAR and challenged for 22 h with vehicle or 1 μg/ml LPS. Oocytes were fixed, probed for the presence of chromatin (blue), α-tubulin and β-tubulin (green) or F-actin (red), and analysed by confocal microscopy. A merged control GVBD image is provided for comparison. Scale bar represents 50 μm.

### **5.3.5 Cholesterol biosynthesis Inhibitors do not alter COC expansion**

Cumulus-oocyte complexes were treated for 22 h with control or 10  $\mu$ M lovastatin, 10  $\mu$ M alendronate or 10  $\mu$ M zaragozic acid, in the presence or absence of 1  $\mu$ g/ml LPS. Experiments were performed in IVM medium in the presence of 20  $\mu$ g/ml FSH and 2  $\mu$ g/ml oestradiol. Following IVM, images of the COCs were captured (**Fig. 5.8A**) and assessed for cumulus cell expansion (**Fig. 5.8B**). There were no significant differences of the treatments on COC expansion. These data suggest that inhibiting the cholesterol biosynthesis pathway in cumulus cells may not affect expansion of the COC during IVM.

### **5.3.6 Alendronate increases the COC innate immune response to LPS**

Groups of 50 COCs (with hormone supplementation) were treated for 22 h with control or 10  $\mu$ M lovastatin, 10  $\mu$ M alendronate or 10  $\mu$ M zaragozic acid, in the presence or absence of 1  $\mu$ g/ml LPS. Experiments were performed in IVM medium in the presence of 20  $\mu$ g/ml FSH and 2  $\mu$ g/ml oestradiol. Treatment with alendronate, but not lovastatin or zaragozic acid increased the LPS-induced secretion of IL-1 $\beta$  by COCs ( $P < 0.01$ ; **Fig. 5.9**). There was no significant effect on the LPS-induced secretion of IL-1 $\alpha$  or IL-8 in response to treatment with lovastatin, alendronate or zaragozic acid.

### **5.3.7 Cholesterol biosynthesis inhibitors impair meiotic competence**

In the presence of hormonal stimulation, 20% of vehicle oocytes were deemed to have failed meiosis (**Fig. 5.10A**). With the limited number of oocytes assessed, we used one-way ANOVA to compare the effects of the treatments on the rate of meiotic failure. There was no significant effect of LPS treatment on the rate of meiotic failure of oocytes, but the rate of meiotic failure did increase to 40%. However, treatment with lovastatin, alendronate or zaragozic acid increased the rate of meiotic failure to 48%, 50% and 53%, respectively ( $P < 0.05$ ; **Fig. 5.10A**). On inspection of the meiotic stages (**Fig. 5.10B**), lovastatin treatment arrested more oocytes at MI (vehicle, 8% vs. lovastatin, 35%) stage of meiosis. Alendronate treatment arrested more oocytes at the MI (vehicle, 8% vs. alendronate, 28% vs. zaragozic acid, 26%) and AI (vehicle, 8% vs. alendronate, 24% vs. zaragozic acid, 35%) stage of meiosis.



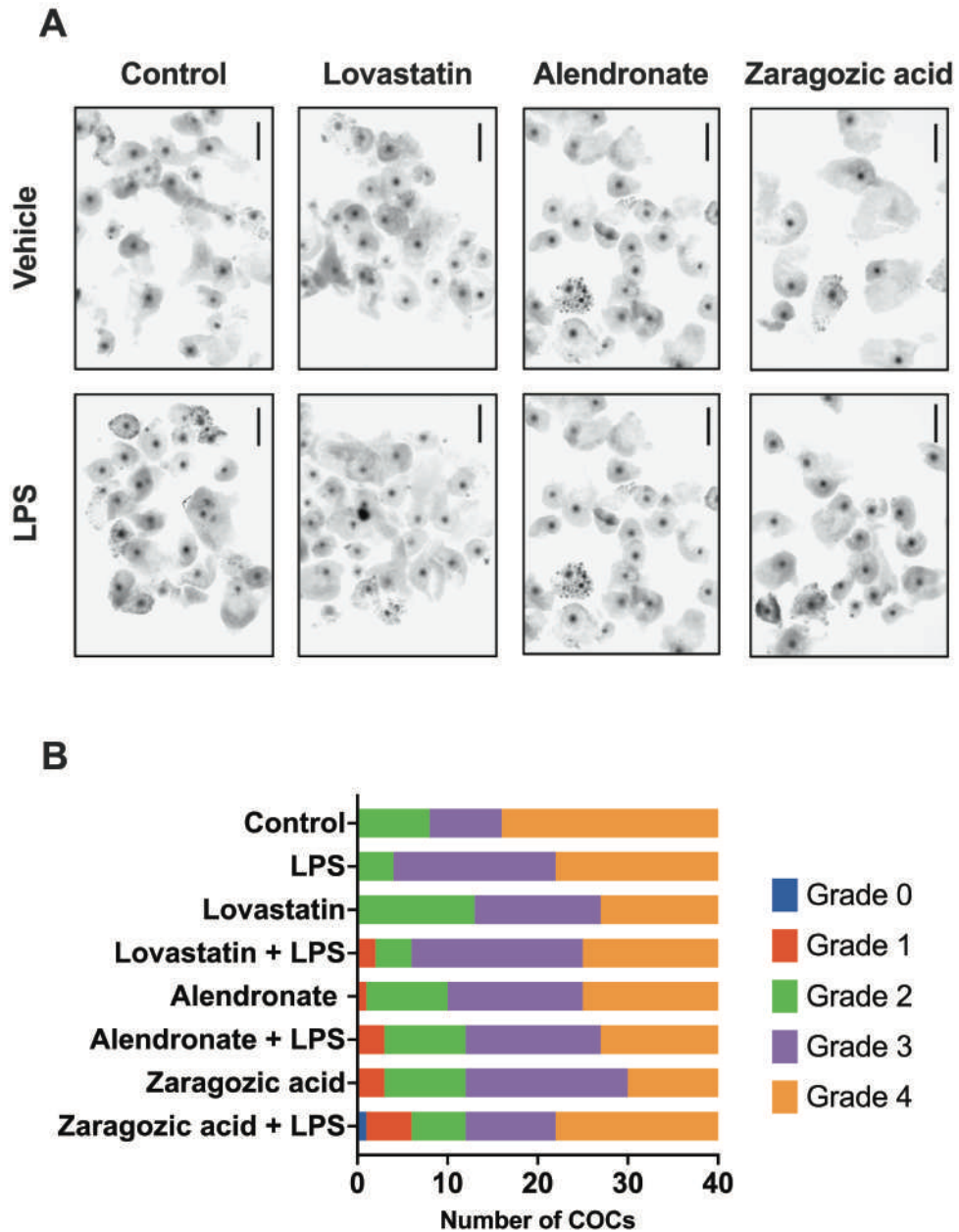


**Figure 5.8. Cholesterol biosynthesis inhibitors do not alter COC expansion**

Cumulus oocyte complexes were treated in IVM medium (supplemented with 20  $\mu\text{g/ml}$  FSH and 2  $\mu\text{g/ml}$  oestradiol) with control, 10  $\mu\text{M}$  lovastatin, 10  $\mu\text{M}$  alendronate or 10  $\mu\text{M}$  zaragozic acid, and challenged with vehicle or 1  $\mu\text{g/ml}$  LPS for 22 h. Following IVM, expansion was assessed (A). Forty COCs were assessed per treatment, on 2 independent occasions, with a total of 320 COCs assessed in total. Data are presented as a spine plot, with the number of COCs in each Grade displayed: Grade 0 (blue), Grade 1 (red), Grade 2 (green), Grade 3 (purple) or Grade 4 (orange) (B). Scale bar represents 1 mm.

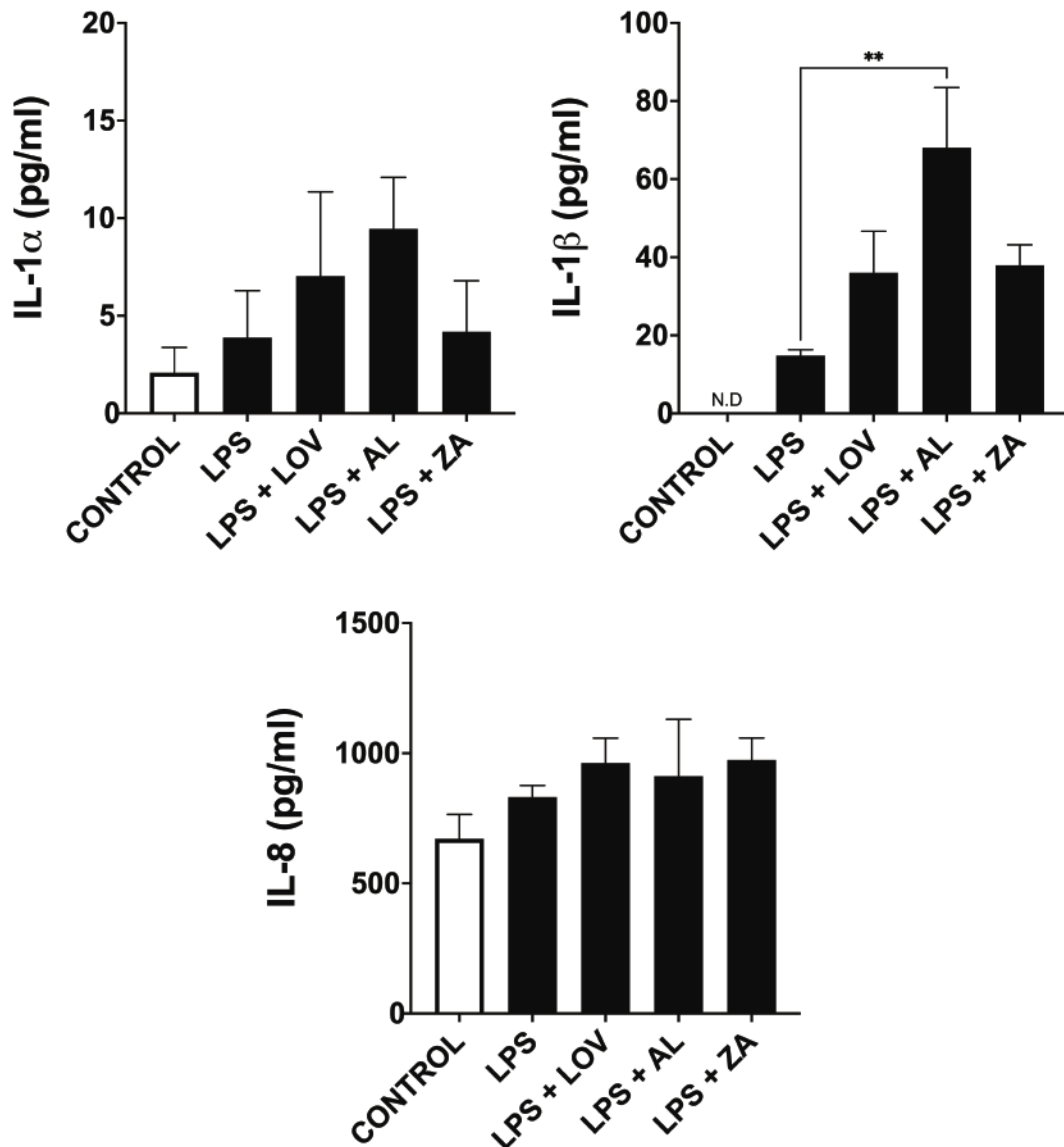


**Figure 5.9. Inhibiting cholesterol metabolism alters the innate immune function of COC's**

Groups of 50 COCs were treated with IVM medium (supplemented with 20 µg/ml FSH and 2 µg/ml oestradiol) containing control, 10 µM lovastatin, 10 µM alendronate or 10 µM zaragozic acid, in combination with vehicle or 1 µg/ml LPS for 22 h. The accumulation of IL-1α, IL-1β or IL-8 was then assessed by ELISA. Data are presented as mean (SEM) and represent 5 independent experiments. Mean values were compared using one-way ANOVA, using Dunnett's post hoc test. Values differ from LPS, \*\*\* P < 0.001, \*\* P < 0.01.

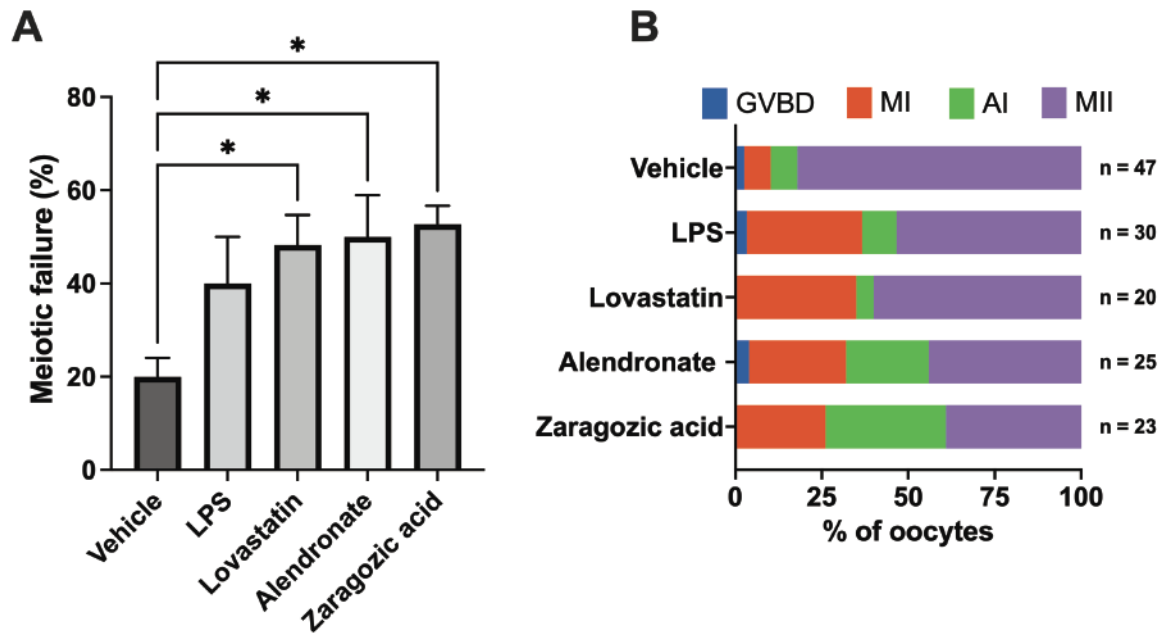


**Figure 5.10. Inhibitors of cholesterol biosynthesis impair meiotic progression during IVM**

Cumulus oocyte complexes were treated in IVM medium (supplemented with 20  $\mu\text{g/ml}$  FSH and 2  $\mu\text{g/ml}$  oestradiol) with vehicle, 1  $\mu\text{g/ml}$  LPS, 10  $\mu\text{M}$  lovastatin, 10  $\mu\text{M}$  alendronate or 10  $\mu\text{M}$  zaragozic acid for 22 h. Oocytes that did not progress to the MII phase of meiosis were deemed to have failed meiosis (A). Oocytes were assessed for meiotic progression using confocal microscopy, according to four main criteria: germinal vesicle breakdown (GVBD), metaphase I (MI), anaphase I (AI) or metaphase II (MII) (B). Data are presented as mean (SEM) from at least three independent experiments. Mean values were compared using one-way ANOVA, using Dunnett's post hoc test. Values differ from treatment, \*  $P < 0.05$ .

## 5.4 Discussion

The hypothesis of this chapter was that energy stress or decreasing the availability of cholesterol would impair the innate immune response of the COC to LPS. We found that treatment with 2-DG, AICAR or Torin 1 reduced the LPS-induced secretion of IL-1 $\beta$  and IL-8 by COCs, suggesting that glycolysis, AMPK and mTOR may regulate innate immunity in bovine COCs. These results are similar to the findings of *Chapter 3*, where treatment of granulosa cells with 2-DG, AICAR or Torin 1 also impaired the innate immune responses to LPS. We also found that treatment with the bisphosphonate, alendronate, increased the LPS-induced secretion of, IL-1 $\beta$  by COCs. Surprisingly, treatment of COCs with lovastatin or zaragozic acid had no significant effect on the LPS-induced secretion of IL-1 $\alpha$  or IL-1 $\beta$ , as observed with mural granulosa cells in *Chapter 4*. Here, bovine COCs secreted IL-1 $\beta$  and IL-8 in response to LPS. Previous studies have detected the LPS-induced secretion of IL-1 $\beta$ , TNF $\alpha$  and IL-6 by bovine COCs (Zhao et al., 2019, Bromfield and Sheldon, 2011). However, we did not observe an increase in IL-1 $\alpha$  secretion in response to LPS, suggesting that either COCs do not secrete IL-1 $\alpha$  in response to LPS, or more likely, that there were insufficient COCs to reach the limit of detection of the assay.

We found that treatment with 2-DG impaired COC expansion. Similarly, mouse COCs treated with 2-DG to mimic acute fasting, exhibited impaired COC expansion during IVM (Han et al., 2012). Glucose and hexosamine are the main substrates for the synthesis of hyaluronic acid, a key component of the extracellular matrix that is secreted by cumulus cells during cumulus expansion (Salustri et al., 1989, Chen et al., 1990). We also found that treatment of bovine COCs with AICAR impaired COC expansion. Activation of AMPK inhibits hyaluronan synthesis (Caon et al., 2021, Vigetti et al., 2014), and treatment of bovine COCs with the AMPK activator, metformin, also impaired the expansion of bovine COCs (Tosca et al., 2007b). Treatment of porcine COCs with AICAR impairs COC expansion, associated with decreased protein synthesis, potentially through inhibition of mTOR (Santiquet et al., 2014). However, when we inhibited mTOR with Torin 1, we did not observe any significant changes in COC expansion.

Inhibition of glycolysis with 2-DG did not alter meiotic progression in the absence of hormone supplementation, however when FSH and oestradiol were present, fewer oocytes progressed to MII, compared with control. The presence of FSH during IVM increases glucose consumption during IVM of bovine (Sutton-McDowall et al., 2004) and porcine COCs (Alvarez et al., 2019). Therefore, the differences in outcomes between COCs cultured with or without hormone supplementation may reflect a crosstalk between metabolic and endocrine pathways. Oocyte meiotic maturation is an energetically expensive process, with higher ATP concentrations detected in bovine oocytes at the MII stage of meiosis, compared with GV stage oocytes (Iwata et al., 2004, Stojkovic et al., 2001, Nagano et al., 2006). Additionally, a recent metabolomics study investigating the metabolic profiles of mouse oocytes found that there was an increase in the abundance of glucose-6-phosphate, as oocytes progressed from GV stage to MII (Li et al., 2020).

Activation of AMPK with AICAR impaired the meiotic progression of oocytes to MII both in the presence and absence of hormones supplementation, with ~90% of oocytes arrested at GVBD stage of meiosis following AICAR treatment. Treatment of bovine COCs with the AMPK activators metformin or AICAR have previously been shown to arrest oocytes at the GV stage of meiosis, after 22 h of IVM (Tosca et al., 2007b, Bilodeau-Goeseels et al., 2007). Signalling molecules, such as cyclic adenosine monophosphate (cAMP) are present in follicular fluid that activate cAMP-dependent protein kinase A (PKA) (Conti et al., 2002). Cyclic AMP can be broken down into AMP by phosphodiesterases, leading to the activation of AMPK (Hardie and Carling, 1997). Oocytes spontaneously resume meiosis when cultured *in vitro* (Pincus and Enzmann, 1935, Edwards, 1965). Therefore, the spontaneous resumption of meiosis *in vitro* may be due to the reduction in signalling molecules, such as cAMP.

One interesting finding was that treatment with AICAR resulted in GVBD failure in some cases. This was characterized by the presence of disorganized actin filaments contracted around the chromatin. Actin filaments are essential for cellular processes during meiosis, such as nuclear positioning, spindle rotation, spindle migration, chromosome segregation and polar body extrusion (Duan and Sun, 2019). Unfortunately, we had insufficient samples to be able to explore this further, but future

studies could investigate this interesting anomaly to investigate the role of AMPK in actin re-organization during meiosis.

Treatment with Torin 1 in the absence of hormone stimulation, did not alter meiotic progression. However, in the presence of hormone stimulation, more oocytes were arrested at AI and fewer oocytes progressed to MII compared, with control. Similar results have been observed in *Mtor* conditional knockout mice, where a significant increase in the percentage of oocytes arrested at telophase I was observed, compared with wild-type mice (Guo et al., 2018b). In mouse oocytes, mTOR localizes around the meiotic spindle (Lee et al., 2012, Kogasaka et al., 2013). Additionally, treatment with rapamycin was associated with inhibition of spindle migration and unusually large polar bodies (Lee et al., 2012).

Finally, treatment with lovastatin, alendronate or zaragozic acid had no significant effect on COC expansion during IVM. Treatment with lovastatin did not alter the percentage of oocytes progressing to MII, however, in combination with LPS there was a significant increase in the percentage of oocytes arrested at AI, compared with control. It has been suggested that metabolites of HMGCR are required for progression from meiosis I in clam oocytes (Turner et al., 1995). A study comparing the expression of target genes in prepubertal (less competent), and mature (more competent) porcine oocytes identified *HMGCR* as a potential marker of increased oocyte competence (Yuan et al., 2011). Treatment with alendronate or zaragozic acid reduced the percentage of oocytes progressing to MII, compared with control.

A recent metabolomics study investigating the metabolic profiles of mouse oocytes found that there a decrease in the abundance of cholesterol, as oocytes progressed from GV stage to MII (Li et al., 2020). Oocytes store cholesterol, along with triglycerides, phospholipids, free fatty acids, and proteins, as lipid droplets (Amstislavsky et al., 2019). Lipid droplets are an energy source for oocytes, and fatty acids and  $\beta$ -oxidation may play an important role in oocyte maturation and development (Ferguson and Leese, 2006, Ferguson and Leese, 1999, Dunning et al., 2014). Bovine oocytes contain around 16.3 pmol of total cholesterol (Kim et al., 2001). Cholesterol may be important for oocyte division following fertilization because the rate of phospholipid synthesis doubles from the 2-cell to the 8-cell stage in mouse embryos (Pratt, 1980). However,

mouse embryos are only capable of synthesizing membrane sterols from the 8-cell stage (Pratt et al., 1980). It is possible that due to the oocyte's inability to synthesize its own cholesterol until the 8-cell blastocyst stage, it relies on the stored cholesterol provided by the cumulus cells up until the time of COC expansion, to maintain its development.

Inhibition of the cholesterol biosynthesis pathway might also alter the concentrations of isoprenoids, such as farnesyl diphosphate or geranylgeranyl diphosphate. Depletion of geranylgeranyl diphosphate in mouse oocytes arrests granulosa cell proliferation and the physical connection between the oocyte and granulosa cells, potentially reducing fertility (Jiang et al., 2017). Additionally, squalene, a product of FDFT1 (squalene synthase), is converted via a series of enzymatic steps to lanosterol, which is then converted to follicular fluid meiosis-activating sterol (FF-MAS) an intermediate of the cholesterol biosynthetic pathway that enhances meiotic maturation of mouse (Marin Bivens et al., 2004, Downs et al., 2001), porcine (Faerge et al., 2006), and bovine (Donnay et al., 2004) oocytes. Future studies could investigate the impact of cholesterol biosynthesis intermediates, such as FPP or GGPP, or cholesterol derivatives, such as oxysterols, on oocyte competence.

The effect of LPS in these experiments on COC expansion and meiotic progression were negligible. This may highlight the importance of glycolysis, AMPK, mTOR and cholesterol biosynthesis during COC expansion and oocyte meiotic maturation. We confirmed that in the absence of hormone supplementation, LPS treatment is associated with increased COC expansion (Bromfield and Sheldon, 2011). However, we found that when COCs were treated with 2-DG, AICAR or Torin 1, the LPS-induced COC expansion was reversed. In summary, we found that inhibiting glycolysis with 2-DG, or activating AMPK with AICAR impaired COC expansion, whereas inhibiting mTOR with Torin 1 did not alter COC expansion. Treatment with 2-DG, AICAR or Torin 1 impaired the innate immune response of COCs to LPS, and the meiotic progression of oocytes to MII during IVM. Whilst inhibitors of cholesterol biosynthesis did not affect COC expansion, meiotic progression of oocytes to MII was impaired. In conclusion, we provide evidence that energy stress or impairing cholesterol biosynthesis might reduce oocyte health which may negatively impact fertility

## 6 Uterine infection alters bovine endometrium, oviduct, granulosa cell and oocyte transcriptome several months later

### 6.1 INTRODUCTION

Infection of the uterus with bacteria is ubiquitous following parturition, and between 15 to 20% of dairy cattle develop clinical endometritis (LeBlanc et al., 2002, Sheldon et al., 2009). Clinical endometritis is characterised by the presence of pus within the uterus and a purulent uterine discharge detectable in the vagina 21 days or more postpartum (Sheldon et al., 2019a). Endometritis is associated with infection of the uterus with *Escherichia coli*, *Trueperella pyogenes*, *Fusobacterium necrophorum*, and *Prevotella* and *Bacteroides* species (Griffin et al., 1974, Noakes et al., 1991, Huszenicza et al., 1991, Sheldon et al., 2002). Notably, endometrial pathogenic strains of *Escherichia coli* are adapted to cause endometritis (Sheldon et al., 2010, Bicalho et al., 2010), and *Trueperella pyogenes* is the pathogen most associated with the severity of endometritis (Bonnett et al., 1991, Westermann et al., 2010). Moreover, intrauterine infusion of endometrial pathogenic *E. coli* and *T. pyogenes* into cattle induces clinical endometritis (Amos et al., 2014, Piersanti et al., 2019c). The clinical disease usually resolves following treatment, or spontaneously resolves after one to two months. However, the importance of endometritis is that even after resolution of the disease, animals remain less fertile than unaffected animals. Compared with unaffected animals, a history of endometritis increases the interval to first insemination by approximately 11 days, delays conception by 32 days, and nearly doubles involuntary culling (Borsberry and Dobson, 1989, LeBlanc et al., 2002). The gap in knowledge is whether uterine bacterial infections lead to long-term changes in the reproductive tract that might help explain the persistence of infertility.

During infection, bacteria or their virulence factors cause short-term inflammation and damage in the reproductive tract (Bromfield et al., 2015, Herath et al., 2009). Endometrial cells mount rapid innate immune responses to bacteria or pathogen associated molecules, such as lipopolysaccharide (LPS), by increasing secretion of prostaglandin E<sub>2</sub>, interleukin (IL)-1, IL-6, and IL-8 (Herath et al., 2006, Cronin et al., 2012, Turner et al., 2014b). Endometrial cells are also susceptible to rapid damage by pore-forming toxins produced by pathogens such as *T. pyogenes* (Amos et al., 2014,



Healy et al., 2014). Oviductal epithelial cells also mount inflammatory responses to LPS, including increased expression of genes associated with inflammation, such as *TNFA* and *IL1B* (Kowsar et al., 2013, Ibrahim et al., 2015). Lipopolysaccharide has been shown to accumulate in the dominant follicle of animals with uterine disease (Herath et al., 2007). Granulosa cells from antral follicles secrete IL-1 $\beta$ , IL-6 and IL-8 in response to LPS (Price et al., 2013, Price and Sheldon, 2013, Bromfield and Sheldon, 2011).

As well as short-term changes, there is *in vivo* evidence that there are long-term residual effects of infection on the tissues of the genital tract (Ribeiro et al., 2016, Piersanti et al., 2019a). Cows that have inflammatory diseases such as metritis, before breeding experienced reduced fertilization and development of oocytes, and increased risk of pregnancy loss, with effects on the developmental biology potentially lasting longer than 4 months (Ribeiro et al., 2016). There appears to be a long-term impact of metritis on the granulosa cells of the dominant follicle. A study of 19 healthy and 15 cows that had been diagnosed with metritis found that there were persistent changes to the transcriptome of the granulosa cells from the dominant follicle, 6 weeks after the resolution of disease (Piersanti et al., 2019a).

Unfortunately, one of the challenges for studying the long-term effects of bacterial infection on the reproductive tract in animals with spontaneous disease is disentangling the effect of infection from the effects of other peripartum problems, metabolic stress and lactation (Chagas et al., 2007, LeBlanc, 2012, Cerri et al., 2012, Girard et al., 2015). Postpartum dairy cattle cannot consume enough food to meet the metabolic demands of lactation, and as a result, body fat and muscle is catabolised to meet the energy requirements (Bauman and Currie, 1980, Coffey et al., 2004). This state of NEB is an altered metabolic state that can lead to metabolic disorders and reduced fertility. This period of NEB may last up to 20 weeks in the postpartum period (Beever et al., 2001). Lactation altered the transcriptome of intercaruncular endometrial tissue, upregulating genes involved in immunity, which may negatively affect the ability of the uterus to support the embryo (Cerri et al., 2012). Additionally, severe negative energy balance can directly affect the granulosa cells of the dominant follicle, possibly contributing to impaired fertility following parturition. Severe negative energy balance altered the transcriptome of granulosa cells at 60 days postpartum, downregulating

genes involved in cellular organization, proliferation, and fatty acid metabolism (Girard et al., 2015).

In the present thesis, we have explored the crosstalk between innate immunity and metabolic energy stress in bovine granulosa cells and cumulus-oocyte complexes, in *Chapter 3* and *Chapter 5*, respectively. In the present chapter, we exploited an *in vivo* model of endometritis in cattle to explore the long-term effects of uterine disease on the transcriptome of the ovary and tissues of the genital tract. Specifically, the hypothesis for this chapter was that intrauterine infusion of pathogenic bacteria leads to changes in the transcriptome of the reproductive tract in dairy cattle several months later.

The model of clinical endometritis in virgin Holstein heifers was initially developed at the University of Florida Dairy Research Unit to investigate the short-term responses to uterine infection, whilst avoiding the confounding effects of periparturient problems, metabolic stress, and lactation (Piersanti et al., 2019c). However, in this chapter, we used the model of endometritis to explore the long-term responses. Briefly, animals were infused intrauterine with either control vehicle or with *E. coli* and *T. pyogenes* to induce endometritis.

Prior to infusion of vehicle or pathogenic bacteria, oestrous cycles were synchronised using the OvSynch protocol to induce ovulation, as previously described (Lima et al., 2013). Similarly, starting 80 days after infusion, the oestrous cycles of all animals were also synchronized, with the second GnRH administered 6 days before sample collection, to induce ovulation. The animals were slaughtered three months (94 days) following the infusion, and the endometrium, oviduct and granulosa cells were collected. The tissues then underwent RNA sequencing at the Interdisciplinary Centre for Biotechnology Research (University of Florida).

## 6.2 MATERIALS AND METHODS

### 6.2.1 Animal model of endometritis

An animal model of endometritis was developed at the University of Florida Dairy Research Unit (Gainesville, FL, USA) (Piersanti et al., 2019c), as described in *Chapter 2*. Briefly, virgin Holstein heifers, 11 to 13 months old received a control intrauterine infusion (n = 6) or intrauterine pathogenic bacteria that induced clinical endometritis (n = 4). Control heifers had no evidence of increased mucus, or echogenic material in the uterus, which would have indicated the presence of endometritis.

### 6.2.2 Collection of reproductive tract tissues

Reproductive tracts and oocytes were collected 94 days and 60 days after bacterial infusion, respectively, as described in *Chapter 2*. Isolation of RNA was carried out at the University of Florida Dairy Research Unit, and RNA sequencing was performed at the Interdisciplinary Centre for Biotechnology Research, University of Florida. Technical problems prevented collection of the oviduct from one bacteria-infused animal and the intercaruncular endometrium from a separate bacteria-infused animal.

The transcripts of *Bos taurus* (76,341 sequences) retrieved from the NCBI genome database (GCF\_002263795.1) were used as reference sequences for RNAseq analysis. The RNAseq data was deposited in NCBI's Gene Expression Omnibus database and is accessible through GEO Series accession number GSE140469 <https://www.ncbi.nlm.nih.gov/geo/query/acc.cgi?acc=GSE140469>. Gene expression was compared between the bacteria-infused and control animals by counting the number of mapped reads for each transcript (Yao and Yu, 2011).

The data generated from this model of endometritis in cattle was analysed by Ingenuity Pathway Analysis (IPA) for the present chapter.

### 6.2.3 Data Analysis

The experimental unit was each individual animal, and comparisons were made between bacteria-infused and control animals. The RNAseq gene expression data for each tissue was used to generate volcano plots, and for principle component analysis, which was performed using Clustvis (<https://biit.cs.ut.ee/clustvis/>) (Metsalu and Vilo, 2015). Genes that were differentially expressed between bacteria-infused and control animals were selected using  $P < 0.05$  and are reported as  $\log_2$  fold-change ( $\log_2\text{FC}$ ); adjusted  $P$ -values for false discovery rate were not used because the values were  $P > 0.10$ . As described previously (Kong et al., 2017), this approach allowed the generation of informative differentially expressed gene (DEG) lists for each tissue, and the identification of pathways and networks that were affected by bacterial infusion. Heatmaps were generated for the DEGs of individual animals with Heatmapper (<http://www.heatmapper.ca>) (Babicki et al., 2016), using Euclidean distance and average linkage (Quackenbush, 2001). Venn diagrams were generated using jvenn to compare the DEGs amongst tissues (<http://jvenn.toulouse.inra.fr/app/index.html>) (Bardou et al., 2014). Unless stated otherwise, figures were generated in GraphPad Prism (GraphPad Software).

Ingenuity Pathway Analysis (Qiagen) was used to identify pathways, gene networks, and upstream regulators of DEGs affected by bacterial infusion (Kramer et al., 2014). Pathways were identified by  $-\log P > 1.3$  and  $\log_2\text{FC} \leq -2$  or  $\geq 2$ , and corresponding z-scores were calculated to predict activation status. Gene networks were identified by assessing the number of DEGs in each network, and gene network scores were calculated by the software (a network score of  $\geq 2$  gives 99% confidence the network was not identified by chance). Upstream regulators of DEGs, and predicted diseases and functions were identified by z-scores  $\geq 2$  or  $\leq -2$  and were considered significant predictors of activation or inhibition of DEGs, respectively (Hatzirodos et al., 2014b, Piersanti et al., 2019a).

## 6.3 RESULTS

### 6.3.1 Effects of bacterial infusion on tissue transcriptomes and differentially expressed genes

**Caruncular endometrium** produced an average of 31,493 mapped transcripts per sample for analysis with an average of 31% of the high-quality reads aligned to the *Bos taurus* reference genome (**Supplemental Table 1**). There were 87 upregulated and 45 downregulated DEGs in bacteria-infused animals compared with controls, as illustrated in a volcano plot of all the caruncular endometrium genes (**Fig. 6.1A**, top panel). Principle component analysis, based on all the genes is presented in **Fig. 6.1A** (middle panel), with principal components 1 and 2 explaining 20% and 16% of the variance, respectively. A heatmap of the distribution of the DEGs across the samples illustrates the separation between the bacteria-infused and control animals (**Fig. 6.1A**, bottom panel). The five most upregulated genes in bacteria-infused animals were *SLC45A1*, *ADARB1*, *RNF38*, *DBNDD1* and *GOLGA3*, and the five most downregulated genes were *MMP3*, *SPAG9*, *NXPE3*, *ATG10* and *VPREB3* (**Supplemental Table 2**).

**Intercaruncular endometrium** produced an average of 32,818 mapped transcripts per sample for analysis with an average of 32% of the high-quality reads aligned to the *Bos taurus* reference genome (**Supplemental Table 3**). There were 34 upregulated and 43 downregulated DEGs in bacteria-infused animals, as illustrated in a volcano plot (**Fig. 6.1B**, top panel). Principle component analysis is presented in **Fig. 6.1B** (middle panel), with principal component 1 and 2 explaining 24% and 16% of the variance, respectively. A heatmap of the DEGs illustrates the separation between the bacteria-infused and control animals (**Fig. 6.1B**, bottom panel). The five most upregulated genes in bacteria-infused animals were *CFAP69*, *CYP11B2*, *FBXW7*, *PDPI* and *CREM*, and the five most downregulated genes were *VNN2*, *FCMR*, *SMIM12*, *VPREB3* and *POU2AF1* (**Supplemental Table 4**).

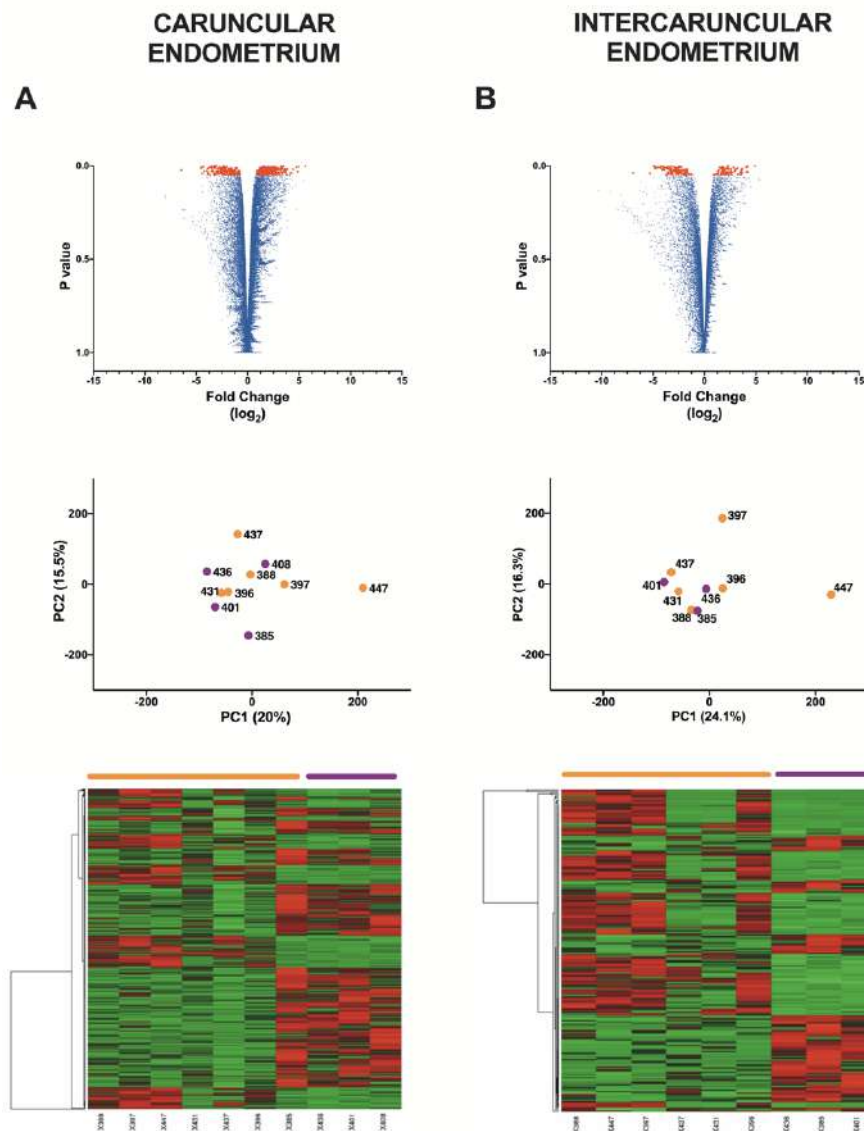


**Figure 6.1. Volcano plots, principal component analysis and heatmap analysis for bacteria-infused and control animals**

Volcano plots (top panel), principal component analysis (middle panel), and heatmap plots (bottom panel) are presented for (A) caruncular endometrium and (B) intercaruncular endometrium. The volcano plots present each gene detected by RNAseq, with differentially expressed genes (DEGs) coloured red. Principal component analyses used all the genes detected by RNAseq in each tissue for control (orange) and bacteria-infused animals (purple). Heatmaps present hierarchical clustering of DEGs, with each column representing an animal and each row a gene; rows were clustered using Euclidian distance and average linkage; gene expression intensities are displayed from green (reduced expression) to red (increased expression) in bacteria-infused compared with control animals.

**Isthmus** produced an average of 29,470 mapped transcripts per sample for analysis with an average of 38% of the high-quality reads aligned to the *Bos taurus* reference genome (**Supplemental Table 5**). There were 45 upregulated and 34 downregulated DEGs in bacteria-infused animals, as illustrated in a volcano plot (**Fig. 6.2A**, top panel). Principle component analysis is presented in **Fig. 6.2A** (middle panel), with principal component 1 and 2 explaining 34% and 16% of the variance, respectively. A heatmap of the DEGs illustrates the separation between the bacteria-infused and control animals (**Fig. 6.2A**, bottom panel). The five most upregulated genes in bacteria-infused animals were *CXCRI*, *CXCL8*, *ATP13A3*, *UBTF* and *PROCR*, and the five most downregulated genes were *GLIPR1L1*, *TNNI3K*, *CEP41*, *FZD5* and *NXPE3* (**Supplemental Table 6**).

**Ampulla** produced an average of 29,662 mapped transcripts per sample for analysis with an average of 39% of the high-quality reads aligned to the *Bos taurus* reference genome (**Supplemental Table 7**). There were 119 upregulated and 197 downregulated DEGs in bacteria-infused animals, as illustrated in a volcano plot (**Fig. 6.2B**; top panel). Principle component analysis is presented in **Fig. 6.2B** (middle panel), with principal component 1 and 2 explaining 34% and 16% of the variance, respectively. A heatmap of the DEGs illustrates the separation between the bacteria-infused and control animals (**Fig. 6.2B**; bottom panel). The five most upregulated genes in bacteria-infused animals were *GSGIL*, *SLP1*, *KCNE4*, *ABCC6* and *KERA*, and the five most downregulated genes were *USP46*, *ZDHHC9*, *ZBTB24*, *ZNF319* and *KIAA0040* (**Supplemental Table 8**).

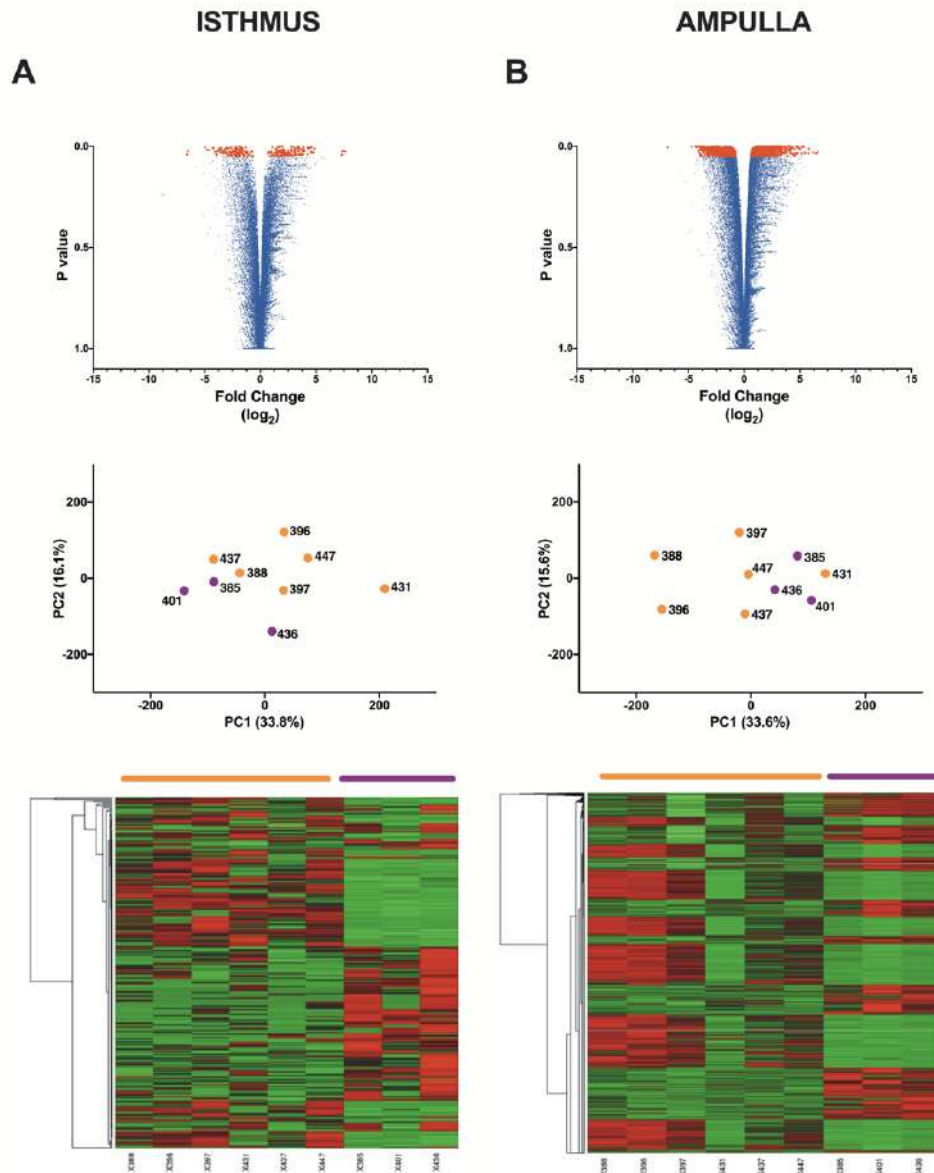


**Figure 6.2. Volcano plots, principal component analysis and heatmap analysis for bacteria-infused and control animals**

Volcano plots (top panel), principal component analysis (middle panel), and heatmap plots (bottom panel) are presented for (A) isthmus and (B) ampulla. The volcano plots present each gene detected by RNAseq, with differentially expressed genes (DEGs) coloured red. Principal component analyses used all the genes detected by RNAseq in each tissue for control (orange) and bacteria-infused animals (purple). Heatmaps present hierarchical clustering of DEGs, with each column representing an animal and each row a gene; rows were clustered using Euclidian distance and average linkage; gene expression intensities are displayed from green (reduced expression) to red (increased expression) in bacteria-infused compared with control animals.



**Granulosa** cells produced an average of 16,978 mapped transcripts per sample for analysis with an average of 30% of the high-quality reads aligned to the *Bos taurus* reference genome (**Supplemental Table 9**). There were 88 upregulated and 1 downregulated DEGs in bacteria-infused animals, as illustrated in a volcano plot (**Fig. 6.3A**; top panel). Principle component analysis is presented in **Fig. 6.3A** (middle panel), with principal component 1 and 2 explaining 42% and 19% of the variance, respectively. A heatmap of the DEGs shows a clear separation between the bacteria-infused and control animals (**Fig 6.3A**; bottom panel). The five most upregulated genes in bacteria-infused animals were *FAM71A*, *EOMES*, *ALKAL2*, *ADAMTS1* and *ARHGAP9*, and the only downregulated gene was *CARD9* (**Supplemental Table 10**).

**Oocytes** produced an average of 24,110 mapped transcripts per sample for analysis with an average of 40% of the high-quality reads aligned to the *Bos taurus* reference genome (**Supplemental Table 11**). There were 287 upregulated and 24 downregulated DEGs in bacteria-infused animals, as illustrated in a volcano plot (**Fig. 6.3B**; top panel). Principle component analysis is presented in **Fig. 6.3B** (middle panel), with principal component 1 and 2 explaining 21% and 14% of the variance, respectively. A heatmap of the DEGs shows a clear separation between the bacteria-infused and control animals (**Fig, 6.3B**; bottom panel). The five most upregulated genes in bacteria-infused animals were *TNFAIP6*, *GPR50*, *CSRP3*, *PALMD* and *TNFSF18* and the five most downregulated genes were *ADAM22*, *CALHM4*, *DNER*, *IL2RG* and *RCVRN* (**Supplemental Table 12**).

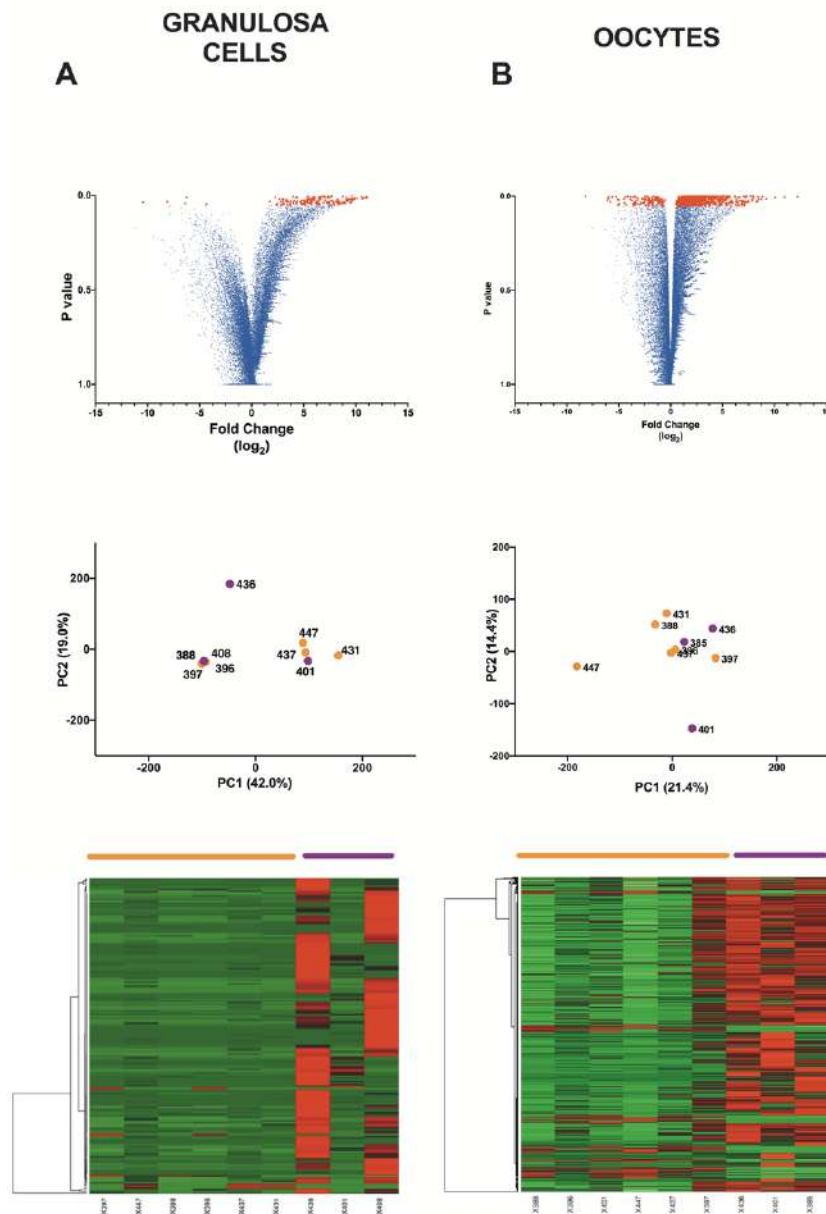


**Figure 6.3. Volcano plots, principal component analysis and heatmap analysis for bacteria-infused and control animals**

Volcano plots (top panel), principal component analysis (middle panel), and heatmap plots (bottom panel) are presented for (A) granulosa cells and (B) oocytes. The volcano plots present each gene detected by RNAseq, with differentially expressed genes (DEGs) coloured red. Principal component analyses used all the genes detected by RNAseq in each tissue for control (orange) and bacteria-infused animals (purple). Heatmaps present hierarchical clustering of DEGs, with each column representing an animal and each row a gene; rows were clustered using Euclidian distance and average linkage; gene expression intensities are displayed from green (reduced expression) to red (increased expression) in bacteria-infused compared with control animals.

### **6.3.2 Shared and unique DEGs between control and bacteria-infused animals.**

The shared and unique DEGs amongst the tissues are presented in **Figure 6.4**. However, none of the DEGs were common across all the tissues and most DEGs were unique to each tissue. There were 103 and 57 unique DEGs in the caruncular and intercaruncular endometrium, 65 and 290 in the isthmus and ampulla, respectively, and 83 and 291 in granulosa cells and oocytes. Taken together, these data (**Fig. 6.1-6.4**) provide evidence that there were tissue-specific alterations in the reproductive tract 3 months after bacterial infusion.

### **6.3.3 Pathway analysis of differentially expressed genes**

Ingenuity Pathway Analysis of DEGs identified 5 canonical pathways with z-scores  $\leq -2$  or  $\geq 2$  in the bacteria-infused animals, including downregulation of phospholipase C signalling in the intercaruncular endometrium, upregulation of 3-phosphoinositide biosynthesis in the caruncular endometrium, and upregulation of the IL-8 pathway in the isthmus (**Fig. 6.5**). When considering pathways below the z-score cut-off (Oguejiofor et al., 2015), there were 18 affected pathways in the caruncular endometrium, 21 in the intercaruncular endometrium, 16 in the isthmus, 24 in the ampulla, 10 in the granulosa cells and 26 in oocytes (**Fig. 6.5**).

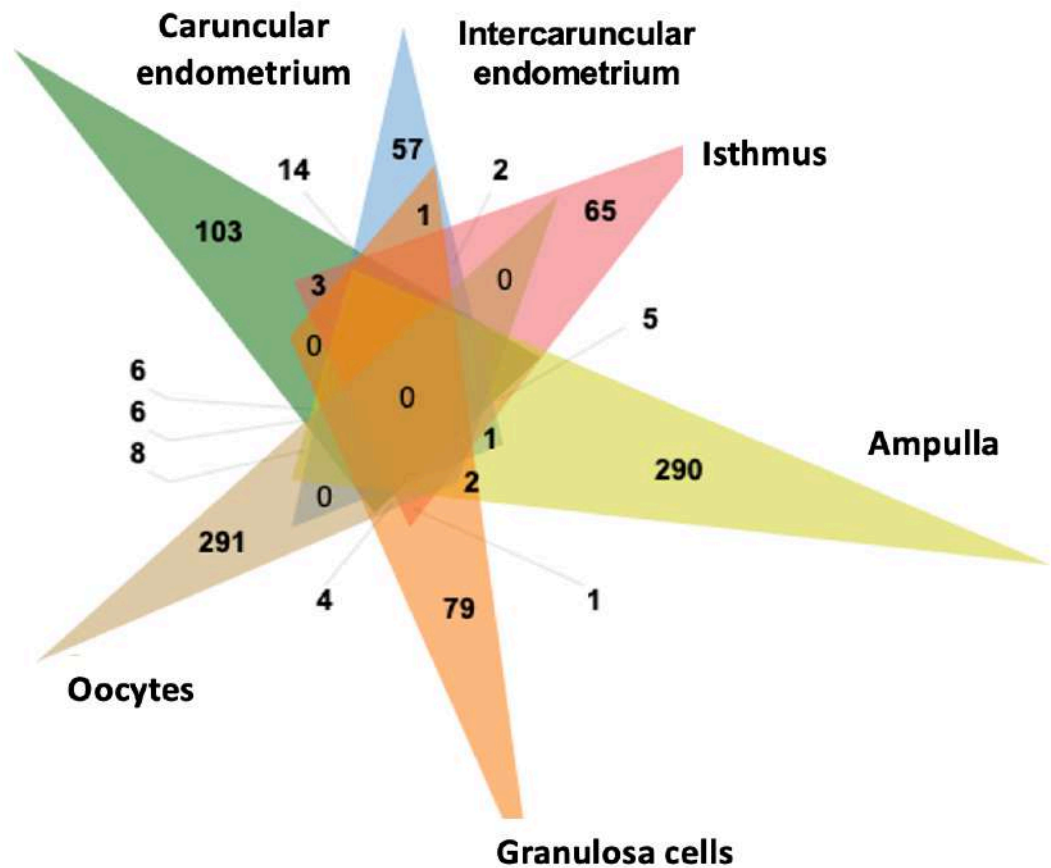


**Figure 6.4. Venn diagram of the common and unique differentially expressed genes 3 months after bacterial infusion**

Differentially expressed genes identified in bacteria-infused compared with control animals are shown for caruncular endometrium (green), intercaruncular endometrium (blue), isthmus (pink), ampulla (yellow), granulosa cells (orange) and oocytes (brown). The number of unique DEGs are reported for each sample and the overlap of common genes are reported at each intersection.

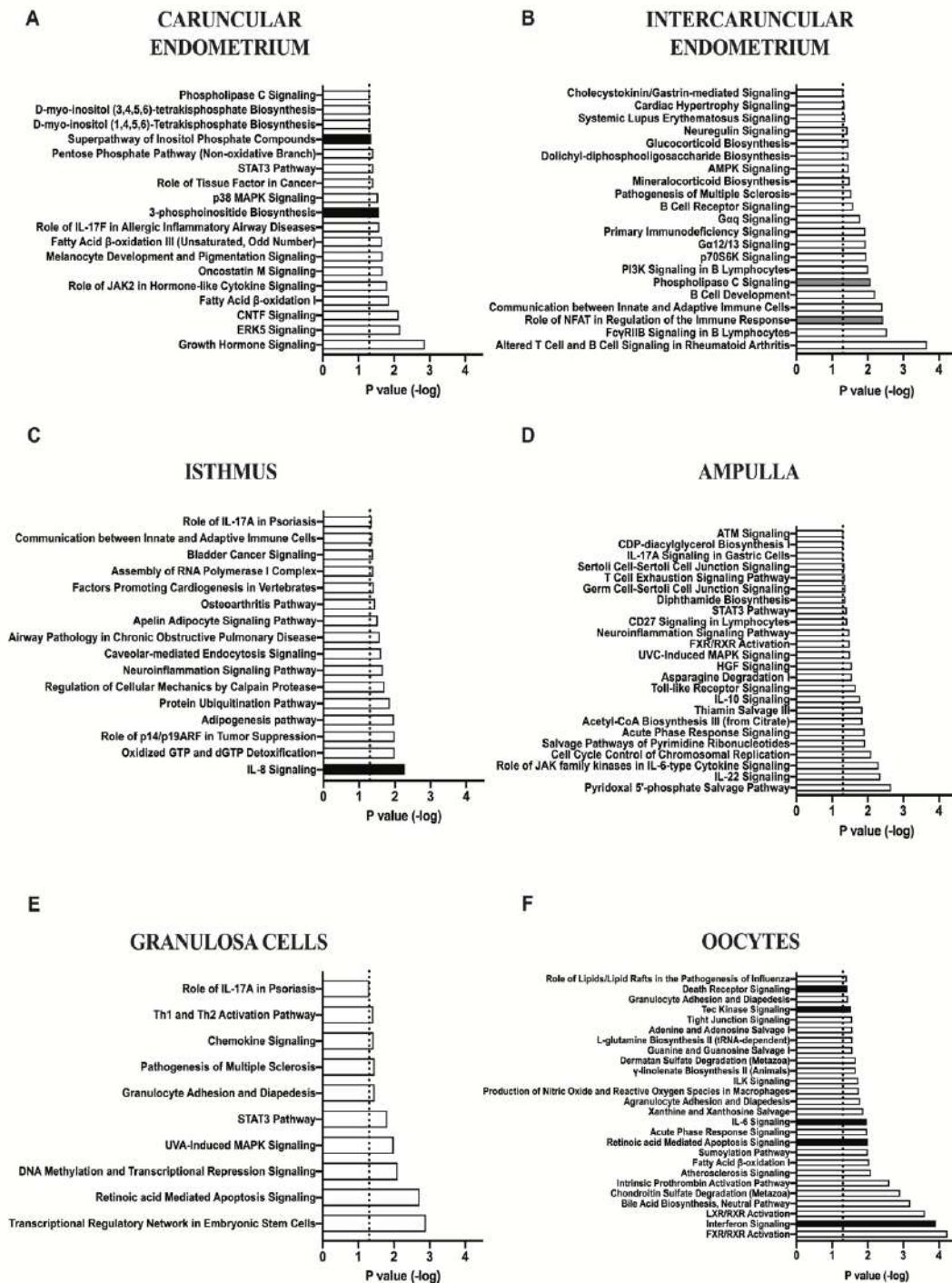


**Figure 6.5. Ingenuity Pathway Analysis of differentially expressed genes**

Ingenuity Pathways Analysis of differentially expressed genes identified canonical pathways affected 3 months after bacterial infusion in (A) caruncular endometrium, (B) intercaruncular endometrium, (C) isthmus, (D) ampulla, (E) granulosa cells and (F) oocytes. Pathways are predicted to be activated (black bars,  $z\text{-score} \geq 2$ ) or inactivated (grey bars,  $z\text{-score} \leq -2$ ). White bars represent canonical pathways that were significantly altered ( $P < 0.05$ ) but did not meet the  $z\text{-score}$  thresholds.

### 6.3.4 Analysis of gene networks effected by bacterial infusion

Ingenuity Pathway Analysis of DEGs in the caruncular and intercaruncular endometrium identified 10 and 8 gene networks affected in bacteria-infused animals, respectively. The highest scoring network in both caruncular and intercaruncular endometrium was cellular development, cellular growth and proliferation and haematological system development and function (network score = 44 and 36, respectively; **Fig. 6.6A-B**). In the isthmus, 8 gene networks were affected with cellular assembly and organization, DNA replication, recombination and repair and cellular development, the highest scoring network (score = 36, **Fig. 6.7A**). In the ampulla, 20 gene networks were affected with developmental disorder, post-translational modification, reproductive system development and function, the highest scoring network (score = 48, **Fig. 6.7B**). In the granulosa cells, 22 gene networks were affected, with endocrine disorders, organ morphology, organismal injury and abnormalities, the highest scoring network (score = 42, **Fig. 6.8A**). In oocytes, 5 gene networks were affected with cell morphology, cellular function and maintenance and reproductive system development and function, the highest scoring network (score = 42, **Fig. 6.8B**).



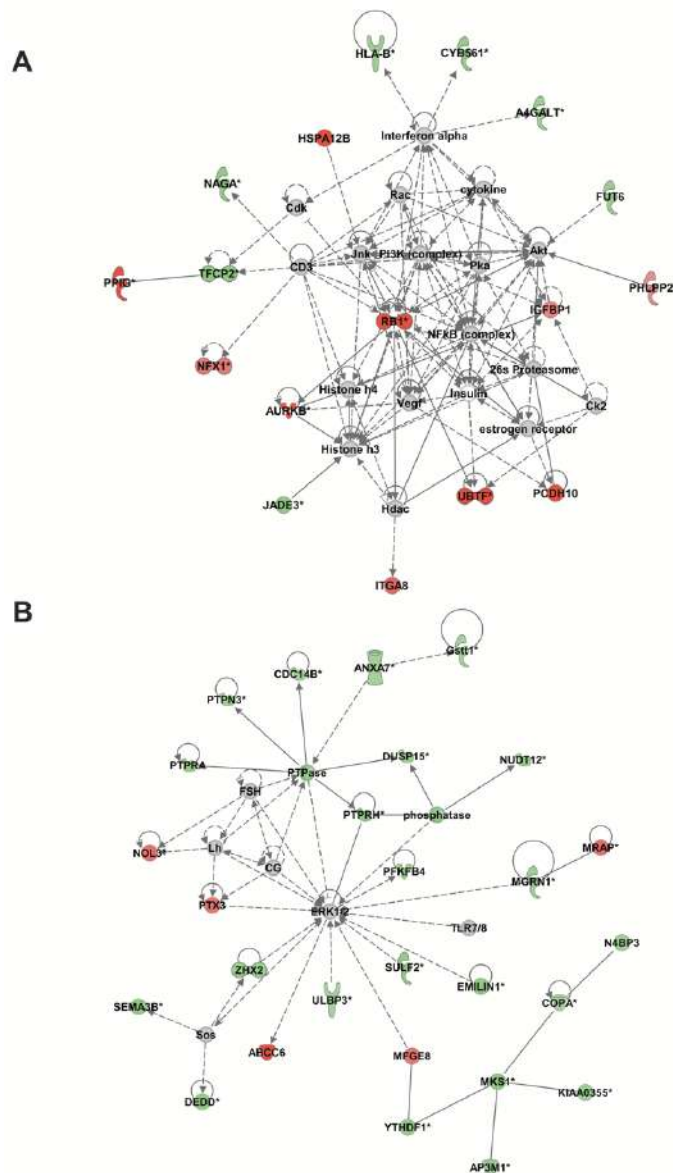


**Figure 6.7. Gene networks of the oviduct affected by bacteria infusion**

Ingenuity Pathways Analysis of differentially expressed genes identified gene networks affected 3 months after bacterial infusion. The highest scoring gene network is presented for (A) isthmus: cellular assembly and organization, DNA replication, recombination and repair, cellular development; (B) ampulla: developmental disorder, post-translational modification, reproductive system development and function. Gene expression is displayed as green (reduced expression) or red (increased expression) in bacteria-infused compared with control animals; grey indicates genes or molecules that are predicted to be part of the network by IPA algorithms but not part of the dataset. Solid lines and dashed lines indicate direct and indirect interactions between nodes, respectively.



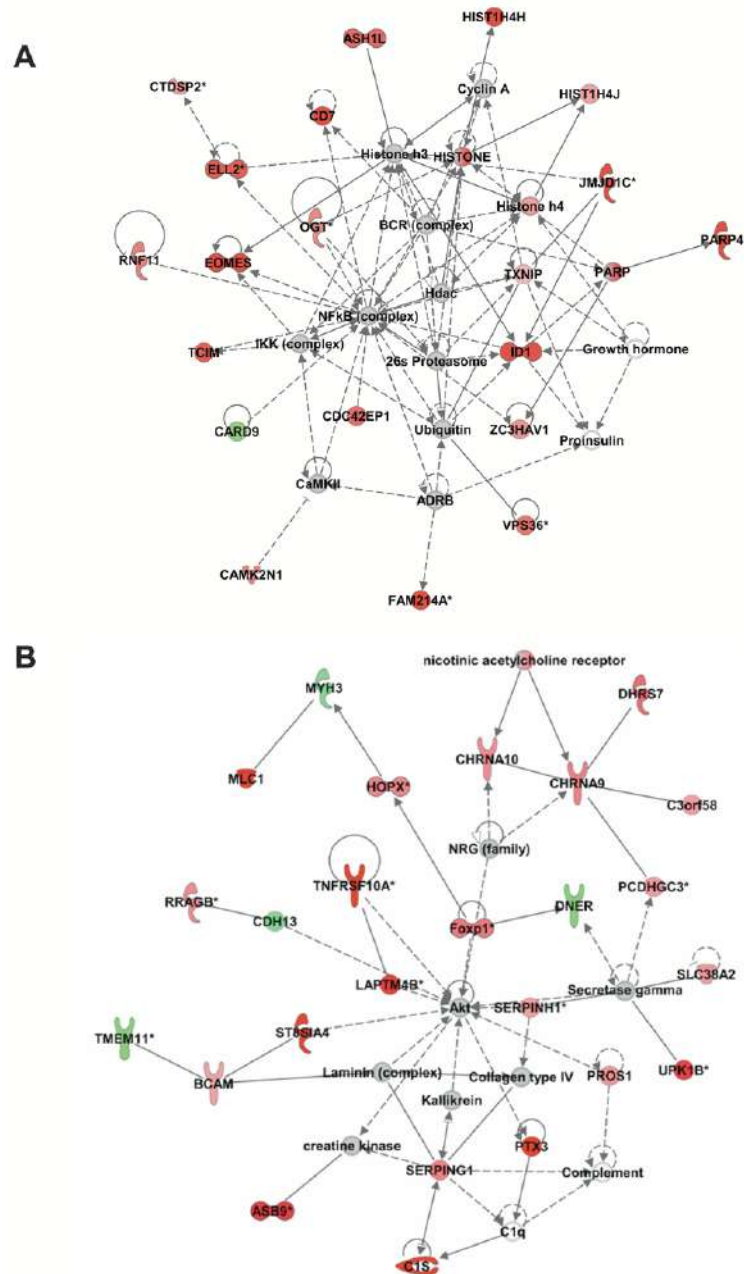


**Figure 6.8. Gene networks of the ovarian follicle affected by bacteria infusion**

Ingenuity Pathways Analysis of differentially expressed genes identified gene networks affected 3 months after bacterial infusion. The highest scoring gene network is presented for (A) granulosa cells: cell cycle, DNA replication, recombination, and repair; (B) oocytes: cell morphology, cellular function and maintenance, reproductive system development and function. Gene expression is displayed as green (reduced expression) or red (increased expression) in bacteria-infused compared with control animals; grey indicates genes or molecules that are predicted to be part of the network by IPA algorithms but not part of the dataset. Solid lines and dashed lines indicate direct and indirect interactions between nodes, respectively.

### **6.3.5 Predicted upstream regulators, diseases and functions associated with bacterial infusion**

Ingenuity Pathway Analysis of the predicted upstream regulators of DEGs in the bacteria-infused animals are reported in **Fig. 6.9**. It was notable that there were 35 upstream regulators in the granulosa cells, and 114 in oocytes including LPS, TLR4, NFκB, IL-6, and IL-1. Other tissues only had between 1 and 4 predicted upstream regulators.

### **6.3.6 Predicted diseases and functions associated with bacterial infusion**

Ingenuity Pathway Analysis of the predicted diseases and functions associated with the DEGs in the bacteria-infused heifers are reported in **Fig. 6.10**. In the caruncular endometrium, functions associated with cancer were predominant with one immune function predicted to be increased, apoptosis of leukocytes. In the intercaruncular endometrium, 16 diseases and functions were significant of which 10 were related to inflammation or immune function. However, few significant diseases and functions were identified in the ampulla and none in the isthmus. In the granulosa cells, 18 disease and functions were significant, of which 6 were related to inflammation or immune function. In oocytes, 47 diseases and functions were significant of which 16 were related to inflammation or immune function.

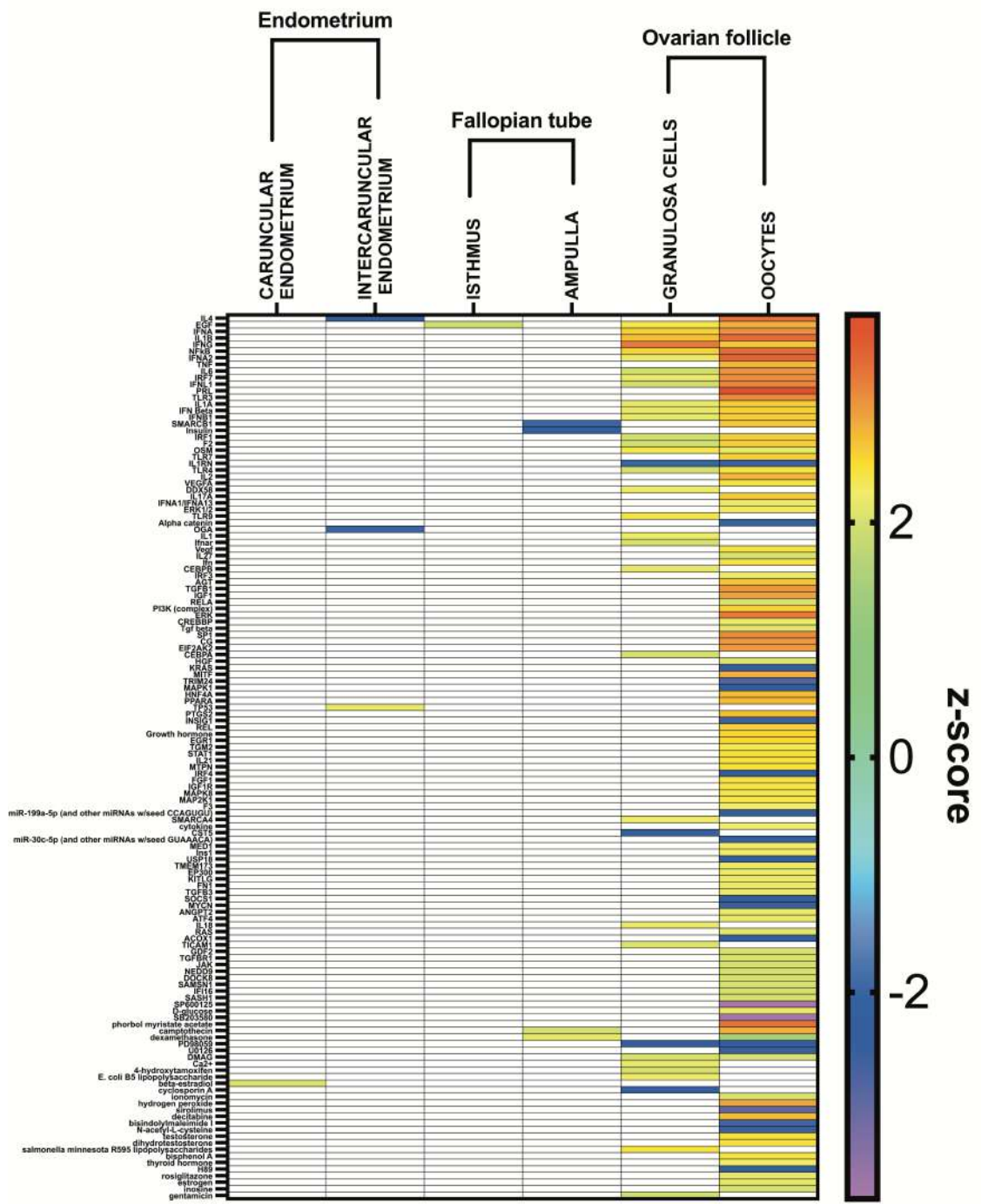


**Figure 6.9. Predicted upstream regulators of differentially expressed genes affected by bacteria infusion**

Ingenuity Pathways Analysis identified predicted upstream regulators of differentially expressed genes affected 3 months after bacterial infusion in caruncular endometrium, intercaruncular endometrium, isthmus, ampulla, granulosa cells and oocytes. The z-score for each regulator is displayed from purple (reduced score) to red (increased score) in bacteria-infused compared with control animals; white blocks represent predicted upstream regulators that did not meet the z-score thresholds.

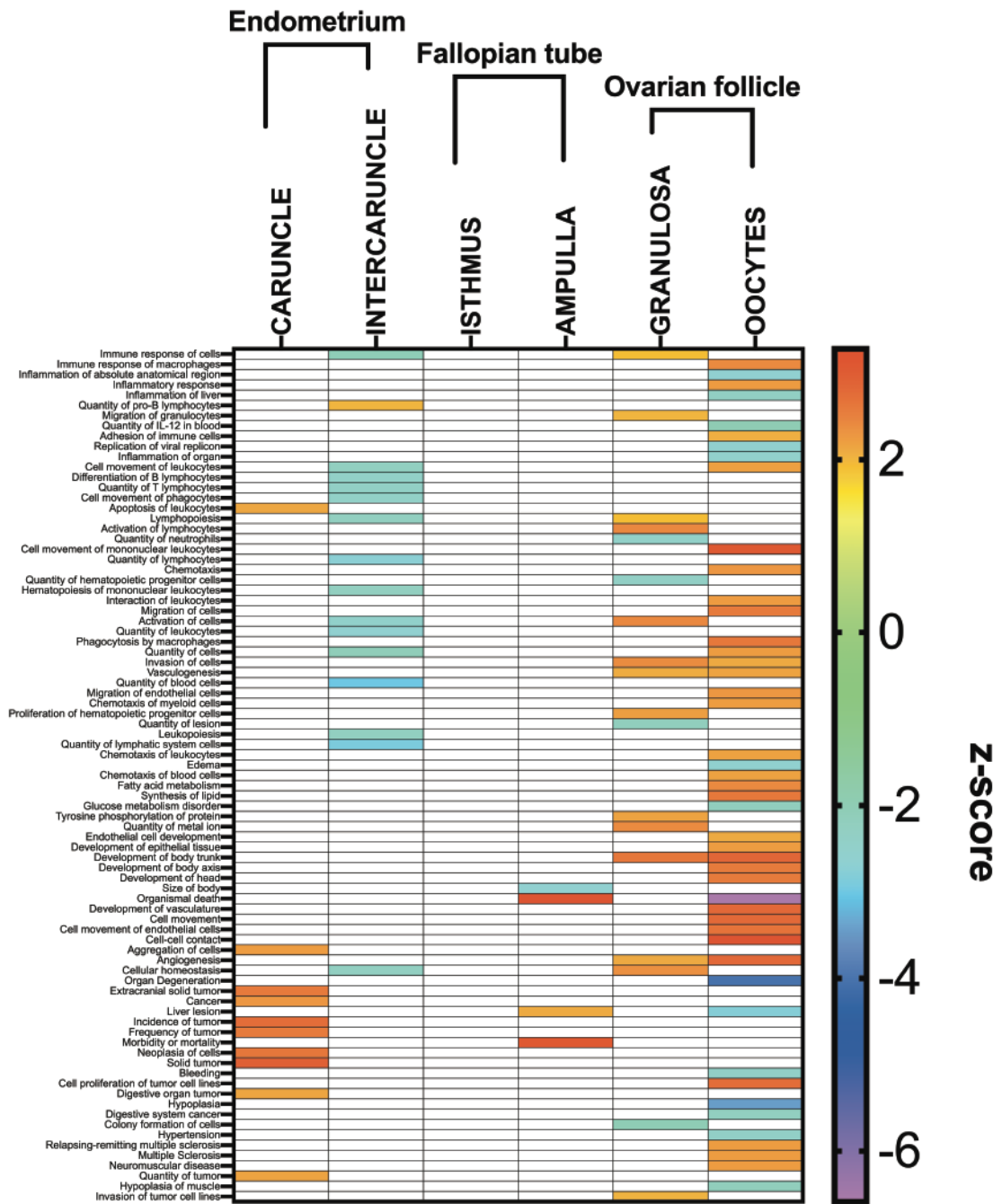


**Figure 6.10. Predicted diseases and functions affected by bacteria infusion**

Ingenuity Pathways Analysis of differentially expressed genes identified predicted diseases and functions affected 3 months after bacterial infusion in caruncular endometrium, intercaruncular endometrium, isthmus, ampulla, granulosa cells and oocytes. The z-score for each disease or function is displayed from purple (reduced score) to red (increased score) in bacteria-infused compared with control animals; white blocks represent predicted upstream regulators that did not meet the z-score thresholds.

### 6.3.7 Inspection of selected genes involved in inflammation, steroid synthesis, and cell viability

The RNAseq data was inspected for genes that have previously been explored when investigating the genital tract of cattle during uterine disease. Genes associated with inflammation (Herath et al., 2009, Foley et al., 2015), steroid synthesis (Magata et al., 2014, de Campos et al., 2017), or cell viability (Piersanti et al., 2019a, Dickson et al., 2020) were selected. There were no significant differences between the bacteria-infused and control animals in the caruncular (**Supplementary Table 13**) or intercaruncular endometrium (**Supplementary Table 14**). In the isthmus (**Supplementary Table 15**), as well as the 7.36 log<sub>2</sub>FC increase ( $P = 0.02$ ) in *CXCL8*, bacterial infusion was associated with a trend for increased expression of *CCL2* (3.47 log<sub>2</sub>FC,  $P = 0.1$ ) and *IL1A* (1.64 log<sub>2</sub>FC,  $P = 0.07$ ). In the ampulla (**Supplementary Table 16**) of bacteria-infused animals, *MHCI* expression increased (2.23 log<sub>2</sub>FC,  $P = 0.01$ ) and *CASP2* expression decreased (-1.12 log<sub>2</sub>FC,  $P = 0.04$ ), and there was a trend for increased expression of *CCNB1* (3.25 log<sub>2</sub>FC,  $P = 0.09$ ) and *CCNB2* (1.12 log<sub>2</sub>FC,  $P = 0.07$ ), which encode cyclin B1 and B2, respectively. In granulosa cells (**Supplementary Table 17**), as well as the -8.09 log<sub>2</sub>FC reduction ( $P = 0.03$ ) in *CARD9* expression, there was a trend for increased expression of *IL1A* (4.59 log<sub>2</sub>FC,  $P = 0.11$ ) and *IL6R* (5.61 log<sub>2</sub>FC,  $P = 0.08$ ), and reduced expression of *HIF1A* (-2.17 log<sub>2</sub>FC,  $P = 0.10$ ). In oocytes (**Supplementary Table 18**), there was increased expression of *MHCI* (2.60 log<sub>2</sub>FC,  $P = 0.004$ ), and a trend for an increase in *MHCII* (3.83 log<sub>2</sub>FC,  $P = 0.11$ ) and *HIF1A* (1.15 log<sub>2</sub>FC,  $P = 0.09$ ). Interestingly, there was also increased expression of *CYP11A1* (1.77 log<sub>2</sub>FC,  $P = 0.01$ ), *CYP19A1* (4.52 log<sub>2</sub>FC,  $P < 0.001$ ), *HSD3B1* (2.30 log<sub>2</sub>FC,  $P = 0.005$ ) and *CCND2* (2.06 log<sub>2</sub>FC,  $P < 0.001$ ).

There was considerable variation in the expression of selected genes amongst the tissues; for example, *STAR* was highly expressed in granulosa cells and oocytes but not the other tissues, but *IL6R* was highly expressed in the endometrium and oviduct but not granulosa cells. However, it was notable that for both bacteria-infused and control animals there were few transcripts for *IL6* or *IL10* and no *TNF* transcripts across all six tissues.

## 6.4 DISCUSSION

The most important finding of this study was that several months after intrauterine infusion of pathogenic bacteria in virgin Holstein heifers there were changes in the transcriptome of the endometrium, oviduct, granulosa cells and oocytes. Most of the genes differentially expressed between the bacteria-infused and control animals were tissue-specific, with very few DEGs common amongst the tissues. Many of the gene networks affected by bacterial infusion in the endometrium and oviduct were involved in cell growth and repair, which might reflect that the tissues were recovering from infection. Despite infusing the bacteria into the uterus, there were more predicted upstream regulators of the DEGs in the granulosa cells and oocytes of bacteria-infused animals than all the other tissues combined. This was particularly striking because, unlike the other tissues, the granulosa cells and oocytes were collected from dominant follicles, which would have developed several weeks after the bacterial infusion. These findings provide evidence that, independent of periparturient problems, metabolic stress, and lactation, infecting the uterus with bacteria that causes endometritis alters the transcriptome of multiple tissues in the reproductive tract several months later, including the granulosa cells and oocyte, which are distant to the site of bacterial infusion.

A novelty of the approach was to use virgin Holstein heifers to separate the effects of bacterial infection on the reproductive tract transcriptome from other peripartum problems, lactation, and metabolic stress (Wathes et al., 2009, Herath et al., 2009, Girard et al., 2015, Cerri et al., 2012). This is particularly important because we have demonstrated throughout this thesis that energy stress has an effect on the innate immune responses in granulosa cells and cumulus-oocyte complexes, *in vitro*. To ensure bacterial infusion was relevant for clinical endometritis, pathogenic strains of *E. coli* and *T. pyogenes* were used, that had been isolated from cows with clinical endometritis previously (Goldstone et al., 2014a, Goldstone et al., 2014b). These pathogenic strains induced clinical endometritis in the heifers 3 to 6 days after intrauterine infusion, determined by the presence of pus in the uterus, a purulent uterine discharge in the vagina, and increased bacterial total 16S RNA in the vaginal mucus compared with controls, as described in the previous publication (Piersanti et al., 2019c).

The bacterial infusion led to multiple DEGs detectable several months later, in the caruncular and intercaruncular endometrium, isthmus, ampulla, granulosa cells and oocytes. Finding DEGs in all the tissues supports the observations that these tissues may contribute to infertility after the resolution of uterine disease in cattle (Ribeiro et al., 2016). However, the DEGs several months after bacterial infusion were tissue-specific with variation across the tissues and no genes common across all the tissues. Furthermore, a striking observation in the present study was that there were few RNA transcripts for *IL6* or *IL10* and no transcripts for *TNF* in any of the tissues of bacteria-infused or control animals several months after infusion. This contrasts with the early inflammatory response to bacteria or LPS amongst the same tissues when genes typical of innate immunity are highly expressed, including *IL1B*, *IL6*, *IL10*, *CXCL8* and *TNF* (Fischer et al., 2010, Gabler et al., 2010, Turner et al., 2014b, Kowsar et al., 2013, Price et al., 2013, Cronin et al., 2012, Herath et al., 2006). However, studies using qPCR also found that whilst there was increased expression of *IL1B*, *IL6*, *IL8*, and *TNF* transcripts in postpartum endometrial samples about 2 weeks postpartum, expression returned to basal levels by 30 to 60 days postpartum (Gabler et al., 2010, Chapwanya et al., 2012). It is likely that the lack of RNA transcripts for cytokines or chemokines observed in the present chapter probably indicates that there is no longer an acute inflammatory response taking place, several months after intrauterine infusion of pathogenic bacteria.

In the endometrium, the lack of DEGs associated with innate immunity between the bacteria-infused and control animals 3 months after bacterial infusion may reflect resolution of infection, and progression to tissue repair and maintenance. Many significant gene networks and pathways in the endometrium were typically involved with cellular development, growth, and proliferation, although some were associated with inflammation. This may not be surprising as tissue repair, cell growth and inflammation are common physiological features of the endometrial transcriptome (Wathes et al., 2011, Arai et al., 2013, Chapwanya et al., 2012, Foley et al., 2012). The 109 and 57 DEGs unique to the caruncular and intercaruncular endometrium, respectively, may also reflect their different physiology. For example, the 3-phosphoinositide biosynthesis pathway was upregulated in caruncular endometrium, and the phospholipase C signalling pathway was downregulated in intercaruncular endometrium. Additional evidence for tissue repair was a trend for increased

expression in the ampulla of genes encoding cyclin B1 and B2, which help drive mitosis in proliferating cells (Fung and Poon, 2005). However, some DEGs contribute to immunity; *VNN2* (Vanin 2) and *POU2AF1* (POU Class 2 Homeobox Associating Factor 1) expression was decreased in the intercaruncular endometrium and *VPREB3* (Pre-B lymphocyte protein 3) was decreased in both the caruncular and intercaruncular endometrium. Vanin 2 plays a role in leukocyte adhesion and migration to inflammatory sites, *VPREB3* is involved in B cell immunoglobulin secretion, and *POU2AF1* is essential for B-cell responses to antigens (Rosnet et al., 2004, Suzuki et al., 1999, Corcoran et al., 2005). Interestingly, *POU2AF1* was expressed between 7 and 21 days postpartum in Holstein-Friesian cows with clinical endometritis, compared with healthy controls (Foley et al., 2015).

The 65 and 298 DEGs unique to the isthmus and ampulla, respectively, may reflect the different functions of the isthmus, supporting fertilization and early embryonic development, and ampulla, facilitating sperm transport (Maillo et al., 2016). As well as a role in innate immunity and angiogenesis, the predicted activation of IL-8 signalling in the isthmus agrees with observations of increased *IL8* expression in the human oviduct during the follicular phase of the menstrual cycle (Hess et al., 2013). In the ampulla, there was greater expression of *SLPI* (secretory leukocyte peptidase inhibitor) in bacteria-infused compared with control animals. As well as a protective role against microbes, *SLPI* is expressed in the human oviduct, where it protects sperm against elastase (Ota et al., 2002). The potassium voltage-gated channel gene (*KNCE4*) was also upregulated in the ampulla. Potassium channels mediate chloride ion secretion in the oviduct, which is important for the production of oviduct fluid, and dysregulated fluid formation has been linked to reduced fertility (Keating and Quinlan, 2012).

The long-term effect of bacterial infusion on the transcriptome was most striking for the granulosa cells derived from dominant follicles, because 3 months earlier these granulosa cells would have been limited to pre-antral follicles (Adams, 1999, Britt et al., 2018). These findings further extend previous observations that 6 weeks after the resolution of metritis there were changes in the transcriptome of granulosa cells from dominant follicles of lactating dairy cows (Piersanti et al., 2019a). Furthermore, the present study adds further knowledge because the effects of infection on the granulosa



cell transcriptome were independent of lactation. One potential mechanism for the effect of bacterial infusion on the granulosa cell transcriptome is that around the time of infusion there was an imprinting effect on the granulosa cells during primordial to primary follicle development, which persisted for 3 months (Britt et al., 2018, Adams, 1999). Indeed, there is *in vitro* evidence that LPS stimulates inappropriate primordial follicle activation (Bromfield and Sheldon, 2013). An alternative mechanism is that bacterial virulence factors persisted to affect the granulosa cells during antral follicle dominance. The latter mechanism seems more likely as the 38 upstream regulators of granulosa cell DEGs included LPS, TLR4, IL-1, and NFκB (nuclear factor kappa-light-chain-enhancer of activated B cells), which are typical of innate immune function (Pahl, 1999, Moresco et al., 2011). The later mechanism is also supported by previous observations that the follicular fluid of dominant follicles contains LPS several weeks after uterine infection (Herath et al., 2007, Piersanti et al., 2019a), and that granulosa cells from antral follicles mount inflammatory responses to LPS (Price et al., 2013, Price and Sheldon, 2013, Bromfield and Sheldon, 2011).

An unusual feature of the DEGs in the granulosa cells was that only one of the 89 DEGs was downregulated. The downregulated gene, *CARD9* is a central regulator of innate immunity that is highly expressed in immune cells and is involved in the activation of mitogen-activated protein kinases and NFκB in response to intracellular pathogens (Ruland, 2008, Hsu et al., 2007). Interesting upregulated DEGs in the granulosa cells included Eomesodermin (*EOMES*) and ADAM Metallopeptidase with Thrombospondin Type 1 Motif 1 (*ADAMTS1*). Eomesodermin is a master regulator of cell-mediated immunity, controlling the production of inflammatory mediators such as interferon and IL-4 (Shimizu et al., 2019). Eomesodermin is also associated with T-cell exhaustion, which occurs during chronic viral infections and cancer (Buggert et al., 2014, Li et al., 2018). In granulosa cells, *ADAMTS1* expression is induced by luteinizing hormone (Robker et al., 2000). Progesterone-regulated genes in the ovulation process: ADAMTS-1 and cathepsin L proteases (Robker et al., 2000), and *ADAMTS1*<sup>-/-</sup> mice had impaired follicle development and ovulated fewer oocytes (Shozu et al., 2005, Mittaz et al., 2004).

Some interesting differentially affected genes in the oocyte of infused animals included increased expression of TNF alpha induced protein 6 (*TNFAIP6*), the G

protein-coupled receptor 50 (*GPR50*) and the cysteine and glycine rich protein 3 (*CSRP3*) and decreased expression of Adam metallopeptidase domain 22 (*ADAM22*) and the delta/notch like EGF repeat containing (*DNER*), compared with control animals. Increased expression of *TNFAIP6* has been suggested to be a predictor of oocyte competence (Matoba et al., 2014, Assidi et al., 2010, Fulop et al., 2003). However, increased *TNFAIP6* expression in poor quality oocytes may be detrimental and therefore may not be a good indicator of oocyte quality (Yuan et al., 2011). *GPR50* is a member of the melatonin receptor subfamily and may be a mechanism by which the oocyte protects itself against oxidative stress caused by infection because melatonin has previously been shown to protect bovine oocytes from LPS-induced oxidative stress (Zhao et al., 2017b, Zhao et al., 2018, Dufourny et al., 2008). *CSRP3* acts as a mechanical stress sensor, triggers autophagy and protects cells from undergoing apoptosis (Rashid et al., 2015). However, the role of *CSRP3* in the oocyte has not been determined. *ADAM22* is thought to function in cell-cell interactions and plays a role in the ovulatory processes in the rainbow trout (Bobe et al., 2006). The delta/notch like EGF repeat containing (*DNER*) can activate the Notch pathway that is important in the ovary for syncytia formation and meiotic entry (Vanorny and Mayo, 2017). Inhibition of the Notch signalling pathway results in delayed meiotic progression and slowed oocyte growth (Feng et al., 2014).

These findings of DEG across all the tissues imply that infection of the uterus with pathogenic bacteria has widespread and long-term effects on the genital tract. Although clinical endometritis normally resolves in the first 60 days following parturition (Sheldon et al., 2009), we found transcriptome changes 3 months after bacterial infusion. Future studies might determine how long the transcriptome changes persist in the genital tract after infection. However, the findings of DEGs in the endometrium 3 months after infection agree with observations that the endometrium has a reduced capacity to support an embryo if animals had uterine disease previously (Ribeiro et al., 2016, Gilbert, 2019). Resilient dairy cows prevent the development of uterine disease using the complimentary defensive strategies of tolerating and resisting infection with pathogenic bacteria (Sheldon et al., 2019a). However, endometritis is currently a problem for the dairy industry, causing infertility, compromising welfare, and reducing profitability (Gilbert, 2019, Ribeiro et al., 2016, Sheldon et al., 2019a). Endometritis is likely to continue to be a risk to fertility and production as farmers

attempt to increase milk yields to meet the need to feed the expanding world population (Britt et al., 2018).

A potential limitation of the present study was that oocytes were collected at day 60 relative to infusion, whereas the other samples were collected at 91 days following infusion. In future studies it would be interesting to collect the oocytes and tissues concurrently to validate our results. Although beyond the scope of the present study, it would also have been interesting to explore the reproductive physiology of the animals, to link the DEGs with mechanisms of infertility. It would also be interesting to extend the transcriptomic studies to the hypothalamus and pituitary because intravenous LPS infusion suppresses the pulsatile release of GnRH and LH, which might also affect ovarian function (Karsch et al., 2002). Future studies utilizing this model of endometritis should quantify endometrial inflammation and uterine microbial populations (Sheldon et al., 2019a), over a larger sample size (as done by (Dickson et al., 2020)), to further establish the validity of the model (Piersanti et al., 2019c). Additionally, further separation of the individual cell types that make up the tissues of the genital tract, such as the epithelial and stromal cells of the endometrium, might be useful to further understand the long-term effects of endometritis on the transcriptome of these tissues.

In conclusion, a model of induced endometritis in heifers was exploited to explore the long-term effects on the reproductive tract of intrauterine bacterial infusion, whilst avoiding the potential confounding effects of periparturient problems, metabolic stress, and lactation. There were changes in the transcriptome of the endometrium, oviduct, granulosa cells and oocytes several months after intrauterine infusion of endometrial pathogenic bacteria. The majority of the DEGs were tissue-specific, with few genes common amongst the tissues. The granulosa cells and oocytes stood out from the other tissues because they had more predicted upstream regulators of DEGs than all the other tissues combined. The evidence of long-term changes to the transcriptome of the endometrium, oviduct, granulosa cells and oocyte implies that each of these tissues may contribute to the persistence of infertility in cattle after endometritis.

## 7 General discussion

During postpartum uterine disease, lipopolysaccharide accumulates in the follicular fluid, and granulosa cells mount an innate immune response to LPS by secreting pro-inflammatory cytokines. *In vitro*, granulosa cells respond to LPS by secreting pro-inflammatory cytokines, such as IL-1 $\beta$ , IL-6 and IL-8, associated with increased phosphorylation of the mitogen activated protein kinases, ERK1/2 and p38 (Price et al., 2013, Price and Sheldon, 2013, Bromfield and Sheldon, 2011). Here, we added to that knowledge by finding that granulosa cells isolated from emerged and dominant follicles also secrete IL-1 $\alpha$  in response to LPS. Additionally, LPS treatment of granulosa cells was associated with increased phosphorylation of JNK.

Negative energy balance in cattle impairs immune cell function, perturbs ovarian follicle growth and function, and increases the risk of uterine disease (Beam and Butler, 1997, Hammon et al., 2006, LeBlanc, 2012, Leroy et al., 2008). Inflammatory responses to LPS are also energetically demanding, further exacerbating NEB. An extra 2.1 Kg/d glucose is required to respond to LPS infusion, which is comparable with 2.7 Kg/d glucose to produce 40 litres of milk (Habel and Sundrum, 2020, Kvidera et al., 2017). Uterine diseases, such as metritis also reduces appetite which further exacerbates negative energy balance (Stojkov et al., 2015).

In *Chapter 3*, we tested the hypothesis was that manipulating glycolysis, AMPK, or mTOR to mimic energy stress, would impair the innate immune responses of granulosa to LPS. In line with the hypothesis, we found that energy stress impaired the innate immune responses of granulosa cells to LPS (**Fig. 7.1**). Specifically, treatment with the AMPK activator AICAR impaired the LPS-induced secretion of IL-1 $\alpha$ , IL-1 $\beta$  and IL-8 by granulosa cells, associated with shortened duration of ERK1/2 and JNK phosphorylation. Consistent with previous studies, we also found that treatment with AICAR reduced the secretion of oestradiol and progesterone by granulosa cells (Tosca et al., 2007a). In addition to regulation of steroidogenesis by AMPK, we also suggest that endocrine function may also be regulated by mTOR because granulosa cells treated with rapamycin or Torin 1 secreted less oestradiol and progesterone (**Fig. 7.1**). The mechanisms by which mTOR inhibition might impair granulosa cell steroidogenesis requires further work and is beyond the scope of the present thesis.

Interestingly, we found that the effects of manipulating granulosa cell energy metabolism on innate immunity and endocrine function were similar between granulosa cells isolated from emerged and dominant follicles, suggesting that energy stress may affect granulosa cell function throughout follicular growth.

Glycolysis, AMPK and mTOR are important regulators of innate immunity in the bovine endometrium, with endometrial explants secreting less IL-1 $\beta$ , IL-6 and IL-8, in response to LPS (Noletto et al., 2017, Turner et al., 2016). Surprisingly, we found that although inhibiting glycolysis with 2-DG impaired the innate immune responses to LPS, glucose deficiency did not alter the innate immune responses of granulosa cells. Bovine granulosa cells have the capability to take up glucose because they express the mRNA for the glucose transporters, GLUT1 and GLUT3, at comparable levels to organs such as the brain or heart; mRNA for GLUT4 is also present, but at much lower levels (Nishimoto et al., 2006). Negative energy balance in cattle is associated with increased insulin resistance, the impaired tissue sensitivity and responsiveness to insulin (Oikawa and Oetzel, 2006, Bell and Bauman, 1997). In the present thesis, we cultured granulosa cells in the presence of insulin, therefore, the lack of effect of glucose depletion on granulosa cell inflammation might be due to differential effects of 2-DG or limiting the availability of glucose on GLUT expression or cellular metabolism.

As well as decreased plasma glucose and cholesterol concentrations, negative energy balance is associated with increased plasma concentrations of non-esterified fatty acids and  $\beta$ -hydroxybutyrate in dairy cows (Fenwick et al., 2008b). Treatment of bovine granulosa cells with NEFAs is associated with reduced proliferation, increased apoptosis, and increased oestradiol secretion (Vanholder et al., 2005). Additionally, treatment of bovine granulosa cells with  $\beta$ -hydroxybutyrate is associated with decreased oestradiol and progesterone secretion (Vanholder et al., 2006). Future studies could investigate the effects of these metabolites on granulosa cell innate immune responses to LPS.

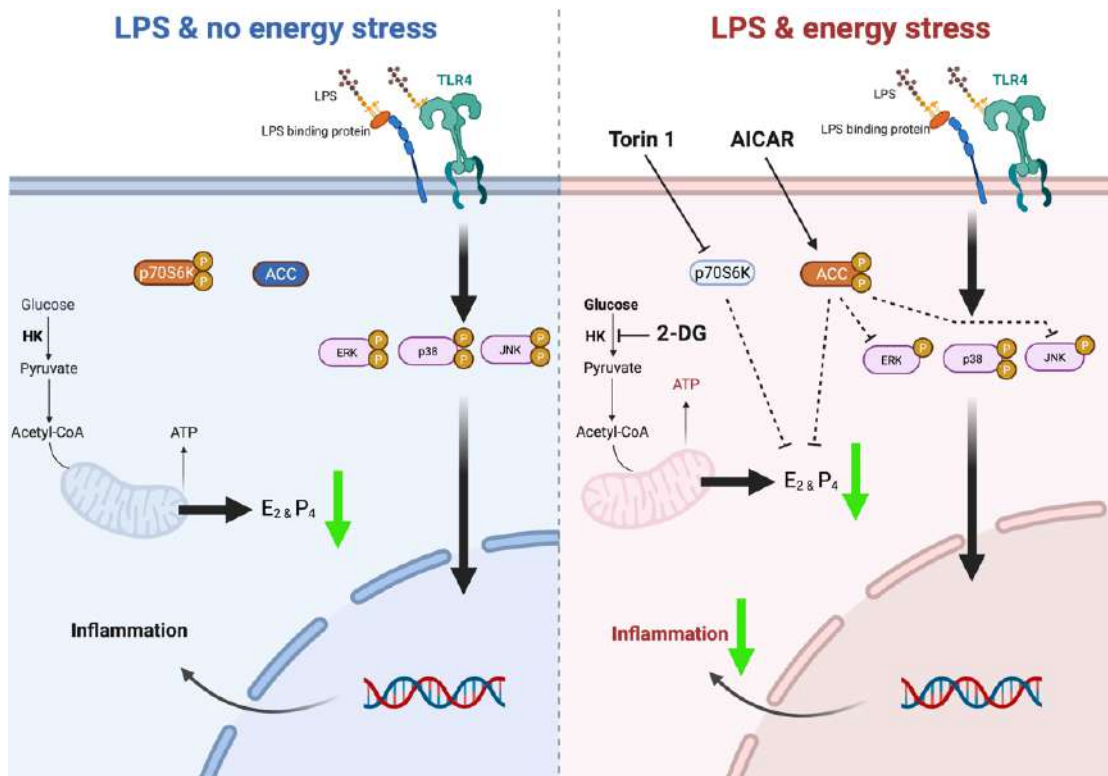


**Figure 7.1. Energy stress impairs granulosa cell innate immunity and endocrine function**

In the absence of energy stress (left), granulosa cells mount an inflammatory response to LPS, associated with increased phosphorylation of ERK1/2, p38 and JNK. Challenge with LPS is also associated with decreased secretion of oestradiol and progesterone by granulosa cells. During energy stress (right), granulosa cell inflammatory responses to LPS are impaired. Energy stress also impairs the endocrine function of granulosa cells as they secrete less oestradiol and progesterone in response to AMPK activation with AICAR, or mTOR inhibition with Torin 1; inhibiting glycolysis with 2-DG impairs progesterone secretion by granulosa cells, but not oestradiol secretion. HK, hexokinase; 2-DG, 2-deoxy-D-glucose; E<sub>2</sub>, oestradiol; P<sub>4</sub>, progesterone; LPS, lipopolysaccharide (Horlock A., 2021; Created with BioRender.com).

Plasma concentrations of total cholesterol (Quiroz-Rocha et al., 2009, Esposito et al., 2014, Cavestany et al., 2005), HDL, LDL and VLDL (Kessler et al., 2014) all decrease around parturition in the dairy cow. Unfortunately, decreases in plasma total cholesterol concentrations are further exacerbated by negative energy balance in the postpartum period (Kim and Suh, 2003, Ruegg et al., 1992, Esposito et al., 2014). Plasma concentrations of cholesterol are reflected in the follicular fluid of dairy cows (Leroy et al., 2004a). Furthermore, reduced plasma cholesterol concentrations in the postpartum period are associated with increased incidence of uterine disease in cattle (Sepulveda-Varas et al., 2015).

In *Chapter 4*, we tested the hypothesis that decreasing the availability of cholesterol would impair the innate immune responses to LPS in granulosa cells. In line with the hypothesis, we found that altering the availability of cholesterol, by supplementing culture medium with FBS (10% providing ~217  $\mu$ M cholesterol) or follicular fluid (5% providing ~75  $\mu$ M cholesterol), augmented the LPS-induced secretion of IL-1 $\alpha$  and IL-1 $\beta$  by granulosa cells. We confirmed previous observations that follicular fluid contains mostly HDL cholesterol (Savion et al., 1982, Brantmeier et al., 1987). Interestingly, we found that treatment of granulosa cells with HDL, but not LDL or VLDL, increased the LPS-induced secretion of IL-1 $\alpha$  and IL-1 $\beta$ . Furthermore, treatment of granulosa cells with the cholesterol lowering agent, methyl- $\beta$ -cyclodextrin, decreased the LPS-induced secretion of IL-1 $\alpha$  and IL-1 $\beta$ . These findings suggest that the availability of cholesterol, particularly in the form of HDL, might regulate the innate immune responses to LPS in granulosa cells. This was surprising because HDL is usually considered to be anti-inflammatory (Catapano et al., 2014). Taken together, our data suggests that the availability of cholesterol may be important for the innate immune function of granulosa cells.

The second hypothesis of *Chapter 4* was that inhibiting the cholesterol biosynthesis pathway would impair the innate immune responses of granulosa cells to LPS. In line with the hypothesis, we found that siRNA targeting *HMGCR*, *FDPS* or *FDFT1* to reduce cholesterol biosynthesis, impaired the innate immune responses to LPS. Surprisingly, small molecule inhibitors of cholesterol biosynthesis, lovastatin, alendronate or zaragozic acid increased the LPS-induced secretion of IL-1 $\alpha$  and IL-

1 $\beta$ . Interestingly, treatment of granulosa cells with lovastatin increased the abundance of SR-BI in granulosa cells, whereas treatment of granulosa cells with siRNA targeting *HMGCR*, *FDPS* or *FDFTI* had no significant effect on the abundance of SR-BI. Whether the increased IL-1 secretion following lovastatin treatment was due to increased uptake of cholesterol esters via SR-BI was not explored. Future studies could explore cholesterol uptake using fluorescent cholesterol or the effect of the treatments following siRNA treatment targeting SR-BI.

The effects of lovastatin or methyl- $\beta$ -cyclodextrin did not appear to be mediated through altered MAPK phosphorylation. Depletion of cholesterol by statins promotes activation of SCAP-SREBP-2, and is associated with increased NLRP3 inflammasome activation and IL-1 $\beta$  secretion by mouse macrophages (Guo et al., 2018a). Whether the differences observed between statins and siRNA treatment are via altered SCAP-SREBP2 activation could be the subject of future studies.

Finally, we explored the interaction between innate immunity and endocrine function because granulosa cells are steroidogenic cells that utilize cholesterol for hormone biosynthesis, in addition to utilizing cholesterol for normal cellular functions. We treated granulosa cells with FSH. Previously, treatment with FSH (2.5  $\mu$ g/ml) has been shown to augment the LPS-induced secretion of IL-8 by granulosa cells from emerged follicles in medium containing 10% serum (Bromfield and Sheldon, 2011). In contrast, we found that FSH increased the innate immune responses to LPS in serum-starved and medium containing 2% FBS; however, the effects of FSH on the innate immune responses to LPS were diminished by 10% FBS.

In summary, we suggest that cholesterol metabolism and innate immunity may be integrated in bovine granulosa cells (**Fig. 7.2**), implying that deficits in cellular cholesterol during the postpartum period may impair the innate immune responses to LPS in the ovarian follicle.



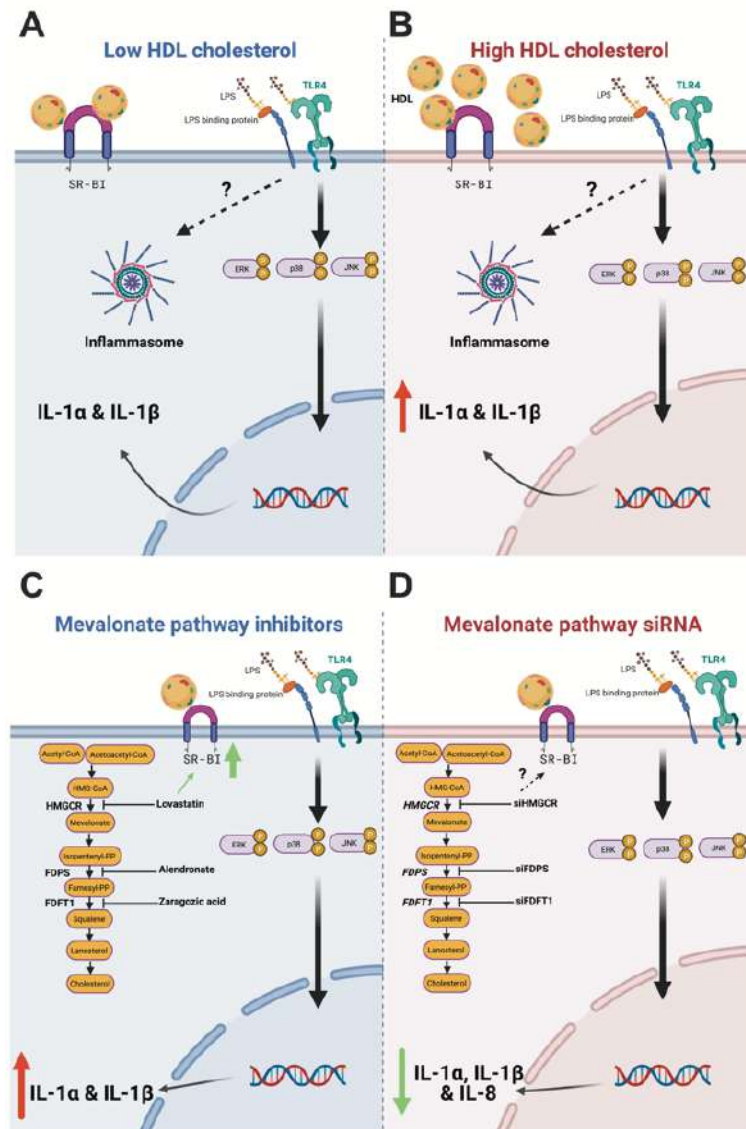


**Figure 7.2. Alterations to HDL concentrations or cholesterol biosynthesis affect the innate immune responses of granulosa cells to LPS**

(A) In conditions where HDL cholesterol concentrations are low or absent, granulosa cells respond to LPS by accumulating IL-1α and IL-1β, via phosphorylation of ERK1/2, p38 and JNK. (B) When HDL concentrations increase, there is an increase in the LPS-induced secretion of IL-1α and IL-1β. (C) Inhibition of the cholesterol biosynthesis pathway with inhibitors increases the LPS-induced secretion of IL-1α and IL-1β; lovastatin treatment is associated with increased SR-BI protein abundance; increased IL-1 may not be associated with increased phosphorylation of ERK1/2, p38 or JNK. (D) Reducing the expression of enzymes of the cholesterol biosynthesis pathway using siRNA decreases the LPS-induced secretion of IL-1α, IL-1β and IL-8 in granulosa cells (Horlock A., 2021; Created with BioRender.com).

In *Chapter 3* and *Chapter 4*, we found that energy stress or impaired cholesterol metabolism altered the innate immune responses to LPS by granulosa cells. Therefore, in *Chapter 5*, we explored how energy stress or impairing cholesterol biosynthesis in the cumulus-oocyte complex might alter innate immune function and affect oocyte health. The hypothesis of *Chapter 5* was that energy stress or decreasing the availability of cholesterol would alter the innate immune response of the COC to LPS. In agreement with the hypothesis, treatment with 2-DG, AICAR or Torin 1, reduced the LPS-induced secretion of IL-1 $\beta$  and IL-8 by COCs. We also found that treatment with the bisphosphonate, alendronate, increased LPS-induced secretion of IL-1 $\beta$  by COCs. However, treatment with lovastatin or zaragozic acid had no significant effect on the innate immune responses to LPS.

Ovulation is an inflammatory process, associated with the release of cytokines such as IL-1, IL-6 and IL-8, and damage of the hyaluronan extracellular matrix (Richards et al., 2008, Espey, 1980). In the bovine ovarian follicle, growth from preantral to small antral follicles is associated with increased expression of *IL1A* and *IL1B*, whilst growth from small antral to large antral follicles is associated with increased *IL1B*, but reduced *IL1A* expression (Passos et al., 2016). Additionally, treatment of bovine granulosa cells isolated from large follicles (> 8.5 mm external diameter) with recombinant IL-8 decreased the FSH-induced secretion of oestradiol, associated with decreased abundance of aromatase; however, treatment with IL-8 increased the LH-induced secretion of progesterone, associated with increased abundance of StAR (Shimizu et al., 2012a). Therefore, disruptions to the release of IL-1 $\alpha$ , IL-1 $\beta$  or IL-8, during periods of energy stress or uterine infection (or both concurrently), might impair the normal physiological processes controlling follicle growth, oocyte development and ovulation.

Maintaining metabolic homeostasis is essential for oocyte health. Utilizing 2-DG to mimic acute fasting suggests that glycolysis may be essential for meiotic progression and COC expansion in mouse oocytes (Han et al., 2012). Activating AMPK with AICAR or metformin in bovine COCs is associated with impaired COC expansion and perturbed meiotic progression (Tosca et al., 2007b, Bilodeau-Goeseels et al., 2007). Additionally, inhibiting mTOR with Torin 1 compromises oocyte developmental

competence of mouse oocytes, with a reduction in the rate of fertilization and blastocyst development (Guo et al., 2016). Similarly, we found that 2-DG or AICAR treatment impaired COC expansion and arrested oocytes at the GVBD stage of development. Interestingly, Torin 1 treatment impaired the meiotic progression of oocytes to MII. Together, this evidence suggests that energy stress in the ovarian follicle might impair oocyte health.

None of the cholesterol biosynthesis inhibitors used in *Chapter 5* altered expansion of COCs during IVM. However, all three of the inhibitors tested in this thesis were associated with decreased meiotic progression during IVM. Hypercholesterolemia is often treated with statins but may negatively affect reproductive outcome. For example, treatment of mouse embryos with mevastatin prevents the development to blastocyst stage (Surani et al., 1983). The prevention of blastocyst formation by statin treatment in mouse embryos can be rescued by the addition of mevalonic acid (Alarcon and Marikawa, 2016, Surani et al., 1983). Statins are listed under the Pregnancy Risk Category X by the Food and Drug Administration, as it is not advisable for pregnant women to use statins (Alarcon and Marikawa, 2016). Due to women conceiving later in life, it is more likely that women of reproductive age may be taking statin treatment for hypercholesterolemia. The present study suggests that inhibitors of cholesterol biosynthesis may also impair oocyte meiotic progression of bovine oocytes to the MII stage. Future work could explore the use of statins or pharmaceutical inhibitors of cholesterol biosynthesis on oocyte health in women of reproductive age.

The limitations of *Chapter 5* were that we did not explore the effects of HDL treatment or utilize siRNA to reduce the expression of genes encoding *HMGCR*, *FDPS* or *FDFT1* in COCs as we did for granulosa cells in *Chapter 4*. Also, it would have been interesting, although beyond the scope of the present thesis, to activate the oocytes following IVM via parthenogenesis, to examine the effects of the treatments on oocyte cleavage.

The work carried out in this thesis provides further understanding of the crosstalk between innate immunity and energy stress in the bovine ovarian follicle (**Fig. 7.3**). We suggest that negative energy balance and uterine infection have both independent and cumulative effects in granulosa cells isolated from emerged or dominant follicles,

and on the cumulus-oocyte complex, providing an insight to the mechanisms by which energy stress and uterine infection cause infertility in cows. This might possibly lead to the development of alternative herd management strategies or therapeutics to reduce impact of negative energy balance on the follicular microenvironment.

In the present thesis, we focused on the granulosa cells of the bovine ovarian follicle, however, theca cells are also essential for ovarian function, producing androgens for steroidogenesis by granulosa cells, supplying nutrients to the growing follicle via the vascular network via the theca interna, and providing structural support to the follicle via the theca externa. The process of ovulation is an inflammatory event, associated with the release of cytokines, chemokines, steroids and prostaglandins by granulosa and theca cells, leading to the activation and infiltration of immune cells into the ovarian follicle (Duffy et al., 2018, Abdulrahman Alrabiah et al., 2021). Temporal regulation of these processes is essential, and RNA sequencing revealed that theca cells displayed a higher frequency of over-represented immune-related pathways during follicle differentiation, compared with granulosa cells (Walsh et al., 2012a). Conversely, during follicle luteinization, granulosa cells displayed a higher frequency of over-represented immune-related pathways, related to inflammation and the innate immune response, compared with theca cells (Walsh et al., 2012a).

Future studies investigating the crosstalk between energy stress and immune function in the ovary might also explore granulosa cell – theca cell interactions. For example, energy stress may also impair ovarian through altered theca cell function; compared with non-lactating heifers, lactating cows under negative energy balance had reduced dominant follicle oestradiol and progesterone secretion, during follicle differentiation and luteinization, respectively (Walsh et al., 2012b). The impaired endocrine function in lactating dairy cows was associated with reduced expression of *STAR* in the theca cells of the ovarian follicle, suggesting a direct link between an altered metabolic environment during energy stress and altered ovarian endocrine functioning in theca cells (Walsh et al., 2012b).

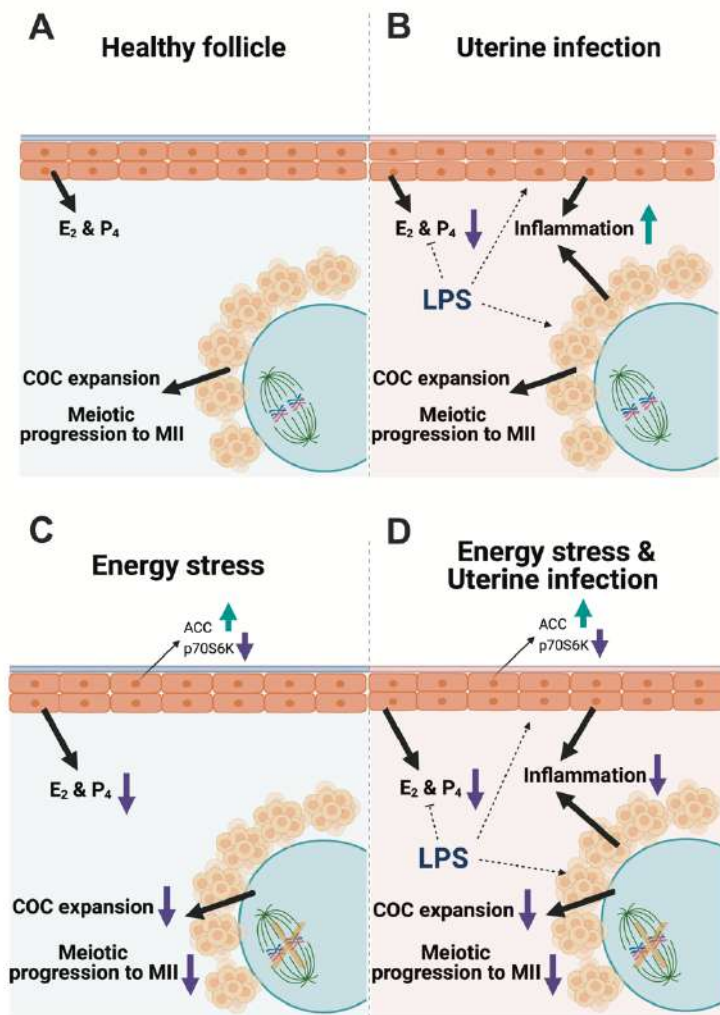


**Figure 7.3. Proposed effects of energy stress and uterine infection on the ovarian follicle**

(A) In healthy growing follicles, mural granulosa cells secrete oestradiol and progesterone and around the time of ovulation, the COC expands, and the oocyte progresses to MII of meiosis. (B) during uterine infection, LPS accumulates in follicular fluid. In response to LPS, mural granulosa cells mount an inflammatory response, and secrete less oestradiol and progesterone; COCs also mount an innate immune response to LPS (C) during energy stress, mural granulosa cells secrete less oestradiol and progesterone, and COC expansion and oocyte meiotic progression are impaired. (D) during energy stress and uterine infection, mural granulosa cells secrete less oestradiol and progesterone, and the innate immune responses of granulosa cells and the COC are impaired; COC expansion and meiotic competence of the oocyte is impaired. GC, granulosa cell; E<sub>2</sub>, oestradiol; P<sub>4</sub>, progesterone; COC, cumulus-oocyte complex (Horlock A., 2021; Created with BioRender.com).

*In vitro* studies, including ours, can only explore the short-term effects of energy stress or LPS challenge during 22 to 24 h of IVM for COCs, or over 48 h for granulosa cells. Unfortunately, it is not possible to explore the long-term effects of energy stress on granulosa cells *in vitro* because they differentiate into luteal cells during prolonged culture. However, throughout this thesis we isolated granulosa cells from both emerged and dominant follicles, representing the different stages of follicular growth to model how energy stress might affect innate immune function of granulosa cells. It is generally agreed that the metabolic health directly impacts the fertility of cows (Leroy et al., 2017). Although serum glucose and cholesterol concentrations are reflected in follicular fluid glucose concentrations (Leroy et al., 2004a, Leroy et al., 2004b), to our knowledge no *in vivo* studies have directly quantified the changes in glucose or cholesterol in follicular fluid during periods of negative energy balance. However, bovine oocytes treated with the follicular fluid obtained from obese women, or women with poor *in vitro* fertilisation (IVF) outcomes, are associated with reduced embryo development, compared with treatment with follicular fluid from positive IVF outcomes (Valckx et al., 2015).

One of the challenges for studying the long-term effects of bacterial infection on the reproductive tract in animals with spontaneous disease is disentangling the effect of infection from the effects of other peripartum problems, metabolic stress and lactation (Chagas et al., 2007, LeBlanc, 2012, Cerri et al., 2012, Girard et al., 2015). Therefore, collaborators at the University of Florida developed an *in vivo* model of endometritis to disentangle uterine disease from other postpartum problems in dairy cows, such as negative energy balance (Piersanti et al., 2019c). We exploited this model of endometritis in *Chapter 6* to test the hypothesis that intrauterine infusion of pathogenic bacteria leads to changes in the transcriptome of the reproductive tract in dairy cattle several months later. In line with the hypothesis, we found that intrauterine infusion of *E. coli* and *T. pyogenes* was associated with altered transcriptome of the caruncular and intercaruncular tissue of the endometrium, the isthmus and ampulla of the oviduct, and the granulosa cells and oocyte of the ovarian follicle, several months following infusion. The most striking finding of this study was that the granulosa cells and oocyte, the most distal to infection, had more predicted upstream regulators, including those involved in innate immunity, than all the other samples combined. Similarly, from the same study, it was found that intrauterine infusion of pathogenic bacteria

alters the transcriptome of the oocyte differently at day 4, compared with day 60, relative to infusion, suggesting that different follicle stages are susceptible to damage (Piersanti et al., 2020). Utilizing the same model, a separate study found that fewer oocytes from bacteria-infused animals developed to morulae stage following IVM and embryo culture, compared with control animals (Dickson et al., 2020). Another study found that natural metritis in cows was associated with changes in the transcriptome of the granulosa cells of the dominant follicle, 6 weeks after the resolution of disease (Piersanti et al., 2019a). We suggest that the *in vivo* model of endometritis analysed in this thesis, may be the first step into disentangling the mechanisms by which uterine infection and energy stress impair the fertility of dairy cows, with the aim to reduce or eliminate the problems of uterine disease and negative energy balance in postpartum dairy cows.

Postpartum negative energy balance or uterine disease experienced by dairy cows is not inevitable. Up to 50% of high milk producing dairy cows maintain or increase body condition score or weight during the first three weeks postpartum (Carvalho et al., 2014). Optimising dairy nutrition during the transition period and genetically selecting against postpartum negative energy balance could eliminate many of the postpartum disease problems experienced by dairy cows (Britt et al., 2021). Feed strategies could be used where feed is formulated provide sufficient vitamins and minerals, as well as meeting metabolic energy and protein requirements for lactation (Mulligan et al., 2006, Sheldon et al., 2020).

Worldwide demand for dairy products is predicted to increase around 37%, from around 87 kg per person to around 119 kg per person by 2067 (Macrae et al., 2019). The increased demand for dairy products, in combination with increased population growth, means that an extra 600 billion kilograms more milk will be needed to be produced in 2067, compared with today (Britt et al., 2018). Sustainable intensification, focusing on selective breeding, or gene editing to select for a balance between fitness and milk yield traits, optimizing nutrition, and minimizing the environmental impacts are essential for the future of the dairy industry (Britt et al., 2021).

In conclusion, this thesis provides novel evidence that innate immunity and metabolism are integrated in bovine granulosa cells and the cumulus-oocyte complex. We found that AMPK and mTOR may regulate innate immune responses to LPS in granulosa cells. Secondly, we found that the availability of cholesterol, or cholesterol biosynthesis may be important for the innate immune responses to LPS in granulosa cell. Thirdly, we found that AMPK, mTOR and cholesterol biosynthesis may regulate the innate immune responses of the cumulus-oocyte complex to LPS. Finally, we exploited an *in vivo* model of endometritis in cattle and found that there are long-term alterations to the transcriptome of the granulosa cells and oocyte, potentially paving the way for further studies to explore the independent and cumulative effects of energy stress and uterine infection in the future. The findings in this thesis might be exploited to manipulate cellular energy metabolism using nutrition or therapeutics to optimize innate immune responses to postpartum bacterial infections, with the aim to prevent negative energy balance and uterine infection in the dairy cow.



## 8 Appendices

**Supplemental Table 1.** Read mapping summary from RNAseq of caruncular endometrium from control (orange) and bacteria-infused (purple) animals

Animal ID	Initial Reads	Quality Reads	Unique Mapped Reads	Aligned (%)	Mapped Transcripts
388C	73,081,076	73,078,831	21,935,268	30	31,691
396C	68,608,160	68,606,827	22,437,030	33	31,320
397C	84,113,672	84,111,047	28,697,193	34	32,086
431C	68,437,970	68,436,035	21,077,607	31	31,509
437C	72,199,870	72,197,481	22,271,578	31	28,382
447C	87,839,708	87,834,656	28,865,531	33	32,777
385C	73,578,076	73,575,015	24,591,389	33	32,711
401C	67,407,462	67,404,309	20,419,794	30	31,647
408C	70,527,082	70,525,202	21,164,579	30	32,260
436C	68,454,398	68,452,906	17,959,506	26	30,544
TOTAL	734,247,474	734,222,309	229,419,475		
AVERAGE	73,424,747	73,422,231	22,941,948	31	31,493
SEM	2,213,750	2,213,501	1,107,905	0.7	405

**Supplemental Table 2.** Top five up and down differentially regulated genes in the caruncular endometrium of bacteria-infused compared with control animals

Gene	Gene name	Control <sup>1</sup>	Bacteria <sup>1</sup>	Log <sub>2</sub> FC	P-value
<i>SLC45A1</i>	Solute Carrier Family 45 Member 1	0.14	7.02	48.64	0.0005
<i>ADARB1</i>	Adenosine Deaminase, RNA-Specific, B1	4.26	26.62	4.73	0.0076
<i>RNF38</i>	Ring Finger Protein 38	0.14	2.80	4.27	0.0037
<i>DBNDD1</i>	Dysbindin Domain Containing 1	0.28	4.06	3.87	0.0019
<i>GOLGA3</i>	Golgin A3	0.19	2.74	3.83	0.048
<i>MMP3</i>	Matrix Metalloproteinase 3 (Stromelysin 1,	1250.70	14.31	-6.45	0.02
<i>SPAG9</i>	Sperm Associated Antigen 9	4.89	0.21	-4.51	0.01
<i>NXPE3</i>	Neurexophilin and principal component	10.41	0.52	-4.45	0.04
<i>ATG10</i>	Autophagy Related 10	6.64	0.52	-3.69	0.008
<i>VPREB3</i>	Pre-B Lymphocyte 3	246.31	20.28	-3.60	0.004

<sup>1</sup>Base mean values determined by RNAseq read number. FC; fold change

**Supplemental Table 3.** Read mapping summary from RNAseq of the intercaruncular endometrium from control (orange) and bacteria-infused (purple) animals

Animal ID	Initial Reads	Quality Reads	Unique Mapped	Aligned (%)	Mapped Transcripts
388IC	90,268,038	90,265,787	26,435,536	29	33,211
396IC	78,276,484	78,274,337	23,948,342	31	32,842
397IC	92,318,102	92,313,575	25,369,421	27	33,478
431IC	72,058,924	72,056,518	24,529,038	34	32,125
437IC	71,020,594	71,018,992	22,143,024	31	32,363
447IC	83,351,184	83,349,152	26,699,219	32	32,618
385IC	76,283,604	76,280,422	25,576,567	34	33,043
401IC	79,919,654	79,916,882	24,945,037	31	32,784
436IC	76,100,358	76,097,110	26,128,390	34	32,896
TOTAL	719,596,942	719,572,775	225,774,574		
AVERAGE	79,955,216	79,952,531	25,086,064	32	32,818
SEM	2,483,464	2,483,325	473,121	0.8	138

**Supplemental Table 4.** Top five up and down differentially regulated genes in the intercaruncular endometrium tissue of bacteria-infused compared with control animals

Gene	Gene name	Control <sup>1</sup>	Bacteria <sup>1</sup>	Log <sub>2</sub> FC	P-value
<i>CFAP69</i>	Cilia and Flagella Associated Protein 69	0.30	8.79	4.89	0.0004
<i>CYP11B2</i>	Cytochrome P450 family 11 subfamily B member	0.17	3.15	4.19	0.03
<i>FBXW7</i>	F-box and WD repeat domain containing 7	0.36	6.60	4.18	0.002
<i>PDP1</i>	Pyruvate Dehydrogenase Phosphatase Catalytic	0.18	3.14	4.11	0.03
<i>CREM</i>	cAMP Responsive Element Modulator	0.30	3.75	3.66	0.03
<i>VNN2</i>	Vanin 2	2279.80	58.91	-5.27	0.04
<i>FCMR</i>	Fc Fragment of IgM Receptor	18.03	0.63	-4.85	0.009
<i>SMIM12</i>	Small Integral Membrane Protein 12	5.99	0.31	-4.26	0.01
<i>VPREB3</i>	Pre-B Lymphocyte 3	273.87	16.62	-4.04	0.003
<i>POU2AF1</i>	POU Class 2 Associating Factor 1	1251.46	81.07	-3.95	0.008

<sup>1</sup>Base mean values determined by RNAseq read number. FC; fold change.

**Supplemental Table 5.** Read mapping summary from RNAseq of the isthmus from control (orange) and bacteria-infused (purple) animals

Animal ID	Initial Reads	Quality Reads	Unique Mapped Reads	Aligned (%)	Mapped Transcripts
388I	72,980,642	72,969,154	28,632,726	39	29,320
396I	84,583,964	84,569,875	33,708,756	40	30,404
397I	87,932,312	87,926,926	32,714,425	37	30,999
431I	94,228,272	94,212,034	40,842,932	43	31,487
437I	74,925,858	74,906,067	25,859,462	35	27,976
447I	85,963,342	85,951,052	36,053,320	42	31,198
385I	57,717,560	57,706,238	23,072,286	40	27,883
401I	76,730,610	76,718,183	20,505,152	27	26,514
436I	71,933,254	71,924,619	28,834,211	40	29,447
TOTAL	706,995,814	706,884,148	270,223,270		
AVERAGE	78,555,090	78,542,683	30,024,808	38	29,470
SEM	3,633,250	3,633,138	2,153,315	2	575

**Supplemental Table 6.** Top five up and down differentially regulated genes in the isthmus of bacteria-infused compared with control animals

Gene	Gene name	Control <sup>1</sup>	Bacteria <sup>1</sup>	Log <sub>2</sub> FC	P-value
<i>CXCR1</i>	Chemokine (C-X-C Motif) Receptor 1	0.29	18.51	7.57	0.02
<i>CXCL8</i>	C-X-C Motif Chemokine Ligand 8	10.60	587.71	7.36	0.02
<i>ATP13A3</i>	ATPase Type 13A3	0.11	3.03	4.81	0.03
<i>UBTF</i>	Upstream Binding Transcription Factor	0.11	2.75	4.67	0.03
<i>PROCR</i>	Protein C Receptor	0.25	5.43	4.43	0.009
<i>GLIPR1L1</i>	GLIPR1 Like 1	18.79	0.69	-4.78	0.02
<i>TNNI3K</i>	TNNI3 Interacting Kinase	8.24	0.34	-4.59	0.02
<i>CEP41</i>	Centrosomal Protein 41kDa	7.92	0.42	-4.23	0.008
<i>FZD5</i>	Frizzled Class Receptor 5	5.84	0.34	-4.09	0.03
<i>NXPE3</i>	Neurexophilin and principal component -esterase	11.24	0.69	-4.04	0.03

<sup>1</sup>Base mean values determined by RNAseq read number. FC; fold change.

**Supplemental Table 7.** Read mapping summary from RNAseq of the ampulla from control (orange) and bacteria-infused (purple) animals

Animal ID	Initial Reads	Quality Reads	Unique Mapped Reads	Aligned (%)	Mapped Transcripts
388A	81,769,028	81,759,542	34,825,372	43	32,503
396A	83,943,082	83,930,886	36,210,308	43	31,535
397A	61,802,508	61,767,551	25,830,356	42	30,401
431A	88,141,482	88,136,830	26,564,487	30	26,945
437A	80,012,734	79,995,007	33,122,086	41	30,137
447A	73,913,602	73,903,650	29,527,164	40	29,989
385A	83,326,282	83,305,891	28,579,873	34	28,457
401A	77,882,744	77,872,656	29,133,389	37	27,475
436A	85,291,892	85,280,588	32,785,207	38	29,513
TOTAL	716,083,354	715,952,601	276,578,242		
AVERAGE	79,564,817	79,550,289	30,730,916	39	29,662
SEM	2,622,024	2,624,306	1,217,516	1	602

**Supplemental Table 8.** Top five up and down differentially regulated genes in the ampulla of bacteria-infused compared with control animals

Gene	Gene name	Control <sup>1</sup>	Bacteria <sup>1</sup>	Log <sub>2</sub> FC	P-value
<i>GSG1L</i>	GSG1 Like	3.66	351.31	6.59	0.03
<i>SLPI</i>	Secretory Leukocyte Peptidase Inhibitor	92.68	8067.41	6.44	0.04
<i>KCNE4</i>	Potassium Voltage-gated Channel Subfamily E	3.66	133.82	5.19	0.004
<i>ABCC6</i>	ATP Binding Cassette Subfamily C Member 6	0.34	11.95	5.13	0.04
<i>KERA</i>	Keratocan	0.90	29.32	5.03	0.01
<i>USP46</i>	Ubiquitin Specific Peptidase 46	8.46	0.32	-4.71	0.003
<i>ZDHHC9</i>	Zinc Finger DHHC-type Containing 9	16.63	0.79	-4.40	0.002
<i>ZBTB24</i>	Zinc Finger and BTB Domain Containing 24	13.17	0.65	-4.35	0.0009
<i>ZNF319</i>	Zinc Finger Protein 319	14.43	0.72	-4.33	0.0005
<i>KIAA0040</i>	KIAA0040 Ortholog	38.48	1.94	-4.31	0.001

<sup>1</sup>Base mean values determined by RNAseq read number. FC; fold change.

**Supplemental Table 9.** Read mapping summary from RNAseq of granulosa cells from control (orange) and bacteria-infused (purple) animals

Animal ID	Initial Reads	Quality Reads	Unique Mapped Reads	Aligned (%)	Mapped Transcripts
388GC	51,635,056	51,635,042	4,928,163	10	7,128
396GC	50,570,650	50,570,639	12,676,007	25	7,741
397GC	52,248,816	52,248,781	12,116,114	23	8,423
431GC	68,360,284	68,360,284	26,838,138	39	25,472
437GC	63,187,200	63,187,198	23,786,029	38	24,307
447GC	59,949,024	59,949,019	23,499,560	39	26,213
401GC	53,693,856	53,693,854	20,780,149	39	24,389
408GC	50,584,752	50,584,743	14,470,484	29	10,615
436GC	62,950,122	62,950,118	19,972,042	32	18,514
TOTAL	513,179,760	513,179,678	159,066,686		
AVERAGE	57,019,973	57,019,964	17,674,076	30	16,978
SEM	2,224,277	2,224,279	2,353,465	3	2800

**Supplemental Table 10.** Top five up and down differentially regulated genes in the granulosa cells of bacteria-infused compared with control animals

Gene	Gene name	Control <sup>1</sup>	Bacteria <sup>1</sup>	Log <sub>2</sub> FC	P-value
<i>FAM71A</i>	Family with sequence similarity 71 member A	0.38	802.61	11.04	0.007
<i>EOMES</i>	Eomesodermin	0.40	812.40	10.99	0.01
<i>ALKAL2</i>	ALK and LTK Ligand 2	0.22	400.53	10.81	0.01
<i>ADAMTS1</i>	ADAM Metallopeptidase with Thrombospondin	0.38	574.73	10.56	0.008
<i>ARHGAP9</i>	Rho GTPase Activating Protein 9	0.32	292.28	9.83	0.02
<i>CARD 9</i>	Caspase Recruitment Domain Family Member 9	143.27	0.52	-8.09	0.03

<sup>1</sup>Base mean values determined by RNAseq read number. FC; fold change.

**Supplemental Table 11.** Read mapping summary from RNAseq of oocytes from control (orange) and bacteria-infused (purple) animals

Animal ID	Initial Reads	Quality Reads	Unique Mapped Reads	Aligned (%)	Mapped Transcripts
436	78,644,926	78,644,926	31,338,811	40	26,278
401	68,166,968	68,166,967	27,299,988	40	24,657
385	72,060,840	72,060,840	28,766,811	40	23,650
388	77,460,136	77,460,129	30,104,986	39	21,758
396	66,547,886	66,547,885	26,227,633	39	26,073
431	77,062,458	77,062,456	30,840,860	40	23,396
447	74,278,946	74,278,940	29,505,343	40	19,153
437	68,200,330	68,200,330	26,955,792	40	25,674
397	77,027,406	77,027,406	30,243,995	39	26,349
TOTAL	659,449,896	659,449,879	261,284,219		216,988
AVERAGE	73,272,211	73,272,209	29,031,580	40	24,110
SEM	1,556,158	1,556,158	608,766	0	809.12

**Supplemental Table 12.** Top five up and down differentially regulated genes in the oocytes of bacteria-infused compared with control animals

Gene	Gene name	Control <sup>1</sup>	Bacteria <sup>1</sup>	Log <sub>2</sub> FC	P-value
<i>TNFAIP6</i>	TNF Alpha Induced Protein 6	1.14	5479.7	12.23	0.003
<i>GPR50</i>	G Protein-Coupled Receptor 50	0.35	716.3	11.0	0.006
<i>CSRP3</i>	Cysteine and Glycine Rich Protein 3	5.27	5656.8	10.07	0.008
<i>PALMD</i>	Palmdelphin	0.35	206.75	9.2	0.01
<i>TNFSF18</i>	TNF Superfamily	0.30	128.17	8.75	0.02
<i>ADAM22</i>	ADAM Metallopeptidase Domain 22	85.41	0.29	-8.20	0.00001
<i>CALHM4</i>	Calcium Homeostasis Modulator Family Member 4	25.66	0.38	-6.09	0.02
<i>DNER</i>	Delta/Notch like EGF Repeat Containing	422.18	6.75	-5.97	0.006
<i>IL2RG</i>	Interleukin 2 Receptor Subunit Gamma	37.19	0.76	-5.62	0.004
<i>RCVRN</i>	Recoverin	32.87	0.87	-5.24	0.003

<sup>1</sup>Base mean values determined by RNAseq read number. FC; fold change.

**Supplemental Table 13.** Expression of target genes of interest in the caruncular endometrium of control and bacteria-infused animals

	<b>Control (Base</b>	<b>Bacteria (Base</b>	<b>Log<sub>2</sub> fold</b>	<b>P-</b>
<b>Inflammation</b>				
<i>CCL2</i>	1604.01	286.60	-2.48	0.47
<i>CXCL2</i>	513.26	60.52	-3.08	0.46
<i>CXCL8</i>	587.38	175.09	-1.75	0.63
<i>IL1A</i>	253.02	92.48	-1.45	0.45
<i>IL1B</i>	1130.18	250.35	-2.17	0.54
<i>IL6</i>	1.77	2.82	0.67	0.61
<i>IL6R</i>	2171.93	2852.57	0.39	0.33
<i>IL10</i>	11.66	6.84	-0.77	0.64
<i>IL12</i>	164.51	182.98	-0.42	0.41
<i>IL18</i>	30.65	24.58	-0.32	0.57
<i>IL22</i>	7.50	1.03	-2.86	0.54
<i>IFNG</i>	22.47	8.47	-1.41	0.30
<i>CARD9</i>	415.77	449.41	-0.30	0.52
<i>MHC I</i>	9049.48	5512.46	-0.71	0.77
<i>MHC II</i>	6949.58	3379.06	-1.04	0.07
<i>HIF1A</i>	11955.34	15499.97	0.38	0.55
<b>Steroid</b>				
<i>CYP11A1</i>	41.73	54.99	0.40	0.46
<i>CYP19A1</i>	1.23	0.26	-2.25	0.46
<i>HSD3B1</i>	N/A	N/A	N/A	N/A
<i>HSD17B2</i>	N/A	N/A	N/A	N/A
<i>STAR</i>	443.10	367.77	-0.27	0.65
<b>Cell viability</b>				
<i>BAK1</i>	107.81	138.37	0.36	0.55
<i>BAX</i>	249.03	207.18	-0.27	0.56
<i>BCL2</i>	22.46	23.79	0.08	0.98
<i>BCL2L12</i>	200.24	271.74	0.44	0.27
<i>CASP1</i>	12.12	10.07	-0.27	0.70
<i>CASP2</i>	249.15	350.36	0.49	0.31
<i>CASP4</i>	32.36	39.92	0.30	0.75
<i>CASP6</i>	1184.73	817.95	-0.53	0.19
<i>CASP8</i>	695.30	710.70	0.03	0.92
<i>CCNB1</i>	1553.93	1480.63	-0.07	0.89
<i>CCNB2</i>	38.56	22.07	-0.81	0.50
<i>CCND1</i>	488.13	404.28	-0.27	0.59
<i>CCND2</i>	306.24	255.92	-0.26	0.55
<i>FADD</i>	1279.54	1152.42	-0.15	0.63

<sup>1</sup>Base mean values determined by RNAseq read number.

**Supplemental Table 14.** Expression of target genes of interest in the intercaruncular endometrium of control and bacteria-infused animals

	<b>Control (Base</b>	<b>Bacteria (Base</b>	<b>Log<sub>2</sub> fold</b>	<b>P-</b>
<b>Inflammation</b>				
<i>CCL2</i>	2402.59	208.59	-3.52	0.49
<i>CXCL2</i>	1456.38	30.72	-5.57	0.36
<i>CXCL8</i>	1300.89	10.03	-7.02	0.26
<i>IL1A</i>	277.71	69.71	-1.99	0.57
<i>IL1B</i>	1309.59	65.98	-4.31	0.41
<i>IL6</i>	2.24	1.88	-0.25	0.97
<i>IL6R</i>	3472.79	4143.23	0.25	0.57
<i>IL10</i>	16.73	9.11	-0.88	0.72
<i>IL12</i>	190.02	161.10	-0.24	0.71
<i>IL18</i>	45.11	33.87	-0.41	0.60
<i>IL22</i>	N/A	N/A	N/A	N/A
<i>IFNG</i>	42.03	6.59	-2.67	0.21
<i>CARD9</i>	467.16	324.27	-0.52	0.35
<i>MHC I</i>	9153.90	11036.98	0.27	0.77
<i>MHC II</i>	8384.16	4527.91	-0.89	0.42
<i>HIF1A</i>	19763.60	20916.35	0.08	0.85
<b>Steroid</b>				
<i>CYP11A1</i>	74.13	78.87	1.06	0.88
<i>CYP19A1</i>	N/A	N/A	N/A	N/A
<i>HSD3B1</i>	0.54	5.00	3.21	0.19
<i>HSD17B2</i>	0.77	4.74	2.63	0.18
<i>STAR</i>	344.64	348.99	0.02	0.96
<b>Cell viability</b>				
<i>BAK1</i>	194.89	202.30	0.05	0.85
<i>BAX</i>	339.46	291.64	-0.22	0.73
<i>BCL2</i>	454.60	419.99	-0.11	0.86
<i>BCL2L12</i>	33.56	31.77	-0.08	0.99
<i>CASP1</i>	13.76	8.81	-0.64	0.52
<i>CASP2</i>	368.63	387.21	0.07	0.85
<i>CASP4</i>	38.15	33.43	-0.19	0.93
<i>CASP6</i>	1271.66	1125.74	-0.18	0.76
<i>CASP8</i>	957.33	888.66	-0.11	0.86
<i>CCNB1</i>	2159.45	2212.04	0.03	0.91
<i>CCNB2</i>	31.56	23.96	-0.40	0.79
<i>CCND1</i>	555.79	449.07	-0.31	0.58
<i>CCND2</i>	276.86	181.39	-0.61	0.37
<i>FADD</i>	1718.89	1611.39	-0.09	0.90

<sup>1</sup>Base mean values determined by RNAseq read number.

**Supplemental Table 15.** Expression of target genes of interest in the isthmus of control and bacteria-infused animals

	Control (Base mean) <sup>1</sup>	Bacteria (Base mean) <sup>1</sup>	Log <sub>2</sub> fold change	P-value
<b>Inflammation</b>				
<i>CCL2</i>	71.98	795.42	3.47	0.10
<i>CXCL2</i>	153.35	159.26	0.05	0.77
<i>CXCL8</i>	10.60	1741.93	7.36	0.02
<i>IL1A</i>	15.60	48.67	1.64	0.07
<i>IL1B</i>	51.18	704.76	3.78	0.09
<i>IL6</i>	11.09	16.85	0.60	0.43
<i>IL6R</i>	1315.12	970.81	-0.44	0.25
<i>IL10</i>	1.93	12.18	2.66	0.14
<i>IL12</i>	0.89	1.37	0.62	0.67
<i>IL18</i>	60.97	68.98	0.18	0.66
<i>IL22</i>	N/A	N/A	N/A	N/A
<i>IFNG</i>	23.04	13.01	-0.82	0.80
<i>CARD9</i>	128.94	175.77	0.45	0.26
<i>MHC I</i>	10058.64	19306.84	0.94	0.18
<i>MHC II</i>	5685.56	10364.17	0.87	0.28
<i>HIF1A</i>	13167.02	11511.57	-0.19	0.70
<b>Steroid synthesis</b>				
<i>CYP11A1</i>	142.93	90.33	-0.66	0.53
<i>CYP19A1</i>	N/A	N/A	N/A	N/A
<i>HSD3B1</i>	0.72	1.69	1.24	0.53
<i>HSD17B2</i>	N/A	N/A	N/A	N/A
<i>STAR</i>	236.33	306.44	0.37	0.26
<b>Cell viability</b>				
<i>BAK1</i>	84.78	87.66	0.05	0.81
<i>BAX</i>	118.78	105.90	-0.17	0.92
<i>BCL2</i>	27.44	27.82	0.02	1
<i>BCL2L12</i>	81.11	102.27	0.33	0.48
<i>CASP1</i>	7.41	3.74	-0.98	0.51
<i>CASP2</i>	127.66	138.65	0.12	0.80
<i>CASP4</i>	15.78	19.13	0.28	0.57
<i>CASP6</i>	1858.33	1854.37	-0.003	0.91
<i>CASP8</i>	788.92	789.49	0.001	0.91
<i>CCNB1</i>	5530.31	6647.42	0.27	0.96
<i>CCNB2</i>	43.77	59.86	0.45	0.34
<i>CCND1</i>	1181.52	1152.13	-0.04	0.91
<i>CCND2</i>	341.56	326.18	-0.07	1
<i>FADD</i>	2967.79	3680.57	0.31	0.30

<sup>1</sup>Base mean values determined by RNAseq read number.

**Supplemental Table 16.** Expression of target genes of interest in the ampulla of control and bacteria-infused animals

	Control (Base)	Bacteria (Base)	Log <sub>2</sub> fold	P-value
<b>Inflammation</b>				
<i>CCL2</i>	269.11	280.90	0.06	0.97
<i>CXCL2</i>	144.32	128.31	-0.17	0.78
<i>CXCL8</i>	31.36	102.48	1.71	0.30
<i>IL1A</i>	16.02	21.61	0.43	0.52
<i>IL1B</i>	67.19	93.62	0.48	0.47
<i>IL6</i>	7.89	4.37	-0.85	0.40
<i>IL6R</i>	1131.81	1190.42	0.07	0.93
<i>IL10</i>	1.86	2.87	0.62	0.72
<i>IL12</i>	0.76	2.27	1.59	0.35
<i>IL18</i>	60.20	73.27	0.28	0.64
<i>IL22</i>	0.29	0.65	1.16	0.70
<i>IFNG</i>	12.38	21.31	0.78	0.43
<i>CARD9</i>	129.39	203.19	0.65	0.19
<i>MHC I</i>	6982.12	32816.29	2.23	0.01
<i>MHC II</i>	8057.06	11192.08	0.48	0.55
<i>HIF1A</i>	12582.91	13781.71	0.13	0.54
<b>Steroid synthesis</b>				
<i>CYP11A1</i>	78.68	126.05	0.68	0.18
<i>CYP19A1</i>	N/A	N/A	N/A	N/A
<i>HSD3B1</i>	N/A	N/A	N/A	N/A
<i>HSD17B2</i>	0.23	2.06	3.15	0.21
<i>STAR</i>	211.49	311.17	0.56	0.24
<b>Cell viability</b>				
<i>BAK1</i>	93.40	65.92	-0.50	0.37
<i>BAX</i>	143.54	161.19	0.17	0.67
<i>BCL2</i>	18.51	16.28	-0.19	0.71
<i>BCL2L12</i>	108.12	65.31	-0.73	0.24
<i>CASP1</i>	9.26	7.60	-0.28	0.71
<i>CASP2</i>	185.78	85.42	-1.12	0.04
<i>CASP4</i>	18.87	9.94	-0.92	0.27
<i>CASP6</i>	1925.44	2281.09	0.24	0.41
<i>CASP8</i>	663.27	772.42	0.22	0.47
<i>CCNB1</i>	761.67	7244.79	3.25	0.09
<i>CCNB2</i>	34.26	74.42	1.12	0.07
<i>CCND1</i>	1506.49	1721.74	0.19	0.83
<i>CCND2</i>	590.24	408.08	-0.53	0.20
<i>FADD</i>	3286.59	3849.54	0.23	0.46

<sup>1</sup>Base mean values determined by RNAseq read number.



**Supplemental Table 17.** Expression of target genes of interest in granulosa cells of control and bacteria-infused animals

	Control (Base)	Bacteria (Base)	Log <sub>2</sub> fold	P-value
<b>Inflammation</b>				
<i>CCL2</i>	3262.20	1936.11	-0.75	0.83
<i>CXCL2</i>	N/A	N/A	N/A	N/A
<i>CXCL8</i>	304.01	67.05	-2.18	0.84
<i>IL1A</i>	4.23	102.00	4.59	0.11
<i>IL1B</i>	20.02	30.73	0.62	0.71
<i>IL6</i>	N/A	N/A	N/A	N/A
<i>IL6R</i>	14.87	726.31	5.61	0.08
<i>IL10</i>	6.29	22.33	1.83	0.43
<i>IL12</i>	N/A	N/A	N/A	N/A
<i>IL18</i>	206.29	49.06	-2.07	0.78
<i>IL22</i>	N/A	N/A	N/A	N/A
<i>IFNG</i>	N/A	N/A	N/A	N/A
<i>CARD9</i>	143.27	0.52	-8.09	0.03
<i>MHC I</i>	3463.25	161.96	-4.42	0.30
<i>MHC II</i>	784.1	77.40	-3.34	0.39
<i>HIF1A</i>	21808.53	4839.27	-2.17	0.10
<b>Steroid synthesis</b>				
<i>CYP11A1</i>	1502.78	906.79	-0.73	0.61
<i>CYP19A1</i>	93.09	109.07	0.23	0.58
<i>HSD3B1</i>	70.34	23.32	-1.59	0.43
<i>HSD17B2</i>	N/A	N/A	N/A	N/A
<i>STAR</i>	5994.15	5215.43	-0.20	0.77
<b>Cell viability</b>				
<i>BAK1</i>	72.99	19.46	-1.91	0.55
<i>BAX</i>	13.99	7.46	-0.91	0.90
<i>BCL2</i>	7.43	51.69	2.80	0.27
<i>BCL2L12</i>	12.53	26.06	1.06	0.69
<i>CASP1</i>	0.19	3.29	4.11	0.20
<i>CASP2</i>	208.02	214.61	0.05	0.85
<i>CASP4</i>	1.03	0.79	-0.39	1
<i>CASP6</i>	5981.83	4554.50	-0.39	0.58
<i>CASP8</i>	375.89	510.36	0.44	0.56
<i>CCNB1</i>	21441.45	21334.06	-0.007	0.81
<i>CCNB2</i>	3081.50	2241.03	-0.46	0.55
<i>CCND1</i>	0.57	10.18	4.15	0.13
<i>CCND2</i>	1153.20	754.79	-0.61	0.60
<i>FADD</i>	681.57	486.79	-0.49	0.92

<sup>1</sup>Base mean values determined by RNAseq read number.

**Supplemental Table 18.** Expression of target genes of interest in the oocytes of control and bacteria-infused animals

	Control (Base mean)	Infected (Base mean)	Log <sub>2</sub> fold change	P value
<b>Inflammation</b>				
<i>IL1A</i>	8.66	12.61	0.54	0.63
<i>IL1B</i>	0.66	1.78	1.42	0.60
<i>IL6</i>				
<i>IL6R</i>	94.06	179.33	0.93	0.30
<i>IL10</i>	35.87	57.91	0.69	0.45
<i>IL12</i>				
<i>IL18</i>	33.08	61.14	0.89	0.52
<i>CARD9</i>	0.69	1.74	1.38	0.54
<i>MHC I</i>	45.57	264.81	2.60	0.004
<i>MHC II</i>	13.02	185.70	3.83	0.11
<i>HIF1A</i>	7696.87	17045.89	1.15	0.09
<b>Steroid synthesis</b>				
<i>CYP11A1</i>	1205.14	4107.34	1.77	0.02
<i>CYP19A1</i>	9.86	225.56	4.52	0.000009
<i>HSD3B1</i>	61.38	301.56	2.30	0.005
<i>STAR</i>	13048.44	13469.61	0.05	0.80
<b>Cell viability</b>				
<i>BAK1</i>	32.11	34.46	0.10	0.81
<i>BAX</i>	20.95	28.32	0.43	0.63
<i>BCL2</i>	3.64	1.16	-1.65	0.75
<i>BCL2L12</i>	57.89	37.92	-0.61	0.58
<i>CASP1</i>	1.26	3.49	1.47	0.52
<i>CASP2</i>	933.64	812.52	-0.20	0.64
<i>CASP4</i>	1.51	0.76	-1.00	0.93
<i>CASP6</i>	14386.85	19528.19	0.44	0.13
<i>CASP8</i>	11.19	14.22	0.34	0.82
<i>CCNB1</i>	81242.97	90242.75	0.15	0.66
<i>CCNB2</i>	11826.77	11620.33	-0.03	1
<i>CCND1</i>	6.97	0.58	-3.59	0.26
<i>CCND2</i>	991.67	4138.71	2.06	0.0004
<i>FADD</i>	1190.27	829.01	-0.52	0.30

## 9 References

- Abdulrahman Alrabiah, N., Evans, A. C. O., Fahey, A. G., Cantwell, N., Lonergan, P., McCormack, J., Browne, J. A. & Fair, T. 2021. Immunological aspects of ovarian follicle ovulation and corpus luteum formation in cattle. *Reproduction*, 162, 209-225. (<https://doi.org/10.1530/rep-21-0165>)
- Acton, S., Rigotti, A., Landschulz, K. T., Xu, S., Hobbs, H. H. & Krieger, M. 1996. Identification of scavenger receptor SR-BI as a high density lipoprotein receptor. *Science*, 271, 518-520. (<https://doi.org/10.1126/science.271.5248.518>)
- Adams, G. P. 1999. Comparative patterns of follicle development and selection in ruminants. *Journal of Reproduction and Fertility Supplement*, 54, 17-32. (<https://doi.org/10.1530/BIOSCIPROCS.4.002>)
- Adhikari, D., Flohr, G., Gorre, N., Shen, Y., Yang, H., Lundin, E., Lan, Z., Gambello, M. J. & Liu, K. 2009. Disruption of Tsc2 in oocytes leads to overactivation of the entire pool of primordial follicles. *Molecular and Human Reproduction*, 15, 765-770. (<https://doi.org/10.1093/molehr/gap092>)
- Adhikari, D., Zheng, W., Shen, Y., Gorre, N., Hamalainen, T., Cooney, A. J., Huhtaniemi, I., Lan, Z. J. & Liu, K. 2010. Tsc/mTORC1 signaling in oocytes governs the quiescence and activation of primordial follicles. *Human Molecular Genetics*, 19, 397-410. (<https://doi.org/10.1093/hmg/ddp483>)
- Akira, S. & Hemmi, H. 2003. Recognition of pathogen-associated molecular patterns by TLR family. *Immunology Letters*, 85, 85-95. ([https://doi.org/10.1016/S0165-2478\(02\)00228-6](https://doi.org/10.1016/S0165-2478(02)00228-6))
- Akira, S., Takeda, K. & Kaisho, T. 2001. Toll-like receptors: critical proteins linking innate and acquired immunity. *Nature Immunology*, 2, 675-680. (<https://doi.org/10.1038/90609>)
- Akira, S., Uematsu, S. & Takeuchi, O. 2006. Pathogen Recognition and Innate Immunity. *Cell*, 124, 783-801. (<https://doi.org/10.1016/j.cell.2006.02.015>)
- Akula, M. K., Shi, M., Jiang, Z., Foster, C. E., Miao, D., Li, A. S., Zhang, X., Gavin, R. M., Forde, S. D., Germain, G., Carpenter, S., Rosadini, C. V., Gritsman, K., Chae, J. J., Hampton, R., Silverman, N., Gravallesse, E. M., Kagan, J. C., Fitzgerald, K. A., Kastner, D. L., Golenbock, D. T., Bergo, M. O. & Wang, D. 2016. Control of the innate immune response by the mevalonate pathway. *Nature Immunology*, 17, 922-929. (<https://doi.org/10.1038/ni.3487>)
- Alam, H., Maizels, E. T., Park, Y., Ghaey, S., Feiger, Z. J., Chandel, N. S. & Hunzicker-Dunn, M. 2004. Follicle-stimulating hormone activation of hypoxia-inducible factor-1 by the phosphatidylinositol 3-kinase/AKT/Ras homolog enriched in brain (Rheb)/mammalian target of rapamycin (mTOR) pathway is necessary for induction of select protein markers of follicular differentiation. *Journal of Biological Chemistry*, 279, 19431-19440. (<https://doi.org/10.1074/jbc.M401235200>)

- Alarcon, V. B. & Marikawa, Y. 2016. Statins inhibit blastocyst formation by preventing geranylgeranylation. *Molecular Human Reproduction*, 22, 350-363. (<https://doi.org/10.1093/molehr/gaw011>)
- Albertini, D. F., Combelles, C. M., Benecchi, E. & Carabatsos, M. J. 2001. Cellular basis for paracrine regulation of ovarian follicle development. *Reproduction*, 121, 647-653. (<https://doi.org/10.1530/rep.0.1210647>)
- Alvarez, G. M., Barrios Exposito, M. J., Elia, E., Paz, D., Morado, S. & Cetica, P. D. 2019. Effects of gonadotrophins and insulin on glucose uptake in the porcine cumulus-oocyte complex during IVM. *Reproduction, Fertility and Development*, 1353-1359. (<https://doi.org/10.1071/RD18321>)
- Alves, B. G., Alves, K. A., Martins, M. C., Braga, L. S., Silva, T. H., Alves, B. G., Santos, R. M., Silva, T. V., Viu, M. A., Beletti, M. E., Jacomini, J. O. & Gambarini, M. L. 2014. Metabolic profile of serum and follicular fluid from postpartum dairy cows during summer and winter. *Reproduction, Fertility and Development*, 26, 866-874. (<https://doi.org/10.1071/RD13102>)
- Amos, M. R., Healey, G. D., Goldstone, R. J., Mahan, S. M., Duvel, A., Schuberth, H. J., Sandra, O., Zieger, P., Dieuzy-Labayé, I., Smith, D. G. & Sheldon, I. M. 2014. Differential endometrial cell sensitivity to a cholesterol-dependent cytolysin links *Trueperella pyogenes* to uterine disease in cattle. *Biology of Reproduction*, 90, 1-13. (<https://doi.org/10.1095/biolreprod.113.115972>)
- Amsterdam, A., Koch, Y., Lieberman, M. E. & Lindner, H. R. 1975. Distribution of binding sites for human chorionic gonadotropin in the preovulatory follicle of the rat. *Journal of Cell Biology*, 67, 894-900. (<https://doi.org/10.1083/jcb.67.3.894>)
- Amstislavsky, S., Mokrousova, V., Brusentsev, E., Okotrub, K. & Comizzoli, P. 2019. Influence of Cellular Lipids on Cryopreservation of Mammalian Oocytes and Preimplantation Embryos: A Review. *Biopreservation and Biobanking*, 17, 76-83. (<https://doi.org/10.1089/bio.2018.0039>)
- Arai, M., Yoshioka, S., Tasaki, Y. & Okuda, K. 2013. Remodeling of bovine endometrium throughout the estrous cycle. *Animal Reproduction Science*, 142, 1-9. (<https://doi.org/10.1016/j.anireprosci.2013.08.003>)
- Argov, N., Moallem, U. & Sklan, D. 2004. Lipid transport in the developing bovine follicle: messenger RNA expression increases for selective uptake receptors and decreases for endocytosis receptors. *Biology of Reproduction*, 71, 479-485. (<https://doi.org/10.1095/biolreprod.104.028092>)
- Argov, N., Moallem, U. & Sklan, D. 2005. Summer heat stress alters the mRNA expression of selective-uptake and endocytotic receptors in bovine ovarian cells. *Theriogenology*, 64, 1475-1489. (<https://doi.org/10.1016/j.theriogenology.2005.02.014>)
- Assidi, M., Dieleman, S. J. & Sirard, M. A. 2010. Cumulus cell gene expression following the LH surge in bovine preovulatory follicles: potential early markers of oocyte competence. *Reproduction*, 140, 835-852. (<https://doi.org/10.1530/REP-10-0248>)

Ayres, H., Ferreira, R. M., De Souza Torres-Júnior, J. R., Demétrio, C. G. B., De Lima, C. G. & Baruselli, P. S. 2009. Validation of body condition score as a predictor of subcutaneous fat in Nelore (*Bos indicus*) cows. *Livestock Science*, 123, 175-179. (<https://doi.org/10.1016/j.livsci.2008.11.004>)

Azhar, S., Nomoto, A., Leers-Sucheta, S. & Reaven, E. 1998a. Simultaneous induction of an HDL receptor protein (SR-BI) and the selective uptake of HDL-cholesteryl esters in a physiologically relevant steroidogenic cell model. *Journal of Lipid Research*, 39, 1616-1628. ([https://doi.org/10.1016/S0022-2275\(20\)32191-X](https://doi.org/10.1016/S0022-2275(20)32191-X))

Azhar, S., Tsai, L., Medicherla, S., Chandrasekher, Y., Giudice, L. & Reaven, E. 1998b. Human granulosa cells use high density lipoprotein cholesterol for steroidogenesis. *The Journal of Clinical Endocrinology and Metabolism*, 83, 983-991. (<https://doi.org/10.1210/jcem.83.3.4662>)

Azzam, K. M. & Fessler, M. B. 2012. Crosstalk between reverse cholesterol transport and innate immunity. *Trends in Endocrinology & Metabolism*, 23, 169-178. (<https://doi.org/10.1016/j.tem.2012.02.001>)

Babicki, S., Arndt, D., Marcu, A., Liang, Y., Grant, J. R., Maciejewski, A. & Wishart, D. S. 2016. Heatmapper: web-enabled heat mapping for all. *Nucleic acids research*, 44, W147-153. (<https://doi.org/10.1093/nar/gkw419>)

Bahrami, M., Morris, M. B. & Day, M. L. 2019. Amino acid supplementation of a simple inorganic salt solution supports efficient in vitro maturation (IVM) of bovine oocytes. *Scientific Reports*, 9, 1-10. (<https://doi.org/10.1038/s41598-019-48038-y>)

Bao, B., Garverick, H. A., Smith, G. W., Smith, M. F., Salfen, B. E. & Youngquist, R. S. 1997a. Changes in messenger ribonucleic acid encoding luteinizing hormone receptor, cytochrome P450-side chain cleavage, and aromatase are associated with recruitment and selection of bovine ovarian follicles. *Biology of Reproduction*, 56, 1158-1168. (<https://doi.org/10.1095/biolreprod56.5.1158>)

Bao, B., Thomas, M. G., Griffith, M. K., Burghardt, R. C. & Williams, G. L. 1995. Steroidogenic activity, insulin-like growth factor-I production, and proliferation of granulosa and theca cells obtained from dominant preovulatory and nonovulatory follicles during the bovine estrous cycle: effects of low-density and high-density lipoproteins. *Biology of Reproduction*, 53, 1271-1279. (<https://doi.org/10.1095/biolreprod53.6.1271>)

Bao, B., Thomas, M. G. & Williams, G. L. 1997b. Regulatory roles of high-density and low-density lipoproteins in cellular proliferation and secretion of progesterone and insulin-like growth factor I by enriched cultures of bovine small and large luteal cells. *Journal of Animal Science*, 75, 3235-3245. (<https://doi.org/10.2527/1997.75123235x>)

Baranova, I. N., Souza, A. C. P., Bocharov, A. V., Vishnyakova, T. G., Hu, X., Vaisman, B. L., Amar, M. J., Chen, Z., Kost, Y., Remaley, A. T., Patterson, A. P., Yuen, P. S. T., Star, R. A. & Eggerman, T. L. 2016. Human SR-BI and SR-BII Potentiate Lipopolysaccharide-Induced Inflammation and Acute Liver and Kidney Injury in Mice. *Journal of immunology (Baltimore, Md. : 1950)*, 196, 3135-3147. (<https://doi.org/10.4049/jimmunol.1501709>)

- Baranova, I. N., Vishnyakova, T. G., Bocharov, A. V., Leelahavanichkul, A., Kurlander, R., Chen, Z., Souza, A. C. P., Yuen, P. S. T., Star, R. A., Csako, G., Patterson, A. P. & Eggerman, T. L. 2012. Class B scavenger receptor types I and II and CD36 mediate bacterial recognition and proinflammatory signaling induced by *Escherichia coli*, lipopolysaccharide, and cytosolic chaperonin 60. *Journal of immunology (Baltimore, Md. : 1950)*, 188, 1371-1380. (<https://doi.org/10.4049/jimmunol.1100350>)
- Baratta, M., Basini, G., Bussolati, S. & Tamanini, C. 1996. Effects of interleukin-1 $\beta$  fragment (163–171) on progesterone and estradiol-17 $\beta$  release by bovine granulosa cells from different size follicles. *Regulatory Peptides*, 67, 187-194. ([https://doi.org/10.1016/S0167-0115\(96\)00123-1](https://doi.org/10.1016/S0167-0115(96)00123-1))
- Bardou, P., Mariette, J., Escudie, F., Djemiel, C. & Klopp, C. 2014. jvenn: an interactive Venn diagram viewer. *BMC Bioinformatics*, 15, 1-7. (<https://doi.org/10.1186/1471-2105-15-293>)
- Batetta, B. & Sanna, F. 2006. Cholesterol metabolism during cell growth: Which role for the plasma membrane? *European journal of lipid science and technology*, 108, 687-699. (<https://doi.org/10.1002/ejlt.200600015>)
- Bauman, D. E. & Currie, W. B. 1980. Partitioning of nutrients during pregnancy and lactation: a review of mechanisms involving homeostasis and homeorhesis. *Journal of Dairy Science*, 63, 1514-1529. ([https://doi.org/10.3168/jds.s0022-0302\(80\)83111-0](https://doi.org/10.3168/jds.s0022-0302(80)83111-0))
- Beam, S. W. & Butler, W. R. 1997. Energy balance and ovarian follicle development prior to the first ovulation postpartum in dairy cows receiving three levels of dietary fat. *Biology of Reproduction*, 56, 133-142. (<https://doi.org/10.1095/biolreprod56.1.133>)
- Beam, S. W. & Butler, W. R. 1999. Effects of energy balance on follicular development and first ovulation in postpartum dairy cows. *Journal of Reproduction and Fertility Supplement*, 54, 411-424.
- Beever, D. E., Hattan, A., Reynolds, C. K. & Cammell, S. B. 2001. Nutrient supply to high-yielding dairy cows. *BSAP Occasional Publication*, 26, 119-131. (<https://doi.org/10.1017/S0263967X00033632>)
- Beg, M. A., Bergfelt, D. R., Kot, K., Wiltbank, M. C. & Ginther, O. J. 2001. Follicular-Fluid Factors and Granulosa-Cell Gene Expression Associated with Follicle Deviation in Cattle. *Biology of Reproduction*, 64, 432-441. (<https://doi.org/10.1095/biolreprod64.2.432>)
- Bell, A. W. & Bauman, D. E. 1997. Adaptations of Glucose Metabolism During Pregnancy and Lactation. *Journal of Mammary Gland Biology and Neoplasia*, 2, 265-278. (<https://doi.org/10.1023/A:1026336505343>)
- Ben-Sahra, I. & Manning, B. D. 2017. mTORC1 signaling and the metabolic control of cell growth. *Current Opinion in Cell Biology*, 45, 72-82. (<https://doi.org/10.1016/j.ceb.2017.02.012>)

Bertavello, P. S., Teixeira-Gomes, A. P., Seyer, A., Vitorino Carvalho, A., Labas, V., Blache, M. C., Banliat, C., Cordeiro, L. a. V., Duranthon, V., Papillier, P., Maillard, V., Elis, S. & Uzbekova, S. 2018. Lipid Identification and Transcriptional Analysis of Controlling Enzymes in Bovine Ovarian Follicle. *International Journal of Molecular Sciences*, 19, 1-31. (<https://doi.org/10.3390/ijms19103261>)

Bertoldo, M. J., Faure, M., Dupont, J. & Froment, P. 2015. AMPK: a master energy regulator for gonadal function. *Frontiers in Neuroscience*, 9, 235. (<https://doi.org/10.3389/fnins.2015.00235>)

Bhattacharyya, S., Brown, D. E., Brewer, J. A., Vogt, S. K. & Muglia, L. J. 2007. Macrophage glucocorticoid receptors regulate Toll-like receptor 4-mediated inflammatory responses by selective inhibition of p38 MAP kinase. *Blood*, 109, 4313-4319. (<https://doi.org/10.1182/blood-2006-10-048215>)

Bicalho, R. C., Machado, V. S., Bicalho, M. L., Gilbert, R. O., Teixeira, A. G., Caixeta, L. S. & Pereira, R. V. 2010. Molecular and epidemiological characterization of bovine intrauterine *Escherichia coli*. *Journal of Dairy Science*, 93, 5818-5830. (<https://doi.org/10.3168/jds.2010-3550>)

Bidne, K. L., Dickson, M. J., Ross, J. W., Baumgard, L. H. & Keating, A. F. 2018. Disruption of female reproductive function by endotoxins. *Reproduction*, 155, R169-R181. (<https://doi.org/10.1530/REP-17-0406>)

Biggers, J. D., Whittingham, D. G. & Donahue, R. P. 1967. The pattern of energy metabolism in the mouse oocyte and zygote. *Proceedings of the National Academy of Sciences of the United States of America*, 58, 560-567. (<https://doi.org/10.1073/pnas.58.2.560>)

Bilodeau-Goeseels, S., Sasseville, M., Guillemette, C. & Richard, F. J. 2007. Effects of adenosine monophosphate-activated kinase activators on bovine oocyte nuclear maturation in vitro. *Molecular Reproduction and Development*, 74, 1021-1034. (<https://doi.org/10.1002/mrd.20574>)

Bloch, K. 1965. The Biological Synthesis of Cholesterol. *Science*, 150, 19-28. (<https://doi.org/10.1126/science.150.3692.19>)

Bobé, J., Montfort, J., Nguyen, T. & Fostier, A. 2006. Identification of new participants in the rainbow trout (*Oncorhynchus mykiss*) oocyte maturation and ovulation processes using cDNA microarrays. *Reproductive Biology and Endocrinology*, 4, 39. (<https://doi.org/10.1186/1477-7827-4-39>)

Bocharov, A. V., Baranova, I. N., Vishnyakova, T. G., Remaley, A. T., Csako, G., Thomas, F., Patterson, A. P. & Eggerman, T. L. 2004. Targeting of scavenger receptor class B type I by synthetic amphipathic alpha-helical-containing peptides blocks lipopolysaccharide (LPS) uptake and LPS-induced pro-inflammatory cytokine responses in THP-1 monocyte cells. *Journal of Biological Chemistry*, 279, 36072-36082. (<https://doi.org/10.1074/jbc.M314264200>)

Bogado Pascottini, O. & Leblanc, S. J. 2020. Metabolic markers for purulent vaginal discharge and subclinical endometritis in dairy cows. *Theriogenology*, 155, 43-48. (<https://doi.org/10.1016/j.theriogenology.2020.06.005>)

Bonnett, B. N., Martin, S. W., Gannon, V. P., Miller, R. B. & Etherington, W. G. 1991. Endometrial biopsy in Holstein-Friesian dairy cows. III. Bacteriological analysis and correlations with histological findings. *Canadian Journal of Veterinary Research*, 55, 168-173.

Borges, A. M., Healey, G. D. & Sheldon, I. M. 2012. Explants of intact endometrium to model bovine innate immunity and inflammation ex vivo. *American Journal of Reproductive Immunology*, 67, 526-539. (<https://doi.org/10.1111/j.1600-0897.2012.01106.x>)

Borsberry, S. & Dobson, H. 1989. Periparturient diseases and their effect on reproductive performance in five dairy herds. *Veterinary Record*, 124, 217-219. (<https://doi.org/10.1136/vr.124.9.217>)

Brännström, M., Wang, L. & Norman, R. J. 1993. Ovulatory effect of interleukin-1 beta on the perfused rat ovary. *Endocrinology*, 132, 399-404. (<https://doi.org/10.1210/endo.132.1.8419137>)

Brantmeier, S. A., Grummer, R. R. & Ax, R. L. 1987. Concentrations of high density lipoproteins vary among follicular sizes in the bovine. *Journal of Dairy Science*, 70, 2145-2149. ([https://doi.org/10.3168/jds.S0022-0302\(87\)80266-7](https://doi.org/10.3168/jds.S0022-0302(87)80266-7))

Braw-Tal, R. & Yossefi, S. 1997. Studies in vivo and in vitro on the initiation of follicle growth in the bovine ovary. *Journal of Reproduction and Fertility*, 109, 165-171. (<https://doi.org/10.1530/jrf.0.1090165>)

Britt, J. H. 1992. Impacts of early postpartum metabolism on follicular development and fertility. *Bovine Practitioners*, 24, 39-43. (<https://doi.org/10.21423/aabppro19916706>)

Britt, J. H., Cushman, R. A., Dechow, C. D., Dobson, H., Humblot, P., Hutjens, M. F., Jones, G. A., Mitloehner, F. M., Ruegg, P. L., Sheldon, I. M. & Stevenson, J. S. 2021. Review: Perspective on high-performing dairy cows and herds. *Animal*, 100298. (<https://doi.org/10.1016/j.animal.2021.100298>)

Britt, J. H., Cushman, R. A., Dechow, C. D., Dobson, H., Humblot, P., Hutjens, M. F., Jones, G. A., Ruegg, P. S., Sheldon, I. M. & Stevenson, J. S. 2018. Invited review: Learning from the future-A vision for dairy farms and cows in 2067. *Journal of Dairy Science*, 101, 3722-3741. (<https://doi.org/10.3168/jds.2017-14025>)

Bromfield, J. J., Santos, J. E., Block, J., Williams, R. S. & Sheldon, I. M. 2015. PHYSIOLOGY AND ENDOCRINOLOGY SYMPOSIUM: Uterine infection: linking infection and innate immunity with infertility in the high-producing dairy cow. *Journal of Animal Science*, 93, 2021-2033. (<https://doi.org/10.2527/jas.2014-8496>)

Bromfield, J. J. & Sheldon, I. M. 2011. Lipopolysaccharide initiates inflammation in bovine granulosa cells via the TLR4 pathway and perturbs oocyte meiotic progression in vitro. *Endocrinology*, 152, 5029-5040. (<https://doi.org/10.1210/en.2011-1124>)

Bromfield, J. J. & Sheldon, I. M. 2013. Lipopolysaccharide reduces the primordial follicle pool in the bovine ovarian cortex ex vivo and in the murine ovary in vivo. *Biology of Reproduction*, 88, 1-9. (<https://doi.org/10.1095/biolreprod.112.106914>)



Brown, M. S. & Goldstein, J. L. 1976. Receptor-mediated control of cholesterol metabolism. *Science*, 191, 150-154. (<https://doi.org/10.1126/science.174194>)

Brown, M. S. & Goldstein, J. L. 1997. The SREBP pathway: regulation of cholesterol metabolism by proteolysis of a membrane-bound transcription factor. *Cell*, 89, 331-340. ([https://doi.org/10.1016/s0092-8674\(00\)80213-5](https://doi.org/10.1016/s0092-8674(00)80213-5))

Buggert, M., Tauriainen, J., Yamamoto, T., Frederiksen, J., Ivarsson, M. A., Michaelsson, J., Lund, O., Hejdeman, B., Jansson, M., Sonnerborg, A., Koup, R. A., Betts, M. R. & Karlsson, A. C. 2014. T-bet and Eomes are differentially linked to the exhausted phenotype of CD8<sup>+</sup> T cells in HIV infection. *PLoS Pathogens*, 10, e1004251. (<https://doi.org/10.1371/journal.ppat.1004251>)

Butler, W. R. 2000. Nutritional interactions with reproductive performance in dairy cattle. *Animal Reproduction Science*, 60-61, 449-457. ([https://doi.org/10.1016/s0378-4320\(00\)00076-2](https://doi.org/10.1016/s0378-4320(00)00076-2))

Butler, W. R. 2001. Nutritional effects on resumption of ovarian cyclicity and conception rate in postpartum dairy cows. *BSAP Occasional Publication*, 26, 133-145. (<https://doi.org/10.1017/S0263967X00033644>)

Butler, W. R. 2003. Energy balance relationships with follicular development, ovulation and fertility in postpartum dairy cows. *Livestock Production Science*, 83, 211-218. ([https://doi.org/10.1016/s0301-6226\(03\)00112-x](https://doi.org/10.1016/s0301-6226(03)00112-x))

Butler, W. R., Everett, R. W. & Coppock, C. E. 1981. The relationships between energy balance, milk production and ovulation in postpartum Holstein cows. *Journal of Animal Science*, 53, 742-748. (<https://doi.org/10.2527/jas1981.533742x>)

Butler, W. R. & Smith, R. D. 1989. Interrelationships between energy balance and postpartum reproductive function in dairy cattle. *Journal of Dairy Science*, 72, 767-783. ([https://doi.org/10.3168/jds.S0022-0302\(89\)79169-4](https://doi.org/10.3168/jds.S0022-0302(89)79169-4))

Cai, L., Ji, A., De Beer, F. C., Tannock, L. R. & Van Der Westhuyzen, D. R. 2008. SR-BI protects against endotoxemia in mice through its roles in glucocorticoid production and hepatic clearance. *The Journal of Clinical Investigation*, 118, 364-375. (<https://doi.org/10.1172/JCI31539>)

Cai, L., Wang, Z., Meyer, J. M., Ji, A. & Van Der Westhuyzen, D. R. 2012. Macrophage SR-BI regulates LPS-induced pro-inflammatory signaling in mice and isolated macrophages. *Journal of Lipid Research*, 53, 1472-1481. (<https://doi.org/10.1194/jlr.M023234>)

Calder, M. D., Caveney, A. N., Smith, L. C. & Watson, A. J. 2003. Responsiveness of bovine cumulus-oocyte-complexes (COC) to porcine and recombinant human FSH, and the effect of COC quality on gonadotropin receptor and Cx43 marker gene mRNAs during maturation in vitro. *Reproductive biology and endocrinology*, 1, 14. (<https://doi.org/10.1186/1477-7827-1-14>)

Canfield, R. W. & Butler, W. R. 1990. Energy balance and pulsatile LH secretion in early postpartum dairy cattle. *Domestic Animal Endocrinology*, 7, 323-330. ([https://doi.org/10.1016/0739-7240\(90\)90038-2](https://doi.org/10.1016/0739-7240(90)90038-2))

Caon, I., Parnigoni, A., Viola, M., Karousou, E., Passi, A. & Vigetti, D. 2021. Cell Energy Metabolism and Hyaluronan Synthesis. *Journal of Histochemistry and Cytochemistry*, 69, 35-47. (<https://doi.org/10.1369/0022155420929772>)

Carneiro, L. C., Ferreira, A. F., Padua, M., Saut, J. P., Ferraudo, A. S. & Dos Santos, R. M. 2014. Incidence of subclinical endometritis and its effects on reproductive performance of crossbred dairy cows. *Tropical Animal Health and Production*, 46, 1435-1439. (<https://doi.org/10.1007/s11250-014-0661-y>)

Carroll, D. J., Grummer, R. R. & Mao, F. C. 1992. Progesterone production by cultured luteal cells in the presence of bovine low- and high-density lipoproteins purified by heparin affinity chromatography. *Journal of Animal Science*, 70, 2516-2526. (<https://doi.org/10.2527/1992.7082516x>)

Carvalho, P. D., Souza, A. H., Amundson, M. C., Hackbart, K. S., Fuenzalida, M. J., Herlihy, M. M., Ayres, H., Dresch, A. R., Vieira, L. M., Guenther, J. N., Grummer, R. R., Fricke, P. M., Shaver, R. D. & Wiltbank, M. C. 2014. Relationships between fertility and postpartum changes in body condition and body weight in lactating dairy cows. *Journal of Dairy Science*, 97, 3666-3683. (<https://doi.org/10.3168/jds.2013-7809>)

Catapano, A. L., Pirillo, A., Bonacina, F. & Norata, G. D. 2014. HDL in innate and adaptive immunity. *Cardiovascular Research*, 103, 372-383. (<https://doi.org/10.1093/cvr/cvu150>)

Cavestany, D., Blanc, J. E., Kulcsar, M., Uriarte, G., Chilibroste, P., Meikle, A., Febel, H., Ferraris, A. & Krall, E. 2005. Studies of the transition cow under a pasture-based milk production system: metabolic profiles. *Journal of Veterinary Medicine. A, Physiology, Pathology, Clinical Medicine*, 52, 1-7. (<https://doi.org/10.1111/j.1439-0442.2004.00679.x>)

Cerri, R. L., Thompson, I. M., Kim, I. H., Ealy, A. D., Hansen, P. J., Staples, C. R., Li, J. L., Santos, J. E. & Thatcher, W. W. 2012. Effects of lactation and pregnancy on gene expression of endometrium of Holstein cows at day 17 of the estrous cycle or pregnancy. *Journal of Dairy Science*, 95, 5657-5675. (<https://doi.org/10.3168/jds.2011-5114>)

Chagas, L. M., Bass, J. J., Blache, D., Burke, C. R., Kay, J. K., Lindsay, D. R., Lucy, M. C., Martin, G. B., Meier, S., Rhodes, F. M., Roche, J. R., Thatcher, W. W. & Webb, R. 2007. Invited review: New perspectives on the roles of nutrition and metabolic priorities in the subfertility of high-producing dairy cows. *Journal of Dairy Science*, 90, 4022-4032. (<https://doi.org/10.3168/jds.2006-852>)

Chang, S. C., Jones, J. D., Ellefson, R. D. & Ryan, R. J. 1976. The porcine ovarian follicle: I. Selected chemical analysis of follicular fluid at different developmental stages. *Biology of Reproduction*, 15, 321-328. (<https://doi.org/10.1095/biolreprod15.3.321>)

Chapwanya, A., Meade, K. G., Foley, C., Narcianti, F., Evans, A. C., Doherty, M. L., Callanan, J. J. & O'farrelly, C. 2012. The postpartum endometrial inflammatory response: a normal physiological event with potential implications for bovine fertility.

*Reproduction, Fertility and Development*, 24, 1028-1039. (<https://doi.org/10.1071/RD11153>)

Chen, H. W. 1984. Role of cholesterol metabolism in cell growth. *Federation Proceedings*, 43, 126-130.

Chen, J., Hudson, E., Chi, M. M., Chang, A. S., Moley, K. H., Hardie, D. G. & Downs, S. M. 2006. AMPK regulation of mouse oocyte meiotic resumption in vitro. *Developmental Biology*, 291, 227-238. (<https://doi.org/10.1016/j.ydbio.2005.11.039>)

Chen, L., Wert, S. E., Hendrix, E. M., Russell, P. T., Cannon, M. & Larsen, W. J. 1990. Hyaluronic acid synthesis and gap junction endocytosis are necessary for normal expansion of the cumulus mass. *Molecular Reproduction and Development*, 26, 236-247. (<https://doi.org/10.1002/mrd.1080260307>)

Chen, Z., Kang, X., Wang, L., Dong, H., Wang, C., Xiong, Z., Zhao, W., Jia, C., Lin, J., Zhang, W., Yuan, W., Zhong, M., Du, H. & Bai, X. 2015. Rictor/mTORC2 pathway in oocytes regulates folliculogenesis, and its inactivation causes premature ovarian failure. *Journal of Biological Chemistry*, 290, 6387-6396. (<https://doi.org/10.1074/jbc.M114.605261>)

Cheong, S. H., Sa Filho, O. G., Absalon-Medina, V. A., Pelton, S. H., Butler, W. R. & Gilbert, R. O. 2016. Metabolic and Endocrine Differences Between Dairy Cows That Do or Do Not Ovulate First Postpartum Dominant Follicles. *Biology of Reproduction*, 94, 1-11. (<https://doi.org/10.1095/biolreprod.114.127076>)

Cheong, S. H., Sa Filho, O. G., Absalon-Medina, V. A., Schneider, A., Butler, W. R. & Gilbert, R. O. 2017. Uterine and systemic inflammation influences ovarian follicular function in postpartum dairy cows. *PLoS One*, 12, e0177356. (<https://doi.org/10.1371/journal.pone.0177356>)

Christian, A. E., Haynes, M. P., Phillips, M. C. & Rothblat, G. H. 1997. Use of cyclodextrins for manipulating cellular cholesterol content. *Journal of Lipid Research*, 38, 2264-2272. ([https://doi.org/10.1016/S0022-2275\(20\)34940-3](https://doi.org/10.1016/S0022-2275(20)34940-3))

Clarke, P. R. & Hardie, D. G. 1990. Regulation of HMG-CoA reductase: identification of the site phosphorylated by the AMP-activated protein kinase in vitro and in intact rat liver. *EMBO Journal*, 9, 2439-2446. (<https://doi.org/10.1002/j.1460-2075.1990.tb07420.x>)

Coffey, M. P., Simm, G., Oldham, J. D., Hill, W. G. & Brotherstone, S. 2004. Genotype and diet effects on energy balance in the first three lactations of dairy cows. *Journal of Dairy Science*, 87, 4318-4326. ([https://doi.org/10.3168/jds.S0022-0302\(04\)73577-8](https://doi.org/10.3168/jds.S0022-0302(04)73577-8))

Cohen, J., Alikani, M., Trowbridge, J. & Rosenwaks, Z. 1992. Implantation enhancement by selective assisted hatching using zona drilling of human embryos with poor prognosis. *Human Reproduction*, 7, 685-691. (<https://doi.org/10.1093/oxfordjournals.humrep.a137720>)

- Combelles, C. M., Cekleniak, N. A., Racowsky, C. & Albertini, D. F. 2002. Assessment of nuclear and cytoplasmic maturation in in-vitro matured human oocytes. *Human Reproduction*, 17, 1006-1016. (<https://doi.org/10.1093/humrep/17.4.1006>)
- Comiskey, M. & Warner, C. M. 2007. Spatio-temporal localization of membrane lipid rafts in mouse oocytes and cleaving preimplantation embryos. *Developmental Biology*, 303, 727-739. (<https://doi.org/10.1016/j.ydbio.2006.12.009>)
- Connelly, M. A. & Williams, D. L. 2003. SR-BI and cholesterol uptake into steroidogenic cells. *Trends in Endocrinology & Metabolism*, 14, 467-472. (<https://doi.org/10.1016/j.tem.2003.10.002>)
- Conti, M., Andersen, C. B., Richard, F., Mehats, C., Chun, S. Y., Horner, K., Jin, C. & Tsafiri, A. 2002. Role of cyclic nucleotide signaling in oocyte maturation. *Molecular and Cellular Endocrinology*, 187, 153-159. ([https://doi.org/10.1016/s0303-7207\(01\)00686-4](https://doi.org/10.1016/s0303-7207(01)00686-4))
- Conti, M. & Franciosi, F. 2018. Acquisition of oocyte competence to develop as an embryo: integrated nuclear and cytoplasmic events. *Human reproduction update*, 24, 245-266. (<https://doi.org/10.1093/humupd/dmx040>)
- Corcoran, L. M., Hasbold, J., Dietrich, W., Hawkins, E., Kallies, A., Nutt, S. L., Tarlinton, D. M., Matthias, P. & Hodgkin, P. D. 2005. Differential requirement for OBF-1 during antibody-secreting cell differentiation. *Journal of Experimental Medicine*, 201, 1385-1396. (<https://doi.org/10.1084/jem.20042325>)
- Correia, B., Sousa, M. I. & Ramalho-Santos, J. 2020. The mTOR pathway in reproduction: from gonadal function to developmental coordination. *Reproduction*, 159, R173-R188. (<https://doi.org/10.1530/REP-19-0057>)
- Corton, J. M., Gillespie, J. G., Hawley, S. A. & Hardie, D. G. 1995. 5-aminoimidazole-4-carboxamide ribonucleoside. A specific method for activating AMP-activated protein kinase in intact cells? *European Journal of Biochemistry*, 229, 558-565. (<https://doi.org/10.1111/j.1432-1033.1995.tb20498.x>)
- Coussens, P. M. & Nobis, W. 2002. Bioinformatics and high throughput approach to create genomic resources for the study of bovine immunobiology. *Veterinary immunology and immunopathology*, 86, 229-244. ([https://doi.org/10.1016/s0165-2427\(02\)00005-3](https://doi.org/10.1016/s0165-2427(02)00005-3))
- Coward, W. R., Marei, A., Yang, A., Vasa-Nicotera, M. M. & Chow, S. C. 2006. Statin-induced proinflammatory response in mitogen-activated peripheral blood mononuclear cells through the activation of caspase-1 and IL-18 secretion in monocytes. *Journal of Immunology*, 176, 5284-5292. (<https://doi.org/10.4049/jimmunol.176.9.5284>)
- Cronin, J. G., Hodges, R., Pedersen, S. & Sheldon, I. M. 2015. Enzyme linked immunosorbent assay for quantification of bovine interleukin-8 to study infection and immunity in the female genital tract. *American Journal of Reproductive Immunology*, 73, 372-382. (<https://doi.org/10.1111/aji.12344>)

- Cronin, J. G., Turner, M. L., Goetze, L., Bryant, C. E. & Sheldon, I. M. 2012. Toll-like receptor 4 and MYD88-dependent signaling mechanisms of the innate immune system are essential for the response to lipopolysaccharide by epithelial and stromal cells of the bovine endometrium. *Biology of Reproduction*, 86, 1-9. (<https://doi.org/10.1095/biolreprod.111.092718>)
- Crowe, M. A., Kelly, P., Driancourt, M. A., Boland, M. P. & Roche, J. F. 2001. Effects of follicle-stimulating hormone with and without luteinizing hormone on serum hormone concentrations, follicle growth, and intrafollicular estradiol and aromatase activity in gonadotropin-releasing hormone-immunized heifers. *Biology of Reproduction*, 64, 368-374. (<https://doi.org/10.1095/biolreprod64.1.368>)
- Da Silva Correia, J., Soldau, K., Christen, U., Tobias, P. & Ulevitch, R. 2001. Lipopolysaccharide is in close proximity to each of the proteins in its membrane receptor complex transfer from CD14 to TLR4 and MD-2. *Journal of Biological Chemistry*, 276, 21129-21135. (<https://doi.org/10.1074/jbc.M009164200>)
- Das, A., Brown, M. S., Anderson, D. D., Goldstein, J. L. & Radhakrishnan, A. 2014. Three pools of plasma membrane cholesterol and their relation to cholesterol homeostasis. *Elife*, 3. (<https://doi.org/10.7554/eLife.02882>)
- Davies, D., Meade, K. G., Herath, S., Eckersall, P. D., Gonzalez, D., White, J. O., Conlan, R. S., O'farrelly, C. & Sheldon, I. M. 2008. Toll-like receptor and antimicrobial peptide expression in the bovine endometrium. *Reproductive biology and endocrinology*, 6, 53. (<https://doi.org/10.1186/1477-7827-6-53>)
- De Campos, F. T., Rincon, J. a. A., Acosta, D. a. V., Silveira, P. a. S., Pradiee, J., Correa, M. N., Gasperin, B. G., Pfeifer, L. F. M., Barros, C. C., Pegoraro, L. M. C. & Schneider, A. 2017. The acute effect of intravenous lipopolysaccharide injection on serum and intrafollicular HDL components and gene expression in granulosa cells of the bovine dominant follicle. *Theriogenology*, 89, 244-249. (<https://doi.org/10.1016/j.theriogenology.2016.11.013>)
- Di Paolo, N. C. & Shayakhmetov, D. M. 2016. Interleukin 1 $\alpha$  and the inflammatory process. *Nature Immunology*, 17, 906-913. (<https://doi.org/10.1038/ni.3503>)
- Dickson, M. J., Piersanti, R. L., Ramirez-Hernandez, R., De Oliveira, E. B., Bishop, J. V., Hansen, T. R., Ma, Z., Jeong, K. C. C., Santos, J. E. P., Sheldon, M. I., Block, J. & Bromfield, J. J. 2020. Experimentally Induced Endometritis Impairs the Developmental Capacity of Bovine Oocytes. *Biology of Reproduction*, 103, 508-520. (<https://doi.org/10.1093/biolre/iaaa069>)
- Dinareello, C. A. 2007. Historical insights into cytokines. *European Journal of Biochemistry*, 37 Suppl 1, S34-45. (<https://doi.org/10.1002/eji.200737772>)
- Donesky, B. W., De Moura, M. D., Tedeschi, C., Hurwitz, A., Adashi, E. Y. & Payne, D. W. 1998. Interleukin-1 $\beta$  Inhibits Steroidogenic Bioactivity in Cultured Rat Ovarian Granulosa Cells by Stimulation of Progesterone Degradation and Inhibition of Estrogen Formation. *Biology of Reproduction*, 58, 1108-1116. (<https://doi.org/10.1095/biolreprod58.5.1108>)

- Donnay, I., Faerge, I., Grondahl, C., Verhaeghe, B., Sayoud, H., Ponderato, N., Galli, C. & Lazzari, G. 2004. Effect of prematuration, meiosis activating sterol and enriched maturation medium on the nuclear maturation and competence to development of calf oocytes. *Theriogenology*, 62, 1093-1107. (<https://doi.org/10.1016/j.theriogenology.2003.12.019>)
- Dorrington, J. H., Moon, Y. S. & Armstrong, D. T. 1975. Estradiol-17 $\beta$  biosynthesis in cultured granulosa cells from hypophysectomized immature rats; stimulation by follicle-stimulating hormone. *Endocrinology*, 97, 1328-1331. (<https://doi.org/10.1210/endo-97-5-1328>)
- Dosogne, H., Meyer, E., Sturk, A., Van Loon, J., Massart-Leen, A. M. & Burvenich, C. 2002. Effect of enrofloxacin treatment on plasma endotoxin during bovine *Escherichia coli* mastitis. *Inflammation Research*, 51, 201-205. (<https://doi.org/10.1007/pl00000293>)
- Downs, S. M. 1989. Specificity of epidermal growth factor action on maturation of the murine oocyte and cumulus oophorus in vitro. *Biology of Reproduction*, 41, 371-379. (<https://doi.org/10.1095/biolreprod41.2.371>)
- Downs, S. M. 2011. Mouse versus rat: Profound differences in meiotic regulation at the level of the isolated oocyte. *Molecular Reproduction and Development*, 78, 778-794. (<https://doi.org/10.1002/mrd.21377>)
- Downs, S. M. & Chen, J. 2006. Induction of meiotic maturation in mouse oocytes by adenosine analogs. *Molecular Reproduction and Development*, 73, 1159-1168. (<https://doi.org/10.1002/mrd.20439>)
- Downs, S. M., Hudson, E. R. & Hardie, D. G. 2002. A potential role for AMP-activated protein kinase in meiotic induction in mouse oocytes. *Developmental Biology*, 245, 200-212. (<https://doi.org/10.1006/dbio.2002.0613>)
- Downs, S. M., Ruan, B. & Schroepfer, G. J., Jr. 2001. Meiosis-activating sterol and the maturation of isolated mouse oocytes. *Biology of Reproduction*, 64, 80-89. (<https://doi.org/10.1095/biolreprod64.1.80>)
- Dror, E., Dalmas, E., Meier, D. T., Wueest, S., Thevenet, J., Thienel, C., Timper, K., Nordmann, T. M., Traub, S., Schulze, F., Item, F., Vallois, D., Pattou, F., Kerr-Conte, J., Lavallard, V., Berney, T., Thorens, B., Konrad, D., Boni-Schnetzler, M. & Donath, M. Y. 2017. Postprandial macrophage-derived IL-1 $\beta$  stimulates insulin, and both synergistically promote glucose disposal and inflammation. *Nature Immunology*, 18, 283-292. (<https://doi.org/10.1038/ni.3659>)
- Drummond, A. E. 2006. The role of steroids in follicular growth. *Reproductive biology and endocrinology*, 4, 16. (<https://doi.org/10.1186/1477-7827-4-16>)
- Duan, X. & Sun, S. C. 2019. Actin cytoskeleton dynamics in mammalian oocyte meiosis. *Biology of Reproduction*, 100, 15-24. (<https://doi.org/10.1093/biolre/iy163>)
- Dubuc, J., Duffield, T. F., Leslie, K. E., Walton, J. S. & Leblanc, S. J. 2010. Risk factors for postpartum uterine diseases in dairy cows. *Journal of Dairy Science*, 93, 5764-5771. (<https://doi.org/10.3168/jds.2010-3429>)

- Duffy, D. M., Ko, C., Jo, M., Brannstrom, M. & Curry, T. E., Jr. 2018. Ovulation: Parallels With Inflammatory Processes. *Endocrine Reviews*, 40, 369-416. (<https://doi.org/10.1210/er.2018-00075>)
- Dufourny, L., Levasseur, A., Migaud, M., Callebaut, I., Pontarotti, P., Malpoux, B. & Monget, P. 2008. GPR50 is the mammalian ortholog of Mellc: evidence of rapid evolution in mammals. *BMC Evolutionary Biology*, 8, 105. (<https://doi.org/10.1186/1471-2148-8-105>)
- Dunning, K. R., Russell, D. L. & Robker, R. L. 2014. Lipids and oocyte developmental competence: the role of fatty acids and beta-oxidation. *Reproduction*, 148, 15-27. (<https://doi.org/10.1530/REP-13-0251>)
- Echternkamp, S. E., Spicer, L. J., Gregory, K. E., Canning, S. F. & Hammond, J. M. 1990. Concentrations of insulin-like growth factor-I in blood and ovarian follicular fluid of cattle selected for twins. *Biology of Reproduction*, 43, 8-14. (<https://doi.org/10.1095/biolreprod43.1.8>)
- Edwards, R. G. 1965. Maturation in vitro of mouse, sheep, cow, pig, rhesus monkey and human ovarian oocytes. *Nature*, 208, 349-351. (<https://doi.org/10.1038/208349a0>)
- Eppig, J. J. 1991. Intercommunication between mammalian oocytes and companion somatic cells. *Bioessays*, 13, 569-574. (<https://doi.org/10.1002/bies.950131105>)
- Eppig, J. J., Chesnel, F., Hirao, Y., O'brien, M. J., Pendola, F. L., Watanabe, S. & Wigglesworth, K. 1997. Oocyte control of granulosa cell development: how and why. *Human Reproduction*, 12, 127-132.
- Erickson, B. H. 1966. Development and senescence of the postnatal bovine ovary. *Journal of Animal Science*, 25, 800-805. (<https://doi.org/10.2527/jas1966.253800x>)
- Erickson, G. F., Casper, R. & Hofeditz, C. 1983. Role of serum-free defined medium in regulation of LH receptor in cultured rat granulosa cells. *Molecular and Cellular Endocrinology*, 30, 37-50. ([https://doi.org/10.1016/0303-7207\(83\)90199-5](https://doi.org/10.1016/0303-7207(83)90199-5))
- Espey, L. L. 1980. Ovulation as an inflammatory reaction--a hypothesis. *Biology of Reproduction*, 22, 73-106. (<https://doi.org/10.1095/biolreprod22.1.73>)
- Esposito, G., Irons, P. C., Webb, E. C. & Chapwanya, A. 2014. Interactions between negative energy balance, metabolic diseases, uterine health and immune response in transition dairy cows. *Animal Reproduction Science*, 144, 60-71. (<https://doi.org/10.1016/j.anireprosci.2013.11.007>)
- Faerge, I., Strejcek, F., Laurincik, J., Rath, D., Niemann, H., Schellander, K., Rosenkranz, C., Hyttel, P. M. & Grøndahl, C. 2006. The effect of FF-MAS on porcine cumulus-oocyte complex maturation, fertilization and pronucleus formation in vitro. *Zygote*, 14, 189-199. (<https://doi.org/10.1017/s0967199406003765>)
- Favier, L. A. & Schulert, G. S. 2016. Mevalonate kinase deficiency: current perspectives. *The application of clinical genetics*, 9, 101-110. (<https://doi.org/10.2147/TACG.S93933>)

- Feng, Y. M., Liang, G. J., Pan, B., Qin, X. S., Zhang, X. F., Chen, C. L., Li, L., Cheng, S. F., De Felici, M. & Shen, W. 2014. Notch pathway regulates female germ cell meiosis progression and early oogenesis events in fetal mouse. *Cell Cycle*, 13, 782-791. (<https://doi.org/10.4161/cc.27708>)
- Fenwick, M. A., Fitzpatrick, R., Kenny, D. A., Diskin, M. G., Patton, J., Murphy, J. J. & Wathes, D. C. 2008a. Interrelationships between negative energy balance (NEB) and IGF regulation in liver of lactating dairy cows. *Domestic Animal Endocrinology*, 34, 31-44. (<https://doi.org/10.1016/j.domaniend.2006.10.002>)
- Fenwick, M. A., Llewellyn, S., Fitzpatrick, R., Kenny, D. A., Murphy, J. J., Patton, J. & Wathes, D. C. 2008b. Negative energy balance in dairy cows is associated with specific changes in IGF-binding protein expression in the oviduct. *Reproduction*, 135, 63-75. (<https://doi.org/10.1530/REP-07-0243>)
- Ferguson, E. M. & Leese, H. J. 1999. Triglyceride content of bovine oocytes and early embryos. *Journal of Reproduction and Fertility*, 116, 373-378. (<https://doi.org/10.1530/jrf.0.1160373>)
- Ferguson, E. M. & Leese, H. J. 2006. A potential role for triglyceride as an energy source during bovine oocyte maturation and early embryo development. *Molecular Reproduction and Development*, 73, 1195-1201. (<https://doi.org/10.1002/mrd.20494>)
- Fernandez, C., Martin, M., Gomez-Coronado, D. & Lasuncion, M. A. 2005. Effects of distal cholesterol biosynthesis inhibitors on cell proliferation and cell cycle progression. *Journal of Lipid Research*, 46, 920-929. (<https://doi.org/10.1194/jlr.M400407-JLR200>)
- Ferreira, E. M., Vireque, A. A., Adona, P. R., Meirelles, F. V., Ferriani, R. A. & Navarro, P. A. 2009. Cytoplasmic maturation of bovine oocytes: structural and biochemical modifications and acquisition of developmental competence. *Theriogenology*, 71, 836-848. (<https://doi.org/10.1016/j.theriogenology.2008.10.023>)
- Fettelschoss, A., Kistowska, M., Leibundgut-Landmann, S., Beer, H. D., Johansen, P., Senti, G., Contassot, E., Bachmann, M. F., French, L. E., Oxenius, A. & Kundig, T. M. 2011. Inflammasome activation and IL-1beta target IL-1alpha for secretion as opposed to surface expression. *Proceedings of the National Academy of Sciences of the United States of America*, 108, 18055-18060. (<https://doi.org/10.1073/pnas.1109176108>)
- Fischer, C., Drillich, M., Odau, S., Heuwieser, W., Einspanier, R. & Gabler, C. 2010. Selected pro-inflammatory factor transcripts in bovine endometrial epithelial cells are regulated during the oestrous cycle and elevated in case of subclinical or clinical endometritis. *Reproduction, Fertility and Development*, 22, 818-829. (<https://doi.org/10.1071/RD09120>)
- Foley, C., Chapwanya, A., Callanan, J. J., Whiston, R., Miranda-Casoluengo, R., Lu, J., Meijer, W. G., Lynn, D. J., C, O. F. & Meade, K. G. 2015. Integrated analysis of the local and systemic changes preceding the development of post-partum cytological endometritis. *BMC Genomics*, 16, 811. (<https://doi.org/10.1186/s12864-015-1967-5>)



Foley, C., Chapwanya, A., Creevey, C. J., Narciandi, F., Morris, D., Kenny, E. M., Cormican, P., Callanan, J. J., O'farrelly, C. & Meade, K. G. 2012. Global endometrial transcriptomic profiling: transient immune activation precedes tissue proliferation and repair in healthy beef cows. *BMC Genomics*, 13, 489. (<https://doi.org/10.1186/1471-2164-13-489>)

Fortune, J. E. 1994. Ovarian follicular growth and development in mammals. *Biology of Reproduction*, 50, 225-232. (<https://doi.org/10.1095/biolreprod50.2.225>)

Fortune, J. E. 2003. The early stages of follicular development: activation of primordial follicles and growth of preantral follicles. *Animal Reproduction Science*, 78, 135-163. ([https://doi.org/10.1016/s0378-4320\(03\)00088-5](https://doi.org/10.1016/s0378-4320(03)00088-5))

Fortune, J. E. & Hansel, W. 1985. Concentrations of Steroids and Gonadotropins in Follicular Fluid from Normal Heifers and Heifers Primed for Superovulation1. *Biology of Reproduction*, 32, 1069-1079. (<https://doi.org/10.1095/biolreprod32.5.1069>)

Fortune, J. E., Rivera, G. M., Evans, A. C. & Turzillo, A. M. 2001. Differentiation of dominant versus subordinate follicles in cattle. *Biology of Reproduction*, 65, 648-654. (<https://doi.org/10.1095/biolreprod65.3.648>)

Franchi, L., Eigenbrod, T., Munoz-Planillo, R. & Nunez, G. 2009. The inflammasome: a caspase-1-activation platform that regulates immune responses and disease pathogenesis. *Nature Immunology*, 10, 241-247. (<https://doi.org/10.1038/ni.1703>)

Frenkel, J., Rijkers, G. T., Mandey, S. H. L., Buurman, S. W. M., Houten, S. M., Wanders, R. J. A., Waterham, H. R. & Kuis, W. 2002. Lack of isoprenoid products raises ex vivo interleukin-1 $\beta$  secretion in hyperimmunoglobulinemia D and periodic fever syndrome. *Arthritis & Rheumatism*, 46, 2794-2803. (<https://doi.org/10.1002/art.10550>)

Fu, H., Alabdullah, M., Großmann, J., Spieler, F., Abdosh, R., Lutz, V., Kalies, K., Knöpp, K., Rieckmann, M., Koch, S., Noutsias, M., Pilowski, C., Dutzmann, J., Sedding, D., Hüttelmaier, S., Umezawa, K., Werdan, K. & Loppnow, H. 2019. The differential statin effect on cytokine production of monocytes or macrophages is mediated by differential geranylgeranylation-dependent Rac1 activation. *Cell Death & Disease*, 10, 880. (<https://doi.org/10.1038/s41419-019-2109-9>)

Fulop, C., Szanto, S., Mukhopadhyay, D., Bardos, T., Kamath, R. V., Rugg, M. S., Day, A. J., Salustri, A., Hascall, V. C., Glant, T. T. & Mikecz, K. 2003. Impaired cumulus mucification and female sterility in tumor necrosis factor-induced protein-6 deficient mice. *Development*, 130, 2253-2561. (<https://doi.org/10.1242/dev.00422>)

Fung, T. K. & Poon, R. Y. 2005. A roller coaster ride with the mitotic cyclins. *Seminars in Cell and Developmental Biology*, 16, 335-342. (<https://doi.org/10.1016/j.semcdb.2005.02.014>)

Funsho Fagbohun, C. & Downs, S. M. 1990. Maturation of the Mouse Oocyte-Cumulus Cell Complex: Stimulation by Lectins. *Biology of Reproduction*, 42, 413-423. (<https://doi.org/10.1095/biolreprod42.3.413>)

- Gabler, C., Fischer, C., Drillich, M., Einspanier, R. & Heuwieser, W. 2010. Time-dependent mRNA expression of selected pro-inflammatory factors in the endometrium of primiparous cows postpartum. *Reproductive biology and endocrinology*, 8, 152. (<https://doi.org/10.1186/1477-7827-8-152>)
- Garcia, D. & Shaw, R. J. 2017. AMPK: Mechanisms of Cellular Energy Sensing and Restoration of Metabolic Balance. *Molecular cell*, 66, 789-800. (<https://doi.org/10.1016/j.molcel.2017.05.032>)
- Gautier, T., Becker, S., Drouineaud, V., Menetrier, F., Sagot, P., Nofer, J. R., Von Otte, S., Lagrost, L., Masson, D. & Tietge, U. J. 2010. Human luteinized granulosa cells secrete apoB100-containing lipoproteins. *Journal of Lipid Research*, 51, 2245-2252. (<https://doi.org/10.1194/jlr.M005181>)
- Gerard, N., Caillaud, M., Martoriati, A., Goudet, G. & Lalmanach, A. C. 2004. The interleukin-1 system and female reproduction. *Journal of Endocrinology*, 180, 203-212. (<https://doi.org/10.1677/joe.0.1800203>)
- Gilbert, R. O. 2019. Symposium review: Mechanisms of disruption of fertility by infectious diseases of the reproductive tract. *Journal of Dairy Science*, 102, 3754-3765. (<https://doi.org/10.3168/jds.2018-15602>)
- Gindri, P., De Avila Castro, N., Mion, B., Garziera Gasperin, B., Catarelli Pegoraro, L. M., Alveiro Alvarado Rincon, J., Diniz Vieira, A., Pradiee, J., Machado Pfeifer, L. F., Nunes Correa, M. & Schneider, A. 2019. Intrafollicular lipopolysaccharide injection delays ovulation in cows. *Animal Reproduction Science*, 211, 106226. (<https://doi.org/10.1016/j.anireprosci.2019.106226>)
- Ginther, O. J., Wiltbank, M. C., Fricke, P. M., Gibbons, J. R. & Kot, K. 1996. Selection of the dominant follicle in cattle. *Biology of Reproduction*, 55, 1187-1194. (<https://doi.org/10.1095/biolreprod55.6.1187>)
- Girard, A., Dufort, I. & Sirard, M. A. 2015. The effect of energy balance on the transcriptome of bovine granulosa cells at 60 days postpartum. *Theriogenology*, 84, 1350-1361 e1356. (<https://doi.org/10.1016/j.theriogenology.2015.07.015>)
- Glauert, A. M. & Thornley, M. J. 1969. The topography of the bacterial cell wall. *Annual Reviews Microbiology*, 23, 159-198. (<https://doi.org/10.1146/annurev.mi.23.100169.001111>)
- Gobel, A., Breining, D., Rauner, M., Hofbauer, L. C. & Rachner, T. D. 2019. Induction of 3-hydroxy-3-methylglutaryl-CoA reductase mediates statin resistance in breast cancer cells. *Cell Death and Disease*, 10, 91. (<https://doi.org/10.1038/s41419-019-1322-x>)
- Goff, J. P. 2006. Major advances in our understanding of nutritional influences on bovine health. *Journal of Dairy Science*, 89, 1292-1301. ([https://doi.org/10.3168/jds.S0022-0302\(06\)72197-X](https://doi.org/10.3168/jds.S0022-0302(06)72197-X))
- Goldstein, J. L. & Brown, M. S. 1990. Regulation of the mevalonate pathway. *Nature*, 343, 425-430. (<https://doi.org/10.1038/343425a0>)

- Goldstein, J. L., Debose-Boyd, R. A. & Brown, M. S. 2006. Protein sensors for membrane sterols. *Cell*, 124, 35-46. (<https://doi.org/10.1016/j.cell.2005.12.022>)
- Goldstone, R. J., Amos, M., Talbot, R., Schuberth, H. J., Sandra, O., Sheldon, I. M. & Smith, D. G. 2014a. Draft Genome Sequence of *Trueperella pyogenes*, Isolated from the Infected Uterus of a Postpartum Cow with Metritis. *Genome Announcements*, 2. (<https://doi.org/10.1128/genomeA.00194-14>)
- Goldstone, R. J., Talbot, R., Schuberth, H. J., Sandra, O., Sheldon, I. M. & Smith, D. G. 2014b. Draft Genome Sequence of *Escherichia coli* MS499, Isolated from the Infected Uterus of a Postpartum Cow with Metritis. *Genome Announcements*, 2. (<https://doi.org/10.1128/genomeA.00217-14>)
- Gong, J. G., Bramley, T. A., Gutierrez, C. G., Peters, A. R. & Webb, R. 1995. Effects of chronic treatment with a gonadotrophin-releasing hormone agonist on peripheral concentrations of FSH and LH, and ovarian function in heifers. *Journal of Reproduction and Fertility*, 105, 263-270. (<https://doi.org/10.1530/jrf.0.1050263>)
- Gong, J. G., Campbell, B. K., Bramley, T. A., Gutierrez, C. G., Peters, A. R. & Webb, R. 1996. Suppression in the Secretion of Follicle-Stimulating Hormone and Luteinizing Hormone, and Ovarian Follicle Development in Heifers Continuously Infused with a Gonadotropin-Releasing Hormone Agonist1. *Biology of Reproduction*, 55, 68-74. (<https://doi.org/10.1095/biolreprod55.1.68>)
- Gong, J. G., McBride, D., Bramley, T. A. & Webb, R. 1993. Effects of recombinant bovine somatotrophin, insulin-like growth factor-I and insulin on the proliferation of bovine granulosa cells in vitro. *Journal of Endocrinology*, 139, 67-75. (<https://doi.org/10.1677/joe.0.1390067>)
- Gonzalez, A., Hall, M. N., Lin, S. C. & Hardie, D. G. 2020. AMPK and TOR: The Yin and Yang of Cellular Nutrient Sensing and Growth Control. *Cell Metabolism*, 31, 472-492. (<https://doi.org/10.1016/j.cmet.2020.01.015>)
- Goto, J., Suganuma, N., Takata, K., Kitamura, K., Asahina, T., Kobayashi, H., Muranaka, Y., Furuhashi, M. & Kanayama, N. 2002. Morphological analyses of interleukin-8 effects on rat ovarian follicles at ovulation and luteinization in vivo. *Cytokine*, 20, 168-173. (<https://doi.org/10.1006/cyto.2002.1987>)
- Gowans, G. J., Hawley, S. A., Ross, F. A. & Hardie, D. G. 2013. AMP is a true physiological regulator of AMP-activated protein kinase by both allosteric activation and enhancing net phosphorylation. *Cell Metabolism*, 18, 556-566. (<https://doi.org/10.1016/j.cmet.2013.08.019>)
- Griffin, J. F., Hartigan, P. J. & Nunn, W. R. 1974. Non-specific uterine infection and bovine fertility. I. Infection patterns and endometritis during the first seven weeks post-partum. *Theriogenology*, 1, 91-106. ([https://doi.org/10.1016/0093-691x\(74\)90052-1](https://doi.org/10.1016/0093-691x(74)90052-1))
- Griffin, S., Healey, G. D. & Sheldon, I. M. 2018. Isoprenoids increase bovine endometrial stromal cell tolerance to the cholesterol-dependent cytolysin from *Trueperella pyogenes*. *Biology of Reproduction*, 99, 749-760. (<https://doi.org/10.1093/biolre/i0y099>)

- Griffin, S., Preta, G. & Sheldon, I. M. 2017. Inhibiting mevalonate pathway enzymes increases stromal cell resilience to a cholesterol-dependent cytolysin. *Scientific Reports*, 7, 17050. (<https://doi.org/10.1038/s41598-017-17138-y>)
- Groß, O., Yazdi, Amir s., Thomas, Christina j., Masin, M., Heinz, Leonhard x., Guarda, G., Quadroni, M., Drexler, Stefan k. & Tschopp, J. 2012. Inflammasome Activators Induce Interleukin-1 $\alpha$  Secretion via Distinct Pathways with Differential Requirement for the Protease Function of Caspase-1. *Immunity*, 36, 388-400. (<https://doi.org/10.1016/j.immuni.2012.01.018>)
- Guo, C., Chi, Z., Jiang, D., Xu, T., Yu, W., Wang, Z., Chen, S., Zhang, L., Liu, Q., Guo, X., Zhang, X., Li, W., Lu, L., Wu, Y., Song, B.-L. & Wang, D. 2018a. Cholesterol Homeostatic Regulator SCAP-SREBP2 Integrates NLRP3 Inflammasome Activation and Cholesterol Biosynthetic Signaling in Macrophages. *Immunity*, 49, 842-856.e847. (<https://doi.org/10.1016/j.immuni.2018.08.021>)
- Guo, J., Shi, L., Gong, X., Jiang, M., Yin, Y., Zhang, X., Yin, H., Li, H., Emori, C., Sugiura, K., Eppig, J. J. & Su, Y. Q. 2016. Oocyte-dependent activation of MTOR in cumulus cells controls the development and survival of cumulus-oocyte complexes. *Journal of Cell Science*, 129, 3091-3103. (<https://doi.org/10.1242/jcs.182642>)
- Guo, J., Zhang, T., Guo, Y., Sun, T., Li, H., Zhang, X., Yin, H., Cao, G., Yin, Y., Wang, H., Shi, L., Guo, X., Sha, J., Eppig, J. J. & Su, Y. Q. 2018b. Oocyte stage-specific effects of MTOR determine granulosa cell fate and oocyte quality in mice. *Proceedings of the National Academy of Sciences of the United States of America*, 115, E5326-E5333. (<https://doi.org/10.1073/pnas.1800352115>)
- Guo, L., Zheng, Z., Ai, J., Huang, B. & Li, X.-A. 2014. Hepatic scavenger receptor BI protects against polymicrobial-induced sepsis through promoting LPS clearance in mice. *The Journal of biological chemistry*, 289, 14666-14673. (<https://doi.org/10.1074/jbc.M113.537258>)
- Guo, Z. & Yu, Q. 2019. Role of mTOR Signaling in Female Reproduction. *Frontiers in Endocrinology*, 10, 692. (<https://doi.org/10.3389/fendo.2019.00692>)
- Gutierrez, C. G., Campbell, B. K. & Webb, R. 1997. Development of a long-term bovine granulosa cell culture system: induction and maintenance of estradiol production, response to follicle-stimulating hormone, and morphological characteristics. *Biology of Reproduction*, 56, 608-616. (<https://doi.org/10.1095/biolreprod56.3.608>)
- Gwynne, J. T. & Strauss, J. F., 3rd 1982. The role of lipoproteins in steroidogenesis and cholesterol metabolism in steroidogenic glands. *Endocrine Reviews*, 3, 299-329. (<https://doi.org/10.1210/edrv-3-3-299>)
- Habel, J. & Sundrum, A. 2020. Mismatch of Glucose Allocation between Different Life Functions in the Transition Period of Dairy Cows. *Animals (Basel)*, 10. (<https://doi.org/10.3390/ani10061028>)
- Hammon, D. S., Evjen, I. M., Dhiman, T. R., Goff, J. P. & Walters, J. L. 2006. Neutrophil function and energy status in Holstein cows with uterine health disorders.

*Veterinary immunology and immunopathology*, 113, 21-29.  
(<https://doi.org/10.1016/j.vetimm.2006.03.022>)

Han, J., Parsons, M., Zhou, X., Nicholson, A. C., Gotto, A. M., Jr. & Hajjar, D. P. 2004. Functional interplay between the macrophage scavenger receptor class B type I and pitavastatin (NK-104). *Circulation*, 110, 3472-3479.  
(<https://doi.org/10.1161/01.CIR.0000148368.79202.F1>)

Han, Y., Yan, J., Zhou, J., Teng, Z., Bian, F., Guo, M., Mao, G., Li, J., Wang, J., Zhang, M. & Xia, G. 2012. Acute fasting decreases the expression of GLUT1 and glucose utilisation involved in mouse oocyte maturation and cumulus cell expansion. *Reproduction, Fertility and Development*, 24, 733-742.  
(<https://doi.org/10.1071/RD10301>)

Hardie, D. G. & Carling, D. 1997. The AMP-activated protein kinase--fuel gauge of the mammalian cell? *European Journal of Biochemistry*, 246, 259-273.  
(<https://doi.org/10.1111/j.1432-1033.1997.00259.x>)

Hardie, D. G., Ross, F. A. & Hawley, S. A. 2012. AMPK: a nutrient and energy sensor that maintains energy homeostasis. *Nature Reviews Molecular Cell Biology*, 13, 251-262. (<https://doi.org/10.1038/nrm3311>)

Hardie, D. G., Scott, J. W., Pan, D. A. & Hudson, E. R. 2003. Management of cellular energy by the AMP-activated protein kinase system. *FEBS Letters*, 546, 113-120.  
([https://doi.org/10.1016/s0014-5793\(03\)00560-x](https://doi.org/10.1016/s0014-5793(03)00560-x))

Hatzirodos, N., Hummitzsch, K., Irving-Rodgers, H. F. & Rodgers, R. J. 2014a. Transcriptome profiling of the theca interna in transition from small to large antral ovarian follicles. *PLoS One*, 9, e97489-e97489.  
(<https://doi.org/10.1371/journal.pone.0097489>)

Hatzirodos, N., Irving-Rodgers, H. F., Hummitzsch, K., Harland, M. L., Morris, S. E. & Rodgers, R. J. 2014b. Transcriptome profiling of granulosa cells of bovine ovarian follicles during growth from small to large antral sizes. *BMC Genomics*, 15, 24.  
(<https://doi.org/10.1186/1471-2164-15-24>)

Hawley, S. A., Boudeau, J., Reid, J. L., Mustard, K. J., Udd, L., Mäkelä, T. P., Alessi, D. R. & Hardie, D. G. 2003. Complexes between the LKB1 tumor suppressor, STRADA $\alpha/\beta$  and MO25 $\alpha/\beta$  are upstream kinases in the AMP-activated protein kinase cascade. *Journal of Biology*, 2, 28. (<https://doi.org/10.1186/1475-4924-2-28>)

Hawley, S. A., Davison, M., Woods, A., Davies, S. P., Beri, R. K., Carling, D. & Hardie, D. G. 1996. Characterization of the AMP-activated protein kinase kinase from rat liver and identification of threonine 172 as the major site at which it phosphorylates AMP-activated protein kinase. *Journal of Biological Chemistry*, 271, 27879-27887.  
(<https://doi.org/10.1074/jbc.271.44.27879>)

Hawley, S. A., Pan, D. A., Mustard, K. J., Ross, L., Bain, J., Edelman, A. M., Frenguelli, B. G. & Hardie, D. G. 2005. Calmodulin-dependent protein kinase kinase- $\beta$  is an alternative upstream kinase for AMP-activated protein kinase. *Cell Metabolism*, 2, 9-19. (<https://doi.org/10.1016/j.cmet.2005.05.009>)

- Healey, G. D., Collier, C., Griffin, S., Schuberth, H. J., Sandra, O., Smith, D. G., Mahan, S., Dieuzy-Labaye, I. & Sheldon, I. M. 2016. Mevalonate Biosynthesis Intermediates Are Key Regulators of Innate Immunity in Bovine Endometritis. *Journal of Immunology*, 196, 823-831. (<https://doi.org/10.4049/jimmunol.1501080>)
- Healy, L. L., Cronin, J. G. & Sheldon, I. M. 2014. Endometrial cells sense and react to tissue damage during infection of the bovine endometrium via interleukin 1. *Scientific Reports*, 4, 7060. (<https://doi.org/10.1038/srep07060>)
- Heidari, M., Kafi, M., Mirzaei, A., Asaadi, A. & Mokhtari, A. 2019. Effects of follicular fluid of preovulatory follicles of repeat breeder dairy cows with subclinical endometritis on oocyte developmental competence. *Animal Reproduction Science*, 205, 62-69. (<https://doi.org/10.1016/j.anireprosci.2019.04.004>)
- Henderson, K. M., Mcneilly, A. S. & Swanston, I. A. 1982. Gonadotrophin and steroid concentrations in bovine follicular fluid and their relationship to follicle size. *Journal of Reproduction and Fertility*, 65, 467-473. (<https://doi.org/10.1530/jrf.0.0650467>)
- Henderson, K. M. & Moon, Y. S. 1979. Luteinization of bovine granulosa cells and corpus luteum formation associated with loss of androgen-aromatizing ability. *Journal of Reproduction and Fertility*, 56, 89-97. (<https://doi.org/10.1530/jrf.0.0560089>)
- Herath, S., Fischer, D. P., Werling, D., Williams, E. J., Lilly, S. T., Dobson, H., Bryant, C. E. & Sheldon, I. M. 2006. Expression and function of Toll-like receptor 4 in the endometrial cells of the uterus. *Endocrinology*, 147, 562-570. (<https://doi.org/10.1210/en.2005-1113>)
- Herath, S., Lilly, S. T., Santos, N. R., Gilbert, R. O., Goetze, L., Bryant, C. E., White, J. O., Cronin, J. & Sheldon, I. M. 2009. Expression of genes associated with immunity in the endometrium of cattle with disparate postpartum uterine disease and fertility. *Reproductive biology and endocrinology*, 7, 55. (<https://doi.org/10.1186/1477-7827-7-55>)
- Herath, S., Williams, E. J., Lilly, S. T., Gilbert, R. O., Dobson, H., Bryant, C. E. & Sheldon, I. M. 2007. Ovarian follicular cells have innate immune capabilities that modulate their endocrine function. *Reproduction*, 134, 683-693. (<https://doi.org/10.1530/REP-07-0229>)
- Hess, A. P., Talbi, S., Hamilton, A. E., Baston-Buest, D. M., Nyegaard, M., Irwin, J. C., Barragan, F., Kruessel, J. S., Germeyer, A. & Giudice, L. C. 2013. The human oviduct transcriptome reveals an anti-inflammatory, anti-angiogenic, secretory and matrix-stable environment during embryo transit. *Reproductive BioMedicine Online*, 27, 423-435. (<https://doi.org/10.1016/j.rbmo.2013.06.013>)
- Hirschfeld, M., Ma, Y., Weis, J. H., Vogel, S. N. & Weis, J. J. 2000. Cutting edge: repurification of lipopolysaccharide eliminates signaling through both human and murine toll-like receptor 2. *Journal of Immunology*, 165, 618-622. (<https://doi.org/10.4049/jimmunol.165.2.618>)
- Hoffmann, E., Dittrich-Breiholz, O., Holtmann, H. & Kracht, M. 2002. Multiple control of interleukin-8 gene expression. *Journal of Leukocyte Biology*, 72, 847-855. (<https://doi.org/10.1189/jlb.72.5.847>)

Horlock, A. D., Ormsby, T. J. R., Clift, M. J. D., Santos, J. E. P., Bromfield, J. J. & Sheldon, I. M. 2021. Manipulating bovine granulosa cell energy metabolism limits inflammation. *Reproduction*, 161, 499-512. (<https://doi.org/10.1530/REP-20-0554>)

Horlock, A. D., Piersanti, R. L., Ramirez-Hernandez, R., Yu, F., Ma, Z., Jeong, K. C., Clift, M. J. D., Block, J., Santos, J. E. P., Bromfield, J. J. & Sheldon, I. M. 2020. Uterine infection alters the transcriptome of the bovine reproductive tract three months later. *Reproduction*, 160, 93-107. (<https://doi.org/10.1530/rep-19-0564>)

Hoshino, K., Takeuchi, O., Kawai, T., Sanjo, H., Ogawa, T., Takeda, Y., Takeda, K. & Akira, S. 1999. Cutting Edge: Toll-Like Receptor 4 (TLR4)-Deficient Mice Are Hyporesponsive to Lipopolysaccharide: Evidence for TLR4 as the Lps Gene Product. *The Journal of Immunology*, 162, 3749-3752.

Hosoe, M., Kaneyama, K., Ushizawa, K., Hayashi, K. G. & Takahashi, T. 2011. Quantitative analysis of bone morphogenetic protein 15 (BMP15) and growth differentiation factor 9 (GDF9) gene expression in calf and adult bovine ovaries. *Reproductive biology and endocrinology*, 9, 33. (<https://doi.org/10.1186/1477-7827-9-33>)

Hou, X., Arvisais, E. W. & Davis, J. S. 2010. Luteinizing hormone stimulates mammalian target of rapamycin signaling in bovine luteal cells via pathways independent of AKT and mitogen-activated protein kinase: modulation of glycogen synthase kinase 3 and AMP-activated protein kinase. *Endocrinology*, 151, 2846-2857. (<https://doi.org/10.1210/en.2009-1032>)

Hsu, Y. M., Zhang, Y., You, Y., Wang, D., Li, H., Duramad, O., Qin, X. F., Dong, C. & Lin, X. 2007. The adaptor protein CARD9 is required for innate immune responses to intracellular pathogens. *Nature Immunology*, 8, 198-205. (<https://doi.org/10.1038/ni1426>)

Hu, J., Zhang, Z., Shen, W. J. & Azhar, S. 2010a. Cellular cholesterol delivery, intracellular processing and utilization for biosynthesis of steroid hormones. *Nutrition and Metabolism (Lond)*, 7, 47. (<https://doi.org/10.1186/1743-7075-7-47>)

Hu, Y. W., Zheng, L. & Wang, Q. 2010b. Regulation of cholesterol homeostasis by liver X receptors. *Clinical Chimica Acta*, 411, 617-625. (<https://doi.org/10.1016/j.cca.2009.12.027>)

Huang, Y., Furuno, M., Arakawa, T., Takizawa, S., De Hoon, M., Suzuki, H. & Arner, E. 2019. A framework for identification of on- and off-target transcriptional responses to drug treatment. *Scientific Reports*, 9, 17603. (<https://doi.org/10.1038/s41598-019-54180-4>)

Hussein, T. S., Thompson, J. G. & Gilchrist, R. B. 2006. Oocyte-secreted factors enhance oocyte developmental competence. *Developmental Biology*, 296, 514-521. (<https://doi.org/10.1016/j.ydbio.2006.06.026>)

Huszenicza, G., Fodor, M., Gacs, M., Kulcsar, M., Dohmen, M. J. W., Vamos, M., Porkolab, L., Legl, T., Bartyik, J., Lohuis, J. a. C. M., Janosi, S. & Szita, G. 1991. Uterine bacteriology, resumption of cyclic ovarian activity and fertility in postpartum

cows kept in large-scale dairy herds. *Reproduction in Domestic Animals*, 34, 237-245. (<https://doi.org/10.1111/j.1439-0531.1999.tb01246.x>)

Ibrahim, S., Salilew-Wondim, D., Rings, F., Hoelker, M., Neuhoﬀ, C., Tholen, E., Looft, C., Schellander, K. & Tesfaye, D. 2015. Expression pattern of inflammatory response genes and their regulatory micrnas in bovine oviductal cells in response to lipopolysaccharide: implication for early embryonic development. *PLoS One*, 10, e0119388. (<https://doi.org/10.1371/journal.pone.0119388>)

Ikonen, E. 2008. Cellular cholesterol trafficking and compartmentalization. *Nature Reviews Molecular Cell Biology*, 9, 125-138. (<https://doi.org/10.1038/nrm2336>)

Ingvarsten, K. L. & Moyes, K. 2013. Nutrition, immune function and health of dairy cattle. *Animal*, 7 Suppl 1, 112-122. (<https://doi.org/10.1017/S175173111200170X>)

Iwata, H., Hashimoto, S., Ohta, M., Kimura, K., Shibano, K. & Miyake, M. 2004. Effects of follicle size and electrolytes and glucose in maturation medium on nuclear maturation and developmental competence of bovine oocytes. *Reproduction*, 127, 159-164. (<https://doi.org/10.1530/rep.1.00084>)

Jabbour, H. N., Sales, K. J., Catalano, R. D. & Norman, J. E. 2009. Inflammatory pathways in female reproductive health and disease. *Reproduction*, 138, 903-919. (<https://doi.org/10.1530/rep-09-0247>)

Jacinto, E., Loewith, R., Schmidt, A., Lin, S., Ruegg, M. A., Hall, A. & Hall, M. N. 2004. Mammalian TOR complex 2 controls the actin cytoskeleton and is rapamycin insensitive. *Nature Cell Biology*, 6, 1122-1128. (<https://doi.org/10.1038/ncb1183>)

Jain, M. K. & Ridker, P. M. 2005. Anti-inflammatory effects of statins: clinical evidence and basic mechanisms. *Nature Reviews Drug Discovery*, 4, 977-987. (<https://doi.org/10.1038/nrd1901>)

Janowski, B. A., Willy, P. J., Devi, T. R., Falck, J. R. & Mangelsdorf, D. J. 1996. An oxysterol signalling pathway mediated by the nuclear receptor LXR alpha. *Nature*, 383, 728-731. (<https://doi.org/10.1038/383728a0>)

Jaspard, B., Collet, X., Barbaras, R., Manent, J., Vieu, C., Parinaud, J., Chap, H. & Perret, B. 1996. Biochemical characterization of pre-beta 1 high-density lipoprotein from human ovarian follicular fluid: evidence for the presence of a lipid core. *Biochemistry*, 35, 1352-1357. (<https://doi.org/10.1021/bi950938i>)

Jiang, C., Diao, F., Sang, Y. J., Xu, N., Zhu, R. L., Wang, X. X., Chen, Z., Tao, W. W., Yao, B., Sun, H. X., Huang, X. X., Xue, B. & Li, C. J. 2017. GGPP-Mediated Protein Geranylgeranylation in Oocyte Is Essential for the Establishment of Oocyte-Granulosa Cell Communication and Primary-Secondary Follicle Transition in Mouse Ovary. *PLoS Genetics*, 13, e1006535. (<https://doi.org/10.1371/journal.pgen.1006535>)

Jiang, S. Y., Li, H., Tang, J. J., Wang, J., Luo, J., Liu, B., Wang, J. K., Shi, X. J., Cui, H. W., Tang, J., Yang, F., Qi, W., Qiu, W. W. & Song, B. L. 2018. Discovery of a potent HMG-CoA reductase degrader that eliminates statin-induced reductase accumulation and lowers cholesterol. *Nature Communications*, 9, 5138. (<https://doi.org/10.1038/s41467-018-07590-3>)



- Jiemtaweeboon, S., Shirasuna, K., Nitta, A., Kobayashi, A., Schuberth, H.-J., Shimizu, T. & Miyamoto, A. 2011. Evidence that polymorphonuclear neutrophils infiltrate into the developing corpus luteum and promote angiogenesis with interleukin-8 in the cow. *Reproductive biology and endocrinology : RB&E*, 9, 79-79. (<https://doi.org/10.1186/1477-7827-9-79>)
- Jorritsma, R., Langendijk, P., Kruij, T. A., Wensing, T. H. & Noordhuizen, J. P. 2005. Associations between energy metabolism, LH pulsatility and first ovulation in early lactating cows. *Reproduction in Domestic Animals*, 40, 68-72. (<https://doi.org/10.1111/j.1439-0531.2004.00558.x>)
- Karsch, F. J., Battaglia, D. F., Breen, K. M., Debus, N. & Harris, T. G. 2002. Mechanisms for ovarian cycle disruption by immune/inflammatory stress. *Stress*, 5, 101-112. (<https://doi.org/10.1080/10253890290027868>)
- Kasimanickam, R., Duffield, T. F., Foster, R. A., Gartley, C. J., Leslie, K. E., Walton, J. S. & Johnson, W. H. 2004. Endometrial cytology and ultrasonography for the detection of subclinical endometritis in postpartum dairy cows. *Theriogenology*, 62, 9-23. (<https://doi.org/10.1016/j.theriogenology.2003.03.001>)
- Kawagoe, T., Sato, S., Matsushita, K., Kato, H., Matsui, K., Kumagai, Y., Saitoh, T., Kawai, T., Takeuchi, O. & Akira, S. 2008. Sequential control of Toll-like receptor-dependent responses by IRAK1 and IRAK2. *Nature Immunology*, 9, 684-691. (<https://doi.org/10.1038/ni.1606>)
- Kawai, T. & Akira, S. 2007. Signaling to NF- $\kappa$ B by Toll-like receptors. *Trends in Molecular Medicine*, 13, 460-469. (<https://doi.org/10.1016/j.molmed.2007.09.002>)
- Kawai, T. & Akira, S. 2010. The role of pattern-recognition receptors in innate immunity: update on Toll-like receptors. *Nature Immunology*, 11, 373-384. (<https://doi.org/10.1038/ni.1863>)
- Kayampilly, P. P. & Menon, K. M. 2007. Follicle-stimulating hormone increases tuberin phosphorylation and mammalian target of rapamycin signaling through an extracellular signal-regulated kinase-dependent pathway in rat granulosa cells. *Endocrinology*, 148, 3950-3957. (<https://doi.org/10.1210/en.2007-0202>)
- Keating, N. & Quinlan, L. R. 2012. Small conductance potassium channels drive ATP-activated chloride secretion in the oviduct. *American Journal of Physiology-Cell Physiology*, 302, C100-109. (<https://doi.org/10.1152/ajpcell.00503.2010>)
- Kessler, E. C., Gross, J. J., Bruckmaier, R. M. & Albrecht, C. 2014. Cholesterol metabolism, transport, and hepatic regulation in dairy cows during transition and early lactation. *Journal of Dairy Science*, 97, 5481-5490. (<https://doi.org/10.3168/jds.2014-7926>)
- Khafipour, E., Krause, D. O. & Plaizier, J. C. 2009. A grain-based subacute ruminal acidosis challenge causes translocation of lipopolysaccharide and triggers inflammation. *Journal of Dairy Science*, 92, 1060-1070. (<https://doi.org/10.3168/jds.2008-1389>)

Kilsdonk, E. P., Yancey, P. G., Stoudt, G. W., Bangerter, F. W., Johnson, W. J., Phillips, M. C. & Rothblat, G. H. 1995. Cellular cholesterol efflux mediated by cyclodextrins. *Journal of Biological Chemistry*, 270, 17250-17256. (<https://doi.org/10.1074/jbc.270.29.17250>)

Kim, B., Lee, Y., Kim, E., Kwak, A., Ryoo, S., Bae, S. H., Azam, T., Kim, S. & Dinarello, C. A. 2013. The Interleukin-1alpha Precursor is Biologically Active and is Likely a Key Alarmin in the IL-1 Family of Cytokines. *Frontiers in Immunology*, 4, 391-391. (<https://doi.org/10.3389/fimmu.2013.00391>)

Kim, D.-H., Sarbassov, D. D., Ali, S. M., King, J. E., Latek, R. R., Erdjument-Bromage, H., Tempst, P. & Sabatini, D. M. 2002. mTOR Interacts with Raptor to Form a Nutrient-Sensitive Complex that Signals to the Cell Growth Machinery. *Cell*, 110, 163-175. ([https://doi.org/10.1016/s0092-8674\(02\)00808-5](https://doi.org/10.1016/s0092-8674(02)00808-5))

Kim, I. H. & Suh, G. H. 2003. Effect of the amount of body condition loss from the dry to near calving periods on the subsequent body condition change, occurrence of postpartum diseases, metabolic parameters and reproductive performance in Holstein dairy cows. *Theriogenology*, 60, 1445-1456. ([https://doi.org/10.1016/s0093-691x\(03\)00135-3](https://doi.org/10.1016/s0093-691x(03)00135-3))

Kim, J. Y. 2012. Control of ovarian primordial follicle activation. *Clinical and experimental reproductive medicine*, 39, 10-14. (<https://doi.org/10.5653/cerm.2012.39.1.10>)

Kim, J. Y., Kinoshita, M., Ohnishi, M. & Fukui, Y. 2001. Lipid and fatty acid analysis of fresh and frozen-thawed immature and in vitro matured bovine oocytes. *Reproduction*, 122, 131-138. (<https://doi.org/10.1530/rep.0.1220131>)

Kimura, K., Goff, J. P., Kehrl, M. E., Harp, J. A. & Nonnecke, B. J. 2002. Effects of Mastectomy on Composition of Peripheral Blood Mononuclear Cell Populations in Periparturient Dairy Cows<sup>1</sup>. *Journal of Dairy Science*, 85, 1437-1444. ([https://doi.org/10.3168/jds.S0022-0302\(02\)74211-2](https://doi.org/10.3168/jds.S0022-0302(02)74211-2))

Kimura, N., Tokunaga, C., Dalal, S., Richardson, C., Yoshino, K., Hara, K., Kemp, B. E., Witters, L. A., Mimura, O. & Yonezawa, K. 2003. A possible linkage between AMP-activated protein kinase (AMPK) and mammalian target of rapamycin (mTOR) signalling pathway. *Genes to Cells*, 8, 65-79. (<https://doi.org/10.1046/j.1365-2443.2003.00615.x>)

Kimura, T., Mogi, C., Tomura, H., Kuwabara, A., Im, D. S., Sato, K., Kurose, H., Murakami, M. & Okajima, F. 2008. Induction of scavenger receptor class B type I is critical for simvastatin enhancement of high-density lipoprotein-induced anti-inflammatory actions in endothelial cells. *Journal of Immunology*, 181, 7332-7340. (<https://doi.org/10.4049/jimmunol.181.10.7332>)

Kogasaka, Y., Hoshino, Y., Hiradate, Y., Tanemura, K. & Sato, E. 2013. Distribution and association of mTOR with its cofactors, raptor and rictor, in cumulus cells and oocytes during meiotic maturation in mice. *Molecular Reproduction and Development*, 80, 334-348. (<https://doi.org/10.1002/mrd.22166>)

Kokia, E., Hurwitz, A., Ben-Shlomo, I., Adashi, E. Y. & Yanagishita, M. 1993. Receptor-mediated stimulatory effect of IL-1 beta on hyaluronic acid and proteoglycan biosynthesis by cultured rat ovarian cells: role for heterologous cell-cell interactions. *Endocrinology*, 133, 2391-2394. (<https://doi.org/10.1210/endo.133.5.8404691>)

Kolmakova, A., Wang, J., Brogan, R., Chaffin, C. & Rodriguez, A. 2010. Deficiency of scavenger receptor class B type I negatively affects progesterone secretion in human granulosa cells. *Endocrinology*, 151, 5519-5527. (<https://doi.org/10.1210/en.2010-0347>)

Kong, B.-W., Hudson, N., Seo, D., Lee, S., Khatri, B., Lassiter, K., Cook, D., Piekarski, A., Dridi, S., Anthony, N. & Bottje, W. 2017. RNA sequencing for global gene expression associated with muscle growth in a single male modern broiler line compared to a foundational Barred Plymouth Rock chicken line. *BMC Genomics*, 18. (<https://doi.org/10.1186/s12864-016-3471-y>)

Koseki, M., Hirano, K., Masuda, D., Ikegami, C., Tanaka, M., Ota, A., Sandoval, J. C., Nakagawa-Toyama, Y., Sato, S. B., Kobayashi, T., Shimada, Y., Ohno-Iwashita, Y., Matsuura, F., Shimomura, I. & Yamashita, S. 2007. Increased lipid rafts and accelerated lipopolysaccharide-induced tumor necrosis factor-alpha secretion in Abca1-deficient macrophages. *Journal of Lipid Research*, 48, 299-306. (<https://doi.org/10.1194/jlr.M600428-JLR200>)

Kowsar, R., Hambruch, N., Liu, J., Shimizu, T., Pfarrer, C. & Miyamoto, A. 2013. Regulation of innate immune function in bovine oviduct epithelial cells in culture: the homeostatic role of epithelial cells in balancing Th1/Th2 response. *Journal of Reproduction and Development*, 59, 470-478. (<https://doi.org/10.1262/jrd.2013-036>)

Koyama, K., Kang, S.-S., Huang, W., Yanagawa, Y., Takahashi, Y. & Nagano, M. 2014. Estimation of the Optimal Timing of Fertilization for Embryo Development of In Vitro-Matured Bovine Oocytes Based on the Times of Nuclear Maturation and Sperm Penetration. *Journal of veterinary medical science*, 76, 653-659. (<https://doi.org/10.1292/jvms.13-0607>)

Kramer, A., Green, J., Pollard, J., Jr. & Tugendreich, S. 2014. Causal analysis approaches in Ingenuity Pathway Analysis. *Bioinformatics*, 30, 523-530. (<https://doi.org/10.1093/bioinformatics/btt703>)

Kuijk, L. M., Mandey, S. H., Schellens, I., Waterham, H. R., Rijkers, G. T., Coffey, P. J. & Frenkel, J. 2008. Statin synergizes with LPS to induce IL-1beta release by THP-1 cells through activation of caspase-1. *Molecular Immunology*, 45, 2158-2165. (<https://doi.org/10.1016/j.molimm.2007.12.008>)

Kvidera, S. K., Horst, E. A., Abuajamieh, M., Mayorga, E. J., Fernandez, M. V. & Baumgard, L. H. 2017. Glucose requirements of an activated immune system in lactating Holstein cows. *Journal of Dairy Science*, 100, 2360-2374. (<https://doi.org/10.3168/jds.2016-12001>)

Lachmandas, E., Boutens, L., Ratter, J. M., Hijmans, A., Hooiveld, G. J., Joosten, L. A., Rodenburg, R. J., Fransen, J. A., Houtkooper, R. H., Van Crevel, R., Netea, M. G. & Stienstra, R. 2016. Microbial stimulation of different Toll-like receptor signalling

pathways induces diverse metabolic programmes in human monocytes. *Nature microbiology*, 2, 16246. (<https://doi.org/10.1038/nmicrobiol.2016.246>)

Lai, W. A., Yeh, Y. T., Lee, M. T., Wu, L. S., Ke, F. C. & Hwang, J. J. 2013. Ovarian granulosa cells utilize scavenger receptor SR-BI to evade cellular cholesterol homeostatic control for steroid synthesis. *Journal of Lipid Research*, 54, 365-378. (<https://doi.org/10.1194/jlr.M030239>)

Larsen, W. J., Chen, L., Powers, R., Zhang, H., Russell, P. T., Chambers, C., Hess, K. & Flick, R. 1996. Cumulus expansion initiates physical and developmental autonomy of the oocyte. *Zygote*, 4, 335-341. (<https://doi.org/10.1017/s096719940000335x>)

Le Goff, D. 1994. Follicular fluid lipoproteins in the mare: evaluation of HDL transfer from plasma to follicular fluid. *Biochimica et Biophysica Acta*, 1210, 226-232. ([https://doi.org/10.1016/0005-2760\(94\)90125-2](https://doi.org/10.1016/0005-2760(94)90125-2))

Leblanc, S. J. 2012. Interactions of metabolism, inflammation, and reproductive tract health in the postpartum period in dairy cattle. *Reproduction in Domestic Animals*, 47 Suppl 5, 18-30. (<https://doi.org/10.1111/j.1439-0531.2012.02109.x>)

Leblanc, S. J., Duffield, T. F., Leslie, K. E., Bateman, K. G., Keefe, G. P., Walton, J. S. & Johnson, W. H. 2002. Defining and Diagnosing Postpartum Clinical Endometritis and its Impact on Reproductive Performance in Dairy Cows. *Journal of Dairy Science*, 85, 2223-2236. ([https://doi.org/10.3168/jds.S0022-0302\(02\)74302-6](https://doi.org/10.3168/jds.S0022-0302(02)74302-6))

Lee, H., Zandkarimi, F., Zhang, Y., Meena, J. K., Kim, J., Zhuang, L., Tyagi, S., Ma, L., Westbrook, T. F., Steinberg, G. R., Nakada, D., Stockwell, B. R. & Gan, B. 2020. Energy-stress-mediated AMPK activation inhibits ferroptosis. *Nature Cell Biology*, 22, 225-234. (<https://doi.org/10.1038/s41556-020-0461-8>)

Lee, S. E., Sun, S. C., Choi, H. Y., Uhm, S. J. & Kim, N. H. 2012. mTOR is required for asymmetric division through small GTPases in mouse oocytes. *Molecular Reproduction and Development*, 79, 356-366. (<https://doi.org/10.1002/mrd.22035>)

Lehmann, J. M., Kliewer, S. A., Moore, L. B., Smith-Oliver, T. A., Oliver, B. B., Su, J. L., Sundseth, S. S., Winegar, D. A., Blanchard, D. E., Spencer, T. A. & Willson, T. M. 1997. Activation of the nuclear receptor LXR by oxysterols defines a new hormone response pathway. *Journal of Biological Chemistry*, 272, 3137-3140. (<https://doi.org/10.1074/jbc.272.6.3137>)

Leroy, J. L., Opsomer, G., Van Soom, A., Goovaerts, I. G. & Bols, P. E. 2008. Reduced fertility in high-yielding dairy cows: are the oocyte and embryo in danger? Part I. The importance of negative energy balance and altered corpus luteum function to the reduction of oocyte and embryo quality in high-yielding dairy cows. *Reproduction in Domestic Animals*, 43, 612-622. (<https://doi.org/10.1111/j.1439-0531.2007.00960.x>)

Leroy, J. L., Vanholder, T., Delanghe, J. R., Opsomer, G., Van Soom, A., Bols, P. E. & De Kruif, A. 2004a. Metabolite and ionic composition of follicular fluid from different-sized follicles and their relationship to serum concentrations in dairy cows. *Animal Reproduction Science*, 80, 201-211. ([https://doi.org/10.1016/S0378-4320\(03\)00173-8](https://doi.org/10.1016/S0378-4320(03)00173-8))

Leroy, J. L., Vanholder, T., Delanghe, J. R., Opsomer, G., Van Soom, A., Bols, P. E., Dewulf, J. & De Kruif, A. 2004b. Metabolic changes in follicular fluid of the dominant follicle in high-yielding dairy cows early post partum. *Theriogenology*, 62, 1131-1143. (<https://doi.org/10.1016/j.theriogenology.2003.12.017>)

Leroy, J. L. M. R., Bie, J., Jordaens, L., Desmet, K., Smits, A., Marei, W. F. A., Bols, P. E. J. & Hoeck, V. V. 2017. Negative energy balance and metabolic stress in relation to oocyte and embryo quality: an update on possible pathways reducing fertility in dairy cows. *Animal Reproduction*, 14, 497-506. (<https://doi.org/10.21451/1984-3143-ar992>)

Levental, I. & Veatch, S. 2016. The Continuing Mystery of Lipid Rafts. *Journal of Molecular Biology*, 428, 4749-4764. (<https://doi.org/10.1016/j.jmb.2016.08.022>)

Li, J., He, Y., Hao, J., Ni, L. & Dong, C. 2018. High Levels of Eomes Promote Exhaustion of Anti-tumor CD8(+) T Cells. *Frontiers in Immunology*, 9, 2981. (<https://doi.org/10.3389/fimmu.2018.02981>)

Li, L., Zhu, S., Shu, W., Guo, Y., Guan, Y., Zeng, J., Wang, H., Han, L., Zhang, J., Liu, X., Li, C., Hou, X., Gao, M., Ge, J., Ren, C., Zhang, H., Schedl, T., Guo, X., Chen, M. & Wang, Q. 2020. Characterization of Metabolic Patterns in Mouse Oocytes during Meiotic Maturation. *Molecular cell*, 80, 525-540 e529. (<https://doi.org/10.1016/j.molcel.2020.09.022>)

Liao, Y. H., Lin, Y. C., Tsao, S. T., Lin, Y. C., Yang, A. J., Huang, C. T., Huang, K. C. & Lin, W. W. 2013. HMG-CoA reductase inhibitors activate caspase-1 in human monocytes depending on ATP release and P2X7 activation. *Journal of Leukocyte Biology*, 93, 289-299. (<https://doi.org/10.1189/jlb.0812409>)

Lima, F. S., Ribeiro, E. S., Bisinotto, R. S., Greco, L. F., Martinez, N., Amstalden, M., Thatcher, W. W. & Santos, J. E. P. 2013. Hormonal manipulations in the 5-day timed artificial insemination protocol to optimize estrous cycle synchrony and fertility in dairy heifers. *Journal of Dairy Science*, 96, 7054-7065. (<https://doi.org/10.3168/jds.2013-7093>)

Liu, C., Peng, J., Matzuk, M. M. & Yao, H. H. 2015. Lineage specification of ovarian theca cells requires multicellular interactions via oocyte and granulosa cells. *Nature Communications*, 6, 6934. (<https://doi.org/10.1038/ncomms7934>)

Liu, T., Zhang, L., Joo, D. & Sun, S.-C. 2017. NF- $\kappa$ B signaling in inflammation. *Signal Transduction and Targeted Therapy*, 2, 17023. (<https://doi.org/10.1038/sigtrans.2017.23>)

Liu, Y. X. & Hsueh, A. J. 1986. Synergism between granulosa and theca-interstitial cells in estrogen biosynthesis by gonadotropin-treated rat ovaries: studies on the two-cell, two-gonadotropin hypothesis using steroid antisera. *Biology of Reproduction*, 35, 27-36. (<https://doi.org/10.1095/biolreprod35.1.27>)

Liu, Z., De Matos, D. G., Fan, H. Y., Shimada, M., Palmer, S. & Richards, J. S. 2009. Interleukin-6: an autocrine regulator of the mouse cumulus cell-oocyte complex expansion process. *Endocrinology*, 150, 3360-3368. (<https://doi.org/10.1210/en.2008-1532>)

- Liu, Z., Shimada, M. & Richards, J. S. 2008. The involvement of the Toll-like receptor family in ovulation. *Journal of Assisted Reproduction and Genetics*, 25, 223-228. (<https://doi.org/10.1007/s10815-008-9219-0>)
- Lombard, J. & Moreira, D. 2011. Origins and early evolution of the mevalonate pathway of isoprenoid biosynthesis in the three domains of life. *Molecular Biology and Evolution*, 28, 87-99. (<https://doi.org/10.1093/molbev/msq177>)
- Lundy, T., Smith, P., O'connell, A., Hudson, N. L. & McNatty, K. P. 1999. Populations of granulosa cells in small follicles of the sheep ovary. *Journal of Reproduction and Fertility*, 115, 251-262. (<https://doi.org/10.1530/jrf.0.1150251>)
- Luo, J., Yang, H. & Song, B. L. 2020. Mechanisms and regulation of cholesterol homeostasis. *Nature Reviews Molecular Cell Biology*, 21, 225-245. (<https://doi.org/10.1038/s41580-019-0190-7>)
- Macrae, A. I., Burrough, E., Forrest, J., Corbishley, A., Russell, G. & Shaw, D. J. 2019. Prevalence of excessive negative energy balance in commercial United Kingdom dairy herds. *Veterinary Journal*, 248, 51-57. (<https://doi.org/10.1016/j.tvjl.2019.04.001>)
- Magata, F., Horiuchi, M., Echizenya, R., Miura, R., Chiba, S., Matsui, M., Miyamoto, A., Kobayashi, Y. & Shimizu, T. 2014. Lipopolysaccharide in ovarian follicular fluid influences the steroid production in large follicles of dairy cows. *Animal Reproduction Science*, 144, 6-13. (<https://doi.org/10.1016/j.anireprosci.2013.11.005>)
- Magata, F. & Shimizu, T. 2017. Effect of lipopolysaccharide on developmental competence of oocytes. *Reproductive Toxicology*, 71, 1-7. (<https://doi.org/10.1016/j.reprotox.2017.04.001>)
- Magoffin, D. A. 2005. Ovarian theca cell. *International Journal of Biochemistry & Cell Biology*, 37, 1344-1349. (<https://doi.org/10.1016/j.biocel.2005.01.016>)
- Maillo, V., De Frutos, C., O'gaora, P., Forde, N., Burns, G. W., Spencer, T. E., Gutierrez-Adan, A., Lonergan, P. & Rizos, D. 2016. Spatial differences in gene expression in the bovine oviduct. *Reproduction*, 152, 37-46. (<https://doi.org/10.1530/REP-16-0074>)
- Malik, A. & Kanneganti, T.-D. 2018. Function and regulation of IL-1 $\alpha$  in inflammatory diseases and cancer. *Immunological reviews*, 281, 124-137. (<https://doi.org/10.1111/imr.12615>)
- Mandey, S. H. L., Kuijk, L. M., Frenkel, J. & Waterham, H. R. 2006. A role for geranylgeranylation in interleukin-1 $\beta$  secretion. *Arthritis & Rheumatism*, 54, 3690-3695. (<https://doi.org/10.1002/art.22194>)
- Mao, Z. & Zhang, W. 2018. Role of mTOR in Glucose and Lipid Metabolism. *International Journal of Molecular Sciences*, 19, 2043.
- Mariathasan, S., Newton, K., Monack, D. M., Vucic, D., French, D. M., Lee, W. P., Roose-Girma, M., Erickson, S. & Dixit, V. M. 2004. Differential activation of the

inflammasome by caspase-1 adaptors ASC and Ipaf. *Nature*, 430, 213-218. (<https://doi.org/10.1038/nature02664>)

Marin Bivens, C. L., Lindenthal, B., O'Brien, M. J., Wigglesworth, K., Blume, T., Grondahl, C. & Eppig, J. J. 2004. A synthetic analogue of meiosis-activating sterol (FF-MAS) is a potent agonist promoting meiotic maturation and preimplantation development of mouse oocytes maturing in vitro. *Human Reproduction*, 19, 2340-2344. (<https://doi.org/10.1093/humrep/deh436>)

Martoriati, A., Duchamp, G. & Gérard, N. 2003. In vivo effect of epidermal growth factor, interleukin-1beta, and interleukin-1RA on equine preovulatory follicles. *Biology of Reproduction*, 68, 1748-1754. (<https://doi.org/10.1095/biolreprod.102.012138>)

Massonnet, B., Normand, S., Moschitz, R., Delwail, A., Favot, L., Garcia, M., Bourmeyster, N., Cuisset, L., Grateau, G., Morel, F., Silvain, C. & Lecron, J. C. 2009. Pharmacological inhibitors of the mevalonate pathway activate pro-IL-1 processing and IL-1 release by human monocytes. *European Cytokine Network*, 20, 112-120. (<https://doi.org/10.1684/ecn.2009.0162>)

Matoba, S., Bender, K., Fahey, A. G., Mamo, S., Brennan, L., Lonergan, P. & Fair, T. 2014. Predictive value of bovine follicular components as markers of oocyte developmental potential. *Reproduction, Fertility and Development*, 26, 337-345. (<https://doi.org/10.1071/RD13007>)

Matsumoto, M., Einhaus, D., Gold, E. S. & Aderem, A. 2004. Simvastatin augments lipopolysaccharide-induced proinflammatory responses in macrophages by differential regulation of the c-Fos and c-Jun transcription factors. *Journal of Immunology*, 172, 7377-7384. (<https://doi.org/10.4049/jimmunol.172.12.7377>)

Matzuk, M. M., Burns, K. H., Viveiros, M. M. & Eppig, J. J. 2002. Intercellular communication in the mammalian ovary: oocytes carry the conversation. *Science*, 296, 2178-2180. (<https://doi.org/10.1126/science.1071965>)

Mayes, M. A., Laforest, M. F., Guillemette, C., Gilchrist, R. B. & Richard, F. J. 2007. Adenosine 5'-monophosphate kinase-activated protein kinase (PRKA) activators delay meiotic resumption in porcine oocytes. *Biology of Reproduction*, 76, 589-597. (<https://doi.org/10.1095/biolreprod.106.057828>)

Mazgaen, L. & Gurung, P. 2020. Recent Advances in Lipopolysaccharide Recognition Systems. *International Journal of Molecular Science*, 21, 1-18. (<https://doi.org/10.3390/ijms21020379>)

Mccarthy, S. D., Waters, S. M., Kenny, D. A., Diskin, M. G., Fitzpatrick, R., Patton, J., Wathes, D. C. & Morris, D. G. 2010. Negative energy balance and hepatic gene expression patterns in high-yielding dairy cows during the early postpartum period: a global approach. *Physiological Genomics*, 42A, 188-199. (<https://doi.org/10.1152/physiolgenomics.00118.2010>)

Mcgillicuddy, F. C., Moya, M. D. L. L., Hinkle, C. C., Joshi, M. R., Chiquoine, E. H., Billheimer, J. T., Rothblat, G. H. & Reilly, M. P. 2009. Inflammation Impairs Reverse

Cholesterol Transport In Vivo. *Circulation*, 119, 1135-1145. (<https://doi.org/10.1161/CIRCULATIONAHA.108.810721>)

McNatty, K. P., Juengel, J. L., Reader, K. L., Lun, S., Myllymaa, S., Lawrence, S. B., Western, A., Meerasahib, M. F., Mottershead, D. G., Groome, N. P., Ritvos, O. & Laitinen, M. P. 2005. Bone morphogenetic protein 15 and growth differentiation factor 9 co-operate to regulate granulosa cell function in ruminants. *Reproduction*, 129, 481-487. (<https://doi.org/10.1530/rep.1.00517>)

McNatty, K. P., Reader, K., Smith, P., Heath, D. A. & Juengel, J. L. 2007. Control of ovarian follicular development to the gonadotrophin-dependent phase: a 2006 perspective. *Society for Reproduction and Fertility Supplement*, 64, 55-68. (<https://doi.org/10.5661/rdr-vi-55>)

Medzhitov, R. & Janeway, C. 2002. Decoding the Patterns of Self and Nonself by the Innate Immune System. *Science*, 296, 298-300. (<https://doi.org/10.1126/science.1068883>)

Metsalu, T. & Vilo, J. 2015. ClustVis: a web tool for visualizing clustering of multivariate data using Principal Component Analysis and heatmap. *Nucleic acids research*, 43, W566-570. (<https://doi.org/10.1093/nar/gkv468>)

Miranda-Jimenez, L. & Murphy, B. D. 2007. Lipoprotein receptor expression during luteinization of the ovarian follicle. *American Journal of Physiology Endocrinology and Metabolism*, 293, E1053-1061. (<https://doi.org/10.1152/ajpendo.00554.2006>)

Mittaz, L., Russell, D. L., Wilson, T., Brasted, M., Tkalcevic, J., Salamonsen, L. A., Hertzog, P. J. & Pritchard, M. A. 2004. Adamts-1 is essential for the development and function of the urogenital system. *Biology of Reproduction*, 70, 1096-1105. (<https://doi.org/10.1095/biolreprod.103.023911>)

Mok, E. H. K. & Lee, T. K. W. 2020. The Pivotal Role of the Dysregulation of Cholesterol Homeostasis in Cancer: Implications for Therapeutic Targets. *Cancers (Basel)*, 12, 1410. (<https://doi.org/10.3390/cancers12061410>)

Monick, M. M., Powers, L. S., Butler, N. S. & Hunninghake, G. W. 2003. Inhibition of Rho family GTPases results in increased TNF-alpha production after lipopolysaccharide exposure. *Journal of Immunology*, 171, 2625-2630. (<https://doi.org/10.4049/jimmunol.171.5.2625>)

Montero, M. a. T., Hernández, O., Suárez, Y., Matilla, J. N., Ferruelo, A. J., Martínez-Botas, J., Gómez-Coronado, D. & Lasunción, M. A. 2000. Hydroxymethylglutaryl-coenzyme A reductase inhibition stimulates caspase-1 activity and Th1-cytokine release in peripheral blood mononuclear cells. *Atherosclerosis*, 153, 303-313. ([https://doi.org/10.1016/S0021-9150\(00\)00417-2](https://doi.org/10.1016/S0021-9150(00)00417-2))

Moresco, E. M., Lavine, D. & Beutler, B. 2011. Toll-like receptors. *Current Biology*, 21, R488-493. (<https://doi.org/10.1016/j.cub.2011.05.039>)

Morin, E. E., Guo, L., Schwendeman, A. & Li, X. A. 2015. HDL in sepsis - risk factor and therapeutic approach. *Frontiers in Pharmacology*, 6, 244. (<https://doi.org/10.3389/fphar.2015.00244>)



- Morris, D. G., Waters, S. M., McCarthy, S. D., Patton, J., Earley, B., Fitzpatrick, R., Murphy, J. J., Diskin, M. G., Kenny, D. A., Brass, A. & Wathes, D. C. 2009. Pleiotropic effects of negative energy balance in the postpartum dairy cow on splenic gene expression: repercussions for innate and adaptive immunity. *Physiological Genomics*, 39, 28-37. (<https://doi.org/10.1152/physiolgenomics.90394.2008>)
- Mosmann, T. 1983. Rapid colorimetric assay for cellular growth and survival: application to proliferation and cytotoxicity assays. *Journal of Immunological Methods*, 65, 55-63. ([https://doi.org/10.1016/0022-1759\(83\)90303-4](https://doi.org/10.1016/0022-1759(83)90303-4))
- Moyes, K. M., Drackley, J. K., Morin, D. E., Rodriguez-Zas, S. L., Everts, R. E., Lewin, H. A. & Loores, J. J. 2010. Mammary gene expression profiles during an intramammary challenge reveal potential mechanisms linking negative energy balance with impaired immune response. *Physiological Genomics*, 41, 161-170. (<https://doi.org/10.1152/physiolgenomics.00197.2009>)
- Mulligan, F. J., O'grady, L., Rice, D. A. & Doherty, M. L. 2006. A herd health approach to dairy cow nutrition and production diseases of the transition cow. *Animal Reproduction Science*, 96, 331-353. (<https://doi.org/10.1016/j.anireprosci.2006.08.011>)
- Murray, P. J., Rathmell, J. & Pearce, E. 2015. SnapShot: Immunometabolism. *Cell Metabolism*, 22, 190-190 e191. (<https://doi.org/10.1016/j.cmet.2015.06.014>)
- Nagano, M., Katagiri, S. & Takahashi, Y. 2006. ATP content and maturational/developmental ability of bovine oocytes with various cytoplasmic morphologies. *Zygote*, 14, 299-304. (<https://doi.org/10.1017/S0967199406003807>)
- Namgoong, S. & Kim, N. H. 2016. Roles of actin binding proteins in mammalian oocyte maturation and beyond. *Cell Cycle*, 15, 1830-1843. (<https://doi.org/10.1080/15384101.2016.1181239>)
- Nguyen, T. M. D. 2019. Role of AMPK in mammals reproduction: Specific controls and whole-body energy sensing. *Comptes Rendus Biologies*, 342, 1-6. (<https://doi.org/10.1016/j.crvi.2018.10.003>)
- Nicholson, A. M. & Ferreira, A. 2009. Increased membrane cholesterol might render mature hippocampal neurons more susceptible to beta-amyloid-induced calpain activation and tau toxicity. *Journal of Neuroscience*, 29, 4640-4651. (<https://doi.org/10.1523/JNEUROSCI.0862-09.2009>)
- Nicklin, P., Bergman, P., Zhang, B., Triantafellow, E., Wang, H., Nyfeler, B., Yang, H., Hild, M., Kung, C., Wilson, C., Myer, V. E., Mackeigan, J. P., Porter, J. A., Wang, Y. K., Cantley, L. C., Finan, P. M. & Murphy, L. O. 2009. Bidirectional transport of amino acids regulates mTOR and autophagy. *Cell*, 136, 521-534. (<https://doi.org/10.1016/j.cell.2008.11.044>)
- Nishimoto, H., Hamano, S., Hill, G. A., Miyamoto, A. & Tetsuka, M. 2009. Classification of bovine follicles based on the concentrations of steroids, glucose and lactate in follicular fluid and the status of accompanying follicles. *Journal of Reproduction and Development*, 55, 219-224. (<https://doi.org/10.1262/jrd.20114>)

- Nishimoto, H., Matsutani, R., Yamamoto, S., Takahashi, T., Hayashi, K. G., Miyamoto, A., Hamano, S. & Tetsuka, M. 2006. Gene expression of glucose transporter (GLUT) 1, 3 and 4 in bovine follicle and corpus luteum. *Journal of Endocrinology*, 188, 111-119. (<https://doi.org/10.1677/joe.1.06210>)
- Noakes, D. E., Wallace, L. & Smith, G. R. 1991. Bacterial flora of the uterus of cows after calving on two hygienically contrasting farms. *Veterinary Record*, 128, 440-442. (<https://doi.org/10.1136/vr.128.19.440>)
- Noletto, P. G., Saut, J. P. E. & Sheldon, I. M. 2017. Short communication: Glutamine modulates inflammatory responses to lipopolysaccharide in ex vivo bovine endometrium. *Journal of Dairy Science*, 100, 2207-2212. (<https://doi.org/10.3168/jds.2016-12023>)
- O'Neill, L. A. & Bowie, A. G. 2007. The family of five: TIR-domain-containing adaptors in Toll-like receptor signalling. *Nature Reviews Immunology*, 7, 353-364. (<https://doi.org/10.1038/nri2079>)
- O'Neill, L. A., Kishton, R. J. & Rathmell, J. 2016. A guide to immunometabolism for immunologists. *Nature Reviews Immunology*, 16, 553-565. (<https://doi.org/10.1038/nri.2016.70>)
- O'Shaughnessy, P. J., Pearce, S. & Mannan, M. A. 1990. Effect of high-density lipoprotein on bovine granulosa cells: progesterone production in newly isolated cells and during cell culture. *Journal of Endocrinology*, 124, 255-260. (<https://doi.org/10.1677/joe.0.1240255>)
- Oguejiofor, C. F., Cheng, Z., Abudureyimu, A., Fouladi-Nashta, A. A. & Wathes, D. C. 2015. Global transcriptomic profiling of bovine endometrial immune response in vitro. I. Effect of lipopolysaccharide on innate immunity. *Biology of Reproduction*, 93, 100. (<https://doi.org/10.1095/biolreprod.115.128868>)
- Oikawa, S. & Oetzel, G. R. 2006. Decreased Insulin Response in Dairy Cows Following a Four-Day Fast to Induce Hepatic Lipidosis. *Journal of Dairy Science*, 89, 2999-3005. ([https://doi.org/10.3168/jds.S0022-0302\(06\)72572-3](https://doi.org/10.3168/jds.S0022-0302(06)72572-3))
- Opsomer, G., Coryn, M., Deluyker, H. & Kruif, A. 1998. An Analysis of Ovarian Dysfunction in High Yielding Dairy Cows After Calving Based on Progesterone Profiles. *Reproduction in Domestic Animals*, 33, 193-204. (<https://doi.org/10.1111/j.1439-0531.1998.tb01342.x>)
- Opsomer, G., Grohn, Y. T., Hertl, J., Coryn, M., Deluyker, H. & De Kruif, A. 2000. Risk factors for post partum ovarian dysfunction in high producing dairy cows in Belgium: a field study. *Theriogenology*, 53, 841-857. ([https://doi.org/10.1016/S0093-691X\(00\)00234-X](https://doi.org/10.1016/S0093-691X(00)00234-X))
- Orisaka, M., Tajima, K., Tsang, B. K. & Kotsuji, F. 2009. Oocyte-granulosa-theca cell interactions during preantral follicular development. *Journal of Ovarian Research*, 2, 9. (<https://doi.org/10.1186/1757-2215-2-9>)

- Orly, J., Sato, G. & Erickson, G. F. 1980. Serum suppresses the expression of hormonally induced functions in cultured granulosa cells. *Cell*, 20, 817-827. ([https://doi.org/10.1016/0092-8674\(80\)90328-1](https://doi.org/10.1016/0092-8674(80)90328-1))
- Orsi, N. M., Gopichandran, N., Leese, H. J., Picton, H. M. & Harris, S. E. 2005. Fluctuations in bovine ovarian follicular fluid composition throughout the oestrous cycle. *Reproduction*, 129, 219-228. (<https://doi.org/10.1530/rep.1.00460>)
- Oshiro, N., Yoshino, K., Hidayat, S., Tokunaga, C., Hara, K., Eguchi, S., Avruch, J. & Yonezawa, K. 2004. Dissociation of raptor from mTOR is a mechanism of rapamycin-induced inhibition of mTOR function. *Genes to Cells*, 9, 359-366. (<https://doi.org/10.1111/j.1356-9597.2004.00727.x>)
- Ota, Y., Shimoya, K., Zhang, Q., Moriyama, A., Chin, R., Tenma, K., Kimura, T., Koyama, M., Azuma, C. & Murata, Y. 2002. The expression of secretory leukocyte protease inhibitor (SLPI) in the fallopian tube: SLPI protects the acrosome reaction of sperm from inhibitory effects of elastase. *Human Reproduction*, 17, 2517-2522. (<https://doi.org/10.1093/humrep/17.10.2517>)
- Ozturk, S. 2020. Selection of competent oocytes by morphological criteria for assisted reproductive technologies. *Molecular Reproduction and Development*, 87, 1021-1036. (<https://doi.org/10.1002/mrd.23420>)
- Pahl, H. L. 1999. Activators and target genes of Rel/NF-kappaB transcription factors. *Oncogene*, 18, 6853-6866. (<https://doi.org/10.1038/sj.onc.1203239>)
- Paiano, R. B., Goncalves, C. G. P., Mendes, J. P. G., Bonilla, J., Birgel, D. B. & Birgel Junior, E. H. 2019. Comparative biochemical profiles, production and reproduction status of the post-partum dairy cows with and without purulent vaginal discharge. *Reproduction in Domestic Animals*, 54, 1188-1194. (<https://doi.org/10.1111/rda.13496>)
- Passos, J. R., Costa, J. J., Da Cunha, E. V., Silva, A. W., Ribeiro, R. P., De Souza, G. B., Barroso, P. A., Dau, A. M., Saraiva, M. V., Goncalves, P. B., Van Den Hurk, R. & Silva, J. R. 2016. Protein and messenger RNA expression of interleukin 1 system members in bovine ovarian follicles and effects of interleukin 1beta on primordial follicle activation and survival in vitro. *Domestic Animal Endocrinology*, 54, 48-59. (<https://doi.org/10.1016/j.domaniend.2015.09.002>)
- Peter, A. T., Bosu, W. T. & Dedecker, R. J. 1989. Suppression of preovulatory luteinizing hormone surges in heifers after intrauterine infusions of Escherichia coli endotoxin. *American Journal of Veterinary Research*, 50, 368-373.
- Piersanti, R. L., Block, J., Ma, Z., Jeong, K. C., Santos, J. E. P., Yu, F., Sheldon, I. M. & Bromfield, J. J. 2020. Uterine infusion of bacteria alters the transcriptome of bovine oocytes. *FASEB bioAdvances*, 2, 506-520. (<https://doi.org/10.1096/fba.2020-00029>)
- Piersanti, R. L., Horlock, A. D., Block, J., Santos, J. E. P., Sheldon, I. M. & Bromfield, J. J. 2019a. Persistent effects on bovine granulosa cell transcriptome after resolution of uterine disease. *Reproduction*, 158, 35-46. (<https://doi.org/10.1530/REP-19-0037>)

Piersanti, R. L., Santos, J. E. P., Sheldon, I. M. & Bromfield, J. J. 2019b. Lipopolysaccharide and tumor necrosis factor-alpha alter gene expression of oocytes and cumulus cells during bovine in vitro maturation. *Molecular Reproduction and Development*, 86, 1909-1920. (<https://doi.org/10.1002/mrd.23288>)

Piersanti, R. L., Zimpel, R., Molinari, P. C. C., Dickson, M. J., Ma, Z., Jeong, K. C., Santos, J. E. P., Sheldon, I. M. & Bromfield, J. J. 2019c. A model of clinical endometritis in Holstein heifers using pathogenic *Escherichia coli* and *Trueperella pyogenes*. *Journal of Dairy Science*, 102, 2686-2697. (<https://doi.org/10.3168/jds.2018-15595>)

Pincus, G. & Enzmann, E. V. 1935. The Comparative Behavior of Mammalian Eggs in Vivo and in Vitro : I. The Activation of Ovarian Eggs. *Journal of Experimental Medicine*, 62, 665-675. (<https://doi.org/10.1084/jem.62.5.665>)

Plewes, M. R., Krause, C., Talbott, H. A., Przygodzka, E., Wood, J. R., Cupp, A. S. & Davis, J. S. 2020. Trafficking of cholesterol from lipid droplets to mitochondria in bovine luteal cells: Acute control of progesterone synthesis. *FASEB journal : official publication of the Federation of American Societies for Experimental Biology*, 34, 10731-10750. (<https://doi.org/10.1096/fj.202000671R>)

Poltorak, A., He, X., Smirnova, I., Liu, M. Y., Van Huffel, C., Du, X., Birdwell, D., Alejos, E., Silva, M., Galanos, C., Freudenberg, M., Ricciardi-Castagnoli, P., Layton, B. & Beutler, B. 1998. Defective LPS signaling in C3H/HeJ and C57BL/10ScCr mice: mutations in Tlr4 gene. *Science*, 282, 2085-2088. (<https://doi.org/10.1126/science.282.5396.2085>)

Pontillo, A., Paoluzzi, E. & Crovella, S. 2010. The inhibition of mevalonate pathway induces upregulation of NALP3 expression: new insight in the pathogenesis of mevalonate kinase deficiency. *European Journal of Human Genetics*, 18, 844-847. (<https://doi.org/10.1038/ejhg.2010.9>)

Pospiech, M., Owens, S. E., Miller, D. J., Austin-Muttitt, K., Mullins, J. G. L., Cronin, J. G., Allemann, R. K. & Sheldon, I. M. 2021. Bisphosphonate inhibitors of squalene synthase protect cells against cholesterol-dependent cytotoxins. *The FASEB Journal*, 35, e21640. (<https://doi.org/10.1096/fj.202100164R>)

Pratt, H. P. 1980. Phospholipid synthesis in the preimplantation mouse embryo. *Journal of Reproduction and Fertility*, 58, 237-248. (<https://doi.org/10.1530/jrf.0.0580237>)

Pratt, H. P., Keith, J. & Chakraborty, J. 1980. Membrane sterols and the development of the preimplantation mouse embryo. *Journal of Embryology and Experimental Morphology*, 60, 303-319.

Price, J. C., Bromfield, J. J. & Sheldon, I. M. 2013. Pathogen-associated molecular patterns initiate inflammation and perturb the endocrine function of bovine granulosa cells from ovarian dominant follicles via TLR2 and TLR4 pathways. *Endocrinology*, 154, 3377-3386. (<https://doi.org/10.1210/en.2013-1102>)

Price, J. C. & Sheldon, I. M. 2013. Granulosa cells from emerged antral follicles of the bovine ovary initiate inflammation in response to bacterial pathogen-associated

molecular patterns via Toll-like receptor pathways. *Biology of Reproduction*, 89, 119. (<https://doi.org/10.1095/biolreprod.113.110965>)

Pryce, J. E., Coffey, M. P. & Simm, G. 2001. The relationship between body condition score and reproductive performance. *Journal of Dairy Science*, 84, 1508-1515. ([https://doi.org/10.3168/jds.S0022-0302\(01\)70184-1](https://doi.org/10.3168/jds.S0022-0302(01)70184-1))

Purcell, S. H., Chi, M. M., Lanzendorf, S. & Moley, K. H. 2012. Insulin-stimulated glucose uptake occurs in specialized cells within the cumulus oocyte complex. *Endocrinology*, 153, 2444-2454. (<https://doi.org/10.1210/en.2011-1974>)

Quackenbush, J. 2001. Computational analysis of microarray data. *Nature Reviews Genetics*, 2, 418-427. (<https://doi.org/10.1038/35076576>)

Quiroz-Rocha, G. F., Leblanc, S., Duffield, T., Wood, D., Leslie, K. E. & Jacobs, R. M. 2009. Evaluation of prepartum serum cholesterol and fatty acids concentrations as predictors of postpartum retention of the placenta in dairy cows. *Journal of the American Veterinary Medical Association*, 234, 790-793. (<https://doi.org/10.2460/javma.234.6.790>)

Rae, M. T., Niven, D., Ross, A., Forster, T., Lathe, R., Critchley, H. O. D., Ghazal, P. & Hillier, S. G. 2004. Steroid signalling in human ovarian surface epithelial cells: the response to interleukin-1 $\alpha$  determined by microarray analysis. *Journal of Endocrinology*, 183, 19-28. (<https://doi.org/10.1677/joe.1.05754>)

Rajapaksha, W. R., McBride, M., Robertson, L. & O'shaughnessy, P. J. 1997. Sequence of the bovine HDL-receptor (SR-BI) cDNA and changes in receptor mRNA expression during granulosa cell luteinization in vivo and in vitro. *Molecular Cell Endocrinology*, 134, 59-67. ([https://doi.org/10.1016/s0303-7207\(97\)00173-1](https://doi.org/10.1016/s0303-7207(97)00173-1))

Rankin, T. L., O'brien, M., Lee, E., Wigglesworth, K., Eppig, J. & Dean, J. 2001. Defective zonae pellucidae in Zp2-null mice disrupt folliculogenesis, fertility and development. *Development*, 128, 1119-1126. (<https://doi.org/10.1242/dev.128.7.1119>)

Rashid, M. M., Runci, A., Polletta, L., Carnevale, I., Morgante, E., Foglio, E., Arcangeli, T., Sansone, L., Russo, M. A. & Tafani, M. 2015. Muscle LIM protein/CSRP3: a mechanosensor with a role in autophagy. *Cell Death Discovery*, 1, 15014. (<https://doi.org/10.1038/cddiscovery.2015.14>)

Reaven, E., Tsai, L. & Azhar, S. 1995. Cholesterol uptake by the 'selective' pathway of ovarian granulosa cells: early intracellular events. *Journal of Lipid Research*, 36, 1602-1617. ([https://doi.org/10.1016/S0022-2275\(20\)39746-7](https://doi.org/10.1016/S0022-2275(20)39746-7))

Revelli, A., Delle Piane, L., Casano, S., Molinari, E., Massobrio, M. & Rinaudo, P. 2009. Follicular fluid content and oocyte quality: from single biochemical markers to metabolomics. *Reproductive biology and endocrinology : RB&E*, 7, 40-40. (<https://doi.org/10.1186/1477-7827-7-40>)

Reverchon, M., Bertoldo, M. J., Ramé, C., Froment, P. & Dupont, J. 2014. CHEMERIN (RARRES2) Decreases In Vitro Granulosa Cell Steroidogenesis and

Blocks Oocyte Meiotic Progression in Bovine Species1. *Biology of Reproduction*, 90. (<https://doi.org/10.1095/biolreprod.113.117044>)

Ribeiro, E. S., Gomes, G., Greco, L. F., Cerri, R. L. A., Vieira-Neto, A., Monteiro, P. L. J., Jr., Lima, F. S., Bisinotto, R. S., Thatcher, W. W. & Santos, J. E. P. 2016. Carryover effect of postpartum inflammatory diseases on developmental biology and fertility in lactating dairy cows. *Journal of Dairy Science*, 99, 2201-2220. (<https://doi.org/10.3168/jds.2015-10337>)

Ribeiro, E. S., Lima, F. S., Greco, L. F., Bisinotto, R. S., Monteiro, A. P., Favoreto, M., Ayres, H., Marsola, R. S., Martinez, N., Thatcher, W. W. & Santos, J. E. 2013. Prevalence of periparturient diseases and effects on fertility of seasonally calving grazing dairy cows supplemented with concentrates. *Journal of Dairy Science*, 96, 5682-5697. (<https://doi.org/10.3168/jds.2012-6335>)

Richards, J. S. 1994. Hormonal control of gene expression in the ovary. *Endocrine Reviews*, 15, 725-751. (<https://doi.org/10.1210/edrv-15-6-725>)

Richards, J. S., Liu, Z. & Shimada, M. 2008. Immune-like mechanisms in ovulation. *Trends in Endocrinology & Metabolism*, 19, 191-196. (<https://doi.org/10.1016/j.tem.2008.03.001>)

Richards, J. S. & Pangas, S. A. 2010. The ovary: basic biology and clinical implications. *Journal of Clinical Investigation*, 120, 963-972. (<https://doi.org/10.1172/JCI41350>)

Riera Romo, M., Pérez-Martínez, D. & Castillo Ferrer, C. 2016. Innate immunity in vertebrates: an overview. *Immunology*, 148, 125-139. (<https://doi.org/10.1111/imm.12597>)

Roberts, A. J. & Echtenkamp, S. E. 1994. In vitro production of estradiol by bovine granulosa cells: evaluation of culture condition, stage of follicular development, and location of cells within follicles. *Biology of Reproduction*, 51, 273-282. (<https://doi.org/10.1095/biolreprod51.2.273>)

Robker, R. L., Russell, D. L., Espey, L. L., Lydon, J. P., O'malley, B. W. & Richards, J. S. 2000. Progesterone-regulated genes in the ovulation process: ADAMTS-1 and cathepsin L proteases. *Proceedings of the National Academy of Sciences of the United States of America*, 97, 4689-4694. (<https://doi.org/10.1073/pnas.080073497>)

Roche, J. R., Macdonald, K. A., Schütz, K. E., Matthews, L. R., Verkerk, G. A., Meier, S., Loor, J. J., Rogers, A. R., McGowan, J., Morgan, S. R., Taukiri, S. & Webster, J. R. 2013. Calving body condition score affects indicators of health in grazing dairy cows. *Journal of Dairy Science*, 96, 5811-5825. (<https://doi.org/10.3168/jds.2013-6600>)

Rosnet, O., Blanco-Betancourt, C., Grivel, K., Richter, K. & Schiff, C. 2004. Binding of free immunoglobulin light chains to VpreB3 inhibits their maturation and secretion in chicken B cells. *Journal of Biological Chemistry*, 279, 10228-10236. (<https://doi.org/10.1074/jbc.M312169-A200>)

- Roth, Z., Dvir, A., Furman, O., Lavon, Y., Kalo, D., Leitner, G. & Wolfenson, D. 2020. Oocyte maturation in plasma or follicular fluid obtained from lipopolysaccharide-treated cows disrupts its developmental competence. *Theriogenology*, 141, 120-127. (<https://doi.org/10.1016/j.theriogenology.2019.09.021>)
- Ruegg, P. L., Goodger, W. J., Holmberg, C. A., Weaver, L. D. & Huffman, E. M. 1992. Relation among body condition score, serum urea nitrogen and cholesterol concentrations, and reproductive performance in high-producing Holstein dairy cows in early lactation. *American Journal of Veterinary Research*, 53, 10-14.
- Ruland, J. 2008. CARD9 signaling in the innate immune response. *Annals of the New York Academy of Sciences*, 1143, 35-44. (<https://doi.org/10.1196/annals.1443.024>)
- Rung, E., Friberg, P. A., Shao, R., Larsson, D. G., Nielsen, E., Svensson, P. A., Carlsson, B., Carlsson, L. M. & Billig, H. 2005. Progesterone-receptor antagonists and statins decrease de novo cholesterol synthesis and increase apoptosis in rat and human periovulatory granulosa cells in vitro. *Biology of Reproduction*, 72, 538-545. (<https://doi.org/10.1095/biolreprod.104.033878>)
- Russell, D. L. & Robker, R. L. 2007. Molecular mechanisms of ovulation: coordination through the cumulus complex. *Human reproduction update*, 13, 289-312. (<https://doi.org/10.1093/humupd/dml062>)
- Ryan, D. G., Murphy, M. P., Frezza, C., Prag, H. A., Chouchani, E. T., O'neill, L. A. & Mills, E. L. 2019. Coupling Krebs cycle metabolites to signalling in immunity and cancer. *Nature Metabolism*, 1, 16-33. (<https://doi.org/10.1038/s42255-018-0014-7>)
- Ryan, K. J., Petro, Z. & Kaiser, J. 1968. Steroid Formation by Isolated and Recombined Ovarian Granulosa and Thecal Cells. *The Journal of Clinical Endocrinology & Metabolism*, 28, 355-358. (<https://doi.org/10.1210/jcem-28-3-355>)
- Salustri, A., Yanagishita, M. & Hascall, V. C. 1989. Synthesis and accumulation of hyaluronic acid and proteoglycans in the mouse cumulus cell-oocyte complex during follicle-stimulating hormone-induced mucification. *Journal of Biological Chemistry*, 264, 13840-13847. ([https://doi.org/10.1016/S0021-9258\(18\)80077-1](https://doi.org/10.1016/S0021-9258(18)80077-1))
- Sanfins, A., Rodrigues, P. & Albertini, D. F. 2018. GDF-9 and BMP-15 direct the follicle symphony. *Journal of Assisted Reproduction and Genetics*, 35, 1741-1750. (<https://doi.org/10.1007/s10815-018-1268-4>)
- Santiquet, N., Sasseville, M., Laforest, M., Guillemette, C., Gilchrist, R. B. & Richard, F. J. 2014. Activation of 5' adenosine monophosphate-activated protein kinase blocks cumulus cell expansion through inhibition of protein synthesis during in vitro maturation in Swine. *Biology of Reproduction*, 91, 51. (<https://doi.org/10.1095/biolreprod.113.116764>)
- Santos, N. R., Lamb, G. C., Brown, D. R. & Gilbert, R. O. 2009. Postpartum endometrial cytology in beef cows. *Theriogenology*, 71, 739-745. (<https://doi.org/10.1016/j.theriogenology.2008.09.043>)

- Sarbassov, D. D., Ali, S. M., Kim, D. H., Guertin, D. A., Latek, R. R., Erdjument-Bromage, H., Tempst, P. & Sabatini, D. M. 2004. Rictor, a novel binding partner of mTOR, defines a rapamycin-insensitive and raptor-independent pathway that regulates the cytoskeleton. *Current Biology*, 14, 1296-1302. (<https://doi.org/10.1016/j.cub.2004.06.054>)
- Savio, J. D., Keenan, L., Boland, M. P. & Roche, J. F. 1988. Pattern of growth of dominant follicles during the oestrous cycle of heifers. *Reproduction*, 83, 663-671. (<https://doi.org/10.1530/jrf.0.0830663>)
- Savion, N., Laherty, R., Cohen, D., Lui, G. M. & Gospodarowicz, D. 1982. Role of lipoproteins and 3-hydroxy-3-methylglutaryl coenzyme A reductase in progesterone production by cultured bovine granulosa cells. *Endocrinology*, 110, 13-22. (<https://doi.org/10.1210/endo-110-1-13>)
- Savion, N., Laherty, R., Lui, G. M. & Gospodarowicz, D. 1981. Modulation of low density lipoprotein metabolism in bovine granulosa cells as a function of their steroidogenic activity. *Journal of Biological Chemistry*, 256, 12817-12822. ([http://doi.org/10.1016/S0021-9258\(18\)42968-7](http://doi.org/10.1016/S0021-9258(18)42968-7))
- Sawyer, H. R., Smith, P., Heath, D. A., Juengel, J. L., Wakefield, S. J. & McNatty, K. P. 2002. Formation of ovarian follicles during fetal development in sheep. *Biology of Reproduction*, 66, 1134-1150. (<https://doi.org/10.1095/biolreprod66.4.1134>)
- Scaramuzzi, R. J., Baird, D. T., Campbell, B. K., Driancourt, M. A., Dupont, J., Fortune, J. E., Gilchrist, R. B., Martin, G. B., McNatty, K. P., Mcneilly, A. S., Monget, P., Monniaux, D., Vinales, C. & Webb, R. 2011. Regulation of folliculogenesis and the determination of ovulation rate in ruminants. *Reproduction Fertility and Development*, 23, 444-467. (<https://doi.org/10.1071/RD09161>)
- Schindelin, J., Arganda-Carreras, I., Frise, E., Kaynig, V., Longair, M., Pietzsch, T., Preibisch, S., Rueden, C., Saalfeld, S., Schmid, B., Tinevez, J. Y., White, D. J., Hartenstein, V., Eliceiri, K., Tomancak, P. & Cardona, A. 2012. Fiji: an open-source platform for biological-image analysis. *Nature Methods*, 9, 676-682. (<https://doi.org/10.1038/nmeth.2019>)
- Schroepfer, G. J., Jr. 2000. Oxysterols: modulators of cholesterol metabolism and other processes. *Physiological Reviews*, 80, 361-554. (<https://doi.org/10.1152/physrev.2000.80.1.361>)
- Semrau, S., Idema, T., Schmidt, T. & Storm, C. 2009. Membrane-mediated interactions measured using membrane domains. *Biophysical Journal*, 96, 4906-4915. (<https://doi.org/10.1016/j.bpj.2009.03.050>)
- Sepulveda-Varas, P., Weary, D. M., Noro, M. & Von Keyserlingk, M. A. 2015. Transition diseases in grazing dairy cows are related to serum cholesterol and other analytes. *PLoS One*, 10, e0122317. (<https://doi.org/10.1371/journal.pone.0122317>)
- Shabankareh, H. K., Kor, N. M. & Hajarian, H. 2013. The influence of the corpus luteum on metabolites composition of follicular fluid from different sized follicles and their relationship to serum concentrations in dairy cows. *Animal Reproduction Science*, 140, 109-114. (<https://doi.org/10.1016/j.anireprosci.2013.06.018>)



- Shalgi, R., Kraicer, P., Rimon, A., Pinto, M. & Soferman, N. 1973. Proteins of human follicular fluid: the blood-follicle barrier. *Fertility and Sterility*, 24, 429-434. ([https://doi.org/10.1016/S0015-0282\(16\)39730-8](https://doi.org/10.1016/S0015-0282(16)39730-8))
- Sharpe, L. J. & Brown, A. J. 2013. Controlling cholesterol synthesis beyond 3-hydroxy-3-methylglutaryl-CoA reductase (HMGCR). *Journal of Biological Chemistry*, 288, 18707-18715. (<https://doi.org/10.1074/jbc.R113.479808>)
- Sheldon, I. M. 2020. Diagnosing postpartum endometritis in dairy cattle. *Veterinary Record*, 186, 88-90. (<https://doi.org/10.1136/vr.m222>)
- Sheldon, I. M., Cronin, J., Goetze, L., Donofrio, G. & Schuberth, H. J. 2009. Defining postpartum uterine disease and the mechanisms of infection and immunity in the female reproductive tract in cattle. *Biology of Reproduction*, 81, 1025-1032. (<https://doi.org/10.1095/biolreprod.109.077370>)
- Sheldon, I. M., Cronin, J. G. & Bromfield, J. J. 2019a. Tolerance and Innate Immunity Shape the Development of Postpartum Uterine Disease and the Impact of Endometritis in Dairy Cattle. *Annual Review of Animal Biosciences*, 7, 361-384. (<https://doi.org/10.1146/annurev-animal-020518-115227>)
- Sheldon, I. M., Cronin, J. G., Pospiech, M. & Turner, M. L. 2018. Symposium review: Mechanisms linking metabolic stress with innate immunity in the endometrium. *Journal of Dairy Science*, 101, 3655-3664. (<https://doi.org/10.3168/jds.2017-13135>)
- Sheldon, I. M., Molinari, P. C. C., Ormsby, T. J. R. & Bromfield, J. J. 2020. Preventing postpartum uterine disease in dairy cattle depends on avoiding, tolerating and resisting pathogenic bacteria. *Theriogenology*, 150, 158-165. (<https://doi.org/10.1016/j.theriogenology.2020.01.017>)
- Sheldon, I. M., Noakes, D. E., Rycroft, A. N., Pfeiffer, D. U. & Dobson, H. 2002. Influence of uterine bacterial contamination after parturition on ovarian dominant follicle selection and follicle growth and function in cattle. *Reproduction*, 123, 837-845. (<https://doi.org/10.1530/rep.0.1230837>)
- Sheldon, I. M., Price, J. C., Turner, M. L., Bromfield, J. J. & Cronin, G. 2019b. Uterine infection and immunity in cattle. *Bioscientifica Proceedings*, 415-430. (<https://doi.org/10.1530/biosciproc.8.029>)
- Sheldon, I. M., Rycroft, A. N., Dogan, B., Craven, M., Bromfield, J. J., Chandler, A., Roberts, M. H., Price, S. B., Gilbert, R. O. & Simpson, K. W. 2010. Specific strains of *Escherichia coli* are pathogenic for the endometrium of cattle and cause pelvic inflammatory disease in cattle and mice. *PLoS One*, 5, e9192. (<https://doi.org/10.1371/journal.pone.0009192>)
- Shen, M., Jiang, Y., Guan, Z., Cao, Y., Li, L., Liu, H. & Sun, S. C. 2017. Protective mechanism of FSH against oxidative damage in mouse ovarian granulosa cells by repressing autophagy. *Autophagy*, 13, 1364-1385. (<https://doi.org/10.1080/15548627.2017.1327941>)

Shen, W.-J., Asthana, S., Kraemer, F. B. & Azhar, S. 2018. Scavenger receptor B type 1: expression, molecular regulation, and cholesterol transport function. *Journal of Lipid Research*, 59, 1114-1131. (<https://doi.org/10.1194/jlr.R083121>)

Shen, W. J., Hu, J., Hu, Z., Kraemer, F. B. & Azhar, S. 2014. Scavenger receptor class B type I (SR-BI): a versatile receptor with multiple functions and actions. *Metabolism*, 63, 875-886. (<https://doi.org/10.1016/j.metabol.2014.03.011>)

Shimada, M., Hernandez-Gonzalez, I., Gonzalez-Robanya, I. & Richards, J. S. 2006. Induced expression of pattern recognition receptors in cumulus oocyte complexes: novel evidence for innate immune-like functions during ovulation. *Molecular Endocrinology*, 20, 3228-3239. (<https://doi.org/10.1210/me.2006-0194>)

Shimada, M., Yanai, Y., Okazaki, T., Noma, N., Kawashima, I., Mori, T. & Richards, J. S. 2008. Hyaluronan fragments generated by sperm-secreted hyaluronidase stimulate cytokine/chemokine production via the TLR2 and TLR4 pathway in cumulus cells of ovulated COCs, which may enhance fertilization. *Development*, 135, 2001-2011. (<https://doi.org/10.1242/dev.020461>)

Shimizu, K., Sato, Y., Kawamura, M., Nakazato, H., Watanabe, T., Ohara, O. & Fujii, S. I. 2019. Eomes transcription factor is required for the development and differentiation of invariant NKT cells. *Communications Biology*, 2, 150. (<https://doi.org/10.1038/s42003-019-0389-3>)

Shimizu, T., Kaji, A., Murayama, C., Magata, F., Shirasuna, K., Wakamiya, K., Okuda, K. & Miyamoto, A. 2012a. Effects of interleukin-8 on estradiol and progesterone production by bovine granulosa cells from large follicles and progesterone production by luteinizing granulosa cells in culture. *Cytokine*, 57, 175-181. (<https://doi.org/10.1016/j.cyto.2011.11.007>)

Shimizu, T., Miyauchi, K., Shirasuna, K., Bollwein, H., Magata, F., Murayama, C. & Miyamoto, A. 2012b. Effects of lipopolysaccharide (LPS) and peptidoglycan (PGN) on estradiol production in bovine granulosa cells from small and large follicles. *Toxicology In Vitro*, 26, 1134-1142. (<https://doi.org/10.1016/j.tiv.2012.06.014>)

Shozu, M., Minami, N., Yokoyama, H., Inoue, M., Kurihara, H., Matsushima, K. & Kuno, K. 2005. ADAMTS-1 is involved in normal follicular development, ovulatory process and organization of the medullary vascular network in the ovary. *Journal of Molecular Endocrinology*, 35, 343-355. (<https://doi.org/10.1677/jme.1.01735>)

Silhavy, T. J., Kahne, D. & Walker, S. 2010. The bacterial cell envelope. *Cold Spring Harbor perspectives in biology*, 2, a000414-a000414. (<https://doi.org/10.1101/cshperspect.a000414>)

Simón, C., Tsafiriri, A., Chun, S. Y., Piquette, G. N., Dang, W. & Polan, M. L. 1994. Interleukin-1 receptor antagonist suppresses human chorionic gonadotropin-induced ovulation in the rat. *Biology of Reproduction*, 51, 662-667. (<https://doi.org/10.1095/biolreprod51.4.662>)

Simpson, E. R., Rochelle, D. B., Carr, B. R. & Macdonald, P. C. 1980. Plasma lipoproteins in follicular fluid of human ovaries. *The Journal of Clinical*

*Endocrinology and Metabolism*, 51, 1469-1471. (<https://doi.org/10.1210/jcem-51-6-1469>)

Sinensky, M. & Logel, J. 1985. Defective macromolecule biosynthesis and cell-cycle progression in a mammalian cell starved for mevalonate. *Proceedings of the National Academy of Sciences of the United States of America*, 82, 3257-3261. (<https://doi.org/10.1073/pnas.82.10.3257>)

Siperstein, M. D. 1984. Role of cholesterologenesis and isoprenoid synthesis in DNA replication and cell growth. *Journal of Lipid Research*, 25, 1462-1468. ([https://doi.org/10.1016/S0022-2275\(20\)34419-9](https://doi.org/10.1016/S0022-2275(20)34419-9))

Sirard, M.-A. 2017. The Ovarian Follicle of Cows as a Model for Human. *Animal Models and Human Reproduction*. (<https://doi.org/10.1002/9781118881286.ch6>)

Sirard, M. A., Florman, H. M., Leibfried-Rutledge, M. L., Barnes, F. L., Sims, M. L. & First, N. L. 1989. Timing of nuclear progression and protein synthesis necessary for meiotic maturation of bovine oocytes. *Biology of Reproduction*, 40, 1257-1263. (<https://doi.org/10.1095/biolreprod40.6.1257>)

Sirard, M. A., Richard, F., Blondin, P. & Robert, C. 2006. Contribution of the oocyte to embryo quality. *Theriogenology*, 65, 126-136. (<https://doi.org/10.1016/j.theriogenology.2005.09.020>)

Sirois, J. & Fortune, J. E. 1988. Ovarian Follicular Dynamics during the Estrous Cycle in Heifers Monitored by Real-Time Ultrasonograph1. *Biology of Reproduction*, 39, 308-317. (<https://doi.org/10.1095/biolreprod39.2.308>)

Sorensen, R. A. & Wassarman, P. M. 1976. Relationship between growth and meiotic maturation of the mouse oocyte. *Developmental Biology*, 50, 531-536. ([https://doi.org/10.1016/0012-1606\(76\)90172-x](https://doi.org/10.1016/0012-1606(76)90172-x))

Spanel-Borowski, K., Rahner, P. & Ricken, A. M. 1997. Immunolocalization of CD18-positive cells in the bovine ovary. *Journal of Reproduction and Fertility*, 111, 197-205. (<https://doi.org/10.1530/jrf.0.1110197>)

Spicer, L. J. & Alpizar, E. 1994. Effects of cytokines on FSH-induced estradiol production by bovine granulosa cells in vitro: dependence on size of follicle. *Domestic Animal Endocrinology*, 11, 25-34. ([https://doi.org/10.1016/0739-7240\(94\)90034-5](https://doi.org/10.1016/0739-7240(94)90034-5))

Spicer, L. J., Chamberlain, C. S. & Maciel, S. M. 2002. Influence of gonadotropins on insulin- and insulin-like growth factor-I (IGF-I)-induced steroid production by bovine granulosa cells. *Domestic Animal Endocrinology*, 22, 237-254. ([https://doi.org/10.1016/S0739-7240\(02\)00125-X](https://doi.org/10.1016/S0739-7240(02)00125-X))

Stojkov, J., Von Keyserlingk, M. A., Marchant-Forde, J. N. & Weary, D. M. 2015. Assessment of visceral pain associated with metritis in dairy cows. *Journal of Dairy Science*, 98, 5352-5361. (<https://doi.org/10.3168/jds.2014-9296>)

Stojkovic, M., Machado, S. A., Stojkovic, P., Zakhartchenko, V., Hutzler, P., Goncalves, P. B. & Wolf, E. 2001. Mitochondrial distribution and adenosine triphosphate content of bovine oocytes before and after in vitro maturation: correlation

with morphological criteria and developmental capacity after in vitro fertilization and culture. *Biology of Reproduction*, 64, 904-909. (<https://doi.org/10.1095/biolreprod64.3.904>)

Su, Y.-Q., Sugiura, K., Wigglesworth, K., O'Brien, M. J., Affourtit, J. P., Pangas, S. A., Matzuk, M. M. & Eppig, J. J. 2008. Oocyte regulation of metabolic cooperativity between mouse cumulus cells and oocytes: BMP15 and GDF9 control cholesterol biosynthesis in cumulus cells. *Development*, 135, 111-121. (<https://doi.org/10.1242/dev.009068>)

Su, Y. Q., Sugiura, K. & Eppig, J. J. 2009. Mouse oocyte control of granulosa cell development and function: paracrine regulation of cumulus cell metabolism. *Seminars in Reproductive Medicine*, 27, 32-42. (<https://doi.org/10.1055/s-0028-1108008>)

Sugiura, K., Pendola, F. L. & Eppig, J. J. 2005. Oocyte control of metabolic cooperativity between oocytes and companion granulosa cells: energy metabolism. *Developmental Biology*, 279, 20-30. (<https://doi.org/10.1016/j.ydbio.2004.11.027>)

Sugiura, K., Su, Y. Q., Diaz, F. J., Pangas, S. A., Sharma, S., Wigglesworth, K., O'Brien, M. J., Matzuk, M. M., Shimasaki, S. & Eppig, J. J. 2007. Oocyte-derived BMP15 and FGFs cooperate to promote glycolysis in cumulus cells. *Development*, 134, 2593-2603. (<https://doi.org/10.1242/dev.006882>)

Sun, D. & Fernandes, G. 2003. Lovastatin inhibits bone marrow-derived dendritic cell maturation and upregulates proinflammatory cytokine production. *Cell Immunology*, 223, 52-62. ([https://doi.org/10.1016/s0008-8749\(03\)00148-5](https://doi.org/10.1016/s0008-8749(03)00148-5))

Surani, M. A., Kimber, S. J. & Osborn, J. C. 1983. Mevalonate reverses the developmental arrest of preimplantation mouse embryos by Compactin, an inhibitor of HMG Co A reductase. *Journal of Embryology and Experimental Morphology*, 75, 205-223.

Sutton, M. L., Cetica, P. D., Beconi, M. T., Kind, K. L., Gilchrist, R. B. & Thompson, J. G. 2003. Influence of oocyte-secreted factors and culture duration on the metabolic activity of bovine cumulus cell complexes. *Reproduction*, 126, 27-34. (<https://doi.org/10.1530/rep.0.1260027>)

Sutton-Mcdowall, M. L., Gilchrist, R. B. & Thompson, J. G. 2004. Cumulus expansion and glucose utilisation by bovine cumulus-oocyte complexes during in vitro maturation: the influence of glucosamine and follicle-stimulating hormone. *Reproduction*, 128, 313-319. (<https://doi.org/10.1530/rep.1.00225>)

Sutton-Mcdowall, M. L., Gilchrist, R. B. & Thompson, J. G. 2005. Effect of hexoses and gonadotrophin supplementation on bovine oocyte nuclear maturation during in vitro maturation in a synthetic follicle fluid medium. *Reproduction, Fertility and Development*, 17, 407-415. (<https://doi.org/10.1071/rd04135>)

Sutton-Mcdowall, M. L., Gilchrist, R. B. & Thompson, J. G. 2010. The pivotal role of glucose metabolism in determining oocyte developmental competence. *Reproduction*, 139, 685-695. (<https://doi.org/10.1530/REP-09-0345>)

- Suzuki, K., Watanabe, T., Sakurai, S., Ohtake, K., Kinoshita, T., Araki, A., Fujita, T., Takei, H., Takeda, Y., Sato, Y., Yamashita, T., Araki, Y. & Sendo, F. 1999. A novel glycosylphosphatidyl inositol-anchored protein on human leukocytes: a possible role for regulation of neutrophil adherence and migration. *Journal of Immunology*, 162, 4277-4284.
- Takehara, Y., Dharmarajan, A. M., Kaufman, G. & Wallach, E. E. 1994. Effect of interleukin-1 beta on ovulation in the in vitro perfused rabbit ovary. *Endocrinology*, 134, 1788-1793. (<https://doi.org/10.1210/endo.134.4.8137743>)
- Takeuchi, O. & Akira, S. 2010. Pattern Recognition Receptors and Inflammation. *Cell*, 140, 805-820. (<https://doi.org/10.1016/j.cell.2010.01.022>)
- Tall, A. R. & Yvan-Charvet, L. 2015. Cholesterol, inflammation and innate immunity. *Nature Reviews Immunology*, 15, 104-116. (<https://doi.org/10.1038/nri3793>)
- Tannahill, G. M., Curtis, A. M., Adamik, J., Palsson-Mcdermott, E. M., McGettrick, A. F., Goel, G., Frezza, C., Bernard, N. J., Kelly, B., Foley, N. H., Zheng, L., Gardet, A., Tong, Z., Jany, S. S., Corr, S. C., Haneklaus, M., Caffrey, B. E., Pierce, K., Walmsley, S., Beasley, F. C., Cummins, E., Nizet, V., Whyte, M., Taylor, C. T., Lin, H., Masters, S. L., Gottlieb, E., Kelly, V. P., Clish, C., Auron, P. E., Xavier, R. J. & O'Neill, L. A. 2013. Succinate is an inflammatory signal that induces IL-1beta through HIF-1alpha. *Nature*, 496, 238-242. (<https://doi.org/10.1038/nature11986>)
- Terranova, P. F. & Rice, V. M. 1997. Review: Cytokine Involvement in Ovarian Processes. *American Journal of Reproductive Immunology*, 37, 50-63. (<https://doi.org/10.1111/j.1600-0897.1997.tb00192.x>)
- Thompson, P. A. & Kitchens, R. L. 2006. Native high-density lipoprotein augments monocyte responses to lipopolysaccharide (LPS) by suppressing the inhibitory activity of LPS-binding protein. *Journal of Immunology*, 177, 4880-4887. (<https://doi.org/10.4049/jimmunol.177.7.4880>)
- Thoreen, C. C., Kang, S. A., Chang, J. W., Liu, Q., Zhang, J., Gao, Y., Reichling, L. J., Sim, T., Sabatini, D. M. & Gray, N. S. 2009. An ATP-competitive mammalian target of rapamycin inhibitor reveals rapamycin-resistant functions of mTORC1. *Journal of Biological Chemistry*, 284, 8023-8032. (<https://doi.org/10.1074/jbc.M900301200>)
- Tobias, P. S., Soldau, K. & Ulevitch, R. J. 1986. Isolation of a lipopolysaccharide-binding acute phase reactant from rabbit serum. *The Journal of experimental medicine*, 164, 777-793. (<https://doi.org/10.1084/jem.164.3.777>)
- Tosca, L., Chabrolle, C., Uzbekova, S. & Dupont, J. 2007a. Effects of metformin on bovine granulosa cells steroidogenesis: possible involvement of adenosine 5' monophosphate-activated protein kinase (AMPK). *Biology of Reproduction*, 76, 368-378. (<https://doi.org/10.1095/biolreprod.106.055749>)
- Tosca, L., Crochet, S., Ferre, P., Fougelle, F., Tesseraud, S. & Dupont, J. 2006. AMP-activated protein kinase activation modulates progesterone secretion in granulosa cells from hen preovulatory follicles. *Journal of Endocrinology*, 190, 85-97. (<https://doi.org/10.1677/joe.1.06828>)

- Tosca, L., Froment, P., Solnais, P., Ferre, P., Fougelle, F. & Dupont, J. 2005. Adenosine 5'-monophosphate-activated protein kinase regulates progesterone secretion in rat granulosa cells. *Endocrinology*, 146, 4500-4513. (<https://doi.org/10.1210/en.2005-0301>)
- Tosca, L., Rame, C., Chabrolle, C., Tesseraud, S. & Dupont, J. 2010. Metformin decreases IGF1-induced cell proliferation and protein synthesis through AMP-activated protein kinase in cultured bovine granulosa cells. *Reproduction*, 139, 409-418. (<https://doi.org/10.1530/REP-09-0351>)
- Tosca, L., Uzbekova, S., Chabrolle, C. & Dupont, J. 2007b. Possible role of 5'AMP-activated protein kinase in the metformin-mediated arrest of bovine oocytes at the germinal vesicle stage during in vitro maturation. *Biology of Reproduction*, 77, 452-465. (<https://doi.org/10.1095/biolreprod.107.060848>)
- Triantafilou, M., Miyake, K., Golenbock, D. T. & Triantafilou, K. 2002. Mediators of innate immune recognition of bacteria concentrate in lipid rafts and facilitate lipopolysaccharide-induced cell activation. *Journal of Cell Science*, 115, 2603-2611. (<https://doi.org/10.1242/jcs.115.12.2603>)
- Trigatti, B., Rayburn, H., Viñals, M., Braun, A., Miettinen, H., Penman, M., Hertz, M., Schrenzel, M., Amigo, L., Rigotti, A. & Krieger, M. 1999. Influence of the high density lipoprotein receptor SR-BI on reproductive and cardiovascular pathophysiology. *Proceedings of the National Academy of Sciences of the United States of America*, 96, 9322-9327. (<https://doi.org/10.1073/pnas.96.16.9322>)
- Turner, J. E., Minkoff, C. G., Martin, K. H., Misra, R. & Swenson, K. I. 1995. Oocyte activation and passage through the metaphase/anaphase transition of the meiotic cell cycle is blocked in clams by inhibitors of HMG-CoA reductase activity. *Journal of Cell Biology*, 128, 1145-1162. (<https://doi.org/10.1083/jcb.128.6.1145>)
- Turner, M. D., Nedjai, B., Hurst, T. & Pennington, D. J. 2014a. Cytokines and chemokines: At the crossroads of cell signalling and inflammatory disease. *Biochimica et Biophysica Acta*, 1843, 2563-2582. (<https://doi.org/10.1016/j.bbamcr.2014.05.014>)
- Turner, M. L., Cronin, J. G., Healey, G. D. & Sheldon, I. M. 2014b. Epithelial and stromal cells of bovine endometrium have roles in innate immunity and initiate inflammatory responses to bacterial lipopeptides in vitro via Toll-like receptors TLR2, TLR1, and TLR6. *Endocrinology*, 155, 1453-1465. (<https://doi.org/10.1210/en.2013-1822>)
- Turner, M. L., Cronin, J. G., Noletto, P. G. & Sheldon, I. M. 2016. Glucose Availability and AMP-Activated Protein Kinase Link Energy Metabolism and Innate Immunity in the Bovine Endometrium. *PLoS One*, 11, e0151416. (<https://doi.org/10.1371/journal.pone.0151416>)
- Uematsu, S., Matsumoto, M., Takeda, K. & Akira, S. 2002. Lipopolysaccharide-Dependent Prostaglandin E2 Production Is Regulated by the Glutathione-Dependent Prostaglandin E2 Synthase Gene Induced by the Toll-Like Receptor 4/MyD88/NF-IL6 Pathway. *The Journal of Immunology*, 168, 5811-5816. (<https://doi.org/10.4049/jimmunol.168.11.5811>)

Uri-Belapolsky, S., Shaish, A., Eliyahu, E., Grossman, H., Levi, M., Chuderland, D., Ninio-Many, L., Hasky, N., Shashar, D., Almog, T., Kandel-Kfir, M., Harats, D., Shalgi, R. & Kamari, Y. 2014. Interleukin-1 deficiency prolongs ovarian lifespan in mice. *Proceedings of the National Academy of Sciences of the United States of America*, 111, 12492-12497. (<https://doi.org/10.1073/pnas.1323955111>)

Valckx, S. D. M., De Bie, J., Michiels, E. D., Goovaerts, I. G., Punjabi, U., Ramos-Ibeas, P., Gutierrez-Adan, A., Bols, P. E. & Leroy, J. L. 2015. The effect of human follicular fluid on bovine oocyte developmental competence and embryo quality. *Reproductive BioMedicine Online*, 30, 203-207. (<https://doi.org/10.1016/j.rbmo.2014.10.008>)

Van Der Vorst, E. P. C., Theodorou, K., Wu, Y., Hoeksema, M. A., Goossens, P., Bursill, C. A., Aliyev, T., Huitema, L. F. A., Tas, S. W., Wolfs, I. M. J., Kuijpers, M. J. E., Gijbels, M. J., Schalkwijk, C. G., Koonen, D. P. Y., Abdollahi-Roodsaz, S., Mcdaniels, K., Wang, C. C., Leitges, M., Lawrence, T., Plat, J., Van Eck, M., Rye, K. A., Touqui, L., De Winther, M. P. J., Biessen, E. a. L. & Donners, M. 2017. High-Density Lipoproteins Exert Pro-inflammatory Effects on Macrophages via Passive Cholesterol Depletion and PKC-NF-kappaB/STAT1-IRF1 Signaling. *Cell Metabolism*, 25, 197-207. (<https://doi.org/10.1016/j.cmet.2016.10.013>)

Van Meer, G., Voelker, D. R. & Feigenson, G. W. 2008. Membrane lipids: where they are and how they behave. *Nature Reviews Molecular Cell Biology*, 9, 112-124. (<https://doi.org/10.1038/nrm2330>)

Vanderhyden, B. C., Caron, P. J., Buccione, R. & Eppig, J. J. 1990. Developmental pattern of the secretion of cumulus expansion-enabling factor by mouse oocytes and the role of oocytes in promoting granulosa cell differentiation. *Developmental Biology*, 140, 307-317. ([https://doi.org/10.1016/0012-1606\(90\)90081-s](https://doi.org/10.1016/0012-1606(90)90081-s))

Vanholder, T., Leroy, J. L., Soom, A. V., Opsomer, G., Maes, D., Coryn, M. & De Kruif, A. 2005. Effect of non-esterified fatty acids on bovine granulosa cell steroidogenesis and proliferation in vitro. *Animal Reproduction Science*, 87, 33-44. (<https://doi.org/10.1016/j.anireprosci.2004.09.006>)

Vanholder, T., Leroy, J. L., Van Soom, A., Coryn, M., De Kruif, A. & Opsomer, G. 2006. Effects of beta-OH butyrate on bovine granulosa and theca cell function in vitro. *Reproduction in Domestic Animals*, 41, 39-40. (<https://doi.org/10.1111/j.1439-0531.2006.00634.x>)

Vanorny, D. A. & Mayo, K. E. 2017. The role of Notch signaling in the mammalian ovary. *Reproduction*, 153, R187-R204. (<https://doi.org/10.1530/REP-16-0689>)

Vasquez, M., Simões, I., Consuegra-Fernández, M., Aranda, F., Lozano, F. & Berraondo, P. 2017. Exploiting scavenger receptors in cancer immunotherapy: Lessons from CD5 and SR-B1. *European Journal of Immunology*, 47, 1108-1118. (<https://doi.org/10.1002/eji.201646903>)

Vigetti, D., Viola, M., Karousou, E., De Luca, G. & Passi, A. 2014. Metabolic control of hyaluronan synthases. *Matrix Biology*, 35, 8-13. (<https://doi.org/10.1016/j.matbio.2013.10.002>)

- Vishnyakova, T. G., Bocharov, A. V., Baranova, I. N., Chen, Z., Remaley, A. T., Csako, G., Eggerman, T. L. & Patterson, A. P. 2003. Binding and internalization of lipopolysaccharide by Cla-1, a human orthologue of rodent scavenger receptor B1. *Journal of Biological Chemistry*, 278, 22771-22780. (<https://doi.org/10.1074/jbc.M211032200>)
- Von Wald, T., Monisova, Y., Hacker, M. R., Yoo, S. W., Penzias, A. S., Reindollar, R. R. & Usheva, A. 2010. Age-related variations in follicular apolipoproteins may influence human oocyte maturation and fertility potential. *Fertility and Sterility*, 93, 2354-2361. (<https://doi.org/10.1016/j.fertnstert.2008.12.129>)
- Walsh, S. W., Fair, T., Browne, J. A., Evans, A. C. & Mcgettigan, P. A. 2012a. Physiological status alters immunological regulation of bovine follicle differentiation in dairy cattle. *Journal of Reproductive Immunology*, 96, 34-44. (<https://doi.org/10.1016/j.jri.2012.07.002>)
- Walsh, S. W., Mehta, J. P., Mcgettigan, P. A., Browne, J. A., Forde, N., Alibrahim, R. M., Mulligan, F. J., Loftus, B., Crowe, M. A., Matthews, D., Diskin, M., Mihm, M. & Evans, A. C. 2012b. Effect of the metabolic environment at key stages of follicle development in cattle: focus on steroid biosynthesis. *Physiological Genomics*, 44, 504-517. (<https://doi.org/10.1152/physiolgenomics.00178.2011>)
- Wandji, S. A., Srsen, V., Voss, A. K., Eppig, J. J. & Fortune, J. E. 1996. Initiation in vitro of growth of bovine primordial follicles. *Biology of Reproduction*, 55, 942-948. (<https://doi.org/10.1095/biolreprod55.5.942>)
- Wang, Y., Huo, P., Sun, Y. & Zhang, Y. 2019. Effects of Body Condition Score Changes During Parturition on the Postpartum Health and Production Performance of Primiparous Dairy Cows. *Animals : an open access journal from MDPI*, 9, 1159. (<https://doi.org/10.3390/ani9121159>)
- Wasko, B. M., Smits, J. P., Shull, L. W., Wiemer, D. F. & Hohl, R. J. 2011. A novel bisphosphonate inhibitor of squalene synthase combined with a statin or a nitrogenous bisphosphonate in vitro. *Journal of Lipid Research*, 52, 1957-1964. (<https://doi.org/10.1194/jlr.M016089>)
- Wathes, D. C., Cheng, Z., Chowdhury, W., Fenwick, M. A., Fitzpatrick, R., Morris, D. G., Patton, J. & Murphy, J. J. 2009. Negative energy balance alters global gene expression and immune responses in the uterus of postpartum dairy cows. *Physiological Genomics*, 39, 1-13. (<https://doi.org/10.1152/physiolgenomics.00064.2009>)
- Wathes, D. C., Cheng, Z., Fenwick, M. A., Fitzpatrick, R. & Patton, J. 2011. Influence of energy balance on the somatotrophic axis and matrix metalloproteinase expression in the endometrium of the postpartum dairy cow. *Reproduction*, 141, 269-281. (<https://doi.org/10.1530/REP-10-0177>)
- Weitz-Schmidt, G. 2002. Statins as anti-inflammatory agents. *Trends in Pharmacological Sciences*, 23, 482-487. ([https://doi.org/10.1016/s0165-6147\(02\)02077-1](https://doi.org/10.1016/s0165-6147(02)02077-1))



Westermann, S., Drillich, M., Kaufmann, T. B., Madoz, L. V. & Heuwieser, W. 2010. A clinical approach to determine false positive findings of clinical endometritis by vaginoscopy by the use of uterine bacteriology and cytology in dairy cows. *Theriogenology*, 74, 1248-1255. (<https://doi.org/10.1016/j.theriogenology.2010.05.028>)

Whitty, A., Kind, K. L., Dunning, K. R. & Thompson, J. G. 2021. Effect of oxygen and glucose availability during in vitro maturation of bovine oocytes on development and gene expression. *Journal of Assisted Reproduction and Genetics*, 38, 1349-1362. (<https://doi.org/10.1007/s10815-021-02218-w>)

Wildman, E. E., Jones, G. M., Wagner, P. E., Boman, R. L., Troutt, H. F. & Lesch, T. N. 1982. A Dairy Cow Body Condition Scoring System and Its Relationship to Selected Production Characteristics. *Journal of Dairy Science*, 65, 495-501. ([https://doi.org/10.3168/jds.S0022-0302\(82\)82223-6](https://doi.org/10.3168/jds.S0022-0302(82)82223-6))

Williams, E. J., Fischer, D. P., Noakes, D. E., England, G. C., Rycroft, A., Dobson, H. & Sheldon, I. M. 2007. The relationship between uterine pathogen growth density and ovarian function in the postpartum dairy cow. *Theriogenology*, 68, 549-559. (<https://doi.org/10.1016/j.theriogenology.2007.04.056>)

Wrobel, K. H. & Suss, F. 1998. Identification and temporospatial distribution of bovine primordial germ cells prior to gonadal sexual differentiation. *Anatomy and Embryology (Berl)*, 197, 451-467. (<https://doi.org/10.1007/s004290050156>)

Xu, Z., Garverick, H. A., Smith, G. W., Smith, M. F., Hamilton, S. A. & Youngquist, R. S. 1995a. Expression of follicle-stimulating hormone and luteinizing hormone receptor messenger ribonucleic acids in bovine follicles during the first follicular wave. *Biology of Reproduction*, 53, 951-957. (<https://doi.org/10.1095/biolreprod53.4.951>)

Xu, Z., Garverick, H. A., Smith, G. W., Smith, M. F., Hamilton, S. A. & Youngquist, R. S. 1995b. Expression of messenger ribonucleic acid encoding cytochrome P450 side-chain cleavage, cytochrome p450 17 alpha-hydroxylase, and cytochrome P450 aromatase in bovine follicles during the first follicular wave. *Endocrinology*, 136, 981-989. (<https://doi.org/10.1210/endo.136.3.7867608>)

Yaba, A., Bianchi, V., Borini, A. & Johnson, J. 2008. A putative mitotic checkpoint dependent on mTOR function controls cell proliferation and survival in ovarian granulosa cells. *Reproductive Sciences*, 15, 128-138. (<https://doi.org/10.1177/1933719107312037>)

Yamamoto, M., Sato, S., Hemmi, H., Hoshino, K., Kaisho, T., Sanjo, H., Takeuchi, O., Sugiyama, M., Okabe, M., Takeda, K. & Akira, S. 2003. Role of Adaptor TRIF in the MyD88-Independent Toll-like Receptor Signaling Pathway. *Science*, 301, 640-643. (<https://doi.org/10.1126/science.1087262>)

Yamashita, H., Murayama, C., Takasugi, R., Miyamoto, A. & Shimizu, T. 2011. BMP-4 suppresses progesterone production by inhibiting histone H3 acetylation of StAR in bovine granulosa cells in vitro. *Molecular and Cellular Biochemistry*, 348, 183-190. (<https://doi.org/10.1007/s11010-010-0653-9>)

- Yang, H., Wang, X., Zhang, Y., Liu, H., Liao, J., Shao, K., Chu, Y. & Liu, G. 2014. Modulation of TSC-mTOR signaling on immune cells in immunity and autoimmunity. *Journal of Cellular Physiology*, 229, 17-26. (<https://doi.org/10.1002/jcp.24426>)
- Yang, M., Wang, X., Wang, L., Wang, X., Li, J. & Yang, Z. 2017. IL-1alpha Up-Regulates IL-6 Expression in Bovine Granulosa Cells via MAPKs and NF-kappaB Signaling Pathways. *Cellular Physiology and Biochemistry*, 41, 265-273. (<https://doi.org/10.1159/000456091>)
- Yang, W., Wang, L., Wang, F. & Yuan, S. 2020. Roles of AMP-Activated Protein Kinase (AMPK) in Mammalian Reproduction. *Frontiers in Cell and Developmental Biology*, 8. (<https://doi.org/10.3389/fcell.2020.593005>)
- Yao, J. Q. & Yu, F. 2011. DEB: A web interface for RNA-seq digital gene expression analysis. *Bioinformatics*, 7, 44-45. (<https://doi.org/10.6026/97320630007044>)
- Yazdi, A. S. & Drexler, S. K. 2013. Regulation of interleukin 1alpha secretion by inflammasomes. *Annals of the Rheumatic Diseases*, 72 Suppl 2, ii96-99. (<https://doi.org/10.1136/annrheumdis-2012-202252>)
- Yesilaltay, A., Dokshin, G. A., Busso, D., Wang, L., Galiani, D., Chavarria, T., Vasile, E., Quilaqueo, L., Orellana, J. A., Walzer, D., Shalgi, R., Dekel, N., Albertini, D. F., Rigotti, A., Page, D. C. & Krieger, M. 2014. Excess cholesterol induces mouse egg activation and may cause female infertility. *Proceedings of the National Academy of Sciences of the United States of America*, 111, E4972-4980. (<https://doi.org/10.1073/pnas.1418954111>)
- Young, J. M. & Mcneilly, A. S. 2010. Theca: the forgotten cell of the ovarian follicle. *Reproduction*, 140, 489-504. (<https://doi.org/10.1530/rep-10-0094>)
- Yu, J., Thomson, T. C. & Johnson, J. 2012. Cross talk between estradiol and mTOR kinase in the regulation of ovarian granulosa proliferation. *Reproductive Sciences*, 19, 143-151. (<https://doi.org/10.1177/1933719111424447>)
- Yu, J., Yaba, A., Kasiman, C., Thomson, T. & Johnson, J. 2011. mTOR controls ovarian follicle growth by regulating granulosa cell proliferation. *PLoS One*, 6, e21415. (<https://doi.org/10.1371/journal.pone.0021415>)
- Yuan, Y., Ida, J. M., Paczkowski, M. & Krisher, R. L. 2011. Identification of developmental competence-related genes in mature porcine oocytes. *Molecular Reproduction and Development*, 78, 565-575. (<https://doi.org/10.1002/mrd.21351>)
- Yvan-Charvet, L., Welch, C., Pagler, T. A., Ranalletta, M., Lamkanfi, M., Han, S., Ishibashi, M., Li, R., Wang, N. & Tall, A. R. 2008. Increased inflammatory gene expression in ABC transporter-deficient macrophages: free cholesterol accumulation, increased signaling via toll-like receptors, and neutrophil infiltration of atherosclerotic lesions. *Circulation*, 118, 1837-1847. (<https://doi.org/10.1161/CIRCULATIONAHA.108.793869>)
- Zhang, G., Meredith, T. C. & Kahne, D. 2013. On the essentiality of lipopolysaccharide to Gram-negative bacteria. *Current Opinion in Microbiology*, 16, 779-785. (<https://doi.org/10.1016/j.mib.2013.09.007>)

- Zhang, J. Y., Wu, Y., Zhao, S., Liu, Z. X., Zeng, S. M. & Zhang, G. X. 2015. Lysosomes are involved in induction of steroidogenic acute regulatory protein (StAR) gene expression and progesterone synthesis through low-density lipoprotein in cultured bovine granulosa cells. *Theriogenology*, 84, 811-817. (<https://doi.org/10.1016/j.theriogenology.2015.05.016>)
- Zhang, Z., Amorosa, L. F., Petrova, A., Coyle, S., Macor, M., Nair, M., Lee, L. Y. & Haimovich, B. 2019. TLR4 counteracts BVRA signaling in human leukocytes via differential regulation of AMPK, mTORC1 and mTORC2. *Scientific Reports*, 9, 7020. (<https://doi.org/10.1038/s41598-019-43347-8>)
- Zhao, Q., Chu, Z., Zhu, L., Yang, T., Wang, P., Liu, F., Huang, Y., Zhang, F., Zhang, X., Ding, W. & Zhao, Y. 2017a. 2-Deoxy-d-Glucose Treatment Decreases Anti-inflammatory M2 Macrophage Polarization in Mice with Tumor and Allergic Airway Inflammation. *Frontiers in Immunology*, 8, 637. (<https://doi.org/10.3389/fimmu.2017.00637>)
- Zhao, S., Pang, Y., Zhao, X., Du, W., Hao, H. & Zhu, H. 2019. Detrimental effects of lipopolysaccharides on maturation of bovine oocytes. *Asian-Australasian Journal of Animal Sciences*, 32, 1112-1121. (<https://doi.org/10.5713/ajas.18.0540>)
- Zhao, S. J., Pang, Y. W., Zhao, X. M., Du, W. H., Hao, H. S. & Zhu, H. B. 2017b. Effects of lipopolysaccharide on maturation of bovine oocyte in vitro and its possible mechanisms. *Oncotarget*, 8, 4656-4667. (<https://doi.org/10.18632/oncotarget.13965>)
- Zhao, X., Zmijewski, J. W., Lorne, E., Liu, G., Park, Y.-J., Tsuruta, Y. & Abraham, E. 2008. Activation of AMPK attenuates neutrophil proinflammatory activity and decreases the severity of acute lung injury. *American Journal of Physiology-Lung Cellular and Molecular Physiology*, 295, L497-L504. (<https://doi.org/10.1152/ajplung.90210.2008>)
- Zhao, X. M., Wang, N., Hao, H. S., Li, C. Y., Zhao, Y. H., Yan, C. L., Wang, H. Y., Du, W. H., Wang, D., Liu, Y., Pang, Y. W. & Zhu, H. B. 2018. Melatonin improves the fertilization capacity and developmental ability of bovine oocytes by regulating cytoplasmic maturation events. *Journal of Pineal Research*, 64. (<https://doi.org/10.1111/jpi.12445>)
- Zhao, Y., Hu, X., Liu, Y., Dong, S., Wen, Z., He, W., Zhang, S., Huang, Q. & Shi, M. 2017c. ROS signaling under metabolic stress: cross-talk between AMPK and AKT pathway. *Molecular Cancer*, 16, 79. (<https://doi.org/10.1186/s12943-017-0648-1>)
- Zheng, D., Liwinski, T. & Elinav, E. 2020. Inflammasome activation and regulation: toward a better understanding of complex mechanisms. *Cell Discovery*, 6, 36. (<https://doi.org/10.1038/s41421-020-0167-x>)
- Zhu, X., Lee, J. Y., Timmins, J. M., Brown, J. M., Boudyguina, E., Mulya, A., Gebre, A. K., Willingham, M. C., Hiltbold, E. M., Mishra, N., Maeda, N. & Parks, J. S. 2008. Increased cellular free cholesterol in macrophage-specific Abca1 knock-out mice enhances pro-inflammatory response of macrophages. *Journal of Biological Chemistry*, 283, 22930-22941. (<https://doi.org/10.1074/jbc.M801408200>)

Zoncu, R., Efeyan, A. & Sabatini, D. M. 2011. mTOR: from growth signal integration to cancer, diabetes and ageing. *Nature Reviews Molecular Cell Biology*, 12, 21-35. (<https://doi.org/10.1038/nrm3025>)